50th ANNUAL
HIGHWAY GEOLOGY SYMPOSIUM

& TRB Karst Meeting

PROCEEDINGS & FIELD TRIP GUIDE

May 20th – 23rd, 1999
The Hotel Roanoke & Conference Center
Roanoke, Virginia

sponsored by

Radford University
Department of Geology / Institute for Engineering Geosciences
Virginia Department of Mines, Minerals and Energy
Division of Mineral Resources
Virginia Department of Transportation

CONTENTS

HIGHWAY GEOLOGY SYMPOSIUM
STEERING COMMITTEE OFFICERS

Mr. Earl Wright, Chair **1999**
Engineering Geology Section Supervisor
Geotechnical Branch
Division of Materials
Department of Highways
Transportation Cabinet
Frankfort, Kentucky 40622
PH: 502-564-2374

Mr. Robert W. Henthorn, Vice Chair **2000**
Kansas Department of Transportation
Box 498
411 W. 14th Street
Chanute, Kansas 66720-0498
PH: 316-431-1000 Ext. 47

Mr. G. Michael Hager, Secretary **2000**
Wyoming Transprotation Dept.
P.O. Box 1708
Cheyenne, Wyoming 82003-1708
PH: 307-777-4475

Mr. Russell Glass, Treasurer **Appointed by Chairman**
Area Geologist
Geotechnical Unit
North Carolina Department of Transportation
Asherville, North Carolina 28802
PH: 828-298-3874

NATIONAL STEERING COMMITTEE 1999
HIGHWAY GEOLOGY SYMPOSIUM

NAME/ADDRESS	PHONE/FAX/E-MAIL
Ken Ashton West Virginia Geological Survey P.O. Box 879 Morgantown, WV 26507-0879	PH 304-594-2331 FX 304-594-2575 E-MAIL ASHTON@geosrv.wvnet.edu
John Baldwin West Virginia Div. of Highways 312 Michigan Ave. Charleston, WV 25311	PH 304-558-3084 FX 304-558-0253 E-MAIL jbaldwin@mail.dot.state.wv.us
Vernon Bump South Dakota DOT Geotech. Engr. Activity 700 E. Broadway Ave. Pierre, SD 57501-2586	PH 605-773-3401 FX 605-773-5867 E-MAIL vern.bump@state.sd.us
Richard Cross New York State Thruway Authority 200 Southern Blvd. P.O. Box 189 Albany, NY 12201-0189	PH 518-471-4277 FX 518-436-3096 E-MAIL cross-r@eng.nystwy.com
Jeff Dean Oklahoma DOT 200 NE 21ST St. Oklahoma City, OK 73015	PH 405-521-2677 FX 405-522-0552 E-MAIL JeffDean ODOT@fd9n01.okladot.state.ok.us
Russell Glass North Carolina DOT Geotechnical Section P.O. Box 3279 Asheville, NC 28802	PH 704-298-3874 FX 704-299-1273 E-MAIL rglass@dot.state.nc.us
Robert Goddard National High Magnetic Field Lab Florida State University 1800 E. Paul Dirac Dr. Tallahassee, FL 32306-4005	PH 850-644-4304 FX 850-644-0687 E-MAIL goddard@magnet.fsu.edu
G. Michael Hager Wyoming DOT P.O. Box 1708 Cheyenne, WY 82003-1708	PH 307-777-4205 FX 307-777-3994 E-MAIL Mhager@missc.state.wy.us

NATIONAL STEERING COMMITTEE
HIGHWAY GEOLOGY SYMPOSIUM 1999

NAME/ADDRESS	PHONE/FAX/E-MAIL
Robert W. Henthorne Kansas DOT P.O. Box 498 411 W. 14TH St. Chanute, KS 66720-0498	PH 316-431-1000 EXT 47 FX 316-431-6946 E-MAIL roberth@dtdist4.wpo.state.ks.us
Richard Humphries Golder Associates 3730 Chamblee Tucker Rd. Atlanta, GA 30341	PH 770-496-1893 FX 770-934-9476 E-MAIL rhumphries@Golder.com
Harry Ludowise 6308 NE. 12TH Ave. Vancouver, WA 98665	PH 206-693-1617 FX 360-696-7842 E-MAIL vusas@teleport.com
A. David Martin Maryland DOT Office of Materials & Research 2323 W. Joppa Road Brooklandville, MD 21022	PH 410-321-3107 FX 410-321-3099 EMAIL dmartin@sha.state.md.us
Henry Mathis, PE Mathis Geotechnical Consulting, Inc. 561 Marblerock Way Lexington, KY 40503	PH 606-296-5664 Home: 606-223-8632 FX 606-296-5664 E-MAIL hmathis@iglou.com
Harry Moore Tennessee DOT P.O. Box 58 Knoxville, TN 37901	PH 423-594-9436 FX 423-594-9310 E-MAIL hmoore@mail.state.tn.us
Christopher A. Ruppen Michael Baker Jr. Inc. 4301 Dutch Ridge Rd. Beaver, PA 15009-9600	PH 724-495-4079 FX 724-495-4017 E-MAIL cruppen@mbakercorp.com
Steve Senior Ministry of Transportation, Ontario 1201 Wilson Ave., Rm 220, Cent bldg. Downsview, ON M3M 1J6 Canada	PH 416-235-3743 FX 416-235-4101 E-MAIL senior@mto.gov.on.ca

NATIONAL STEERING COMMITTEE
HIGHWAY GEOLOGY SYMPOSIUM, 1999

NAME/ADDRESS	PHONE/FAX/E-MAIL
Willard L. Sitz Alabama DOT 1409 Coliseum Blvd. Montgomery, AL 36110-2060	PH 334-206-2279 FX 334-264-6263 E-MAIL sitzw@dot.state.al.us
Jim Stroud Vulcan Materials Co. 4401 N. Patterson Ave. P.O. Box 4239 Winston-Salem, NC 27115	PH 336-767-4600 FX 336-744-2019 E-MAIL stroudj@vmcmail.com
Steven E. Sweeney New York State Thruway Authority 200 Southern Blvd. Albany, NY 12209	PH 518-471-4378 FX 518-436-3060 E-MAIL steve_sweeney@thruway.state.ny.us
Robert Thommen Brugg Cable Products, Inc. RR 31, Box 197E, 11 E. Frontage Rd. Santa Fe, NM 87505	PH 505-438-6161 FX 505-438-6166 E-MAIL geobrugg@aol.com
Sam I. Thornton 3712 Hwy. 112 N. Fayetteville, AR 72704	PH 501-521-1331 FX 501-521-0429 E-MAIL samthornton@earthlink.net
Michael P. Vierling New York State DOT State Office Building Campus Bldg. 7, Rm. 106 1220 Washington Ave. Albany, NY 12232	PH 518-457-4727 FX 518-457-8080 E-MAIL mvierling@gy.dot.state.ny.us
Skip Watts Institute for Engineering Geosciences Radford University Radford VA 24142	PH 540-831-5637 FX 540-831-5732 E-MAIL cwatts@runet.edu
Terry West Earth and Atmospheric Science Dept. Purdue University West Lafayette, IN 47907-1297	PH 765-494-3296 FX 765-496-1210 E-MAIL trwest@omni.cc.purdue.edu

NATIONAL STEERING COMMITTEE
HIGHWAY GEOLOGY SYMPOSIUM, 1999

W. A. Wisner
Martin Marietta Aggregates
P.O. Box 30013

PH 919-783-4649
FX 919-783-4552
E-MAIL Raleigh, NC 27622

Earl Wright
Kentucky Dept. of Highways,
Geotech Branch
1236 Wilkinson Blvd.
Frankfort, KY 40601-1200

PH 502-564-2374
FX 502-564-4839
E-MAIL ewright@mail.kytc.state.ky.us

HIGHWAY GEOLOGY SYMPOSIUM
MEDALLION AWARD WINNERS

The Medallion Award is presented to individuals who have made significant contributions to the Highway Geology Symposium over many years. The award, instituted in 1969, is a 3.5-inch medallion mounted on a walnut shield and appropriately inscribed. The award is presented during the banquet at the annual Symposium.

Hugh Chase*	-	1970
Tom Parrott*	-	1970
Paul Price*	-	1970
K. B. Woods*	-	1971
R. J. Edmonson*	-	1972
C. S. Mullin*	-	1974
A. C. Dodson*	-	1975
Burrell Whitlow*	-	1978
Bill Sherman	-	1980
Virgil Burgat*	-	1981
Henry Mathis	-	1982
David Royster*	-	1982
Terry West	-	1983
Dave Bingham	-	1984
Vernon Bump	-	1986
C. W. "Bill" Lovell	-	1989
Joseph A. Gutierrez	-	1990
Willard McCasland	-	1990
W. A. "Bill" Wisner	-	1991
David Mitchell	-	1993
Harry Moore	-	1996
Earl Wright	-	1997
Russell Glass	-	1998

*Deceased

HIGHWAY GEOLOGY SYMPOSIUM
EMERITUS MEMBERS OF THE STEERING COMMITTEE

Emeritus Status is granted by the Steering Committee.

R. F. Baker*
David Bingham
Virgil E. Burgat*
Robert G. Charboneau*
Hugh Chase*
A. C. Dodson*
Walter F. Fredericksen
Joseph Gutierrez
Charles T. Janik
John Lemish
George S. Meadors, Jr.*
Willard McCasland
David Mitchell
W. T. Parrot*
Paul Price*
David L. Royster*
Bill Sherman
Mitchell Smith
Berke Thompson*
Burrell Whitlow*
Ed J. Zeigler

*Deceased

HIGHWAY GEOLOGY SYMPOSIUM

FUTURE SCHEDULE

YEAR	ANNUAL	LOCATION	COORDINATORS
2000	51st	Washington	Prof. Robert Holtz Univ. of Washington & Steven Lowell Washington DOT
2001	52nd	TBD	
2002	53rd	California	John Duffy CALTRANS (805) 549-3663
2003	54th	TBD	
2004	55th	Minnesota	Chuck Howe Minnesota MDOT (612) 779-5602
2005	56th	Vermont	Tom Eliassen Vermont DOT (802) 828-2561

PREFACE

W. T. Parrott, a long time geologist with the Virginia Department of Transportation, was instrumental in organizing the first Highway Geology Symposium in 1950. In recognition of Tom Parrott's contribution to the Annual Highway Geology Symposium, the following short paper is reprinted from the October 1957 issue of "Virginia Minerals".

THE GEOLOGIST'S ROLE IN HIGHWAY ENGINEERING

W. T. PARROTT, Highway Geologist
Virginia Department of Highways

The role of the geologist in highway engineering is not new, but within the past 20 years the use of geology in the field of highway construction has been steadily increasing. As far back as 1898 the Maryland Highway Division was a part of the Maryland Geological Survey, but in 1910 the Maryland State Roads Commission incorporated the highway division into its organization. In 1955, Dr. J. T. Singewald, Jr., Director, Maryland Department of Geology, Mines and Water Resources, sent a questionnaire to the Association of American State Geologists, requesting information on the employment of geologists by their respective highway departments. The replies indicated that 23 highway departments employed from 1 to 10 geologists. This questionnaire also revealed that Ohio was the first State, 1914, to employ a geologist in its highway department, and that the first highway geological section was established in 1923 by Missouri. On January 1, 1947, the Virginia Department of Highways established a geological section within the Testing Division, with the writer as the highway geologist. Since then, the staff has been increased to eight geologists.

The duties of a highway geologist are numerous; however, an analysis of the work done by a highway geological section and that done by a geological survey shows that there is no duplication or competition. The function of a state highway department is to build and maintain highways and necessary structures. The construction materials are geologic in origin and the structures rest on geologic foundations. The more costly the road and more exacting the traffic requirements, the more essential it is to use geologic knowledge in the design and construction of the highway.

The functions of a highway geologist are:

1. To locate stone quarries and sand and gravel pits
2. To conduct local or statewide surveys for aggregate
3. To supervise core drilling and interpret core drill data
4. To make geophysical surveys, either seismic or electrical resistivity
5. To make vibration studies in connection with potential blast damage
6. To investigate slides or areas of potential sides and suggest either preventive or remedial measures
7. To assist in design of slopes and benches
8. To investigate alleged blast damage to wells, springs and dwellings
9. To act as a expert witness in ligation
10. To instruct engineer trainees in refresher courses in general geology.

An examination of these primary functions will show what specific knowledge is required and that a specially trained geologist, preferably one with some engineering experience, is needed to appraise accurately the existing conditions. Such training is gained by experience or a course in engineering geology.

In the location of a quarry, the most important items are the quantity, quality, and availability of the stone. Generally, the most important physical properties of good highway aggregate are low abrasion loss, freedom from injurious minerals, and affinity for bituminous material. Depending on the purpose for which the stone is to be used, an abrasion loss up to 43% is acceptable for most primary construction and maintenance work. Almost all granite, granite gneiss, limestone, dolomite, basalt, and greenstone will meet these specifications. Aggregates that contain a high percentage of mica, chlorite, or talc will give a poor bond with bituminous material and their adhesive qualities in various bituminous mixes should be predetermined by laboratory tests.

In conducting an aggregate survey for either a specific project or on a statewide basis, a comprehensive knowledge of the previously mentioned physical properties of the stone is necessary so that the material selected will meet specifications. In this manner, the geologist assists the engineer in locating the materials that are available nearest the project, thus eliminating long hauls and reducing the cost of the project.

Superficial rod soundings for bridges have been replaced by detailed exploration by core drills, and probably one of the biggest jobs of the highway geologist is correlating and interpreting core drill data. In rock, the core drilling entails the cutting of a rock core, which is examined for fractures, mineral content, and degree of weathering. In unconsolidated materials, samples of sand, clay, or gravel are taken and examined for moisture content and degree of plasticity, and the resistance the materials offered to drill casing or sampling spoon is noted. Once these data are obtained, an accurate appraisal of the results by the geologist gives a picture of the subsurface conditions to the bridge designer and a bridge can be designed for the best as well as the worst, conditions that may be encountered, with substantial savings in the design.

Geophysical advances that have aided the geologist and the engineer are electrical and seismic subsurface surveys. The old method of estimating the amount of rock and soil which may be encountered has given way to the more accurate determination by either resistivity or seismic methods. Both of these methods are used by state highway departments. The seismic method is a small scale utilization of the reflection principle which is used by oil companies in exploratory work. A small charge of dynamite is exploded, setting up seismic waves, which are recorded on special instruments placed a various distance from the shot point. The interval between time of shot and arrival of the seismic waves at recording stations is measured and the velocity of waves determined. Because various materials transmit the waves at different velocities, this information is used with the known geology of the region to interpret the subsurface conditions. The electrical resistivity method is probably more popular because it requires less equipment, eliminates the danger from explosives, and affords greater portability. This method measures the resistance that material will offer a given amount of electrical current. By correlating this information with the known geology, aided by one or two test holes, a very accurate rock-soil profile can be developed. From cross sections drawn of the proposed construction, the highway designer can calculate the over-all amount of cut and fill he may have in a given area; however, with the rock-soil profile, it is possible to determine the amount of rock available for the base of the fill and the amount of material available for capping or for borrow purposes. The Virginia Department of Highways has been using the resistivity method since 1950, and predictions based on this rock-soil profile have averaged 98 percent correct as proved by actual construction.

One of the greatest bugbears with which a highway department may be faced is an enormous number of claims from property owners who live in areas adjacent to construction limits, that their wells, springs, or dwellings have been injured by blasting during construction. Vibration studies have come to the aid of the engineers in such cases. In the past, the determination of alleged damage has been based on personal observation and the reports of the people on the construction project and of the property owners. However, there was rarely concrete evidence, except in a few cases, that would support the contention of either side. Within the past few years the development of an instrument for the measurement of vibration and the acceleration of shock waves through the earth and rock has gone far to eliminate potential court cases, as well as substantiate the claims of the state or property owner. In fact, the science of vibration study is rapidly developing a branch of specialists who can render great aid to any individual or corporation faced with potential blast damage. The use of these experts, plus their recording machine, has, in at least two cases, saved the state and the taxpayers thousands of dollars in refuting the claims of private individuals who claimed that their property had been damaged. With the expanding use of these instruments it is believed that virtually all claims will be placed on a scientific basis and each can be decided upon its own merits.

One of the natural phenomena that can be very time consuming to the highway geologist is landslides and rock falls. Contrary to popular opinion, a landslide need not be a catastrophic occurrence, but may take the form of relatively small amounts of rock and earth that plague the highway engineers in either old or new construction. It is the duty of the highway geologist to inform the design engineer of any area that offers a slide potential and to suggest preventive measures which would eliminate or at least reduce the danger of slides. Once a slide has occurred, it is also the highway geologist's duty to suggest remedial measures which will prevent future slides. Some of these measures are benching, flattening the slope, stabilizing the area by vegetation, and last, but far from least, is proper drainage. In some instances vertical sand drains, which are drill holes filled with sand to remove excess moisture, are used. Grouting is also used: that is, a mixture of sand, water and cement is pumped into the ground and the mixture, or grout, forces out excessive moisture and occupies the former voids. Upon setting, the grout binds the soil together and prevents water from entering the area treated. In grouting as area, adequate provision must be made for escape of ground water; otherwise, the building of hydrostatic pressure may wreck all efforts to control the slide.

With the inauguration of the new federal highway program, the proper design of slopes and benches that will conform to the standards of the Federal specifications has increased the work of the highway geologist. Each of these cases is an individual one and the benching and sloping must be tailored to suit the existing conditions.

Another facet of the highway geologist's duties is that of acting as an expert witness in litigation between property owners or contractors and the state. Any of the aforementioned functions may be used as a basis of litigation, and the testimony of the geologist may lead to a favorable judicial decision. The two subjects on which the highway geologist is called upon to testify most frequently are damage to water supplies and dwellings.

A very important function of the highway geologist is to offer a short refresher course in general geology to engineer trainees. Most of these men have had at least one course in general geology while in college, but it is a duty of the geologist to point out the more special aspects of geology as applied to highway engineering. In this course the young engineer learns that geology is another tool with which the adverse conditions and agents of nature may be more successfully controlled. Within the past ten years, at least 100 or more engineer trainees have been given this refresher course.

This resume of the geologist's role in highway engineering presents a brief picture of his part in the world of highway construction. As the highway program progresses, it is becoming more and more apparent that the advice and studies of the geologist regarding highway problems are a great aid to the construction engineer. It is not claimed for one instance that geology in itself is a panacea for all highway problems, but if used intelligently it can go far in helping to eliminate some of the vexing problems with which the highway engineers are confronted.

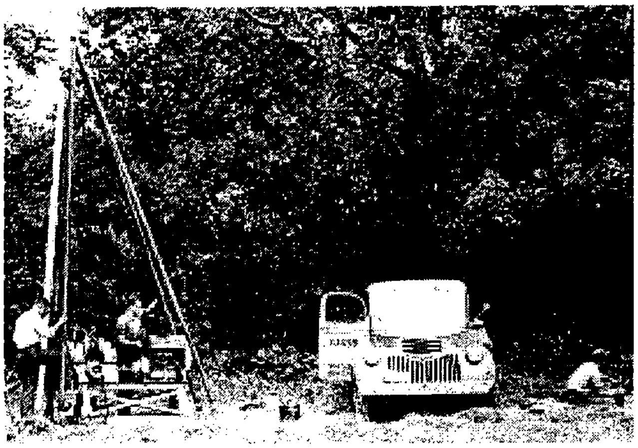

Figure 1. Core drilling for bridge foundation at Cedar Creek, Frederick-Shenandoah county line.

Figure 2. Resistivity unit is use to check depth of river gravel over bedrock in Alleghany County.

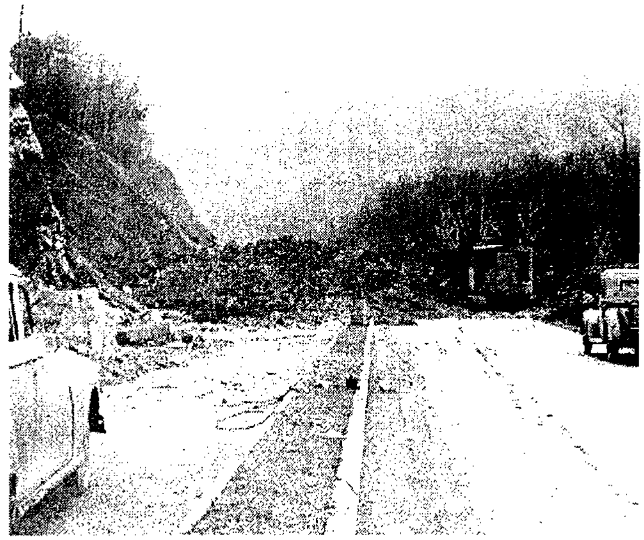

Figure 3. Slide on U.S. Highway 60, east of Covington, Allehany County. This slide was caused by movement of supersaturated clay and sand, and it covered the 4-lane highway with 3 to 11 feet of debris.

Figure 4. Grouting on U.S. Highway 460, two miles northeast of Narrows, Giles County. The mixture of water, sand, and cement is being pumped into a fill.

WELCOME TO VIRGINIA

Stanley S. Johnson, State Geologist
Department of Mines, Minerals and Energy
Division of Mineral Resources

It is a great opportunity to welcome you to Virginia and the 50th Highway Geology Symposium. This symposium is quite an honor to host, as Virginia was where the first meeting of the association was held. Your local Steering Committee has spent many long hours in ensuring that this meeting will be one of your most memorable.

Your field trip on Saturday has been carefully planned to show you some of the geology of the area and how it affects you as engineers. Your meeting site is at the northern end of the southern Appalachians, an area of classic geology for over a hundred and fifty years. In that you will only see a small part of some of the geology in the local areas, please take time to read the brief geologic summary of the geology of Virginia in your proceedings volume.

Again, Welcome. If any of us can make your meeting more enjoyable, please contact any of us on the Committee.

Virginia Geology and Mineral Resources

Virginia is characterized by perhaps the most varied terrain of any state east of the Mississippi River. Parts of five major physiographic provinces are encompassed including, from east to west, the Atlantic Coastal Plain, the Piedmont, the Blue Ridge, the Valley and Ridge, and the Appalachian Plateaus.

The Coastal Plain Province. The Coastal Plain, extending inland for more than 100 miles, is monotonously flat. The surface slopes gently eastward from elevations of less than 200 feet along its western margin to the Atlantic Ocean and Chesapeake Bay shores. Created by the flooding of the ancestral valley of the Susquehanna River which flowed across the present continental shelf to a coastal margin much lower and farther east, the Chesapeake Bay is the dominant topographic feature of the province. The melting of the last continental glacier caused a rise in sea level, so that tidal waters currently occupy, not only the lower valley of the Susquehanna, but also the lower portions of its primary tributaries, the James, York, Rappahannock and Potomac Rivers. Consequently, all are estuarine in character, with salt- and brackish-water marshes bordering much of the system. Sea cliffs eroded by the rising seas overlook the bay and associated estuaries in many places. The Atlantic side of the Eastern Shore and the coast south of Virginia Beach are fringed by barrier islands and longshore bars, which shelter extensive lagoons and associated swamps and marshes.

Economic materials mined in the province are sand, gravel, and clay. Mining will probably start within two years for heavy mineral sands (ilmenite, leucoxene, and zircon) in world class deposits discovered in Dinwiddie, Sussex, and Greenville Counties by Division geologic mapping.

The Piedmont Province. Largest of Virginia's physiographic provinces, the Piedmont extends from the Fall Line westward to the Blue Ridge Mountains. Structurally, it is comprised of a complex of metamorphic and plutonic rocks, overlain in a number of places by Triassic-age sedimentary beds. Elevations range from around 100 feet in the east to more than 1000 feet in the foothills of the Blue Ridge. Local relief generally is low but becomes less gentle to the west.

The rock types in this province are schists, gneisses, metamorphosed basalts, slates, phyllites, marble, and quartzites. These metamorphic rocks have been altered by intrusions of granite, gabbro, diabase, pegmatite and other igneous rocks. These metamorphic/igneous rocks continue under the Coastal Plain sediments. The rocks/minerals mined from the Piedmont are kyanite, slate, vermiculite, granite, gabbro, diabase, and feldspar. Some gem "mining" occurs in pegmatite. Former mining activity includes gold, lead, zinc, copper, soapstone, manganese, iron, and pyrite.

Mesozoic-age basins composed of relatively more erodible sedimentary rocks in north northeast trending; faulted troughs are present within the Piedmont terrane. These basins are parts of a belt of similar northeast-trending structures, all of Early Mesozoic age, in eastern North America. Such areas stand out, not only because they are generally lowland areas, but also because of the striking red color of the surface soils. The most extensive Triassic-age beds are found in the Culpeper basin, which extends from the Potomac River south to the Culpeper area; the Richmond basin just west of Richmond; and the Danville basin, which extends from North Carolina into Virginia to just west of Danville and from there northeastward into Campbell and Appomattox Counties. The basins contain sandstone, siltstone, shale, and conglomerate. Some of the basins contain coal and gas and oil (currently non-commercial). The first coal mining in North America occurred in the Richmond basin. The sedimentary rocks in these Mesozoic-age basins have been intruded by igneous rocks of Triassic and Jurassic age (basalts occur in the Culpeper basin).

The Blue Ridge Province. The rocks that form the Blue Ridge Province or mountains include a basement complex of Precambrian granite and gneiss along with late Precambrian metamorphosed sedimentary rocks. This old terrane of Precambrian-age metamorphosed sedimentary and volcanic rocks with igneous intrusions contains the "oldest" rock in Virginia. The Old Rag Granite is the oldest unit dated in Virginia at approximately 1.2 billion years. The complex of interbedded volcanic and sedimentary rocks in the Mount Rogers-White Top area are different from the rocks in central and northern Blue Ridge.

The Blue Ridge rocks are quarried for quartzite and dolostone for use as crushed stone. Past mining occurred for copper, iron, manganese, and a limited amount of tin.

The Blue Ridge follows a northeast-southwest alignment of the Appalachians across the west-central portion of the state. The Roanoke River, the southernmost of the three major rivers flowing eastward through the Blue Ridge, divides the province into two distinct parts. North of the river a central ridge dominates the topography, with spurs and associated ridges reaching outward from it. In addition to the Roanoke, both the James and the Potomac Rivers rise west of the Blue Ridge and flow eastward to the Chesapeake Bay. Several windgaps suggest that earlier streams did likewise. South of Roanoke, the Blue Ridge province becomes broader and higher, reaching a width of more than 50 miles along the North Carolina border. Here, the province becomes a mountainous upland, with the term Blue Ridge largely restricted to the sharply defined escarpment overlooking the Piedmont. Nevertheless, the Blue Ridge forms the drainage divide, with all streams flowing west through the higher mountains either into the north flowing New River or the south flowing Holston River system, both a part of the Mississippi drainage system. The two highest mountains in the state, Mt. Rogers (elevation 5,720 ft.) and White Top (elevation 5,520 ft.) are located in southern Blue Ridge.

The Valley and Ridge Province. This is the most varied region of the state, both topographically and geologically. Thick sedimentary layers accumulated during the Paleozoic Era, with strata comprised generally of sandstone, siltstone, and shale on the east grading westward into strata comprised generally of shale, dolostone, and limestone. The age of the rocks in this province is 570 to 335 million years. Diabase dikes and other exotic dike types are present. Toward the end of the Paleozoic, sediments accumulated faster and littoral to non-marine deposits similar to those of the present Coastal Plain spread westward across the older marine formations. Similar to the present Coastal Plain, large swampy areas developed with the thick residues of fast-growing plants accumulating in marsh and swamp environments; the origin of the numerous coal beds in western Virginia and the other Appalachian Plateaus states.

At the end of the Paleozoic, the crystalline rocks of the Blue Ridge and Piedmont were thrust westward, overriding the Paleozoic sedimentary rocks of the Valley and Ridge and deforming the beds into northeast-trending linear folds broken by numerous eastward-dipping thrust faults. The eastern portion of the province is characterized by wider, more open valleys and less prominent ridges. This Great Valley area is broader and lower to the northeast, becoming narrower and higher to the southwest. Karst features are common throughout the Valley and Ridge province. Sinkholes and sinking creeks are common throughout the province.

With the exception of the lower valley of the Shenandoah River, the Great Valley gives way to the west to a complex of northeast-trending ridges and narrow valleys, with the ridges rather than the valleys dominating the landscape. Sandstones are the primary ridge formers, and the valleys are cut into less resistant limestone and shale formations. Several summits of more than 4,000 feet are found in this area.

Resources currently utilized from this province are limestone, dolostone, sandstone, gypsum, iron oxides, clay, oil, natural gas, and shale. Past resources included salt, manganese, iron, lead, zinc, and barite.

The Appalachian Plateaus Province. The Allegheny and Cumberland Plateaus fringe the Ridge and Valley along much of the western margin of the state. Only in the southwest is it significant in any way other than as a topographic break. This area of the plateau, encompassing Dickenson, Buchanan, and part of Wise, Scott, Russell, Lee, and Tazewell Counties, and lying west of Sandy Ridge, can easily be identified by the dendritic drainage pattern west of the drainage divide, this in contrast with the predominantly linear pattern associated with the linear, narrow folds of the Valley and Ridge. Downcutting by the streams in the plateau region has created a maturely dissected landscape, with eroded valley slopes exposing the horizontal or gently dipping sedimentary beds. The sedimentary units are coal, shales, siltstones, and sandstones. The province generally contains 320 to 280 million-year-old units. The southwest Virginia coalfields are totally contained within this province. In addition to the coal, this province contains valuable resources of coal-bed methane, natural gas, and oil. Crushed stone is also produced.

MINERAL RESOURCES

In terms of contribution to the economy of the State, the most important mineral resources of Virginia area coal, crushed stone, sand and gravel, lime (limestone and dolostone), and natural gas. Virginia contains a world-class deposit of kyanite that is mined in Buckingham County. This is the only deposit of kyanite currently being mined in the United States. Virginia is also the only producer of a feldspar marketed as "Virginia Aplite" and the second leading producer of vermiculite. In 1994, Virginia ranked 21st in non-fuel mineral production.

Although the last metal mine in Virginia, the zinc and lead mine at Austinville, closed in December, 1981, there is continuing interest in the Commonwealth's precious and base metal metallic resources.

Virginia, as well as several other Appalachian states, were important gold producers during the last century, but declined as more economic deposits were discovered elsewhere. The high price of fold in the 1980s renewed interest in eastern U. S. deposits. Massive sulfide deposits of the Piedmont, especially those bearing copper, lead, and zinc as well as precious metals (gold and silver), are of interest, with that interest fluctuating in accordance with world metal prices.

A wide variety of non-metallic deposits, the industrial minerals and rocks, are of great interest and importance to Virginia. These include crushed and dimension stone, sand and gravel, limestone for cement and lime production, kyanite, soapstone, feldspar, iron-oxide pigments, vermiculite, gemstones, and clay materials.

ACTIVITIES

- - - Thursday, May 20 - - -

TRB pre-meeting Karst Field Trip: Thursday, May 20. The Transportation Research Board committees A2L01 & A2L05 are sponsoring a ½-day field trip to view the world-class karst features of southwest Virginia. Hydrogeologist Dr. Ernst Kastning will lead the excursion departing from the hotel lobby area at 12:30 pm and returning about 5:30 pm. The cost is $35.00. Pre-registration is required.

Exhibitor Setup: 2:00 pm to 5:00 pm
HGS Registration: 3:00 pm to 7:00 pm
Welcoming Icebreaker: Thursday, May 20, 7:00 pm to 9:00 pm in exhibitors' area.

- - - Friday, May 21 - - -

HGS Registration: 7:00 am to 5:00 pm
Exhibit area open: 8:00 am to 6:00 pm **Visit the Exhibits**
Technical Sessions: 7:00 am to 5:30 pm
Steering Committee Meeting: 5:30 – 7:00 pm

Guest Trip: Friday, May 21. A trip for spouses and guests is planned for the Blue Ridge Parkway. Featured will be tour & lunch at the Chateau Morrissette Winery and a tour of historic Mabry Mill. The group will depart at 10:00 am and return by 5:00 pm. The cost is $30.00. Pre-registration is required.

- - - Saturday May 22 - - -

HGS 50 Field Trip: ***Geology and Engineering Challenges of Southwest Virginia***. Departing promptly at 7:00 am from The Hotel Roanoke & Conference Center. The trip explores a beautiful and complex geologic setting. The metamorphic mountains of the Blue Ridge Province lie just to the east. The folded and faulted Paleozoic rocks of the Valley and Ridge Province lie just to the west. The trip will provide an overview of the geology and geologic challenges of these unique provinces. Stops will include Mill Mountain overlook in the Blue Ridge, Dixie Caverns and Spring Hollow roller compacted concrete dam in the karst area, lunch at the ancient landslide of the Mountain Lake Resort area (filming location for the movie Dirty Dancing) and the galloping highway landslide on Rt 460 at Narrows on the beautiful New River. The field trip centerpiece will be informative stops along the Smart Road test bed near Blacksburg, Va., including the 200'+ rock cuts presently under construction. Guests may attend the field trip for a $20.00 fee.

Social Time: Saturday, May 22, 6:30 pm to 7:30 pm in exhibitors' area.

Banquet: Saturday, May 22, the social hour will occur from 6:30 to 7:30 pm. The banquet will begin at 7:30 pm. The banquet speaker will be Dr. Bob Whisonant who will talk on ***Salt, Lead, and Rails: Geology and the Civil War in Southwestern Virginia.*** Guests may attend the banquet for an additional $30.00.

- - - Sunday, May 23 - - -

Exhibit area open: 8:00 am to 10:00 am **Visit the Exhibits**
Technical Sessions: 8:00 am to 3:30 pm
Exhibits taken down: 10:00 am to 12:00 am

PROGRAM

- - - Friday, May 21 - - -

Visit the exhibits

7:00 am Welcoming Remarks to HGS

7:20 am *A Brief History of the Highway Geology Symposium,* ..... **p. 1**
Harry Moore, Tennessee DOT

7:40 am *Virginia Geology*
Stanley Johnson, State Geologist

Technical Session I: TRB-Sponsored Session on Karst / General Site Assessments

8:00 am *Highways in Virginia Karst: Resource and Hazard Considerations,* ..... **p. 13**
David A. Hubbard, Jr., Virginia Speleological Society and Virginia Division of Mineral Resources

8:20 am *Karst Considerations in Final Design of Interstate 99 from State College, Pennsylvania, to Interstate 80,* **p. 23**
Donald V. Gaffney, Michael Baker Jr, Inc.
Jeffrey G. Dippel, Patel Chen Associates, Inc.

8:40 am *Use of Geophysical Techniques to Evaluate Karst Features for Roadway Design,* ..... **p. 32**
Joel C. Daniel, P.G., Virginia Geotechnical Services, P.C., Richmond, Virginia
Richard C. Benson, C.P.G., Technos, Inc., Miami, Florida
Ann M. Samford, P.E., P.G., Virginia Geotechnical Services, P.C., Richmond, Virginia

9:00 am *A Case History on the Use of Compaction Grouting for Roadway Improvements in Mature Karst Topography,* ..... **p. 42**
Marcia V. Prowell, P.W., Virginia Geotechnical Services, P.C., Richmond, Virginia
Hugh C. Garst, P.G., Hayes, Seay, Mattern and Mattern, Roanoke, Virginia
Ann M. Samford, P.G., P.E., Virginia Geotechnical Services, P.C., Richmond, Virginia

9:20 am **Break - visit exhibits** (sponsor to be announced)

9:40 am *Electrical Imaging: A Method for Identifying Potential Collapse and Other Karst Features Near Roadways,* ..... **p. 52**
Heather L. Reccelli-Snyder, Beth A. Stahl, Jeffrey L. Leberfinger, Science Applications International Corporation

10:00 am *Resistivity Imaging: Getting the Big Picture in Karst,* ..... **p. 61**
Eric Rehwoldt, P.E., P.G., Schnabel Engineering Assoc., Bethesda, MD
Gordon M. Matheson, Ph.D., P.E., P.G., Schnabel Engineering Assoc., Bethesda, MD
Mark H. Dunscomb, P.G., Schnabel Engineering Assoc., West Chester, PA

10:20 am *Near Surface Cavity Detection Logan Co., Ohio,* ..... **p. 68**
Ethan Nowak, Wright State University, Dayton, Ohio

10:40 am *Geophysical Techniques to Locate Old Coal Mines Beneath Highways,* ..... **p. 85**
B.H. Richard, P.J. Wolfe, E.C. Hauser, and J.D. Hicks, Department of Geological Sciences, Wright State University

11:00 am *Detailed Subsurface Explorations Facilitate Cost Saving Designs for Transportation Projects,* ..... **p. 93**
Aaron L. Zdinak, P.E., Virginia Geotechnical Services, P.C., Richmond, Virginia
David A. Kaulfers, P.E., Virginia DOT
Thomas W. Pelnik, III, P.E., Virginia Geotechnical Services, P.C., Richmond, Virginia

11:20 am *Use of Environmental Site Assessments to Facilitate Roadway Design and Construction in the Church Street Urban Corridor, Norfolk, Virginia,* ..... **p. 104**
David M. Sayre, P.G., Virginia Geotechnical Services, P.C., Richmond, Virginia
Bill Nash, P.E., Kimley-Horn and Associates, Inc., Virginia Beach, Virginia

11:40 am *Protection and Preservation of an Archaeological Site below a Constructed Highway Fill,* ..... **p. 113**
Christopher C. Mathewson, Lloyd E. Morris, Department of Geology and Geophysics, Texas A&M University

12:00 **Lunch** (Sponsor to be announced)

Technical Session II: Bridges / Foundations / Aggregates

1:10 pm *An Overview of NDT Methods for Characterization of Roads and Bridges,* ..... **p. 123**
Richard C. Benson, C.P.G., Technos, Inc., Miami Florida

1:30 pm *Replacement of Bridge B-451, Milepost 78.98, Carrying S.R. 0819 Over the Pennsylvania Turnpike,* **p. 132**
Lawrence J. Artman, II, P.G., HDR Engineering, Inc., Pittsburgh, Pennsylvania
Matthew L. McCahan, Project Geologist, Pennsylvania Turnpike Commision

1:50 pm *Pile Relaxation in Soft Shales – A Critical Evaluation of the Effectiveness of Various Remedial Strategies based on Experience on the Airport Busway Project in Pittsburgh, Pennsylvania,* .... **p. 144**
Keith Wargo, P.E., Port Authority of Allegheny County
Scott D. Zang, P.E., Michael Baker, Jr., Inc., Beaver, Pennsylvania

2:10 pm *Soil Modification and Stabilization Utilizing Lime,* .... **p. 154**
Henry Mathis, P.E., Mathis Geotechnical Consulting, Inc.

2:30 pm *Multivariable Statistical Techniques Applied to Aggregate Inventory Testing Program in Northwestern Ontario,* .... **p. 166**
Peter P. Hudec, University of Windsor
Andrew Mitchell, DST Consulting Engineers Inc.

2:50 pm *The Effect of Aggregate Type and Mix Design on Wet Pavement Skid Resistance,* .... **p. 176**
W. Cullen Sherwood, David C. Mahone, L. Scott Eaton, James Madison University

3:10 pm **Break - visit exhibits** (sponsor to be announced)

Technical Session III: Landslides

3:30 pm *Grid-based model for prediction of debris flow susceptibility applied to the Appalachian Valley and Ridge, Spruce Run Mountain, Giles County, Virginia,* .... **p. 190**
Rupe, C. and Knight, K.L., Radford University

3:50 pm *Evaluation of a Suspected Ancient Mass Movement Using Electrical Resistivity,* .... **p. 200**
W.T. Dean, ATS International, Inc., Christiansburg, VA
C.F. Watts, Radford University, Radford, VA
W.J. Seaton, ATS International, Inc., Christiansburg, VA

4:10 pm *A Reconnaissance Survey of Hazard Potential of Slope Movements Along the Karakoram Highway, Northeast Pakistan,* .... **p. 206**
Abdul Shakoor, Department of Geology, Kent State University

4:30 pm *1997 California Storm Damage: The Gorda Landslide,* .... **p. 218**
John D. Duffy, Mike Finegan, California DOT

4:50 pm *Last Chance Grade and Wilson Creek Wall Landslides, Del Norte County, California,* .... **p. 225**
Timothy J. Beck, John K. Bowman, California DOT

5:10 pm Information about the Saturday field trip

Adjourn Technical Sessions for the day

5:30 – 7:00 pm Steering Committee Meeting

- - - Saturday, May 22 - - -

Field Trip: 7:00 am to 5:00 pm
Steering Committee: 5:30 pm to 7:00 pm
Social Hour/Visit the Exhibits: 6:30 pm to 7:30 pm
Banquet: 7:30 pm

- - - Sunday, May 23 - - -

Exhibit area open: 8:00 am to 10:00 am **Visit the Exhibits**
Technical Sessions: 8:00 am to 3:30 pm
Exhibits taken down: 10:00 am to 12:00 am

Technical Session IV: Landslide Remediation / Rock Slope Engineering

8:20 am *Soil Nail Wall for Stabilization of the Elbow Fill Slide, Snake River Canyon, Wyoming,* .... **p. 232**
W.G. Jensen, Department of Civil and Architectural Engineering, University of Wyoming
J.P. Turner, Hayward-Baker, Inc. Roswell, Georgia
J.R. Wolosick, M. Falk , Wyoming DOT

8:40 am *Geogrid Reinforced Slope Repairs Airport Service Road Tri-State Airport Huntington, West Virginia,* **p. 247**
B. Dan Marks, Ph.D., P.E., S&ME, Inc., Arden, North Carolina

9:00 am *I-279 Landslide Repair,* .... **p. 254**
F. Barry Newman, P.E., GAI Consultants, Inc., Monroeville, Pennsylvania
William R. Adams, Jr., Ph.D., P.E., P.G., Pennsylvania DOT

9:20 am *Rock Slope Engineering and Management Process on the Canadian Pacific Railway,* .... **p. 264**
A.J. Morris, P.Geol., Canadian Pacific Railway
D.F. Wood, P.Eng., D.F. Wood Consultants, Ltd.

9:40 am *Rockfall Hazard Remediation Along Ontario Highways,* .... **p. 276**
S.A. Senior, P.Eng., Ministry of Transportation Ontario

10:00 am **Break - visit exhibits** (sponsor to be announced)

10:20 am *Design and Construction of Major Cuts on US 460 in Virginia,* .... **p. 287**
James M. Sheahan, HDR Engineering, Inc. Pittsburgh, Pennsylvania
Stan L. Hite, Sam Graybeal, Virginia DOT

10:40 am *Rock Slope Engineering in Complex Geology: Jenkins By Pass,* .... **p. 297**
Earl Wright P.G., Kentucky Department of Highways

HGS EXHIBITORS AND HOSTS:

Supporters:

Field Trip Lunch – Brugg Cable Products
Field Trip Drinks – Golder Associates

Additional exhibitors and supporters will be gratefully acknowledged in forthcoming announcements.

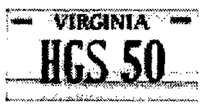

Visit our website often for regular updates:
http://www.runet.edu/~geol-web/hgs50

HGS SPONSORS:

Radford University, Department of Geology
Institute for Engineering Geosciences

Virginia Department of Mines, Minerals and Energy
Division of Mineral Resources

Virginia Department of Transportation

A BRIEF HISTORY OF THE HIGHWAY GEOLOGY SYMPOSIUM

By Harry Moore
Tennessee Department of Transportation
P.O. Box 58,Knoxville, Tennessee 37901

ABSTRACT

The highway Geology Symposium (HGS) was instituted in 1950 in order to foster the exchange of ideas between highway engineers and geologists on problems relating to highway construction. The first Highway Geology Symposium was sponsored by the Virginia Department of Highways and was held in Richmond, Virginia on April 14, 1950.

Since the initial meeting in 1950, 49 consecutive symposia have been held in various parts of the United States. Between 1950 and 1962, the meetings were held east of the Mississippi River. Beginning in1962 the Symposium was held in Phoenix, Arizona and has rotated, for the most part, back and forth from east to west since that time.

The governing body of the Symposium is a steering committee composed of approximately 20 to 25 engineering geologists and geotechnical engineers. Members of the steering committee are from state and federal agencies, colleges and universities, as well as private service companies and consulting firms.

The meetings are usually composed of one and a half days of technical presentations and a day for a field trip excursion. The field trip usually visits areas of geological and highway related subjects and ends that evening with a banquet and speaker.

The Highway Geology Symposium celebrates the 50th Highway Geology Symposium in Roanoke, Virginia, May 20-23, 1999. This golden anniversary culminates many years of friendships and exchanging technical ideas beginning in Virginia in 1950 and continuing through many states to return to Virginia again in 1999.

HISTORY, ORGANIZATION, AND FUNCTION

Cutting through hills of rock and soil and filling across valleys and plains characterize the process of building roads throughout these great United States. Ribbons of asphalt and concrete that wind through the valleys and plains and across the mountains and hills and connect the Atlantic Coast with the Pacific Coast are the lifelines of our country.

The process of building these roads and highways involves many people and professions. Two of the many professions involved with transportation/highway construction include engineers and geologists who have worked together in partnership to bring about a product that connects our nation together – our highway and transportation system.

Established to foster a better understanding and closer cooperation between geologists and civil engineers in the highway industry, the Highway Geology Symposium (HGS) was organized and held its first meeting on March 14, 1950, in Richmond, Virginia. Attending the inaugural meeting were representatives from state highway departments (as referred to at the time) from Georgia, South Carolina, North Carolina, Virginia, Kentucky, West Virginia, Maryland, and Pennsylvania. In addition, a number of federal agencies and universities were represented. A total of nine technical papers were presented.

W.T. Parrott, an engineering geologist with the Virginia Department of Highways, chaired the first meeting. It is Mr. Parrott who originated the Highway Geology Symposium.

In 1956 the national steering committee for the Highway Geology Symposium was composed of the following:

*W.A. Warrick, Chairman, Chief Construction Engineer, Pennsylvania Highway Department, Harrisburg, Pennsylvania.

*R.S. Edmundson, School of Geology, University of Virginia, Charlottesville, Virginia.

*Allen Lee, Research Engineer, Maryland State Roads Commission, Baltimore, Maryland.

*Harry Marshall, Geologist, Ohio Department of Highways, Columbus, Ohio.

*J.L. Stucky, State Geologist for North Carolina and professor, North Carolina State College, Raleigh, North Carolina.

It was at the 1956 meeting that future HGS leader, A. C. Dodson, began his active role in participating in the Symposia. Mr. Dodson was the Chief Geologist for the North Carolina State Highway and Public Works Commission, which sponsored the 7th HGS meeting.

Since the initial meeting, 49 consecutive annual meetings have been held in 31 different states. Between 1950 and 1962, the meetings were held east of the Mississippi River, with Virginia, Ohio, West Virginia, Maryland, North Carolina, Pennsylvania, Georgia, Florida, and Tennessee serving as the host states.

In 1962, the Symposium moved west for the first time to Phoenix, Arizona where the 13th annual HGS meeting was held. Since then, it has alternated, for the most part, back and forth from east to west. Following meetings in Texas and Missouri in 1963 and 1964, the Annual Symposium moved to different locations as follows:

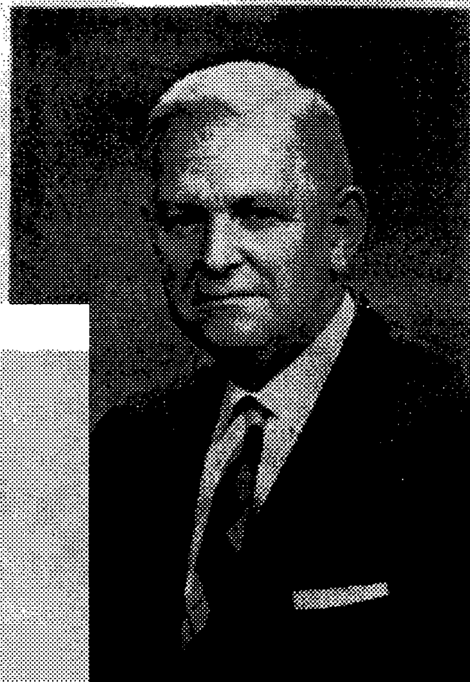

W. T. Parrott

in founding HGS while serving as Chief
ginia Highway Department. Mr. Parrott
loyed as Materials Engineer with the
ighway Commission.

Hugh Chase

oyed as Geologist in Georgia Highway Department for man
s and served a long term as Secretary of HGS. Mr. Chas
ow retired.

Pictured are two very important men in the history of the HGS. Upper right is W.T. Parrott who was instrumental in founding the HGS while with the Virginia DOT (later working with the North Carolina DOT). Lower left is Hugh Chase, retired geologist with Georgia DOT who served as HGS secretary for many years during the 50's and 60's.

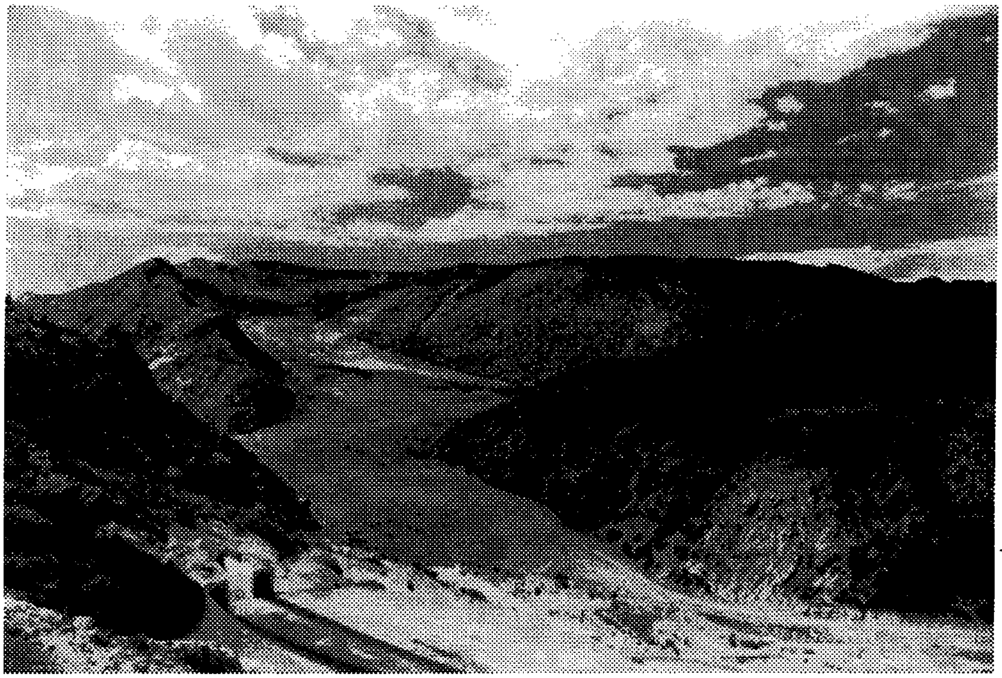

The Thistle Landslide as seen on the field trip of the 39th HGS in Utah, August, 1988.

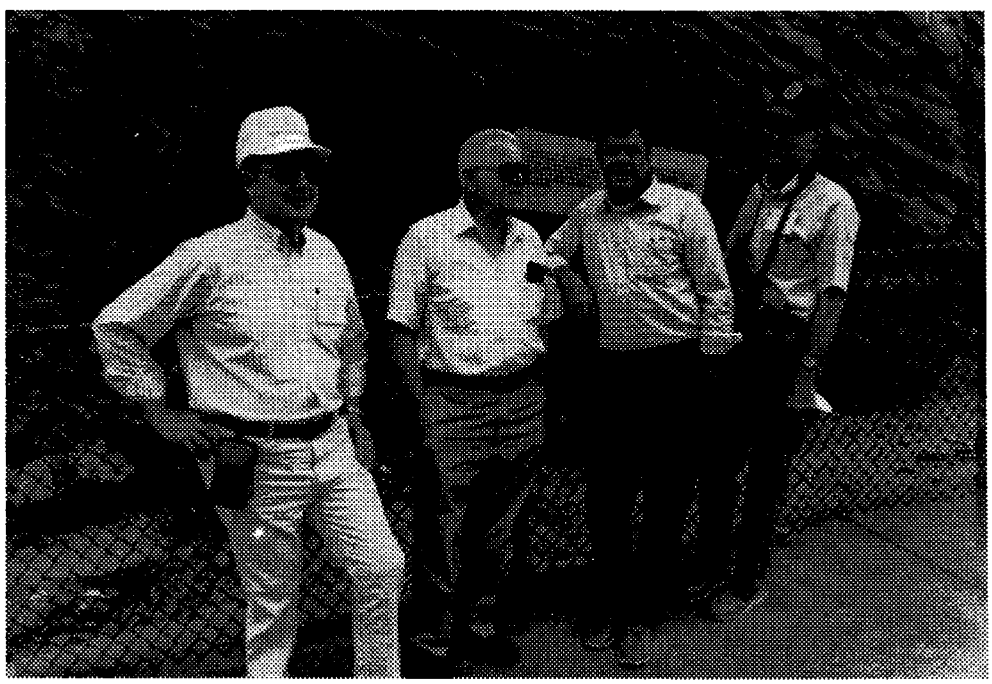

National Steering Committee members on a field trip stop during the 40th HGS meeting in Birmingham, Alabama. Pictured (L to R) : Willard McCasland (Okla. DOT), Joe Guterieriez (Vulcan Materials, Inc.), Dave Bingham (N.Carolina DOT), and Vernon Bump (S.Dakoata DOT).

List of Highway Geology Symposium Meetings

NO.	Year	HGS Location	NO	Year	HGS Location
1st	1950	Richmond, VA	2nd	1951	Richmond, VA
3rd	1952	Lexington, VA	4th	1953	Charleston, W VA
5th	1954	Columbus, OH	6th	1955	Baltimore, MD
7th	1956	Raleigh, NC	8th	1957	State College, PA
9th	1958	Charlottesville, VA	10th	1959	Atlanta, GA
11th	1960	Tallahassee, FL	12th	1961	Knoxville, TN
13th	1962	Phoenix, AZ	14th	1963	College Station, TX
15th	1964	Rolla, MO	16th	1965	Lexington, KY
17th	1966	Ames, IA	18th	1967	Lafayette, IN
19th	1968	Morgantown, WV	20th	1969	Urbana, IL
21st	1970	Lawrence, KS	22nd	1971	Norman, OK
23rd	1972	Old Point Comfort, VA	24th	1973	Sheridan, WY
25th	1974	Raleigh, NC	26th	1975	Coeur d'Alene, ID
27th	1976	Orlando, FL	28th	1977	Rapid City, SD
29th	1978	Annapolis, MD	30th	1979	Portland, OR
31st	1980	Austin, TX	32nd	1981	Gatlinburg, TN
33rd	1982	Vail, CO	34th	1983	Stone Mountain, GA
35th	1984	San Jose, CA	36th	1985	Clarksville, IN
37th	1986	Helena, MT	38th	1987	Pittsburgh, PA
39th	1988	Park City, UT	40th	1989	Birmingham, AL
41st	1990	Albuquerque, NM	42nd	1991	Albany, NY
43rd	1992	Fayetteville, AR	44th	1993	Tampa, FL
45th	1994	Portland, OR	46th	1995	Charleston, WV
47th	1996	Cody, WY	48th	1997	Knoxville, TN
49th	1998	Prescott, AZ	50th	1999	Roanoke, VA

Unlike most groups and organizations that meet on a regular basis, the Highway Geology Symposium has no central headquarters, no annual dues, and no formal membership requirements. The governing body of the Symposium is a steering committee composed of approximately 20-25 engineering geologists and geotechnical engineers from state and federal agencies, colleges and universities, as well as private service companies and consulting firms throughout the country. Steering committee members are elected for three-year terms, with their elections and re-elections being determined principally by their interests and participation in and contribution to the Symposium. The officers include a chairman, vice chairman, secretary, and treasurer, all of whom are elected for a two-year term. Officers, except for the treasurer, may only succeed themselves for one additional term.

A number of three-member standing committees conduct the affairs of the organization. The lack of rigid requirements, routing, and the relativity relaxed overall functioning of the organization is what attracts many of the participants.

Meeting sites are chosen two or four years in advance and are selected by the Steering Committee following presentations made by representatives of potential host states. These

HGS Steering Committee members David Royster (Tenn. DOT), Ed Garner (Texas DOT), and Mitchell Smith (Okla. DOT) enjoying refreshment on the field trip near Mount Hood at the 30th HGS meeting in Portland, Oregon, 1979.

The New River Gorge Bridge in West Virginia (over 800 feet high) as seen on the field trip during the 46th HGS meeting in Charleston, West Virginia, 1995.

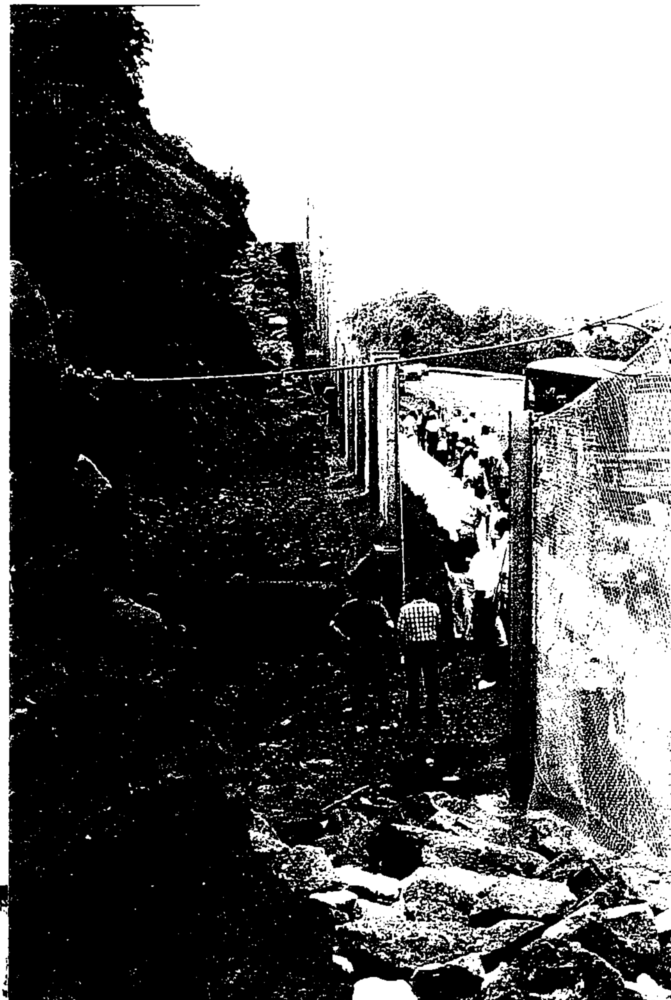

Upper Photo: Field trip of the 42nd HGS in Albany, New York (1991); attendees are looking at wire rope rock catchment fences along the New York thruway. **Lower Photo:** HGS Steering Committee members (L To R) Burrell Whitlow (Geotechnics, Virginia), Willard McCasland (Okla. DOT), Earl Wright (Kentucky DOT).

presentations are usually made at the steering committee meeting, which is held during the Annual Symposium. Upon selection, the state representative becomes the state chairman and a member protem of the Steering Committee.

The symposia are generally for two and one-half days, with a day-and-a-half for technical papers and a full day for the field trip. The Symposium usually begins on Wednesday morning. The field trip is usually Thursday, followed by the annual banquet that evening. The final technical session generally ends by noon on Friday. In recent years this schedule has been modified to better accommodate climate conditions and tourism benefits.

The field trip is the focus of the meeting. In most cases, the trips cover approximately from 150 to 200 miles, provide for six to eight scheduled stops, and require about eight hours. Occasionally, cultural stops are scheduled around geological and geotechnical points of interest. To cite a few examples: in Wyoming (1973), the group viewed landslides in the Big Horn Mountains; Florida's trip (in 1976) included a tour of Cape Canaveral and the NASA space installation; the Idaho and South Dakota trips dealt principally with mining activities; North Carolina provided stops at a quarry site, a dam construction site, and a nuclear generating site; in Maryland, the group visited the Chesapeake Bay hydraulic model and the Goddard Space Center; the Oregon trip included visits to the Columbia River Gorge and Mount Hood; the Central Mineral Region was visited in Texas; and the Tennessee meeting in 1981 provided stops at several repaired landslides in Appalachia regions of East Tennessee.

The Colorado field trip (1982) consisted of stops at geological and geotechnical problem areas along Interstate 70 in Vail Pass and Glenwood Canyon, while the Georgia trip in 1983 concentrated on highway design and construction problems in the Atlanta urban environment. The 1984 field trip had stops in the San Francisco Bay area, which illustrated the planning, construction and maintenance of transportation systems. In 1985, the one-day trip illustrated new highway construction procedures in the greater Louisville area. The 1986 field trip was through the Montana Rocky Mountains on recent interstate construction in the Boulder Batholith. The trip highlight was a stop at the Berkeley Pit in Butte, Montana, an open pit copper mine.

In Utah (1988) the field trip visited sites in Provo Canyon and stopped at the famous Thistle Landslide, while in New Mexico in 1990 the emphasis was on rockfall treatment in the Rio Grand River canyon and included a stop at the Brugg Wire Rope headquarters in Santa Fe. The field trip in New York in 1991 included a stop at the famous Army school West Point on the banks of the Hudson River.

In 1992 the field trip visited ongoing construction of highways in the Ozark Mountains. The field trip in Tampa in 1993 visited the beautiful Sunshine Skyway Tampa Bay Bridge and included a visit inside the segmental suspension bridge. Mount St. Hellens was visited by the field trip in 1994 when the meeting was in Portland, Oregon, while in 1995 the West Virginia meeting took us to the New River Gorge bridge that has a deck elevation 876 feet above the river.

Top: HGS Steering Committee members (L to R) Terry West, Sam Thornton, and Harry Ludowise discussing scenery on the field trip in Wymoing, 47th HGS meeting, 1996. Center: Mike Hagar, Wyoming DOT, explaining geology on the field trip in 1996 in Wyoming. Field trip attendees overlooking city of Pittsburgh, Pennsylvania during the 38th HGS meeting in 1987.

In Cody, Wyoming the 1996 field trip visited the Chief Joseph Scenic Highway and the Beartooth uplift in northwestern Wyoming. In 1997 the Meeting in Tennessee visited the newly constructed future I-26 highway in the Blue Ridge of East Tennessee. The Arizona meeting in 1998 visited Oak Creek Canyon near Sedona and a mining ghost town at Jerrome, Arizona.

At the technical sessions, case histories and state-of-the-art papers are most common; with highly theoretical papers the exception. The papers presented at the technical sessions are published in the annual proceedings. Some of the more recent proceedings may be obtained from the Treasurer of the Symposium.

Banquet speakers are also a highlight and have been varied through the years. In 1964 at the Rolla, Missouri meeting, Mr. Jerry Vineyard gave a slide-illustrated talk on the caves of Missouri. At the 18th HGS meeting (1967) Dr. G.A. Leonards, Head of the School of Civil Engineering, Purdue University, presented a talk on the Aswan Dam. In 1970 at the 21st annual meeting in Kansas, Dr. Wakefield Dort, Jr. showed color slides and described enthusiastically his "Recent Experiences in Antarctica". In 1977 at the 28th HGS meeting Paul Gnirk, consultant in rock mechanics, spoke on radiological waste disposal. The late Dr. James Quinlan spoke at the 36th HGS meeting (1985) in Clarksville, Indiana on the hydrology of the Mammoth Cave Kentucky Region. The history of the New Madrid Earthquake was discussed by the banquet speaker at the 43rd HGS meeting in Fayetteville, Arkansas while at the 45th meeting in Portland, Oregon the banquet speaker was Sue D'Agnese who presented a slide show and talk on the Wilson River Landslide. At the 48th HGS meeting in Knoxville, Tennessee in 1997 Dr. David Hunter, University of Tennessee, presented a humorous perspective on growing up in the south.

A Medallion Award was initiated in 1970 to honor those persons who have made significant contributions to the Highway Geology Symposium. The selection was and is currently made from the members of the national steering committee of the HGS.

The first three Highway Geology Symposium Medallion Awards were presented at the 21st meeting in Lawrence, Kansas in 1970. They were presented to W.T. Parrott, North Carolina Highway Department; Dr. Paul Price, West Virginia Geological and Economic Survey; and Hugh D. Chase, Georgia State Highway Department.

W.T. Parrott was instrumental in founding the HGS while serving as Chief Geologist of the Virginia Highway Department (he later transferred to the North Carolina Highway Commission). Dr. Price was on the HGS steering committee for several consecutive terms and was very influential on the success of the HGS. Hugh Chase served a long term as secretary of the HGS steering committee. To date, a total of 23 Medallion Awards have been presented to various individuals who have served on the National Steering Committee.

HGS Steering Committee members discussing construction techniques on the field trip during the 34th meeting in Stone Mountain, Georgia. (L to R): David Royster (Tennessee DOT), Bob Leary (FHWA, not a HGS Steering Committee member), Dave Bingham and Russell Glass (both with North Carolina DOT).

Earl Wright, Kentucky DOT and Bob Henthorne, Kansas DOT enjoy a moment of refreshment on the field trip in Wyoming, 1996.

MEDALLION AWARD WINNERS

Hugh Chase* 1970, Tom Parrott* 1970, Paul Price* 1970, K.B. Woods* 1971, R.J.Edmonson* 1972, C.S. Mullin* 1974, Carter Dodson* 1975, Burrell Whitlow* 1978, Bill Sherman 1980, Virgil Burgat*1981, Henry Mathis 1982, David Royster* 1982, Terry West 1983, Dave Bingham 1984, Vernon Bump 1986, C.W. "Bill" Lovell 1989, Joseph A. Gutierrez 1990, Willard McCasland 1990, W.A. "Bill" Wisner 1991, David Mitchel 1993, Harry Moore 1996, Earl Wright 1997, and Russell Glass 1998. (*deceased)

A number of past members of the National Steering Committee have been granted Emeritus status. These individuals, usually retired, resigned from the HGS Steering Committee, or are deceased, have made significant contributions to the Highway Geology Symposium. A total of 20 persons have been granted the Emeritus status. Ten are now deceased (see above list *).

EMERITUS MEMBERS OF THE STEERING COMMITTEE

R.F. Baker*, David Bingham, Virgil E. Burgat*, Robert G. Charboneau*, Hugh Chase*, A.C. Dodson*, Walter F. Fredericksen, Joseph Gutierrez, John Lemish, George S. Meadors,Jr.*, Willard McCasland, David Mitchell, W.T. Parrot*, Paul Price*, David L. Royster*, Bill Sherman, Mitchell Smith, Berke Thompson, Burrell Whitlow*, Ed Zeigler. (* deceased)

Several Proceedings volumes have been dedicated to past HGS Steering Committee members who have passed away. The 36th HGS Proceedings were dedicated to David L. Royster (1931-1985, Tennessee) at the Clarksville, Indiana meeting in 1985. In 1991 the Proceedings of the 42nd HGS meeting held in Albany, New York was dedicated to Burrell S. Whitlow (1929-1990, Virginia).

ACKNOWLEDGEMENTS

The writer wishes to thank the many persons involved with the Highway Geology Symposium for the past fifty years who have made this group the nationally respected organization that it is. Mr. David Bingham is credited with the idea of having a special proceedings volume to celebrate the Golden Anniversary of the Highway Geology Symposium. He stated his idea to me during the 39th Symposium in Utah. I also wish to thank Dr. Terry West, Purdue University and senior member of the current HGS National Steering Committee, for reviewing the manuscript. It is with great enthusiasm that I thank the current HGS National Steering Committee for pursuing the idea of a Special Proceedings Volume. The work on the Special Proceedings Volume enabled the writer to produce this paper, A Brief History of the Highway Geology Symposium.

The writer also acknowledges the many writers and editors (too numerous to list and some are unknown) of proceedings volumes of past meetings as those proceedings were used to generate the historical details presented in this paper.

HIGHWAYS IN VIRGINIA KARST: RESOURCE AND HAZARD CONSIDERATIONS

David A. Hubbard, Jr., Virginia Speleological Survey and Virginia Division of Mineral Resources, P.O. Box 3667, Charlottesville, VA 22903 dhubbard@geology.state.va.us

ABSTRACT

Highways in Virginia's karst have impact on cave and karst resources and are impacted by karst processes and features. Most of Virginia's karst is developed on folded and faulted rocks with a range of expression of surficial features such as karren, sinkholes, cave entrances, and sinking streams. Although numerous scenic karst features, such as natural bridges, a natural tunnel, commercial caves, sinking streams, springs, and travertine waterfalls, are well known to Virginia's highway travelling karstland residents and visitors, other significant karst resources abound. Virginia's 3600 caves contain a plethora of archaeological, biological, geological, historical, hydrological, and paleontological resources. Undoubtedly, the most significant karst resource is water. Karst is the result of the interaction of water and soluble bedrock (predominantly limestone and dolostone). Water drives the processes active in karst. The three natural hazards of karst are associated with water movement: subsidence, flooding, and groundwater contamination. Human induced changes to the local hydrology can trigger or exacerbate these hazards.

Highway construction in Virginia has impacted cave and karst resources. Past highway construction projects have impacted a range of cave resources, including archaeological, biological, and hydrological (groundwater) resources, at Front Royal Caverns, Young-Fugate Cave, and Bone Cave. Active highway projects are or will impact biological, historical, and hydrological (groundwater) resources at Rigg's Chapel and Gibson No. 1 Caves. Virginia Highways have been and will continue to be impacted by karst processes in the form of subsidence and flooding hazards. Of paramount importance to the successful mitigation and remediation of karst hazard impacts to highways is an understanding of karst processes and water movement in the epikarst and site specific solutions compatible with karst processes. The current practice of channeling storm water runoff from highways directly into sinkholes and caves is environmentally unsound because such designs channel leaked and spilled hazardous waste and other contaminants transported along highways directly into the groundwater resource.

INTRODUCTION

The focus of this paper is the interaction between highways and karst in Virginia's Valley and Ridge physiographic province. Karst is a terrain that develops by the action of water with soluble bedrock and characteristically features karren, sinkholes, caves, and subsurface drainage. Although the natural processes active in karst result in subsidence, sinkhole flooding, and surface water recharge of groundwater aquifers, human induced changes to the local hydrology can trigger and exacerbate subsidence, flooding, and groundwater contamination hazards.

Scenic karst features, such as commercial caves, natural bridges, sinking streams, springs, and travertine waterfalls are well known to Virginia's highway travelling karstland residents and visitors. The Commonwealth is richly endowed with diverse and significant karstland resources. Significant karst resources have been impacted by Virginia highways in the past and certain active construction projects assure that impacts will continue to occur. Karst processes are active along some highway corridors; however the degree of activity may be exacerbated by land-use and landscape modifications.

KARST SETTING

Solution of the relatively impermeable Paleozoic carbonate rocks of the Appalachian Valley and Ridge physiographic province occurs on the surface of exposed rock, at the soil-bedrock interface, and along partings and fractures in the rock. Folding and faulting of these rocks has enhanced the development of bedding partings, joints, cleavage, and a plethora of other fractures along which seeping waters solutionally modify flowpaths into conduits. Characteristic features of Virginia's karst include solutional forms on rock referred to as karren, closed depressions, caves, and subsurface drainage (Hubbard, 1983 and 1988). In the covered karst of the Appalachians, soils or sediments mantle much of the carbonate terrain and disguise the nature of the epikarst and the pattern of movement of water at the irregular soil-bedrock interface. Sinkholes, blind valleys, and other natural closed-contour depressions characterize areas of subsidence. This subsidence is usually of the unconsolidated mantle materials overlying the bedrock and is associated with drainage topographically funneled to the subsidence area and drained through the epikarst into an underlying conduit. In covered karst, much of the drainage is along the irregular soil-bedrock interface toward epikarstic drains, which may or may not be marked by sinkholes or other subsidence features. Landscaping changes, which alter the surficial drainage pattern or the amount of runoff, may trigger sinkhole formation as soils are winnowed into epikarst drains previously unmarked by subsidence features.

The evolution of the subsurface drainage in karst is ongoing. Subsurface conduits (caves) may range from active (water filled or free water surface) to segmented and abandoned paleo-features (dry caves) no longer connected to active epikarst drains. As bedrock partings and fractures are solutionally enlarged by groundwater, they may pirate increasing amounts of the flow from existing conduits to the point that the older conduits are abandoned as flowpaths; however, these conduits may become active during extremely wet weather or human induced changes to the drainage pattern or volume. The connectivity of springs to sinking streams is frequently recognized during flashy high volume flows from springs accompanied by increased turbidity, the emergence of trash, or vegetation debris.

KARST RESOURCES

It may seem ironic that water is illusive in a terrain shaped by water, yet this scarcity dictates that it, especially as groundwater, is the most significant resource in karst. The scenic, water-sculpted karst features, including Natural Bridge, Little Natural Bridge, Natural Chimneys, Natural Tunnel, Falling Springs, Caverns of Natural Bridge, Crystal Caverns, Dixie Caverns, Grand Caverns, Endless Caverns, Luray Caverns, Shenandoah Caverns, Skyline Caverns, are popular natural features to Virginia's karstland residents and visitors. A unique aspect of karst is that it is a 3-dimensional terrain, not just in that it frequently attains considerable topographic relief, but in that a significant amount of it is naturally accessible underground. Presently, over 3600 caves are known in the Commonwealth. The resources in these caves virtually span the sciences and have proven important in historic human activities.

Virginia caves have been used by Native Americans as burial sites, ceremonial sites, a source for lithic materials and minerals, and for shelter (Hubbard and Boyd, 1997). Other archaeological resources include evidence of historical use by the multitude of willing and unwilling immigrants for food storage, mining, and shelter. The historical mining aspects include the extraction of saltpetre for the manufacture of black powder during the Revolutionary War, the War of 1812, and the Civil War.

Biologically, the Commonwealth's caves contain a diverse fauna. Three of the species of bats that use caves, are on the Federal List of Endangered Species. Virginia caves contain more than 137 species of troglobitic invertebrates, including 73 species of cave-limited insects and 33 species of cave-limited crustaceans (amphipods and isopods), that have been described and published (Holsinger and Culver, 1988; Christiansen and Bellinger, 1996a and b; Thibaud, 1995 and 1996). Geological and hydrological boundaries are important in defining the distribution of the various troglobitic invertebrate fauna.

Caves offer opportunities to observe structural and other geological details of the host rocks, which are commonly covered by the soil mantle in karst. These solutional features also contain important clues to the nature of the karst aquifers. Preferential solution of faults, joints, or particular fracture patterns offer important clues to the nature of the aquifer, its recharge, and resurgences. In the past, speleologists debated about whether particular caves were developed in vadose (in the unsaturated zone above the "water table") and or phreatic (in the saturated zone) conditions (Davis, 1930; Bretz, 1942; Bögli, 1980). Palmer (1991) proposed that many caves actually develop in both vadose and phreatic phases existing simultaneously in different parts of a cave. The dual phase development is commonly seen in Virginia caves, however a series of caves that formed under phreatic conditions and still access phreatic waters were recognized in the 1990s. A single distinctive species of crustacean exists in these phreatic caves (Holsinger and others, 1994). The implication is of an integrated phreatic conduit network spanning 72 miles of the Great Valley of Virginia.

Virginia caves have yielded the remains of vertebrate taxa of Pleistocene age. These fossils are paleontologically significant and convey information about climate, vegetation, and other conditions in the past. Significant records include the Arctic shrew, Jefferson's ground sloth, beautiful armadillo, pica, yellow-cheeked vole, northern bog lemming, dire wolf, short-faced bear, mastodon, wooly mammoth, vero tapir, flat-headed peccary, camel, and caribou (Hubbard and Grady, 1997).

Only a fraction of Virginia's caves have been studied scientifically and the interrelationships of processes and materials pose a problem in these studies. For example, an archaeological study in a cave may disturb limited sediment deposits which also may contain biological, paleontological, sedimentological, etc. materials that may be even more sensitive and significant, but their recognition and interpretation are beyond the expertise of most highly trained archaeologists.

Most cave resources are protected under the Virginia Cave Protection Act. The degree of protection afforded groundwater is much less and landowners may be exempt from sinkhole and cave dumping prohibitions.

KARST HAZARDS AND THEIR IMPACTS ON HIGHWAYS

The three natural hazards in karst are subsidence, sinkhole flooding, and groundwater contamination. Each is associated with water movement and can be triggered or exacerbated by human activities. As has been the case with karstland residents, the karst hazard of greatest concern to highway personnel traditionally has been subsidence (Figure 1).

Figure 1. Sinkhole in New Hope Road in Waynesboro. Photograph by T.M. Gathright, II.

Sinkhole formation is a natural process in karst and is usually associated with changes in groundwater levels or drainage. Such changes may occur naturally from weather variation or can be induced by causes ranging from groundwater level fluctuations associated with water-well pumping to landscape altered surficial drainage patterns. Sowers (1996) notes that much of the increased sinkhole activity in the southeastern U.S. is related to changes in the groundwater levels and infiltration caused by human activity. Sinkholes induced by highway construction have been extensively reported in the past, however these papers contain a wide array of concepts of karst processes and how they relate to sinkhole formation. Three such papers presented at the First Multidisciplinary Conference on Sinkholes demonstrate this point. Newton (1984) includes these sinkholes in his category of "Construction" induced, although he conceptualizes that "Grading results, in cuts, in the thinning of unconsolidated deposits. Emplacement of weight on thinned roofs of existing cavities in residual clay or on those shallow bedrock cavities can cause their failure." Myers and Perlow (1984) note that "Excavation…exposes an underlying material that is more granular and consequently more permeable and with less shear strength than the overlying materials. Surface waters, which can be introduced naturally, or during construction processes, can rapidly erode these silty, granular materials and, in areas where the underlying bedrock is highly pinnacled and riddled with solution enhanced openings, sinkholes will readily develop." Moore (1984) observed the formation of collapse features along unpaved ditches in excavated cuts. He reports "The prevention of karst related subsidence and collapse of highways is centered around controlling the drainage…." Of even more importance is his discussion of subsidence, flooding, and runoff contaminants and their interrelationships in highway construction and design function. Hubbard (1999) notes that "During highway construction, cuts and fills alter the local surficial drainage and infiltration patterns. Infiltrating water is channeled through the epikarst, along the soil/bedrock interface to solutionally modified fractures, into under-draining conduits. Soil piping at the soil/bedrock interface creates voids, which may continue to enlarge or stope upward depending on the soil properties, size and configuration of modified fractures, the amount of infiltration, and the elevation and variability of the local "water table." The soil arch roofs of these voids may progressively fail to the surface creating a sinkhole during construction or later."

Sinkhole flooding is not as common a hazard to Virginia karstlands and highways as in other U.S. karstlands in Kentucky (Crawford, 1984; Currens and Graham, 1993), Missouri (Aley, 1981), etc. however it does occur. The two types of sinkhole flooding are due to ponding, when under-draining occurs at a slower rate than surficial drainage into the feature (Figure 2), and back-flooding, when estavelle type flow results from high head pressures in the under-draining conduit. The ponding type of sinkhole flooding is usually associated with altered land-use or where inadequate sediment control contributes to siltation of the sinkhole drain and increased runoff from vegetation changes and impermeable surfaces overwhelm the drainage capacity of a sinkhole. Sinkhole flooding as a back-flooding condition during extremely wet weather is known in Virginia (Hubbard and Brown, 1997). In this situation high head pressures in the conduit under-draining the sinkhole have resulted in water rising into the sinkhole from below and overflowing from the sinkhole. These incidents have been known to lag after a precipitation event and may be related to high head pressures generated by other sinkholes draining into the same conduit system. The use of sinkholes as outfalls for altered terrain generated runoff enhances subsidence, flooding, and groundwater quality problems.

Figure 2. Sinkhole flooding obstructing State Road 763 in Rockingham County.

Karst groundwater has a high risk of contamination because of the nature of the recharge from sinking streams, sinkholes and other subsidence features, and the general lack of filtering within conduits that are large enough to accommodate cavers or divers. A further concern is that solutional pathways from the soil-bedrock interface to active aquifer conduits are not all marked by subsidence features or otherwise identifiable. Some of the contaminants that have degraded Virginia's karst aquifers include: the leachate of improperly disposed wastes; spills or leaks or use of petroleum products, herbicides, solvents, fertilizers, sheep and cattle dip, sewage, and milk (Hubbard and Sterrett, 1994).

HIGHWAY IMPACTS TO KARST RESOURCES

Highways have impacted Virginia karst perhaps even before the first road was built across Natural Bridge. The impacts of greatest concern are those on caves and groundwater. Five case studies of highway construction impacts to cave resources are presented below, two of these projects are still underway. A limited number of examples of highway associated contamination of caves and groundwater are noted below. The continued use of sinkholes and other groundwater recharge features as drainage outfalls for highway runoff exacerbates the groundwater contamination hazard inherent in karst.

FRONT ROYAL CAVERNS

Front Royal Caverns is located along U.S. Highway 340 in Warren County. In the spring of 1990, this cave was known to have three entrances, 1,185 feet of passage, had failed an attempt at commercialization, and was considered a mud hole by some speleologists. One of the three entrances was accepting runoff from the two-lane highway. Unfortunately, the cave's location was directly in the path of a planned expansion to a 4 lane divided highway with a 130 foot-wide median for a scenic upgrade of the approach to the Northern Entrance of Skyline Drive. A "last rights" inventory of the doomed cave (all three entrances were slated for destruction) revealed some significant resources.

The cave was determined to be of phreatic origin and within the active epiphreatic zone. As groundwater levels rose in response to sinkhole recharge, extensive flooding occurred in the cave. An adjacent sinkhole already had been observed by Highway personnel to back-flood with a minimum head change of 40 feet before upwelling waters breached it's rim and flowed from the sinkhole (Hubbard and Brown, 1997). Even more significant was the discovery of a population of the troglobitic isopod *Antrolana lira* Bowman, a crustacean known for thirty years from only two caves in Cave Hill some 60 miles away (Holsinger and others, 1994). *Antrolana lira* Bowman was, and remains, on the Federal List of Threatened Species.

As a result of the resource and hazard considerations, the highway plans were modified. The road was built within the originally planned right-of-way, but with a smaller median. Only one entrance to the cave was sealed and a curb and culvert drain system was designed and built. The drainage system was designed to carry runoff, including road salt and other contaminants, from the highway and median to a basin and outfall draining to an area isolated hydrologically from the isopod's aquatic habitat. The road was successfully upgraded and previously existing groundwater pollution hazards were mitigated by construction with only the loss of a single entrance to this sensitive cave. The remaining cave entrances are privately owned and closed to the public.

YOUNG-FUGATE CAVE

Young-Fugate Cave is located under U.S. Highway 58 in Lee County. In the fall of 1991, this cave was known to extend under the highway, contain over a mile of passage including a 4,000-foot stream passage, was the domestic water supply for two households, and contained a complex ecosystem. Runoff from the two-lane highway drained into the blind valley near the Fugate insurgence of the surface stream that becomes the cave stream and emerges as a spring/domestic water supply some 4,000-foot downstream. The known cave biological inventory included two species of troglobitic aquatic crustaceans and a globally and state rare (G1, S1) troglobitic cave beetle. Plans for a four-lane expansion of U.S. 58 included a fill across the active blind valley and encroachment of the insurgence, but no provisions to keep runoff of road salt or leaks and spills from accessing the Fugate insurgence and impacting the cave ecosystem or the domestic water supply. A survey of the cave to determine distances between the proposed roadbed and cave passages revealed hazards to the highway and cave resources.

The survey established that the proposed route would cross over the cave in a segment in which upper level cave passages were found and a small tributary stream joined the main passage. The upper level passage was roofed with breakdown (a jumble of collapsed rock) and found to extend within 16 feet (vertically) of the proposed roadbed. During one survey trip, the carbide lamp (open-flame cap lamp) equipped surveyors encountered gasoline fumes at the tributary-main cave stream juncture.

One of three gasoline USTs at a service station on the existing road was found to be leaking and replaced, eliminating the fume and product problems in the cave. A re-alignment was proposed within the existing and proposed alignments, which would cross a more stable roof segment and also displace the service station (Hubbard and Balfour, 1993). The highway was built over the more stable passage, the service station was removed eliminating future petroleum leaks along a known input path, and drainage control measures were constructed to divert runoff and contaminants away from the Fugate blind valley and sinkholes within a designated critical area. The cave ecosystem was determined to be even more complex and sensitive than previously known and the resurgent groundwater continues to serve as a domestic water supply. This privately owned cave remains closed to the public.

BONE CAVE

Bone Cave is located along U.S. Highway 58 in Lee County. Prior to the spring of 1993, it was known only as a very small cave (50 to 75 foot of passage) to the speleological community and was inaccurately located. It was subsequently visited and determined to contain disturbed, exposed, human skeletal remains. Local lore held that Art Faulkerson buried his slaves there. The cave's location not only was within the footprint of the planned expanded four-lane highway, but the roof of the cave was above the elevation of the proposed roadbed. A phase II archaeological investigation was negotiated prior to the implementation of a proffered preservation solution of removing the ceiling and grading. Two test pits yielded 1494 probable human skeletal fragments and prehistoric artifacts. Dental characteristics and the artifacts indicated that the skeletal remains were of Native Americans, an osteological analysis determined that the minimum number of individuals represented in the test holes was six (Kimball and Whyte, 1994). The report concluded "...Bone Cave is an extremely significant archaeological and biological resource." Plans were made to move the road slightly to avoid this 75-foot long cave, a compromise that had been characterized previously by VDOT personnel as not possible. The cave was gated and the protection of the resource began to look feasible. Just over a year later, the cave was blasted during construction. A drill hole through the cave roof was found and determined to be leaking water onto the burials. Five feet away from the hole was a collapse precipitated by a blast in the cave ceiling. "Further investigation revealed fresh rock fragments distributed around the interior of the cave as well as many impact marks on the cave walls" (Hubbard and Barber, 1997). Two seeps of a dark viscous fluid were observed dripping from a ceiling fracture and were believed to be motor oil or hydraulic fluid from construction equipment.

The new, improved U.S. 58 road is in use. The roof of Bone Cave sags on the gate, beyond which the pile of rubble from the blast can be seen without the aid of artificial light. Within the test pits, the remains of Native Americans and their artifacts lay in plastic sample bags awaiting reburial. This sensitive, and now unstable, cave remains gated and closed to the public.

RIGG'S CHAPEL CAVE

Rigg's Chapel Cave is located along State Road 649 in Scott County. The pit entrance, the terminus of the dry end of a sinking stream that sinks upstream except in very wet weather, drops into a 430-foot stream passage that ends in siphons both up and downstream. The cave has been at risk to contaminants in runoff from the road for decades. Tracer studies have established that the Rigg's Chapel Cave waters rise approximately 7,000 feet to the NE at a spring along Cove Creek (Terri Brown, written communications, 5 November 1998). Recent construction along State Road 649 rerouted and channeled upstream portions of the sinking stream, but provided little if any relief to the groundwater contamination risks the road design has enhanced. Suggestions of employing curbs and culverts draining to an adequate retention basin were countered with rip rap lining of the drainage. A solution, which may temporarily trap particulate contaminants transported from road surfaces by runoff, but which offers no remediation to liquid leaks or spills associated with vehicular traffic or dissolved deicing chemicals.

GIBSON CAVE NO. 1

Gibson Cave No. 1 is located in Lee County. Prior to the fall of 1993, it was known to contain about 700 foot of passage and to contain a small stream. Word of a planned road in the vicinity, prompted a subsequent assessment of resources. The cave was found to contain evidence of historic saltpetre mining during the Civil War. Biologically, the cave also proved to be significant, containing both terrestrial as well as aquatic fauna. The aquatic fauna was found to include two troglobitic crustaceans and *Holsingeria unthanksensis*, an extremely rare and critically imperiled troglobitic cave snail (G1, S1). This stream was subsequently traced to a spring rising some 1500 feet to the SW along Fleenortown Creek (Terri Brown, oral communication, 1999). The recharge area for this small cave stream probably involves diffuse recharge as well as sinkhole drainage and has yet to be defined.

Presently, plans for the Jonesville bypass will physically alter an unknown extent of the cave and probably impact it hydrologically and biologically.

OTHER IMPACTED KARST RESOURCES

A limited number of examples of Virginia highway associated contamination impacts to Virginia karst resources are noted to capture the range of problems. UST petroleum leak impacts to Chimney Rock Cave (1970s – 1990s) by the Pounding Mill VDOT shop in Tazewell County. Groundwater contamination by a petroleum spill, from a tanker wreck (1980) on U.S. Highway 23 in Wise County, that passed through Wildcat Caverns. Groundwater contamination by milk from a 3,000-gallon spill from a tanker truck (1977) along U.S. Highway 33 in Rockingham County. Groundwater contamination by herbicide application (1983) by VDOT personnel along a segment of State Road 720 in Augusta County. Past use of Roadside Trash Pit, a cave along U.S. Highway 71 in Scott County, for refuse disposal by the Nickelsville VDOT shop. Groundwater contamination from salt storage and use along the roads and highways of Virginia's karstlands.

The most severe hazard that highways poise to Virginia's karstlands is that of groundwater contamination. Storm water runoff transports contaminants such as heavy metals, road salts, nutrients, bacteria, and hydrocarbons from road surfaces (Stephenson and Beck, 1995). An even greater potential hazard is the hazardous materials and other potential contaminants that are transported along highways. U.S. Department of Transportation (DOT) and Environmental Protection Agency (EPA) data indicate that highway transportation of hazardous materials is a relatively high-risk industry (Padgett, 1993). Designs that commit highway drainage into sinkholes and caves, potentially endangering karst water resources, may lead to increased litigation as environmentally unsound yet still accepted design practices are challenged by karstland residents.

CONCLUSIONS

Virginia's karstlands contain a wealth of resources, however they are limited and many are unique. The most significant of these resources is groundwater, which is highly susceptible to contamination due to the nature of the processes and features characteristic of karst. Those resources found in caves are only fractionally known due to their multidisciplinary relationships and the technical difficulty in access and assessment. Karst resources are impacted by road construction and site specific functional designs.

Highways, in construction and design function, are also subject to karst processes that can result in subsidence, flooding, and groundwater contamination problems on site or on neighboring properties. Control of runoff, including the specifics of disposal and quality are crucial in minimizing environmental disasters that are commonly avoidable with due diligence to site specific conditions. The current practice of channeling storm water runoff from highways into sinkholes and caves is environmentally unsound because such designs channel leaked and spilled hazardous waste and other contaminants transported along highways into the groundwater resource.

ACKNOWLEDGEMENTS

Thanks to the owners of Virginia's privately owned caves for access to study and document their caves and to the cavers that have helped in the recognition and documentation of Virginia's cave resources. Additional thanks to Frank Gilmer, Clay Stowers, Sam Greybill, and other VDOT field personnel who have strived toward environmentally sound site specific solutions to our karst hazards. Special thanks to Terri Brown, of VDCR, for her dye tracing work.

REFERENCES

Aley, T. and Thomson, K.C., 1981, Hydrogeologic mapping of unincorporated Green County, Missouri, to identify areas where sinkhole flooding and serious groundwater contamination could result from land development: Project Summary prepared for the Green County Sewer District, 11 p., 5 plates.

Bögli, A., 1980, Karst Hydrology and Physical Speleology. Springer-Verlag, New York, 284 p.

Bretz, J.H., 1942, Vadose and phreatic features of limestone caverns. Journal of Geology 50: 675-811.

Christiansen, K. and Bellinger, P., 1996a, Cave *Pseudosinella* and *Oncopodura* new to science. Journal of Cave and Karst Studies 58(1): 38-53.

Christiansen, K. and Bellinger, P., 1996b, Cave *Arrhopalites*: new to science. Journal of Cave and Karst Studies 58(3): 168-180.

Crawford, N.C., 1984, Sinkhole flooding associated with urban development upon karst terrain: Bowling Green, Kentucky: *in* Beck, B.F., ed., Sinkholes: Their Geology, Engineering & Environmental Impact, Proceedings of the First Multidisciplinary Conference on Sinkholes, Orlando, FL. A.A. Balkema, Rotterdam, p. 283-292.

Currens, J.C. and Graham, C.D., 1993, Flooding of the Sinking Creek karst area in Jessamine and Woodford Counties, Kentucky. Kentucky Geological Survey, Report of Investigations 7, 33 p.

Davis, W.M., 1930, Origin of limestone caverns. Geological Society of America Bulletin 41: 475-628.

Holsinger, J.R. and Culver, D.C., 1988, The invertebrate cave fauna of Virginia and a part of eastern Tennessee: Zoogeography and ecology. Brimleyana 14, 162 p.

Holsinger, J.R., Hubbard, D.A., Jr., and Bowman, T.E., 1994, Biogeographic and ecological implications of newly discovered populations of the stygobiont isopod crustacean *Antrolana lira* Bowman (Cirolanidae). Journal of Natural History 28: 1047-1058.

Hubbard, D.A., Jr., 1983, Selected karst features of the northern Valley and Ridge province, Virginia. Virginia Division of Mineral Resources, Publication 44, one sheet.

Hubbard, D.A., Jr., 1988, Selected karst features of the central Valley and Ridge province, Virginia. Virginia Division of Mineral Resources, Publication 83, one sheet.

Hubbard, D.A., Jr., 1999, Remediation of sinkholes along Virginia's highways: *in* Beck, B.F., Pettit, A.J., and Herring, J.G., ed.s, Hydrogeology and Engineering Geology of Sinkholes and Karst-1999, Proceedings of the Seventh Multidisciplinary Conference on Sinkholes and the Engineering and Environmental Impacts of Karst, Harrisburg/Hershey, PA. A.A. Balkema, Rotterdam, 413-417.

Hubbard, D.A., Jr. and Balfour, W.M., 1993, An investigation of engineering and environmental concerns relating to proposed highway construction in a karst terrane. Environmental Geology 22: 326-329.

Hubbard, D.A., Jr. and Barber, M.B., 1997, Virginia burial caves: An inventory of a desecrated resource. Journal of Cave and Karst Studies 59(3): 154-159.

Hubbard, D.A., Jr. and Boyd, C.C., 1997, Archaeological cave resources in Virginia, USA. Proceedings of the 12th International Congress of Speleology, La Chaux-de-Fonds, Switzerland 3: 37-40.

Hubbard, D.A., Jr. and Brown, T., 1997, Sinkhole back-flooding: A localized karst hazard in Virginia (abs.). Journal of Cave and Karst Studies 59(1): 53.

Hubbard, D.A., Jr. and Grady, F., 1997, Vertebrate paleontological cave resources in Virginia, USA. Proceedings of the 12th International Congress of Speleology, La Chaux-de-Fonds, Switzerland 3: 175-177.

Hubbard, D.A., Jr. and Sterrett, R.M., 1994, Ground-water contamination in Virginia karst: Case studies (abs.). Program and Abstracts, 37th Annual Meeting of the Association of Engineering Geologists, Williamsburg, VA, p. 49.

Kimball, L.R. and Whyte, T.R., 1994, Phase II archaeological investigations at Bone Cave (44LE169), Lee County, Virginia. Report prepared for the Virginia Department of Transportation by Appalachian State University Laboratories of Archaeological Science, Boone, N.C., 53 p.

Moore, H.L., 1984, Geotechnical considerations in the location, design, and construction of highways in karst terrain- "The Pellissippi Parkway extension," Knox-Blount Counties, Tennessee: *in* Beck, B.F., ed., Sinkholes: Their Geology, Engineering & Environmental Impact, Proceedings of the First Multidisciplinary Conference on Sinkholes, Orlando, FL. A.A. Balkema, Rotterdam, p. 385-389.

Myer, P.B., Jr. and Perlow, M., Jr., 1984, Development, occurrence, and triggering mechanisms of sinkholes in the carbonate rocks of the Lehigh Valley, eastern Pennsylvania: *in* Beck, B.F., ed., Sinkholes: Their Geology, Engineering & Environmental Impact, Proceedings of the First Multidisciplinary Conference on Sinkholes, Orlando, FL. A.A. Balkema, Rotterdam, p. 111-115.

Newton, , J.G., 1984, Review of induced sinkhole development: *in* Beck, B.F., ed., Sinkholes: Their Geology, Engineering & Environmental Impact, Proceedings of the First Multidisciplinary Conference on Sinkholes, Orlando, FL. A.A. Balkema, Rotterdam, p. 3-9.

Palmer, A.N., 1991, Origin and morphology of limestone caves. Geological Society of America Bulletin 103(1): 1-21.

Padgett, D.A., 1993, Remote sensing applications for identifying areas of vulnerable hydrogeological and potential sinkhole collapse within highway transportation corridors: *in* Beck, B.F., ed., Applied Karst Geology, Proceedings of the Fourth Multidisciplinary Conference on Sinkholes and the Engineering and Environmental Impacts of Karst, Panama City, FL. A.A. Balkema, Rotterdam, p. 285-290.

Sowers, G.F., 1996, Building on Sinkholes: Design and construction of foundations in karst terrain. ASCE Press, New York, 202 p.

Stephenson, J.B. and Beck, B.F., 1995, Management of the discharge quality of highway runoff in karst areas to control impacts to ground water – A review of relevant literature: *in* Beck, B.F., ed., Karst Geohazards, Proceedings of the Fifth Multidisciplinary Conference on Sinkholes and the Engineering and Environmental Impacts of Karst, Gatlinburg, TN. A.A. Balkema, Rotterdam, p. 297-321.

Thibaud, J.-M., 1995, Une nouvelle espèce de *Schaefferia* d'une grotte des États-Unis D'Amérique [Collembola, Hypogastrurida]. Revue fr. Ent., (N.S.) 17(2): 77-78.

Thibaud, J.-M., 1996, Une nouvelle espèce de *Typhlogastrura* de deux grottes des États-Unis D'Amérique [Collembola, Hypogastrurida]. Revue fr. Ent., (N.S.) 18(1): 11-12.

Karst Considerations in Final Design of Interstate 99 from State College, Pennsylvania, to Interstate 80

by
Donald V. Gaffney, Michael Baker Jr., Inc.
and
Jeffrey G. Dippel, Patel Chen Associates, Inc.

Abstract

One of the gaps in the interstate highway system is being closed with final design and construction of this section of roadway, which includes over twelve miles of new pavement and nearly 50 new structures in Pennsylvania's Nittany Valley. The local terrain is well known for its karst features, and has been the subject of many studies due in part to the proximity of Pennsylvania State University. Sensitivity to the impacts of construction on karst was heightened by local development and trout hatcheries on nearby high-quality streams.

Geotechnical design was guided by Pennsylvania Department of Transportation (PennDOT) Design Manuals and related publications, including a PennDOT "Geotechnical Engineering Manual." During preliminary design of the roadway, an Environmental Impact Statement identified karst processes and groundwater quality as major concerns. An associated mitigation report put forth strategies which were followed during final design. The strategies included discussion of options with interested parties, direct treatment of sinkholes and other solution features, and provision of adequate soil cover to prevent direct highway runoff migration into the groundwater.

Geotechnical investigations started with a review of available literature, maps and air photos. Pennsylvania Geological Survey Open-File Report OF92-01, "Sinkholes and Karst Related Features of Centre County, Pennsylvania," became a primary reference for karst evaluation. Field reconnaissance and mapping confirmed major lineament trends and joint patterns, although some local features were obscured by farming activity. Geophysical studies included both electromagnetic terrain conductivity and seismic refraction surveys. Geotechnical soil and rock borings were performed to define the subsurface conditions at structure locations and throughout the areas of major earthwork. A series of test pits in one potentially critical area was very beneficial to the design team's understanding of karst. The information gathered from these investigations allowed assessments of the intensity of local karst activity and development of detailed design and construction recommendations. Recommendations took the form of design details and two dozen technical specifications for construction which are incorporated as contract special provisions.

Cooperative work with the various engineering disciplines and reviewing agencies was essential to successful completion of the final design effort. The design will minimize infiltration of potentially contaminated surface water, improve the stability of the pavement subgrade, treat sinkholes and voids during construction, optimize use of excavated materials, allow flexibility during structure foundation construction, and provide the option of additional karst investigation during construction.

Acknowledgments

The authors appreciate the support provided by their companies, the Pennsylvania Department of Transportation, and the FHWA in the preparation and presentation of this paper. However, the views and conclusions presented are those of the authors and should not be interpreted as necessarily representing official policies or positions of Michael Baker Jr., Inc., Patel Chen and Associates, Inc., the Pennsylvania Department of Transportation, or the FHWA.

Project Overview

This paper discusses the final design of 8.3 miles of four-lane, limited access freeway in Centre County, PA. The completed project will be the principal route from the North into State College, PA, and will eventually become a segment of Interstate System as I-99. During design the roadway was identified as S.R. 0026, but the designation was changed prior to construction to S.R. 6026. In addition to the four-lane roadway, there were junctions with exiting four-lane roadways at both ends, one full and one partial interchange, and several miles of ancillary roads. The project required 46 bridges, walls and major culverts. Figure 1 shows the layout of the project. The central section of the project traverses an active State Penitentiary, complicating the design and construction.

The project was designed in four sections for PennDOT Engineering District 2-0 by Erdman Anthony Associates, Inc.(Erdman), with Benatec Associates, Inc.(Benatec) and KCI Technologies, Inc. (KCI) as subconsultants. During design the sections were designated C02, A02, C03, and C05, from south to north. All of the geotechnical design was performed by Patel Chen Associates, Inc. (PCA). Michael Baker Jr., Inc. (Baker) served as design manager, providing consultant management and review services.

The entire project is on karst terrain, a fact well known by the residents of Centre County. Pennsylvania Geological Survey Open-File Report 92-01, "Sinkholes and Karst-related Features of Centre County, Pennsylvania," provided an excellent basis for understanding the local terrain. Figure 2, modified from that report, illustrates the project's location from a regional perspective. Pennsylvania State University has conducted research in the general area and has provided groundwater expertise to local governmental agencies. Well systems provide water for the communities in the area. Local high-quality streams support trout, and a number of fish hatcheries operating on them. Concern for potential impacts due to roadway construction were raised during the environmental clearance process, documented in the final Environmental Impact Statement (EIS), and written into the associated Mitigation Report. The Mitigation Report committed to:

1. Capping sinkholes and areas of active solution activity with concrete to prevent surface water infiltration.
2. Covering excavations with potential for contamination with sufficient soil to prevent direct migration of the contaminants into the groundwater.
3. Discussing mitigation options to address groundwater concerns with interested parties.
4. Identifying and assessing all water wells within 1000 feet of the project.

During the design period, other construction activities in the area created significant local sinkhole activity and fish-kills. This reinforced the environmental concerns and the need for mitigation.

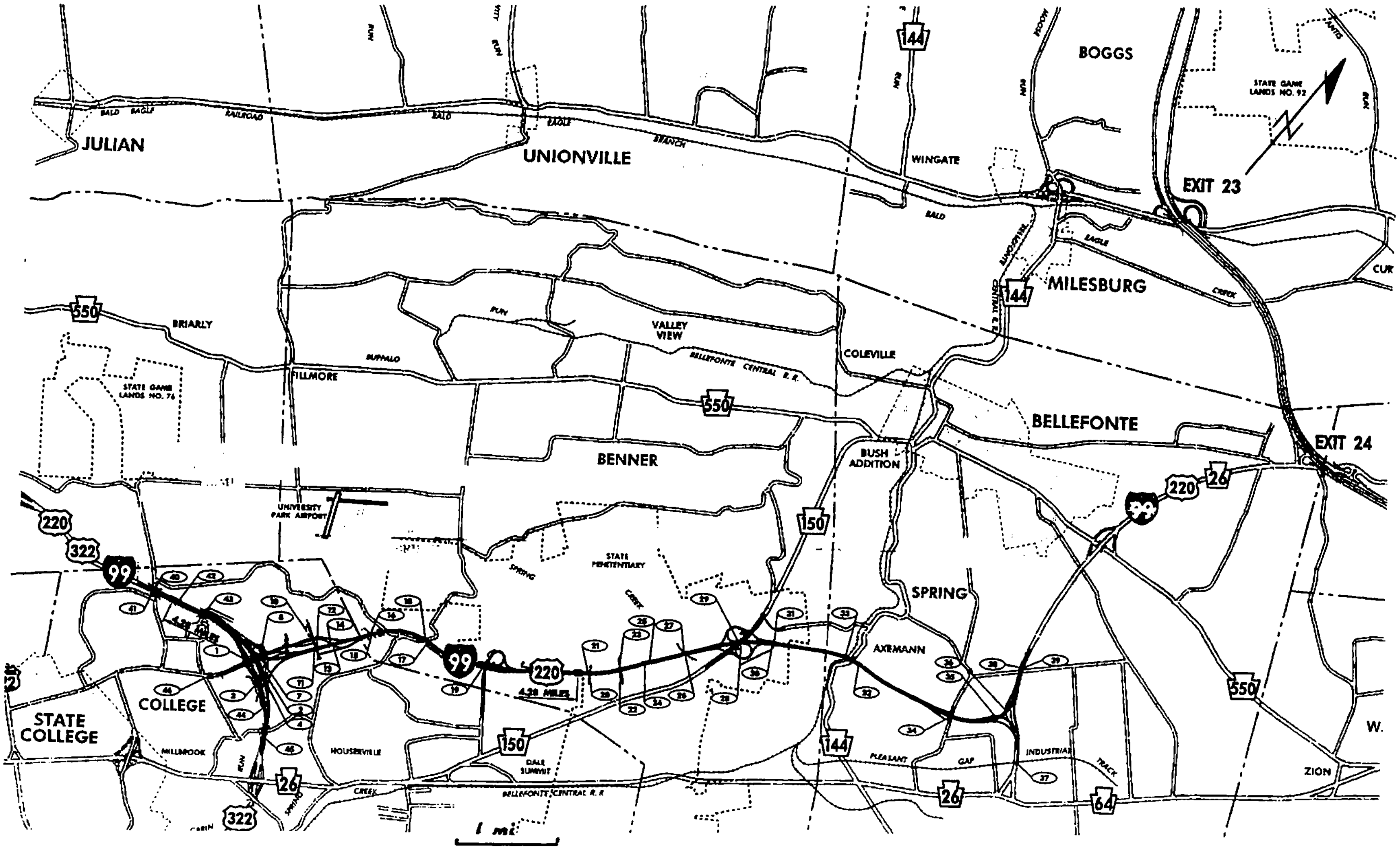

FIGURE 1. Project layout. The ovals indicate major structures.

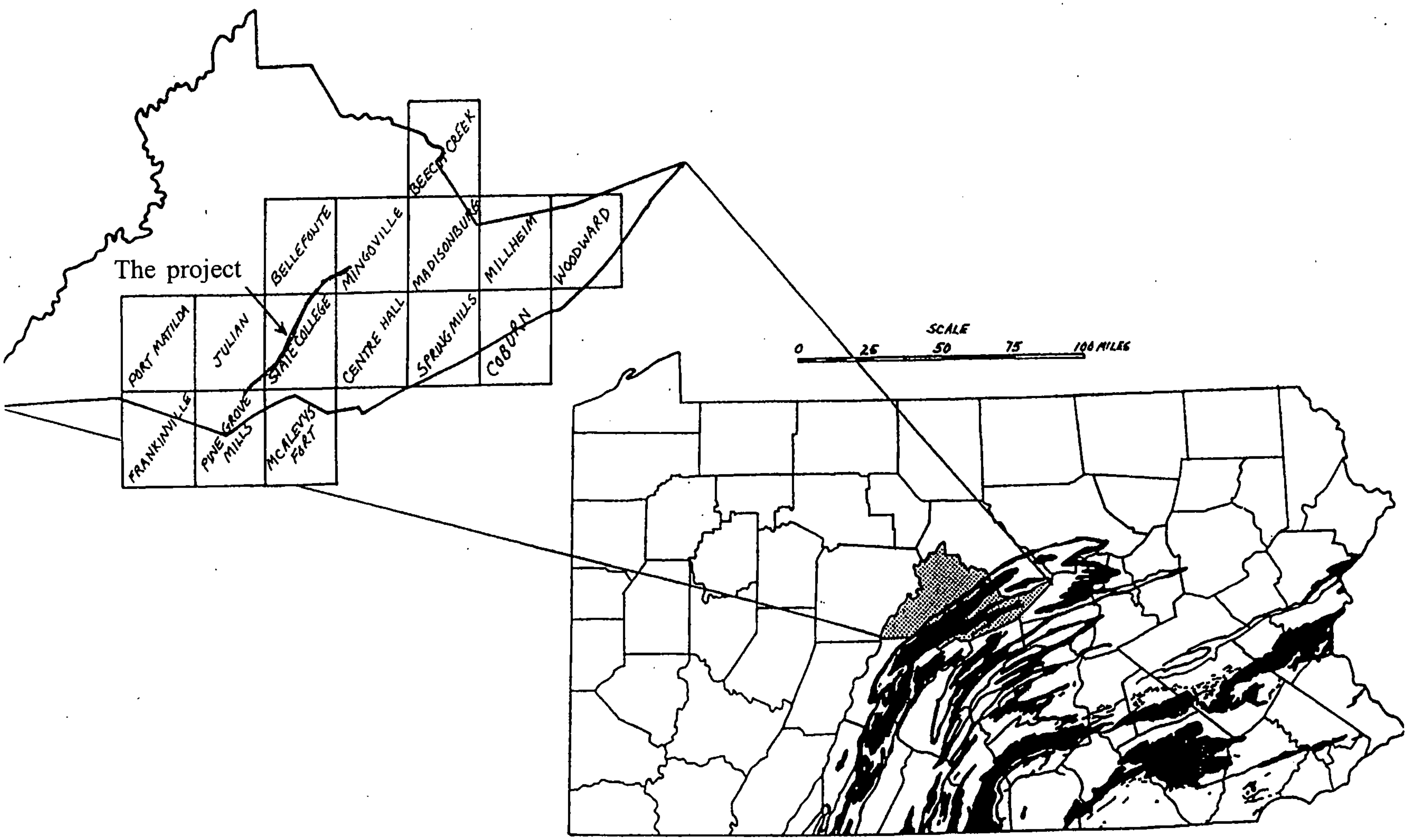

FIGURE 2. The project from a regional perspective. Black areas on the PA map show locations of carbonate bedrock. (Modified from OFR 92-01)

Geotechnical Investigations

The geotechnical investigations were performed in general conformance with PennDOT Design Manuals and other PennDOT geotechnical publications. The investigations involved preliminary study, geological mapping, subsurface exploration, laboratory testing, and analysis.

Initially, available project literature, engineering reports, geological maps, and information helpful for understanding the geology of the project route were reviewed. Useful data was abstracted and compiled on a base map. During the geological mapping, the topography, rock outcrops, springs, streams, and distinctive features were identified, mapped and photographed as appropriate. A full program of strike and dip measurement was also undertaken. Several lines of geophysical surveys were run with both electromagnetic terrain conductivity and seismic techniques employed.

Roughly 8.1 miles of soil sampling and rock coring were performed. Generally, boring depths were extended to 20 feet below the proposed grade in cut sections and 20 feet below the rock surface in embankment sections. When cavities were encountered, borings were extended to 20 feet below the cavity bottom. Borings for structures had similar termination criteria, extending a minimum of 20 feet into bedrock below the anticipated bottom of footing and also requiring ten continuous feet of sound rock prior to boring termination.

Laboratory testing included classification, compaction, and CBR tests on bag samples; consolidation and triaxial compression tests on undisturbed thin-walled tube samples; and point load and uniaxial compression tests on rock core samples.

As expected, classical karst subsurface conditions were confirmed throughout the length of the project. This was supported when a series of test pits were dug in an especially critical area after borings had been drilled along a proposed wall. The test pits reminded everyone that borings just provide a nominal 3-inch picture of the subsurface, and another boring six inches away would easily show different conditions. In general, most of the current karst activity and open voids appear to be at the edges of major sinkhole clusters. These clusters were labeled early in the project as "Sinkhole Problem Areas." The interiors of the clusters appear to be relic sinks filled with soft, wet, fine-grained soils. Very few open voids remain, but the soils can lead to erratic settlement under embankment loading. A plan of sinkhole areas at the north end of the project is shown in Figure 3.

Karst treatments, settlement and stability were analyzed as the primary geotechnical concerns related to the roadway construction. Geotechnical concerns analyzed for structures included determination of adequate bearing locations, selection of appropriate foundation types and foundation treatments.

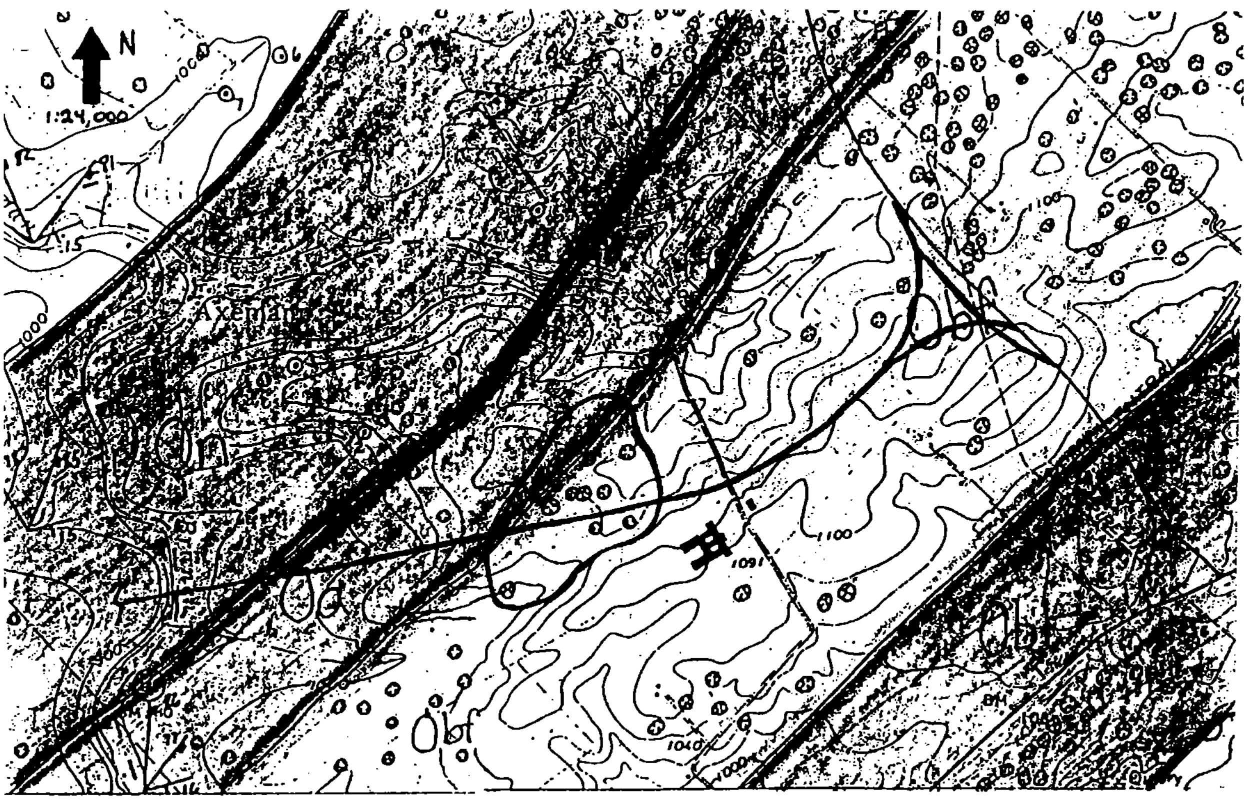

FIGURE 3. Portion of OFR 92-01 showing sinkhole locations, with geology and alignment added. Note encircled "sinkhole problem area" cluster.

Geotechnical Recommendations

Geotechnical recommendations typically were developed into details and special provisions for construction, and addressed karst issues for both roadways and structures. PennDOT has guideline details for sinkhole treatment, some of which are shown in Figure 4. Minor modifications were made to the details to adapt them to this project, and a special provision was written to accompany them

To address the environmental concern of contaminant infiltration into the groundwater, details and specifications were developed. Cut areas are to be over-excavated, and ditches and swales are to be lined. A geosynthetic clay liner (GCL) is to be used through sinkhole problem areas, while the fine-grained site soil is considered to be adequate elsewhere. This approach is illustrated in Figure 5. Toe-of embankment ditches and storm water facilities were treated similarly.

Where the roadway subgrade will be in cut, provision has been made for undercutting or lime-treating the subgrade. Where the roadway is to be on fill, lower portions of the embankment are to be constructed of best available rock from excavations. Where settlement was determined to be a problem, programs were developed for quarantining and monitoring embankments prior to potentially impacted subsequent construction.

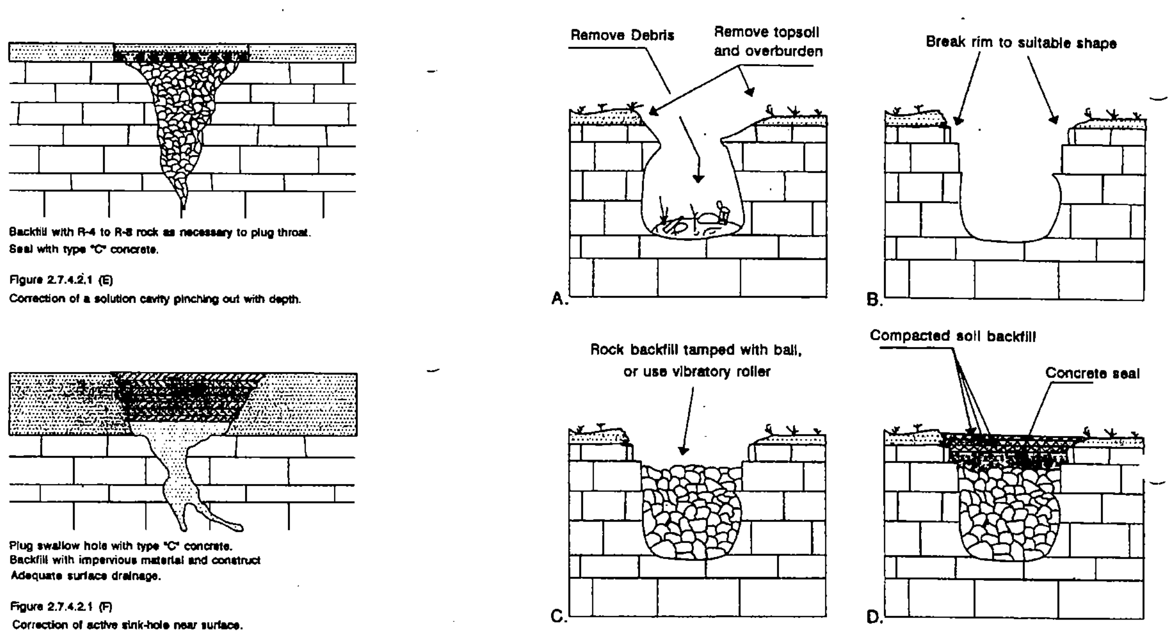

FIGURE 4. Typical Sinkhole Treatment Guideline Drawings from PennDOT Pub. 293. These details were modified and adapted for this project.

Project special provisions require more extensive clearing and grubbing than PennDOT standards typically require. This will expose the subsoil conditions for the full roadway footprint and allow detailed visual inspection prior to major earthmoving. If the inspection indicates potential karst activity, the contractor will be directed to provide exploratory air-track drilling, soil sampling and rock core boring, or test pitting as appropriate. If sinkholes are uncovered, they are to be treated as directed.

The structure foundations were designed conservatively, with a maximum of 4 TSF allowable bearing capacity for spread footings. Pre-drilled H-piles or pipe-piles were allowed for deep foundations, with 6 ksi allowable in steel and the pile cap designed to withstand the loss of one-third of the piles. Disallowed from consideration as foundation types were caissons, pin-piles and other deep foundations where grout or concrete is injected 'blindly' with the potential for uncontrolled material loss. All foundations must bear on sound rock at least 10 feet thick. This is to be confirmed by the contractor through a program of exploratory drilling on a 10-foot or closer grid under the foundations. Preparation of rock bearing surfaces, detailed inspection of foundation rock, excavation of soft seams and treatment of voids below foundation level are all addressed with special provisions. Examples of structure foundations are presented in Figure 6.

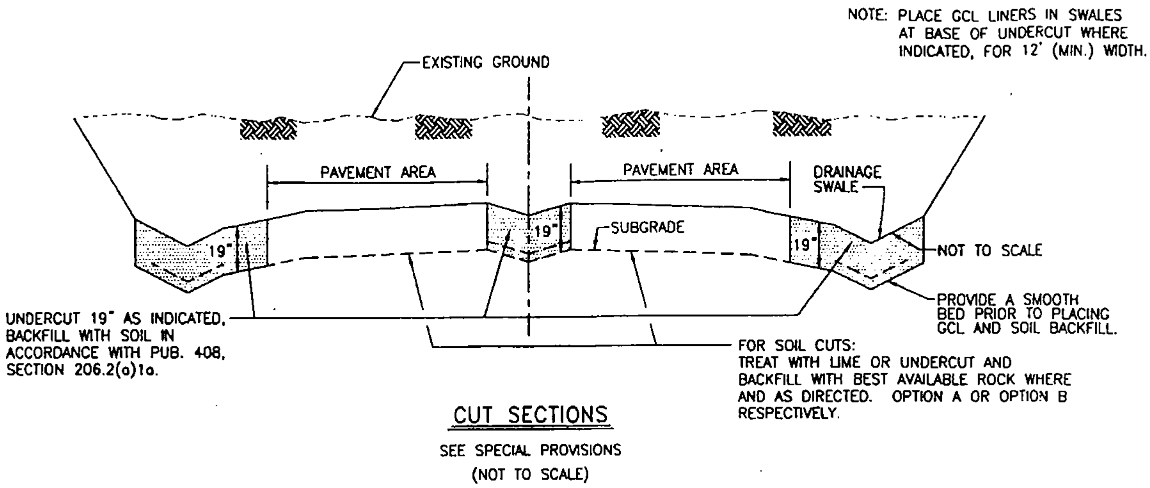

FIGURE 5. Treatment of Swales and Ditches. GCL to be used only in Sinkhole Problem Areas.

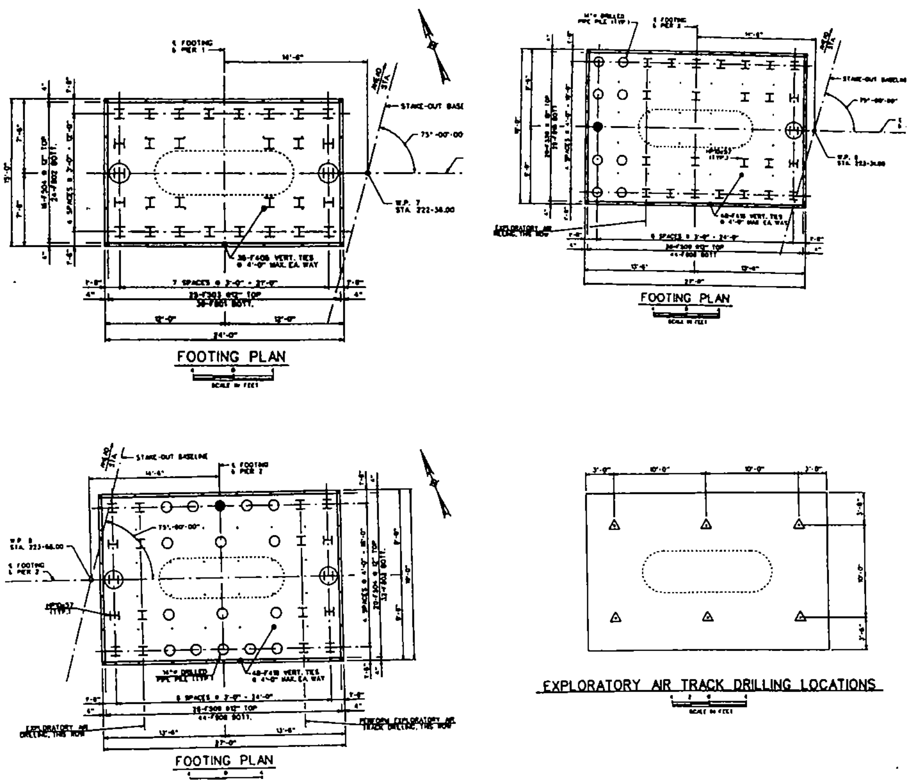

FIGURE 6. Typical pier column footings: H-Pile (good bedrock at depth), Pipe-Pile/H-Pile (void under footing edge), H-Pile / Pipe-Pile / H-Pile (void under footing center), Spread (good bedrock at bottom of footing)

Continuing Coordination

During construction, there is to be a geotechnical site representative. The representative is responsible for proper implementation of the geotechnical details and specifications, and is available to resolve geotechnical issues which typically arise during construction in karst. This representative's involvement was initially set at half-time, but once construction started the value of a geotechnical presence was quickly realized and full-time status established.

Bibliography

Benatec Associates, Inc., 1998, Plans for Construction of S.R. 6026, Section C03, Supplemental Drawings - Bridge Plans, New Cumberland, PA

Kochanov, W. E., 1992, Sinkholes and Karst-Related Features of Centre County, Pennsylvania, Pennsylvania Topographic and Geologic Survey, Harrisburg, PA

McCormick, Taylor & Associates, Inc., 1996, Mitigation Report, S.R. 0026, Section C02, Harrisburg, PA

Moore, H., 1988, Treatment of Karst Along Tennessee Highways, *in* Geotechnical Aspects of Karst Terrains, N. Sitar (ed.), ASCE Geotechnical Special Publication No. 14, ASCE, New York, NY

Patel Chen Associates, Inc., 1998, Geotechnical Engineering Reports for Roadway Construction and Structure Foundations - S.R. 0026, Sections C02, C03 and C05, Grantville, PA

PennDOT, 1994, Specifications, Publication 408, Pennsylvania Department of Transportation, Harrisburg, PA

PennDOT, 1997, Geotechnical Engineering Manual, Publication 293, Pennsylvania Department of Transportation, Harrisburg, PA

PennDOT, latest editions, Design Manuals - Volumes I through IV, Pennsylvania Department of Transportation, Harrisburg, PA

Weber, L. C., 1988, Exploring Karst Terrain with Air Track Drilling, *in* Geotechnical Aspects of Karst Terrains, N. Sitar (ed.), ASCE Geotechnical Special Publication No. 14, ASCE, New York, NY

White, W.B., 1988, Geomorphology and Hydrology of Karst Terrains, Oxford University Press, New York, NY

Use of Geophysical Techniques to Evaluate Karst Features for Roadway Design

Joel C. Daniel, PG
Virginia Geotechnical Services, PC, Richmond Virginia

Richard C. Benson, CPG
Technos, Inc., Miami, Florida

Ann M. Samford, PE, PG
Virginia Geotechnical Services, PC, Richmond, Virginia

A major Federal facility was proposed for an undeveloped site in southwestern Virginia. The site is located in a mature karst area of the Valley and Ridge Physiographic Province. The site is underlain by highly soluble carbonates of the Dot and Poteet Limestones. The main access road to the site and main utilities for the site cross a "saddle" area between two major coalescing sinkholes. Data collected during a test boring program at the site indicated possible subsurface instability in the saddle area. Because of the importance for maintaining the road and utilities for the site, additional subsurface information was necessary in the saddle area.

We completed a geophysical exploration program using microgravity, electromagnetics (EM31 and EM34) and electrical resistivity to supplement the test boring program, and to develop a more detailed conceptual model of the subsurface conditions. Test boring data collected in the "saddle" area corroborated measured geophysical anomalies. The major anomaly in the "saddle" area appeared to follow the contact between the Dot and Poteet Limestones. The data also indicate this area is likely a significant recharge zone to wetlands located in the bottoms of the sinkholes.

Data collected by geophysical and traditional drilling techniques identified potential stability problems. As part of the roadway design considerations, we recommended compaction grouting as the preferred remedial alternative for the karst problems.

INTRODUCTION

The United States Federal Bureau of Prisons (FBoP) is building a maximum security prison on a 200-acre site in Dot, Virginia, which is located in Lee County (Fig. 1). This project is part of an effort by Lee County to provide economic growth to this rural, low-income area of Virginia. The majority of the area readily available for development is valley pastureland and forests, underlain by soluble carbonate rocks.

Development in carbonate terrain can present significant geotechnical and construction challenges. If care and thoroughness are not utilized in the initial stages of site evaluation, unforeseen site conditions can result in significant design changes and cost overruns. As part of the geotechnical investigation for the maximum security prison, we completed an extensive subsurface exploration program consisting of test borings and geophysical surveys. The subsurface data revealed significant stability concerns in the area of the proposed roadway/utility corridor. Because this was a planned Federal maximum security prison, we recommended that additional geophysical exploration be completed in the roadway area to ensure we had a sound understanding of the subsurface conditions. This information would be essential to designing any remedial programs for the roadway area.

GEOLOGIC SETTING OF THE SITE

The site is located in the Valley and Ridge Physiographic Province of Virginia. The Valley and Ridge is characterized by broad valleys underlain by limestone, dolomite and some shale, with narrow ridges composed of more resistant sandstone and conglomerate. Stratigraphic ages of these rocks range from Cambrian to Devonian, and they are generally folded and thrust-faulted.

The site is underlain by the near-horizontal Poteet and Dot Limestones. The western portion of the site is underlain by the more-resistant Dot Limestone, and the eastern portion by the less-resistant Poteet Limestone. The Poteet Limestone has undergone more extensive weathering and karst development than the Dot Limestone. Consequently, the eastern portion of the site is characterized by a mature karst topography, with two caves located in the southeastern corner of the site.

The geologic contact between the Dot and Poteet Limestones crosses the middle of the site in an approximately north to south direction. The entrance roadway (Fig. 2) also crosses this contact. In the north-central portion of the site, the contact corresponds to the locations of two large sinkholes which are separated by a topographic "saddle" (Fig. 2). In this report, we have defined sinkholes to include all closed solution features

The saddle area is the location of the prison entrance roadway. Field observations made on June 15, 1997 after a heavy rainstorm indicated that the northern sinkhole contained a 3-acre pond with a water level approximately 6 feet above grade. We observed this pond to be completely drained after 24 hours, which suggested the presence of a significant drainage pathway beneath the ground surface. The pond was estimated to have held approximately 4 million gallons of water. A dye trace was completed in 1996 by others, where dye was introduced into the subsurface within this sinkhole, and was subsequently detected a various locations in the northeastern central and southeastern portions of the site. This indicated groundwater flowed beneath the saddle area as it left the large sinkhole, and proceeded across the site. We attributed this drainage pathway in the saddle area to considerable secondary porosity along joints and bedding planes corresponding to the Dot-Poteet contact.

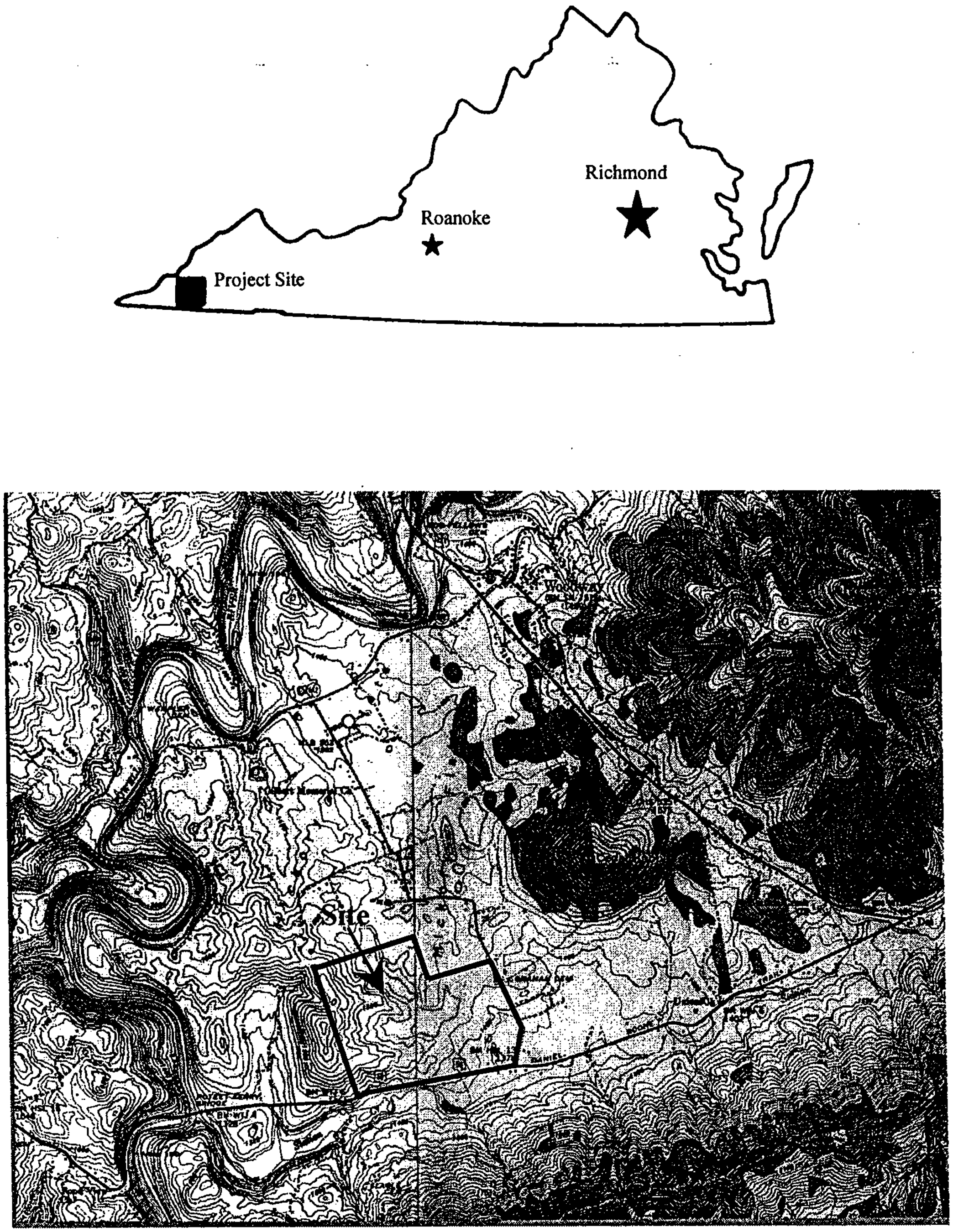

Figure 1. Location of Site Area in Southwest Virginia. 7.5- Minute USGS Topographic Quadrangle Showing Site.

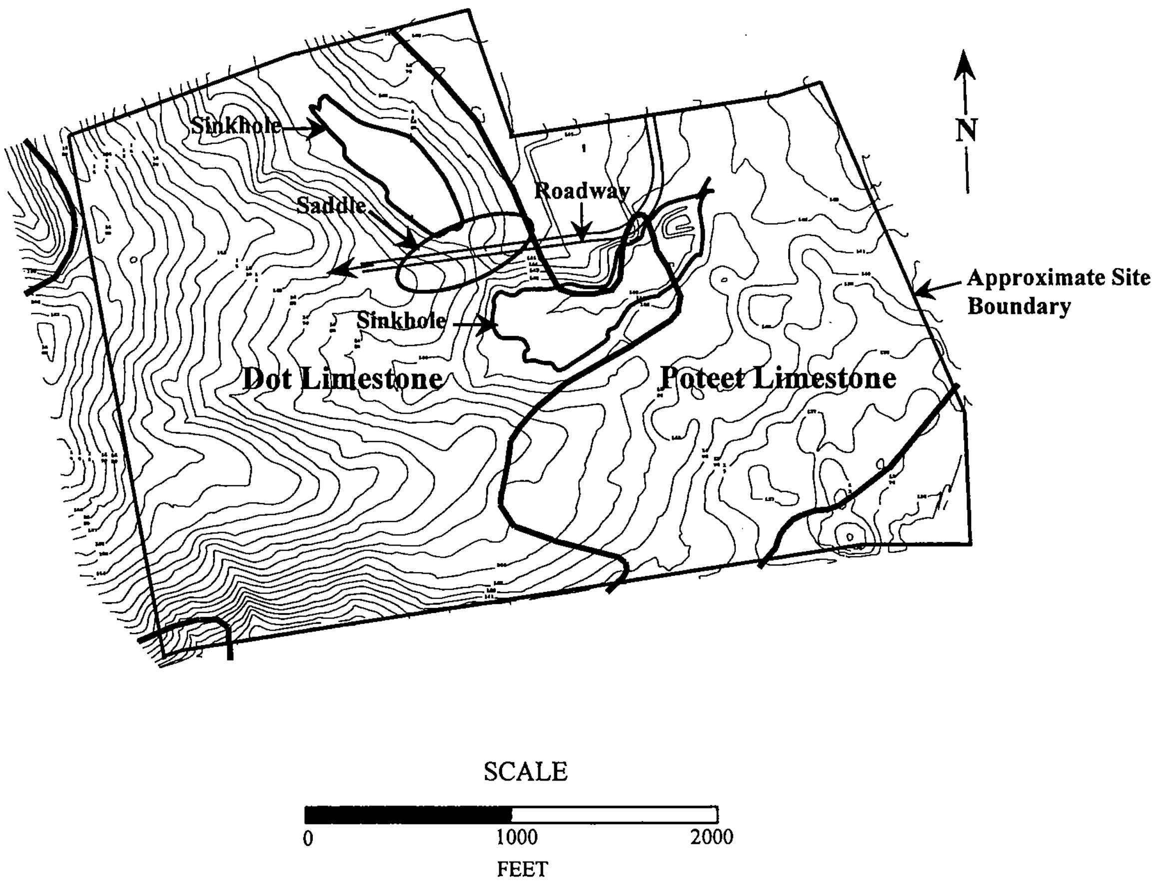

Figure 2. Site Map with Geologic Contacts and Saddle Area.

SUBSURFACE EXPLORATION PROGRAM

Several test boring exploration programs have been completed on and adjacent to this site since 1988. The original exploration program for this site, completed by Law Engineering in 1996, consisted of several borings and test pits, and an electromagnetic (EM31) survey.

GENERAL EXPLORATION

A total of 141 borings and test pits have been completed around the 200-acre site. This has produced a wealth of information with a total of over 4,100 feet of drilling including over 2,500 feet of rock core. Soil thickness, from borings where rock was encountered, ranged from 1.1 to 43.1 feet. A total of 40 cavities and smaller voids were encountered during drilling and coring, with heights of the cavities and voids ranging from 0.2 to 5 feet.

We completed five borings (G10, RD1, RD5, G13 and RD6) in an east-west line (1400N) along the saddle (Fig. 3). We completed three additional borings (RD7, RD8 and RD9) near line 1400N, with two of these located north and south of this line. The data from these eight borings indicated soil thickness ranging from 6.7 to 33.8 feet, and thickness was observed to gradually increase from west to east, with an abrupt decrease at the eastern end of the saddle.

GEOPHYSICAL EXPLORATION OF SADDLE AREA

Geophysical exploration programs at the site have included electromagnetic surveys using EM31 and EM34 methods, microgravity profiles and electrical resistivity soundings. A thorough description of these methods is beyond the scope of this paper.

Microgravity involves collecting measurements of the earth's gravitational field at the microGal level (1/1000 of a milliGal or 10^{-9} Gal). Gravity data are collected along a profile at discrete stations, and must be corrected for various effects such as terrain and minor fluctuations in the Earth's gravitational field. After corrections are made, the resulting gravity anomalies are directly related to variations in subsurface density.

Electromagnetic surveys involve measuring variations in electrical conductivity of subsurface materials using one or more electromagnetic instruments, including the EM31 and EM34 used in this study. Basically, data is collected continuously along parallel profiles with the EM31 instrument, with the overall "depth" of electrical penetration remaining "constant". In comparison, data is collected along profile lines, but at discrete stations, using the EM34 instrument. The EM34 has two coils which can be reoriented (vertical and horizontal dipole positions) to achieve different "depths" of electrical penetration. The spatial variability of electrical conductivity is directly related to changing subsurface conditions such as clay and moisture content.

Electrical resistivity surveys involve measuring variations in electrical resistivity of subsurface materials. This technique is typically used in areas where higher resistivities are expected, and electromagnetics may, therefore, be less appropriate. However, this method may be used to corroborate other geophysical data such as electromagnetics, if natural conditions permit successful surveys with multiple methods. Overall, the electrical resistivity technique is more labor-intensive than the more popular electromagnetic methods.

The results from geophysical surveys must be confirmed with actual discrete, invasive data, such as test borings and test pits. Geophysics gives a more continuous assessment of subsurface conditions than the discrete data. This can have significant implications in geologically-variable environments such as karst, where discrete exploration can possibly "miss" important subsurface features such as caverns.

MICROGRAVITY SURVEY

We completed the microgravity survey in the saddle area using an EDCON SuperG gravimeter. We completed a total of four microgravity profiles in the saddle area, with the largest measured anomaly being 180 μGals at station 1600N, 1800E. Field observations of shallow rock in the vicinity of this station indicated that this anomaly was not entirely attributable to thick soils. The density of soil is lower than that of rock; therefore, the presence of thick soils overlying bedrock may provide a lower gravity anomaly than expected for the bedrock. After accounting for soil thickness changes and terrain effects during gravity modeling, a residual gravity anomaly of 150 μGals remained (Fig. 4). We interpreted this to be due to a heavily weathered and dissolved zone of bedrock. This interpretation was corroborated by 1) the reconnaissance dye trace completed in 1996, 2) the rapid drainage of June 15, 1997, and 3) a localized zone of lower groundwater levels as compared to the rest of the site.

We measured a second gravity anomaly at station 1415N, 2050E (Fig. 3, near the saddle borings) as 150 μGals (Fig. 4). As described previously, the eight saddle borings generally showed an increasing soil thickness from station 1800E to approximately 1950E. However, the soil thickness rapidly increases east of station 1950E. This variation in soil thickness was interpreted to account for the majority of this anomaly. The thick soils here are likely the result of rock weathering and the presence of smaller voids in soils. We concluded that the presence of these conditions implies the existence of a highly-weathered contact between the Dot and Poteet Limestones.

ELECTROMAGNETIC SURVEY

We completed the electromagnetic surveys on all gravity survey lines around the site using the EM31 instrument, to aid in the gravity interpretation. We also completed electromagnetic surveys using the EM34 at 10 and 20 meter coil spacings in both horizontal and vertical dipole orientations.

Based on the data collected from the test borings in this area, we interpreted higher electrical conductivities to indicate thin soils and a shallow, highly-weathered epikarst zone at the top-of-rock. Similarly, we interpreted lower measured conductivities as thicker soils with lesser influence from a deeper epikarst zone. We have defined epikarst to be a weathered, high-moisture clay which tends to be "draped" across the irregular bedrock surface. This wet material has a higher electrical conductivity due to its high moisture and resulting dissolved ion content than overlying drier soils.

Investigation of the saddle area using EM31 methods along line 1415N (Fig. 3) indicated a minimal change in electrical conductivity from west to east, until around station 1950E. At this station, electrical conductivity showed an abrupt decrease (Fig. 4). This overall trend in rapid decrease followed by eventual rapid increase in conductivity indicated a zone of thicker soils, which corroborates the interpretation of the measured gravity anomaly at this location.

ELECTRICAL RESISTIVITY SOUNDINGS

We collected electrical resistivity data at seven locations around the site using a Bison Instruments Model 2390 resistivity system. We used standard Wenner and Lee electrode geometries.

We completed two of the electrical resistivity soundings in the vicinity of the saddle area (Fig. 3). We completed one sounding at station 1415N, 1550E where the EM31 data indicated high conductivities. We completed a second sounding at station 1415N, 2200E where the EM31 data indicated low conductivities. We interpreted the measured apparent resistivities by inverse modeling the data with RESIXP software by Interpex Ltd. Inverse modeling of apparent resistivity data presents a "non-unique" solution of resistivities and depths to corresponding layers. Generally, alternative solutions are also presented and evaluated during inverse modeling.

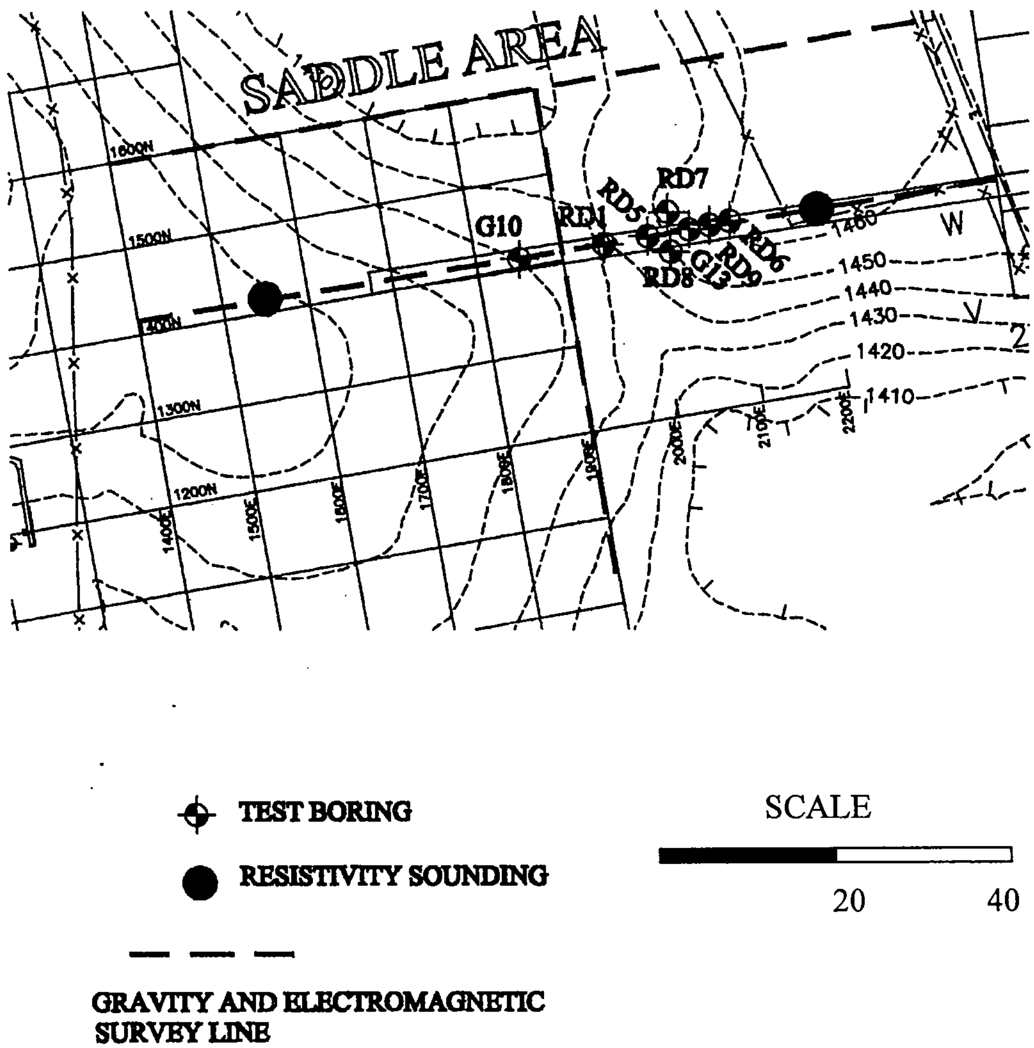

Figure 3. Saddle Area with Exploration Locations.

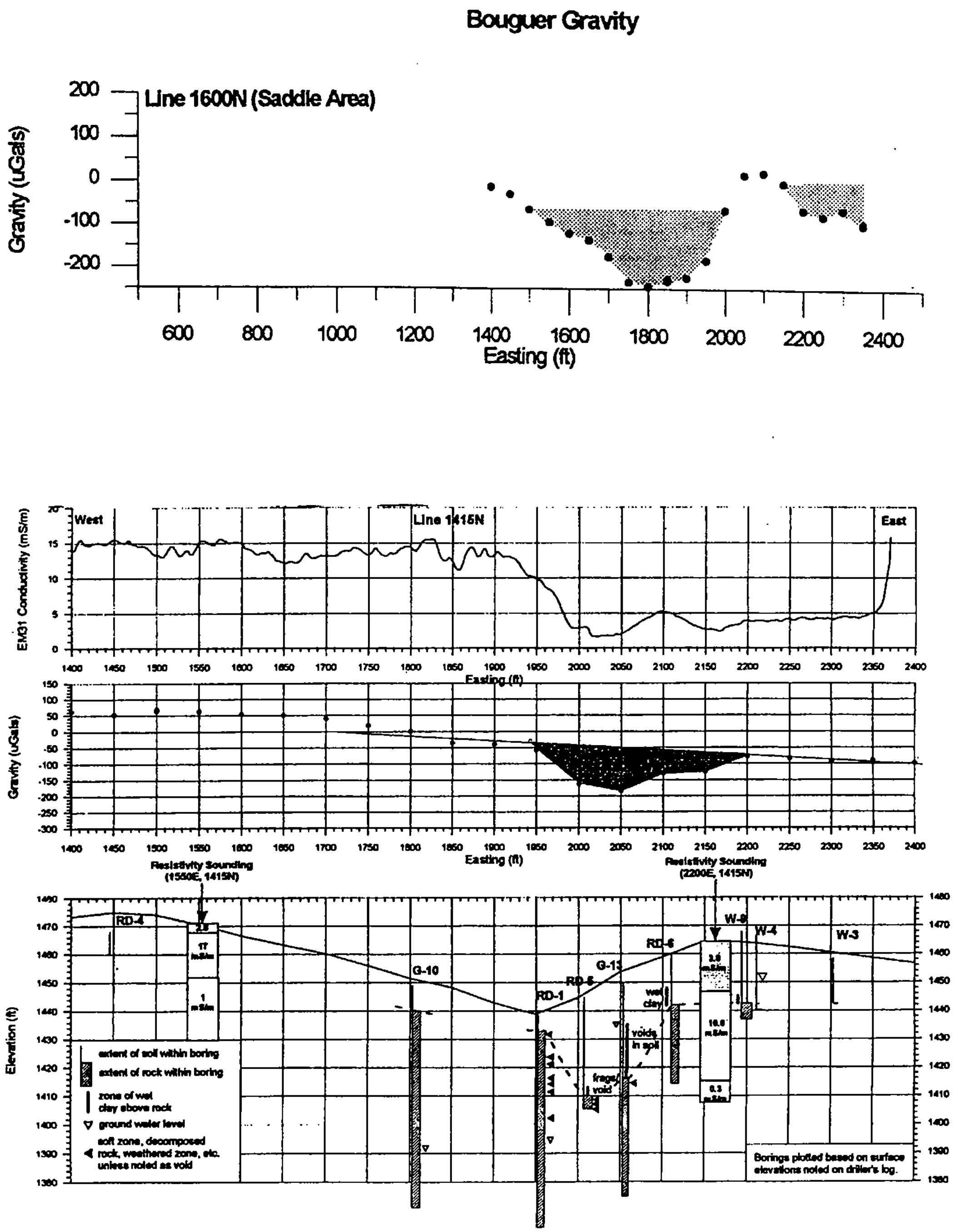

Figure 4. Top - Gravity Anomaly Along Line 1600N.
Bottom - Geophysical Results and Interpretations along Line 1415N.

Inverse modeling of both resistivity soundings showed a low-resistivity zone associated with the soil/bedrock interface (epikarst zone). For station 1550E, the modeling indicated the top of the low-resistivity epikarst zone (179.2 ohm-ft) to be at 1.6 feet below the ground surface. This is shown on Figure 4 as high conductivity (17 mS/m). In comparison, the modeling indicated the top of the low-resisitivity epikarst zone at station 2200E to be at a depth of 18.6 feet (278.8 ohm-ft). This is also shown on Figure 4 as high conductivity (10.8 mS/m). This observation supports the correlation of shallow rock with high conductivities noted across the site.

DESIGN CONSIDERATIONS FOR THE ENTRANCE ROADWAY

The test borings and geophysical surveys indicate a substantial geotechnical stability concern in the vicinity of the saddle area. Since this roadway functions as the sole entrance and exit to the site, and to serve as the site utility route, it was important to make every effort to ensure the stability of this area.

All data collected in this portion of the site, along with the rapid surface discharge and dye trace observations, and the general karst geomorphology indicate the presence of a significant groundwater recharge zone north of the saddle area. This zone is attributed to the dissolution-enlarged joints and bedding planes interpreted for this area.

The geophysical data indicate a heavily weathered and dissolved zone of bedrock located beneath the saddle area, and connecting the recharge zone to the sinkhole south of the saddle area. It is our interpretation, based on the data, that this weathered zone is associated with the contact between the Dot and Poteet limestones. Therefore, the highly weathered rock and soil voids in the contact zone are particularly susceptible to soil piping and subsidence. Consequently, a geotechnical stability problem in the saddle area could be detrimental to the overall function of the prison facility, with the loss of the entrance road and the possible loss of all site utilities.

The project team presented the Federal Bureau of Prisons with four remedial alternatives based on the data and observations from the saddle area. Option 1 involved no remedial activity and accepting the risk of sinkhole development or other stability problems. Option 2 involved excavating poor soils and replacing them with controlled rock fill. Option 3 involved supporting the roadway on a pile supported/geosynthetic reinforced embankment. Option 4 involved in-situ ground improvement by compaction grouting. Following review of the relative technical merits and potential costs of the alternatives, ground improvement by compaction grouting was recommended for mitigating potential sinkhole instability in the saddle area.

It becomes evident when we look at the overall additional costs and scheduling difficulties that would have been incurred from drilling alone that geophysics provided a significant value to the success of the project. The test boring data from the saddle area indicated the need for special consideration of the design of the roadway, and we would have required significantly more test boring data in this area to obtain the same quality of information as obtained with the geophysics. The project schedule did not allow for substantial increase in the test boring program, and the use of geophysics provided rapid, quality data at a fraction of the potential cost of drilling.

ACKNOWLEDGEMENTS

The authors wish to thank the United States Federal Bureau of Prisons and Hayes, Seay, Mattern & Mattern, Inc., prime consultant, for their thoughtful review of this paper, and extending the permission to present this information. The opinions expressed herein are the authors', and should not be taken to reflect those of the United States Federal Bureau of Prisons or Hayes, Seay, Mattern & Mattern, Inc.

BIBLIOGRAPHY

Technos, Inc., 1998. Final Report, Subsurface Karst Investigation and Characterization for Geotechnical Purposes, U.S. Penitentiary and Satellite Camp, Lee County, Virginia. Consultant Report.

Technos, Inc., 1997. Preliminary Data Report, Subsurface Karst Investigation and Characterization, U.S. Penitentiary and Satellite Camp, Lee County, Virginia. Consultant Report.

Virginia Geotechnical Services, P.C., 1998. Geotechnical Engineering Report, Federal Bureau of Prisons - USP, FPC and CSF, Lee County, Virginia. Consultant Report.

Virginia Geotechnical Services, P.C., 1998. Addendum 1 - Geotechnical Engineering Report, Federal Bureau of Prisons - USP, FPC and CSF, Lee County, Virginia. Consultant Report.

A Case History on the Use of Compaction Grouting for Roadway Improvement in Mature Karst Topography

Marcia V. Prowell, P.E., Virginia Geotechnical Services, P.C., Richmond, VA
Hugh C. Garst, P.G., Hayes, Seay, Mattern & Mattern, Inc., Roanoke, VA
Ann M. Samford, P.G., P.E., Virginia Geotechnical Services, P.C., Richmond, VA

ABSTRACT

A large development was proposed for a 267-acre site in southwestern Virginia. The site is located in the Valley and Ridge Physiographic Province and was underlain by highly soluble carbonates of the Dot and Poteet Limestones. The main entrance to the site crossed a ridge between two major sinkholes. These sinkholes generally were aligned parallel to the contact between the Dot and Poteet Limestones. The subsurface exploration program supplemented with a geophysical study revealed an excessive thickness of very soft epikarst in the eastern flank of the ridge. Stability analyses indicated that the soils were not strong enough to support the embankment fills required to achieve adequate grade for the main roadway.

Following an evaluation of several remediation alternatives, in-situ ground improvement was determined to be the most effective solution. A compaction-grouting program with primary and secondary grout holes was ultimately designed and implemented. Tertiary holes were installed in a limited area due to large grout uptakes in several primary and secondary holes.

INTRODUCTION

The Federal Bureau of Prisons (FBOP) is currently constructing a maximum security United States Penitentiary (USP), a minimum security Federal Prison Camp (FPC) and a Central Shared Facility (CSF) in Lee County, Virginia. The site is located in the Valley and Ridge Physiographic Province and is underlain by highly soluble carbonates of the Dot and Poteet Limestones. Mature karst geology and topography, including surface sinkholes and subsurface enlarged joints and voids, characterize the site. The depth to bedrock varies across the site. Bedrock outcrop is present, as well as areas with thicker soil layers overlying bedrock. Epikarst was present in some of the overburden soils.

Within the context of this paper, epikarst is defined as "The soft zone of unconsolidated residual soil immediately above the rock surface, and in deeper slots between the solutioned pinnacles." (Sowers) From a practical perspective, very soft to soft soils were considered epikarst.

Generally, the Dot Limestone underlies the western half of the site and the Poteet Limestone underlies the eastern half of the site. The Poteet Limestone exhibits more severe karst activity that the Dot Limestone. The contact between the two limestone formations generally follows a regional lineament of sinkholes. The main entrance road to the site crosses a small ridge of land between two major coalescing sinkholes along the contact between the Dot and Poteet Limestones. The ridge was referred to as a "saddle" between the two sinkholes. Figure 1 shows the existing contours around the saddle area and the adjacent sinkholes.

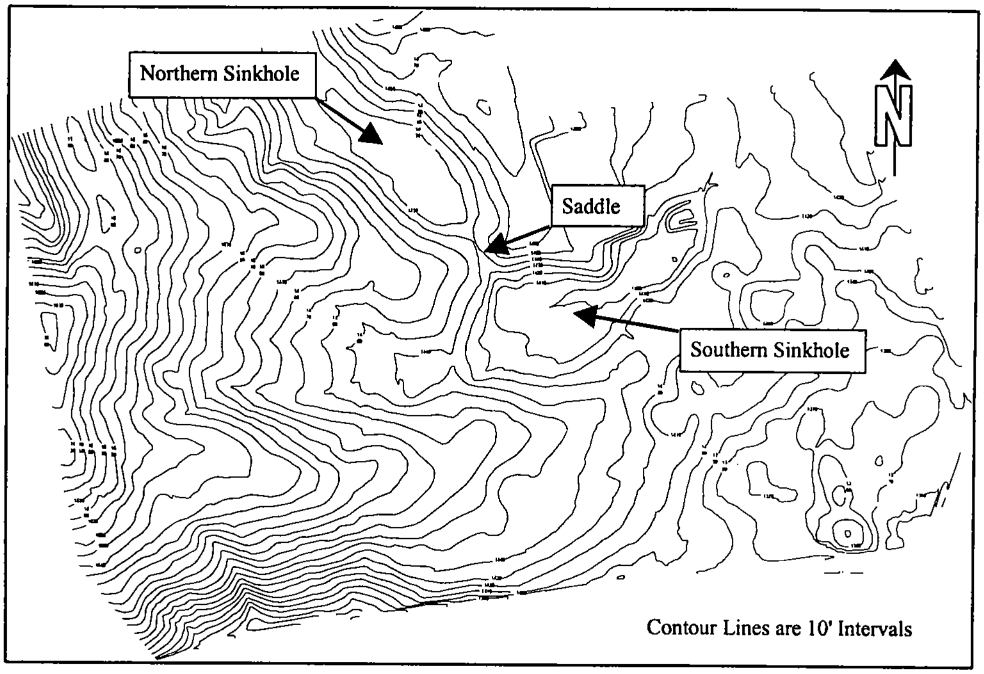

Figure 1: Site Topography

The two sinkholes are believed to be hydraulically connected. A dye study, completed in 1996 by others, indicated that the subsurface flow from the sinkhole was generally in a southeast trend. Following heavy rains, the northern sinkhole was observed to form a pond up to 3 acres in size with water up to 6 feet deep. The water in the pond drained in less than 24 hours indicating that significant subsurface drainage exists under the saddle.

SUBSURFACE EXPLORATION

The initial subsurface exploration program for the roadway across the saddle included one hollow stem auger boring with NX rock core and two air rotary borings. The hollow stem auger boring (RD1) and the western air rotary boring (G10) indicated a relatively shallow soil profile. The underlying rock was decomposed to unweathered, but no voids were detected. The results of the eastern air rotary boring (G13) indicated a deep soil profile. Furthermore, the drillers reported several voids in the soil, including when the drill rods dropped about 1.5 feet during drilling. The bottom 20 feet of the soil profile consisted of zones of very soft soil.

The depth of the ground water was observed between 10 and 15 feet above the soil/rock interface in the eastern borings. The depth of the ground water was observed between 40 and 50 feet below the soil/rock interface in the western borings. The difference in elevation of the ground water between borings RD1 and G13 was more than 40 feet in a distance of about 100 feet. The elevation of the top of rock changed by about 15 feet in a distance of about 100 feet.

Based on the significant change in the soil thickness between borings, two additional hollow stem auger borings and a geophysical survey were completed across the axis of the saddle. At a later time, three additional borings were advanced to try to quantify the strength of the epikarst. A cross-section showing the variability of the soil and rock profile is shown on Figure 2.

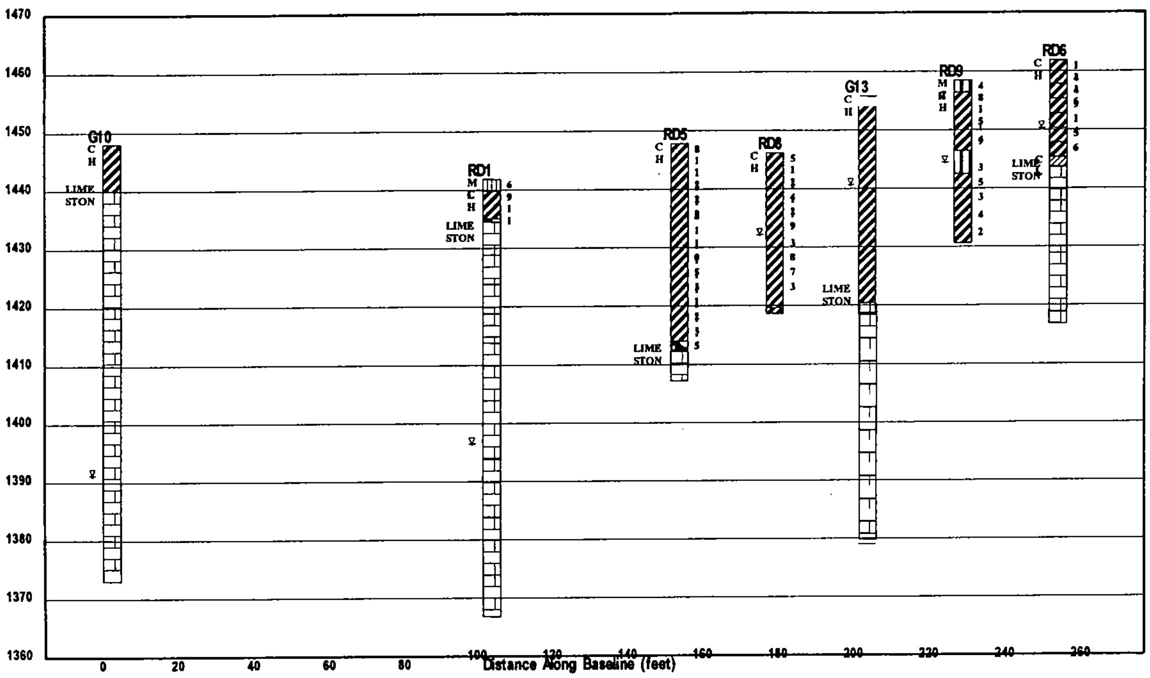

Figure 2: Cross-Section of Selected Borings

The results of the geophysical survey defined the extent of the deep, soft soils. Additional information about the geophysical survey is discussed in the paper by Daniel in these proceedings. The additional borings also indicated the same deep soil profile with varying amounts of epikarst. Several thin wall tube samples were collected for laboratory testing. Results of undrained shear strength tests ranged between 450 and 600 psf. A graphical summary of the subsurface exploration locations is shown on Figure 3.

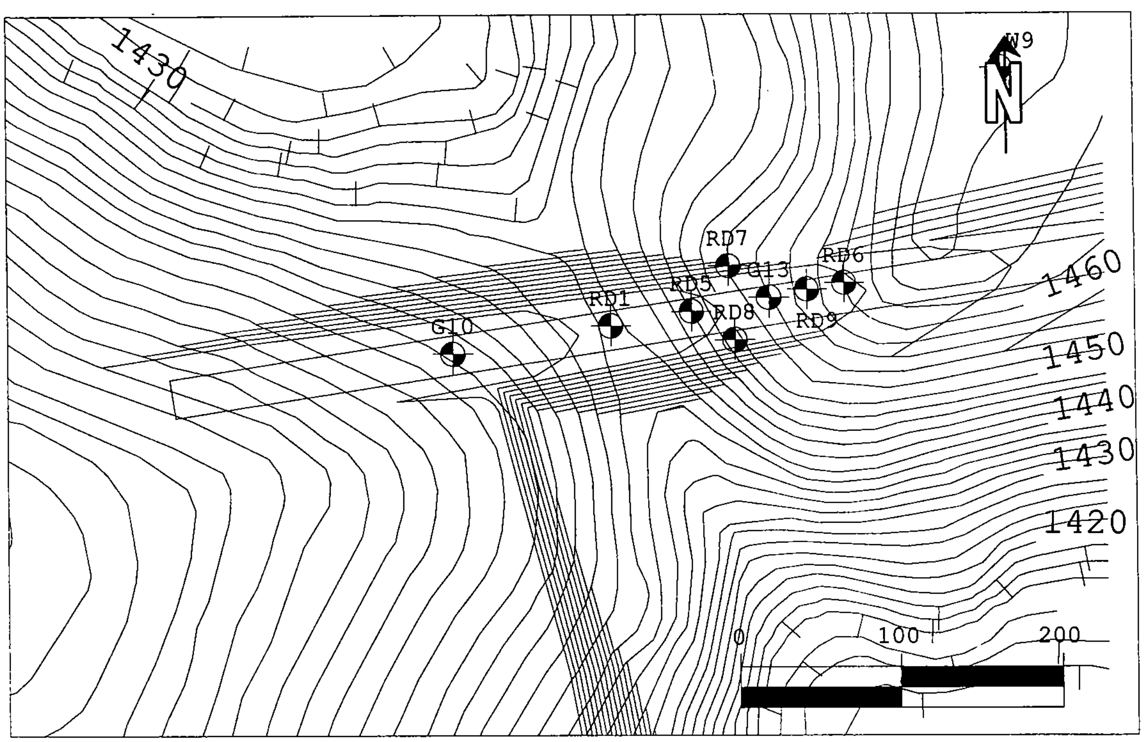

Figure 3: Boring Locations

GEOTECHNICAL CONSIDERATIONS

The proposed roadway is the only entrance into the maximum-security facility. In addition, several of the utilities for the facility will be constructed in the embankment across the saddle. The embankment was determined to be a critical structure in the development of the property. Loss of the roadway or the utilities would be unacceptable both in terms of cost and security.

The proposed construction for the roadway includes almost 25 feet of fill at the highest point. The side slopes of the roadway embankment extend toward wetlands in both of the adjacent sinkholes. Accordingly, the footprint of the roadway embankment was restricted to minimize disturbance to the wetlands.

The stability of the subgrade soils was analyzed under the proposed embankment load. Evaluation of the borings indicates that the location and strength of the epikarst varied under the proposed embankment. The stability of the embankment assuming a limited amount of epikarst with overlying stiffer clay soils resulted in a short-term factor of safety of 1.2. A slope stability evaluation assuming a more extensive epikarst stratum resulted in a short-term factor of safety below 1.0. An acceptable factor of safety for the embankment would be 1.3, based on the available data. Accordingly, the embankment could not be constructed as designed without subgrade modification.

Although the voids reported in boring G13 were not observed in any of the subsequent borings, soft soils were observed and the possible development of soil domes under the embankment was still a concern. Soil domes may form as water erodes soil particles into the voids and enlarged joints of underlying rock. Even if the subgrade soils were stabilized to allow construction of the roadway, the subsequent development of soil domes could lead to failure of the roadway embankment.

Based on the subsurface exploration, the geophysical study and the stability analyses, it was determined that the soils in the area of the saddle should be remediated or replaced prior to the construction of the road. The proposed improvement should address both short-term and long-term stability. Short-term stability will allow construction of the embankment and long-term stability will reduce the potential formation of soil domes.

CONSTRUCTION ALTERNATIVES CONSIDERED

Several alternatives were considered to remediate the epikarst in the saddle area. Cost, schedule and the geometry of the roadway embankment were major considerations when remediation alternatives were evaluated.

Stability evaluations at other locations on the site showed that the embankment could be stabilized with the construction of a berm at the toe of the embankment. The availability of on-site borrow soils made this an inexpensive solution. At the saddle, the toe berms would extend into the wetlands and this alternative was rejected.

Another possible solution was to excavate the soil to the top of rock and replace with rock fill. With this alternative, any voids or defects in the rock could be evaluated and remediated. Based on the borings advanced across the saddle area, the maximum excavation would extend up to 35 feet (El 1410). This elevation is well below the elevation of the adjacent wetlands (El 1424). Furthermore, the water level in the borings was about 20 feet above the top of rock.

In order to remove the epikarst that could be affected by the weight of the roadway embankment, the excavation would have to extend beyond the toe of the embankment and towards the wetlands. The north side of the excavation would be at a low enough elevation that water ponding in the upstream wetlands could wash out the excavation following a rain. Furthermore, the porous rock fill could result in drainage of the upstream wetlands.

Surcharging was not a viable alternative because the project was being constructed on a fast-track basis and the roadway was needed early in the project to support construction traffic. Furthermore, while this method could collapse any existing soil voids it would not address the potential for formation of soil domes.

Several other ground improvement techniques were evaluated as remediation alternatives. Stone columns were rejected since they would create a location for water to pond and could accelerate the formation of soil domes. The use of a pile and geosynthetic supported embankment was eliminated due to high costs. Following review of the relative technical merits and potential cost of the noted alternatives, ground improvement by compaction grouting was recommended. Compaction grouting could be implemented to mitigate potential for sinkhole development below the main access road across the saddle. In addition, compaction grouting would create columns of grout that would help transfer the load of the embankment fill to the bedrock below the soft soils. Therefore, compaction grouting could address concerns for short-term embankment stability as well as long-term sinkhole development.

COMPACTION GROUTING PROGRAM

Compaction grouting involves pressure injection of low slump (0- to 2-inch slump) concrete grout at high pressures to fill or collapse voids, and displace or compact soft or loose soil. Compaction grouting can also be used to fill voids in rock and seal off potential paths for water travel. At this site, compaction grouting was not extended into the bedrock as it was not intended to block the flow paths that connected the two large sinkholes on either side of the road.

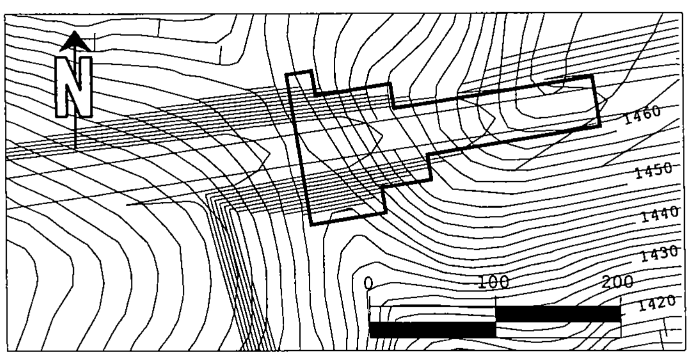

Figure 4: Footprint of Compaction Grout Area

Compaction grouting on a regularly spaced grid was designed for the saddle. The grid was located on the eastern half of the saddle area. It started at the low point on the saddle and extended 240 feet to the east. The toe of the proposed embankment defined the outer edges of the compaction grouting. The footprint of the compaction grouting is shown as Figure 4.

It is believed that the grouting would collapse existing soil voids and displace very soft soils overlying voids in rock. Due to the grouts low slump, compaction grouting forms a discrete bulb of grout local to the grout pipe instead of infiltrating into the pore space of the soil. More grout will be injected at locations where soft epikarst soils exist resulting in larger grout bulbs. Therefore the most improvement is achieved in the weakest zones. Another potential improvement resulting from the compaction grouting process is to provide a column of stiff grout to transfer load to the bedrock.

The primary grout holes were located on a 20-foot grid. The secondary grout holes were also located on a 20-foot grid, offset from the primary grout holes. Grout pipes were driven to the top of the bedrock surface. The depth that the pipes were driven showed a trough in the top of rock surface verifying the trend observed during the subsurface exploration. The approximate width of the trough is 60 to 70 feet. The location of the trough follows the trend of the large sinkholes on either side of the saddle. The ground surface elevations were not available from the construction records. Based on the original ground surface elevations the top of rock in the trough is believed to be between El 1410 to El 1420, similar to that observed in the subsurface exploration.

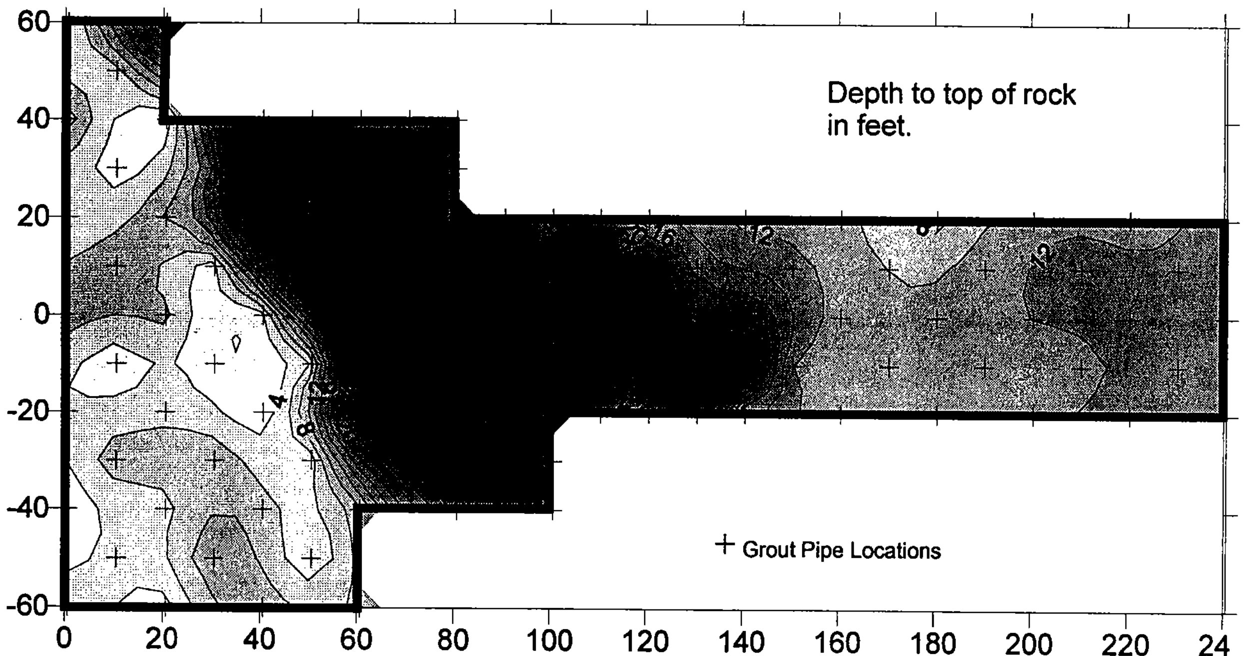

Figure 5: Depth to Top of Rock (Based on Grout Pipe Records)

Grout was injected from the soil/rock interface in one or two foot stages, working upwards to within 6 feet of the existing ground surface. The rate of grout injection was limited to reduce the increase in pore pressures in the clay soils. The specifications defined cutoff criteria for ending any particular stage of grouting and the grout hole. The termination criteria were: when grout volumes were exceeded based on injection pressure, a pressure greater than 600 psi, if the pipe was ejected from the ground, when grout was observed at the ground surface or when the ground heaved or cracked. In general, the volume criteria terminated stages in epikarst, the 600 psi pressure terminated stages in stiffer soils and ground heave or cracking was responsible for terminating a hole. One problem observed during construction was the grout mix. The grout was obtained from local ready-mix sources and contained angular sand. The grout mixture clogged the grout pipes stopping operations several times. To be effective, the grout mixture should include rounded sands and enough fines to provide a pumpable mixture.

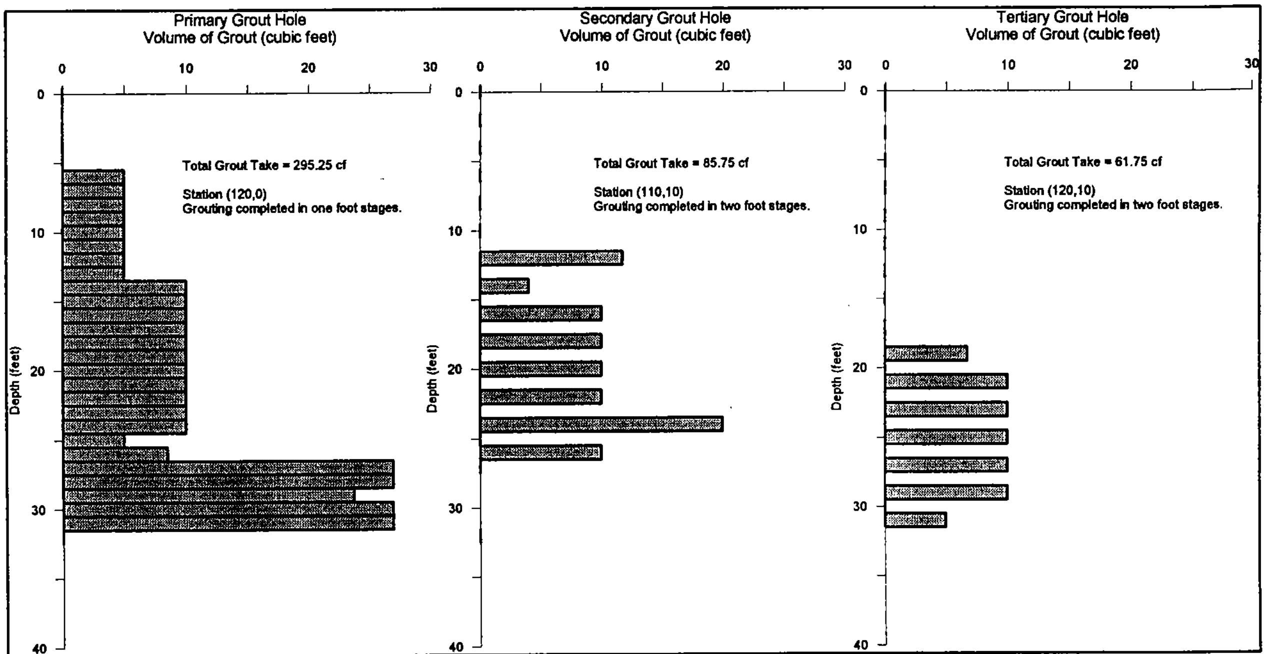

Figure 6: Grout Records for Primary, Secondary and Tertiary Grout Holes

During the primary grouting phase of the project, a distinct trend was noticed in the grout take. For planning purposes, 2 cubic feet of grout per linear foot was assumed. In general, the grout holes in the trough area showed a significant increase in the volume of grout take per linear foot of grout injection pipe. This was especially evident in the lower half of the grout hole. Three grout records are summarized in Figure 6. Each bar represents volume of grout in a single stage.

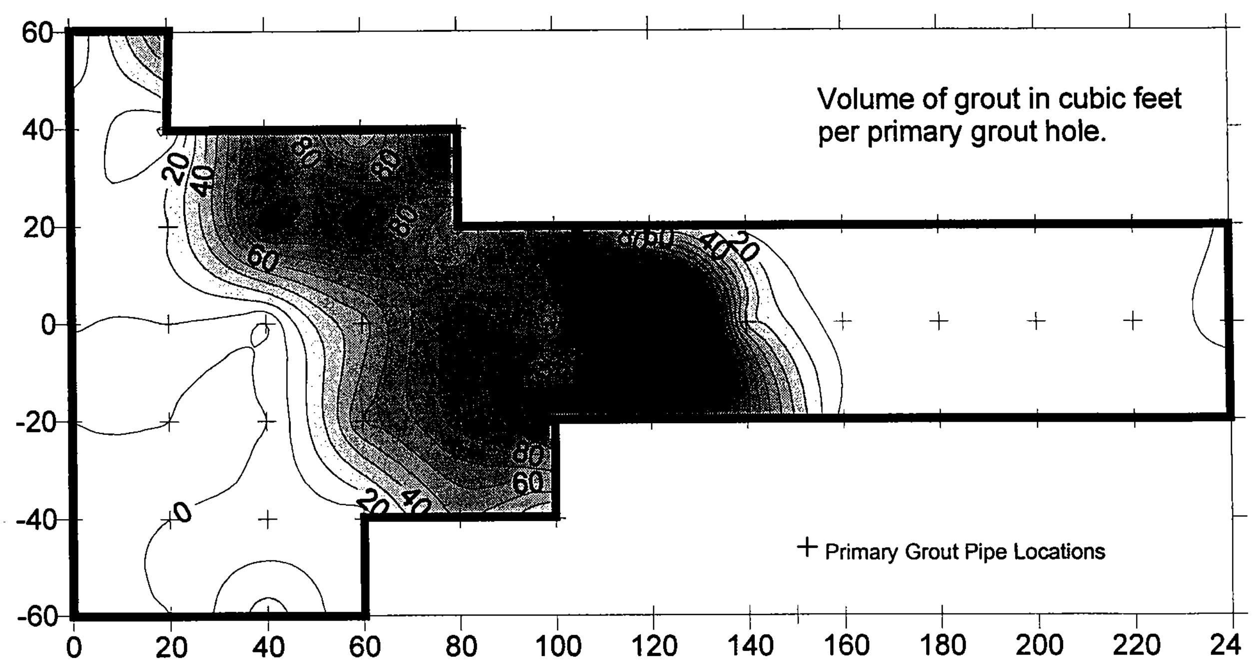

Figure 7: Volume of Grout Injected in Primary Grout Holes

Following the completion of the primary grout holes, secondary grout holes were installed with the same criteria as the primary holes. In the majority of the secondary grout holes, the grout take was significantly lower than the adjacent primary grout holes. However, the grout take in the trough was still very high in the secondary holes. Where grout takes in the secondary holes 4was large, tertiary holes were added between the primary and secondary holes.

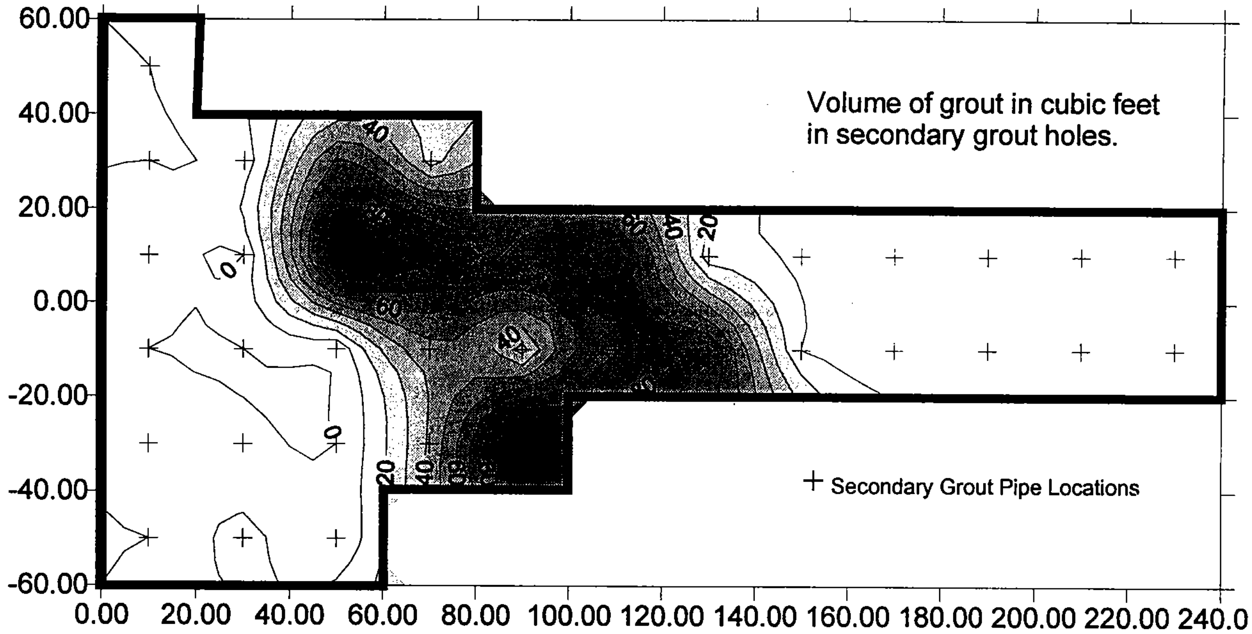

Figure 8: Volume of Grout Injected in Secondary Holes

While a significant decrease in the volume of grout was observed in the tertiary holes, the volume of grout per linear foot in the lower portions of the holes were still much larger than the grout holes located west of station 45 or east of station 150. Most of the grout holes in the tertiary phase of the project were terminated at depths of 10 to 23 feet below existing grade due to ground heave and cracking.

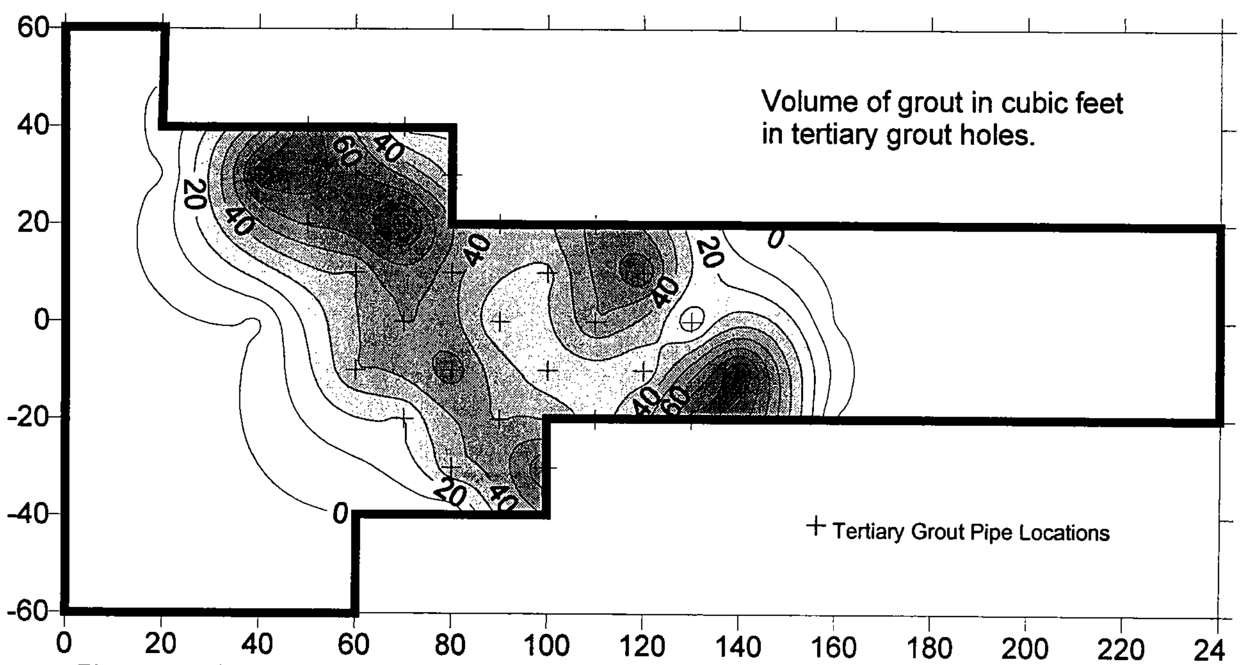

Figure 9: Volume of Grout Injected in Tertiary Holes

SUMMARY AND CONCLUSIONS

An entrance road for a maximum-security penitentiary crossed a thin ridge of land separating two large sinkholes to the north and south. The subsurface exploration and a subsequent geophysical survey indicated a deep soil profile on the eastern half of the ridge. Stability analyses indicated that the soft soils would not support the proposed embankment construction and the underlying enlarged joints in the limestone bedrock presented an unacceptable risk for development of the roadway.

After evaluating several ground improvement alternatives, a compaction grouting program was implemented. The compaction grouting was completed on a grid pattern including primary, secondary and tertiary grout holes. The compaction grout holes encountered a trough of deeper soils similar to that observed in the subsurface exploration. The trough was situated in the same linear trend as the northern and southern sinkholes and the presumed interface between the Dot and Poteet Limestone. Larger quantities of grout were injected in this area, specifically in the lower portion of each grout hole. Tertiary holes were added to the compaction grouting program in this vicinity to further improve the soil.

The compaction grouting was successfully implemented to improve both short and long term stability of the entrance road. The total grout volume and pressures observed during grouting operations indicate that the soft soils were improved. The roadway embankment has been successfully constructed and supported construction traffic without incident.

ACKNOWLEDGEMENTS

The authors wish to thank the United States Federal Bureau of Prisons for allowing us to present this information. We would also like to thank Technos, Inc. for their assistance during the project with the geophysical study.

BIBLIOGRAPHY

Daniel, Joel C., et.al, *Use of Geophysical Techniques to Evaluate Karst Features for Roadway Design*, Proceedings of the 50th Highway Geology Symposium, 1999.

Sowers, George F., *Building on Sinkholes*, ASCE Press, 1996.

Technos, Inc., *Final Report, Subsurface Karst Investigation and Characterization for Geotechnical Purposes, U.S. Penitentiary and Satellite Camp, Lee County, Virginia.* Consultant Report, 1998.

Virginia Geotechnical Services, P.C., *Geotechnical Engineering Report, Federal Bureau of Prisons - USP, FPC and CSF, Lee County, Virginia,* Consultant Report, 1998.

Virginia Geotechnical Services, P.C., *Addendum 1 - Geotechnical Engineering Report, Federal Bureau of Prisons - USP, FPC and CSF, Lee County, Virginia,* Consultant Report, 1998.

Warner, James, *Compaction Grouting - The First Thirty Years,* Proceedings on the Conference on Grouting In Geotechnical Engineering, ASCE Press, 1982.

ELECTRICAL IMAGING:
A Method for Identifying Potential Collapse and other Karst Features Near Roadways

By

Heather L. Reccelli-Snyder,
Beth. A. Stahl , Jeffrey L. Leberfinger, P.G., and Jeffrey J. Warren

Science Applications International Corporation
Middletown, Pennsylvania

Abstract

Electrical Imaging (EI) is a geophysical method developed over the past several years that provides a two or three dimensional resistivity model of the subsurface. EI can provide information about distinct subsurface boundaries and conditions, which can indicate soil or bedrock lithology variations. In particular, EI can be very effective in characterizing potential collapse features associated with sinkhole activity. Frequently, in karst systems, boreholes drilled without regard to the variability of karst geology do not intersect areas of interest, such as developing collapse features in the subsurface. Poor location of borings can result in inadequate subsurface data, and could misrepresent the subsurface system leading to additional costs for remedial design or additional investigation of developing sinkholes.

In the past, electrical resistivity techniques performed by experienced geophysicists had proven to be effective tools for characterizing the subsurface but certain limitations caused theses techniques to be utilized less over the years. These limitations were the following: 1) the technique was very labor intensive. A resistivity crew could range from three to five people. 2) Interpretation of the data was time-intensive, and methods differed as to ways of obtaining accurate subsurface representations. Recently, the development of computer-controlled multi-electrode resistivity survey systems and the development of resistivity inversion modeling software have allowed for more cost-effective EI surveys and better representation of the subsurface. With these two factors improved, electrical resistivity is starting to be employed more often. New advances in EI have allowed for three-dimensional surveys and cross-borehole surveys which will make this technique even more successful for sinkhole and fracture characterization in complex systems.

Introduction

Sinkholes are often a major development hazard in areas underlain by carbonate rocks. Road and highway subsidence, building foundation collapse, and dam leakage are a few of the problems associated with sinkholes. Structural instability associated with sinkholes can occur as a sudden collapse of the ground surface or as a less catastrophic, but recurring drainage problem. Within karst regions, either scenario can be expensive to design and implement controls for present and future structures. Frequently, borings drilled within karst regions do not intersect areas of concern in the subsurface. Misplaced borings can provide inadequate subsurface data, and could misrepresent the subsurface system leading to additional costs for remedial design or additional investigation. Rapid reconnaissance surveys using remote sensing (e.g. Aerial Photograph Evaluation) and surface geophysical techniques integrated with a boring plan are best used to aid in the proper location of test borings to identify subsurface features related to karst development.

Electrical resistivity techniques have been utilized successfully for characterizing the subsurface for many years (Roman, 1951). Certain limitations of this technique have caused resistivity to be utilized less over recent years. These limitations are: 1) The technique was very labor intensive. A resistivity crew could range from three to five people. 2) Interpretation of the data was time-intensive, and methods differed as to ways of obtaining accurate subsurface representations. These methods have limitations because they are largely based upon individual subjective interpretation.

The development of computer-controlled multi-electrode resistivity survey systems and the development of resistivity inversion modeling software (Loke and Barker, 1996) have allowed for more cost-effective resistivity surveys and better representation of the subsurface. These surveys are typically referred to as Electrical Imaging (EI) surveys. Most EI surveys are collected as two-dimensional surveys. The inversion modeling software also processes three-dimensional surveys as well. These factors allow data to be collected and processed quickly, within a few hours, and as a result EI is becoming a valuable tool in subsurface investigations.

Electrical Resistivity Methods

EI surveys are typically conducted to determine the resistivity of the subsurface. Resistivity data can be used to determine the location of variations in geologic and soil strata, soil/bedrock interface topography, bedrock fractures, faults, and voids. The method has been used effectively to delineate old waste sites and landfill boundaries and to map hydrogeologic and mineral resource boundaries.

Resistivity values are found for earth materials to cover a wide range. This variety of resistivities is what makes resistivity surveying a viable technique for many applications. Table 1 describes typical resistivities of earth materials.

Table 1: Typical Electrical Resistivities of Earth Materials

Material	Resistivity (ohmmeter)
Clay	1-60
Sand, Wet to Moist	20-200
Shale	1-500
Sandstone	150-450
Porous Limestone	100-1,000
Dense Limestone	1,000-1,000,000
Metamorphic Rocks	50-1,000,000
Igneous Rocks	100-1,000,000

Fundamental to all resistivity methods is the concept that current (I) can be impressed into the ground and the effects of this current within the ground can be measured. The effect of potential (V) or differences of potential, ratio of potential differences, or some other parameter that is directly related to these variables is the commonly measured effect of the impressed current. The principal differences among various methods of EI lie in the number and spacing of the current and potential electrodes, the variable quantity determined, and the manner of presenting the results.

In application, a series of measurements is made between a variety of current electrode pairs and potential electrode pairs. In general, as the distance between the two electrodes increase, the apparent resistivity p_a is measured at greater depths and across increasing volumes of ground as shown in Figure 1.

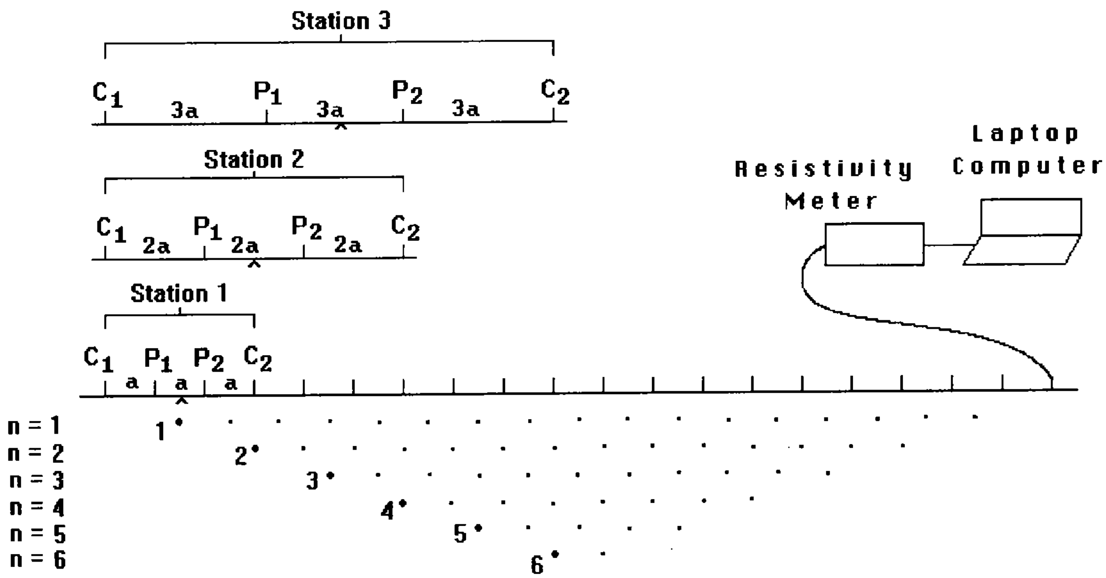

Figure 1 – Example of data measurement locations for 2D surveys (from AGI, Inc, 1999).

EI Data Collection

For EI data collection, SAIC uses a Sting/Swift multielectrode system manufactured by Advanced Geosciences, Inc. (AGI) of Austin, Texas. The EI equipment is composed of three primary components: 1) the Sting R1 resistivity meter with data storage capability; 2) the Swift automatic multielectrode switching system, which is an accessory for the Sting; and 3) the Sting/Swift cables which contain fixed cylindrical stainless steel switches that attach to stainless steel electrodes placed into the ground.

2D Data Collection

The EI system automatically energizes different electrodes to measure apparent resistivities at new horizontal locations and depths. Commonly, a series of 28 to 112 stainless steel electrodes are driven 6 to 12 inches into the ground at a fixed interval to establish earth contact. At most sites, the interval is established to be from 1 to 10 meters. Although the system can be programmed to use any electrode arrangement, the data are collected typically in a dipole-dipole electrode arrangement. The dipole-dipole arrangement provides increased resolution over other electrode array configurations. In the dipole-dipole arrangement, two electrodes are used to provide current to the subsurface, while two other electrodes some distance away are used to measure the voltage. The current and voltage electrodes do not overlay each other as in other electrode arrangements.

During preparation for data collection, the operator programs the Sting for the chosen number of current pairs (in electrode spacing measurements) to energize and the maximum separation (in electrode spacing measurements) to measure the potentials. These two numbers determine the total number of measurement to be collected along the electrode spread and the total depth of investigation. The Sting digitally records this information for use in data processing and quality assurance. The 2-D model assumes that all structures are infinitely long and perpendicular to the EI survey line. Because not all structures can be characterized in this manner and can be considerably more complex, 3-D surveys can be conducted.

3D Data Collection

As stated above, to compensate for subsurface complexity 3-D data can be collected. The amount of current, potential, and the configuration of electrodes are analyzed to yield an apparent resistivity value between electrodes. The electrodes for such a survey are arranged in a rectangular grid (Figure 2). The EI system automatically energizes different electrodes to measure apparent resistivities at new horizontal locations and depths. The EI system can be used to determine a three-dimensional (3-D) resistivity model for the subsurface using the data obtained from a 3-D electrical imaging E-SCAN type of survey (Li and Oldenburg 1992).

As with a 2-D survey, the operator programs the Sting for the chosen number of current pairs (in electrode spacing measurements) to energize and the maximum separation (in electrode spacing measurements) to measure the potentials. These two numbers determine the total number of measurement to be collected along the electrode spread and the total depth of investigation. The Sting digitally records this information for use in data processing and quality assurance.

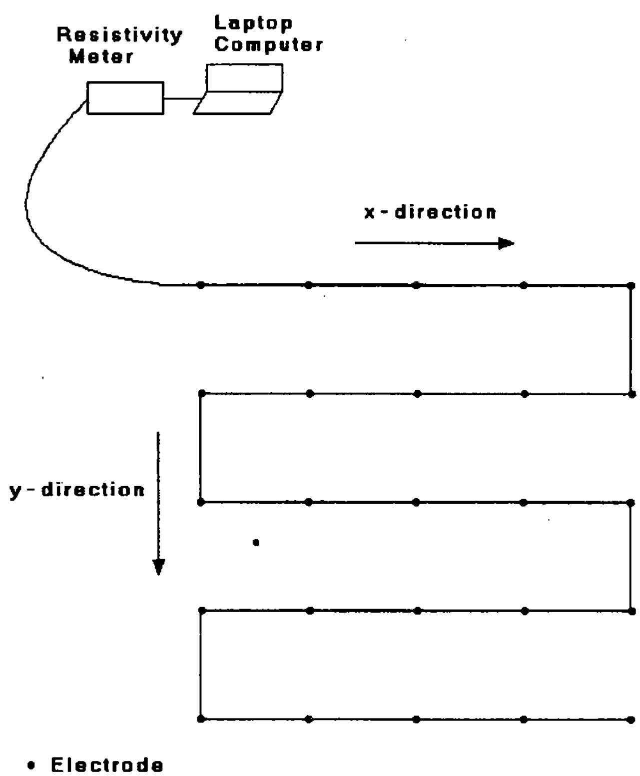

Figure 2. A schematic diagram for one possible layout for a 3D survey (Loke, 1997).

The most commonly used electrode configuration for 3D surveys is the pole-pole array. As presented in Figure 3, each electrode is used as a current electrode and the potentials at all the other electrodes are measured It can be very time-consuming to make such a large number of measurements with typical single-channel resistivity meters commonly used for 2D surveys. For large survey grids, it is common to limit the maximum spacing used in the measurements to about 8 to 10 times the minimum electrode spacing. To map large areas with a limited number of electrodes in a multi-electrode resistivity meter system, the roll-along technique can be used (Dahlin and Bernstone, 1997) a).

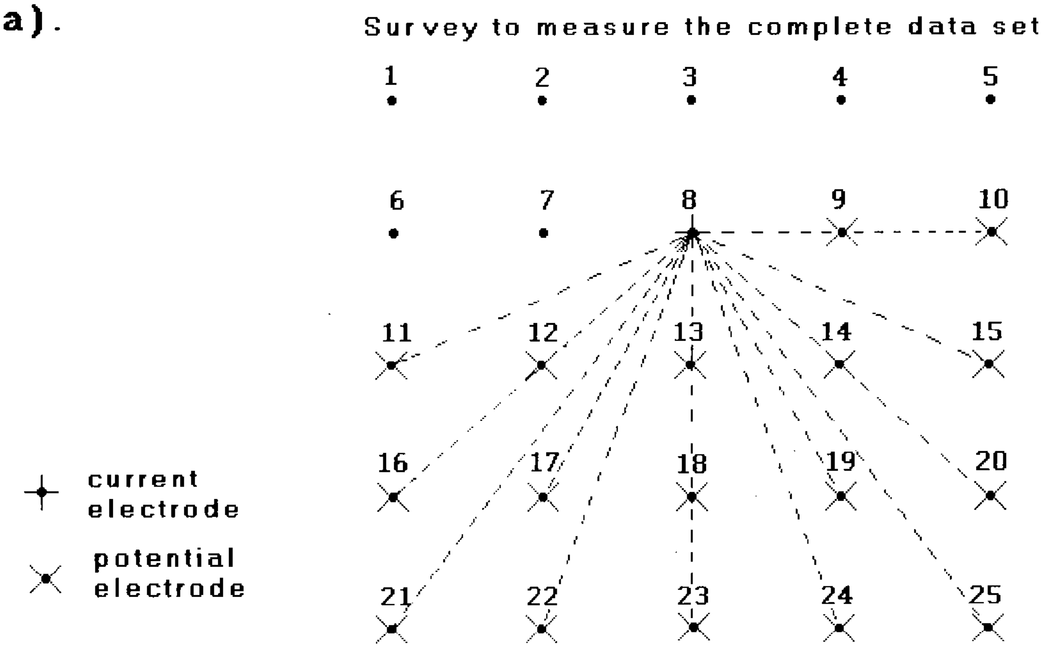

Figure 3. The location of potential electrodes corresponding to a single current electrode in the arrangement used by a survey to measure the complete data set (Loke, 1997).

Data Modeling and Interpretation

The apparent resistivity p_a, as measured by the EI system, is the product of a large area of the subsurface responding to the impressed current. Interpretation of apparent resistivity data collected in the field without reduction provides a qualitative product very similar to many electromagnetic (EM) methods. Because the earth is not homogeneous, it is useful to model the resistivities at discrete locations in order to make a more quantified interpretation. Inverse modeling of the data is performed using RES2DINV/RES3DINV™ (Loke, 1997) to produce a three-dimensional resistivity model based on the apparent resistivity data.

Final data processing involves the generation of color-enhanced contour maps of the data using a two-dimensional mapping program. EI resistivity models are presented in cross-section or 3D model blocks, with inline distance shown along the horizontal axis, depths, or elevation along the vertical axis. The geoelectrical model presents the electrical stratigraphy (electrostratigraphy) of the subsurface.

Following the data collection and inversion modeling, the EI electrostratigraphy information is used to interpret the potential gross stratigraphy of the traverses. In general, dry materials have higher resistivity than similar wet materials because moisture increases their ability to conduct electricity. This resistivity change, if indicated in the observed electrostratigraphy, can represent water table depths. Beneath the water table, silt, clay-free sands, and gravels will have a much higher resistivity than silts or clays under similar moisture condition because fine-grained materials are better conductors. In the bedrock, competent rock will have a high resistivity. Saturated fractured or weathered rock would show a much lower resistivity than the competent rock. Very high resistivities can indicate air filled voids.

The identified electric boundaries separating layers of different resistivities may or may not coincide with boundaries separating layers of different lithologic composition. These differences may result from the gradational presentation of the electrostratigraphy. Therefore, the electrostratigraphy can vary from the geologic stratigraphy, and caution should be exercised when reviewing and applying the electrical profiles.

2D EI Survey Case History

At a petroleum tank farm in Mechanicsburg, Pennsylvania, the Above Ground Storage tanks (ASTs) sit on solution-prone limestone bedrock. An investigation was performed to evaluate the location and distribution of potential collapse features near the ASTs and to define migration pathways of hydrocarbon in the soil and ground water for remedial design. As such, the location and trend of bedrock fractures were critical to placing monitoring wells where they would accurately characterize groundwater flow for designing a remedial approach.

Several geophysical surveys had been performed on the site with ground penetrating radar, gravity, terrain conductivity, and seismic refraction, but all had prove ineffective in producing subsurface models consistent with boring and well information. EI was performed to identify targets for a confirmatory boring and well program. The specific EI investigation included measurement and analysis of four parallel traverses within the tank farm, along roadways, and parking lots. The four profiles resulted in approximately 685 linear m of surveyed section to a depth of approximately 15 m.

The electrostratigraphy model from processing Traverse 2 is presented on Figure 4. Areas of high resistivity (greater than 300 ohm meters) were interpreted as competent limestone. Areas of moderate resistivity (200 to 300 ohmmeters) were interpreted as less competent (partially fractured and/or dissolved) limestone. Zones with lower resistivity (between 50-200 ohm meters) were interpreted as areas of soil, fractured limestone, and/or dissolved limestone. However, these areas may also be interpreted as soil where low resistivities occur near the ground surface. Finally, areas where resistivity was less than 50 ohmmeters were interpreted to represent potential soils, very fractured rock, or mud filled voids.

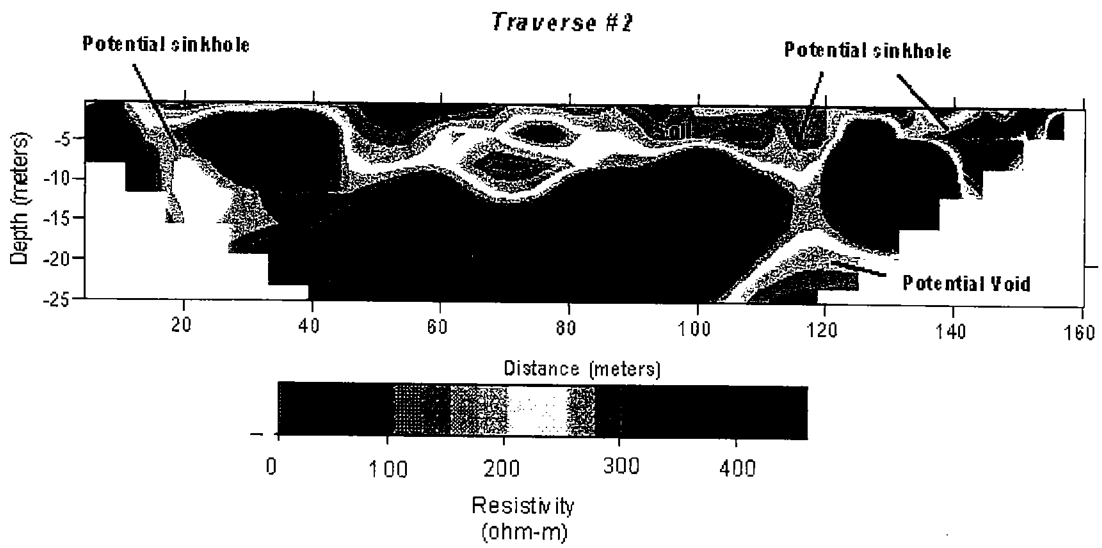

Figure 4 – 2-D Electrical Imaging model for Traverse 2.

Data evaluation at Traverse 2 suggested shallow bedrock from 0 to 40 meters (m) inline distance. Resistivity readings suggest that approximately 2 to 7 m of soil cover is present from 40 to 160 m inline distance. A zone of competent limestone was interpreted along the traverse from 40 to 100 meters at depth. Two zones of fractured limestone were suggested at inline distances of 20 meters and 120 meters. Within the feature at an inline distance of 120 m, a low resistivity zone was measured at 15 m below grade level (bgl). This zone could be interpreted as very fractured limestone and/or a mud-filled void in the bedrock. A shallow high resistivity zone underlain by a low resistivity zone was observed from an inline distance of 60 to 80 meters. This feature was interpreted as isolated blocks of competent limestone underlain by very weathered rock or soil.

Numerous direct push soundings were obtained to confirm bedrock depth and several rock borings/wells were installed to verify deeper features. There appeared to be a good correlation between the confirmatory intrusive program, air photographs, and the interpreted EI sections.

3D EI Survey Case History

A three dimensional survey was completed over Indian Echo Caverns in Hummelstown, PA (Figure 5) to identify the cavern morphology. The cavern is contained within the Ordivician Epler Formation, an interbedded limestone and dolomite. The cave maps indicate that the cavern entrance is along the Swatara Creek and the cave gets progressively wider with distance from the entrance (Figure 5). Near the Wilson Room, the cave narrows and speleothems are prevalent. Further from the entrance, greater than 100 feet, the cave widens again and breakdown and ceiling height increases. The 3-D grid overlies this described area and is shown on Figure 5.

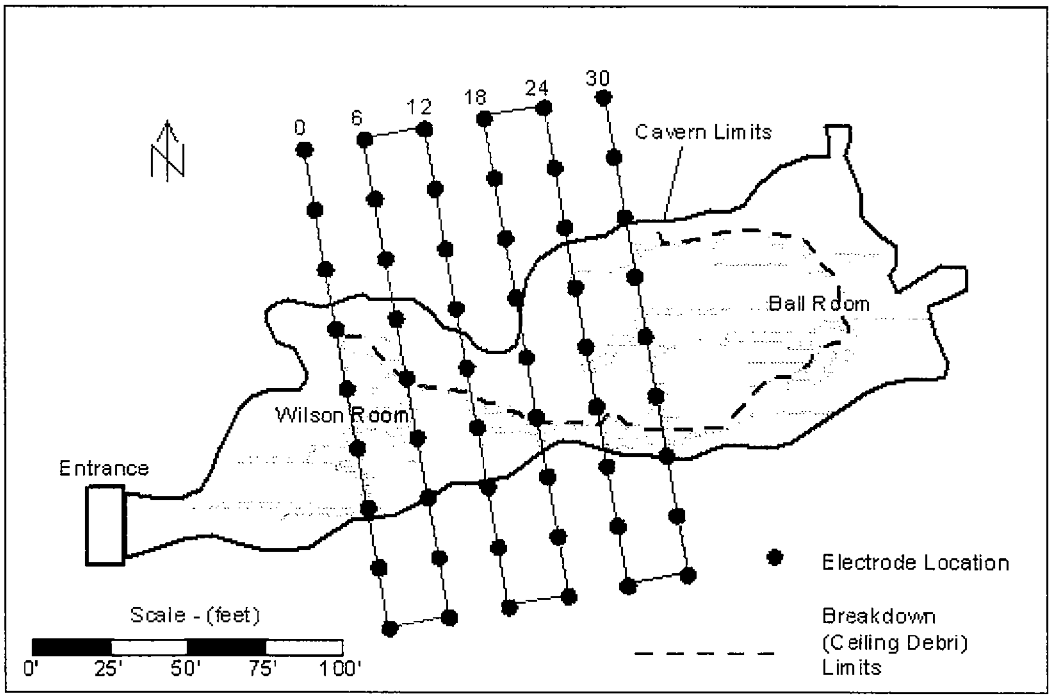

Figure 5- 3-D Electrical Imaging survey grid over Indian Echo Caverns.

The rectangular survey grid was configured so that maximum depth could be attained from a limited number of electrodes with a six meter electrode spacing. The grid was 48 meters by 30 meters, or 9 electrodes by six electrodes, and allowed for a maximum depth of 40 meters to be collected. The pole-pole method was used for this survey, which placed the B and N electrodes over 400 meters from the grid. Data was collected for approximately 6 hours.

Inversion modeling software, RES3DINV™ (Loke, 1997), was utilized to convert the apparent resistivities collected to modeled resistivity. The results are displayed in Figure 6 and are presented as vertical 2-D slices along the following locations of the model: y=0-6 meters, y=6-12 meters, etc.

The results presented in Figure 6 indicate a high resistivity zone directly beneath the survey grid. The high resistivity zone (greater than 18,000 ohm-meters), as shown on the profiles, changes size and shape and corresponds to distinct changes within the cavern. This zone appears smaller within the middle of the survey grid, profile y=12-18 meters and likely corresponds to the narrower cave passageway and the presence of numerous speleothems. The high resistivity zone widens and becomes larger in the last profile and corresponds to the widening of the cavern at the beginning of the ballroom. The smaller size of the high resistivity zone can also be related to the increase of breakdown material that occurs from the end of the Wilson Room to the Ballroom because of decreased void space.

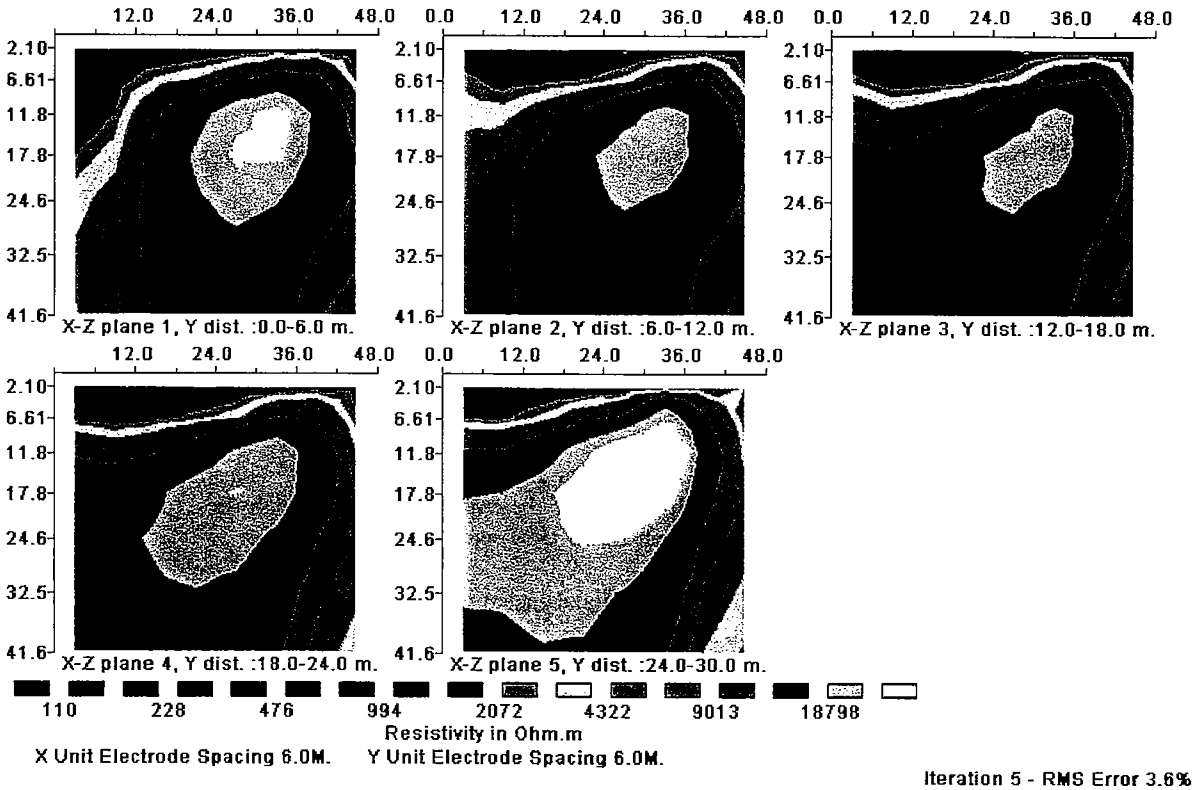

Figure 6- 3-D Electrical Imaging model showing vertical slices in the X-Z plane.

The resistivity profiles were examined closely to determine if changes in the overburden were present specifically in those areas that overly breakdown and rock debris. By using the EI system significant overburden changes, such as increased fracturing and water movement, should be noticeable on the resistivity profiles. This kind of information can provide some information into the potential weaknesses within the void ceiling and possibly future sinkhole development. Although the grid configuration provided a resolution that was not ideal for this type of analysis, significant changes within the overburden were not observed near the breakdown areas. These preliminary results suggest that the changes within the cavern ceiling are likely due to bedrock bedding changes and not increased fracturing.

Conclusions

Electrical Imaging techniques can be utilized to provide a cost effective characterization of the subsurface in karst environments. The EI method has been successful in identifying features of concern, in particular sinkholes, fractures, and voids. Both 2-D and 3-D surveys can be conducted along roadways, parking lots, developments, and airport runways to identify and monitor problematic areas that may cause structural damage. Furthermore, new developments in the EI system can allow for increased resolution with depth.

These new developments, such as cross-hole surveys can better characterize the subsurface and problem areas. New downhole cables have recently been developed to allow for downhole data collection. These techniques will allow for the use of EI for a much wider range of applications to obtain subsurface information.

Bibliography

Loke, M.H. and Barker R.D., 1996, *Rapid Least-squares inversion of apparent resistivity pseudosections by a quasi-Newton Method,* Geophysical Prospecting, V.44, p.131-152.

Loke, M.H., 1997, RES3DINV ver. 2.0 for Windows 3.1, 95, and NT, Advanced Geosciences, Inc., pp. 66.

Loke, M.H., 1997, RES2DINV ver. 3.3 for Windows 3.1, 95, and NT, Advanced Geosciences, Inc., pp. 66.

Roman, Irwin, 1951, *Resistivity Reconnaissance in American Society of Testing and Materials*, Symposium on Surface and subsurface reconnaissance: American Society of Testing Materials Special Technical Publication 122, p. 171-220.

Van Nostrand, R.G. and Cook, K.L., 1966, *Interpretation of Resistivity Data,* Geological Survey Professional Paper 499.

Dahlin, T. and Bernstone, C., 1997, A roll-along technique for 3D resistivity data acquisition with multi-electrode arrays, Procs. SAGEEP'97 (Symposium on the Application of Geophysics to Engineering and Environmental Problems), Reno, Nevada, March 23-26 1997, vol 2, 927-935.

Griffiths D.H. and Barker R.D. 1993, Two-dimensional resistivity imaging and modeling in areas of complex geology. Journal of Applied Geophysics, 29, 211-226.

Li Y. and Oldenburg D.W. 1992, Approximate inverse mappings in DC resistivity problems. Geophysical Journal International, 109, 343-362.

Loke M.H. and Barker R.D.,1996, Practical techniques for 3D resistivity surveys and data inversion. Geophysical Prospecting, 44, 499-523.

RESISTIVITY IMAGING: GETTING THE BIG PICTURE IN KARST

Eric Rehwoldt, P.E., P.G., Schnabel Engineering Assoc., Bethesda, MD, 20817, U.S.A.
Mark H. Dunscomb, P.G., Schnabel Engineering Assoc., West Chester, PA, 19380, U.S.A.
Gordon M. Matheson, Ph.D., P.E., P.G., Schnabel Engineering Assoc., Bethesda, MD, 20817, U.S.A.

ABSTRACT

The two-dimensional resistivity imaging method is an effective geophysical tool for evaluation of complex subsurface geologic conditions in karst terrain. The images of the subsurface provided by this method may be used to supplement existing boring data, extrapolate subsurface conditions into areas where no borings have been performed, or to characterize the subsurface non-intrusively on sensitive sites where test borings or wells are not feasible. The resistivity imaging method takes advantage of contrasting material electrical properties to map zones of anomalously high or low resistivity that may be related to potential targets of interest in the karst subsurface. This technique has very good resolving capabilities in karst to image geologic features such as pinnacled bedrock surfaces, "overhanging" rock ledges, fracture zones, and voids (open, or clay and/or water-filled) within the rock mass and within the soil overburden.

The resistivity imaging method uses an automatic, multi-electrode switching system to pass electric current into the ground and record the resulting voltage along a linear array of electrodes coupled to the ground at a constant spacing. A computer-guided resistivity meter automatically takes the measurements along the electrode array until all possible combinations of electrodes within given parameters are used. Where site conditions allow, the electrode array can be advanced along the ground in a line by "rolling along" the array and extending the subsurface resistivity profile. Following collection of raw, apparent resistivity data in the field, the data is processed using an inversion modeling algorithm to determine the estimated distribution of true earth resistivity and the location and extent of subsurface targets.

The depth of typical resistivity imaging data for engineering applications can extend to over 100 feet. However, resolution of subsurface targets decreases as the depth of the investigation increases. Effective interpretations of subsurface conditions can be made based on existing geologic and ground water data and aerial photography to put together the "big picture" of the karst subsurface. New advances in this technique in the future are expected to include the capability of faster field data collection methods and performing cost-effective, three-dimensional subsurface resistivity models.

INTRODUCTION

Characterization and mapping of complex subsurface conditions in karst terrain using surface geophysical techniques has been implemented for many years to estimate conditions beneath the ground for engineering and environmental applications. Typically, geophysics is used to help select locations for more invasive investigative techniques such as drilling, or to supplement existing information on subsurface conditions from drilling data and observations of surface features such as sinkholes, springs, fracture trends and lineaments. Features commonly associated with karst geologies that are the target of geophysical investigations include depth to bedrock, pinnacled bedrock profile conditions, ledge rock conditions, location and size of voids or cavities in soil overburden and rock, saturated "enhanced weathered zones", and the location and size of dry or water-bearing bedrock fracture systems (i.e., joints or faults) and solution pathways.

Relatively fast, two-dimensional, electrical resistivity tomography (or profiling or imaging) applications have been very successful in geologic terrain, such as karst, where other geophysical methods, including ground penetrating radar (GPR), electromagnetics and seismic methods, have had limited success. The resistivity imaging method enables mapping of relatively complex subsurface conditions in greater detail and depth than what could be reasonably assessed using more traditional geophysical techniques. A continuous image of the subsurface resistivity conditions is provided, reducing the number of borings or wells that may otherwise be required to characterize subsurface conditions. The techniques can serve to minimize potentially costly unknowns, particularly in karst, that may be located between borings or undetected by other geophysical investigation methods. The method can also serve to characterize the subsurface non-intrusively on sensitive sites where test borings or wells are not feasible.

FIELD DATA COLLECTION

The resistivity geophysical method has been used in exploration for about a century. One-dimensional resistivity sounding methods have traditionally used four metal stakes (electrodes) which are driven about a foot into the ground. A resistance measurement is obtained by passing an electrical current between a pair of current and potential electrodes (see Figure 1 on following page) and then the electrodes are moved to gain data at different depths or in different locations. Field data collection is often slow due to the need to maneuver long electrical cables associated with resistivity data collection through wooded or hilly terrain. With the advent of sophisticated, accurate, and relatively easy-to-handle EM instruments in the 1960's and 1970's, the resistivity technique lost popularity to faster EM methods.

Recently, computers have made it economically possible to obtain and manipulate large, detailed resistivity data sets. Now, many electrodes (generally 20 to 150) can be driven into the ground at a constant spacing along a line. A computer guided resistivity meter can automatically take measurements along the "array" of electrodes using four at a time until all the possible combinations of electrodes within given parameters are used. Where the site constraints allow, the electrode array can be advanced along the ground in a line by "rolling along" the array (AGI, 1997). This is done when all the measurements in the original array are completed and the data set is extended along the profile line by "leap-frogging" the beginning portion of the array to the end of the array. When all possible measurements have been taken using the new arrangement, the beginning portion of that array is again leap-frogged to the end. In this way, measurements may be obtained indefinitely without leaving gaps in the data. These techniques quickly provide resistivity information with depth and distance along the ground surface, hence two-dimensional resistivity.

Inversion modeling of the resulting data set is completed using a finite difference or finite element subroutine that provides an approximation of the true earth resistivity distribution. Anomalies identified within the modeled subsurface image may then be used to help identify voids, rock ledges, bedrock fractures and thickness of soil overburden in karst terrain. Due to the advantages stated above related to the technique, the resistivity method has begun to regain its popularity, especially in the near surface engineering and environmental geophysics industry, and shows great promise for further expansion.

ANALYSIS PROCEDURE

As previously stated, the resistivity technique uses four electrodes at a time. One pair of electrodes is used to direct electricity into the subsurface. The second pair of electrodes is used to measure the potential drop (voltage) in the earth. The resistance of the ground circuit is calculated using Ohm's Law (Resistance = Voltage ÷ Current). Next, the resistivity is calculated using the electrode geometry and the resistance. Resistivity is a measurement of resistance normalized for distances through the conducting circuit (i.e., the subsurface). The units of resistivity are therefore ohm-length (typically ohm-meters). In general, the farther apart the electrodes are placed, the deeper the electricity flows through the subsurface. Therefore, resistivity depth sounding can be conducted by obtaining measurements at successively greater electrode separations. However, the resistivity measurements are influenced by the specific method of obtaining them, and the positions of the four electrodes with respect to each other (i.e., the electrode array geometry.) Empirical curves have been developed for specific geologic situations and may be consulted in an effort to determine the actual distribution of resistivity within the subsurface. Numerical models have been developed to solve this problem. This is sometimes called an "inverse" problem. Instead of knowing the characteristics of an object and calculating its resistivity, we know the resistivity and are trying to determine the characteristics (i.e., shape, depth and true resistivity) of the object in the subsurface.

The most commonly used computer modeling procedures for resistivity imaging are based on the approach as described by M. H. Loke and R. D. Barker (1995). The application of the procedure relies on use of finite-difference or finite element solution methods to calculate the average earth resistance for an array of rectangular subsurface cells. The procedure develops a model of the subsurface conditions based on the measured resistivity and then calculates a resistivity profile based on the modeled subsurface. If the modeled subsurface resistivity is close to matching the resistivity profile measured in the field, the resistivity profile calculated from the model is assumed similar to the measured profile. The measured resistivity and calculated resistivity are compared by means of a root mean square (RMS) error. If the RMS error is high, the program then modifies the model and iterates through the same process again to minimize the RMS error. This process is continued until the model converges to a relatively stable RMS error value, or until a specified number of iterations are completed. Most models converge within three to seven iterations. The modeled data can then be exported in an ASCII data format for contouring using standard graphical contouring software to create the final modeled resistivity cross sections. It is important to note that the resulting modeled resistivity profile is theoretically based, and as such does not provide a unique solution to the actual subsurface conditions. Therefore, the model results should be verified by physical field truthing such as drilling. Based on our experience applying this method in karst, and as illustrated in the examples that follow, the interpreted model results have closely matched the actual subsurface conditions.

RESISTIVITY ARRAY CONFIGURATIONS

Several different electrode configurations are commonly used to collect resistivity data. These configurations include dipole-dipole, Schlumberger (or modified Wenner), Wenner, pole-pole, pole-dipole, and square arrays in general order of popularity. Each of these array types can be modeled with the exception of the square array.

Figure 1 presents a typical dipole-dipole set up for resistivity electrodes. The dipole-dipole array is most popular because it generally provides the highest precision, provides a reasonable depth of investigation [about 18% of the maximum allowable electrode separation (Roy and Apparao, 1971) depending upon the measured subsurface resistivity values (Edwards, 1977)], and has the greatest sensitivity to vertical resistivity boundaries (Loke, 1998) as are commonly found in karst terrain at pinnacle interfaces. For the field setup for the dipole-dipole array, the distance between the two current electrodes and the two potential electrodes is kept the same and is called "a". The two sets of electrodes are separated from each other and the distance between the two sets of electrodes is typically a multiple ("n") of "a". In accordance with standard convention, the two current electrodes are indicated as "A" and "B", and the potential electrodes as "M" and "N".

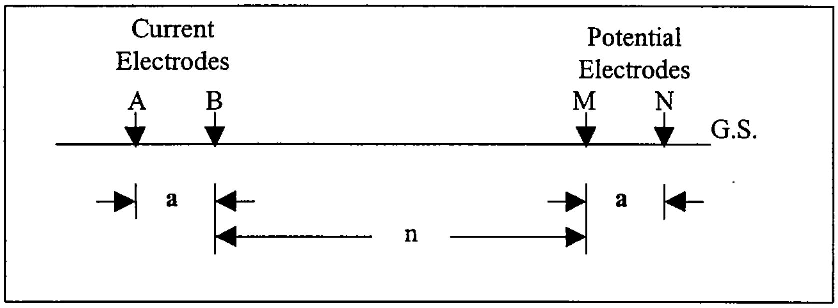

Figure 1: Typical four-electrode dipole-dipole array.

One drawback of the dipole-dipole array, is that it does not provide a very high signal for measurement and therefore can produce somewhat noisy data. Other array geometries can provide a better signal to noise ratio but do not have quite the resolving power as the dipole-dipole array, especially at depth. For Example, the Schlumberger array is not as sensitive to vertical resistivity boundaries as the dipole-dipole array but is more sensitive to horizontal boundaries. The Wenner array is most sensitive to horizontal resistivity boundaries, but is much less sensitive to vertical boundaries than either the Schlumberger or dipole-dipole arrays. The Wenner array provides good average resistivity measurements with depth, but does not resolve specific subsurface features well. As such, the Wenner array is most often used in obtaining information for purposes such as grounding design. The pole-pole and pole-dipole arrays provide the greatest depth of exploration (about 35% of the maximum allowable electrode spacing depending upon the subsurface conditions) but also provides the worst resolution of the common array configurations. The square array is sometimes used where there is very high subsurface resistivity anisotropy (Tsokas, et al., 1997).

DATA INTERPRETATION

Data interpretation of two-dimensional resistivity information is done by the geophysicist through manipulation of the measured data by inverse modeling, comparison of the modeled results to the measured data, error estimate analyses, and consideration of potential sources of cultural or natural noise. Modeled results are calibrated by comparing observed anomalies with physical data such as mapped sinkholes, rock outcrops, and boring data. However, there are some specific points to consider and general resistivity anomaly patterns to look for to aid in understanding the data.

In order to understand the two-dimensional resistivity profiles, it is important to understand how electricity is conducted through the subsurface. Most earth materials are either good insulators or dielectrics. That is to say, in general, they do not conduct electricity very well. Rather, electricity is conducted through interstitial water by ionic transport. Rock typically has a significantly higher resistivity than soil because it has a much smaller primary porosity with fewer interconnected pore spaces. Earth materials, such as clays, that tend to hold more moisture and have a higher concentration of available ions generally conduct electricity better and, therefore, exhibit lower resistivity values. The conditions in carbonate geologies favor the use of two-dimensional resistivity methods because of the typically high contrast in resistivity values between carbonate rock and the typically moist, clayey residual soil overlying it, or karstic features such as voids or very moist deep enhanced weathered zones.

Before reviewing specific resistivity values in a profile, it is important to consider that resolution of resistivity data decreases with depth. This is because the concentration of measured data points decreases with depth as a function of the electrode spacing, type of geometric array used, and the signal to noise ratio. Thus, it is possible that potentially significant features may not be resolved in the resistivity profile, especially as observed near the bottom of the profile. In addition, edge effects at the margins of the model should be considered. Edge effects occur where the finite elements or finite difference blocks at the edges of the model only have data on one side and exhibit anomalously high or low resistivity values that are not indicative of the true subsurface condition.

In karst terrain, our experience suggests that resistivity values of between about 150 to 600 ohm-meters generally delineate the bedrock surface. Because of the generally high contrasts in resistivities among earth material in karst terrain, we have found that contouring the data using logarithmic contours works well. This range of resistance values that define the rock surface can be influenced by the thickness of the enhanced weathered zone overlying the rock, the condition of the bedrock, and the thickness of a saprolitic rock zone, if present. This is especially true where pinnacled rock is highly jointed.

Voids or solution cavities in carbonate bedrock are generally found to be of two types. The two types include those that are air-filled and empty, and those that are filled with residual soil or water. Isolated zones of anomalously low resistivity measurements within the bedrock mass may indicate a clay-filled void; whereas very high anomalies in the bedrock mass (10,000 to 15,000 ohm-meters or more) may indicate an air-filled void, especially if the observed anomaly lies at or near the bedrock interface. We have observed that these isolated, very high resistivity areas, at or just above the bedrock interface, often correlate with air-filled voids where soil has raveled into a seam or fracture in the bedrock. However, carbonate bedrock tends to exhibit relatively high resistivity values. Therefore, isolated high resistivity anomalies deeper within the rock zone may also indicate very low porosity, unfractured bedrock.

In addition to subsurface karst features such as voids and pinnacled rock conditions, dry or water-bearing bedrock fractures may also be identified by resistivity imaging methods. Narrow zones of lower resistivity within the bedrock mass very often indicate clay- or water-filled fractures or faults.

EXAMPLE RESULTS

To illustrate the results of two-dimensional resistivity profile models in karst terrain and their interpretations, examples of karst features identified at four separate sites are presented below. Dipole-dipole electrode arrays were used at each site to maximize penetration depth while maintaining resolution of vertical features. Electrode spacings range from 2 to 5 meters (about 6.5 to 16.4 ft) depending upon the site conditions, anticipated depth to rock, and resolution desired for specific subsurface targets (e.g., fractures and voids).

Bedrock Surface and Fault, Frederick County, Maryland

The resistivity survey conducted at this site was performed at the edge of the paved shoulder of a State highway north of Frederick, Maryland. The highway traverses a line of developing sinkholes that follow regional bedrock structure. The fault identified in the resistivity profile shown in Figure 2 was traced crossing the highway at this location by aerial photography, and was observed on-strike within a nearby quarry highwall. Additionally, EM data obtained over the profile confirmed the presence of a deep, near vertical, fault-like conductive sheet at the same location.

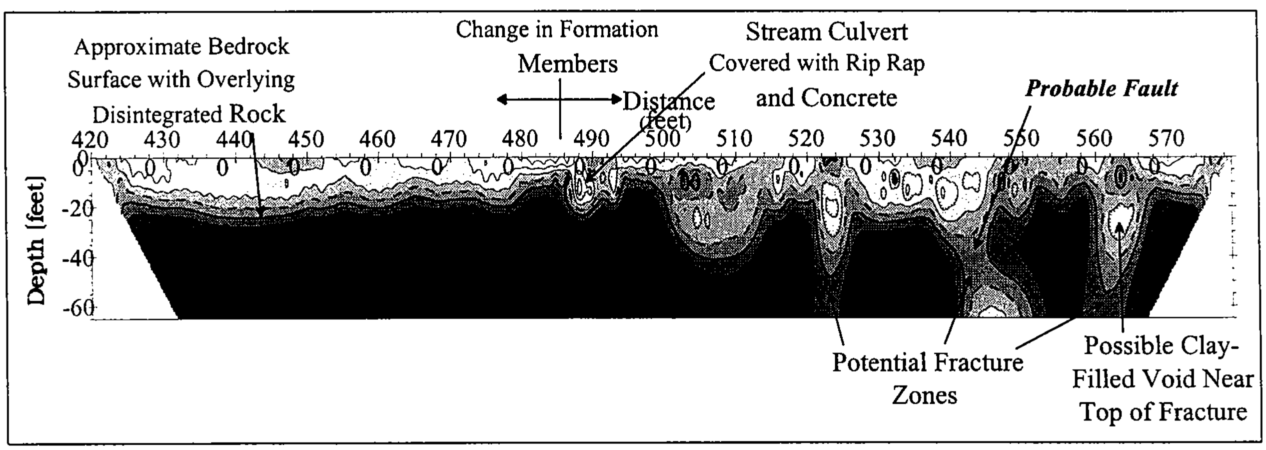

Figure 2: Example of fault zone in modeled resistivity profile in karst.

The fault feature, deep weathered zone, and adjoining bedrock surfaces shown in Figure 2 were later confirmed during drilling and grouting operations conducted by the Maryland State Highway Administration to mitigate sinkhole formation within the roadway. Also noteworthy is the difference in karst development between geologic formation members and the presence of cultural noise from a stream culvert crossing beneath the highway.

Weathered Rock/Hardrock Interface, Lebanon County, Pennsylvania

Air-track drilling verified depth to bedrock and weathered rock conditions within karst from resistivity imaging data at a future power plant site in Pennsylvania. Figure 3 below shows the depth to the bedrock surface interpreted from the resistivity model, the results of the air-track borings performed along the resistivity profile location, and the presence of "overhanging" pinnacles in the bedrock surface.

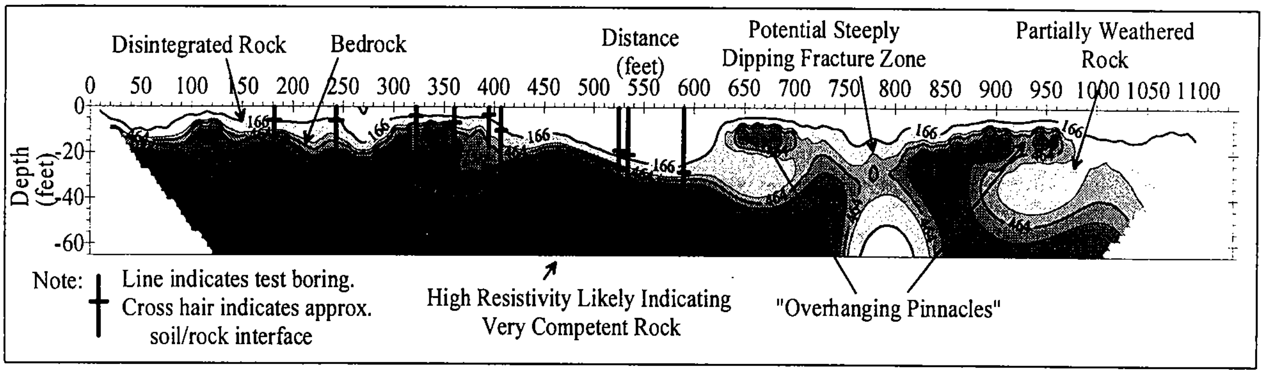

Figure 3: Example of air-track boring data overlain on modeled resistivity profile in karst.

The cross shown on the air-track boring location and depth symbol indicates the approximate bedrock surface interface as recorded from the air-track drill logs. The agreement between the bedrock surface depth estimated from the resistivity model and the results of the air-track borings are generally very good. However, some variation in rock and weathered rock interface depths from the borings is apparent.

Bedrock Cavity and Sinkhole Formation, Pulaski County, Virginia

A remarkable resistivity model profile is shown in Figure 4 that identifies a large bedrock cavity below ground, an opening to the cave at the ground surface, and a large sinkhole developed nearby. The bedrock cavity was well documented in this case and could be accessed to verify its dimensions.

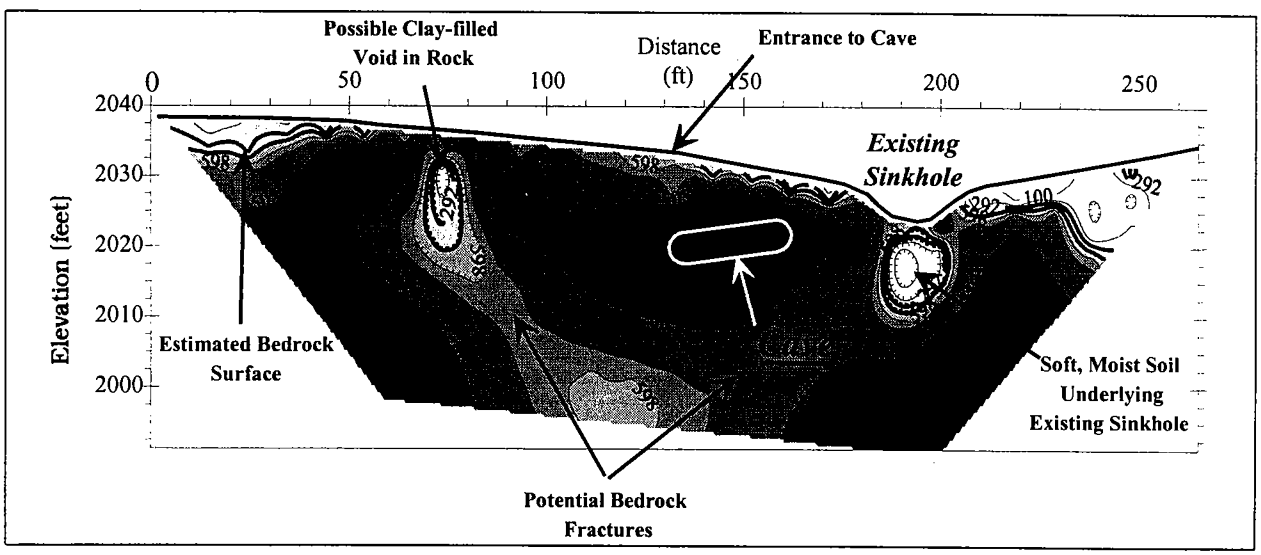

Figure 4: Example of bedrock cavity and adjacent sinkhole developed in karst.

This model profile was utilized for comparison in delineating similar features including additional voids, depth to rock, and rock ledge conditions for a large commercial development site nearby the cave shown in Figure 4. Air-track probes were conducted to confirm the resistivity data for this study and were found to be in excellent agreement with the resistivity data.

Soil Void Formation Over Bedrock Fracture, Mineral County, West Virginia

Large surface sinkhole features were present in the area of the resistivity profile shown in Figure 5 below. A small depression at the ground surface marked by an exposed section of scrap lumber was all that warned of the voided condition located only a few feet below the ground surface.

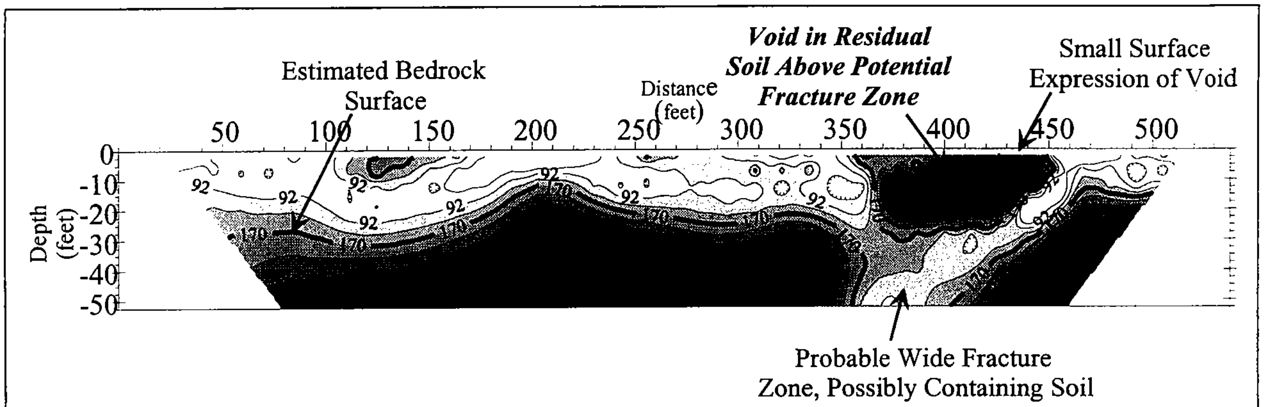

Figure 5: Example of void in soil overburden above major bedrock fracture in karst.

Additional voids were observed to form in an area of concentrated highway stormwater drainage that happened to coincide with a major bedrock fracture. The fracture identified in Figure 5 could be traced from low altitude aerial photography of the site.

CONCLUSIONS

Engineering and environmental geophysicists have struggled for many years in karst terrain because of the inherent difficulties associated with attempting to characterize highly variable subsurface conditions. Two-dimensional resistivity provide a method of imaging the subsurface in karst terrain with accuracy and precision unmatched by other standard geophysical methods. This method also has important applications in the evaluation of abandoned underground mine subsidence, dam seepage studies, mapping of contaminant plumes, location of tunnels, and ground water studies.

Although the modeled resistivity profile does not provide a unique solution to actual geologic conditions, physical ground truthing in the field indicates that the resistivity model is very close to being unique. The two-dimensional resistivity method is relatively quick and measurements can be downloaded to a computer and modeled for a "first cut" look at the data in the field. For example, typical data collection time for a 28 electrode array [135 m (442.8 ft) total length for 5 m (16.4 ft) electrode spacing] in average field conditions may take just over 2 hours (45 minutes for setup, about 1 hour for data collection, and 20 minutes for takedown). Downloading and modeling of that data for a field review takes about 20 minutes. Therefore, a line could be conducted and modeled for initial analysis in one morning.

The two-dimensional resistivity technique, like any other, does have limitations. Primary among those limitations is that the method produces a two-dimensional "slice" of the subsurface, and karst features are generally also highly variable in the third dimension. This is amplified by the fact that although the data is modeled and presented two-dimensionally, the measurements include some influences from features in the third dimension and are dependent upon the direction of measurement movement and three-dimensional anisotropy such as bedding planes. Although the technique has been shown to provide excellent information on subsurface features, there are resolution limits with respect to potentially significant but small karst features. A feature like this could be, for example, a thin, partially open or clay-filled fracture in the bedrock surface that could potentially become a route for raveling soil and a subsequent sinkhole. Resolution does increase when the electrode spacing is decreased, but the trade off is less depth of evaluation. As with any geophysical method, accurate interpretation of the modeled resistivity data is facilitated by knowledge of the geologic conditions, site history, sources of natural and cultural noise, and method limitations, as well as experience in the use of the method and equipment in various geologic terrain.

Areas for future exploration with respect to resistivity include three-dimensional resistivity tomography (Loke and Barker, 1996). Three-dimensional resistivity tomography has the ability to correct for resistivity anisotropy and three-dimensional features in the geology to provide a larger and more accurate image of the subsurface. At present, three-dimensional resistivity requires significantly more time to collect and interpret the data and is uneconomical for most sites. However, improvements in data collection instrumentation program algorithms, and computer models should continue to decrease the time needed to obtain and process this type of data. Cross-borehole resistivity in conjunction with induced polarization also could provide a future improvement for locating smaller potentially significant features in karst terrain.

ACKNOWLEDGEMENTS

The authors wish to acknowledge Mr. A. David Martin and Mr. Bruce Boyer of the Maryland State Highway Administration who provided ample opportunity to compare modeled resistivity data with other geophysical survey methods, and who allowed our use of data presented in this paper. The authors also wish to acknowledge Mr. Tomasz Labuda (Schnabel Engineering Associates, Bethesda, Maryland) who provided modeled resistivity data for the Mineral County, West Virginia, example site for this paper.

REFERENCES

Advanced Geosciences, Inc., 1997, *Sting R1 Instruction Manual, Release 2.5.5,* AGI, Austin, TX.

Edwards, L.S., 1977, A modified pseudosection for resistivity and IP: GEOPHYSICS, Vol. 42, no. 5 (August 1977); pp. 1020-1036.

Loke, M.H., pers. comm., October 1998; mhloke@pc.jaring.my

Loke, M.H., and Barker, R.D., 1996, Practical techniques for 3D-resistivity surveys and data inversion: Geophysical Prospecting, vol. 44, pp. 499-523.

Loke, M.H., and Barker, R.D., 1995, Least-squares deconvolution of apparent resistivity pseudosections: GEOPHYSICS, Vol. 60, No. 6 (November-December 1995); pp. 1682-1690.

Roy, A. and Apparao, A., 1971, Depth of investigation in direct current methods, GEOPHYSICS, Vol. 36, No. 5, pp. 943-959.

Telford, W.M., Geldart, L.P., and Sheriff, R.E., 1990, *Applied Geophysics,* Second ed., New York, U.S., Cambridge University Press, 770 p.

Tsokas, G.N., Tsourlos, P.E., and Szymanski, J.E., 1997, Square array resistivity anomalies and inhomogeneity ratio calculated by the finite-element method: GEOPHYSICS, Vol. 62, No. 2 (March-April 1997); pp. 426-435.

Near Surface Cavity Detection-Logan County, Ohio

Ethan Nowak
Vibra-Tech Engineers, Inc.
Wright State University

INTRODUCTION

An exhaustive geophysical study was performed along a section of the proposed alignment of New Route 33 in Logan county, Ohio. The study was authorized by Mr. Steve Kremer of the Ohio Department of Transportation. Field work was carried out from August 1997 through February 1998.

The purpose of the geophysical study was to assess the subsurface conditions at the above referenced site, which is prone to solution activity. Various geophysical prospecting techniques were employed to determine which would reduce the number of costly core samples needed to adequately assess the subsurface in such a problematic setting. Ground penetrating radar (GPR) was employed as a reconnaissance survey. An 80 MHz antenna provided a depth of investigation of approximately 20 to 25 feet. Diffraction patterns associated with subsurface cavities in the GPR profiles would designate areas for special attention. A gravity survey was conducted to determine if relative gravity lows, associated with voids, corresponded with the location of diffraction patterns identified in the GPR data. A seismic P-wave refraction profile was conducted over the same traverses to search for velocity lows and bedrock depressions that could indicate a karst feature. Continuous resistivity profiles and automated vertical electrical resistivity sounding scan (resistivity imaging) were performed to determine whether the anomalies previously mentioned are dissolution voids occupied by air (high resistivity anomalies) or occupied by either dirt or water (low resistivity anomalies). These methods were conducted on the West bound shoulder of New Route 33. The profiles are compared and correlated to the parallel array of core logs.

STATEMENT OF PROBLEM

Subsurface cavities and their final expression, sinkholes, frequently occur in carbonate rock types. These rocks are different from other rock types on which cultural structures are built in that they weather predominately by solution. The dissolution process involves the formation of bicarbonates from the reaction of carbonic acid and calcite or dolomite. The resulting bicarbonate is 30 times more soluble in water then the original carbonate. Water seeping through joint patterns in limestone bedrock dissolves the carbonate and forms subsurface channels. The enlargement of these channels can lead to the development of cavities in the rock and soil overburden. These cavities become progressively larger until they can no longer support the overlying roof material. This lack of integrity results in the formation of depressions in the ground surface and ultimately sinkholes. The dissolution of carbonate rock ceases only if the water table (approximately 70% saturation) or an insoluble strata such as an impervious shale is encountered, or if the drainage of internal water is impeded by clogging from silts or clays (Way,1973).

It is estimated that karst landscapes occupy up to 10% of the Earth's land surface. The instability of karst surfaces annually causes millions of dollars in damages to roads, buildings, and other structures in North America alone. Surface features and soils in karst terrains are notoriously unstable and can change at catastrophic rates. In humid climates, most surface collapse occurs during or soon after floods, when soil has been eroded above potential sinkholes (Way,1973).

There are two common misconceptions regarding solution activity. First, a solution cavity is not a single occurrence but rather part of a network of enlarged fractures, bedding planes, vertical pipes, horizontal conduits, and large rooms. This can be observed in commercial caves such as Ohio Caverns located in Champaign County and Zane Caverns located in Logan County, Ohio (Vibra-Tech). These particular cave systems are mentioned due to their close proximity to the study area and because they exist within the Columbus limestone, which is the rock unit at this survey site. Secondly, the dissolution of limestone is a rapid on going process. An area that, historically, has been unaffected by solution activity may develop a karst topography in a relatively short period of time. It has been estimated that one year of rainfall on one acre of land in the region of Mammoth Cave, Kentucky, dissolves 25 cubic feet of limestone bedrock in one year. If this activity is concentrated to a particular area, a sizable cavity can form in a relatively short period of time (Way,1973).

THE SITE AND PREVIOUS STUDY

Geology

The study site is located on the Bellefountaine Outlier and is underlain by the upper portion of the Columbus Limestone. The Columbus Limestone ranges in thickness from 80 to 105 feet in Logan County, Ohio. This unit consists of two distinct rock types. The basal Bellepoint Member is a slightly argillaceous dolomite. The overlying Delhi Member is typically a very fossiliferous massively bedded limestone that contains greater than 80 percent calcium carbonate. The upper 40 to 65-feet of the Columbus exhibits vuggy porosity and hosts many commercial caves, as previously stated, due to the high calcium carbonate concentration (Swinford,1995).

Direct Measurement Methods

Direct measurement methods, coring or boring, reveal the presence of subsurface cavities through direct contact with the cavity. For example, a loss in drilling fluid or an abrupt drop in the drill stem during the operation identifies the presence of a cavity. The number of corings required to provide an acceptable level of confidence for detecting cavities can be calculated by the site-to-cavity ratio (Benson,1984). The site-to-cavity ratio, as shown in Equation 1, is determined by dividing the length of the traverse, $L_{traverse}$, by the diameter of the smallest cavity of concern, L_{cavity}. The number of required core locations, N, can then calculated to achieve a specified probability of detection, C. The cavities in this model are assumed to be cylindrical. Equation 4.1a was derived assuming that the coring stations are uniformly spaced and on center, this conforms with typical coring operations for evaluating the subsurface.

Equation 1: Probability of cavity detection by drilling.

$$N = \left(\frac{L_{traverse}}{L_{cavity}}\right) \times \left(\frac{C}{100}\right)$$

The following Table 1 shows how the number of drilling locations increase as a higher level of confidence is desired and as the detection of smaller cavities is necessary. The station spacing can be determined simply by dividing the length the traverse, in this case 1,000 feet, by the number of drilling locations.

Table 1: Probability of detecting cavities of various size by a calculated number of sample points.

Cavity Diameter (ft)	Probability of Detection for a 1000 ft Traverse							
	10%	25%	50%	75%	90%	95%	98%	100%
1	100	250	500	750	900	950	980	1,000
2	50	125	250	375	450	475	490	500
3	33	83	167	250	300	316	326	333
5	20	50	100	150	180	190	196	200
10	10	25	50	75	90	95	98	100

It is obvious from the Table 1 that an unrealistic number of cores must be drilled to achieve an acceptable level of confidence that all subsurface cavities have been detected. Even after the extensive coring program was implemented at this site for the 1000-foot section of the proposed highway alignment the probability that all cavities at least five feet in diameter were detected is only 50%. Most subsurface investigations that are limited to drilling achieve less than 20% (Benson,1984) confidence and yet this is a common occurrence as in this case in Logan County, Ohio.

Results of the Drilling Program

The data obtained from the core logs are presented as a contoured cross-sectional profile (Figure 1). The dirt zones identified in the driller's log are contoured in orange; shot, soft, and weathered rock zones identified in the core logs were contoured in green as incompetent rock, solid rock zones are displayed in blue, and the voids encountered during the drilling project are identified in black. This figure is not meant to be misleading, the employed contouring algorithm contains some unavoidable error with respect to the actual core log data.

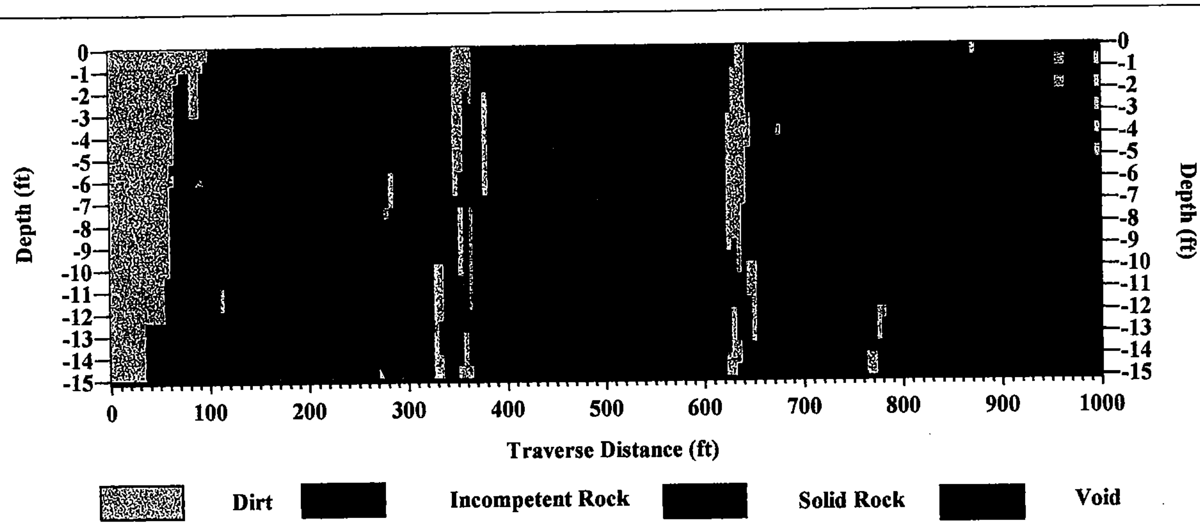

Figure 1: Core Log Profile WB 542+00 through WB 552+00

As previously stated, the coring program identified many subsurface cavities, the presence of a dirt zone beneath incompetent or solid rock was interpreted as a solution cavity that has been clogged and filled with superficial silts and clays. The coring program identified 11 air filled cavities along the west bound center line. The ceiling height of the largest air filled cavity is unknown. According to the core logs in one (1) instances the drilling operation ended in a void. With this exception, the largest air filled cavity observed in the core logs occurred along the west bound center line at station WB 545+60. This particular cavity was located beneath three feet of broken rock and had an eight foot ceiling height. The coring program also identified four (4) dirt filled cavities along the west bound center line. The ceiling height of the largest dirt filled cavity is also unknown. According to the core logs, at one drilling location rock was encountered and a subsequent a dirt zone extended past the depth of the core. The process of superficial silts and clays (noted on the driller's log as dirt filling subsurface cavities was evidenced in the core logs. According to the core logs, four (4) drilling locations encountered a void partially occupied by dirt. The maximum vertical extent of this occurrence is also unknown. At one (1) location, the last medium encountered during the drilling operation was dirt occupying the bottom of a void.

GEOPHYSICAL METHODS

Currently, commercial operations utilize pattern drilling to locate cavities. This is typically insufficiently intensive to ensure all possible targets are identified and adversely affects local ground conditions. A much more effective and economic solution is to employ geophysical techniques to locate drilling targets. This study made use of gravity, continuous electrical resistivity profiling, resistivity imaging, ground penetrating radar, and seismic P-wave refraction techniques. The geophysical data were collected along a 1000-foot traverse that paralleled the

West bound lane of the four lane highway. The traverses were located approximately 70 feet on center from the centerline within the shoulder.

Gravity Profiling

Gravity exploration measures the variations in the earth's gravitational field due to differences in the density of subsurface materials. However, the earth's gravitational field is also effected by the procession of solar and lunar gravitational fields, latitude, elevation, and topographic relief. These effects must be removed so variations in subsurface density can be evaluated. Overburden thickness, porosity, and voids are the primary contributors to variations in shallow subsurface density. The resultant data will show gravity lows over dissolution cavities because the material occupying these voids are lower in density then the hosting limestone (Table 2). Localized depressions in bedrock topography can form as a result of solution activity. These depressions allow for an increase in overburden thickness which in turn also reduces the overall density of the shallow subsurface. For a complete explanation on the theory behind gravity exploration consult (Reynolds,1997).

Table 2: Density contrast of dissolution cavity materials (data from Reynolds,1997).

Limestone: 2.55	$\frac{\text{limestone}}{\text{limestone}}$	0
Dirt: 1.92	$\frac{\text{limestone}}{\text{regolith}}$	-0.63
Water: 1.0	$\frac{\text{limestone}}{\text{water}}$	-1.55
Air: 0.0	$\frac{\text{limestone}}{\text{air}}$	-2.55

Gravity Field Procedure

The gravity study utilized the LaCoste and Romberg model G gravimeter which has a 0.01 mGal precision. Relative gravity measurements were taken on a 10-foot station spacing and a return to base station every hour to assure an adequate drift correction. Because the gravity lows were anticipated to be quite small, very precise elevation control was necessary. The stations needed a vertical surveying accuracy of at least 0.1 feet. These locations were established with a digital theodolite.

Expected Gravity Anomalies

The density contrast between limestone/regolith, limestone/water, and limestone/air (listed in Table 2) were used to produce a gravity model (Figure 2) to determine the magnitude of the expected anomalies. This model was produced using the vertical sheet method (Equation 2).

Equation 2: Vertical gravitational component of a vertical sheet (Dobrin,1988).

$$g_z = 4.68\rho t\left(\log \frac{1+\frac{z_2^2}{x^2}}{1+\frac{z_1^2}{x^2}}\right)$$

Where 'Z_1 and Z_2' are the depth, in feet, to the top and bottom of the cavity (respectively), 't' is the width of the cavity, in feet, and 'ρ' is the density contrast, in milligals per cubic centimeter, between limestone and the appropriate material occupying the cavity. This equation was chosen because dissolution cavities often occur along fractures and this model assumes the third dimension is infinite.

The largest cavity observed in the core logs was approximately 5 feet beneath the surface and had a ceiling height of 8 feet. The width of the void was estimated to be 10 feet across. These dimensions were used to create the subsequent model shown in Figure 2. The largest expected gravity low for this void is -0.1 mGal in the case of an air filled void, -0.06 mGal for a water filled void, and -0.02 mGal with respect to a dirt filled void of the previously described dimension.

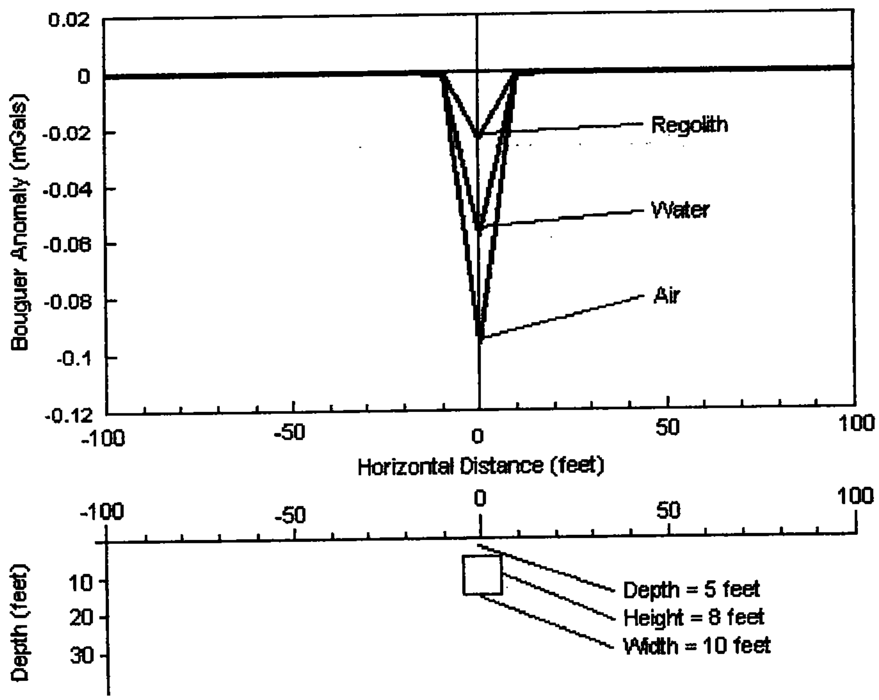

Figure 2. Gravity anomaly model of a dirt, water, and air fill cavity

<u>Observed Gravity Anomalies</u>

A total of nine (9) low gravity anomalies were observed in the subsequent gravity profile, Figure 3. The magnitude of these gravity lows ranged from -0.01 to -0.06 milligals, deviations of this nature do correspond with the expected anomalies modeled in Figure 2. Table 3 describes these anomalous areas found on Figure 3.

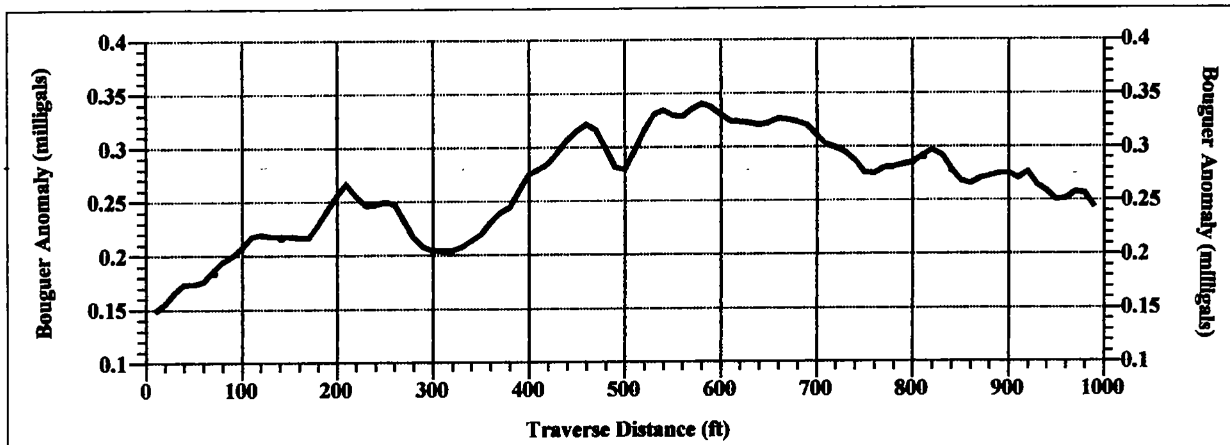

Figure 3: Gravity Profile WB 542+00 through WB 552+00

Table 3: Gravity anomalies observed on the west bound traverse (Figure 3)

WB 543+60	160	-0.02
WB 544+45	245	-0.03
WB 545+20	320	-0.06
WB 547+00	500	-0.04
WB 547+65	565	-0.01
WB 548+30	630	-0.01
WB 549+60	760	-0.03
WB 550+60	860	-0.02
WB 551+55	955	-0.01

Electrical Resistivity Profiling

An electrical resistivity survey measures changes in the ease at which an electric current can flow through the subsurface. When an electrical current is artificially induced into the ground a potential difference can be measured between two points at the surface. As the resistance to current flow varies vertically and/or horizontally, changes in the electrical potential reflect these differences. These material dependent changes provide an indication of horizontal and vertical heterogeneity in the subsurface. Subsurface conductivity, the inverse of resistivity, is a function of several parameters. The three primary contributors to subsurface electrical conductivity are clay content, moisture content, and void space. For a complete understanding of electrical resistivity theory consult (Burger,1992).

In this geologic setting, the nominal resistivity should be that of limestone assuming a homogeneous subsurface. Changes in electrical resistivity measurements in this area can be attributed to the presence of dissolution cavities. These cavities may be air, water or dirt filled depending on their position relative to the water table. This leads to two different measurable resistivity anomalies; air which is highly resistive, and water and dirt which is highly conductive with respect to the hosting limestone (Table 4).

Table 4. Electrical resistivities of materials associated with dissolution cavities (data from Reynolds,1997).

Material	Electrical Resistivity	
	Ω*ft	Ω*m
Limestone	164 - 1.64×10^8	50 - 5.0×10^7
air	∞	∞
water	64.6 - 328	19.7 - 100.1
dirt	26.2 - 108	7.98 - 32.9

The high resistivity of air is apparent because it is infinite. The low resistivity of ground water results from the dissolution process. As water dissolves carbonate rock the resultant solution becomes highly ionized which is characteristically very conductive. Dirt may be composed of up to 40% clay, clays typically possesses a residual electric charge which renders it a conductive material.

Continuous Resistivity Profile Field Procedures

Two electrical resistivity profiles were conducted during this study. The Sting resistivity meter was used to perform a pair of continuous electrical resistivity profiles over both traverses. Each survey utilized the Wenner electrode configuration (Figure 4), where each of the four electrodes are equally separated with an a-spacing of 10 and 20 feet. A less then 2% reproducibility error limit was set for each of the continuous resistivity profiles to ensure accurate readings at each station. Once the averaged readings at a particular station fell within this error limit the array was advanced one a-spacing. This process was repeated until the end of the traverse was reached.

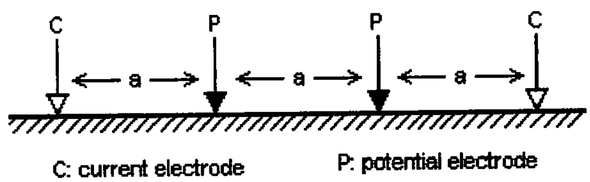

Figure 4: The Wenner electrode configuration (Burger,1992).

The profile conducted with a 20-foot a-spacing will average a larger hemisphere of the subsurface to produce an apparent resistivity measurement than the 10 foot a-spacing profile. Hence, if an anomaly is present in the 20-foot a-spacing profile but not the 10-foot a-spacing profile, it can be assumed that the sought-after feature is beyond the limitations of the 10 foot a-spacing configuration but within the depth of investigation of the 20-foot a-spacing. Also, if an anomaly is present in both profiles, a-spacings of 10 and 20 feet, then in all likelihood the anomaly is shallow, determined by the 10 foot a-spacing profile, and real, as it was confirmed by the 20 foot a-spacing profile. These assumptions allow for a qualitative depth estimation of anomalies present in the data.

Resistivity Imaging Field Procedure

The second electrical resistivity survey employed in this study was an automated vertical electric resistivity sounding scan (resistivity imaging). The Sting resistivity meter, in conjunction with the Sting Swift multi-electrode coordinating unit was used to perform this resistivity imaging survey over the west bound traverse. This survey utilized the Dipole-dipole electrode configuration (Figure 5), where the two current and potential electrodes are at a constant a-spacing but the dipole separation is variable.

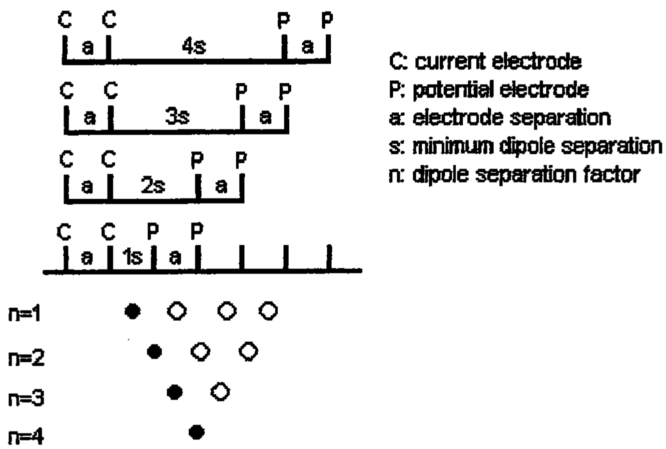

Figure 5: The Dipole-dipole multi-electrode configuration.

The survey was conducted with a 28 electrode spread where the minimum dipole separation is 10 feet. Initially, the two current electrodes were kept at the same location as the potential electrodes are advanced as shown in Figure 5. When the maximum dipole separation is reached the current electrodes are advanced one a-spacing and the cycle repeats. After the array of electrodes have progressed to the far end of the spread the next spread overlaps the previous by 50%. This allows for continuous deep resistivity measurements and tests the reproducibility of shallow readings.

A less then 2% reproducibility error limit was set for the resistivity imaging survey to ensure accurate readings at each station. Once the averaged readings at a particular station achieved this criteria the array advanced to the next measurement.

Expected Resistivity Anomalies

Since air is infinite in resistivity (Table 4) an air filled cavity is expected to produce a high resistivity anomaly in both of the electrical resistivity profiling techniques employed in this study. The magnitude of the high resistivity anomaly is dependent solely on the size of the cavity.

The average electrical resistivity observed in all the profiles is approximately 700 Ω*ft (213.4 Ω*m) this is assumed to be the resistivity of the limestone unaffected by cavities. Groundwater has an electrical resistivity of 64.6 - 328 Ω*ft (19.7 - 100.1 Ω*m) and dirt has an electrical resistivity range of 26.2 - 108 Ω*ft (7.98 - 32.9 Ω*m). Since these resistivity values are much lower then that of the static, 700 Ω*ft (213.4 Ω*m), resistivity associated with the limestone, a low resistivity anomaly will suggest the presence of a water or dirt filled cavity. The magnitude of the low resistivity anomaly is dependent on the size and contents of the cavity.

Observed Electrical Resistivity Anomalies

A total of eight (8) electrical resistivity anomalies were observed in the data resulting from the continuous electrical resistivity survey (Figure 6). The data collected with the 10-foot a-spacing is designated with a solid line and the data collected with the 20-foot a-spacing is designated with a dashed line on the profiles. The magnitude of these anomalies were based on a resistivity datum, the resistivity of the limestone at this site unaffected by cavities, which was determined to be 700 Ω*ft (213.4 Ω*m). The electrical resistivity deviations from the limestone datum are either positive (high resistivity anomalies), or negative (low resistivity anomalies). Table 5 summarizes the anomalous areas found on Figure 6.

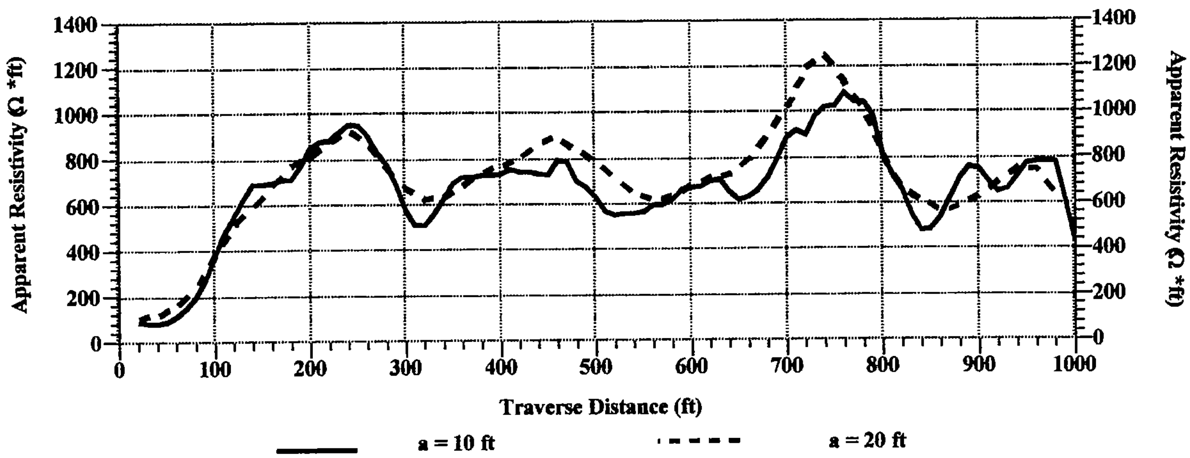

Figure 6: Continuous Electrical Resistivity Profile WB 542+00 through WB 552+00

Table 5: Electrical resistivity anomalies observed on the west bound traverse (Figure 6).

Station	Location (ft)	Magnitude (Ω*ft)	
		a = 10 ft	a = 20 ft
WB 544+45	245	241.4	206.9
WB 545+20	320	-206.9	-86.2
WB 546+60	460	86.2	172.4
WB 547+40	540	-137.9	-86.2
WB 548+20	620	103.4*	103.4*
WB 549+40	740	379.3	517.2
WB 550+55	855	-224.1	-137.9
WB 551+60	960	68.9	34.5

* this anomaly was not observed from the 700 Ω*ft resistivity datum but rather a predominate inflection in the profile.

A total of fifteen electrical resistivity anomalies were observed in the data resulting from the resistivity imaging survey (Figure 7). The profile is color contoured with respect to the spatial variability of subsurface electrical resistivity. The colder colors, violet and dark blue, represent low resistivity zones, while the warmer colors, yellow and red, indicate areas of high resistivity. All the anomalies present in the data were of high resistivity values which ranged from 2300 to 5100 Ω*ft (701 to 1554 Ω*m). Table 6 summarizes the results of this survey.

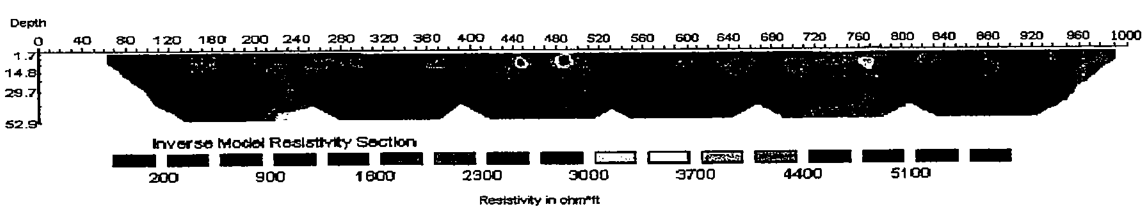

Figure 7: Resistivty Imaging Profile WB 542+00 through WB 552+00

Table 6: Electrical resistivity anomalies observed on the west bound traverse (Figure 7).

WB 543+50	150	2,650
WB 544+10	210	2,300
WB 544+50	250	3,350
WB 544+85	285	3,350
WB 545+60	360	2,650
WB 546+35	435	5,100
WB 546+75	475	5,450
WB 547+85	585	1,950
WB 548+40	640	3,000
WB 548+90	690	2,300
WB 549+25	725	3,000
WB 549+55	755	4,750
WB 550+10	810	2,650
WB 550+70	870	2,300
WB 551+70	970	2,650

Ground Penetrating Radar

Ground penetrating radar (GPR) is a useful technique for identifying near surface cavities. The GPR system is capable of imaging horizontal and vertical discontinuities due to changes in material dependent dielectric constants. As pulse electromagnetic waves are emitted into the ground they are reflected from boundaries where there is a change in dielectric properties. During a GPR survey the radar antenna is pulled along the traverse as the electromagnetic energy is emitted from the source antenna. The energy disperses in the ground taking the shape of a tear drop. The reflected energy is detected by a receiver antenna and recorded as a time history. For a further discussion on ground penetrating radar theory can be found in (Reynolds,1997).

In the case of dissolution cavities, the boundaries of concern are limestone/air, limestone/water, and limestone/regolith. Knowing the dielectric constants (ε) of these four materials enables the reflectivity (k) of the radar signal to be calculated for each of these interfaces (Equation 3). The reflectivity is the portion of incident radar energy that is reflected (Schwaiger,1997).

Equation 3: Reflectivity

$$k = \frac{1-\sqrt{\frac{\varepsilon_2}{\varepsilon_1}}}{1+\sqrt{\frac{\varepsilon_2}{\varepsilon_1}}} \times 100\%$$

Table 7: Comparison between dielectric constants and reflectivity for various dissolution cavity interfaces (Schwaiger,1997).

$\varepsilon_{limestone} = 7\text{-}9$	$\frac{\text{limestone}}{\text{limestone}}$	0 %
$\varepsilon_{air} = 1$	$\frac{\text{limestone}}{\text{air}}$	-47 %
$\varepsilon_{water} = 81$	$\frac{\text{limestone}}{\text{water}}$	52 %
$\varepsilon_{regolith} = 8\text{-}12$	$\frac{\text{limestone}}{\text{regolith}}$	6 %

As displayed in Table 7 the contrast in dielectric constants between limestone and air, and limestone and water is large therefore much of the incident radar energy is reflected. Where there is little to no change in dielectric constants at a subsurface interface, as in the case between limestone and limestone, and limestone and dirt, only a minute amount of radar energy is reflected.

Ground Penetrating Radar Field Procedure

The SIR system 2 ground penetrating radar system needed to be equipped with an antenna that would provide the depth of penetration to image the sought-after anomalies. The voids were present in the 15 foot deep core logs. The skin depth (Equation 4) is regarded as an approximate effective depth of penetration of electromagnetic energy (Sheriff,1973).

Equation 4: Skin depth

$$Skin\ Depth = \sqrt{\frac{2}{\sigma\mu_0\omega}}$$

Where the conductivity (σ) was calculated from the inverse average resistivity from the electrical resistivity surveys also conducted during this study. The angular frequency (ω) is of the antenna and the magnetic permeability (μ_0) is a constant. In this particular environment, where broken limestone is present at the surface, an 80 MHz monostatic antenna would investigate to a depth of at least 8 feet. This frequency antenna is common in shallow subsurface prospecting and was utilized during this radar reflection profiling survey over both traverses.

Expected Ground Penetrating Radar Anomalies

Due to the tear drop shape of the electromagnetic energy, subsurface objects are often observed in data before the antenna is directly over its superficial location. This will cause a subsurface cavity to appear as a parabolic reflector where the apex of the parabola will designate the superficial location. In the processed data an air or water filled cavity is expected to appear as a high amplitude parabolic reflection. Referring to Table 7, at least 47% of the incident radar energy is reflected with respect to limestone/air, and limestone/water interfaces these reflections should be very pronounced in the data. In the case of a dirt filled cavity the small difference in dielectric constants leaves only 8% of the incident radar energy to be reflected therefore cavities of this nature are anticipated to be difficult to resolve.

Observed Ground Penetrating Radar Anomalies

A total of eight (8) predominate radar anomalies were observed in the GPR profile (Figure 8). The reflections on the radar profiles are color contoured with respect to the reflection amplitude. The purple and red colors represents high amplitude reflections caused by interfaces of large contrasting dielectric constants. The yellow, and gray colors indicate low amplitude reflections caused by slightly varying dielectric constants. The white colored designates areas of no radar reflections, indicating zones of homogeneous dielectric properties. The following Tables 8 summarize the radar anomalies observed on Figure 8.

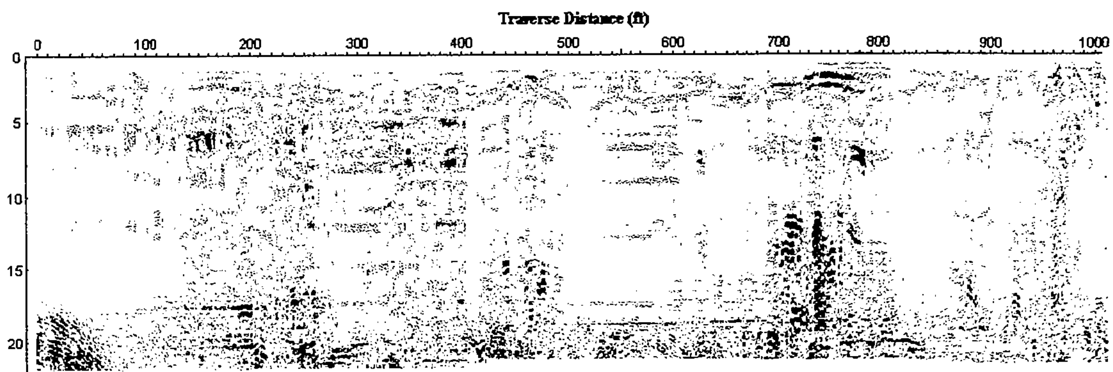

Figure 8: Ground Penetrating Radar profile WB 542+00 through WB552+00

Table 8: Ground Penetrating Radar anomalies observed on the west bound traverse (Figure 8).

Station	Traverse Location (ft)	Depth (ft)	Magnitude Assessment
WB 543+60	160	6	Medium to High
WB 544+40	240	7-10	Medium to High
WB 545+90	390	5-8	Medium to High
WB 546+60	460	2	Low to High
WB 548+25	625	7	High
WB 549+50	750	2.5-20	High
WB 551+70	970	2	Low to Medium
WB 552+00	1,000	3-5	High

Seismic P-wave Refraction

Seismic velocities in a medium is a function of the density and elastic moduli of the material they are traveling through. As a refracted seismic wave is traveling along a subsurface interface it produces secondary head waves to the surface. The arrival of these refracted head waves are detected at the surface before the remaining spectrum of seismic wave energy, i.e. ground roll, reflected waves, direct waves, air blast, etc. Localized density changes, within a layer overlying a refracting interface will impede or promote their arrival to the surface. For a complete explanation of seismic refraction theory consult (Renolds,1997).

The large reduction in seismic velocity between limestone/air, limestone/water, and limestone/regolith (Table 9) will retard the arrival of the secondary head waves to the surface. This reduction would be very pronounced compared to the head waves adjacent to a particular cavity.

Table 9: Velocity comparison of dissolution cavity materials (data from Reynolds,1997).

Medium	Mean Seismic Velocity $(\frac{ft}{s})$
Limestone	13,800
Dirt	3,490
water	4,850
air	1,100

Seismic P-wave Refraction Field Procedure

The StrataView 36 channel seismograph was utilized to collect the raw field records. The survey was designed with a 5 foot geophone spacing and a 5 foot in-line shot offset. A 5 foot geophone separation was chosen to provide sufficient detail of subsurface structure. The forward and reverse shots, supplied by a 12 pound sledge hammer, were vertically stacked 16 times to ensure an adequate signal to noise ratio.

Expected Seismic P-wave Refraction Anomalies

Seismic velocities in bedrock typically decrease in areas of solution activity. Velocities in the soil overburden, however is variable depending on the state of stress in the soil. Low velocity anomalies would be observed on the provided travel-time plots as areas on the curve that deviate above the best-fit line designating a layer of uniform velocity. In addition, depressions in the bedrock topography can also be indicative of solution activity. These depressions would be observed in the provided cross-sectional profiles. Regions of depressed bedrock topography coupled with decreases in seismic velocities will suggest the presence of a dissolution cavities.

Observed Seismic P-wave Refraction Anomalies

The results of the seismic refraction survey yielded a three (3) layer model on the west bound traverse. The seismic stratigraphy beneath the west bound traverse (Figure 9) consisted of a shallow Layer 1, an intermediate Layer 2, and a deep Layer 3. Layer 1 varied from 0 to 12 feet thick, and consisted of an unconsolidated, unsaturated soil overburden material. This Layer 1 was identified by a compressional wave velocity of 1,450 ft/sec. Layer 2 ranged from 5 to 37 feet thick, and was composed of an unconsolidated, unsaturated talus overburden material. This Layer 2 was identified by a compressional wave velocity of 3,300 ft/sec. Layer 3 was characterized as a competent limestone bedrock, which varied from 18 to 40 feet beneath the surface. This Layer 3, expected to be the Columbus limestone, was identified by a seismic velocity of 11,560 ft/sec. The undulating bedrock topography along the west bound traverse displayed many minor, less than 3-foot, depressions. Four (4) significantly larger depressions were also observed in the seismic refraction data along this traverse. In addition, five (5) low velocity zones (LVZ's) were observed on the Time-Distance plots for the west bound traverse. Table 9 summarizes the seven (7) anomalous areas along the west bound traverse.

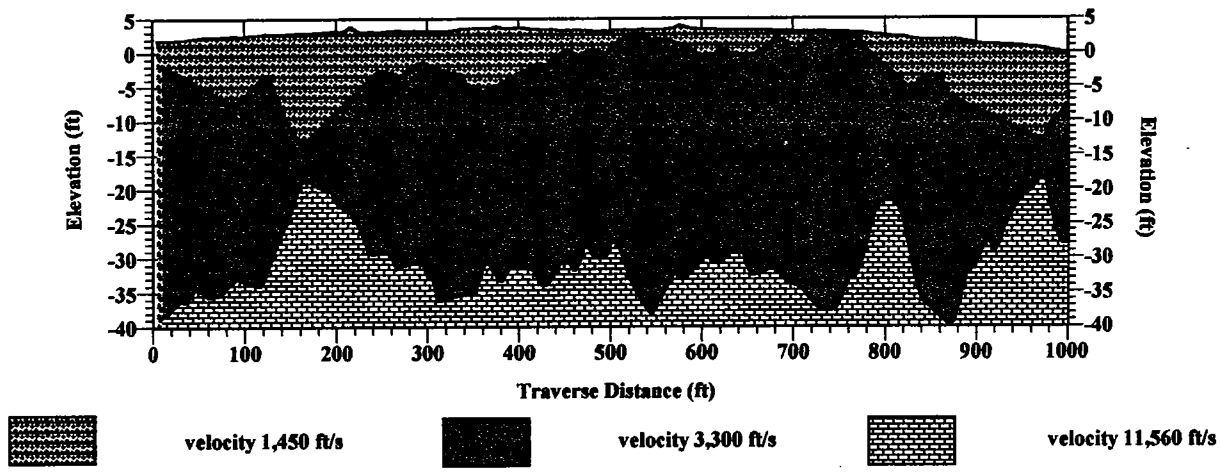

Figure 9: West Bound Seismic Refraction Profile WB 542+00 through WB 552+00

Table 9: Observed seismic refraction anomalies along the west bound traverse (Figure 9).

Station	Traverse Location (ft)	Magnitude (ft)	LVZ Observed
WB 542+79	79	minor	yes
WB 545+20	320	-6	no
WB 545+85	385	minor	yes
WB 547+40	540	-10	yes
WB 547+81	581	minor	yes
WB 549+40	740	-9	no
WB 550+70	870	18	yes

INTERPRETATION OF RESULTS

The interpretation of results consist of the identification of geologically consistent anomalies observed in the geophysical data collected during this study, and their subsequent correlation with the core log data. It is important to remember that the cores were drilled along the centerline of the highway which paralleled the geophysical traverses on approximately 45-foot centers. If these cavities developed along linear fractures in the limestone bedrock it would not be a safe assumption that the geophysical traverse were perpendicular to the orientation of the fractures. Because of this, a little latitude was required when correlating the results of the investigation with the core log data.

The geophysical techniques employed during this study were complimentary, meaning they measured different properties of subsurface material as they relate to the development to sinkholes. The criteria for identifying a subsurface cavity, with a high level of confidence, relies on the coincidence of anomalies observed in the profiles produced from these complimentary geophysical techniques. Based on the physical characteristics of an air filled void a zone of: high electrical resistivity, high amplitude radar reflections, low relative gravity, low compressional wave velocity, and depressed bedrock topography would suggest the presence of such a cavity. Similarly, the physical characteristics of a dirt filled cavity would cause a zone of: low electrical resistivity, low amplitude radar reflections, low relative gravity, low compressional wave velocity, and depressed bedrock topography would suggest the presence of a dirt filled cavity. Thirdly, the physical characteristics of a water filled cavity would produce a zone of: low electrical resistivity, high amplitude radar reflections, low relative gravity, low compressional wave velocity, and depressed bedrock topography would suggest the presence of a water filled cavity. Finally, the presence of a cavity partially occupied by dirt would be identified by a zone exhibiting: a low gravity anomaly, low electrical resistivity measurements, high amplitude radar reflections, depressed bedrock topography coupled with a low compressional wave velocity. The confidence bestowed in the interpretation of the geophysical anomalies is a function of the number of corroborating events.

West Bound Traverse

The west bound profiles are displayed on Plate 1 in Appendix G. As per careful scrutiny of the geophysical data, a total of eight (8) locations along the west bound traverse exhibit sinkhole characteristics.

Station WB 543+56 (156 feet) exhibited: a low (-0.02 milligal) gravity anomaly, a high (2,650 ohm*ft) electrical resistivity anomaly in the resistivity imaging profile, and medium to high amplitude radar reflections. The driller's log indicated that small 1 to 2-foot air filled cavities were centered around WB 543+20 (120 feet). Based on the previously described criteria, the geophysical anomalies observed at WB 543+56 suggest that an air filled cavity or cavities lie approximately 7 feet beneath the surface.

Station WB 544+45 (245 feet) exhibited: a low (-0.03 milligal) gravity anomaly, high (241 and 207 ohm*ft) electrical resistivity anomalies in the continuous electrical resistivity profiles conducted with a 10 and 20-foot a-spacing (respectively), an additional high (2,825 ohm*ft) electrical resistivity anomaly in the resistivity imaging profile, and medium to high amplitude radar reflections. Small dirt and air filled cavities were identified in the driller's log at approximately WB 544+30 (230 feet). The nature of the geophysical anomalies at WB 544+45 suggest the presence of another air filled cavity located approximately 7 feet beneath the surface.

Station WB 545+20 (320 feet) exhibited: a low (-0.06 milligal) gravity anomaly, low (-207 and -86 ohm*ft) electrical resistivity anomalies in the continuous electrical resistivity profiles conducted with 10 and 20-foot a-spacings, and a 6-foot bedrock depression identified in the seismic refraction profile. According to the driller's log a void partially filled with dirt was identified at WB 545+30 (330 feet). Also at this particular station, a large dirt zone was observed in the road-cut outcrop which extended sub-grade. The nature of the geophysical anomalies and the outcrop observation at WB 545+20 suggest the presence of a substantial superficial dirt filled cavity.

Station WB 546+57 (457 feet) exhibited: a high (86 and 172 ohm*ft) electrical resistivity anomalies in the continuous electrical resistivity profiles conducted with a 10 and 20-foot a-spacing (respectively), an additional high (5,100 ohm*ft) electrical resistivity anomaly in the resistivity imaging profile, and medium amplitude radar reflections. Although the anomalies at this station did not display many subsurface cavity characteristics, the localized and extremely high electrical resistivity measured during the resistivity imaging survey coupled with the parabolic radar reflections suggest the presence of an air filled cavity located less than 5 feet beneath the surface.

Station WB 548+29 (629 feet) exhibited: a low (-0.01 milligal) gravity anomaly, high (103 ohm*ft) electrical resistivity anomaly in the pair of continuous electrical resistivity profiles, an additional high (3,000 ohm*ft) electrical resistivity anomaly in the resistivity imaging profile, and medium amplitude radar reflections. According to the driller's log multiple air filled cavities were found to be centered around station WB 548+40 (640 feet). The nature of the geophysical anomalies at WB 548+29 suggest the presence of a single air filled cavity located approximately 8 feet beneath the surface.

Station WB 549+46 (746 feet) exhibited: a low (-0.03 milligal) gravity anomaly, high (379 and 517 ohm*ft) electrical resistivity anomalies in the continuous electrical resistivity profiles conducted with a 10 and 20-foot a-spacing (respectively), an additional high (4,750 ohm*ft) electrical resistivity anomaly in the resistivity imaging profile, high amplitude radar reflections, and a 9-foot bedrock depression was noted on the seismic refraction profile. According to the driller's log, an air filled cavity extended past the depth of the core at WB 549+75 (775 feet). The nature of the geophysical anomalies at WB 549+46 suggest the presence of a large air filled cavity located approximately 12 feet beneath the surface.

Station WB 550+60 (861 feet) exhibited: a low (-0.02 milligal) gravity anomaly, low (-224 and -137 ohm*ft) electrical resistivity anomalies in the continuous electrical resistivity profiles conducted with 10 and 20-foot a-spacings, and an 18-foot bedrock depression identified in the seismic refraction profile coupled with a pronounced low velocity zone on the time-distance plot. The nature of the geophysical anomalies at WB 550+60 suggest the presence of a dirt filled cavity.

Station WB 551+63 (963 feet) exhibited: a low (-0.02 milligal) gravity anomaly, high (69 and 36 ohm*ft) electrical resistivity anomalies in the continuous electrical resistivity profiles conducted with a 10 and 20-foot a-spacing (respectively), an additional high (2,650 ohm*ft) electrical resistivity anomaly in the resistivity imaging profile, and low to medium amplitude parabolic radar reflections. The nature of the geophysical anomalies suggest the presence of an air filled cavity located less than 5 feet beneath the surface.

CONCLUSIONS

The results of this geophysical investigation suggest that there are eight (8) areas of concern for sinkhole development within the limits of this study. These locations, listed in ascending order of importance, are Stations WB 549+46, WB 550+61, WB 544+45, WB 546+57, WB 551+63, WB 543+56, WB 548+29, and WB 545+20. These areas were characterized by a combination of low gravity measurements, electrical resistivity anomalies, ground penetrating radar reflections, observed bedrock depressions in the seismic refraction data, and low compressional wave velocity zones associated with a deeper bedrock horizon. These anomalous areas correlated reasonably well with the core logs, which paralleled the geophysical traverses. Given the nature of the subsurface material at this site, these are areas that should be investigated further through the coring program in order to establish ground truth and confirm the validity of the claims made during this investigation.

The non-uniqueness of these techniques stresses the importance of complimentary geophysical surveys to corroborate the nature of observed anomalies. Thus, successfully imaging the subsurface in a nondestructive, unenvasive manner.

REFERENCES

Benson, Richard C., 1984, Evaluation of Subsidence or Collapse Potential Due To Subsurface Cavities, Proceedings of the First Multidisciplinary Conference on Sinkholes, Orlando, Florida, 204-206 p.

Burger, H. Robert, 1992, Exploration Geophysics of the Shallow Subsurface: Prentice Hall, Englewood Cliffs, New Jersey, 241, 289 p.

deGroot-Hedlin,C. and Constable, S., 1990, Occam's inversion to generate smooth, two- demensional models from megnetelluric data, Geophysics, 55, 1613-1624 p.

Dorbin, Milton B. and Savit, Carl H., 1988, Introduction to Geophysical Prospecting Fourth Edition: McGraw Hill, New York, 617 p.

Palmer, Derecke, 1986, Handbook of Geophysical Exploration, Section I. Seismic Exploration, Volume 13. Refraction Seismics, The lateral resolution of structure and seismic velocity: Geophysical Press, London, 90-94 p.

Reynolds, John M., 1997, An Introduction to Applied and Environmental Geophysics: John Wiley & Sons, West Sussex, England, 32,422, 681 p.

Sasaki, Y., 1992, Resolution of resistivity tomography inferred from numerical simulation, Geophysical Prospecting, 40, 453-464 p.

Schwaiger, Hans F.; Murray, Craig; Brown, Larry; 1997, Effectiveness of Ground Penetrating Radar in Detecting Caves in Karst Limestone of the Yucatan Peninsula, Mexico, Symposium on the Application of Geophysics to Engineering and Environmental Problems: Environmental and Engineering Geophysical Society, Wheat Ridge, Colorado, 577 p.

Sheriff, Robert E., 1973, Encyclopedic Dictionary of Exploration Geophysics: Society of Exploration Geophysicists, Tulsa, Oklahoma, 198 p.

Swinford, E. Mac, and Slucher, Ernie R., 1995, Regional Bedrock Geology of the Bellefountaine, Ohio, 30x60 Minute Quadrangle: Ohio Department of Natural Resources, Ohio.

Vibra-Tech Engineers, Inc., unpublished documents.

Way, Douglas S., 1973, Terrain Analysis Second Edition: Dowden, Hutchinson, and Ross Inc., Pennsylvania 102 p.

GEOPHYSICAL TECHNIQUES TO LOCATE OLD COAL MINES BENEATH HIGHWAYS

by

Richard, B. H., , Wolfe, P. J., Hauser, E. C., and Hicks, J. D.,

Department of Geological Sciences, Wright State University

ABSTRACT

Several years ago, Interstate 70 in eastern Ohio collapsed over old coal mine workings. The remediation of this event cost millions of dollars. This paper gives the results of a study currently in progress that is funded by the Ohio Department of Transportation over old coal mines.

In the late 1800's and early 1900's, mining of shallow, thin coal seams was common. The maps of these mines were, at best, incomplete. Though the area of coal deposits is generally known, little is known about the extent of the old mines. Since that time many highways have been constructed over these mines. We conducted a geophysical study of an area where coal mines were believed to exist beneath a highway. Radar, P-wave seismic refraction, S-wave seismic refraction, seismic reflection, dipole-dipole 2-D resistivity, gravity, and surface wave data were gathered and analyzed. The purpose was to find an inexpensive technique that would focus on probable areas of future collapse.

The success of these different geophysical methods varied. The less successful methods were:

1) Radar - there was too much attenuation because of the high percentage of clay in the overburden.
2) Gravity - The voids were too small to be resolved.
3) Seismic reflection - The frequency of the waves was too low to find the small voids.

More successful were the observation of diffractions and velocity and amplitude attenuation anomalies in the seismic refraction data, as well as anomalies in the dipole-dipole 2-D resistivity data. These anomalies were correlated with each other and with drilling at these sites. Results of the surface wave studies are not yet available.

Of the geophysical methods tested, it appears the P and S wave seismic refraction and dipole-dipole resistivity techniques will be the most useful inexpensive methods to locate possible unstable mines beneath highways. This summer, we will test improved survey designs resulting from the studies presented in this paper.

INTRODUCTION

In 1994 subsidence features were identified on Interstate 70 in Ohio (Hoffmann et al., 1994). These features were caused by collapse of old mine workings beneath the highway. At that time, geophysical studies attempted to delineate these features without much success. Ground penetrating radar, seismic refraction and electromagnetics were attempted. Drilling was used as the primary technique to delineate the voids. The collapse was believed to be caused by dewatering of old mines. At this site there was too much overburden for the radar to penetrate, the shafts were too deep to be detected by the electromagnetic technique used and the seismic refraction lacked adequate resolution to delineate the voids.

Is there a geophysical technique that will focus on areas of possible future collapse? There are many miles of highway that have been built over shallow coal seams that were mined in the late 1800's and early 1900's with inadequate mapping of the voids produced. Therefore, there are many sites where potential future collapse could occur. Drilling would be prohibitively expensive as a searching tool. This study tests various geophysical tools to focus on areas of possible future highway collapse. We hope to be able to locate sites where future drilling can detail the problem. The geophysical tools we investigated were gravity, ground penetrating radar, seismic reflection, P-wave and S-wave seismic refraction, dipole-dipole 2-D resistivity, and surface wave studies. A site was selected in Jackson County, Ohio, where abandoned coal mines did exist beneath a highway and there was some evidence to suggest future failure (see figure 1).

METHODS

Gravity was measured at ten foot intervals along the highway. Elevations were surveyed to an accuracy of +/- 0.1 ft. Measurements were made with a Lacoste and Romberg gravity meter with precision of 0.01 mGal. These readings were then corrected to a Bouguer anomaly. This survey was not expected to delineate individual voids but it might show zones of reduced rock density due to mining.

Ground penetrating radar data were gathered in profiles along the highway using a GSSI SIR-2 system with an 80 megahertz and a 300 megahertz antenna. It was expected that the clay content in the soil might attenuate the signals before the voids were reached.

Seismic reflection data were gathered using a 36 channel Geometrics Strataview seismic system with a minivibrator and an elastic wave generator as sources. The geophone spacing was 10 feet. We recognized that a very close spaced survey would probably be required to detect small voids, but this would not meet the project goals of finding an economical search method.

Both P and S wave seismic refraction data were gathered. We used the same system with a ten foot station spacing. The Minivibrator was used as a P-wave source and then modified to an S-wave source. In addition we used the elastic wave generator to acquire a set of P-Wave data and a sledge hammer to acquire a set of S-wave data. The data were examined for unusual attenuation and anomalous velocities. In addition we calculated depth to refracting layers using the Rimrock Geophysical refraction software. This software uses a delay time method with ray path tracing to refine the data. Eight elastic wave generator weight drops or hammer blows were usually adequate to obtain energy for a good seismic record. For the S-wave survey, four blows in one direction and then four blows in the opposite direction produced adquate energy for a record. By reversing the polarity of the second set of records and then adding them together, we removed the P-waves from the data.

Dipole-dipole 2-D resistivity surveys were acquired with the Sting-Swift system. This system uses an array of electrodes driven by a computer program which selects numerous different arrangements of these electrodes to record apparent resistivities. These electrodes were spaced at ten and five foot intervals. The data are then inverted with 2DINV software by Advanced Geosciences, Inc. to produce a 2-D resistivity cross section.

Surface wave data were gathered using two 4.5 hertz geophones with a two channel Dynamic Signal Analyzer, Stanford Research Systems SR-780, and hammers and the elastic wave generator as sources. Data were gathered with receiver spacings of 0.5, 1, 2, 4, 8, 16, and 32m at six different locations. This was designed to test the value of the technique. Profiles were also acquired by stepping the source and geophones along the surface with a fixed separation between them (Avar and Luke, 1999).

GEOLOGY OF THE SITE

The Ohio Department of Transportation did several borings in the area. Figure 2 is a description of a boring near the middle of the site. The soil cover is very thin with as little as two feet of unconsolidated material. Below this is a three foot thick limestone unit that is not continuous across the area and then a 2 foot thick shale. This hole then encountered a three foot thick void where coal had been removed. Below that is a fireclay. The series of borings show that the depth to the coal ranges due to differences in the thickness in the soil. The reason for the discontinuous limestone is unknown but probably relates to erosion before the soil profile developed. The boring for the log shown was 62 feet south of the center line of the highway about 1/3 of the distance from the west end of the survey. The north side of the highway indicates there was material removed. If blasting occurred before removal of the material, this would effect the geophysical results producing a deeper than normal depth to competent rock.

RESULTS

Both the P and S wave seismic refraction results correlated well with the dipole-dipole 2-D resistivity. Areas of low resistivity correlated with areas where the seismic ray path was either diffracted, attenuated or the velocity reduced. In addition these areas were indicated by greater apparent depth to the refracting horizon. Because the voids are filled with moist material, the resistivity cross section shows these voids as a low resistivity (see figure 3). Where collapse is starting to occur, the seismic ray path will be traveling through zones where the roof is at least partially collapsed which will increase the attenuation and slow the velocity. This, in turn, will cause the refraction program to produce a greater apparent depth to the refractor (see figure 4). The P-wave refraction showed these areas better than the S-wave. This may be because the P-wave velocity is effected by water content and the S-wave is not. The main refractor in the area studied appears to be the underlay beneath the coal, which was a surprise. The geology of the area indicates there is a thin limestone and shale above the coal. Observation of the material at the site demonstrates that the limestone is discontinuous. Was it not present at this site? If it is present would we have seen it? We also saw a gravity low that correlated well with the mined zone. This low was substantially greater than expected. Is it possible that ground water could have removed enough of the roof material to produce the lows recorded. Ground penetrating radar provided no useful information on the mines or collapse features due to high attenuation in the clay-rich soil.

Seismic reflection has been shown to be effective for identifying subsurface voids in detailed studies. In our survey, which was designed to cover long sections of highway economically, seismic reflection did not provide useful information.

The surface wave data are being analyzed by our colleagues at the University of Nevada at Las Vegas. We do not have results to report at this time.

CONCLUSIONS

Seismic refraction (P and S wave) and dipole-dipole 2-D resistivity surveys were effective in studying the effects of mining under the highway. The Minivib did not show any significant advantage over the less expensive weight drop and hammer sources.

The intent of this study was not to model the detail of the voids or collapses but to demonstrate that geophysics would be a good reconnaissance tool to identify anomalous areas under highways where coal is known to exist below the surface and thus potential mines may exist.

ACKNOWLEDGMENT

We wish to thank the Ohio Department of Transportation (ODOT) for funding this project and especially Rich Ruegsegger from ODOT for his helpful support. We also want to thank Manooch Zoghi of the University of Dayton for his help evaluating the surface materials on Burcin Avar and Barbara Luke of the University of Nevada, Las Vegas for their work on surface waves.

REFERENCES

Avar, Burcin B. and Luke, Barbara A., 1999, Roadside application of seismic surface waves over abandoned mines: Proc.SAGEEP-99 (Oakland, CA) p. 31-40.

Hoffman, A.G., Clark, D.M., and Bechtel, T.D., 1994, Abandoned deep mine subsidence investigation and remedial design: Proc. 46th Highway Geology Symposium (Charleston, WV) p. 137 -151.

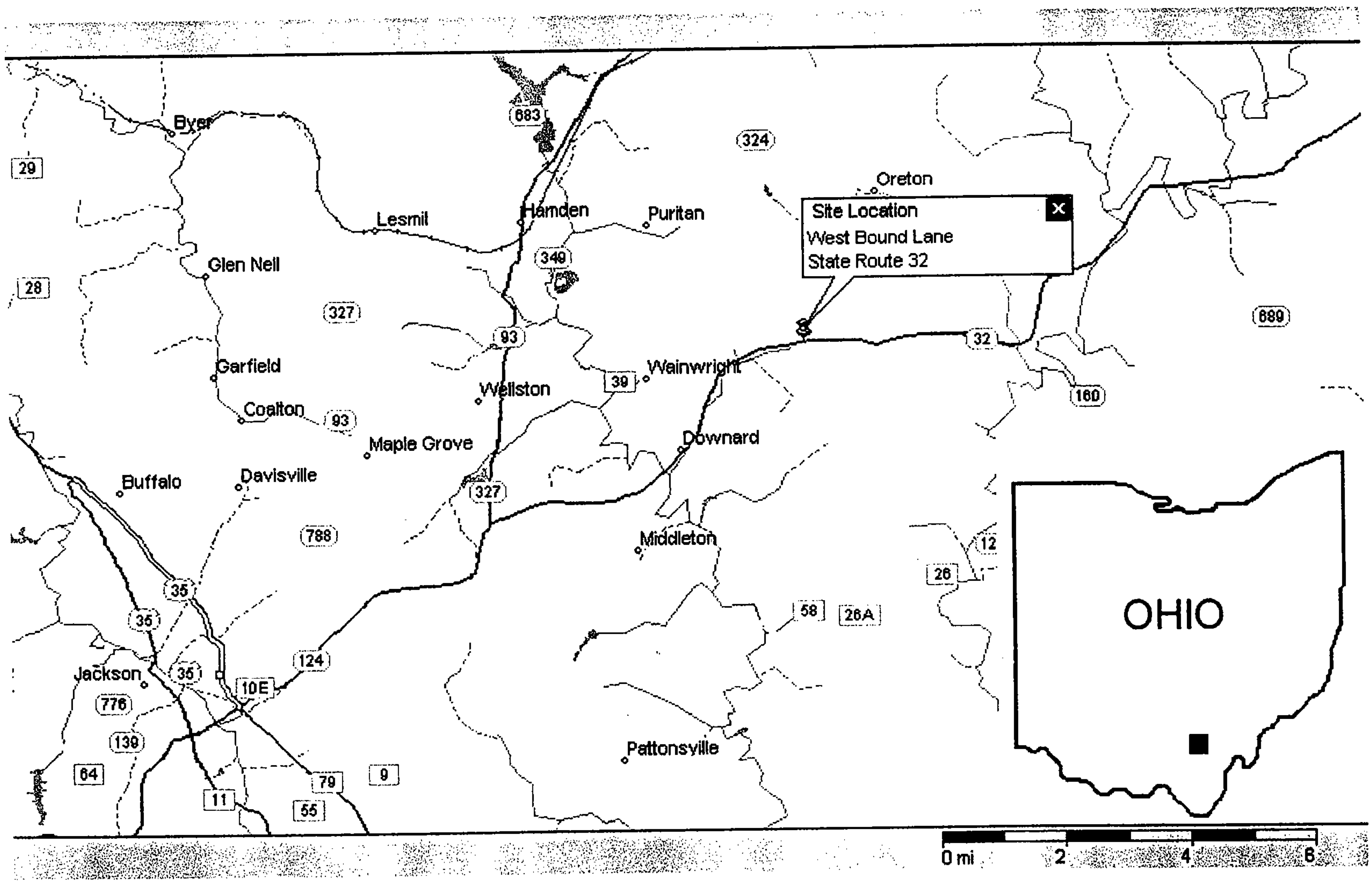

FIGURE 1 - LOCATION OF THE TEST AREA IN JACKSON COUNTY, OHIO

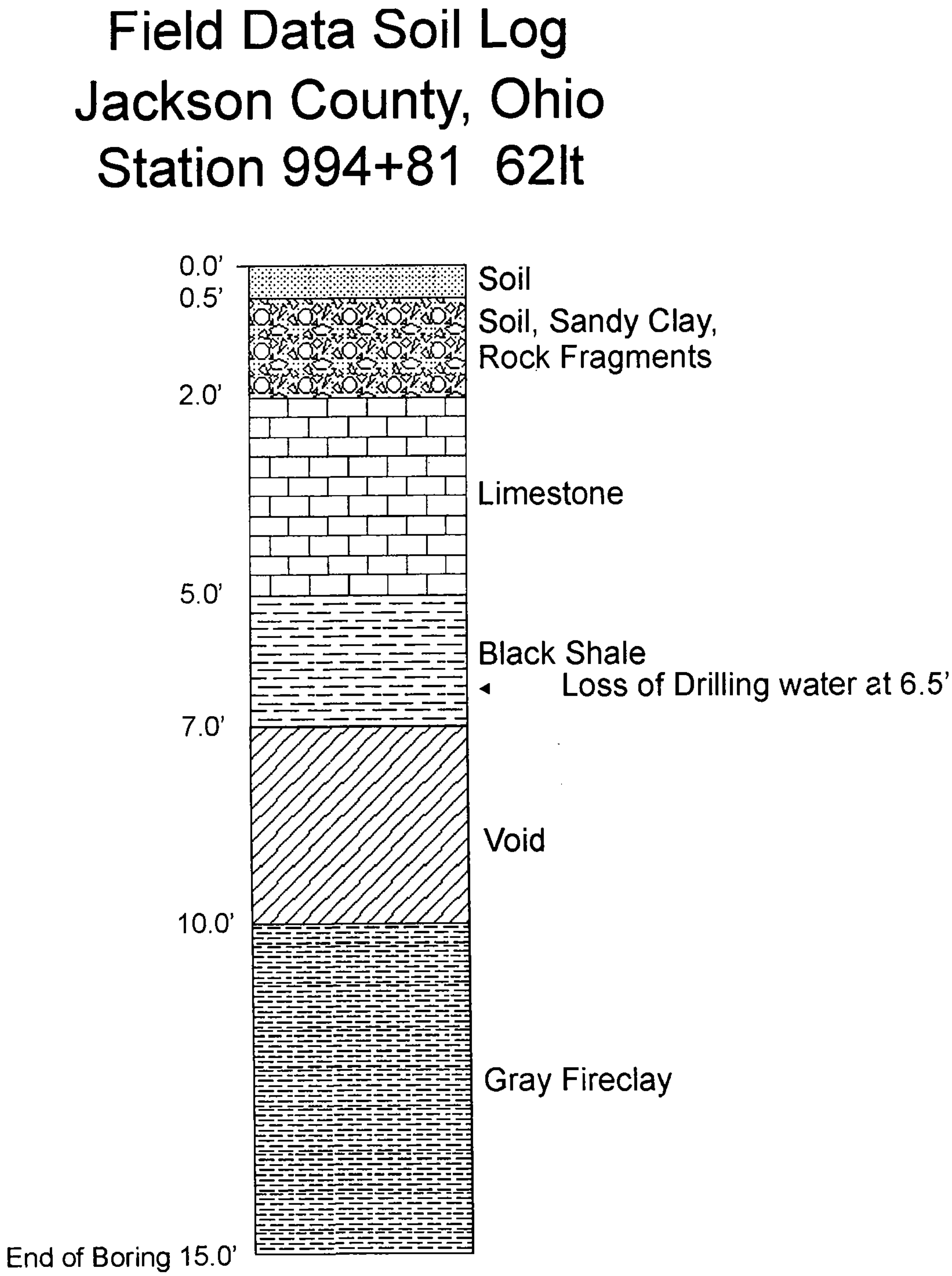

FIGURE 2 - LOG OF A BORING AT TEST SITE

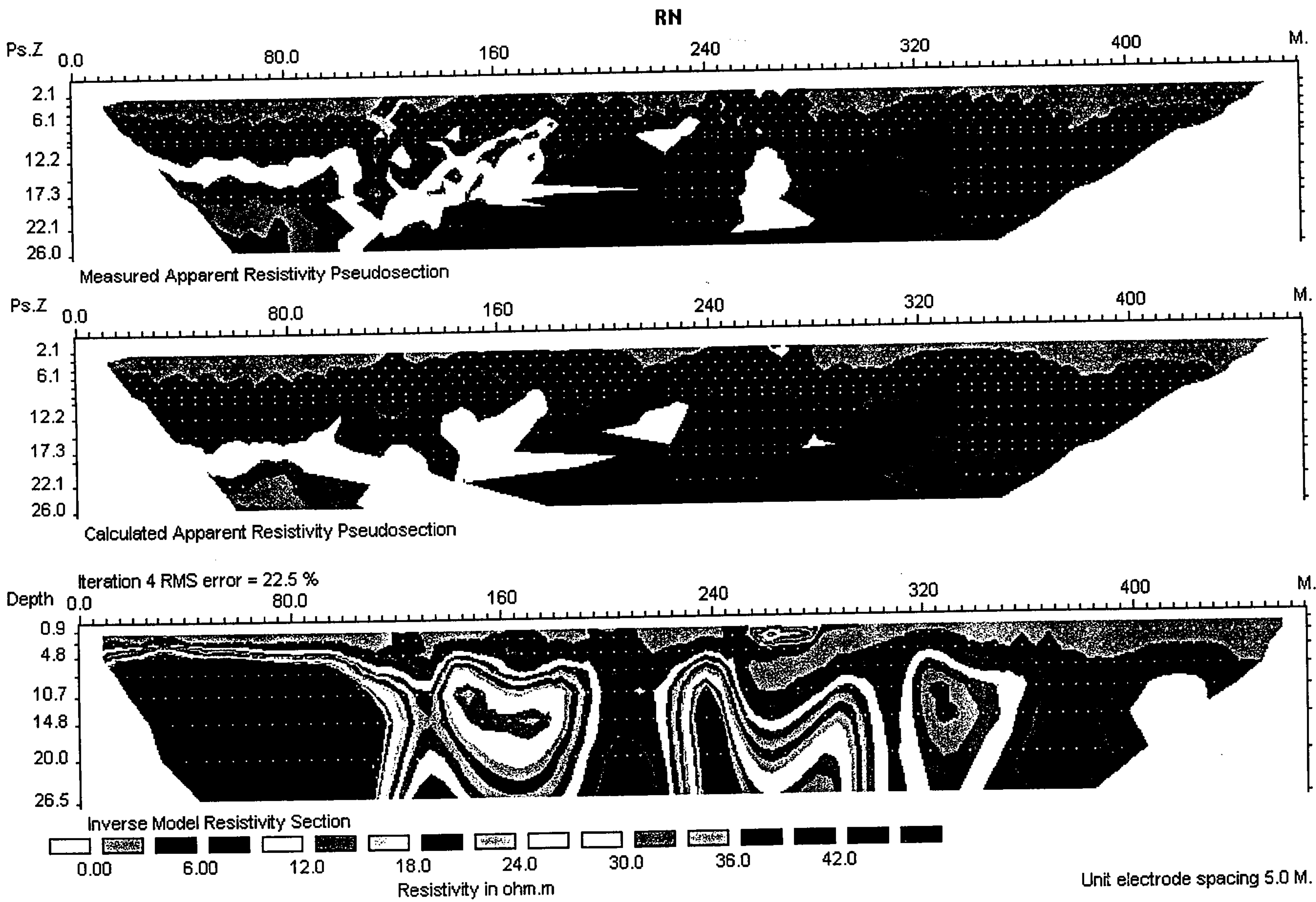

FIGURE 3 - RESISTIVITY MODEL OF THE AREA BENEATH THE HIGHWAY

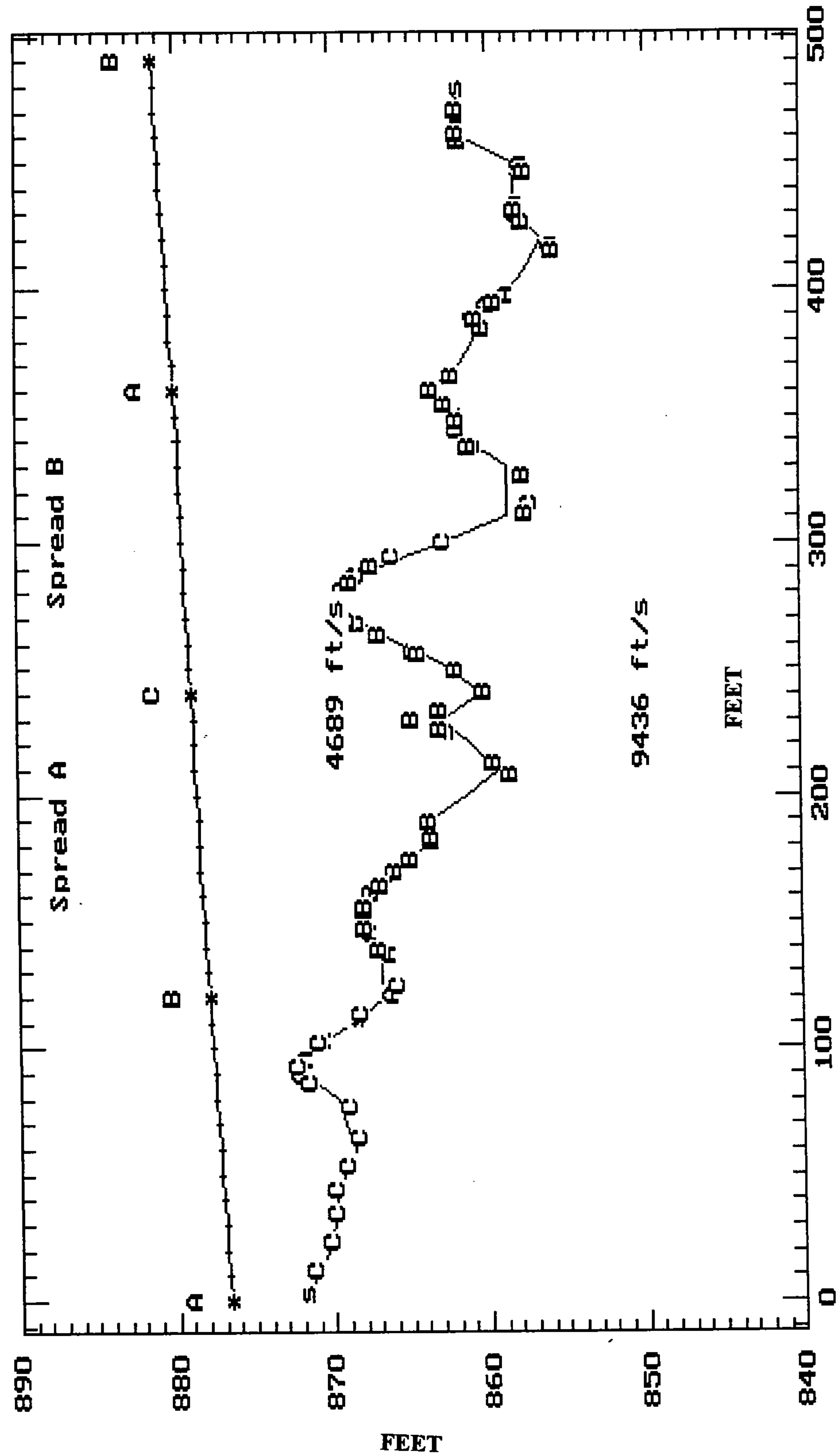

FIGURE 4 - PROFILE TO THE P-WAVE REFRACTOR BENEATH THE HIGHWAY

IN SITU TESTING ADDS VALUE TO COASTAL PLAIN FOUNDATION DESIGNS

Aaron L. Zdinak, P.E., Virginia Geotechnical Services, P.C., Richmond, VA
David A. Kaulfers, P.E., Virginia Department of Transportation, Sandston, VA
Thomas W. Pelnik, III, P.E., Virginia Geotechnical Services, P.C., Richmond, VA

ABSTRACT: Stratigraphy and engineering parameters of soils in the Coastal Plain of Virginia are difficult to characterize. Thick deposits of compressible clay soils are commonly interbedded with sand soils of varying relative density. Although the subsurface conditions are complex, many subsurface exploration programs are developed utilizing only conventional (Standard Penetration Test) borings and corresponding laboratory tests. As a result, many generalizing assumptions must be made with regard to the stratigraphy and engineering properties of the site specific subsurface soils. Foundation designs, may consequently, become overly conservative.

In situ testing has been used effectively in the Coastal Plain of Virginia for characterizing complex stratigraphy and the engineering parameters of site specific soils. Flat Plate Dilatometer, Piezocone Penetrometer, and Pressuremeter tests quickly provide geotechnical engineers with large amounts of reliable data that can be integrated into design efforts.

Two case histories (South-West Suffolk Bypass and Pinners Point Interchange) of projects in the Coastal Plain of Virginia illustrate the value in situ testing adds to specific foundation designs. Each case evaluates potential construction costs based on two comparable foundation design alternatives. One design alternative is based on the results of Standard Penetration Test borings and corresponding laboratory testing, while the other design alternative incorporates in situ testing. The large Return On Investment for the design alternative incorporating in situ test results clearly shows the benefit of supplementing SPT boring programs with in situ tests.

INTRODUCTION

The complexity of Coastal Plain stratigraphy is difficult to characterize by Standard Penetration Test (SPT) borings and is often over generalized by geotechnical engineers. As a result, many foundation designs are completed without thoroughly defining actual subsurface conditions. These designs are adequate, most of the time. Occasionally, inadequate evaluation of subsurface conditions will result in a failed pile load test, intolerable settlement, instability during construction, or maintenance problems.

Fortunately, in our experiences, "failures" do not occur with high frequency. Designs are generally deemed adequate if they perform well. However, adequacy should not be the goal of the geotechnical engineer. The geotechnical engineer should strive to provide a design that is of long lasting value to the client. Although, "value" has a client driven definition, one critical component of a good geotechnical design is low life-cycle costs.

In general, projects include both objective and subjective costs. Objective costs include those which can be directly measured (design services, construction, maintenance, etc.). Other costs are subjective (aesthetics, traffic delays, public perception, etc.). Both objective and subjective costs must be considered and evaluated prior to selecting to a particular design. This paper focuses on geotechnical design services and construction cost savings supported by in situ testing.

The South-West Suffolk Bypass and Pinners Point Interchange case histories illustrate that implementation of in situ tests result in more cost effective designs as reflected by a positive Return On Investment (ROI). The ROI is the ratio of construction costs saved to cost of additional geotechnical exploration and design work. Each case evaluates potential construction costs based on two comparable design alternatives for a specific aspect of each project. Within each case, one design alternative is based on the results of Standard Penetration Test borings and corresponding laboratory testing, while the other alternative incorporates in situ testing.

IN SITU TESTING METHODS

The Flat Plate Dilatometer (DMT), Piezocone Penetrometer (CPTU), and Pressuremeter (PMT) are three in situ tests that are used to reliably determine stratigraphy and engineering parameters of soils relative to planned construction. Figure 1 presents schematics of the DMT, CPTU, and PMT testing apparatus.

Common engineering parameters readily interpreted from DMT, CPTU, and PMT test data include settlement parameters (magnitude and time rate) and strength parameters (friction and cohesion) Soil settlement parameters, specifically Tangent Modulus (M_t) and Coefficient of Consolidation (c_v), relate a specific soil's tendency to deform and how much time such deformation will take with a specific increase in load. The effective angle of internal friction (ϕ') and undrained shear strength (S_u) relate a specific soil's ability to carry load without "failure" under drained and undrained loading conditions, respectively. Settlement parameters are used to calculate magnitude and time rates of foundation settlement. Strength parameters are used to calculate ultimate capacities of foundations.

For specific applications, in situ test results may be used with direct or indirect methods to estimate foundation settlement and allowable capacity. Soil properties are interpreted by comparing the in situ data to common correlations that have been "calibrated" to the specific site. In situ tests are often correlated to specific site conditions by comparing their results to data obtained in conjunction with a conventional SPT boring and laboratory testing program.

Briaud and Miran (1992) and Briaud (1989) developed technical reports (design manuals) for the Federal Highway Administration (FHWA) that outline the theory, interpretation, and integration of in situ test data (DMT, CPTU, and PMT) into foundation design. These reports are particularly useful to design engineers responsible for evaluating the applicability of in situ test methods relative to specific geotechnical design scenarios.

Flat Plate Dilatometer (DMT)

DMT testing consists of pushing a flat blade located at the end of a series of conventional drill rods into the soil. Practitioners in the United States commonly measure the applied vertical thrust required to advance the sampler. For each testing depth (typically every 0.2 meters), a circular steel membrane, located on one side of the blade, is expanded horizontally (1 mm) into the soil and the pressure exerted on the membrane is recorded. The operator records the pressure at three particular moments during each test; as the membrane contacts the soil, at full expansion, and upon complete deflation (Briaud and Miran, 1992).

Piezocone Penetrometer (CPTU)

CPTU testing consists of pushing a cone into the soil at a constant rate of 2 cm/s. Electronic instrumentation collects measurements of soil penetration resistance on the cone tip, soil friction on a friction sleeve, and pore pressures through a porous element (located on or just above the cone shaped tip of the penetrometer) as soil penetration progresses (Briaud and Miran, 1992).

Pressuremeter (PMT)

PMT testing (pre-bored type) consists of placing a flexible, cylindrical probe into a carefully prepared borehole and expanding the cylinder. The pressure on the soil and the relative increase in probe volume are measured. In effect, the PMT gives an in situ stress-strain curve of the soil (Briaud, 1989).

CASE HISTORIES

The South-West Suffolk Bypass project illustrates the benefits of utilizing DMT soundings to further evaluate stratigraphy and the magnitude and time rate settlement characteristics of subsurface soils. The Pinners Point project illustrates the benefit of using DMT, CPTU, and PMT data to complete deep foundation design. The benefits of in situ testing are clear in both cases.

The case histories do not represent all projects or reflect all advantages or disadvantages of in situ testing for site characterization. For each of the projects, the in situ testing supplemented a traditional SPT boring program. The results of the in situ testing were "calibrated" to the specific sites based on the SPT borings and laboratory testing program.

SOUTH-WEST SUFFOLK BYPASS

The Virginia Department of Transportation (VDOT) plans to build a four lane, limited access connector between US 13 and US 58 in the city of Suffolk, Virginia. This connector is approximately 4.4 km in length and includes seven bridges. The majority of the alignment will be constructed on embankments with heights reaching 10 meters at the bridges.

Soil Conditions

Geologically, the proposed alignment crosses the Chuckatuck and Charles City Formations. These formations are typically characterized by interbedded layers of clayey sand and sandy clay overlying silty clay with traces of shells. Foundation and soil survey borings revealed the general stratigraphy presented in Figure 2. The results of the SPT borings indicate that some of the clay below five meters in depth is highly compressible.

Design Approach

Traditionally, geotechnical engineers evaluate the compression characteristics of clay soils with laboratory consolidation tests. Based on the results of the consolidation tests, geotechnical engineers calculate the magnitude of anticipated settlement as well as the amount of time required to complete primary consolidation. Thus, a series of nine laboratory consolidation tests were run on soil samples collected from the clay (below 5 meters depth) in the vicinity of the highest embankment fills on the job.

The interpreted consolidation test results indicate a Tangent Modulus (M_t) from 2,200 kN/m^2 (23 tsf) to 5,600 kN/m^2 (59 tsf), an Overconsolidation Ratio (OCR) from 1.5 to 2.5, and a Coefficient of Consolidation (c_v) from 0.02 m^2/day to 0.07 m^2/day. Based on the results of the consolidation tests, the magnitude of settlement was calculated to be 0.2 meters to 0.5 meters. The estimated time to complete 90% of the primary consolidation settlement is at least 700 days.

The results of the consolidation tests indicate that the clay soils will consolidate sufficiently to cause downdrag loads on abutment piles installed before settlement is complete. Downdrag loads effectively negate any capacity the piles may develop within the consolidating soils. The amount of time to reach 90% consolidation, thus preventing detrimental downdrag loads, does not fit the proposed construction schedule.

To accelerate consolidation settlements, ground modification consisting of wick drains and a surcharge fill was evaluated. However, ground modification is costly. Based on the parameters obtained from the borings and consolidation tests, installing wick drains and a surcharge fill adds approximately $400,000 in direct cost to the project. In addition to the direct cost, the wick drain modified clay layer requires at least three months to reach 90% consolidation.

To further study the consolidation settlement at the highest embankments, the geotechnical engineers completed DMT soundings and dissipation tests to re-evaluate the design assumptions based on the SPT borings and the laboratory consolidation results. The M_t (magnitude of settlement) and c_v (time rate of settlement) values calculated from the DMT soundings and dissipation tests confirm the consolidation test derived values.

However, the DMT soundings identified an interbedded, thin sand layer below the compressible clay layer that was not detected in the SPT borings. A comparison of the generalized stratigraphy interpreted from the SPT borings relative to the DMT data is illustrated in Figure 2. The contrast in stratigraphic detail between the SPT and the DMT methods is primarily due to the sampling interval of both methods. DMT tests are typically performed every 0.2 meters (8-in) while SPT borings are typically sampled every 1.5 meters (5 ft).

Selected Design Alternative

The time rate of primary consolidation is based on c_v and the length of the drainage path in each layer of slow draining clay. Interpretation of the laboratory consolidation tests and the DMT results reflects similar consolidation parameters (M_t and c_v). However, the interbedded layer of sand identified by the DMT soundings supports the use of a shorter drainage path (than originally identified by the SPT borings) in the time rate calculations. As a result, the time required to complete 90% primary consolidation within the layer is less. Time to complete primary consolidation based on the DMT data is up to approximately three months, which fits the proposed construction schedule.

The contract documents specify installation of settlement plates at each approach fill and along ramps where embankment heights exceed six meters. Once construction of the embankments is complete, the settlement plates will be monitored for ninety days while the embankments settle. If the observed settlement data confirms the DMT based calculations, the abutment piles will be installed 90 days after embankment construction is complete.

Cost Savings

The calculations based on the DMT data indicate that settlement can be completed within the allotted construction schedule without implementing an expensive and time consuming ground modification program. The additional cost of completing DMT soundings, dissipation tests, and related geotechnical analyses was approximately $10,000. By comparing the cost of the additional geotechnical exploration and analyses to the avoided cost of the ground modification alternative ($400,000), a ROI of 4,000% is clear.

PINNERS POINT INTERCHANGE – ROUTE 58 BRIDGE OVER THE CSX RAILROAD

Pinners Point is a VDOT project located in Portsmouth, Virginia where the Western Branch of the Elizabeth River flows into the Elizabeth River. This project consists of a three-legged interchange connecting State Route 164, Martin Luther King Freeway (Route 58), and the Norfolk Midtown Tunnel. The project requires a new West Norfolk Bridge Extension (760 meters of overwater bridge), six new overland bridges, and widening of the existing Route 58 bridge over the CSX Railroad.

The widened Route 58 Bridge will be a four span structure with two piers. The southern abutment of the new bridge will coincide with the existing southern abutment. The new northern abutment will be approximately 15 meters north of the existing abutment. The widened bridge will be approximately 108 meters long and 64 meters wide. The abutments and piers are approximately 86 meters wide because they are parallel to the railroad and skewed with the Route 58 centerline. Adequate clearance over the railroad is maintained with embankment fills up to approximately 10 meters high.

The preliminary foundation design for the Route 58 Bridge Widening (R58BW) includes evaluation of drilled shafts. Each of the 40 drilled shaft foundations for the R58BW piers must be designed to carry vertical loads of 4,850 kN (545 tons). Vertical loads are the critical factor relative to the minimum shaft size and bearing depth. Lateral loads and potential downdrag at the abutments will be evaluated for final design.

Soil Conditions

The subsurface geology in the project area is characterized by the Sandbridge Formation, the Norfolk Formation, and the Yorktown Formation. The Sandbridge Formation consists of up to approximately 6 meters of fine to coarse sand, silty sand, and clayey sand, sometimes containing decaying plant material. The Norfolk Formation consists of gravel, sand, silt, clay, and peat deposits. This formation is up to 20 meters thick in the project area. The aggregate thickness of the compressible clay soils of the Norfolk Formation is up to 10 meters. The Yorktown Formation generally consists of silty to clayey fine sand with high strength and low compressibility. The Yorktown Formation is considered the "bearing" stratum for most deep foundations installed in the general project area.

Historical boring records and a recent SPT boring program confirm the approximate extent of each formation in the vicinity of the R58BW. Based on the results of the SPT borings, the clay soils of the Norfolk Formation are thickest in the vicinity of the R58BW (southern leg of the interchange).

In 1998, VDOT and Virginia Geotechnical Services (VGS) completed eight CPTU and six DMT soundings across the site to supplement the traditional subsurface information collected by the SPT borings. In 1999, twelve PMT tests were completed at three interchange pier locations. One CPTU and one DMT sounding are within 50 meters of the proposed Route 58 Bridge Widening (R58BW). Six of the twelve PMT tests are in the soils of the Yorktown Formation. Results of the site wide PMT tests are consistent with the DMT and CPTU test results near the R58BW.

Design Approach

The engineering parameters of primary concern relative to bridge pier foundation design for the R58BW are compressibility (soil modulus or $C_{\varepsilon c}$), stress history (OCR), and shear strength (S_u). These parameters are used to determine the appropriate foundation types considering likely settlement and allowable bearing pressure.

The clay soils of the Norfolk Formation are well suited for careful sampling and laboratory testing. Laboratory strength tests were completed on six, thin-walled tube samples of the clay collected from the SPT borings. Consolidation tests were completed on seven, thin-walled tube samples. Figure 3 summarizes the results of the SPT boring and laboratory testing program.

Laboratory strength and compression tests were not completed on samples from the Yorktown Formation. The coarse grained characteristics of the Yorktown Formation precluded obtaining quality, thin-walled tube samples. Correlations of strength and compressibility parameters of the Yorktown Formation were based on SPT N-values and soil classification data.

The average N-value documented in the R58BW SPT borings in the Yorktown Formation is 26 blows per 0.3 meters (N_{ave} = 26 blows per foot). The typical percentage of shell fragments is low and determined not to influence the N-values. Based on the drilled shaft design procedure outlined by the FHWA (1988), the allowable average unit shaft friction ($q_{fa\,SPT}$) is about 32 kN/m^2 (0.34 tsf).

Several methods (summarized in the next section) were used to calculate an allowable unit end bearing. The SPT methods are less than satisfactory because the results are highly variable. The engineers' prefer the method by Reese and O'Neill (1988). However, comparisons with other SPT based methods indicate that the Reese and O'Neill method yields unconservative results. The large range of results yields an allowable end bearing resistance ($q_{ta\,SPT}$) of approximately 224 kN/m^2 (3 tsf).

Thus, to support the design load of 4,850 kN (545 tons) utilizing the SPT derived allowable unit values, a 1.52 meter (5 ft) diameter drilled shaft must be founded 29 meters (95 ft) below the ground surface (approximately 8.5 meters into the Yorktown Formation). The controlling criterion is allowable settlement. The estimated settlement, corresponding to the SPT analysis, is less than 2.5-cm (1-in). Considering a unit cost of \$650/m^3 (\$500/yd^3), this design results in a construction cost of approximately \$1.38 million (for the 40 drilled pier shafts at the two piers).

CPTU, DMT, and PMT tests were completed to further characterize the in situ properties of the overburden and bearing stratum soils. Figure 4 compares the results of the in situ testing to the laboratory tests. The allowable unit shaft friction was determined using the CPTU data in conjunction with the method proposed by Laboratoire des Ponts et Chaussees (LPC) in France. FHWA recommends using the LPC method relative to other CPTU methods based on statistical correlations between observed (studied pile load tests) and predicted ultimate capacities (Briaud and Miran, 1992). Based on the CPTU data, the allowable average unit shaft friction ($q_{fa\,CPTU}$) was determined to be about 30 kN/m^2 (0.31 tsf). The CPTU derived unit shaft friction is comparable to that determined with SPT data.

The allowable unit end bearing ($q_{ta\,insitu}$) was calculated using the LPC method and M_t data obtained directly from the in situ tests. The M_t data was used in settlement analyses with a limiting settlement of 2.5-cm (1-in). The calculations based on CPTU correlations have significant variation. The engineers' judgment is that the DMT, PMT, and SPT (Reese and O'Neill) methods yield the most reasonable results. The in situ tests confirm the higher end of the SPT based calculations and enable design for a higher end bearing resistance and smaller shaft diameter.

Based on in situ tests, the allowable unit end bearing is nearly 275% higher than the allowable value developed exclusively from the SPT data. To support the design load of 4,850 kN (545 tons) utilizing the in situ confirmed allowable unit values, a 1.37 meter (4.5 ft) diameter drilled shaft must be founded 30 meters (100 ft) below the ground surface (approximately 10 meters into the Yorktown Formation).

Selected Design Alternative

Martin et al. (1987) and Mayne (1989) indicate the Yorktown Formation has time-dependent strength characteristics and is sensitive to disturbance by conventional SPT sampling. In situ strengths of the Yorktown Formation soils are often higher than indicated by SPT N-values. Therefore, standard correlations between SPT N-values in the Yorktown Formation often result in overly conservative designs.

The allowable unit end bearing resistance confirmed by the in situ test methods results in a smaller shaft than the design based exclusively on SPT data. The following table summarizes the results of the SPT and in situ methods used to calculate the allowable unit end bearing.

Summary of Unit End Bearing Calculations

Unit End Bearing Analysis Method	Low Value (kN/m^2)	High Value (kN/m^2)	Trend (kN/m^2)
SPT Methods			
AREA Manual, Volume 2 (1996)	---	---	153
NAVFAC, DM-7.2 (1983)	---	---	211
Meyerhof (1976)	326	565	441
Reese and Wright (1977)	680	1,178	910
Reese and O'Neill (1988)	613	1,063	824
Average SPT Unit End Bearing ≈ 599 kN/m^2	Std. Deviation ≈ 375 kN/m^2	**Recommended ≈ 224 kN/m^2**	
In Situ Methods (Including SPT Methods)			
SPT - Reese and Wright (1977)	680	1,178	910
SPT - Reese and O'Neill (1988)	613	1,063	824
CPTU (Briaud and Miran, 1992)	546	1,015	---
DMT (Briaud and Miran, 1992)	---	---	766
PMT (Briaud, 1989)	---	---	881
Average of In Situ Unit End Bearing ≈ 842 kN/m^2	Std. Deviation ≈ 228 kN/m^2	**Recommended ≈ 614 kN/m^2**	

Notes:
- Recommended values shown are one standard deviation below the mean value.

When used for design, both of the recommended allowable unit end bearing values yield effective foundation systems. However, if in situ tests were not completed, the design engineer is faced with recommending an allowable end bearing as low as 153 kN/m^2 (1.6 tsf) and as high as 1,178 kN/m^2 (12.3 tsf). The closer data spread of the in situ test methods gives the designer a much higher level of confidence in selecting an allowable bearing pressure. Thus, 1.37 meter (4.5 ft) diameter shafts founded 30 meters (100 ft) below the ground surface are recommended for preliminary design.

Cost Savings

A reduction in shaft diameter of 0.15 meters seems marginal. However, a 0.15 meter reduction in diameter correlates to a reduction of approximately 17% of the design shaft volume. This corresponds to a savings of over $200,000 in construction costs for the 40 drilled shaft pier foundations. The additional cost of the in situ testing and associated geotechnical analyses completed in connection with the R58BW were less than $4,000. This additional work shows a ROI of approximately 5,000% ($200,000 construction savings with $4,000 worth of additional testing and geotechnical analyses).

SUMMARY

Geotechnical engineers are hired to provide foundation solutions for their clients. Clients rely on a geotechnical engineer's judgment, experience, and technical expertise to develop an economic, structurally sound foundation. Geotechnical engineers should consider the impact of their design on construction costs when negotiating design phase services, and should educate the client to not be content with an expensive, "adequate" design. In situ testing methods, when applied appropriately, can reduce the uncertainty in characterizing complex subsurface conditions and soil properties. By more thoroughly characterizing the subsurface, geotechnical engineers may develop designs based on specific site conditions and not general correlations.

In situ testing yields detailed data for approximately the same fee of SPT borings and associated laboratory work. In situ test data may be used for design within hours of completing a test as compared to several days or weeks with conventional SPT sampling and laboratory testing. When completed by properly trained personnel, in situ test methods will produce quality data with less statistical variation than conventional SPT borings.

The two case histories demonstrate the tremendous Return On Investment (4,000% to 5,000%) that is possible when in situ testing is used correctly. Numerous other case histories could be cited to support the same conclusion: when used appropriately, in situ testing adds value to coastal plain foundation designs. As knowledge of subsurface conditions and soil properties increase at a specific site, so should the efficiency of the design. Geotechnical engineers who understand the capabilities and limitations of in situ testing can ultimately provide a more economical design for the traveling public.

REFERENCES

[1] Briaud, J-L. (1989). *The Pressuremeter Test for Highway Applications*. Report No. FHWA-IP-89-008. Federal Highway Administration. U.S. Department of Transportation.

[2] Briaud, J-L., and J. Miran (1992). *The Flat Plate Dilatometer Test.* Report No. FHWA-SA-91-044. Federal Highway Administration. U.S. Department of Transportation.

[3] Briaud, J-L., and J. Miran (1992). *The Cone Penetrometer Test.* Report No. FHWA-SA-91-043. Federal Highway Administration. U.S. Department of Transportation.

[4] Clarke, B. (1995). *Pressuremeters in Geotechnical Design*. Blackie Academic & Professional, London. 20.

[5] Electrical Power Research Institute (1990). *Manual on Estimating Soil Properties for Foundation Design.* EPRI EL-6800, Project 1493-6, Final Report. Cornell University, Ithaca New York. 4-37.

[6] Federal Highway Administration (1988). *Drilled Shafts: Student Workbook.* Publication No. FHWA HI-88-042. Federal Highway Administration.

[7] Lunne, T., P. Robertson, and J. Powell (1997). *Cone Penetration Testing in Geotechnical Practice.* Blackie Academic & Professional, London. 71-72.

[8] Martin, R., J. Seli, G. Powell, and M. Bertoulin (1987). Concrete Pile Design in Tidewater Virginia. *Journal of Geotechnical Engineering.* 113(6). American Society of Engineers.

[9] Mayne, P. (1995). Profiling Yield Stresses in Clays by In Situ Tests. *Transportation Research Record No. 1479, Engineering Properties and Practice in Overconsolidated Clays.* Transportation Research Board. National Academy Press, Washington, D.C.. 45.

[10] Mayne, P. (1989). Site Characterization of Yorktown Formation for New Accelerator. *Foundation Engineering: Current Principles and Practices.* Volume 1. American Society of Civil Engineers.

[11] Meyerhof, G. (1976). Bearing Capacity and Settlement of Pile Foundations. *Journal of Geotechnical Engineering.* 102(3). American Society of Civil Engineers.

[12] Reese, L. and S. Wright (1977). *Drilled Shaft Manual – Construction Procedures and Design for Axial Loading*, Volume 1, United States Department of Transportation, Implementation Division, HDV-22, Implementation Package 77-21.

[13] Strutynsky, A. (1999). *STRATIGRAPHICS Marketing Brochure.* Glen Ellyn, Illinois.

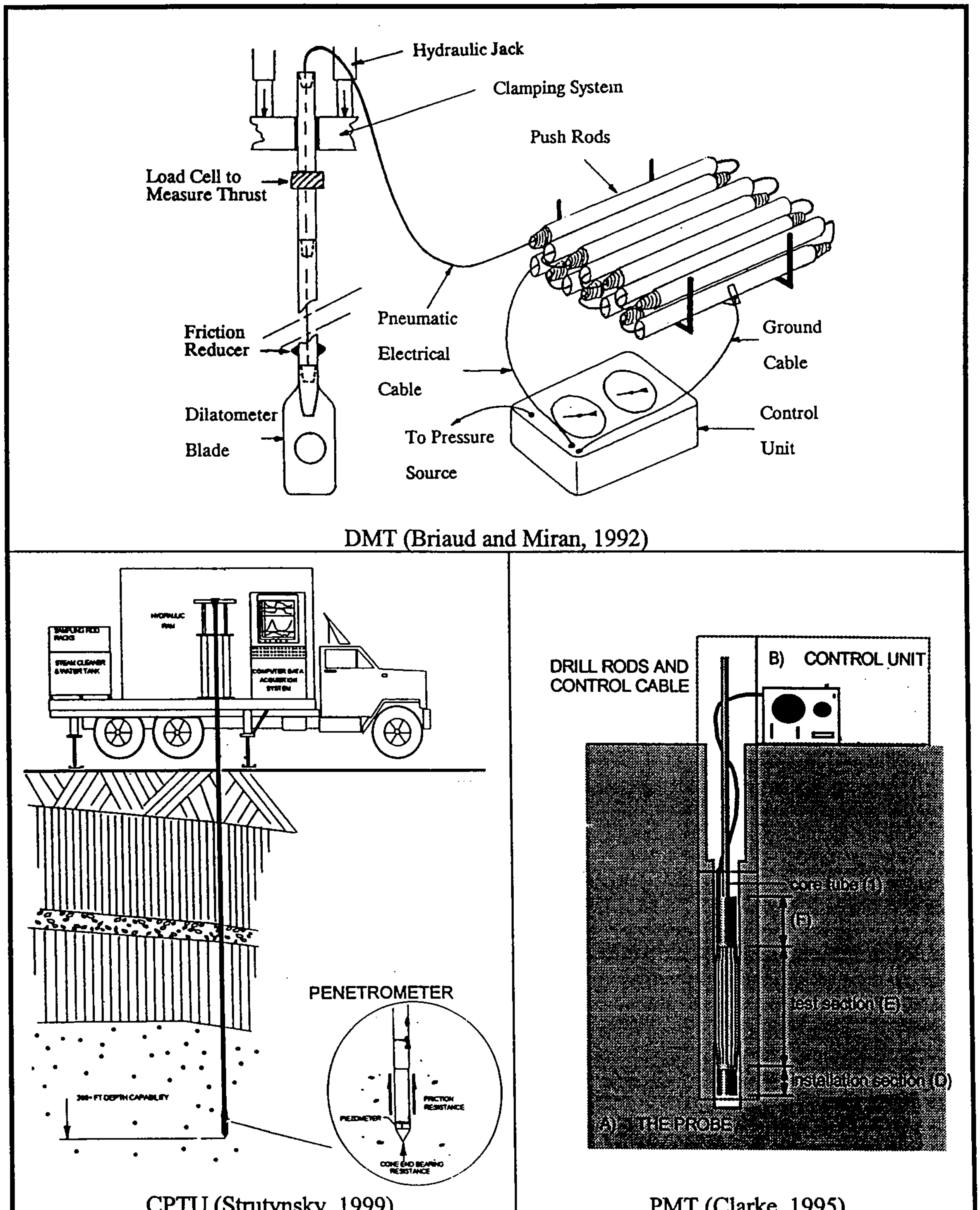

Figure 1: Schematic of DMT, CPTU, and PMT Testing Apparatus

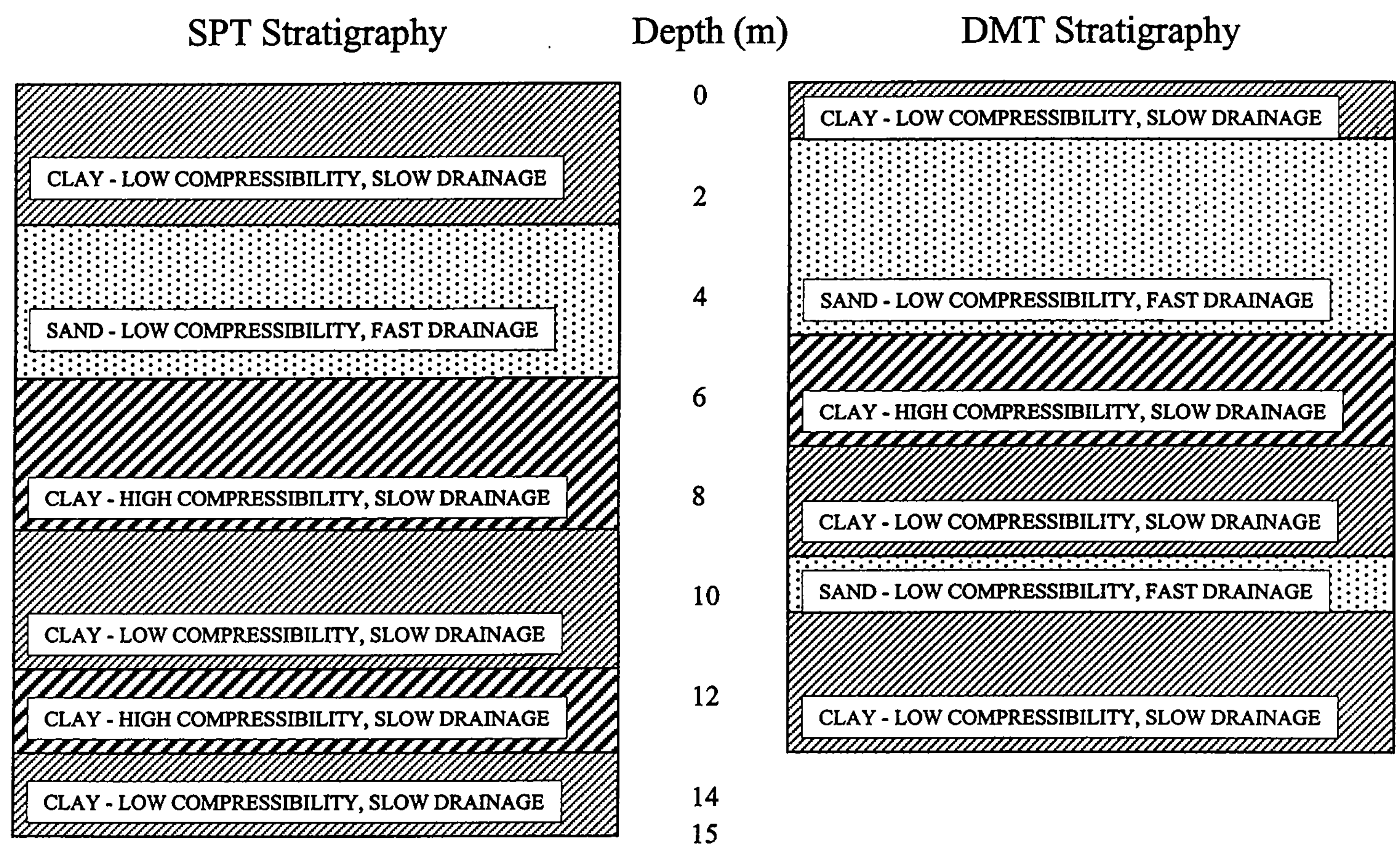

Figure 2: Comparison of Stratigraphy Characterized by SPT and DMT Test Methods
South-West Suffolk Bypass

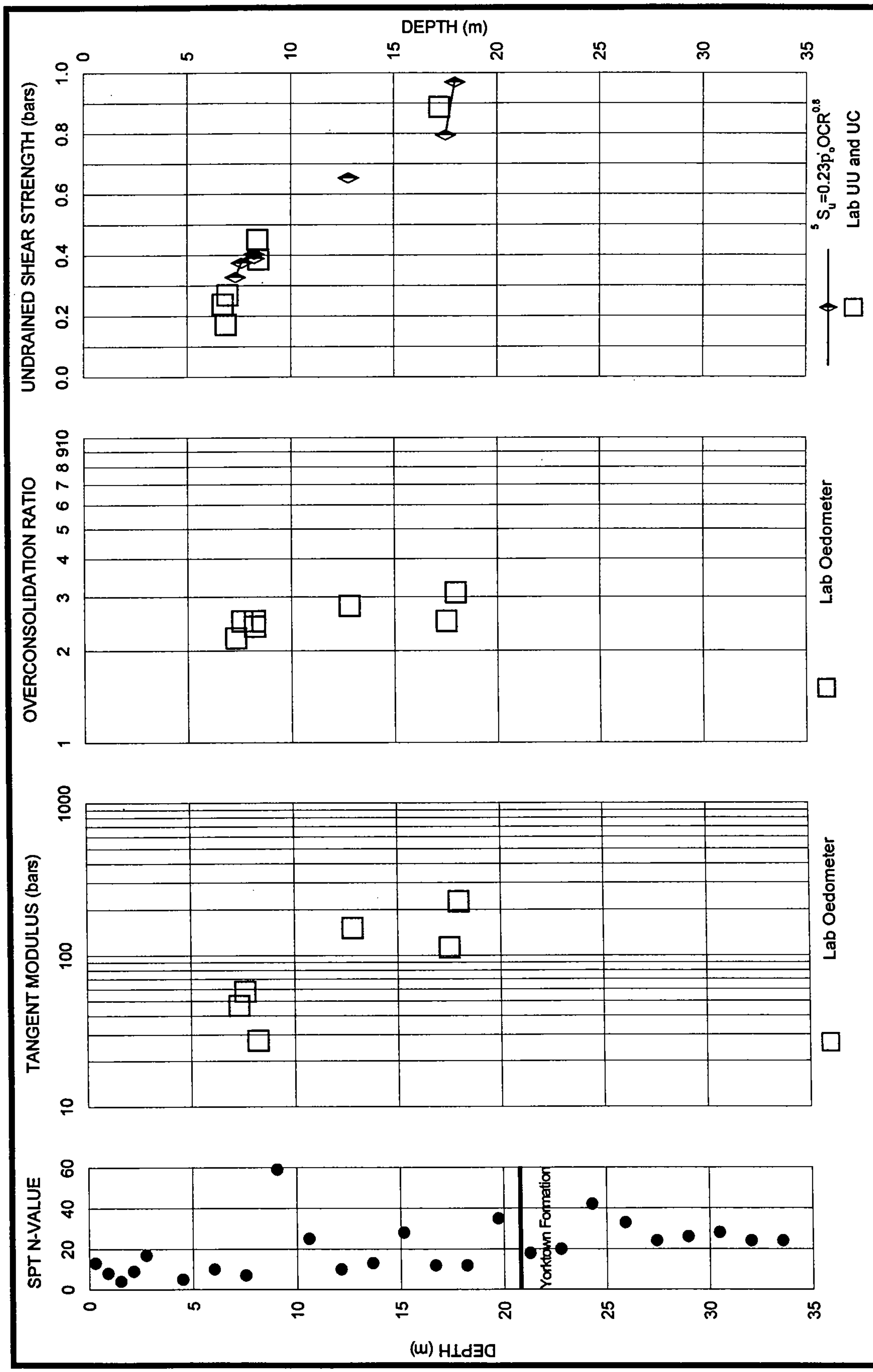

Figure 3: Summary of SPT Boring and Laboratory Data -Route 58 Bridge Over CSX Railroad

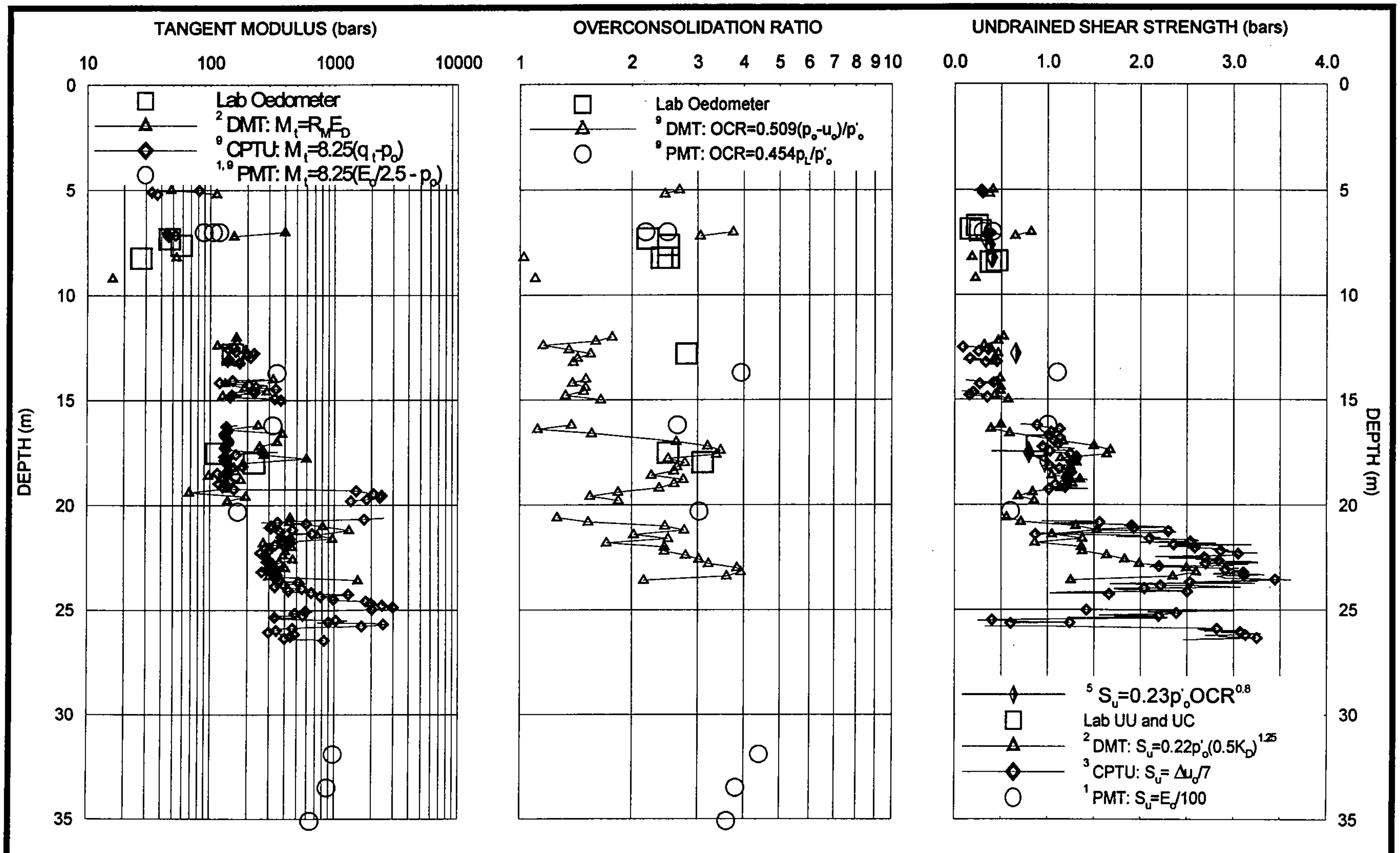

Figure 4: Comparison of Laboratory and In Situ Test Results - Route 58 Bridge Over CSX Railroad

Use of Environmental Site Assessments to Facilitate Roadway Design and Construction in the Church Street Urban Corridor, Norfolk, Virginia

David M. Sayre, P.G., Virginia Geotechnical Services, P.C., Richmond, Virginia

Bill Nash, P.E., Kimley-Horn Associates, Inc., Virginia Beach, Virginia

ABSTRACT

The City of Norfolk is currently widening Church Street from Goff Street to 33rd Street. This project is upgrading 6,500 feet of two-lane urban roadway to four lanes. The City of Norfolk, Virginia Department of Transportation, and design consultants recognized a significant potential for construction problems associated with the environmental impact of over 100 years of property use as residential, commercial, and industrial real estate. These concerns were magnified by knowledge of regional geology characterized by sandy near-surface soils with high permeability and shallow groundwater. The design team completed 168 Phase I Environmental Site Assessments (ESAs) prior to selection of the alignment for the widening. The Phase I ESAs allowed the design team to select an alignment that avoids the most significantly impacted sites.

We performed Phase II ESAs on 24 properties after the preliminary alignment was selected to identify the nature of environmental impact of the highest risk sites. A construction management plan was developed to deal with documented contamination of soils and groundwater at impaired sites. Knowledge of the local geology obtained from research and site specific studies facilitated the design of the construction management plan. The Virginia Department of Environmental Quality participated in the environmental analysis of the project and gave regulatory approval and concurrence for planned construction activities.

Completion of the ESAs prior to right-of-way acquisition and design provided a number of economic and operational benefits to the project. The highest risk sites were identified and avoided. The early environmental studies reduced the possibility of acquiring properties that could require costly remediation. Property values could be more accurately determined based on extent of impairment. The construction management plan reduced the cost associated with excavation, storage, and disposal of contaminated media. Construction delays resulting from encountering unexpected contamination were avoided. Comprehensive planning and management of potential environmental hazards protected human health and the environment.

PROJECT DESCRIPTION

In 1994 VIRGINIA GEOTECHNICAL SERVICES P. C. (VGS) and Kimley-Horn and Associates participated on a design team for the City of Norfolk, Virginia to design the Church Street Widening Project. Church Street was to be widened from a two-lane undivided urban roadway to a four-lane divided profile. The project extended from Goff Street on the south to 33rd Street on the north and included two major intersections at Broadway Street and at Granby Street. The alignment was approximately 6,500 feet in length. Previous roadway reconstruction projects in the City of Norfolk encountered numerous schedule delays and budget overruns caused by the discovery of environmental contamination during construction.

VGS prepared Phase I and Phase II Environmental Site Assessments for the Church Street Corridor. The corridor was defined as 100 feet on either side of the centerline of Church Street. Several additional blocks were included in the study in the vicinity of the Broadway and Granby Street intersections. VGS completed Phase I ESAs during the pre-design phase of the project prior to selection of a preliminary alignment. This allowed the design team to identify and avoid the most potentially impaired sites.

Phase II ESAs were completed during the design phase after selection of the alignment. This allowed the design team to develop a quantitative understanding of the nature and extent of contamination of property that would be acquired during the procurement of the right-of-way. Specific knowledge of site impairment was also useful during construction planning and implementation.

SITE LOCATION AND DESCRIPTION

Norfolk is located on the Chesapeake Bay, south of Hampton Roads, in an area frequently described as "Tidewater" Virginia (Drawing Number 1). The site is located in the south-central part of the City of Norfolk, Virginia. The area surrounding the site is a mixture of residential, commercial, and industrial properties. A tributary to the Lafayette River is located approximately 1,000 feet east of the Church Street Corridor. The Lafayette River itself is located about 2,200 feet east of the site. The Eastern Branch of the Elizabeth River is located approximately 1.2 miles south of Goff Street.

Church Street is a throughway for traffic from Interstate 64 to the economically revitalized and renovated portions of downtown Norfolk. Church Street south of the project area has been recently widened and beautified. The first urban development in the project area occurred in the southern portion and was documented on an 1887 Sanborn Fire Insurance Map. A long history of development was documented by the record research during the preparation of the Phase I ESAs. The study area included vacant lots, commercial, residential, and industrial properties. The golden years of the Church Street Corridor occurred some time in the past and the area could be described as one suffering from urban decline.

The site is located in the Coastal Plain geologic province of Virginia. The Coastal Plain is characterized by a wedge of recent to late Cretaceous age unconsolidated sediments starting at the Fall Zone to the west and thickening to several thousand feet along the Atlantic coast. The unconsolidated sediments dipping to the east consist of interbedded layers of clay, silt, sand, and gravel. Subsurface formations are frequently semi-consolidated or partially cemented and contain deposits of marine shells and/or glauconite. The thick wedge of sediments beneath the study area is underlain by Precambrian to late Paleozoic crystalline basement. Drawing Number 2 shows the relationship of the site to the Coastal Plain geologic features.

A water supply well drilled two to three miles northeast of the site encountered bedrock at approximately 2,700 feet. Several significant aquifers are located within permeable subsurface strata of silt, sand, and gravel. The site is underlain by the upper Pleistocene age Lynnhaven Member of the Tabb Formation. The Lynnhaven Member is approximately zero to twenty feet in thickness and is composed of pebbly to cobbly, fine to coarse gray sand grading upward into clayey and silty fine sand and sandy silt. Locally, medium to coarse cross-bedded sand and clayey silt containing abundant plant material fill channels cut into underlying stratigraphic units. The Lynnhaven Member is underlain by approximately 800 feet of similar mid-Quaternary age fluvial and marine deposits

Seven major aquifers underlie the site: the Columbia, Yorktown-Eastover, Chickahominy-Piney Point, Aquia, Upper Potomac, Middle Potomac, and Lower Potomac aquifers. Shallow groundwater beneath the site is part of the unconfined Columbia Aquifer. The Columbia Aquifer is also referred to as the Water Table or Quaternary Aquifer. The Columbia Aquifer (thickness: 20 - 30 feet) is underlain by the semi-permeable Yorktown confining unit (thickness 20 - 30 feet). Confining units between major aquifers are frequently composed of glauconitic silt and clay. The semi-permeable, compressed, and partially cemented sediments greatly retard the vertical migration of groundwater between water-bearing formations. The aquifers below the Columbia are considered confined water bearing units. Four water supply wells are located near the study area at depths of 75, 135, 735, and 830 feet.

The long history of previous site use and the presence of relatively high-risk commercial and industrial businesses along the corridor suggested that significantly impaired sites could be present. The knowledge that the regional geology was characterized by sandy near-surface soils with high permeability and shallow groundwater increased the design team's and project owners' desire to explore the environmental impact of past activities near the project site.

Drawing Number 1
Site Location Map Showing Major Roads

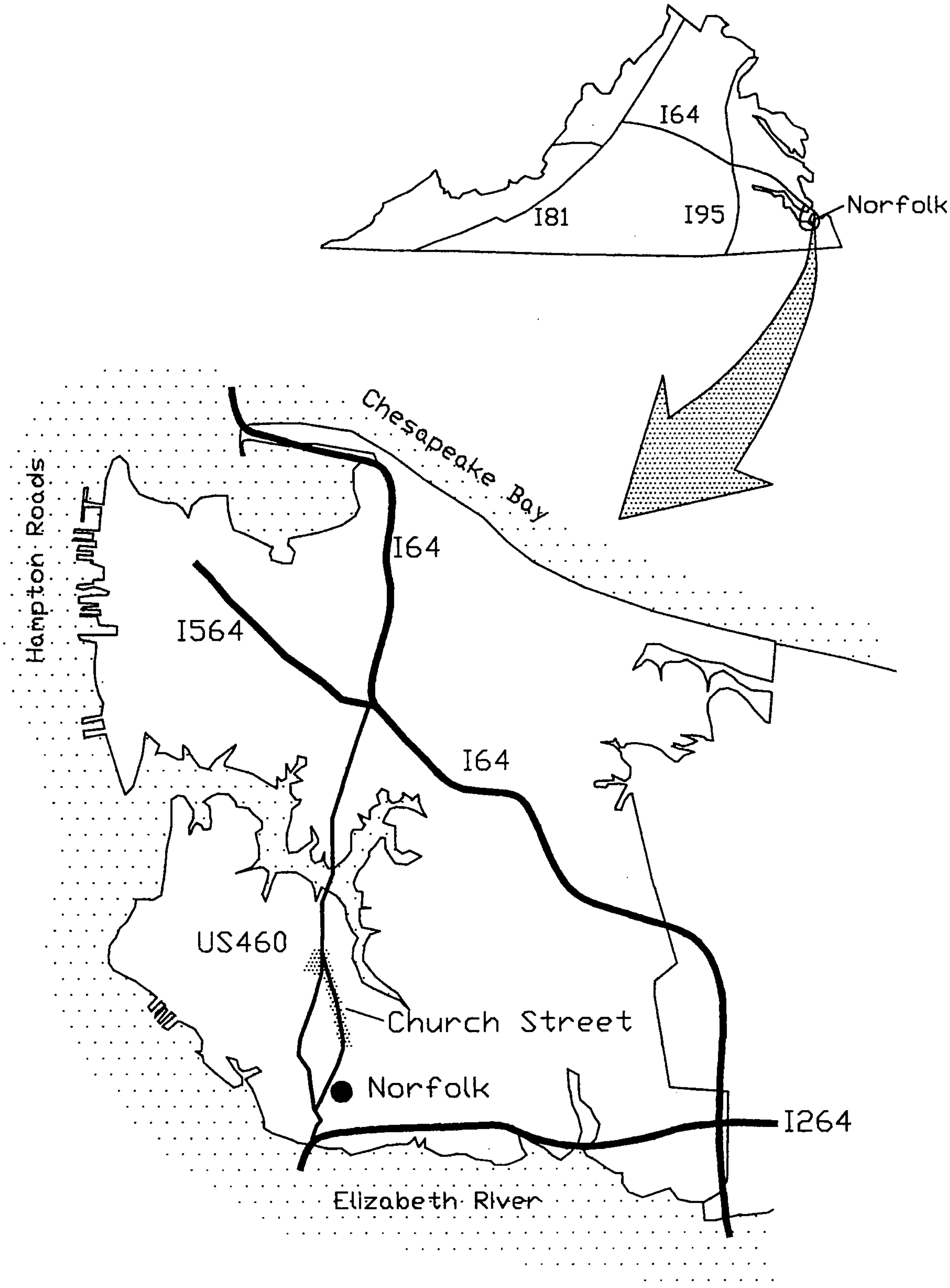

Drawing Number 2
Geologic Setting of the Church Street Project

Geologic Provinces of Virginia

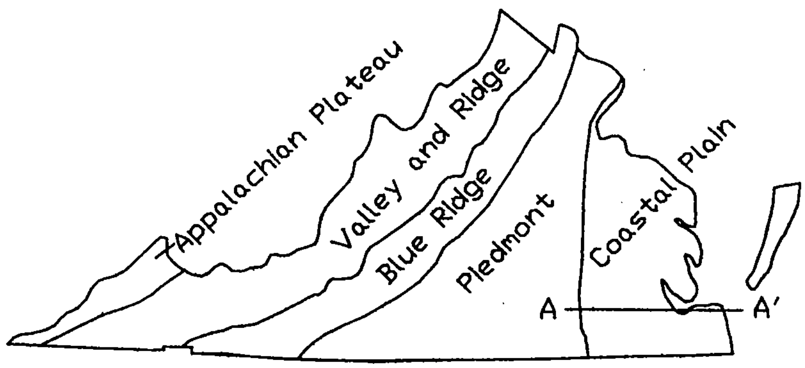

Generalized Geologic Cross Section

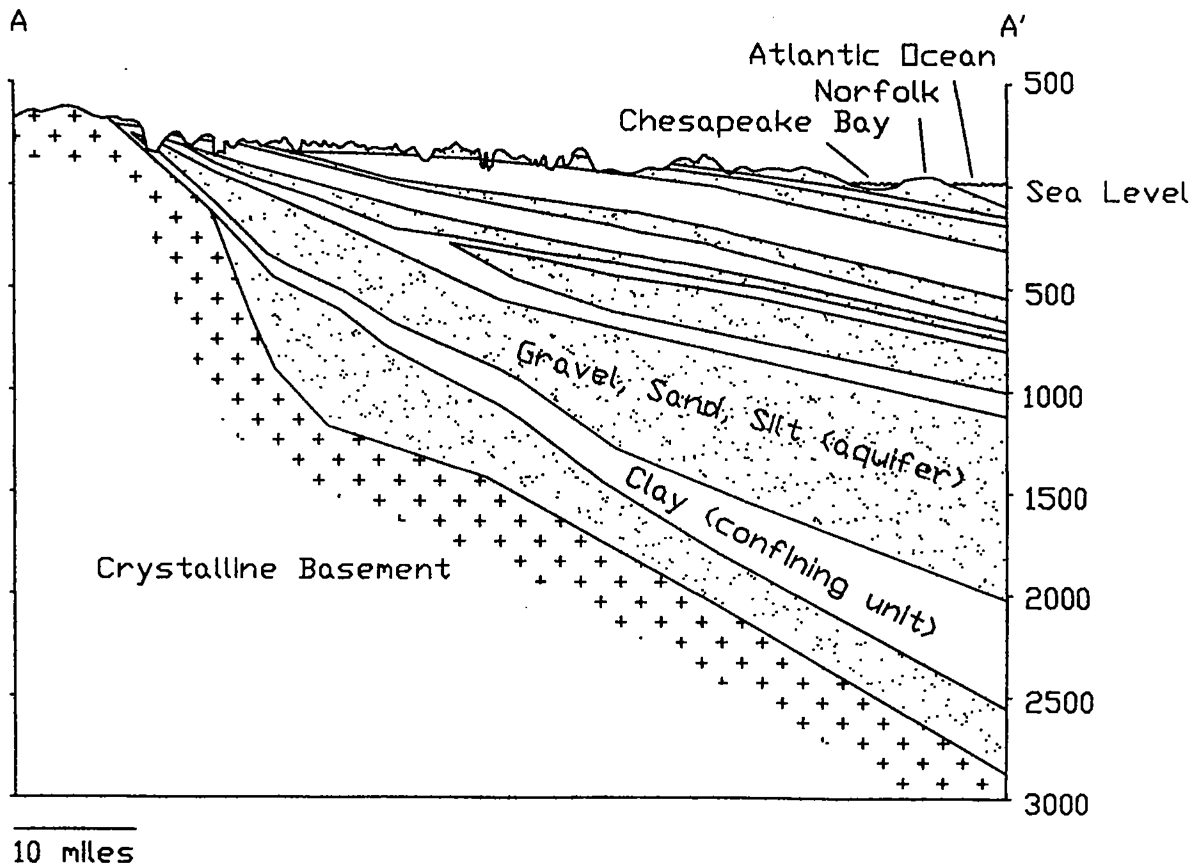

PHASE I ENVIRONMENTAL SITE ASSESSMENTS

The Phase I ESAs were conducted to identify known or potential sites which might be contaminated or adversely environmentally impacted. The Phase I ESAs included records research and on-site interviews and observations. Phase II strategies for sampling and characterizing known or potentially impacted sites were developed during the Phase I ESA. One hundred sixty-eight Phase I ESAs were completed. Table Number 1 shows the number of Phase I ESAs completed for various types of properties.

Table Number 1:
Church Street Corridor Phase I ESA

Property Use	**Number of Phase I ESAs**
Commercial	72
Church	7
Residential	55
Vacant	34
TOTAL	**168**

VGS personnel conducted office research prior to conducting site visits. The Phase I ESAs were completed in pre-design, prior to survey and title research of the alignment. Property boundaries were not available prior to conducting fieldwork. VGS reviewed aerial photography collected for survey to identify sites for Phase I activities. City blocks were numbered and sites were given letter designations to organize research and field activities. We also contacted various state, city, and private agencies to gather information on the sites during the record research. Table Number 2 shows the various agencies contacted and the information obtained.

Table Number 2
Sources and Types of Information for Phase I ESAs

Agency	Available Information
Virginia Department of Environmental Quality, Water Division	UST, Incident Reports
Virginia Department of Environmental Quality, Waste Division	RCRA, CERCLA, Solid Waste, Incident Reports
Virginia Department of Environmental Quality, Air Division	Permits, Incident Reports
Virginia State Library	Sanborn Fire Insurance Maps
Virginia Department of Transportation	Aerial photographs past and present
Virginia Department of Mineral Resources	Geologic literature
Fire Marshall, City of Norfolk Fire Department	HAZMAT incidents, Fires
Health Department, City of Norfolk	Miscellaneous complaint reports: litter, pests, pets, junk cars, dumping
Virginia Natural Gas	Utility Maps
C&P Telephone	Utility Maps
City of Norfolk Water and Sewer	Utility Maps
City of Norfolk Public Utilities	Trolley Maps

Record research identified many past and present potential contaminant sources. Past commercial and industrial sites that are not currently observable on the corridor include a brewing company, a public school, a trolley car barn (horse-drawn rail trolley), a motor truck warehouse, a bagging and tie manufacturer, a sheet metal facility, a hotel, a bowling alley, vulcanizing, dye works, coal and wood yard, autos and wagons, lumber company, and ice factory. Existing facilities included residential, commercial, restaurants, gasoline stations, car washes, automotive repair facilities, laundry, dry cleaning, steel fabrication, paper recycling, and roofing companies.

Numerous site visits were conducted to perform on-site assessments of each property. Assessment activities included interview of a site representative, observations of site conditions, and documenting observations with site photography. An attempt was made to interview a site representative at each site. In some cases, it was necessary to conduct a telephone interview at a later date. Interviews may not have been completed if sites were abandoned, site representatives could not be identified, or site representatives were unwilling to speak with interviewers.

Standard forms were developed to facilitate and standardize data collection. A Block Observation Form was completed for each city block giving a general description of bounding sites/streets, buildings, vacant properties, topography, and surface water flow direction (drainage). An on-site questionnaire was completed for each site identified from aerial photography. The questionnaire included general information about the site and site operations, and adjacent properties from interviews with site contacts. A detailed questionnaire was completed for high-risk industrial and commercial sites or potentially contaminated sites. The detailed questionnaire included specifics regarding the use and disposal of hazardous materials and wastes. A site observation form was also completed for each site. The site observation form was a checklist that considered 26 site characteristics such as: presence of hazardous materials, waste material, evidence of spills or stains, stressed vegetation, drainage, tanks, and etc. Descriptive comments were recorded for any item checked on the form. Photographs of every site were taken to show the site and document observations of potential environmental impairment.

Information obtained from record research, interviews, and observations were used to identify and evaluate potential contaminants and sources of potential contaminants. Some potential contaminants were so likely to be present at numerous sites with a hundred-year development history, that we did not believe that identification of all potential sources of these contaminants was likely. These contaminants or wastes were commonly used in urban environments at different times in the past. Contaminants from non-specific sources included those which we felt were likely to be encountered at any point along the alignment regardless of documented site history. Contaminants from non-specific sources included asbestos, lead based paint, fuel oil, coal ash and cinders, pesticides, herbicides, polychlorinated biphenyls, and household hazardous wastes.

Thirty-five specific sites were identified with documented sources of potential contaminants. Specific types of sources were identified: laundries, UST sites and repair facilities, roofing companies, and miscellaneous. Sites with potential impairment were grouped by industry. Table Number 3 shows the distribution of identified sites of concern in the various categories. Some of the 35 sites were listed as potential sources in more than one category.

Table Number 3

Sites of Concern by Category

Source Type	Number of Sites
UST Site and Auto Repair	32
Miscellaneous	6
Laundries	3
Roofing Companies	3

A list of potential contaminants was developed for each group of sites. Based on the list of potential contaminants from non-specific and specific sources a limited scope qualitative risk assessment was developed. The risk assessment identified possible receptors, identification of exposure pathways, qualified possible exposure levels, and evaluated the risk of exposure to environmental media during roadway construction activities. Sites were ranked based on the risk assessment and graphically represented on maps (Drawing Number 3a).

Phase II sampling strategies were developed for further study of potentially impacted sites. The design team felt that avoiding sites with potential impairment was a valid strategy for reduction of risk associated with the project. Potentially impacted sites which could not be avoided were proposed for Phase II ESAs. One site was identified by Phase I ESAs as potentially the most significant environmental hazard on the alignment.

Based on the results of the Phase I ESAs and other design criteria, the design engineer and the City of Norfolk agreed on a proposed alignment for the roadway improvements.

PHASE II ENVIRONMENTAL SITE ASSESSMENTS

After selection of the proposed alignment and preparation of design plans, plans were reviewed and 23 sites were identified which fell within the limits of right of way acquisition (Drawing Number 3b). Phase II ESAs involve collection of samples from various environmental media, chemical analysis of the samples and analysis of the resulting data. The purpose of the Phase II ESA is to further understand the nature and extent of contamination. Data analysis included qualitative risk assessment and remediation assessment.

We developed three scopes of services for site investigation at Phase II sites. Table Number 4 details the scope of services for various sites.

Table Number 4

Scope of Services for Phase II ESAs

Scope	UST Site 17	Roofing Companies 3	Repair/ Miscellaneous 8
Confirm UST presence	X		
3 Hollow Stem Auger borings	X		
Collect surface soil samples	X	X	X
Collect subsurface soil samples	X		
Collect groundwater samples	X		
Document all field activity	X		
Preparation of detail report	X		
If free product encountered or contamination obvious			
Install, develop, and sample monitoring wells	X		
Subcontract chemical analysis			
Total Petroleum Hydrocarbons	X	TCLP	X
Benzene, Ethylbenzene, Toluene, Xylene	X		
Volatile Organic Compounds		TCLP	X
Lead	X		
RCRA Metals (total)		TCLP	X

Drawing Number 3
Church Street Potential and Confirmed Sources of Contaminants

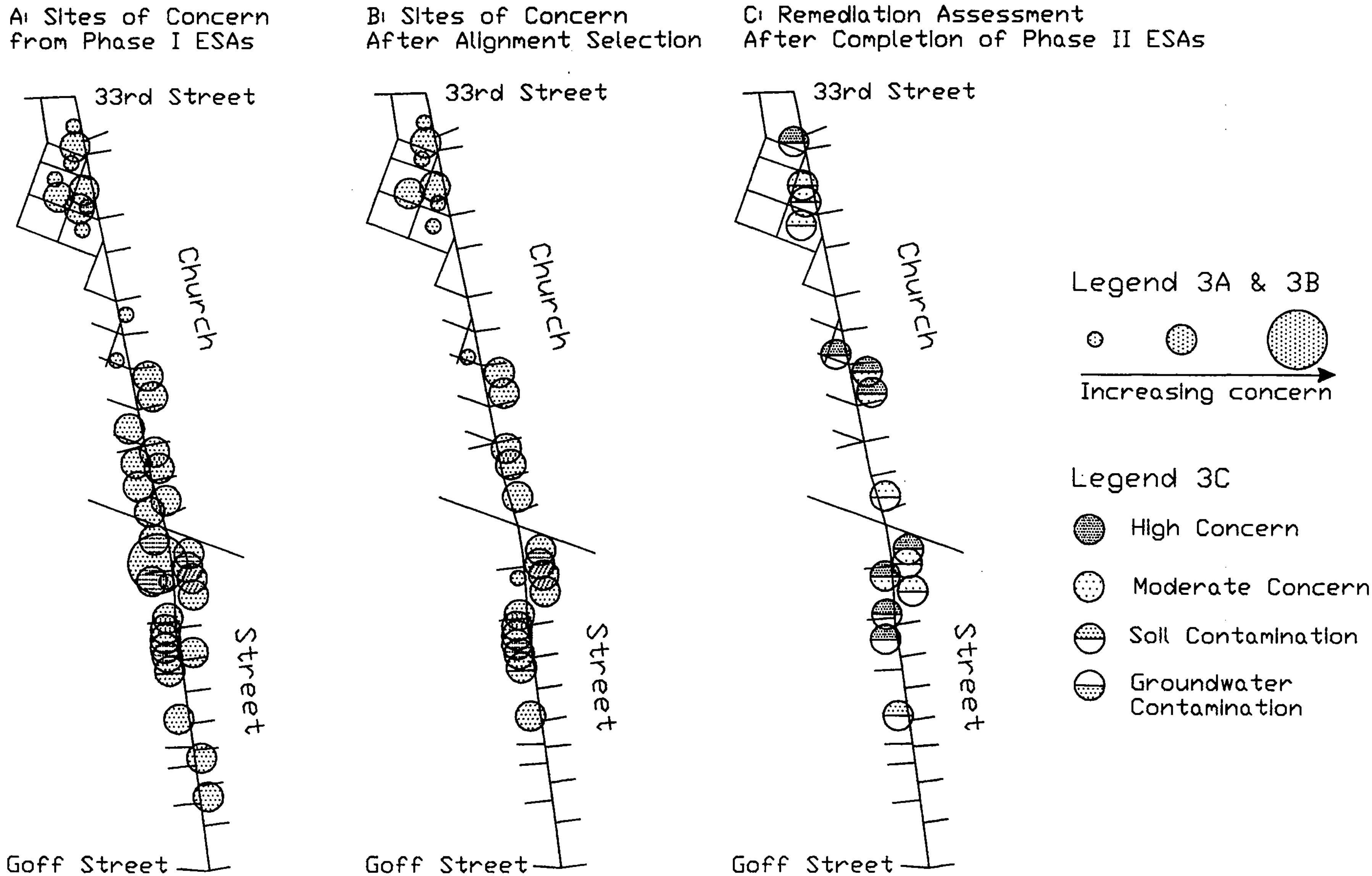

Many site visits were made to collect samples from Phase II ESA sites. All field work was documented with report of soil sampling forms, boring logs, monitoring well as-builts, report of groundwater sampling forms, report of static water level forms, and chain of custody forms. Chemical analytical data was tabulated and assessed for each site Qualitative risk assessment was repeated with identification of receptors, identification of exposure pathways, quantification of exposure levels, and evaluation of existing and potential risks. A qualitative assessment of potential remedial requirements was developed for surface soils, subsurface soils, and groundwater (Drawing Number 3c).

OPERATIONAL BENEFITS

Numerous operational benefits were realized by completing ESAs early during this roadway construction project. The design team avoided the most contaminated sites during right-of-way acquisition, reducing the project owners financial risk associated with ownership and requirements to remediate significantly impaired sites. We identified potentially contaminated sites prior to unanticipated discovery of hazardous waste during construction. Meetings with design consultants, owners, and regulatory agencies facilitated regulatory acceptance of construction-related issues associated with management of hazardous wastes generated during construction activities. The project team obtained regulatory concurrence that grading and excavation did not constitute waste generation if soils were replaced in their original location

CONCLUSIONS

VGS identified 17 sites out of 168 which were considered possible candidates for remedial activies during the construction phase of the Church Street widening. It is possible that significant sources of contamination or undocumented USTs could be discovered during subgrade preparation at any site along the corridor. Contingencies to deal with contaminated soil, groundwater, and undocumented USTs were recommended. Preparation of a detailed Health and Safety Plan was also recommended.

REFERENCES

Barker, William, J., and Bjorn, Eric D., 1978, Geology of the Norfolk South Quadrangle, Virginia, Virginia Division of Mineral Resources, Publication 9.

Hawthorne, D. W., May, A. E., and Siudyla, E. A., 1981, Groundwater Resources of the Four Cities Area, Virginia, Commonwealth of Virginia State Water Control Board, Bureau of Water Control Management, Tidewater Regional Office, Richmond, Virginia Planning Bulletin 331.

Meng, Andrew,A. , and Harsh, John F., 1989, Hydrogeologic Framework of the Virginia Coastal Plain, Regional Aquifer System Analysis, Department of the Interior, United States Geological Survey Professional Paper 1404-C.

Mixon, R. B., Berquist, C. R., Newell, W. L., Johnson, G. H., Powars, D. S., Schindler, J.S., Rader, E. K., 1989, Geologic Map and Generalized Cross Sections of the Coastal Plain and Adjacent Parts of the Piedmont, Virginia, Department of the Interior, United States Geological Survey Miscellaneous Investigations Series, Map 1-2033.

PROTECTION AND PRESERVATION OF AN ARCHAEOLOGICAL SITE BELOW A CONSTRUCTED HIGHWAY FILL

Christopher C. Mathewson and Lloyd E. Morris
Department of Geology and Geophysics
Texas A&M University
College Station, TX 77843-3115

ABSTRACT

Archaeological sites can be protected and preserved through intentional burial below an engineered cover. An investigation of the physical and chemical changes that occur in buried soils was carried out at historic engineering fills, ranging in age from 40 to 130 years. If was found that buried soils differ taxonomically from unburied soils at the suborder and lower levels. Buried soils have thicker soil profiles; yellower hues, lower values and lower chromas; increased gleying and mottling; coarser structure; fewer calcium carbonate concretions; and preserved organic carbon. A related field test using burial to protect against construction equipment loading was carried out at an artificial archaeological site. Protection against equipment loading increases as the thickness or stiffness of the cover increases. Burial was found to cause some breakage of the test artifacts. Physical and chemical changes in the buried soils are controlled by the site geology, climate, hydrogeology and local geomorphology. Artifact breakage is controlled by the depth of burial, the compressibility of the burial matrix and artifact orientation. Full-scale load tests carried out during the construction of FM-2953 in Montague County, Texas indicate that low-ground pressure equipment can be used to place cover materials. These tests further demonstrate that the impact of dynamic loading from vehicular traffic is effectively filtered out below about 5 ft (1.7 m) of cover. Burial of an archaeological site tends to increase the moisture content, induce reducing conditions, increase site compression, reduce dynamic loading on the cultural materials, reduce site erosion and weathering, and limit human and animal intrusion into the site.

ARCHAEOLOGICAL SITE PROTECTION THROUGH BURIAL

The objective of site preservation is to strike a delicate balance between the systematic data and artifact recovery and the long-term protection of artifacts that can be preserved in-situ (Moratto, 1977). Site excavation should be reduced to a minimum where long-term protection is feasible; and many cultural deposits should remain intact and be visually indistinguishable from the surrounding environment. When protected from natural or human destruction, archaeological data can be preserved for the future, to be studied and interpreted with fresh insights using the most up-to-date information and technology available. The concept of site protection through burial maintains the total archaeological resource in place.

Any definition of site protection and preservation should also have legal implications (Mathewson and Gonzalez, 1988; Mathewson, 1989a), which include:

- The goal of preservation is not to prevent change, but to reduce or shield a site from adverse human and natural impacts.
- Preservation involves what is technologically and financially feasible at present; i.e., "is it an achievable goal?"
- Preservation is limited to the length of time that the technique utilized will afford protection.

Because sites have been in place for hundreds or even thousands of years, we often assume that the site exists as a relatively constant entity. Whereas the excavator may choose to view a site as a fixed entity at the time of excavation, in fact, a site is located along a continuum of change over time. Therefore, preservation cannot be defined as non-change, but instead should be defined as "any action that reduces or eliminates detrimental changes resulting from site impacts." The goal then is that preservation activities should reduce the rate of change of the ongoing natural processes on the site matrix and contents (Mathewson and Gonzalez, 1988; Mathewson, 1989a).

Ample evidence exists to suggest that the burial of an archaeological site provides long-term protection and preservation of the archaeological materials. Archaeological investigations and excavations of burial mounds throughout the world have recovered numerous artifacts, materials, and skeletal remains. The successful preservation of these materials and remains in and below burial mounds indicates that engineered fills could provide a similar degree of protection to a site buried for preservation. The concern about burial as a site preservation technique is not that burial preserves a site, but that adverse physical, biological and chemical conditions may be induced within the site upon burial.

The changes observed in the buried soils appear to have occurred shortly after burial, at least within the first 40 or so years (Gonzalez, 1989; Mathewson, et. al, 1992). The amount of change observed appears to be controlled by site-specific geologic, climatic, hydrologic, and most importantly, geomorphic conditions. The changes in buried soils described herein may differ from changes observed in buried soils in drier or more humid geographic locations. Comments on the effects of burial on various soil properties are presented below:

- **Thickness**: Most of the buried soils analyzed have thicker soil profiles and thicker horizons than the unburied soils.
- **Color**: Buried soil horizons have yellower hues, lower values, and lower chromas than unburied soils, although the change in chroma is not statistically significant. The differences in color are associated with gleying, and in some sites, with the preferential preservation of organic carbon in the buried soils.
- **Gleying and Mottling**: Gleying and associated mottling are more common in buried soils. Buried soils were often wetter than the unburied soils.
- **Texture**: Burial has no noticeable effect on the texture of the buried soils.
- **Structure**: Buried soil horizons, particularly clay-rich horizons, show a coarsening of their structure as a result of burial.
- **Calcium Carbonate**: Buried soils have less calcium carbonate concretions than unburied soils.
- **Organic Carbon**: Saturated horizons preserve organic carbon.

EFFECTS OF COMPRESSION

Very limited research has been carried out to determine the relationship between soil stress and damage to archaeological materials. In 1981, the California Department of Transportation (Caltrans) conducted a study on the effects of burial on an engineered archaeological site (Garfinkel et al., 1983). The results of burial of materials under 75 ft (26 m) of embankment fill for two years suggests that limited gross morphological changes do occur upon burial. The organic objects, including shells, bones, and charcoal sticks suffered the most damage by breaking or bending as the fill compacted.

Texas Eastern Gas Pipeline Company contracted with Battelle to carry out an analysis and laboratory testing of compaction-induced damages to archaeological materials. Concerns were expressed about the potential impacts of pipe-laying equipment on the Kauffman II site in Chester County, Pennsylvania. Olson and others (1988) carried out two different laboratory test programs. In the first test, modern pottery samples were buried in soil placed in a 24 in. (61 cm) diameter steel pipe and loaded using a MTS 130-kip universal tension-compression machine. The test pottery cracked at soil pressures ranging from 7.6 psi, for a straight sided pot filled with soil, to 15.6 psi, for a rounded pot that was filled with cotton to prevent soil entry. In the second test, manufactured and natural archaeological materials were placed in an excavated pit in a 48 in. (122 cm) diameter steel pipe and loaded using a MTS 1000-kip universal tension-compression machine. In this test, none of the archaeological materials were damaged. In fact, it was found that excavation of the materials caused more damage than the soil loading did (Olson, 1989; Skinner, 1989).

Laboratory experiments of compressive loading and artifact breakage were carried out using twenty different arrangements of archaeological materials placed in a sand box (Mathewson et al., 1992). The results of this testing program indicate that clay pots and ceramic sherds approximately 0.23 in. (6 mm) thick buried 9.8 in. (25 cm) below the surface, will fracture under a surface load of approximately 30 psi. General conclusions that can be drawn from these tests include:

- Thin walled pottery will fracture more readily than thick walled pottery.
- Pottery oriented horizontally will break more frequently than pottery standing vertically.
- Rapid loading tends to cause more damage than slow loading.
- Pottery in contact with more dense materials or in contact with other pottery are more susceptible to failure than isolated pottery.
- The controlling factor causing breakage appears to be related to total strain (displacement) rather than total stress (loading).
- Weaker, more brittle, charcoal sticks tend to fracture more readily than more ductile materials.

A field scale test of various protection techniques that would protect an archaeological site from construction equipment loading was carried out by Mathewson and others (1992) at the Texas Engineering Extension Service, Heavy Equipment Training School site in Brazos County, Texas. In this experiment, a series of twelve test pits, 3 ft (1 m) wide, 12 ft (4 m) long, and 3 ft (1 m) deep, were excavated and filled with test artifacts. The pits were organized in parallel pairs, with four pairs aligned along a construction road, one pit in each lane of traffic. This arrangement made it possible to place the test artifacts in two different types of backfill material - a fine sand and a silty loam.

An "archaeological site" was constructed in each test pit using 4-in. (10 cm) and 6-in. (15 cm) clay flower pots, 4-in. and 6-in. clay pot trays, artist charcoal sticks, 30-in. long glass rods and a 30-in. (76 cm) long strip of sheet metal. The flower pots were manufactured in the same production batch to minimize differences in the firing and treatment of the pots. Laboratory strength tests indicated that the flower pot sherds behaved in a similar manner as aboriginal sherds. A 6-in. pot to represent a "skull" was located in the center of the arrangement, with two "burials" and two "cooking" arrangements in each corner.

The test artifacts were arranged in four replicate test arrangements and buried approximately 36 in. (91 cm), 24 in. (60 cm), and 12 in.(30 cm) below the ground surface. Each test arrangement was rotated 90 degrees between each successive cell, A through D. To facilitate post-excavation analyses of the damages caused by construction loading, each pot was color coded on both the outside and inside. The outside color identified the layer depth and the inside color identified the pot use. The artist charcoal sticks were also color coded using the layer color. Site burial was performed by a Texas Department of Highways Heavy Construction School using conventional construction techniques. All students in the school were experienced Highway Department heavy equipment operators.

A board road was constructed on-site from three crossed layers of 2 x 12 lumber. The 18-in. (46 cm) and 36-in. (92 cm) soil covers were placed using a front end loader to place the cover material without driving directly on the site. A motor grader with the blade extended to the side was used to spread the material. Once an access ramp was constructed, the cover was extended by placing new cover material from the end of the ramp. The cover material was a locally available clay. A motor grader was used to construct a clay road on top of the soil cover, which was compacted by the traffic loads. The road was periodically maintained and low spots were refilled to keep the road at the desired grade. A total of 1300 vehicle axle passes were made across the road using loaded and unloaded scrapers, dozers, pick-up trucks, crew bus, rubber tired front end loaders, tractor backhoes, and motor graders.

Following the heavy equipment school, the test sites were excavated by experienced field archaeologists from the Department of Anthropology at Texas A&M University. Damage of each pot was classified for each test cell and averaged to obtain the damage for a specific burial depth, pot orientation, matrix type and protective method. Data from the laboratory analysis can be found in Mathewson and others (1992). The saturated artists charcoal sticks were generally found intact but deformed because the charcoal sticks became very ductile upon saturation. The glass rods buried at shallow depths in unprotected pits were broken into as many as five pieces. Rods buried at greater depths in each pit and in the control pits were intact or broken into two pieces. The three-feet (1 m) depth layer was not excavated in the sand-filled pit protected by the board road because no breakage was detected in any of the test artifacts in the two-ft (66 cm) depth layer.

Compressive breakage of the test artifacts indicates that original depth of burial has a direct controlling effect on the amount of breakage caused by surface loading. The amount of damage to the test pots drops off rapidly with increasing depth of original burial, except in a few rare cases. For example, the average number of broken pieces of the 6-in. diameter "skull" pot in an unprotected site in a silty loam matrix at a one-foot depth is 28.25, at a two-feet (66 cm) depth is 22.75 and at a three-feet (1 m) depth it is 12.50.

Breakage of the test artifacts appears to be related to both the size and orientation of the artifacts. The 6-in. pot lying on its side experienced more breakage than a similar 4-in. diameter pot. Pots lying on their side are more susceptible to breakage because the pot must carry the entire vertical load rather than transfer it to the matrix material. Pots set vertically, either open upward or inverted, are able to transfer the load to the underlying matrix material and thereby, experience less breakage. In the case of the covered pot, the pot transferred the load by penetrating the underlying matrix and therefore, reducing the total strain on the pot; however, both the pot and the capping lid fractured. The inverted 4 in. pot resting in a 6 in. tray tended to cause greater breakage to the underlying tray by punching a circular hole in the tray because it was not able to penetrate into the underlying matrix. The 4 in. diameter upright pot, filled with matrix material, experienced the least amount of breakage.

The amount of breakage in the more compressible silty loam matrix material was greater than in the less compressible fine sand matrix. Glass rods in the silty loam matrix always showed greater breakage than in the sand matrix, indicating greater differential movement within the silty loam. Compressibility of the matrix appears to be a significant factor in the amount of artifact breakage both in the test pits and in natural burial mounds. The relationship between burial depth and matrix material shows that the amount of breakage is greater in the silty loam than in the sand.

The maximum amount of pot breakage occurred in the unprotected site in all cases. The constructed board road, which spreads the vehicle load over a larger area and does not significantly load the site, provided the best protection against breakage caused by moving construction equipment. Some pot breakage was caused by the construction of the 36-in. thick protective cover. In some cases, greater damage was caused by the construction of the 36-in. control cover than was caused by the cover plus the vehicle loading. Artifact breakage in the sites protected by the 18-in. thick soil cover were generally greater than that in the 36 in. cover control sites and in the 36 in. protected sites.

The field experiments indicate that the breakage of archaeological materials is controlled by the interaction of the original burial depth, the orientation and interrelationship between artifacts, the compressive characteristics of the burial matrix, and the type of protective cover.

MONTAGUE COUNTY HIGHWAY CONSTRUCTION

The Texas Department of Transportation (TXDoT) contracted with Texas A&M University to bury two archaeological sites below an engineered fill in Montague County, Texas. Archaeological significance testing was carried out by the Texas Department of Transportation (Price, 1992). The two sites, designated 41MU60 and 41MU62, are located in northeastern Montague County about 300 ft (100m) south of the Red River. The sites have been interpreted to be the remains of single occupations of unknown duration that date from the Late prehistoric II period. A radiocarbon data for site 41MU60 yielded date of AD 1310 +/- 90 while one for site 41MU62 yielded a date of AD 1380 +/- 60.

Site 41MU60 contains bone, shell, charcoal, granular lithics, ceramics, and features that are generally scattered and dispersed throughout the site. Stratigraphic relationships are generally poorly defined, with the upper horizon disturbed by recent human activities. The primary archaeological horizon exists between about 12 and 30 in. (30 -70 cm) below the ground surface. The upper horizon is a plow zone. Part of the site is situated within an agricultural field that has been plowed and the other part is situated below a non-agricultural area containing oaks, brush, and grasses.

Site 41MU62 contains bone, shell, plants/ecofacts, granular lithics, ceramics, and features that are generally scattered and dispersed throughout the site. Stratigraphic relationships are generally poorly defined, with the upper horizon disturbed by recent human activities. The primary archaeological horizon lies between approximately 12 and 50 in. (30 - 125 cm) below the ground surface. Approximately one-half of the site is situated below a short-grass pasture while the other half is situated below a long-grass pasture. A portion of the site was exposed during the construction of a County Road that cuts into the ridge along the northern boundary. This area is known to "pot hunters", who dig for arrow heads and other archaeological components of the site.

The design concept of the burial was controlled by the site decay matrix (Mathewson and Gonzalez, 1988; Mathewson, 1989b) which established the desired site conditions to preservation (Figure 1). The site components included bone materials, shell, granular lithics, ceramics and features. The site was subjected to cyclic wet-dry and freeze-thaw events, human intrusion and burrowing by organisms.

SITE CONDITIONS	**Animal Bones**	**Shell**	Plants, Ecofacts	**Charcoal**	Crystalline Lithics	**Granular Lithics**	**Ceramics**	**Features**	Soil Attributes	Metals	Context	Isotopic Content
Acidic Environment	A	A	E	N	N	A	N	N	A	A	N	A
Basic Environment	E	E	A	N	N	E	N	N	A	A	N	N
Continuously Dry	E	E	E	E	N	E	N	N	N	E	N	E
Continuously Wet, Anaerobic	E	E	E	A	A	A	A	A	A	A	N	A
Continuously Wet, Aerobic	A	A	A	A	N	A	A	A	A	A	N	A
Cyclic Wet-Dry	A	A	A	A	A	A	A	A	A	A	N	A
Cyclic Freeze-Thaw	A	A	A	A	A	A	A	A	A	N	A	A
Freeze	A	A	A	A	N	A	A	N	E	N	A	E
Thaw	N	N	N	N	N	A	N	N	A	N	A	A
Compression	A	A	A	A	N	N	A	A	A	N	A	N
Movement	N	N	N	A	N	N	N	A	A	N	A	N
Microorganisms	A	N	A	A	N	N	N	N	N	A	A	A
Macroorganisms	A	A	A	A	N	A	N	A	A	N	A	N
Human Intrusion	A	A	A	A	A	A	N	A	A	A	A	A

SITE COMPONENTS

Notes
E = Condition Enhances Preservation
A = Condition Accelerates Decay
N = Condition is Neutral or Has No Effect
= Existing Site Characteristics

Figure 1. Archaeological site protection matrix for site 41MU60 in Montague County, Texas.

The burial was designed to direct all surface water away from the site area, prevent ponding and concentration of surface water, reduce freeze-thaw and prevent human and animal intrusion into the site. Preconstruction engineering analyses indicate that the geogrid and burial would greatly reduce the dynamic traffic loading on the site components (Figure 2).

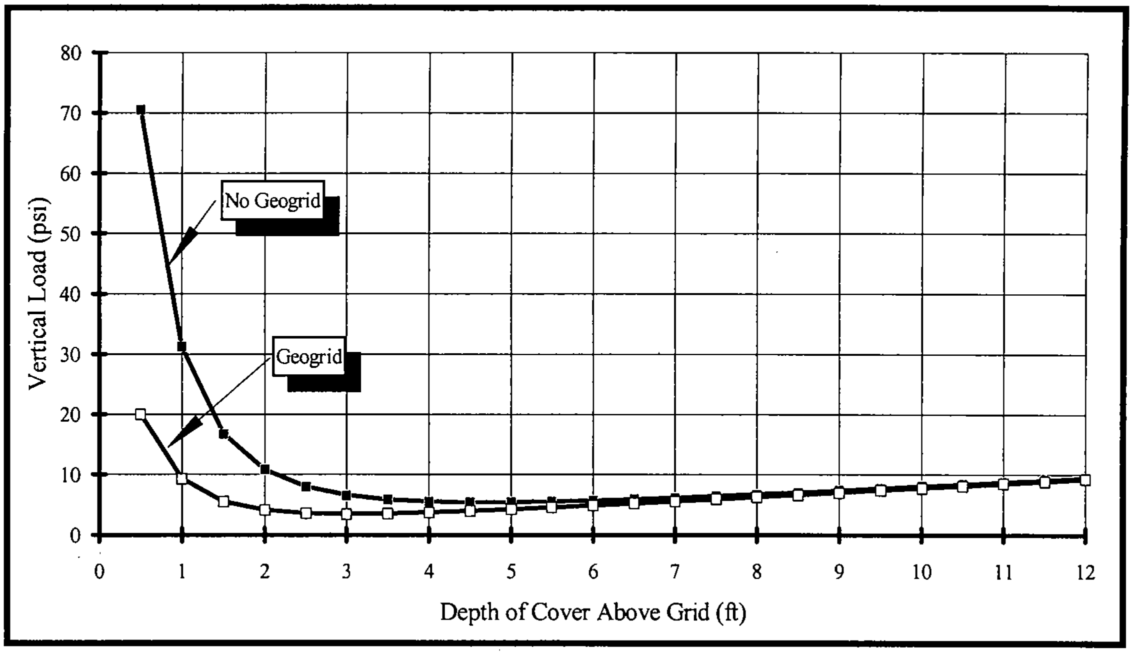

Figure 2. Calculated total load (dead + live) on cultural materials situated below an engineered fill showing the protection gained through the application of a geogrid placed directly on top of the site.

The project specifications for burial included:

- **Site clearing:** limited to spray with a herbicide to kill all vegetation on the site. Trees and large brush to be removed by hand methods. All stumps to be cut flush with the ground surface. Following removal of large vegetation, the site was to be burned in order to remove all remaining surface organic matter.
- **Surface preparation:** placement of sand (limestone screenings) to fill low spots to smooth the surface for construction vehicle traffic and prepare the surface for a geogrid. The screenings to be placed using a small, low ground-pressure dozer. Upon placement, screenings are to be compacted using a pneumatic or non-vibrating steel wheel roller.
- **Geogrid:** hand placed over the entire section to provide lateral strength to the base of the cover material and to mark the top of the original ground surface
- **Limestone protection course:** placed over the geogrid to a minimum thickness of 0.5 ft (15 cm) and compacted using a pneumatic roller. No equipment to be allowed to travel on top of the unprotected geogrid.
- **Fill and Road Section:** local material spread over the site to bring the site up to the design grade with the road surface placed on top.

Each site was instrumented with three total pressure cells and one total settlement (vertical movement) monitor prior to the placement of any cover material. The sensors were placed on top of the cultural horizon and buried with native soil to detect loading conditions at this level and to provide some protection to the sensors. Vertical loads (pressure) were recorded following both a dynamic and static procedure. Dynamic loads were recorded at a rate of 100 readings/sec for a 5 sec burst in order to obtain the full range of dynamic loads as a test vehicle passed over a selected load cell. Dynamic load readings were made at selected times during the construction period while static loads read at the rate of 1 reading/10 min were monitored throughout the construction process.

Land uses in the area indicate that the maximum historic loads that the site experienced are related to farm equipment used for pasture management, hay production and a family garden. The depth of the plow horizon was found to be approximately 0.5 ft (15 cm) below the existing ground surface. A stomping man and standing horse and rider generated loads of about 5 to 7 psi at the top of the cultural horizon, 0.5 ft (15 cm) below the surface. At the same depth, a 1/2-ton pickup truck generated a maximum load of about 12 psi, while a John Deere 2950 farm tractor generated a load of about 16 psi. These data were used to establish the maximum historic load at 16 psi.

A CAT D4 LGP (Caterpillar D4 low-ground pressure) dozer was tested across the load cells to determine its suitability for moving the screenings onto the site. Maximum ground pressures on top of the cultural horizon were within the maximum historic loads. The contractor was authorized to use the LGP dozer for all on-site work with the stipulation that the dozer blade avoid excavating into the cultural horizon. However, loading tests in the laboratory demonstrated that rapid loading caused greater artifact breakage that slow loading. Because the vibratory character of the loading signal generated by the LGP dozer has the potential to cause breakage of artifacts the contractor was also instructed to operate the dozer at 1/2-speed while on the site to minimize the impact loads that cause artifact breakage.

Additional construction equipment can be allowed on the site as soon as the screenings have been placed and smoothed by the LGP dozer, however, speeds must be at a minimum to reduce impact loads on the site. A loaded IH S2500 water truck can be allowed on the site to maintain moisture content control necessary to obtain optimum density of the screenings. A CAT 140G motor grader, 12-yard belly dump hauler, Ingram 11-5400Q pneumatic roller and an Ingersol SD-100D steel wheel roller, not vibrating, can be used over the screenings. The vibrating load generated by the Ingersol steel wheel roller is a "sharp impact" type of load that exceeded the allowable level and can cause significant artifact damage.

Once the limestone screenings had been placed and compacted, the geogrid was placed by hand. Because no equipment was allowed to drive directly on top of the geogrid, the D4 LGP dozer was used to push a locally obtained crushed limestone protection coarse over the grid. Once the fill thickness reached 3 ft (1 m), a CAT 815 pad foot compactor was used to compact the fill to TXDoT specifications. At shallower thicknesses, the pneumatic and steel wheel roller was used to obtain desired compaction of the fill. A CAT 973 track loader can be used to transport fill material if the existing fill exceeds 1.5 ft (50 cm) in thickness.

As the thickness of the fill section increases, the dynamic loading associated with passing traffic sharply decreases. For example, the dynamic load from the loaded water truck driving on top of the screenings (0.7 ft (21 cm) above the cultural horizon) was approximately 15 psi. The load of the water truck decreases to about 2 psi when the fill is about 3 ft (1 m) thick and to less than 1 psi at a fill thickness of 7 ft (2.3 m).

CONCLUSIONS

Archaeological sites are a complex system of geographic, stratigraphic, and ethnographic relationships that are over-printed with a mixture of different archaeological materials. Each site is, in turn, preserved within a unique physical, biological, and chemical environment. A change in the physical, biological, or chemical environment of a site induced through burial may result in the enhanced preservation or accelerated decay of the site components.

Burial can be used as an effective site preservation technique. However, burial will effect the site in both beneficial and deleterious ways, as follows:

- Burial will increase the vertical load on archaeological sites.
- Artifact breakage decreases as the depth of burial increases.
- Artifacts that are oriented in such a manner that they can transfer the compressive load to the matrix are less susceptible to breakage.
- Artifacts that are in contact with other artifacts are more susceptible to breakage.
- As the matrix material becomes more compressible, the amount of artifact breakage increases.
- Protective covers that minimize the amount of differential strain on the buried artifacts will provide greater protection than those that cause or allow the transfer of strain downward.
- Burial limits site erosion and reduces the rate of near-surface weathering of archaeological materials.
- Burial will reduce the impact of microorganisms and burrowing macro-organisms on archaeological sites.
- Burial will usually increase the moisture content of the soil matrix.
- Burial can induce a limited change in the pH of the soil matrix.
- Burial of a site limits the deleterious effects of freeze-thaw and wet-dry cycles, the two most damaging natural agents to archaeological sites.
- Burial of a site reduces the amount of vertical strain (displacement) related to construction equipment loading.
- Burial reduces the significance of dynamic loading from vehicular traffic.
- Burial projects can be constructed using conventional construction techniques and methods if care is exercised in equipment selection and operation.

REFERENCES

Garfinkel, A.P.; Lister, B.L.; and Boost, A., 1983, *Effects of High Embankment Construction on Archaeological Materials*: California Department of Highways, Construction Division, Sacramento, CA, 84 p.

Gonzalez, Tania, 1989, *Study of Soils Buried Under Embankments to Determine the Potential for Burial as a Preservation Technique for Archaeological Sites*: unpublished Master of Science thesis, Texas A&M University, College Station, TX, 331 p.

Mathewson, Christopher C., 1989a, Introduction to the Workshop and the Concept of a Site Decay Model: in Mathewson, C.C. (editor), *An Interdisciplinary Workshop on the Physical-Chemical-Biological Processes Affecting Archaeological Sites to Develop and Archaeological Site Decay Model*: Technical Report EL-89-1 for the U.S. Army Engineer Waterways Experiment Station, Vicksburg, MS, 238 p.

Mathewson, Christopher C., 1989b, Logic-Based Qualitative Site Decay Model for the Preservation of Archaeological Sites: in Mathewson, C.C. (editor), *An Interdisciplinary Workshop on the Physical-Chemical-Biological Processes Affecting Archaeological Sites to Develop an Archaeological Site Decay Model*: Technical Report EL-89-1 for the U.S. Army Corps of Engineer, Waterways Experiment Station, Vicksburg, MS, pp. 227-238.

Mathewson, Christopher C. and Gonzalez, Tania, 1988, Burial of Archaeological Sites for Protection and Preservation: in Proceedings, *24th Annual Symposium on Engineering Geology and Soils Engineering*: University of Idaho Press, Coeur d'Alene, ID, pp. 443-452.

Mathewson, Christopher C.; Gonzalez, Tania; and Eblen James S., 1992, *Burial as a Method of Archaeological Site Protection*, Contract Report EL-92-1: US Army Engineer Waterways Experiment Station, Vicksburg, MS, 125 p.

Moratto, J.C., 1977, Research Prospects: New Melones Archaeological Project: in Schiffer, M.B. and Gumerman, G.J. (editors), *Conservation Archaeology: A Guide for Cultural Resource Management Studies*: Academic Press, New York, NY, pp. 401-411.

Olson, R.J., 1989, *Soil-Structure Interaction Testing for Assessing the Impact of Pipe Lying Operations at the Kauffman II Archaeological Site*: unpublished report prepared for Texas Eastern Gas Pipeline Company by Battelle, Columbus Division, Columbus, OH, 35 p.

Olson, R.J.; Guerrieri, D.A.; and Jones, D.J., 1988, *The Impact of Pipe Lying Operations on the Kauffman II Archaeological Site*: unpublished report prepared for Texas Eastern Gas Pipeline Company by Battelle, Columbus Division, Columbus, OH, 24 p.

Price, Dennis G. R., 1992, *Archaeological Significance Testing at Sites 41MU60, 41MU61, 41MU62 and 41MU63 Montague County, Texas*: Texas Department of Transportation, Division of Highway Design, Austin, TX, 6 Sections.

Skinner, Shanne M., 1989, *Experimental Study to Assess the Effects of Compaction and Pressure on Artifacts in Archaeological Sites*: unpublished report prepared for Texas Eastern Gas Pipeline Company by Archaeological Services Consultants, Inc., Columbus, OH, 25 p.

AN OVERVIEW OF NON-DESTRUCTIVE METHODS FOR CHARACTERIZATION OF ROADS AND BRIDGES

Richard C. Benson, Technos, Inc., Miami, Florida

ABSTRACT

A variety of remote sensing, surface geophysical, borehole geophysical and other non-destructive methods can be used to determine conditions of roads and bridges. Some of these methods can be utilized to determine subsurface conditions prior to construction. Some can be applied to QC measurements during construction, and many can be applied after construction to determine as-built conditions, as well as degradation and monitoring.

The benefits of such measurements compared to discrete point measurements or tests are that they: are non-destructive, provide in-situ measurements of a number of physical properties, sample larger areas or volumes, provide continuous measurements in some cases, and provide faster measurements. All of this results in a greater sample density, which can more readily identify uniform conditions as well as locate anomalous conditions. Once anomalous conditions are identified, those areas requiring further tests, borings or repairs can be accurately and quickly located.

THE SITE CHARACTERIZATION PROCESS

Site characterization is the process of understanding the hydrologic/geologic framework for engineering projects, and the contaminant distribution for environmental projects. Site characterization is the corner stone of all geotechnical and environmental projects. Proper site characterizations provide the basis for sound engineering designs and optimal remediation strategies. Incomplete and inaccurate site characterizations are often responsible for engineering and environmental failures (Shuirman and Slosson, 1992; Freeze and Cherry, 1989).

A solid base of appropriate types of data, adequate data and accurate data (Figure 1) enables us to carry out subsequent efforts such as modeling, risk assessment, remediation, engineering design and maintenance with much greater confidence and accuracy while minimizing uncertainties, assumptions, and opinions.

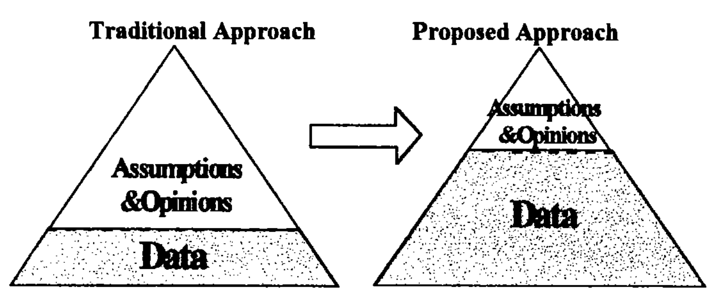

Figure 1. Increasing the data and minimizing assumptions and opinions forms a solid basis for understanding site conditions.

The primary factor affecting the accuracy and completeness of any site characterization is the limited number of data points available to spatially and or temporally describe site conditions. Achieving a reasonable spatial sampling of hydrogeologic conditions for geotechnical investigations requires borings and/or sampling in a close-order grid, which would reduce the site to "Swiss cheese" (Benson, 1993).

While direct sampling methods provide detailed data at discreet locations within a site, they do little to describe overall site conditions in a heterogeneous environment. The strategy should be to concentrate direct sampling methods in areas where problems occur. In order to obtain a sufficiently complete picture of site conditions, measurements must be taken over denser spacings than direct sampling can feasibly provide. Remote sensing, geophysical methods and non-destructive testing (NDT) methods can economically provide this denser spacing.

There is a wide range of usage for terms such as remote sensing, geophysics, and NDT. In the broad sense of the term, they are similar since they all make in-situ measurements. These in-situ measurements can be made relatively quickly, in some cases continuous data acquisition along a traverse line can be employed at speeds up to several miles per hour (and in some cases at highway speeds). Because of the greater sample density, anomalous conditions (problem areas) are more likely to be detected.

This paper provides an overview of remote sensing, geophysical, and NDT methods that can and have been applied to characterizing conditions of roads and bridges.

A WIDE RANGE OF REMOTE SENSING, GEOPHYSICAL AND NDT METHODS

Remote sensing, geophysical and NDT methods encompass a wide range of airborne, surface and downhole measurement techniques which provide a means of investigating subsurface geologic and hydrologic conditions, and obtaining engineering properties.

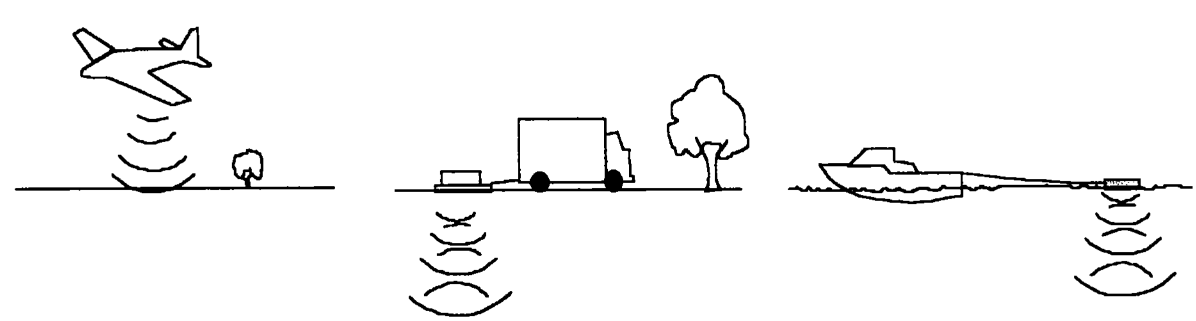

Figure 2. Measurements can be made from the air, surface, and over water.

Satellite data, aerial photography and other airborne geophysical measurements are used to provide reconnaissance level data over large areas and can provide some site specific data. These methods clearly have merits in terms of spatial coverage per unit time and cost. The *imaging* methods (photographic, infrared, and thermal imagery) provide a "picture" of the site and the surrounding area and can quickly establish the regional setting.

While surface geophysical methods yield much less spatial coverage per unit time than the airborne methods, they significantly improve resolution (the ability to detect smaller features) while providing subsurface information up to a few 100 feet. With some methods, continuous data acquisition can be obtained at speeds up to several miles per hour. In certain situations total site coverage is technically and economically feasible. An inherent limitation of all surface geophysical methods is that their resolution decreases with depth. Most of the surface geophysical methods can be used on water (rivers, lakes, estuaries, and coastal) or over frozen bodies of water as well as on land. ASTM PS 78-97 provides a brief description of the surface geophysical methods and their application.

Downhole geophysical methods are used to provide very localized details down a borehole, core hole in concrete or a well (Figure 3a). The volume sampled by downhole methods is usually limited to the area immediately around the boring (a cubic foot to a cubic yard). Unlike surface geophysical methods where resolution decreases with depth, the resolution of downhole logging is independent of depth. If holes are already in place or if they are to be drilled for other purposes, the overall cost of downhole logging is relatively low. Measurements between boreholes (Figure 3b) provide a means of measuring conditions between two or more boreholes and increasing the volume being measured. Tomographic imaging can also be done between boreholes (Figure 3c). ASTM D5753 provides a brief description of the downhole geophysical methods and their application.

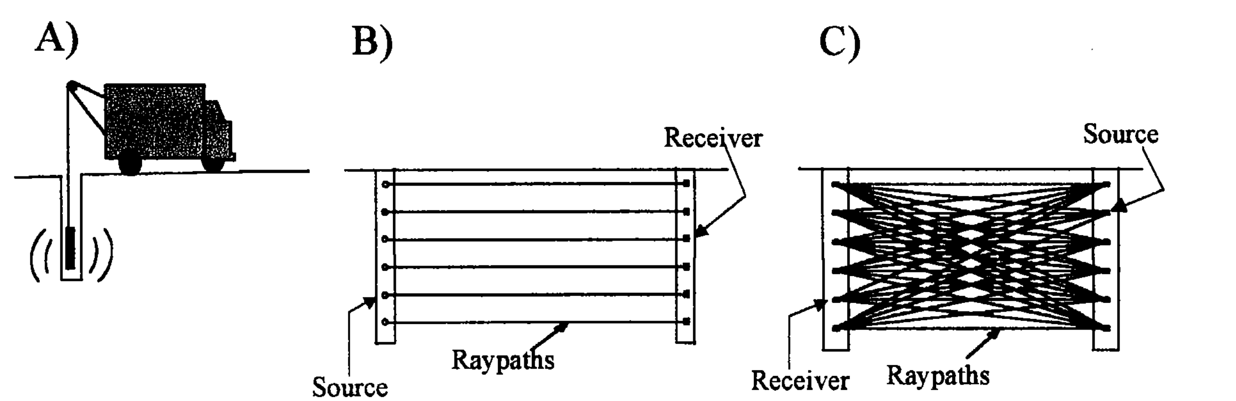

Figure 3. Borehole logging, surface to borehole, hole to hole and tomography

Unlike direct sampling, such as obtaining a soil sample and sending it to a laboratory, the geophysical methods provide nondestructive, in-situ measurements. These methods measure some physical, electrical, or chemical property of the soil, rock and pore space fluids or some property of the subbase, asphalt or concrete. Benson (1993) describes the application of geophysical measurements to a number of geologic, hydrologic and environmental problems. Olson (1998) discusses some of the many seismic and sonic tests used in NDT. O'Connor (1999) presents applications for the TDR methods to monitor site stability.

There is a surprising similarity between many medical techniques and the geophysical methods. The wide range of tools available to a medical professional measure different physical, chemical or electrical parameters of the body, such as x-ray, ultrasound, EKG or CAT scan. The doctors use these tools to collect a sufficient amount of data and insight on the patients internal conditions. These data along with blood tests, personal observations and discussion with the patient are used to provide a diagnosis of the patient's condition prior to prescribing a medication or surgery. A similar approach should also be used in the engineering field to minimize assumptions and opinions (Figure 1).

THESE METHODS CAN BE APPLIED TO A WIDE RANGE OF APPLICATIONS FOR ROADS AND BRIDGES

Remote sensing, geophysical and NDT methods are routinely applied to four areas:

- Mapping natural hydrogeologic conditions such as depth to rock or potential sinkhole areas;
- Detection and mapping of buried objects and contaminant plumes associated with new right of ways;
- Evaluation of soil and rock properties, and non-destructive testing of man-made structures, and
- Temporal measurements for monitoring conditions and remediation management

The following tables identify a wide range of methods that can be applied to various aspects of site characterization and NDT of roads and bridges. This listing is not intended to be complete, but cites the more commonly used methods.

Some of these methods can be utilized to determine subsurface conditions prior to construction. Some can be applied to QC measurements during construction and many can be applied after construction to determine as-built conditions, as well as degradation of conditions.

Mapping Natural Hydrogeologic Conditions

The mapping of natural hydrogeologic conditions is applicable to right of way selection and more specifically to roadway and bridge design and construction. Identifying problems ahead of time we can avoid costly surprises during construction.

Satellite imagery, remote sensing or aerial photo interpretation can establish the regional setting and aid in route selection, identifying direct routes and minimizing cut and fill. Once a route selection has been made, incorporating surface geophysical techniques with geotechnical borings, borehole logging, and hole to hole methods along the right of way can effectively provide reliable subsurface information for design and construction (Tables 1, 2 and 3). Whether it is as simple as mapping the top of rock or as complicated as determining the presence of karst features, surface and borehole geophysics can greatly improve spatial sampling and the accuracy of an assessment.

Table 1
Summary of Methods Applied to Right of Way Selection

Method	Parameter/Condition Measured
Satellite Imagery	Surface image documentation and terrain interpretation
Aerial Photo Imagery	Surface image documentation and terrain interpretation
Thermal Imagery	Temperature of surface (moisture/seeps/karst)
Video	Surface image documentation

Table 2
Summary of Surface Geophysical Methods Applied to Hydrogeologic Characterization

Method	Parameter/Condition Measured
Ground Penetrating Radar	Dielectric constant (stratigraphy/top of rock/karst)
Electromagnetic	Electrical conductivity (lateral variation in soil and rock/ inorganic contaminants)
Resistivity	Electrical resistivity (spatial variation in soil and rock/ inorganic contaminants)
SP (spontaneous potential)	Electrochemical and streaming potential (seepage/karst)
Seismic Refraction	Seismic velocity (top of rock/rippability)
Seismic Reflection	Seismic velocity (stratigraphy)
Seismic Surface Wave Analysis	Seismic velocity/dispersion (S-wave/stratigraphy)
Gravity	Density (bedrock channels/karst)
Thermal Imagery	Temperature of surface (moisture/seeps/karst)

Table 3
Summary of Borehole Methods Applied to Hydrogeologic Characterization

Method	Parameter/Condition Measured
Single Hole	
Natural Gamma Logging	Natural gamma radiation (stratigraphy – clays/shales)
Gamma Gamma Logging	Density (stratigraphy/voids/fractures)
Neutron Neutron Logging	Porosity (stratigraphy/permeable zones)
Induction/resistivity Logging	Electrical conductivity /resistivity (stratigraphy/contaminants)
Spontaneous Potential (SP) Logging	Electrochemical and streaming potential (stratigraphy/voids/fractures/flow)
Resistance Logging	Resistance (stratigraphy/voids/fractures/flow)
Caliper Logging	Borehole diameter (voids/cavities)
Temperature Logging	Borehole fluid temperature (groundwater flow)
Conductivity Logging	Borehole fluid electrical conductivity (flow/contaminants)
Flow Logging	Fluid flow within borehole (groundwater flow)
Sonic Logging	P and S shear wave velocity (near borehole)
Borehole Imagery Methods TV/ATV/BIPS	Voids and fractures in core holes
Hole to Hole	
P-S Wave Measurements	P and S wave velocity (elastic moduli between holes)
Sonic Tomography	Image of conditions between holes
Radar Tomography	Image of conditions between holes

Detection and Mapping of Buried Objects and Contaminant Plumes

Establishing new roadways or expanding existing ones, often involves traversing previously developed properties with few records or documentation. Prior to roadway development, environmental issues such as waste disposal areas and underground storage tanks may also need to be addressed.

Surface geophysical methods can significantly aid in the detection and mapping of landfills, construction debris, pipelines/utilities, underground storage tanks, old building foundations and contaminant plumes (Table 4). These methods provide a high degree of spatial sampling to ensure that buried objects and environmental concerns are adequately characterized before construction.

Table 4
Summary of Methods Applied to Location of Buried Materials and Contaminants

Method	Parameter/Condition Measured
Ground Penetrating Radar	Dielectric constant (utilities/tanks/debris)
Electromagnetic	Electrical conductivity (utilities/tanks/debris/contaminants)
Resistivity	Electrical resistivity (utilities/tanks/debris/contaminants)
Magnetics	Magnetic susceptibility (ferrous utilities/tanks/drums/metal debris)
Metal Detector	Electrical conductivity of metal (utilities/tanks/metallic debris)

Evaluation of Soil and Rock Properties, and Non-Destructive Testing of Structures

A wide variety of applications fall into this category and include: rock stability, soil properties, pile length and integrity, bridge scour assessment and roadbed evaluations (Tables 5, 6, 7, 8 and 9). The insight that the measurements provide by detecting features or determining properties within roadbeds, structures, etc. allows the maintenance and repairs to be more effectively carried out. These methods often are used to provide localized, detailed measurements.

Table 5
Summary of Methods Applied to Monitoring During and After Construction

Method	Parameter/Condition Measured
Nuclear density gauges	Density (attenuation of gamma rays) (shallow in situ density)
TDR	Displacement and/or changes in fluids levels (monitor stability)
Acoustic Emission	Sonic noise due to fluid flow or structural movement (monitor stability)
Thermal Infrared Imagery	Temperature of surface (moisture/seeps)
Ground Penetrating Radar	Dielectric constant (thickness of roadbed)
Laser Rugosity	Reflection (Surface roughness of roadbed)
Video	Surface image (documentation of road bed conditions)
Via Boreholes in Drilled Shafts and Slurry Walls	See borehole logging methods in a single hole or between holes (monitor stability)

Table 6
Summary of Methods Applied to Pile Length Determination and Integrity Assessment

Method	Parameter/Condition Measured
Pile Length Determination	
Sonic Impulse (reflection)	P wave Velocity (Length of pile and or discontinuity within the pile)
Magnetometer/Induction Log	Presence of rebar (length of pile)
Sonic (refraction)	P wave velocity (length of pile)
Pile Integrity Assessment	
Sonic Impulse (reflection)	P wave reflection (Discontinuities within the pile)
Cross-hole Sonic Logging	P Wave velocity – (quality and uniformity of concrete)
Sonic Tomography	P wave velocity (tomographic image of quality and uniformity of concrete)
Gamma-gamma (density log)	Density (quality and uniformity of concrete)
Neutron-neutron (porosity log)	Porosity (quality and uniformity of concrete)
Corrosion Potential	Voltage due to galvanic action (areas of rebar corrosion)
Caliper	Diameter of core holes (Voids/fractures)
Borehole Imagery Methods TV/ATV/BIPS	Image of core hole (Voids and fractures)

Table 7
Summary of Methods Applied to Concrete Structure Integrity Assessment

Method	Parameter/Condition Measured
Rebar Corrosion Potential	Voltage due to galvanic action (areas of rebar corrosion)
Ground Penetrating Radar	Dielectric constant (slab thickness/rebar)
Seismic Surface Wave Analysis	Seismic velocity/dispersion (S-wave velocity/thickness)
Slab impulse respond	Vibration frequency of concrete slab (voids/thickness)
Ultrasonic Velocity	P wave velocity (concrete strength)
P-S Wave Measurements (hole to hole)	P and S wave velocity (elastic moduli/integrity))
Borehole Imagery Methods TV/ATV/BIPS	Image of core hole (Voids and fractures intersecting the borehole)
Sonic Tomography	P wave velocity (Image of conditions between boreholes based upon sonic measurements)
Radar Tomography	Radar velocity (Image of conditions between boreholes based upon radar measurements)

Table 8
Summary of Methods Applied to Bridge Scour Assessment

Method	Parameter/Condition Measured
Various Monitoring Attachments (electrical, TDR)	Changes in resistivity or dielectric properties (Monitor changes in sediment thickness)
Bathymetry	P wave travel time (Acoustic profile of bottom scour)
Side scan sonar	P wave travel time (Broad acoustic image of bottom scour)
Divers or ROV with TV	Visual image (Document bottom conditions)
Subbottom profiling (seismic reflection) to establish depth to rock	P wave travel time (Determine stratigraphy/depth to rock)

Table 9
Summary of Methods Applied to Roadbed Condition/Thickness/Voids/Deterioration

Method	Parameter/Condition Measured
Rebar Corrosion Potential	Voltage due to galvanic action (area of rebar corrosion)
Ground Penetrating Radar	Dielectric constant (asphalt, concrete, and subbase thickness/voids/rebar)
Seismic Surface Wave Analysis	Seismic velocity/dispersion (S-wave); (asphalt, concrete, and subbase thickness/uniformity)
Slab impulse respond	Vibration frequency of concrete slab (voids/thickness)
Nuclear Density/Porosity	Density/Porosity (quality and uniformity of material)
Thermal Imagery	Temperature of surface (porous areas/voids/moisture)
Shallow Electromagnetics	Conductivity of subbase (voids/porous zones/moisture)
Laser Rugosity	Reflection (Surface roughness)
Video	Surface image documentation

Temporal Measurements for Monitoring of Conditions and Remediation Management

Many of these methods can be used to monitor changes in conditions with time. Such data can be incorporated into a database to guide management decisions for maintenance and repairs. Maintenance and repairs on roads, bridge decks and bridge scour is becoming ever important as our infrastructure ages. Monitoring changes over time allows an assessment of frequency and distribution of potential problems. Monitoring can be accomplished in two ways: by measurements which are repeated at suitable intervals in time or by in-situ measurements (made by implanting sensors) to provide semi-continuous monitoring of any change in conditions.

CONCLUSIONS

There are a variety of roadway and bridge problems that can be solved by integrating the use of remote sensing, geophysical and non-destructive testing techniques. The benefits of such measurements compared to discrete point measurements or tests are that they: are non-destructive, provide in-situ measurements of a number of physical properties, sample larger areas or volumes, provide continuous measurements in some cases, and provide faster measurements.

All of this results in a greater sample density, which can more readily identify uniform conditions as well as locate anomalous conditions. Once anomalous conditions are identified, those areas requiring further tests, borings or repairs can be accurately and quickly located.

These methods, like any other means of measurement, have advantages and limitations. There is no single, universally applicable method that can be used to meet all site characterization needs. Some methods can be adapted to a wide range of measurements. For example, radar can be adapted to identify the locations and depth of rebar in concrete, evaluate thickness and uniformity of pavement and provide stratigraphy data to depths of 10's of feet. If we are looking for details we must use a method that will provide the level of detail (resolution) needed. While many methods can be adapted to a wide range of scale, there is usually one or two optimum methods that can be applied. Methods must be selected and applied by professionals with the necessary knowledge and experience.

REFERENCES

American Society for Testing and Materials, 1995. Standard guide for planning and conducting borehole geophysical logging. ASTM D5753.

American Society for Testing and Materials, 1997. Provisional Guide for Selecting Surface Geophysical Methods, ASTM PS 78-97

Benson, R. C., 1993. Geophysical Techniques for Subsurface Site Characterization, Chapter 14, In: Geotechnical Practice for Waste Disposal, David Daniel, Ed., Chapman and Hall, pp. 311-357

Olson, Larry, 1998. Short course on Nondestructive Testing (NDT). Symposium on the Application of Geophysics to Environmental and Engineering Problems, Environmental and Engineering Geophysical Society, Wheat Ridge, Colorado, March 22.

O'Connor, K.M., and Dowding, C. H., 1999. GeoMeasurements by Pulsing TDR Cables and Probes, CRC Press LLC, Boca Raton, FL, 402 p.

Freeze, A. and J. Cherry, 1989. What has gone wrong - A guest editorial. Groundwater Vol. 27 #4, July-August.

Shuirman, G. and Slosson, J. E., 1992. Forensic engineering, environmental case histories for civil engineers and geologists. Academic Press, Inc., San Diego, California, 296 p.

Replacement of Bridge B-451, Milepost 78.98, Carrying S.R. 0819 Over the Pennsylvania Turnpike

Lawrence J. Artman, II, P.G.
Senior Geologist
HDR Engineering, Inc.

Matthew L. McCahan
Project Geologist
Pennsylvania Turnpike Commission

ABSTRACT

This project is part of the Pennsylvania Turnpike Commission's continuing efforts to upgrade its facilities. The work included design of a replacement structure which eliminates the median pier and improves vertical and horizontal clearances under the new bridge in preparation for a mainline reconstruction project between Mileposts 76 and 85. The new structure and approaches will be constructed along the same general horizontal alignment of existing S.R. 0819, but with a grade increase to provide additional vertical clearance under the structure. The extreme skew of the alignment requires a single-span, 172-foot long structure providing a clear distance of 96.3 feet between the faces of the new abutments. Modifications to the vertical geometry results in the addition of a maximum 9 feet of new fill that will completely envelop the existing embankments. The new embankments will be constructed of random and rock embankment materials keyed into the existing approach embankments.

Bridge B-451 carries S.R. 0819 over the Pennsylvania Turnpike mainline at Milepost 78.98 in Westmoreland County, approximately 3 miles east of the New Stanton Interchange (No. 8). The existing structure was built during original construction of the mainline Turnpike (circa 1940). The existing structure is a two-span, simply-supported structure skewed approximately 35 degrees to mainline with an intermediate pier located in the median of the turnpike. Existing abutment and wingwall foundations consist of buried concrete buttresses (counterforts) founded on spread footings (on rock) at a depth of approximately 50 feet below existing Turnpike grade. The buttresses were constructed within a deep-mine undercut created to remove mined Pittsburgh Coal from beneath the mainline roadway and structure foundations. The pier is also founded on spread footings bearing on rock at the base of the undercut.

H-pile foundations utilizing battered piles would interfere with the buried buttresses (to remain) and highwall and would significantly increase the length of the structure. Spread footings would pose similar constructability problems and introduce long-term stability concerns into the design. Consequently, the new abutments and wingwalls will be founded on 48-inch diameter drilled shafts installed through the undercut backfill to the base of the Pittsburgh Coal undercut with 42-inch diameter rock sockets founded in competent bedrock below the coal. The shafts will be installed in a line 4.5 feet behind the existing buttresses and will be capped with a footing tangent to and at the approximate elevation of the top of the existing buttresses. Some lateral support will be provided by the buttresses. Permanent casing will be used for the shaft section due to the soft, wet conditions of the undercut backfill. Type II sulfate resistant cement and epoxy-coated reinforcement will be used due to the corrosive nature of the backfill materials and groundwater. Deep-mine grouting will be performed at Wall B since it will straddle the buried highwall. Evidence of chimney collapse was encountered in the boring at this wall. Construction began in January of 1999, with a scheduled duration of eleven (11) months.

PROJECT SCOPE

The Bridge B-451 Replacement project is part of the Pennsylvania Turnpike Commission's continuing efforts to upgrade its facilities. The work performed by HDR included design of a replacement structure to eliminate the median pier and provide additional horizontal and vertical clearance under the new bridge. The design effort was to be completed prior to and in preparation for a mainline Turnpike reconstruction project between Mileposts 76 and 85. The Project Location Map in Figure 1 shows the bridge location relative to the nearby New Stanton Interchange (No. 8).

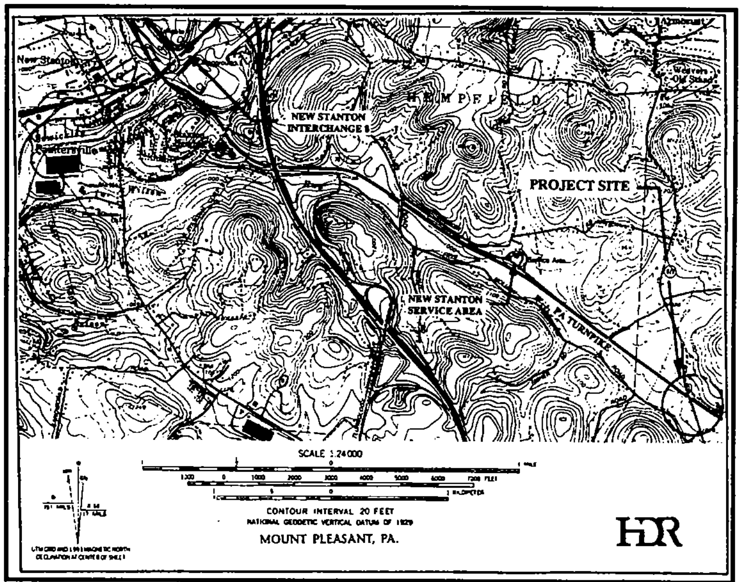

Figure 1 – Project Location Map

To meet the horizontal clearance requirements of 92.0 feet between the abutment faces for the reconstruction project, a minimum 165-foot long structure was required to span the width of the Turnpike due to the extreme skew of the alignment. The horizontal clearance between the existing abutments is 78.0 feet. To minimize the required structure length, alternate foundation types were analyzed, including drilled shafts, driven (or pre-drilled) piles, and spread footings. Because of space restrictions caused by the existing abutment and wingwall foundations, drilled shaft foundations were ultimately selected as the design foundation type. Modifications to the approach embankments to accommodate the structure and provide the necessary vertical clearance under the bridge required the addition of approximately 9 feet of new fill along the southern approach. Along both approaches, the new fill consisting of either random or rock fill materials will completely envelop the existing embankments.

A detailed site investigation was conducted by HDR geotechnical personnel that included a thorough review of the site geological information and available design information from the original construction. A test boring program was developed to investigate conditions around the new structure location and in the approach areas. Borings were also taken to delineate the limits of the buried undercut highwall around the existing foundations. Laboratory testing focused on rock unconfined compression testing for developing allowable loads in the proposed shafts. Corrosion testing was conducted on soil and water samples from the undercut backfill materials and groundwater, and approach embankment materials, to determine if additional measures would be required to protect the new foundations. A limited number of classification tests were performed on project soils to correlate soils types across the site. Project special provisions, geotechnical details, and geotechnical treatment quantities were ultimately developed for construction of the new bridge and approaches.

This paper presents the results of these investigations and the foundation design methodologies employed to accommodate the new structure, while accounting for the impacts from the deep mining performed in the project area and construction techniques used to build the existing bridge.

HISTORICAL PERSPECTIVE

The Pennsylvania Turnpike, America's first super highway, was constructed between 1938 and 1940. The original Turnpike alignment was 160 miles long and stretched from Carlisle, PA, near the state capital of Harrisburg, to Irwin, Pennsylvania, a municipality approximately 20 miles southeast of Pittsburgh (*Cupper, 1995*). The original route follows much of the abandoned right-of-way of the South Pennsylvania Railroad which became defunct in 1885. With 60 percent of the grading and a significant portion of tunneling work completed for the railroad, the line was abruptly abandoned and remained that way until the mid-1930's when there became increased interest in developing a major east-west route across the state due to changing demographics and commerce. The first members of the Pennsylvania Turnpike Commission were appointed on June 4, 1937, and the search for funding for the new road began. Design work started shortly thereafter. Incorporated into the WPA work programs of the Roosevelt administration, funding for construction was in place on October 10, 1938, and the first contract let on October 26 of the same year. Opened to traffic on October 1, 1940, the total cost of the original 160-mile alignment was around $70,000,000.

In order to maintain existing drainage and traffic on local and state highways intersected by the Turnpike, a total of 307 bridges and culverts were designed and constructed. The design for 21 of the original overpasses consisted of two simple spans supported on a median pier. Federal officials objected to this design citing potential collision hazards with the median pier, but only after many of these structures were already completed. One of these structures was the B-451 bridge shown in Figure 2, completed prior to switching to a single-span arrangement for the remaining overpass structures. Aside from minor rehabilitation projects to maintain the original structure, the current bridge remains as it was originally designed and constructed in 1940.

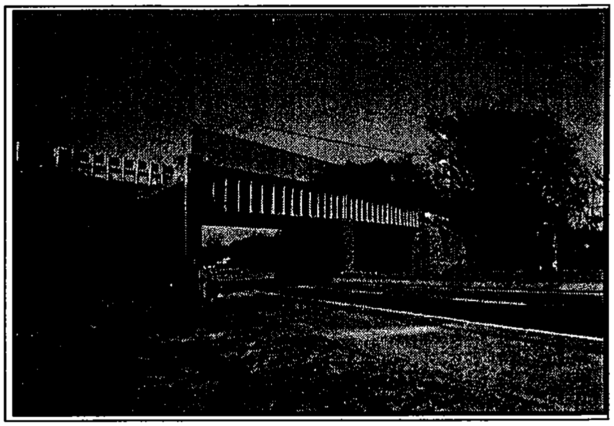

Figure 2 – Existing Bridge

PROJECT SETTING

Located around 3 miles east of Turnpike Interchange No. 8 (New Stanton) at Milepost 78.98, Bridge B-451 carries State Route 0819 (S.R. 0819) over the Turnpike between the communities of Mount Pleasant and Armbrust in Westmoreland County. The existing structure is a two-span, simply-supported structure skewed approximately 35 degrees to mainline with an intermediate pier located in the current 10-foot wide median. The existing abutments consist of cantilevered walls supported on buried concrete buttresses (counterforts) founded on spread footings. The existing abutments and wingwalls are a maximum 20-feet high and are supported directly on the buried buttresses. The footings for both the abutments and median pier are founded on rock approximately 45 to 50 feet below Turnpike grade. The existing approach fills follow the same general alignment as the original S.R. 0819 roadway and are currently standing at 2:1 slopes. Some areas of the approaches are oversteepened to a 1:1 sideslope as a result of the addition of new fill during subsequent approach and pavement rehabilitation projects.

GEOLOGIC SETTING

The project site is located in the Pittsburgh Plateaus Section of the Appalachian Plateaus Province of Western Pennsylvania. Rocks underlying the site are typical of formations found in the western part of the state and consist of Pennsylvanian-Aged, cyclothemic siltstones, shales, claystones, limestones, and coals of the Conemaugh and Monongahela Formations. Separating these formations is the Pittsburgh Coal seam, one of the numerous economically attractive coal seams characteristic to this sequence of Appalachian stratigraphy. The Pittsburgh Coal separates the formations into the Little Pittsburgh and Pittsburgh members, respectively. The Pittsburgh Coal typically ranges from 10 to 13 feet in thickness across the region but is 5 to 13 feet thick at the project site.

Structurally, the project site is situated between the Fayette Anticline and the Uniontown (Latrobe) Syncline, both of which are gently-folded structures trending generally to the northeast (*Skema, 1988*). Structural mapping on the Pittsburgh Coal (see Figure 3) indicates that the Turnpike is aligned perpendicular to strike of bedrock, which is dipping toward the southeast at a rate of approximately 7 percent. The alignment of the existing B-451 structure and approaches cuts across strike and up-dip toward the northwest as evidenced from the geologic mapping and the boring information which indicates a general rise in elevation of the coal toward the northwest. Due to the folded nature and differential erosion characteristics of the stratigraphy, as well as the geomorphological processes acting on the various formations, the coal crops in the subsurface along a northeast-trending crop line nearly perpendicular to the Turnpike and 500 feet west of the existing bridge. The coal has been removed by erosion west of the crop line in the Fayette Anticline.

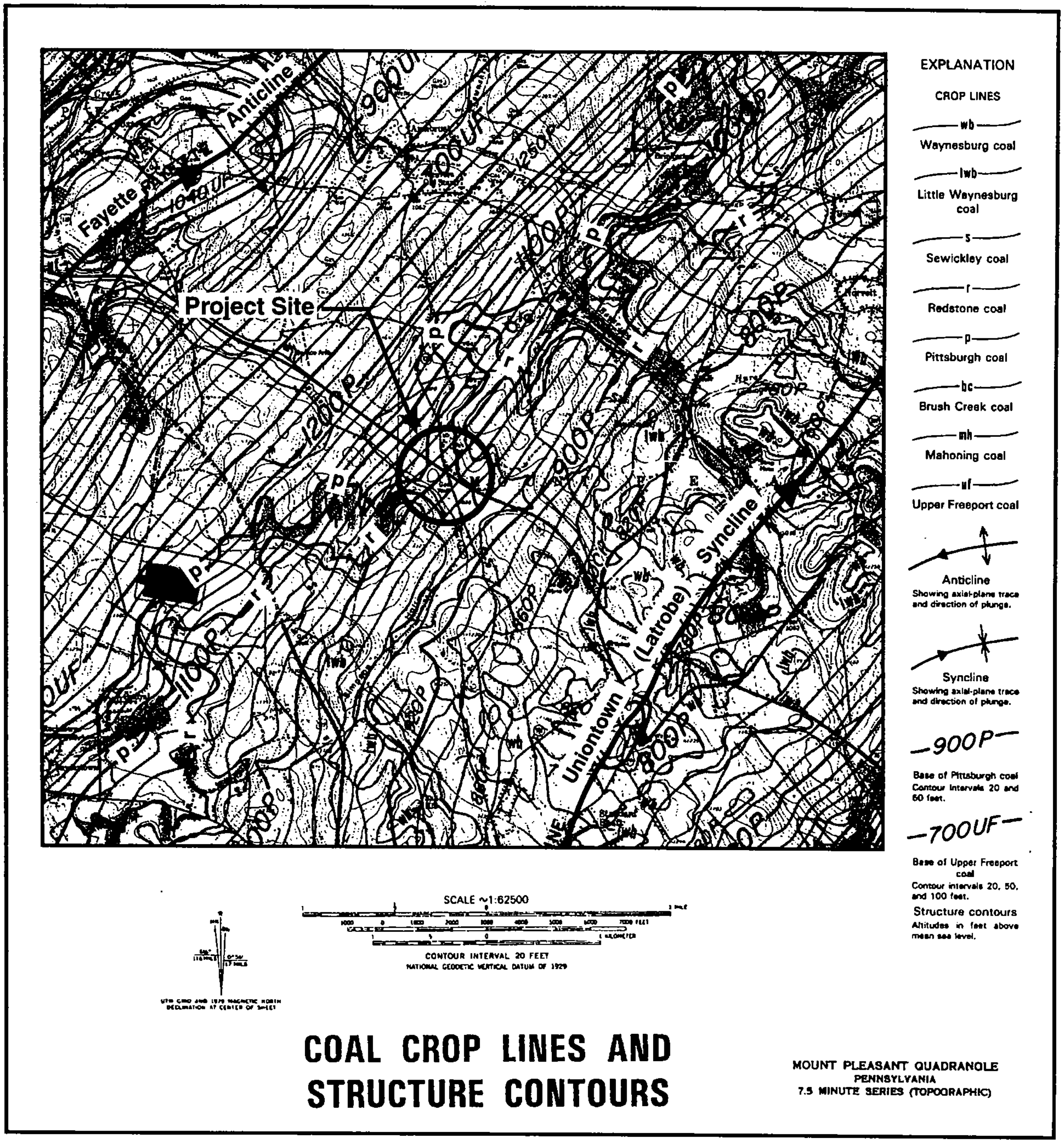

Figure 3- Structure Contours on the Pittsburgh Coal

COAL GEOLOGY AND MINING IMPACTS

Mining of the Pittsburgh coal has been extensive in the project area. While both deep-mining and strip-mining methods have been used in the region, deep-mining by the room-and-pillar method has been the prevalent form of extraction, particularly in the project area. Available mine mapping indicates that the entire Pittsburgh seam has been mined east of the crop line in the Uniontown Syncline. Based on borings taken during original design efforts, the bottom of the coal is located between Elevations 1005 and 975 along the Turnpike and ranges from 5 to 13 feet in thickness. Original borings drilled at the abutment locations indicate that the bottom of the coal is located between Elevations 995 and 992 at Abutment 1 (southern abutment), and 996 and 990 at Abutment 2 (northern abutment). These elevations were generally confirmed in borings taken during the current investigations.

Several of the original borings encountered both open voids and voids filled with gob and collapse materials. To mitigate potential mine collapse beneath the bridge and the Turnpike, an undercut was excavated to the base of the coal. This method of stabilizing the roadway was used at several other locations along the original Turnpike alignment. Stretching from the crop line to approximately 100 feet east of the bridge, the undercut followed the dip of the coal to a depth of around 50 feet below Turnpike grade or to a depth at which engineers believed sufficient support was provided by the remaining rock overburden. The limits of the undercut provided sufficient clearance for forming the concrete buttresses. The original plans indicate by a detail that a ½:1 slope was to be used for the highwall around the perimeter of the undercut. The photos in Figures 4 and 5 show the undercut during construction and the room-and-pillars of the mines. Note the west to east dip of the coal in Figure 4 and the chimney collapse zones above the coal in Figure 5. Soft gob materials are visible along the undercut floor in both photos.

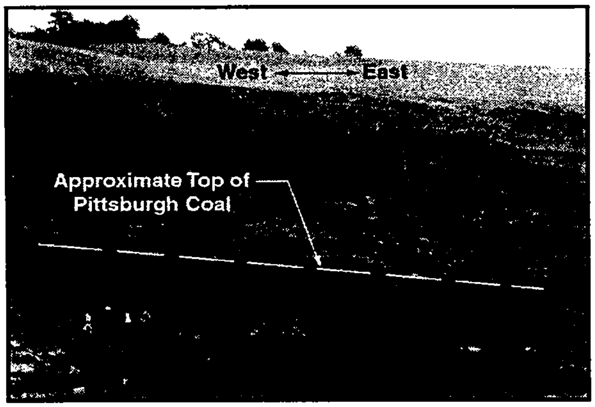

Figure 4 – Northern Highwall Slope of Undercut During Construction

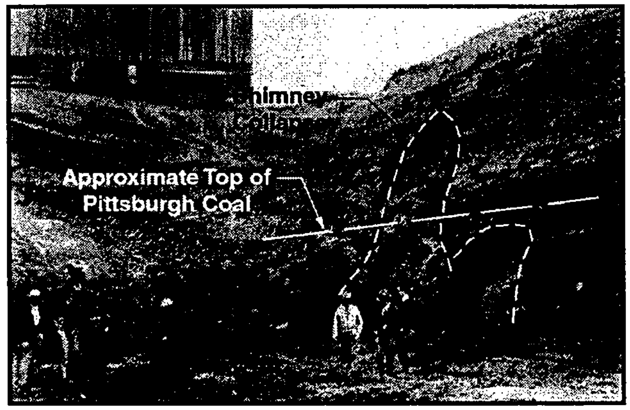

Figure 5 – Southern Highwall Slope of Undercut During Construction

Upon removal of the coal and preparation of the base of the undercut, the foundations were constructed and the undercut backfilled with materials from the pit. Additional backfill materials were likely needed to replace the removed volume of coal and excavated materials from the buttress foundations. According to local residents, an area adjacent to the bridge was used as a borrow pit. The pit was never backfilled and has subsequently filled with discharge waters from the mines as they are outletted at the surface. These discharges have been channeled to the pit which, over time, have formed a pond. The mine waters are being treated by the U.S. Department of Energy (formerly the U.S. Bureau of Mines) and a local watershed association by passive treatment methods. Treatment techniques include periodic addition of lime and aeration of the mine waters as they exit the ground. The pond acts as a settlement basin prior to release of the discharges into the local stream system.

The original plans delineated several sinkholes below the northern bridge approach which were likely grouted or backfilled prior to embankment construction. Several sinkholes are currently visible in the open fields surrounding the site. One of the current borings drilled near the southeastern wall of the existing bridge penetrated a chimney collapse zone. The boring was advanced through the collapse zone and into the base of the mine. Due to the expected density of rooms in the mine workings and the relatively high percentage of undisturbed areas on the surface around the project site, it is inferred that complete collapse of the overlying overburden into the mines has not occurred and is an ongoing process.

Two other prominent Pennsylvanian-Aged coal seams have been mined in the project area. Located approximately 650 feet below the Pittsburgh Coal, the Upper Freeport Coal has been mined extensively west of the project in the New Stanton area (Fayette Anticline) where the coal crops at the surface. Both strip- and deep-mining methods have been used for mining the Upper Freeport. However, due to its depth below the Pittsburgh Coal at the site, it should not impact the project. As shown in Figure 3, the Redstone Coal crops in the subsurface to the east of the Pittsburgh Coal crop line and the project site. Located 40 to 70 feet above the Pittsburgh seam, with a thickness of approximately 48-inches, the Redstone crop line generally parallels the Pittsburgh crop and follows the local topography. Stripping of the Redstone has occurred at several locations near the project site, but will not affect the project design.

SUBSURFACE INVESTIGATIONS AND LABORATORY TESTING

A total of 16 test borings for approximately 500 lineal feet of drilling were taken as part of the current geotechnical investigations. Locations for these recent borings are shown in the Plan and Location of Borings drawing included as Figure 6. Locations for borings taken as part of the original investigations (circa 1939) are also shown on the plans. Drilling was conducted in December, 1997, by the Pennsylvania Drilling Company of McKees Rocks, Pennsylvania. Continuous and 5-foot interval Standard Penetration Tests (SPT) were typically taken to refusal in project soils which was defined as an SPT penetration of 50 blows for intervals less than 0.1 foot. In some instances, refusal was met more than once before coring was begun. This typically occurred in highly weathered shale units or in the soft claystone/underclay, in-place coal, or gob materials at the Pittsburgh Coal horizon at the base of the undercut. Coring was started when, in the judgment of the inspector and driller, it was believed that coring would result in good recovery and SPT-sampling methods were no longer required. Pocket penetrometer readings were taken on SPT samples in cohesive materials for estimating unconfined compressive strength. Rock was cored using NQ2-sized wireline equipment. NQ2 concrete coring was also conducted through one of the buttresses at Abutment 1, through the existing footing, and into the underlying bearing materials. Core recoveries and RQD's were measured for all core runs. Stratum RQD's were computed for each rock type encountered.

Borings were taken to investigate foundation conditions in the structure area and the foundation areas of the new approach embankments. Structure borings S-1 through S-10 were drilled to investigate foundation conditions at the existing and proposed abutments, and conditions under the proposed wingwall extensions (see Figure 6). The borings were also located to establish the limits of the deep-mine undercut, the type of backfill materials used, and to determine whether the new wingwall foundations would clear the buried highwall. One boring, S-2, was drilled through one of the buried buttresses to investigate the condition of the concrete and the footing contact with the underlying bearing material. Borings S-3 and S-8 were drilled behind the abutment walls through the S.R. 0819 embankment and into rock below the base of the undercut.

All structure borings, with the exception of S-1, S-5R, and S-6R penetrated the full depth of the undercut and backfill materials. The backfill varied between 40 and 50 feet in thickness and consisted of multi-layered, typically fine-grained soils with varying amounts of rock fragments derived from the local rock types. SPT samples tested classified as clayey sands with gravel [SC/ A-4(1) to A-2-4(0)], clayey gravels with sand [GC/ A-1-b to A-6(2)], and sandy lean clays [CL/ A-6(9 to 10)], all with varying amounts of rock fragments. Many of the soil layers were dark gray to black, which has been attributed to the carbonaceous nature of the parent materials. Upon reaching the base of the undercut, residual coal and mine gob was encountered in several of the borings, while soft underclay and coal fragments or very soft claystone was encountered at others. Hard, competent bedrock formed a clearly definable layer at the base of the softer materials and consisted of hard to very hard siltstone and limestone. Stratum RQD's of 10 to 84 percent and 10 to 92 percent were measured in the siltstone and limestone units, respectively. Groundwater was generally first encountered during SPT sampling in a granular, water-bearing layer near the base of the undercut. Artesian conditions did not develop, but groundwater rapidly rose in the augers until it stabilized approximately 10 feet below Turnpike grade (Elevation 1035).

Corrosion potential of soil and water samples in the undercut was determined with respect to minimum resistivity, sulfate and chloride content, and pH following ASTM, CalDOT, and PennDOT testing methods. For design purposes, criteria established in PennDOT Design Manual 4 (DM-4) (*PennDOT, 1993*) were used for estimating corrosive potential with respect to both steel and concrete foundations. Results of the testing relative to the criteria used in DM-4 are presented in Table 1. Shaded values in the table indicate test values considered corrosive with respect to the DM-4 criteria. Based on these results, it was concluded that the existing soil/groundwater regime in both the embankment and undercut backfill materials was potentially corrosive for either concrete or steel and that protective measures would be required for the selected foundation type.

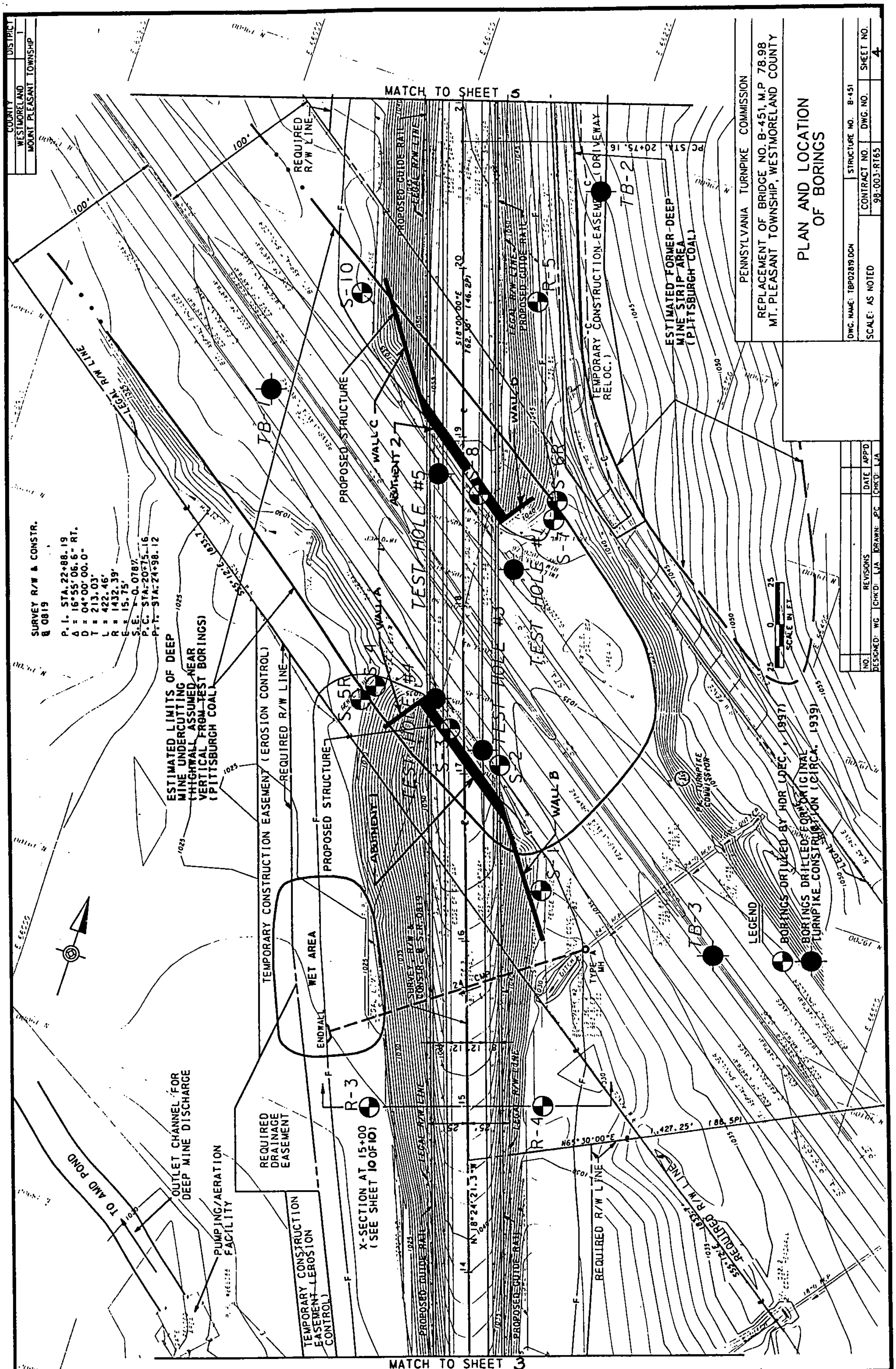

Figure 6 - Plan and Location of Borings

Borings S-5R and S-6R were drilled in section with borings S-4 and S-7, respectively, to delineate the highwall slope (see Figure 6). Refusal on rock was met at 6.6 and 16.6 feet indicating that the highwall was located between the paired borings and rose approximately 40 feet vertically within a 10-foot horizontal distance (i.e., ¼:1).

TABLE 1 – SUMMARY OF CORROSION TESTING RESULTS

TB#/ GENERAL MATERIAL TYPE	SAMPLE NO.	SAMPLE DEPTH (feet)	MINIMUM RESISTIVITY (ohm-cm)	SULFATES (ppm)	pH (Standard Units)	CHLORIDES (ppm)
S-3/ SR 819 EMBANKMENT	B-1	1.5 – 1.9	13,885	148	7.2	108
S-3/ SR 819 EMBANKMENT	B-2	15.0–16.5	2,700	<50	6.2	54
S-10/ UNDERCUT BACKFILL	B-1	4.5 - 10.5	3,650	131	6.5	102
S-10/ UNDERCUT BACKFILL	B-2	15.0-24.0	11,412	238	6.5	22
S-10/ UNDERCUT BACKFILL	B-3	24.0-30.0	605	207	6.5	323
S-3/ GROUNDWATER	W-1	31.5	0.37	108	7.2	1,550
S-10/ GROUNDWATER	W-1	33.0	0.39	626	6.5	1,440
DM-4 CORROSIVITY THRESHOLD			*<10,000*	*>150*	*<5.5*	*>1,000*

Boring S-1 drilled near proposed Wall B hit bedrock at a depth of approximately 17 feet indicating that the new wingwall will straddle the buried highwall. Rock coring was begun at SPT refusal. The top of a chimney collapse zone was penetrated at a depth of approximately 36 feet in a dark gray siltstone unit overlying the coal. The collapsed zone was identified by the high-angle bedding in the core, the uneven tool advance through hard and soft layers, the loss of drill water, and poor core recoveries. These materials were encountered to a depth of approximately 50 feet until in-place coal was recovered and the bedding again became horizontal. An interbedded underclay and carbonaceous shale was penetrated beneath the coal followed by a hard, thinly-bedded limestone unit with a stratum RQD of 80 percent. An unconfined compression test on a sample of the limestone indicated a compressive strength of 2,670 psi.

Boring S-2 was drilled through one of the buried concrete buttresses and into the underlying bearing materials. Figure 7 shows a sectional view of one of the buttresses redrawn from the original plans. The buttress was penetrated at a depth of approximately 5 feet below Turnpike grade to a total depth of around 50 feet. The concrete was slightly iron-stained and vuggy, but was generally in good condition. An unconfined compression test on a sample of the concrete indicated a compressive strength of 6,300 psi. The drill rods deviated from vertical during the coring, exited the side of the buttress stem at a depth of approximately 36 feet and were completely out of the concrete at a depth of approximately 38 feet. No sample was recovered between a depth of 38 and 48 feet as the tools penetrated the undercut backfill materials surrounding the stem. The tools again seated on concrete (top of footing) at a depth of approximately 48 feet (elevation 986) and penetrated bedrock at the bottom of the footing at a depth of approximately 50 feet (Elevation 984). The limestone unit penetrated in the other borings was encountered at the base of the footing. The bottom of footing elevation in the boring differed from the proposed elevation of 991 in the original plans. It has been inferred that the soft materials (underclay/claystone) overlying competent bedrock were overexcavated under the footings prior to constructing the buttress. It appears that the decision to lower the footing elevation was a field decision made during construction to provide suitable bearing.

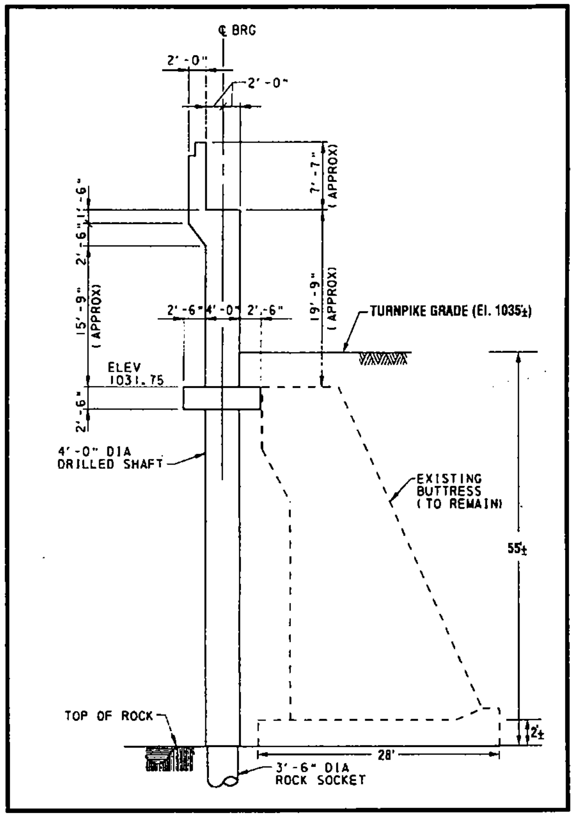

Figure 7 – Buttress Section View

Borings S-3 and S-8 were drilled immediately behind the backwalls of the existing abutments from S.R. 0819 grade. Taken to total depths of 70 and 72 feet, respectively, both borings penetrated approach fill materials to Turnpike grade elevation and then undercut backfill materials to mine level. Approach fill materials tested were mixed-grained soils consisting of silty sands with gravel [SM/ A-1-a] and sandy lean clays [CL/ A-7-6(8)]. Backfill materials behind both abutment walls were similar to those encountered in the borings drilled in the undercut. Bedrock was encountered approximately 60 feet below grade and consisted of the limestone and siltstone units previously described. Stratum RQD's ranged from 43 to 92 percent in the limestone and 10 to 37 percent in the siltstone. In-place coal (gob) and underclay/claystone was penetrated before hitting good rock in boring S-10, but was missing in boring S-3. Unconfined compressive strengths of 7,300 and 8,100 psi were measured in the siltstone in borings S-3 and S-8, respectively. Similarly, compressive strengths of 8,100 and 7,200 psi were measured in the limestone in each boring.

FOUNDATION DESIGN CONSIDERATIONS

Drilled shafts, driven (or pre-drilled) steel H-piles, and spread footings were considered early on in the investigations as potential foundation types. However, space restrictions, foundation stability, and cost issues were determining factors in the foundation type ultimately selected. Driven piles and spread footings were eliminated for several reasons. Preliminary calculations indicated that lateral loads would be relatively high for any deep foundations due to the span length required to clear the Turnpike. Driven piles would have to be battered to handle the anticipated lateral loads. Because of the space restrictions posed by the buried buttresses, tip locations for new piles would be determined from estimating the limits of the rear side of the buttresses and translating the batter (3:12) to the pile cap near Turnpike grade. This would have significantly increased the span length and ultimately required a more costly, multi-span structure. Since the goal of the project was to eliminate the median pier, use of a multi-span structure would have negated the project goals while significantly increasing costs.

The use of pre-drilled vertical piles installed through the rock overburden above the coal was considered since some resistance to lateral loading would be provided by the in-situ rock. However, this option would have also required a longer, multi-span structure (with median or shoulder piers) to push the pile caps behind the limits of the buried highwall (see Figure 6). In addition to the substructure costs (including piles), other costs associated with pre-drilling, additional piles for handling lateral loads, and grouting of the mine workings under the abutments to improve stability would have increased the total cost of the new structure. Consequently, both driven and pre-drilled piles were eliminated from further consideration.

The use of spread footings would have posed many of the same problems as the pile foundations. Because of the proximity of the undercut and the need to limit structure length, spread footings on rock would not have been possible over the undercut area behind the abutments. Using the soft, inconsistent undercut backfill materials for bearing would have resulted in low calculated allowable bearing capacities and increased the potential for differential settlement across the footings. Pushing the abutment footings back behind the buried highwall would have been possible, but would have also required a multi-span structure, significant overexcavation to reach bedrock, and grouting of the mines to improve stability under the foundation footprints. Consequently, spread footings were also eliminated as an alternate foundation type.

After further analysis, drilled shafts bearing in the competent rock units below the coal appeared to be the most feasible foundation system of the three considered. The shafts could be installed vertically behind the buttresses in the undercut backfill materials which would minimize the required span length while maintaining the single-span arrangement. Since the buried buttresses were to remain, the analyses focused on incorporating them into the new structure to provide some of the required lateral resistance. As shown in Figure 7 and the structure plan in Figure 8, a single row of 48-inch shafts with 42-inch rock sockets will be installed in a line behind the buttresses. This configuration results in a horizontal clearance of 96.3 feet between the abutment faces. The shafts will be capped with a footing tangent to and at the approximate elevation of the tops of the buttresses. The abutment backwalls will be constructed directly on the cap beam. Permanent, sacrificial casing will be used in the soil zone and will be drilled into bedrock to stabilize the anticipated soft, wet backfill soils of the undercut. Because of the flooded condition in the mines, the casing should mitigate some of the groundwater inflow into the shafts from the water-bearing layer at the base of the undercut. It was also recommended for construction that the casing be advanced quickly through the water-bearing layer into rock to minimize the volume of water in the shafts. Groundwater inflow is to be monitored at each shaft and allowed to stabilize before placing concrete into the shafts by tremie methods. Type II sulfate-resistant cement and epoxy-coated reinforcement will be used due to the corrosive nature of the backfill and groundwater. The contract also included a special provision and quantities for deep-mine grouting around Wall B to stabilize the open voids and collapse zones in the overburden prior to installation of the shafts along the wall.

The rock sockets will be founded in the competent limestone and siltstone units below the softer coal and underclay deposits at the base of the undercut. Based on the unconfined compression testing results and stratum RQD measurements from the borings, an allowable side resistance, q_{sr}, of 32 psi was calculated for the shafts at both abutments using AASHTO methods (*AASHTO, 1992*). Using a 10-foot embedment depth for each rock socket resulted in an allowable load in side resistance of 253 tons per shaft (i.e., 25.3 tons per lineal foot of rock socket). Actual vertical loads calculated in the structural analysis were calculated to be 295 tons per shaft.

Additional load bearing capacity was required for the computed vertical loads. An allowable bearing capacity for end bearing was calculated using AASHTO methods for broken and jointed rock. Based on these calculations, an allowable bearing capacity, q_{all}, of 8.5 tsf was calculated for shafts at both abutments. Using the 42-inch rock socket end area, an additional 82 tons (per shaft) was provided in end bearing. Because of the soft, wet conditions in the undercut, it is expected that complete cleanout of the shaft bottoms may be difficult. However, the project special provisions provide for using probings and down-hole videography for monitoring shaft cleanout.

Lateral loads were analyzed using the COM624 computer program (*FHWA, 1993*). Lateral load capacity of the shafts was computed by modeling the drilled shafts, surrounding backfill materials, and buried buttresses as one system. Based on the analysis, the buttresses were adequate to resist 48 tons each, requiring each drilled shaft to resist 82 tons each of lateral load. No uplift load was computed in any of the drilled shafts. The controlling design loadings were computed for AASHTO Group I loading. Based on the proposed shaft spacing and information in the

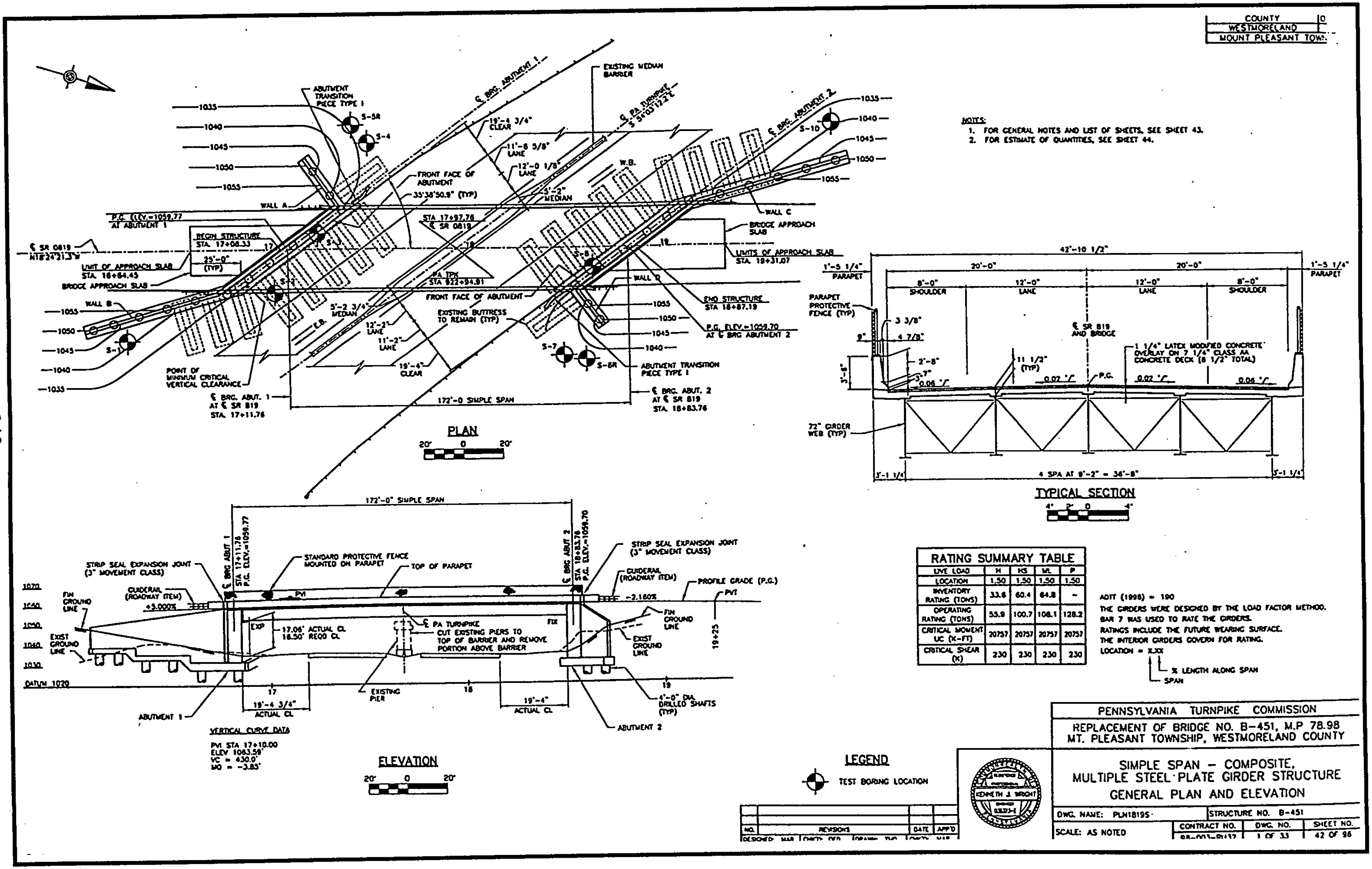

Figure 8 - Structure General Plan and Elevation

available literature (*AASHTO, 1992; FHWA, 1984; Wang, 1997*), group effect reductions in lateral capacity were to be minimal.

CONCLUSIONS

The Bridge B-451 Replacement Project posed several unique and interesting geotechnical and structural design challenges due to the mining in the project area, and the techniques used for constructing of the existing structure. Through review of the geological literature, original design plans, test borings, and laboratory testing, a design was prepared that efficiently re-used the existing buttress foundations while meeting the requirements of a single-span replacement structure. Construction on the replacement structure began in January, 1999, and is to be completed in November, 1999. Through HDR's construction services contract with the Turnpike Commission, the design will be followed through construction. Results of the construction may be presented in a subsequent paper.

REFERENCES

AASHTO, 1992, *"AASHTO Standard Specifications for Highway Bridges, Fifteenth Edition, 1992,"* American Association of State Highway Transportation Officials (with Interims)

Cleaves, 1949, *"Guidebook to the Geology of the Pennsylvania Turnpike, Carlisle to Irwin,"* by Cleaves, A.B., and Stephenson, R.C., Pennsylvania Topographic and Geological Survey, Bulletin G-24, 1949 (Including photos used in paper)

Cupper, 1995, *"The Pennsylvania Turnpike – A History, 55th Anniversary Edition, Authorized History of the Pennsylvania Turnpike Commission,"* by Cupper. D., Applied Arts Publishers, 1995

FHWA, 1993, *"COM624P – Laterally Loaded Pile Analysis Program for the Microcomputer, Version 2.0,"* Manual FHWA-SA-91-048, Federal Highway Administration, August, 1993

FHWA, 1984, *"Handbook on the Design of Piles and Drilled Shafts Under Lateral Loads,"* Manual FHWA-IP-84-11, Federal Highway Administration, July, 1984

Skema, 1988, *"Coal Resources of Westmoreland County, Pennsylvania, Part 1. Coal Crop Lines, Mined-Out Areas, and Structure Contours,"* by Skema, V.W., Mineral Resources Report 94, Part 1, Pennsylvania Topographic and Geologic Survey, 1988

Wang, 1997, *"Chapter 6, Reduction Factor for Soil Resistance in Closely-Spaced Pile Groups Under Lateral Loading,"* by Wang, S., excerpt from *Documentation of Computer Program LPILE, Version 4.0*, by Reese, L.C., and Wang, S., Ensoft, Inc., 1993

Pile Relaxation in Soft Shales

A Critical Evaluation of the Effectiveness of Various Remedial Strategies based on Experience on the West Busway Project in Pittsburgh Pennsylvania

Keith Wargo , P.E. , Port Authority of Allegheny County
Scott D. Zang, P.E., Michael Baker Jr., Inc., Beaver, Pennsylvania

1 INTRODUCTION

The Port Authority of Allegheny County is constructing a Busway From West Carson Street in the City of Pittsburgh to the Borough of Carnegie with a connection to I-279. The Busway is an exclusive roadway for bus traffic which will serve the communities west of Pittsburgh and will allow buses from these communities to bypass daily traffic jams at the Fort Pitt Tunnel on I-279. It will also help relieve traffic on detour routes when the Fort Pitt Tunnel and Bridge are closed for major rehabilitation early in the next decade. The busway also includes six stations to permit patron boarding.

One such station, Bell Avenue Station, is located in the section of the project just north of the connection to I-279 (see Figure 1). Construction began on this section in the spring of 1998 and is expected to be completed in November of 2000.

The Bell Avenue Station is situated atop an existing railroad embankment about fifteen feet above the adjacent ground. It consists of a patron platform on either side of the busway and is accessed via stairs and an ADA accessible ramp on the east side of the Busway. Multiple retaining walls were required to support the platform, stairs and ramp within the available right-of-way. These walls are identified as Wall 13403R and Wall 13665R (see Figure 2). Wall 13403R consists of multiple concrete walls supported on a single continuous foundation and Wall 13665R is a typical single concrete cantilever wall.

During installation of the pile foundations for these walls, dynamic testing and field observations indicated that the piles in some portions of the wall were experiencing significant relaxation; that is, the loss of capacity over time. This paper discusses the geologic conditions that led to this relaxation, the various remedial strategies considered, and the effectiveness of several of these remedial strategies.

2 SUBSURFACE CONDITIONS

The walls are situated at the toe of the existing railroad embankment and fill will be placed behind these walls to widen the embankment for the station. Soils beneath the footing consist mainly of residual clays derived from weathering of the underlying shale and claystone. Silty fill underlies the south end of Wall 13403R where a stream valley had been filled in to construct Bell Avenue.

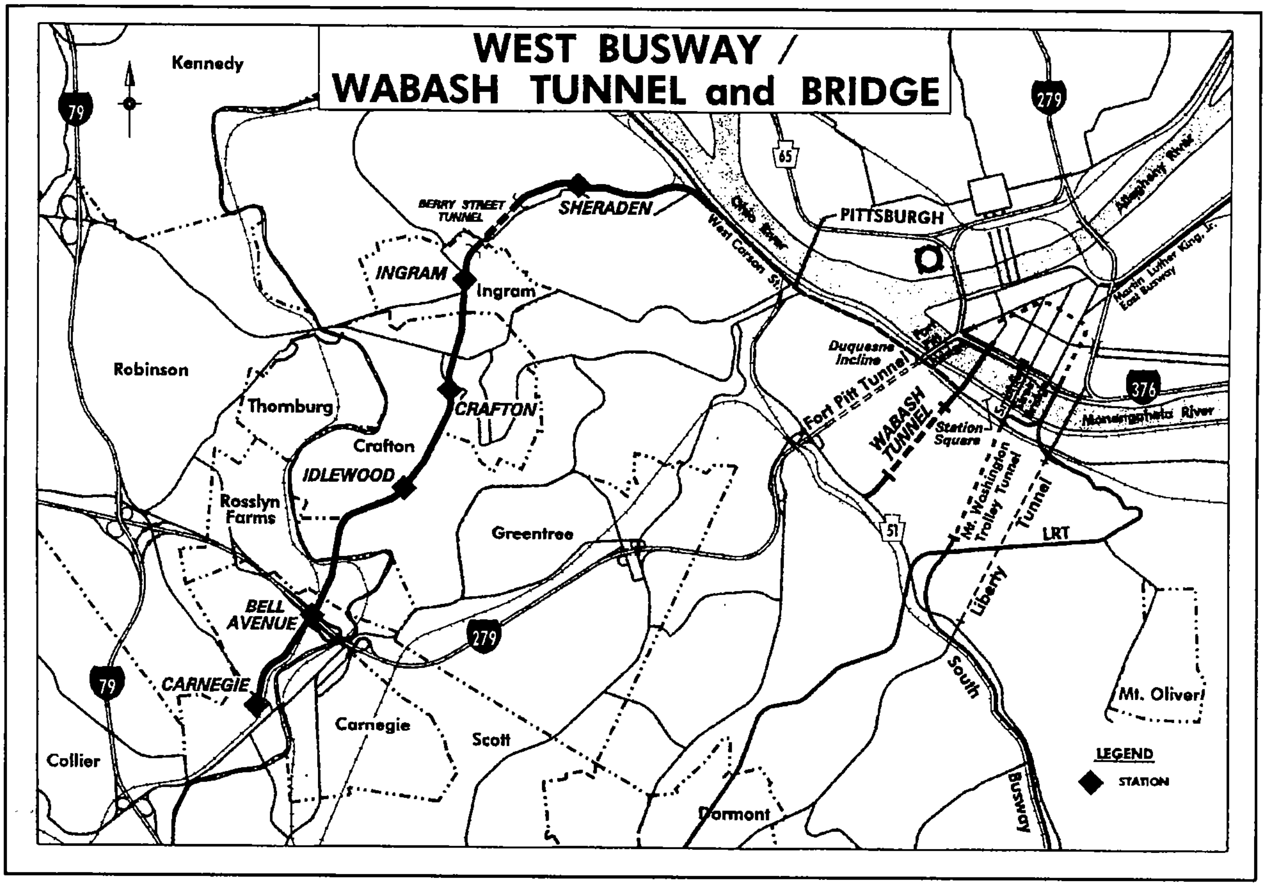

Figure 1 - Site Location map

Bedrock at the site consists predominately of the Morgantown member of the Conemaugh Group; represented by a medium hard siltstone and very fine grained sandstone in this case. The contact with the overlying Clarksburg Member was identified as a soft red claystone beneath the northern two thirds of the wall using the test borings. See Figure 2 for a generalized geologic cross section.

The water table fluctuates with rainfall but ranges between elevation 765 and 775; or about 5 to 15 feet below the existing ground.

3 RECOMMENDED FOUNDATIONS AND DESIGN

The potential for differential settlement of walls supported on spread footings on soil was high due to the variable subsurface conditions and the weight of the backfill that would be placed behind the walls. The depth to rock (7-20 feet) and the water table made pedestal type foundations impractical. Therefore, pile foundations were recommended for support of these walls. Steel H-piles driven to end bearing on rock, which have been used successfully for many years in the Pittsburgh area, were selected as the most economical foundation.

The top of bedrock is highly weathered thus piles were expected to penetrate up to 2' below the top of rock. Experience with similar soft red claystones on other jobs in the Pittsburgh area and the descriptions on the test boring logs led to the conclusion that the claystone would have insufficient

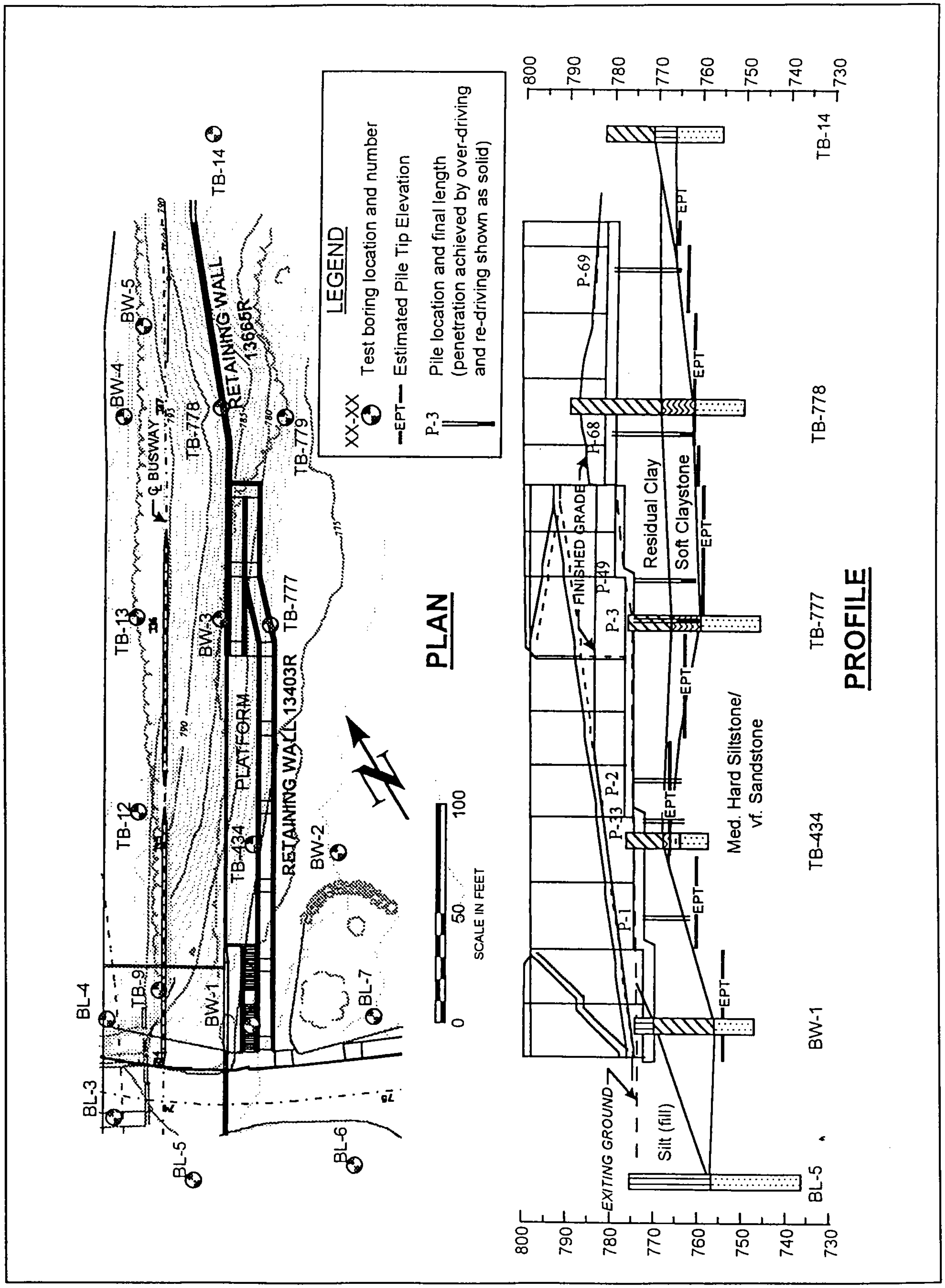

Figure 2 - Plan and Profile

strength to support an end bearing pile of the required capacity, thus the pile tip elevations were specified near the top of the underlying siltstone. Estimated Pile tip elevations are shown in Figure 2.

A relatively heavy pile section (HP12x74) and steel pile shoes were specified to help the pile penetrate through the soft claystone to the medium hard siltstone. A test pile program was not conducted during design due to restricted site access and because it was not cost effective for the number of piles (124) at this location. Test piles and dynamic monitoring during construction were specified to confirm design allowable pile capacities.

4 CONSTRUCTION

4.1 TEST PILE DRIVING

Piles were driven with a Delmag D12-32 open end diesel hammer. This hammer has a 4 position throttle and a maximum rated energy of 31.33 ft-lbs. A 2 inch synthetic cushion was used in the drive helmet.

On 8/11/98, the contractor drove three of six test piles scheduled for the subject walls. These piles are designated as P-1, P-2, and P-3 on Figure 2. Dynamic monitoring during driving of these piles indicated that more than adequate capacity was achieved at case 2 refusal, defined as 20 blows per inch. Actual tip elevations for P-1 and P-2 were 762.1 and 764.8 compared to estimated tip elevations of 760 and 766; which is within expected deviations. Actual tip elevation of P-3 was 765.2 compared to an estimated tip elevation of 759.0 or 6.2 feet higher than expected. Examination of the test boring logs in the vicinity of P-3 indicated that the tip was bearing in the soft red claystone. This type of material degrades on contact with water and loses a significant amount of its strength. Strength loss in the claystone will lead to "relaxation" (loss of pile capacity) over time.

To assess the potential for pile relaxation, test pile P-3 was restruck on 8/14/98, three days after the initial drive to refusal. Restriking resulted in the pile penetrating an additional 1.4 feet to elevation 763.8 before again meeting refusal. Penetration resistance for the first 3 inches of redrive averaged 12 blows per inch which represented a significant drop from 20 blows per inch achieved at refusal. The average hammer stroke during redrive was 8.6 feet compared to 8.7 feet at the end of initial drive, thus the observed drop in penetration resistance could not be attributed to variations in hammer operating characteristics. On 8/17/98, P-3 was again restruck with the Pile Driving Analyzer (PDA) attached to better quantify initial capacity on restrike. The PDA confirmed an ultimate capacity on restrike of 375 kips which represents about a 30% loss of capacity from that observed at initial refusal and is less than the 440 kips required by the design. Additional piles were restruck to define the extent of the problem and showed similar performance. Driving records and PDA results of representative piles are presented in Figure 3.

Test piles P-68 and P-69 in wall 13665R were driven on 8/18/98 with PDA monitoring. These piles were driven first to case 2 refusal, then over-driven in an attempt to drive them to the estimated tip elevation. A total of 343 and 76 additional blows beyond case 2 refusal were applied to Pile P-68 and P-69 respectively; resulting in additional penetrations of 1.2 And 0.2 feet. Over driving was halted when penetration resistance exceeded 40 blows per inch. Neither of these test piles reached

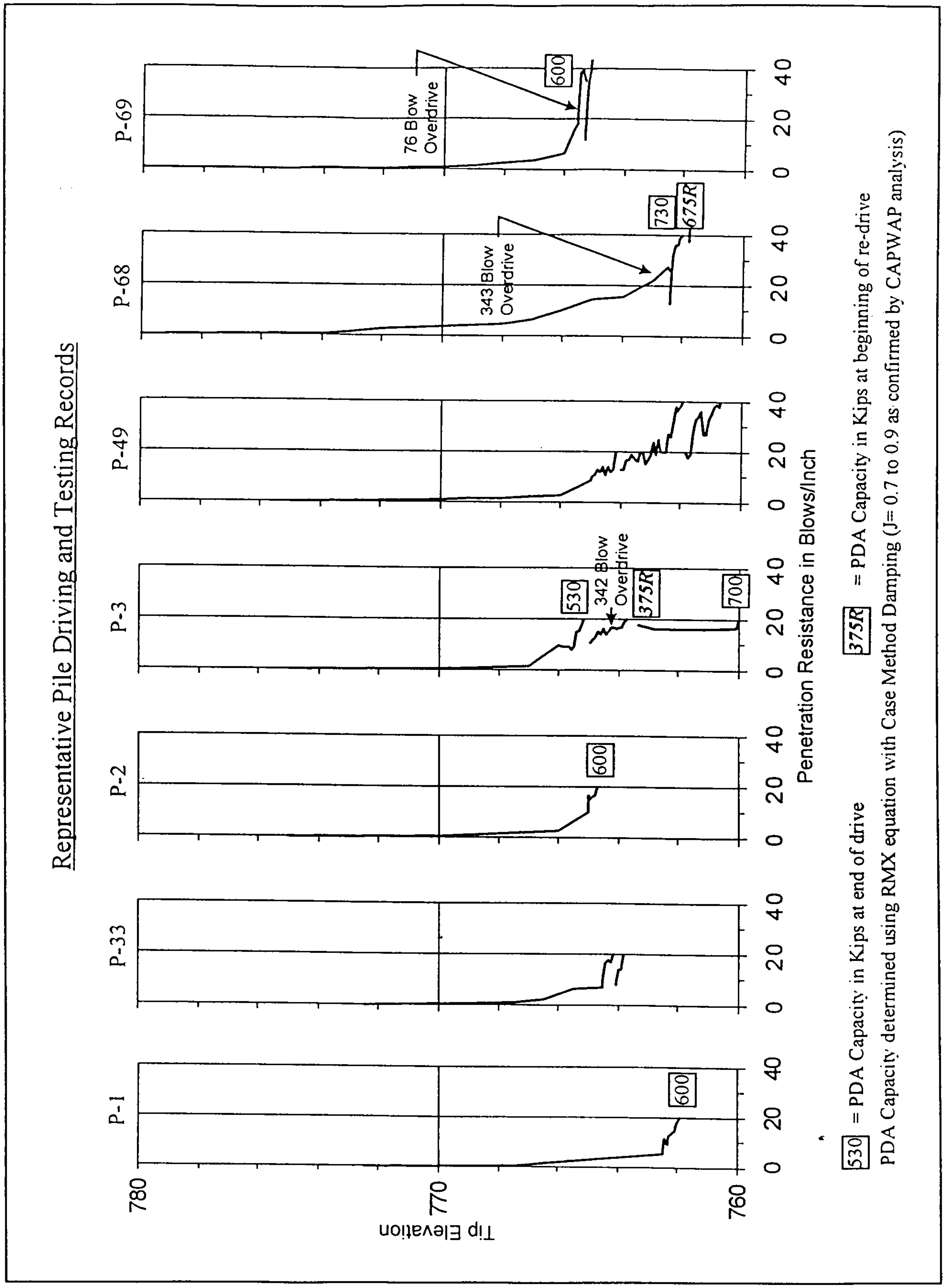

Figure 3 - Pile Driving Records

the estimated tip elevation, even after extensive over driving beyond refusal. Case 2 refusal was achieved with the tip in the claystone above the intended bearing stratum. PDA capacities at the end of this initial drive far exceeded those required by the design.

Pile P-68 was restruck on 9/15/98 and advanced at a penetration resistance of 13 blows per inch for the first inch. The average stroke for the first inch was 9.2 feet compared to 9.4 feet observed at the end of initial drive, thus the reduction in penetration resistance can not be attributed to operating characteristics of the hammer. Due to the observed relaxation, the pile was again over driven and an additional 0.5 feet of penetration was achieved. This placed the tip very close to the estimated tip elevation. On 9/30/98 Pile P-68 was again restruck with PDA monitoring to evaluate relaxation. Restrike showed about a 10% reduction in capacity from that achieved during the initial drive but still exceeded the required ultimate capacity, thus the pile was considered acceptable. Based on the PDA results and the driving records, it was concluded that this pile was bearing on the medium hard siltstone at the end of the second over drive on 9/15/98

Two restrikes on pile P-69 produced an additional 0.3 and 0.1 feet of penetration. Initial penetration resistance on the second redrive was 40 blows per inch which is similar to the penetration resistance at the end of the first redrive. Based on the nominal movement during the second redrive and the high penetration resistance, this pile was considered acceptable even though it was still above the estimated tip elevation. It was concluded that this pile is also bearing on the medium hard silt stone and that the difference between the estimated tip elevation and the as driven tip elevation is due to variations between borings.

Based on the results of the test piles, it was determined that piles located north of pile P-2 would have difficulty penetrating the soft claystone and would require special attention to reduce the potential for relaxation. Remedial action was required to address those production piles that had already been installed to case 2 refusal in claystone (located in Wall 13403R), and a plan had to be developed to address piles that had not yet been driven (located in Wall 13665R)

4.2 REMEDIAL STRATEGIES

Five different strategies were considered to address the situation as discussed below.

Accept reduced capacities

A 30% to 40% reduction in ultimate capacity was observed in the PDA results and the driving records (penetration resistance). The ultimate capacity at case 2 refusal ranged between 530 and 630 kips. This would result in a relaxed ultimate capacity between 370 and 440 kips, assuming 30% relaxation. The maximum design ultimate capacity was 440 kips thus the piles would have inadequate capacity if nothing was done. This was not considered acceptable.

Over drive pile to higher capacity

A typical approach to relaxation in soft shales in western Pennsylvania is to over drive the pile a specified number of blows past case 2 refusal. This has the effect of forcing some additional penetration and developing a higher initial ultimate capacity thus giving more "room" for relaxation.

This was tested with pile P-68 and P-69 which developed ultimate capacities of 600 to 730 kips at the end of practical over drive. Since relaxation was observed but not quantified in pile P-68, even after driving 343 blows beyond case 2 refusal, it must be assumed that relaxation similar to that measured on other piles would occur. This would yield 420 to 500 kip ultimate relaxed capacities, assuming 30% relaxation. Additionally, pile P-3 was observed to have significantly less capacity than required (375 kips) even after being over driven 342 blows during the second redrive. Thus it was concluded that an unacceptable amount of relaxation would occur as long as the pile tip was embedded in the soft claystone and that overdriving would be successful only if it resulted in the tip penetrating the soft claystone to the medium hard siltstone as was the case in pile P-69.

Use multiple redrives until tip penetrates soft claystone

Since it was concluded that a pile would relax so long as it was bearing in the soft claystone, and since we had shown that the piles could be driven 1-2 feet on each redrive, it was determined that it should be possible to simply redrive each pile as far as possible, wait, and redrive again until the pile tip reaches the siltstone. This was the approach selected for those piles that had already been installed to case 2 refusal and that had not penetrated to the siltstone.

Use a stiffer pile to allow driving through soft claystone

A stiffer pile and larger hammer could be used to allow easier penetration of the soft claystone, however, this would have required mobilization of additional equipment, ordering new piles, and may not have been successful. This approach was not selected due to time constraints, unproven results, and costs associated with both the work and delays to the contractor.

Predrill through soft claystone

Predrilling a hole to the estimated pile tip elevation, backfilling it with sand, and then driving the pile through the sand is also commonly used in western Pennsylvania when excessive driving resistance or obstructions are encountered. Since this approach could use the on-site piles, had proven results, and was already incorporated into the contract documents, it was selected for those piles that had not yet been driven in Wall 13665R.

4.3 IMPLEMENTATION AND RESULTS

Multiple redrives, including overdriving beyond case 2 refusal

Criteria for redriving the piles was established as follows:

> Minimum tip elevations were established for each pile based on the results of the test piles and interpretation of the borings. Piles were to be repeatedly redriven until this minimum tip elevation was achieved and the penetration resistance was at least 20 blows per inch.
>
> The throttle was to be adjusted to keep the hammer stroke below 10.5 feet. This was required to prevent over-stressing the pile as shown by the PDA results.

Redriving was to cease if penetration resistance reached 40 blows per inch as a way of maximizing the efficiency of redriving.

All of the previously driven piles that required remediation were successfully treated and reached the minimum tip elevation established with from one to three redrives.

4.3.1 Predrilling

Predrilling was successful in allowing the piles to be driven to the established minimum tip elevation. Driving through the sand was easy and piles reached refusal within 0.5 feet of the bottom of the predrill hole on average.

5 CONCLUSIONS

5.1 RELAXATION MECHANISMS AND MAGNITUDE

The generally cited cause for relaxation is the development of negative pore pressures due to shearing of very dense materials which increases the effective stress. When the negative pore pressures equalize, the effective stress decreases and relaxation is observed. Dense silts and glacial tills are thought to be most likely to exhibit this type of behavior. Ultimate capacity losses between 20% and 50% have been reported (Hannigan, 1996) under these conditions. It is not felt that this is the mechanism that produced the observed relaxation at this site.

Thompson (1985) has attributed relaxation of shales to release of locked in stresses in the material. Driving a pile into the weak rock formation fractures and displaces the rock. As water enters the fractures, the rock will lose strength and relax into the fractures. This is thought to be the mechanism producing the observed results at this site. Core samples of this rock degrade into clay when placed in water after only a few hours. Release of the confining stress and exposure to water produces a dramatic change in strength properties. Ultimate capacity losses between 10% and 50% have been reported (Hannigan, 1996) under these conditions.

Some cases of "apparent relaxation" (lower penetration resistance on restrike but no accompanying loss of capacity) have been attributed to the operating characteristics of single acting diesel hammers (Thompson, 1985). These hammers may lose efficiency after extended hard driving which results in higher observed penetration resistances at the end of initial driving. On restrike, when the hammer is not overheated and operates more efficiently, lower penetration resistances are observed which may be interpreted as pile relaxation. PDA measurements in these cases confirm equal or higher capacities on restrike rather than lower capacities. Based on observation of hammer stroke at the end of initial drive and at the beginning of redrive, the operating characteristics of the single acting diesel hammer did not produce an "apparent relaxation" at this site. The PDA results confirmed that the relaxation observed at this site was indeed "real".

5.2 THE EFFECTIVENESS OF OVERDRIVING

Overdriving the pile was only found to be effective if the overdriving resulted in the pile tip bearing on a unit not susceptible to relaxation. Typical overdriving specifications require driving a set number of blows beyond absolute refusal, typically 300 or less. At a driving resistance of 20 to 30 BPI this would result in an additional foot of penetration. If a layer not susceptible to relaxation is not encountered in that extra foot of penetration, as was the case for many of the piles at this location, overdriving does not substantially reduce the possibility of relaxation.

5.3 THE EFFECTIVENESS OF MULTIPLE REDRIVES

Redriving multiple times until the pile tip reaches a layer not susceptible to relaxation was shown to be effective at this site. This method is commonly used in Toronto (Thompson, 1985). Though effective, the method is not efficient since the pile driving equipment must be mobilized to each pile several times and waiting periods must be incorporated which can affect the project schedule.

5.4 THE EFFECTIVENESS OF PREDRILLING

Predrilling was shown to be effective in reducing the driving resistance through the soft claystone and allowing the pile to bear on the medium hard siltstone at this site. Predrilling and backfilling with sand could proceed independently from the pile driving operation thus allowing greater efficiency.

5.5 COST EFFECTIVENESS

A comparison of the crew hours required to perform multiple restrikes and the hours required to predrill indicates that an average of 1.3 crew hours was used for each restrike (including time to move the rig to the pile location and set up to drive) which equals 2.6 crew hours per pile based on two restrikes per pile. Predrilling averaged 1 crew hour per pile (including time to move to each pile location, set up and drill). Thus, predrilling appears to be a more cost effective solution to reducing the effects of relaxation at this site.

6 SUGGESTIONS FOR DESIGN OF PILES IN RELAXATION PRONE ROCK

A pre-design test pile program is the best way to quantify the impacts of relaxation and the ability of driving equipment to penetrate relaxation prone materials. The cost of such programs, the unavailability of the site prior to construction, and the fact that the successful contractor may wish to use different driving equipment than that used during the test pile program make them useful and justifiable only on those projects with large numbers of piles.

In general, stiffer piles (larger cross sectional area) will penetrate soft rock better than piles with small cross sectional area. The stiffer piles allow the use of a larger hammer and transmit more energy to the pile tip. This can only be quantified by a pre-design test pile program. The piles selected for this job represent the mid point of the range of H-pile sections but were not stiff enough to allow penetration of the soft claystone without overdriving, redriving or predrilling. While stiffer piles penetrate better, it has been shown that very high displacement piles tend to increase the effects of relaxation due to increased fracturing and displacement of the bedrock (Thompson, 1985). Thus selecting the right pile becomes a trade off between stiffness and low displacement.

Predrilling, or the option of predrilling should be considered anytime it is necessary to penetrate more than a few feet of relaxation prone material.

Pile load testing, either dynamic or static, is necessary to allow evaluation of relaxation effects and should be included in the contract where relaxation prone materials are expected.

REFERENCES

Hannigan, P.J., Gobel, G.G., Thendean, G., Likins, G.E., and Rausche, F. (1996). Design and Construction of Driven Pile Foundations - Volume I. US DOT Federal Highway Administration, Office of Technology Application, Report No. FHWA-H1-96-033

Thompson, C.D. and Thompson, D.E. (1985). Real and Apparent Relaxation of Driven Piles. American Society of Civil Engineers, Journal of Geotechnical Engineering, Vol. 111, No. 2, 225-237

SOIL MODIFICATION AND STABILIZATION UTILIZING LIME

PRESENTED BY:
HENRY MATHIS, P.E.
MATHIS GEOTECHNICAL CONSULTING, INC.

SPONSORED BY:
DRAVO LIME COMPANY

Abstract

The Kentucky DOT has experienced subgrade "pumping" problems during base and pavement construction for many years. The "pumping" has been a direct result of the saturated soil subgrade due to the lack of proper drainage and the heavy construction equipment overloading the soil subgrade during construction. Geotextiles and aggregate, geogrids and aggregate, mechanical modification using aggregate, lime and cement have been used by the Kentucky DOT to establish a working platform. Chemical stabilization with lime and cement is currently being used in the structural design of pavements.

Included in this paper is all phases of soil modification and stabilization utilizing lime for highway subgrades. Products used, manufacturing of lime, soil-lime reactions, Kentucky DOT design practices, Kentucky geotechnical mix design procedures, long term durability, and cost comparisons are some of the topics that will be discussed.

Introduction

This paper basically covers the same points as discussed in the slide presentation but to a greater detail. The information discussed and data shown is a result of many years experience the author, Henry Mathis, had while working with the Kentucky DOT, Division of Materials, Geotechnical Branch. The opinions and facts expressed in the paper and during the slide presentation by the author, may not reflect the official views or policies of the Kentucky DOT.

Ward Blakefield, Vice President of Commercial Sales, Dravo Lime Company, was very instrumental in getting lime stabilization started in Kentucky. In 1986 Dravo Lime Company sponsored a study, "Lime Stabilization of Pavement subgrade Soils of Section AA - 19 of the Alexandria - Ashland Highway," KTC-86-24, in cooperation with the Kentucky Transportation Center, College of Engineering , University of Kentucky, and the Kentucky Transportation Cabinet, that assisted greatly in the implementation of using hydrated lime for subgrade treatment. Since this study hydrated lime has been utilized very successfully for treating clay subgrades.

Several research reports namely "Bearing Capacity Analysis of Pavements," KTC-91-8, "Evaluation of Lime Stabilized Subgrade (AA-19) ,"KTC-93-25, and "Modification of Highway Soil Subgrades", KTC-94-11, have contributed to the Kentucky DOT's policy and procedures.

Soil Modification and Stabilization

The initial reaction between the soil and lime results in a cation exchange. This reaction absorbs water from the clay, breaks down the clay lumps and reduces the clay content of the soil which makes the soil more workable for compaction. Therefore, mixing 2 percent of quicklime by weight with the wet soil using light farm tractors, modifies the soil. This process may take a mellowing period of a few hours or longer for the reaction to take place. Since the lime has a high affinity for water the reaction dries up the soil and the following benefits are realized for soil modification:

- Heavy clayey soils become friable and workable.
- Wet soils dry and when compacted they form a working platform for construction.
- Unit weight of most soils are reduced.
- Swell potential of swelling soils or soil-like shales are reduced.
- Collapse potential of collapsing soils are eliminated.

A second very complex chemical reaction called pozzolanic, results from lime being added to the soil. This is a cementation reaction which acts similar to portland cement, thus the soil is stabilized. Hydrated lime, approximately 5 or 6 percent by weight, shall be mixed with the soil for the pozzolanic reaction to take place. The following benefits are realized for soil **stabilization**:

- Same as outlined above.
- Increased **strength** and **durability**, therefore, mixture can be given structural credit.

The main difference between modification and stabilization is that no structural credit is given to the soil- lime modified mixtures in highway pavement design. Due to the low percentage of lime used for the soil modification, the mixtures are not as durable and have less strength than the stabilized mixtures. However, the soil modified mixtures could be upgraded for stabilization with the addition of larger quantities of lime. The larger quantities of lime are necessary for the pozzolanic reaction to take place for additional strength and durability.

What is Lime

Lime is one of the oldest chemicals known to man as it was used in building the pyramids of ancient Egypt. Calcium Oxide (Quicklime) is produced by the calcination of limestone or dolomitic limestone at a high temperature, thus evaporating nearly half of the stone's weight in carbon dioxide. In other words, lime is burned limestone. During its transformation from limestone to lime, material being calcined takes on a distinctly different physical appearance. No longer gray, hard and sharp-edged, the creamy white newly calcined pebbles have distinctively rounded contours, and soft, porous surfaces.

- Limestone + Heat = Calcium Oxide (Quicklime) + Carbon Dioxide
- $CaCO_3$ + Heat (~ 1315°C) = $CaO + CO_2$
- Dolomitic Limestone + Heat = Dolomitic Quicklime + Carbon Dioxide
- $CaCO_3 \cdot MgCO_3$ + Heat (~ 1315°C) = $CaO \cdot MgO + CO_2$

High calcium lime is more reactive with the soil than the dolomitic lime. It should be noted that agricultural lime ($Ca\ CO_3$) has not been calcined and does not react with the soil and water to modify or stabilize the soil like calcium oxide or dolomitic lime. Agricultural lime mainly is used to neutralize soil acidity.

CaO (calcium oxide or quicklime) is highly reactive in the presence of moisture, even the moisture in the air will cause slaking. Dropped in a beaker of water the lime will react quickly with the water, hence, the name quicklime. Sufficient heat is generated in this chemical reaction to boil water. Therefore, handling the quicklime during construction requires gloves, and eye protection, to reduce the danger of burns. A safety program should be administrated to the workers before this material is used on construction and emergency equipment should be available at the job site for the workers protection.

Particle sizes for the quicklime range from approximately 8 inches (lump lime) to 95 percent passing a number 100 sieve (pulverized lime). Pebble lime, (2 inches to 1/4 inch) is generally the most common size of quicklime utilized for soil modification and stabilization. The color ranges from white to light gray depending on the purity of the quicklime. The quicklime is shipped in bags, or in bulk by rail or truck. Quicklime can be slaked at the construction site and applied to the soil subgrade in a slurry form. In this process the resulting hydrated lime is suspended in a slurry with ~ 30 to 35 percent solids and 65 to 70 percent water. The advantage of this process is the quicklime slakes into hydrated lime with no remaining unhydrated particles to present problems at a later date.

Hydrated lime is produced by hydrating quicklime with water, and this form of lime is less reactive because additional water does not change its composition.

- $CaO + H_2O = Ca(OH)_2$ Calcium Hydroxide or Hydrated lime.

Hydrating the quicklime with water at the plant produces a fine dry white powder. The dry hydrated lime is often shipped in either bulkbags, 50 lb. bags or in bulk.

A unit measure of CaO(Quicklime) contains approximately 25 percent more calcium for the reaction than $Ca(OH)_2$ (Hydrated Lime). Therefore, Kentucky DOT and most other states use a factor to determine the amount of dry hydrated lime for payment. This factor can be calculated based on a standard molecular weight ratio and the available calcium oxide as measured at the plant. However, when quicklime is furnished for a slurry or slaking application for the Kentucky DOT, they will measure the quantity in tons at 1.25 times the actual quantity.

On most of the Kentucky DOT projects, quicklime is pumped into a Porta Batch slaker which is a large tank filled with water and equipped with an agitator. The paddles stir the water as the quicklime is pneumatically discharged from the truck. As the quicklime is slaked, the temperature of the mixture is approximately 200^{o}F. The resulting hydrated lime slurry is pumped into distributor trucks equipped with continuous agitation to ensure a uniform mixture from the mixing site until applied to the soil subgrade. This method of application eliminates the dust problem that may be undesirable in an urban environment, and provides for better distribution of the lime.

Another acceptable way is to mix dry hydrated lime and water in a tank truck and spray the mixture on the soil subgrade using the same type of equipment for application. The slurry method may not be practical if the soils are saturated or during the wet, cool, time of the year. In this case dry hydrated or quicklime may be a more appropriate method of applying the lime.

Lime Manufacturing

Dravo Lime's distinctive approach to the production and distribution of lime products, first took shape more than 20 years ago. A group of chemical engineers affiliated with a large engineering firm, whose services included combustion and industrial process technology, developed a lime-based gas scrubbing process to assist coal - fired power plants in meeting the clean air regulations under the original Federal Clean Air Act. This team developed a production plant near Maysville, Kentucky, capable of producing one million tons of lime per year to support the lime-based stack gas scrubbing technology. This lime production enterprise was called Dravo Lime Company and it came on line in the middle 1970's. The Maysville operation was the largest and most efficient lime ever built at that time. Rigorous testing ensured that Maysville shipments met the quality specifications required for successful scrubber operations at customer power plants. In the late 1970's the Longview plant in Saginaw, Alabama, just south of Birmingham became part of Dravo Lime Company. In the 1980's the Black River plant became part of the Dravo Lime Company. This plant is located in Northern Kentucky on the Ohio River in Augusta, Kentucky which is between Maysville, Kentucky and Cincinnati, Ohio approximately 30 miles from downtown Cincinnati.

Black River's surface facilities overlay a 552 acre underground limestone mining operation. Limestone rock, of the Ordovician Age in the Camp Nelson formation, which extends in an arch through much of Northern Kentucky, is mined 800 ft. below the surface. The limestone is drilled and blasted in such a way to leave in place 50 ft. x 70 ft. pillars at 50 ft. intervals to support the roof of the mine as the face advances. Crushed limestone is conveyed to the surface along a 9 ft. x 21 ft. x 2300 ft. slope. which is also traveled by the cable car that carries men and equipment into and out of the mine. Passing through a series of crushing and sizing stations, the mined limestone eventually reaches the kiln feed storage piles. From there, material is conveyed to one of the lime plant's two 500 tons per day rotary kilns or the longer 1,000 tons per day kiln. Two kilns are approximately 330 ft. in length and 15 ft. in diameter and the other is 400 ft. in length and 15 ft. in diameter. Entering the kiln, the limestone is calcined at 2,000^{O}F for more than 2 hours. The heated limestone emerges from the kiln as calcium oxide or quicklime. Exhaust heat from the kilns is dissipated by the lime plant's distinctive radiant coolers, and fine dust particles are captured in one of the baghouses before the exhaust gas is vented to the atmosphere. Crushed and screened to an appropriate size the quicklime is stored in one of the lime plant's storage silos. The kilns are coal-fired for maximum fuel efficiency and burn approximately 300,000 tons of Eastern Kentucky coal per year. It takes three tons of limestone to produce one ton of lime. The annual production capacity of the plant is in excess of 600,000 tons. Strict attention is paid to environmental regulations during every phase of production operations, with special efforts made in the areas of dust suppression and collection as well as waste products disposal.

Dravo Lime Company merged with Carmeuse Lime Company and Lafarge Lime Company at the first of this year. The merged companies together have 16 plants in North America with a total production capacity of 7.5 million tons of lime per year. Due to the merger of the three companies, they are capable of producing and selling all types of lime.

Soil - Lime Reaction

Hydrated lime, when mixed with the soil in the presence of water, reacts with the soil to initiate a cation exchange immediately. The calcium ion in the soil is exchanged with the weaker sodium, potassium, or other ions in the soil. This reaction results in reducing the adsorbed water on the clay particle and it reorients the clay particles from an edge-to-edge form rather than a stacked form. This reaction creates a flocculated structure and the texture of the soil is changed. A soil originally classified as a clay, when mixed with lime, may be then classified as silt, or sand. Since the lime has a strong affinity for water, wet soils can be mixed with the lime and the reaction breaks down the clay lumps by drawing water from the clay, which results in a drier and more workable soil. The results of the cation exchange and flocculation of particles is as follows:

- Reduces the size of the absorbed water layer.
- Reduces the plasticity of the soil.
- Lowers the unit weight of the soil.
- Increases the workability due to the textural change from clay to silt or sand.
- Increases the soil strength and stability.

If quicklime is mixed with the soil, in the presence of water, it goes thru hydration first and produces $Ca\ (OH)_2$ or hydrated lime. This reaction takes several hours in the field, and this time period is known as mellowing. During the mellowing period the reaction produces heat and steam. Soil mixed with the quicklime should be allowed to complete the mellowing period prior compaction. After this reaction is complete, and the soil has been allowed to mellow, the soil is **modified.**

Pozzolan is defined as a naturally occurring material which contains Silica and Alumina. When combined with water and hydrated lime in a high ph environment, through a very complex chemical reaction, forms a natural cement similar to portland cement. The natural cement is formed by the reaction which results in combining Ca^{++} and OH^- and Silica in the soil, or $Ca^{++}$and OH^-, and Alumina in the soil forms CSH (Calcium Silicate Hydrate) and / or CAH (Calcium Aluminate Hydrate.) This pozzolanic action with the soil particles produces a cemented material with substantial strength and durability and the soil is **stabilized.** As long as there is sufficient calcium in the system to combine with the clay soil (Silica and Alumina), and the ph remains sufficiently high to produce this pozzolanic reaction strength gain and durability will continue. The strength of the mixture may increase to more than 100 psi over a 28 day curing period with the temperatures over $70^{\circ}F$. Research field data indicates additional strength gains may occur for ten years or more.

Why Modify Or Stabilize Soil Subgrades

Kentucky DOT has experienced many subgrade pumping problems during base and pavement construction, and premature pavement failures that have resulted in lost of construction time, inconvenience of the traveling public, and millions of dollars of revenue that could have been spent for other highway uses. Clayey subgrades absorb moisture and swell over the long period of time, thus causing an increase in volume and loss of strength over time. To prevent this from occurring, they have used lime and cement, depending on the soil type, as soil stabilizers. This has been very effective creating a solid working platform during construction and providing long term strength and durability for the soil subgrade, thus eliminating the premature pavement failures. Stabilization has also been economical because the structural pavement thickness is reduced thus creating a cost savings.

Kentucky DOT Design Considerations for Subgrade Stabilization

The Kentucky DOT, Division of Design is responsible for the pavement design and the Division of Materials, Geotechnical Branch, provides the recommended California Bearing Ratio (CBR) for subgrade design and type of soil subgrade stabilization, if necessary. Some of the items that are considered for stabilization are:

- Subgrade stabilization will be considered for all subgrade soils with a design CBR of 6 or less.
- Alternate methods of subgrade stabilization will be considered on a site specific basis. Methods of subgrade stabilization typically considered include chemical, (lime and cement), mechanical (mixing of soil with aggregate), fabric and Geogrids with aggregrate and removal and replacement with improved materials.
- Subgrade stabilization shall be for the full roadbed width (shoulder edge to shoulder edge.)
- A stabilized base material may be considered as an alternate for subgrade stabilization.
- Subgrade stabilization will not normally be considered for pavements with annual ESAL'S less than 50,000 (low volume roads.)
- Subgrade stabilization will be considered but will not be required for pavements with annual ESAL'S greater than or equal to 50,000 and less than 250,000. (high type state secondary , and primary routes.)
- Subgrade stabilization will normally be considered for pavements with annual ESAL'S greater than or equal to 250,000 (interstate and parkways.)

The Kentucky DOT uses the "AASHTO Design Guide" for pavement design. A CBR design value of 9 is assigned to the lime and cement soil stabilized susbgrades and from this value a resilient modulus is calculated. The following AASHTO structural layer coefficients are used :

- Untreated soil subgrade Depends on CBR design value.
- Lime or cement treated soil subgrade .11
- Aggregate base course .14
- Flexible Pavement .40

Kentucky DOT Geotechnical Design Procedures for Soil Stabilization

Soil tests performed on site specific samples are soil classifications, moisture-density and unconfined compression tests. The criteria for chemical selections are as follows:

- Cement: P.I. less than 20 and percent passing the 200 sieve less than 35.
- Lime P.I. greater than 20 and percent passing the 200 sieve greater than 35.

In order to determine the percent of chemicals required for stabilization the soil is remolded to 95 percent of AASHTO T-99 and unconfined compression tests are performed using various percentage of chemicals. The treated samples are cured in the oven for 48 hours at 120°F and compared to the compressive strength of the untreated soil. The minimum strength desired is 100 psi., however, in most cases the lime treated specimens will not obtain the 100 psi minimum strength in the 48 hour quick curing time. Therefore, the percent of lime that provides the highest strength gain is selected. Another consideration, is the percent of lime that provides a strength gain of greater than 50 psi over the untreated soil. Generally, the depth of stabilization is 8 inches, however, greater depths may be necessary not to exceed approximately 16 inches. If the depth of treatment is increased the pay quantity for the stabilization (per square yard) is increased as follows:

- Four inches additional multiply by 1.33.
- Eight inches additional multiply by 1.50.

In order to estimate the design quantities for the chemicals a figure of 6 percent, (based on the dry weight of soil), is used for the 8 inch depth, however, the exact amount, and type of chemicals are based on the soil strength test data obtained from the in place subgrade samples. Generally the strength tests on lime treated soils indicate approximately 5 percent by weight is sufficient. For cement treated soils, generally 4 to 8 percent by weight is necessary to meet the criteria.

Summary of Moisture-Density Tests Using AASHTO T-99

Based on 584 laboratory test samples, the following are mean values for lime treated samples:

% Lime	0%	3%	6%
Moisture-Density PCF	105 PCF	101 PCF	100 PCF

Based on 145 laboratory test samples, the following are mean values for cement treated samples:

Moisture-Density PCF	115 PCF	115 PCF	115 PCF

These test results indicate the soil weight (pounds per cubic foot) lowers with the addition of lime, however, the soil weight of the cement treated samples does not change with additional cement. Therefore, when using lime it is very important to perform the laboratory moisture-density test on the same type soil, and using the percent of lime that is being added to the field mixture, in order to have a correct target density for the field density test. It is also very important to use the same mellowing time for the moisture - density test in the laboratory as is used in the field. Following these guidelines will produce a better comparison between the laboratory and field density test.

Laboratory Compressive Strength Test Data of Soil with Lime

The folowing represents the average compressive strength values obtained compacting 766 samples at 95 % of AASHTO T-99 and curing the samples in an oven for 48 hours at 120° F.

Percent Lime	Minimum PSI	Mean PSI	Maximum PSI
0%	25	30	40
2%	50	72	95
3%	65	95	125
4%	80	110	140
5%	82	115	150
6%	73	96	115

Laboratory Compressive Strength Test Data of Soil with Cement

The following represents the average compressive strength values obtained compacting 145 samples at 95 % of AASHTO T-99 and curing the samples in an oven for 48 hours at 120^{O} F.

Percent Cement	Minimum PSI	Mean PSI	Maximum PSI
0%	20	33	45
3%	88	119	150
4%	106	165	239
6%	169	200	300
8%	215	289	375

Average Compressive Strengths of Core Samples From Lime Stabilized Soils

Below is a chart depicting average strengths of core samples obtained from lime stabilized soil subgrades These core samples were oftained from the subgrade using a pavement core drill rig equipped to drill with air, in order to limit disturbance of the core sample. The strength values were derived using the results from 503 cores.

Values	Strength PSI	Moisture Percent	Curing Age Days
Minimum	57	17.8	9
Mean	90	22.5	10
Maximum	130	26.9	12

Average Compressive Strengths of Core Samples From Cement Stabilized Soils

Below is a chart depicting average strengths of core samples obtained from cement stabilized soil. These core samples were also obtained from the cement soil subgrade using a pavement core drill rig equipped to drill with air. Values from 200 cores were used to obtain the results shown below:

Values	Strength PSI	Moisture Percent	Curing Age Days
Minimum	99	10.7	12
Mean	172	13.7	13
Maximum	275	16.6	13

CBR Values For Swelling Shales

Four samples of swelling shales were obtained from the New Providence Formation in Jefferson County, and CBR tests were performed on these samples in accordance with Kentucky Test Method 64-501-95. These shales are among the worst materials in the state for subgrade construction. The results of these tests are as follows:

- Soaked Un-Treated CBR = **2.6**
- Un-soaked Un-Treated CBR = **10.8**
- Soaked (7 days) Lime-Treated CBR = **12.5**
- Soaked (7 Months) Lime-Treated CBR = **32.0**

The CBR plugs from these samples have been kept moist in plastic containers. The un-soaked un-treated CBR (**10.8**) has absorbed moisture and is very soft, similar to the soaked un-treated CBR, (**2.6**), therefore, the sample that was once a CBR of **10.8** is now probably less than **3.0.** This is a model of what happens when the samples are subject to moisture beneath the pavement. The lime treated samples are gaining strength with time. **Therefore, when the subgrades are treated with lime they gain strength, instead of swelling and losing strength as do the non-treated samples.**

Cost Comparisons Using Different Types of Stabilization

Below is a cost comparison using lime, cement, and fabric-aggregate. A depth of 8 inches was assumed for all three types of stabilization. Lime cost per ton was $90 and the cement was $83.53 / ton. Prices based on 1998 Kentucky DOT average bid prices.

Lime

Soil Wt. lbs. / cu.ft.	% Lime by weight	Manipulation Cost / sq.yd.	Lime Cost / sq.yd.	Bit. Curing Seal/sq.yd.	Total Cost Per sq.yd. / 8 inches	Cost / sq.yd. Per inch Depth
107	5%	$1.44	$1.43	$0.31	$3.18	**$0.40**

Cement

Soil Wt. lbs./ cu.ft.	% Cement by weight	Manipulation Cost / sq. yd.	Cement Cost / sq.yd.	Bit. Curing Seal/sq.yd.	Total Cost Per sq.yd. / 8 inches	Cost / sq.yd. Per inch Depth
115	6%	$1.24	$1.73	$0.31	$3.28	**$0.41**

Fabric and Aggregate

Excavation cost / cu.yd.	Aggregate Cost / Ton	Fabric Cost / sq.yd.	Excavation Cost / sq.yd	Aggregate Cost / sq.yd.	Total Cost Per sq.yd./ 8 inches	Cost / sq.yd. Per inch Depth
$3.77	$14.97	$1.38	$0.84	$4.48	$6.70	**$0.84**

Benefits of Utilizing Lime For Soil Modification and Stabilization

- Aide in drying wet soils.
- Provides an excellent working platform.
- Improves workability.
- Controls volume changes in soil.
- Allows marginal soils (low bearing) to be used.
- Improves strength and durability.
- Creates a water resistant barrier.
- Very cost effective.

Long Term Durability

The Kentucky Transportation Center conducted a series of long term in-situ CBR tests on the subgrade of Section 19 of Alexandria-Ashland Highway. The subgrade of this section was constructed with soil-like shales of the Crab Orchard Shale Formation. These soil-like shales are very low bearing and swelling shales. Typically, these shales are one of the worst subgrade materials in the state. Therefore, these subgrades were treated with 6 % hydrated-lime during construction in 1987. In-situ CBR tests were performed over a period of seven years to determine the long term durability of the hydrated-lime treated subgrades. These tests were performed in 1991 and 1994, four years and seven years respectively, after construction. The in-situ CBR tests were performed through boreholes in the asphalt pavement on top of the treated subgrade. Borings were also advanced through the treated subgrade and in-situ CBR test were performed on top of the untreated subgrade.

Results of in-situ CBR values, of the untreated subgrade found below the treated subgrade, ranged from only 1.9 to 3.7 in 1991, while in 1994 the values ranged from 1.2 to 2.5. In 1991, the in-situ CBR bearing strengths of the treated subgrade layer ranged from **40 to 106.** In 1994, some seven years after construction, the in-situ CBR values ranged form 48 to 94. Therefore, the strengths of the hydrated lime-treated subgrade, continue to be exceptionally large. Future long term monitoring of these subgrades, is being planned by the Kentucky Transportation Center as part of another research study.

Do's and Don't

The following recommendations are suggested for the lime stabilization of soils:

- Perform recommended tests on each soil to determine if the soil will react with the lime, and percent of lime necessary to produce the desired strength.
- Remember more lime may not give you the best results.
- Don't use lime in high sulfate soils. The sulfates will react with the calcium and expand.
- Make sure the lime meets ASTM specifications and fresh lime is used.
- Be sure and protect the workers from lime burns, if quicklime is used. Gloves and eye protection are recommended when using this type of lime.

- Be careful spreading hydrated lime in an urban environment. Another method is slaking quicklime, or using a lime slurry. Also another alternate is using quicklime in pebble form.
- If quicklime is used, make sure that **sufficient water** is added in order to hydrate the lime or expansion can take place.
- Uniform distribution of lime, both horizontal and vertical, in the soil is very important.
- Compare the field density test with the appropriate laboratory test. Use the same percent of lime and mellow the soil in the laboratory to match field conditions.
- Set the grade low to account for the swell in the lime. An approximate estimate is a 10 % swell factor.
- Allow 7 days, above 50 degrees, for the curing period. No heavy construction equipment should be allowed on the grade during the curing period.
- Keep the roadbed moist, by continuous sprinkling, until the curing seal is applied. Apply the curing seal no later than 24 hours after completion of finishing operations.
- Cover the stabilized roadbed with the pavement courses before suspending work for winter.

Acknowledgments

The author wishes to recognize Ara Arman, Dr.Dallas Little, Dr.Jim Eades, and Dr.Marshall Thompson, whose major contributions have greatly advanced the use of lime for soil modification and stabilization. The National Lime Association has sponsored many studies, seminars, and publications for lime stabilization. The comprehensive handbook, entitled "Stabilization of Pavement Subgrades and Base Courses with Lime," written by Dr. Dallas Little and sponsored by The National Lime Association, is an excellent comprehensive source of information concerning lime stabilization. In fact, some of the information in this paper, came from the handbook. Ward Blakefield, Vice President of Dravo Lime Company , should also be recognized for his efforts in bringing lime stabilization to the starting point in Kentucky. Thanks to Dravo Lime Company for sponsoring this publication, and slide presentation, and the research projects responsible for the lime stabilization beginning. Doug Smith, Michael Weitlauf, and others in the Geotechnical Branch of the Kentucky DOT, contributed in a large part to the success we have experienced in Kentucky with lime stabilization, and for much of the data in this paper. Tom Hopkins, Tony Beckman, David Hunsucker, David Allen, and Bobby Meade, all of the Kentucky Transportation Center, College of Engineering, University of Kentucky, provided valuable information to the Kentucky DOT as a results of their research studies.

References

Arman, Ara, (1997), **"Recent Advances in Soil-Cement and Soil-Lime Mixtures as Applied to Flexible Pavement Systems,"** 50 Jahre Betonstrassen, Ag (50 th. Year of Concrete Roads Association, "of Switzerland,") pp.57-60.

Dravo Lime Company,(Oct. 1992), **"Black River Division,"** Brochure.

Dravo Lime Company, (Nov. 1992), **"Dravo Lime Company,"** Brochure.

Hopkins, T.C.; Allen, D.L.; (Oct. 1986), **" Lime Stabilization of Pavement Subgrade Soils of Section AA-19 of the Alexandria - Ashland Highway,"** Research Report UKTRP-86-24, Kentucky Transportation Research Program, College of Engineering, University of Kentucky, Lexington, Kentucky.

Hopkins, T.C.; Beckham,T.L.; (June 1995), **"Modification of Highway Soil Subgrades,"**Research Report KTC- 94-11, University of Kentucky Transportation Center, College of Engineering.

National Lime Association, **"Lime Stabilization Construction Manual,"** (1987), Bulletin 326.

National Lime Association, **"Lime in Soil Stabilization,"** FHWA-HI-93-031,Federal Highway Administration, American Association of State Highway and Transportation Officials.

Little, D.N., (1995), "**Stabilization of Pavement Subgrades and Base Courses With Lime**," National Lime Association.

Little, D.N., (1987), **"Fundamentals of the Stabilization of Soil with Lime,"** Bulletin 332, National Lime Association.

Mathis, H. A., (1991), **"Modification of Soil Subgrades Utilizing Chemicals",** Kentucky Transportation Cabinet, Department of Highways, Division of Materials, Geotechnical Branch, presentation made at the 1991 Southeastern Transportation Geotechnical Engineering Conference in Charleston, South Carolina.

Meade, B.W.; Allen, D.L.; (Oct.1993), **"Evaluation of Lime Stabilized Subgrade (AA-19),"** Research Report KTC-93-25, Kentucky Transportation Center, College of Engineering, University of Kentucky, Lexington, Kentucky.

National Lime Association, (1951)**"Chemical Lime Facts,"** Bulletin 214.

Federal Highway Administration,"**Soil Stabilization in Pavement Structures**," FHWA-1P-80-2.

Thompson, M.R., **"Lime Treated Soils for Pavement Construction,"** 50 Jahre Betonstrassen, Ag (50 th. Year of Concrete Roads Association, "of Switzerland,") pp. 61-64.

Multivariate Statistical Techniques Applied to Aggregate Inventory Testing Program in Northwestern Ontario.

Peter P. Hudec, University of Windsor, Windsor, ON
Andrew Mitchell, DST Consulting Engineers, Thunder Bay, ON

ABSTRACT

Over six hundred samples of unprocessed aggregate were recently collected from 62 sites in NW Ontario by DST Consulting Engineers Inc. as part of an aggregate inventory project for the Ministry of Transportation of the Province of Ontario, Canada. The sites represent glacial sand and gravel deposits derived from gneissic/volcanic/metasedimentary terrain of the Precambrian Shield. The collected samples were subjected to the following tests: gradation, micro-Deval abrasion (coarse and fine aggregates), petrographic analyses of fine and coarse aggregates, absorption, relative density, magnesium sulphate soundness (coarse and fine aggregates), and plasticity.

The results obtained were analyzed by multivariate statistical techniques (factor and cluster and discriminant analyses, multivariate stepwise regression, etc.) to evaluate and group the samples according to their durability and general quality, and to determine the effect of glacial environments of formation on the sample properties. The statistics were also used to judge the relationships of the aggregate properties and test methods. The results show that river terrace, outwash, ice-margin delta and esker deposits contain significantly better aggregates than other environments. The K-cluster analysis procedure is capable of classifying sources into 'excellent', 'good', 'fair' and 'poor' categories. Among the tests, coarse PN analysis and microDeval test are most significant in aggregate classification.

INTRODUCTION

INVENTORY PROGRAM

The provincial highway authority in Ontario is the Ministry of Transportation of Ontario (MTO). On an annual and/or as needed basis the MTO conducts exploration and evaluation of gravel pits and quarries. These evaluations are used in the planning of maintenance and capital construction programs. The MTO thoroughly investigates existing and new sites and provides data on the quality and volumes of aggregates available to contractors and to maintenance patrols. The inventory program is ongoing and quantifies reserves for a range of granular materials including crushed gravel, pit run sand and gravel, sand for winter ice control operations, concrete and asphalt aggregates, etc.

The MTO has recently started to contract out the function of conducting geological evaluations of their aggregate sources to private consulting firms. In the fall of 1998, DST Consulting Engineers Inc. was awarded a contract to conduct geological exploration and evaluation of 62 aggregate sources located throughout northwestern Ontario. Figure 1 shows the location of these sources. The data derived in this exploration program will be catalogued in the MTO's Northwester Region office in Thunder Bay. During the course of this contract the authors identified the opportunity to conduct a meaningful statistical analysis and obtained the permission of the MTO to use the data for this purpose.

Sampling and Testing

In the evaluation of granular resources, the MTO has developed a number of specific guidelines for completing geological evaluations of sand and gravel deposits. In this program, samples were recovered from test pits excavated to approximately 4.5 m depth. Samples were channeled from the walls of the excavations in such a manner as to be representative of the materials in the test pit as a whole. A 15 kg (33 lb) sample was collected for sand and a 30 kg (66 lb) sample was collected for gravels. Test pit are spaced on a grid of between 30 m (100 ft) and 50 m (160 ft) depending on geological continuity.

For assigning laboratory testing, the samples are divided into "crushable" and non-crushable" materials. A

Figure 1 - Site Locations

"crushable" material is defined as raw material with a minimum of 35 % retained on the 4.75 mm (#4) sieve and also having a minimum of 25 % retained on the 25 mm (1") sieve. In this sampling program, a total of 683 samples were collected. This included 370 non-crushable and 314 crushable samples. Non-crushable materials were assigned grainsize analysis (MTO LS-602), Plasticity tests (MTO LS704), and the Micro-Deval Abrasion test for fine aggregate (MTO LS-619). Crushable samples awere assigned these tests plus the MTO Petrographic Analysis of Coarse Aggregate (MTO LS-609), the MTO Petrograpic Examination of Fine Aggregate (MTO LS-616), Relative Density and Absorption tests (MTO LS-604), Magnesium Sulphate Soundness tests (MTO LS-606) and the Micro-Deval Abrasion test for Coarse Aggregate (MTO LS-618). All testing was done in DST's laboratory located in Thunder Bay, Ontario.

For a detailed discussion of the above test methods, the reader is referred to the appropriate MTO or ASTM test specifications.

GEOGRAPHIC SETTING

The study area is located throughout northwestern Ontario between the latitudes of 48° and 50° N and the longitudes of 83° and 95° W. The area is located in the Canadian Shield physiographic region of Canada (Bostock, 1972). The topography in the region is characterized by a monotonous series of rounded ranges of hills. Locally relief is up to 60-200 m (200-600 ft). The topography resulted from extensive and deep erosion and deposition due to continental glaciation.

GEOLOGICAL SETTING

Surficial Geology

The surficial geology of the region is dominated to a large part by prominent ridges of shallow drift cover or exposed bedrock knobs and ridges. In the intervening lower lying areas, surficial deposits of largely glacial origin are deposited. These include glacio-lacustrine plains, glacio-fluvial deposits such as esker, kame, outwash, delta, etc. and morainal deposits including ground moraine, end moraine, stagnation moraine, etc. (Barnett, 1991).

The key areas for exploration for aggregate resources are the glaciofluvial deposits. The bulk of the aggregate sources tested lie within these types of deposits including kames, eskers, outwash deposits, ice-margin delta deposits, and reworked moraine deposits. In the area along the north shore of Lake Superior, lake terrace, stranded beach and alluvial deposits were sampled. These deposits would have formed during times when Lake Superior was at a much higher level than its current day state (by as much as several hundred metres).

Bedrock Geology
The bedrock in the region is characterized dominantly by Archean rocks of the Superior Province of the Canadian Shield. (Thurston, 1991). There are two distinct structural/lithological terrains in the Superior Province. These are basement rock suites including granitic gneiss, schists, migmatites, etc and supracrustal sequences ("greenstone belts") which include a variety of lithologies including meta-volcanic and meta-sedimentary rocks and plutonic rocks of a variety of composition. Proterozoic rocks of the Southern Province also occur in the study area, although in much less abundance (Sutcliffe, 1991). These rocks include flat lying, stratified sedimentary rocks including shale, mudstone, chert, sandstone, arkose, dolostone, etc., extensive intrusive sheets of diabase and small amounts of volcanic rocks. Southern Province rocks within the study area largely found in the Thunder Bay-Lake Nipigon area and in the Sault Ste. Marie area.

To the north of the study area, a large sedimentary basin occurs surrounding the southern shore of James and Hudson Bays. The Hudson-James Bay Lowlands consist of flay lying, Paleozoic sedimentary strata including a range of clastic rocks, carbonates and chert (Johnson et. al., 1991).

The petrography of the majority of the aggregates sampled reflects a source region largely from the Superior Province of the Shield. In some specific areas, there may be up to 30% Southern Province (sites 32 to 34) or Hudson-James Bay Lowlands rock types (sites 35-45).

STATISTICAL ANALYSIS

The ultimate purpose of testing the 684 samples from the 62 pits was to evaluate, categorize, and catalogue the pit material. The catalogue could be a simple list of test results; however, much more information can be wrung from the expensive and time-consuming testing than can be found in a simple list. The large number of samples allows for statistical evaluation not only of the material, but also of the test methods as they apply to the materials. All of the materials are glacial in origin, and the general provenance (source material) is the Precambrian Shield. Statistical treatment allows us to determine the influence of the provenance and the influence of the agents and environments of deposition on material quality.

The usual approach to statistical treatment of data is the univariate description of data to give mean, median, the range, and standard deviation for the pit, area, glacial type, provenance, etc. The plots are usually simple bar plots. Although of some value, this approach is rather simplistic.

The next level of sophistication is bivariate comparison. Statistics such as scatter plots and correlation between, for instance, two tests or two deposit types, coupled with regression lines and equations if appropriate, and perhaps significance of means comparisons, give some insight into the interdependency (or the lack of it) between pairs of variables. This can result in an effective comparison of material in pit A vs pit B, or the relationship of test X vs test Y. However, if too many sites and too many test comparisons are involved, the discussion can become quite tedious.

The advent of powerful desk-top computers and software allows us to use multivariate statistical approach, where a large number of cases and variables can be treated simultaneously. A number of statistical procedures can be applied to the data set, and each will yield an output; the trick is to select the proper procedure, set proper parameters within it, and, most importantly, analyze and understand the significance of the output produced. This paper will illustrate how a relatively simple data set can yield significant, and perhaps unexpected results about the sand and gravel sources, about the tests used, and the quality control potential of multivariate statistical approach. It will show how statistics can classify aggregate, and predict its behaviour based on aggregate properties of sources with known service history. An article by Hudec (1997) gives a brief explanation of many of the statistical procedures used. A more in-depth, but non-technical explanation can also be found in Williams, 1986.

The statistical package used was SYSTAT 8.0, a Windows-based program from SPSS Inc.

STATISTICAL PROCEDURES AND RESULTS:

Basic Statistics:

The basic statistics for the data are given in **Table 1.** Although the database has some test results for over 680 samples, only the cases that have the full test complement can be used for multivariate analysis. This reduced the number to 314 cases (depending on combination of variables used), as shown in Table 1. Chert and Mica percentages are determined as part of fine aggregate PN analysis. **Figure 2** shows the means and ranges as a function of glacial source of the material. River terrace and glacial outwash material are seen as the best overall in quality, with moraine, lake terrace and kame sources as the worst.

Table 1. Descriptive Statistics

	MicroDeval, Fine	MicroDeval Coarse	$MgSO_4$ Loss	PN Concrete	PN Granular
N of cases	314	314	311	314	314
Mean	10.152	8.331	2.733	127.739	101.844
Stand. Dev.	3.89	2.925	2.607	13.12	6.326
	Bulk Density	App.Density	24h Absorption	Chert %	Mica %
N of cases	314	314	314	311	311
Mean	2.694	2.76	0.9	0.314	1.586
Stand. Dev.	0.056	0.059	0.351	0.557	1.191

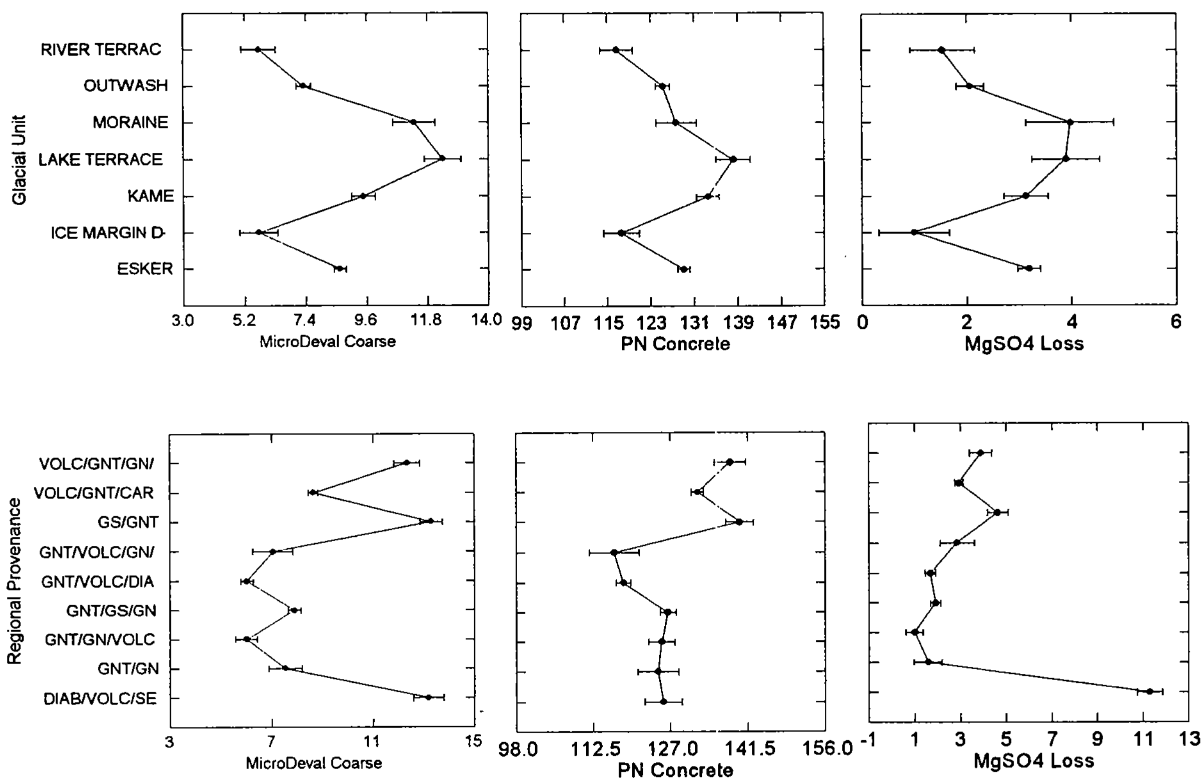

Figure 2. Effect of glacial origin and provenance on test results of coarse aggregate.

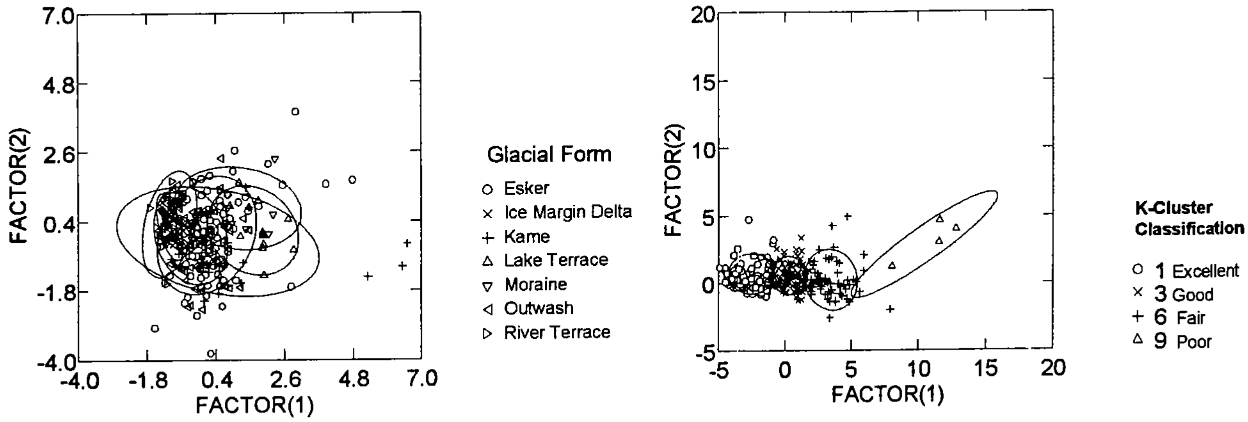

Figure 3. Canonical analyses of glacial forms and of K-Cluster classification.

Figure 3 is the Canonical Scores plot that shows the spacial distribution of the test results expressed as canonical factors. Canonical factors are the degree of similarity or differences between samples grouped, in this case, according to the glacial environment of deposition (see discussion in Factor Analysis section). The enclosing ellipses mark the 65% significance limit - i.e., all samples within the ellipse have 65% commonality. The canonical plot for coarse and microDeval variables (where these are the two discriminant variables grouping all other variables) shows that the properties of outwash are different from esker and terrace materials, whereas there is some commonality between lake terrace and esker material. Where PN Concrete and coarse microDeval properties serve as canonical variables, all materials have a similar response to tests.

Correlation Matrix:
A measure of dependancy or relationship between variables (tests) can be obtained from a simple bivariate correlation matrix. Two matrices are given in **Table 2** - one for coarse and one for fine aggregate tests. To the latter, some results from the coarse aggregate testing have been added for comparison purposes.

Table 2. Pearson correlation matrix			**Number of observations: 311**			
COARSE AGGREGATE						
	MicroDeval	**$MgSO_4$ Loss**	**PN Concrete**	**PN Granular**	**Bulk Density**	**App.Density**
MicroDeval Coarse	1.000					
$MgSO_4$ Loss	**0.595**	1.000				
PN Concrete	**0.571**	0.256	1.000			
PN Granular	**0.581**	0.206	**0.480**	1.000		
Bulk Density	0.050	0.075	-0.228	-0.026	1.000	
App.Density	**0.365**	**0.357**	-0.037	0.176	**0.909**	1.000
24h Absorption	**0.720**	**0.620**	**0.462**	**0.462**	-0.198	0.187
FINE AGGREGATE						
		MicroDeval	**Chert %**	**Mica %**		
MicroDeval, Fine		1.000				
Chert %		0.080	1.000			
Mica %		-0.025	0.155	1.000		
Apparent Density		**0.545**	-0.209	-0.167		
24h Absorption		**0.587**	0.288	-0.086		

For the number of cases, the significant correlation at 1 percent significance level is any correlation coefficient with a value of greater than 0.228. The higher the value, the greater the correlation. Examination of the table for coarse aggregate shows that, for instance, microDeval abrasion test correlates significantly with all the other tests. The surprising finding is that absorption, which normally correlates well with density, does not do so for the rock types found withing the study area. Fine aggregate matrix shows that the fine aggregate microDeval test correlates significantly with absorption and apparent density of coarse aggregate, and with nothing else. The fine PN values for chert and mica have no relationship to any other test, and the test's significance should perhaps be re-examined.

Factor Analysis:

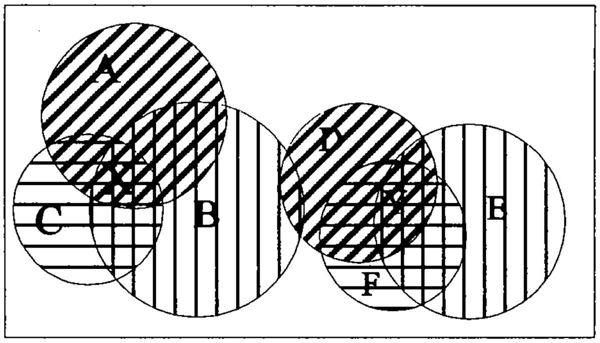

Figure 4. Schematic of factor analysis.

Rock materials have certain properties in common. These properties combine to give the material a specific response to a given test. In the hypothetical example in **Figure 4** (similar to the canonical plots of Figure 2), the response of the material to six different tests (A - F) may fall within circles that overlap to a different degree when plotted on an x-y scatter diagram (using normalized data). Tests A, B, and C overlap in an area X, i.e., they would exhibit a certain amount of correlation, and form a distinct set. Likewise, tests D, E, and F also overlap at Y, have certain mutual correlation, and form a distinct set. The two sets overlap only marginally with tests B and D. The multivariate statistical technique that finds the above groupings is FACTOR ANALYSIS. All physical tests on aggregate material depend on one or more physical characteristic of the rock, such as strength, hardness, porosity, absorption, density, etc. That is why a correlation exists between the results of some tests, such microDeval abrasion test, as shown in Table 2. However, the relationship can extend to more than two tests. Factor analysis is a technique that measures the degree of interdependence between the test results which is based on the physical properties of the aggregate. The procedure considers all the results of a square matrix, the columns of which are tests, and the rows are samples (cases). It groups the variables (tests) in "factors" so that variables within each factor are more highly correlated with each other than with variables in other factors. Each factor can then be interpreted in terms of the correlated variables.

Table 3. Factor Analysis of Coarse and Fine Aggregate

COARSE AGGREGATE				
	Durability	**Density**	**Pore Vol.**	**Petrography**
microDeval, Coarse	**0.661**	0.177	***0.444***	***0.421***
PN Granular	**0.917**	0.163	-0.045	0.078
PN Concrete	0.214	-0.120	0.239	**0.932**
Absorption, %	0.165	0.044	**0.936**	0.226
Bulk Density	-0.089	**0.988**	-0.039	-0.091
Apparent Denisty	***0.256***	**0.951**	0.113	-0.011
MgSO4 Loss, %	**0.816**	-0.105	***0.364***	0.189
% Variance Explained:	29.9	28.1	18.3	16.4
			Total	92.6
FINE AGGREGATE				
	Mineralogy	**Abrasion**		
microDeval, Fine	0.005	**0.939**		
Chert %	**0.725**	***0.307***		
Mica %	**0.793**	-0.236		
% Variance Explained:	38.4	34.4	72.9	

Table 3 gives the results of factor analysis. The procedure found that all the variables (tests) for coarse aggregate can be grouped into 3 factors. The first factor accounts for almost 30% of the total variance; i.e., the high coefficients, shown in **bold**, and the related tests, define up to 30% of the properties of the sample. Lower, but still significant coefficients are shown in *italics*. The first

factor has been named Durability Factor, since the high coefficient tests can be broadly defined as durability tests. Factor 2, accounting for additional 28% of variance, is Density Factor. The Pore Volume factor shows that Absorption, reflecting porosity, is mostly related to microDeval and the $MgSO_4$ loss. The Petrography Factor includes microDeval and PN Concrete as significant variables.

For fine aggregate, only two factors have been identified, since there are only three variables (tests). As expected from the correlation matrix, microDeval loss and chert content form a strong factor, which can be termed the Abrasion Factor. Chert and mica form what can be termed the Mineralogy Factor.

Cluster Analysis:
The multivariate statistical technique that groups samples rather than variables is called CLUSTER ANALYSIS. The results of cluster analysis are commonly expressed as a hierarchical tree, or a dendogram. However, for a large number of samples, a dendogram becomes undecipherable. A variant, called K-cluster analysis groups the samples (cases) into several broad groups. The character of the group can be identified by the means of the tests (variables). This is shown in **Table 4.** The means of variables can be used to interpret the characteristics of the group, i.e., in this case, is the overall durability or quality of the material. This is perhaps the most powerful statistic that can be used to classify samples and differentiate between sources. Examining the means of PN

Table 4. K-CLUSTER ANALYSIS & GROUPING								
	Excellen	N=123	Good	N=120	Fair	N=66	Poor	N=5
VARIABLE	Mea	St.Dev	Mea	St.Dev	Mea	St.Dev	Mea	St.Dev
MicroDeval Coars	6.91	2.04	8.44	1.89	9.88	2.93	20.0	4.80
$MgSO_4$ Loss	2.03	1.67	2.95	2.54	3.38	3.53	7.18	3.07
PN Concrete	115.6	4.85	129.1	3.77	144.0	5.78	174.8	9.23
PN Granular	100.5	1.61	101.1	2.22	102.0	3.86	146.4	10.9
Bulk Density	2.71	0.05	2.69	0.06	2.68	0.05	2.63	0.04
Apparent Density	2.76	0.06	2.76	0.07	2.75	0.05	2.80	0.02
24h Absorption	0.76	0.21	0.92	0.30	1.02	0.37	2.27	0.32

Concrete and micoDeval in each group, for instance, shows that the values parallel closely the acceptance limits imposed for this test. Similar results were obtained for fine aggregate. The K-Cluster groupings were assigned categories, based on the means of the test results in each group, as Excellent, Good, Fair and Poor.
The members of each group are clearly identified by case number, and can be identified by pit, location, producer, or whatever ID is used. If a new sample from the area is tested, the results are simply appended to the database, the analysis is re-run (a matter of minutes), and the sample will be placed in one of the four categories. The category in which it appears clearly classifies the sample. As new samples are added and the database grows, the classification of samples improves.

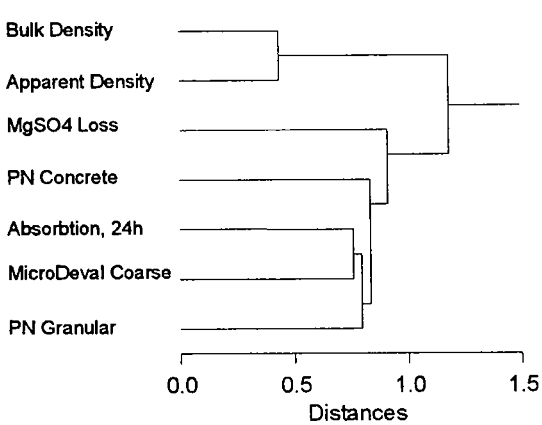

Figure 4 Cluster Analysis Dendogram

The ability of the procedure to classify aggregates is shown by the means of some of the more significant tests, such as the microDeval, magnesium sulphate, and petrographic number tests. The means in the four categories are, interestingly, close to the passing limits that have been assigned to the three tests.

Another variant of cluster analysis groups variables (tests) rather than cases. The results of cluster analysis of tests for coarse aggregate is given in dendogram of **Figure 4** and shows yet in another way the common traits among the tests. The calculations were done on normalized data. The distance along the x-axis shows the degree of commonality - the smaller the distance, the closer are the variables correlated. Thus, the two density tests form a common cluster with shortest distance, as expected. MicroDeval and absorption also form a common cluster, but with longer distance. The more removed member of a larger cluster is PN Granular, and then PN Concrete. Magnesium sulphate forms a lone member, related more distantly to the preceding variables. The cluster analysis gives graphical results which are similar to the numeric factor analysis.

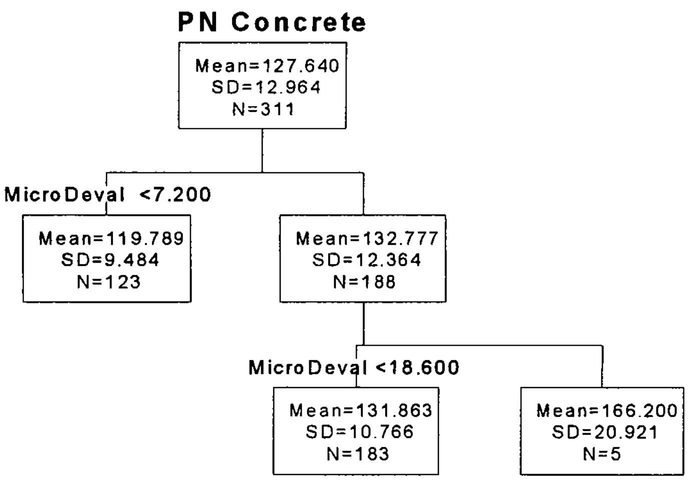

Figure 5. Tree analysis of PN for concrete.

Tree Analysis:
Tree analysis can be applied to tests (variables), and to samples (cases). When applied to tests, the analysis effectively subdivides the chosen test (dependent variable) into segments which are based on properties of the samples as determined by other tests (independent variables). The independent variables (tests) are chosen by the procedure on the basis of having the greatest influence on the dependent variable. A tree is formed, as shown in **Figure 5,** that progressively narrows down the test value limits which define the groups.

In the case of PN for Concrete (in Figure 5), microDeval test classifies the PN test. Tthe first limb of the tree divides the PN results into two groups: those in which microDeval data are less than 7.2 (left branch) and those in which microDeval loss is greater than 7.2. Note that the mean of PN is lower in the left branch than in the right, and that the standard deviation also drops, indicating a closer fitting group. The right branch is

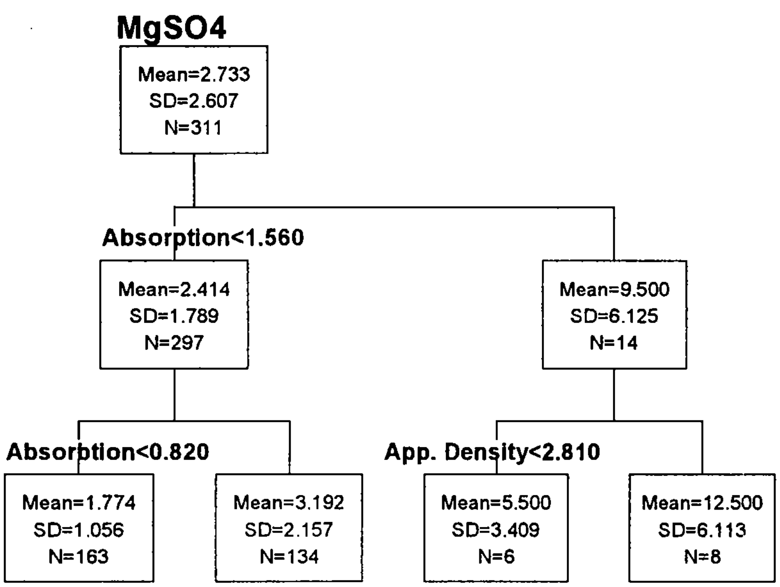

Figure 6. Tree analysis of $MgSO_4$ test results.

further divided into two sub-branches, in which microDeval on the left sub-branch is less than 18.6, compared to that on the right. The PN correspondingly increases in the right sub-branch.

Although performed randomly by the TREE procedure, the division of the PN results into groups is very close to what are the currently acceptable PN passing limits for various uses of coarse aggregate. The analysis thus divides coarse aggregate into three groups: left-most group with PN of <119 and microDeval of <7.2 represents the best aggregate, whereas that of PN >166 and microDeval >18.6 represents the worst material.

A similar tree was constructed for magnesium sulphate soundness tests as given in **Figure 6.** In the case of $MgSO_4$, absorption and apparent density are the distinguishing variables. The last row of Figure 6 subdivides the coarse material into four soundness groups that can be applied to this particular material from Precambrian Shield sources. The subdivision also clearly shows the dependance of the $MgSO_4$ test on absorption and density properties.

Stepwise Regression Analysis

Stepwise regression is a relatively simple procedure that allows the calculation of a categorical variable (such as a quality estimate) from standard test results. In this case, the categorical variable was derived from the K-cluster analysis grouping, in which all the samples (cases) that fell into the 'Excellent' group were given a category value of 1. The 'Good', 'Fair', and 'Poor' groups were given the categories of 3, 6, and 9 respectively. This category designation is similar to that used in the calculation of PN for Concrete.

Using the categorical designation as a dependent variable, a stepwise regression analysis was run using all the test results as independent variables. The results of the analysis are shown in **Table 5.** The regression coefficient was very significant, suggesting high a confidence in the relationship. Of all the variable, the procedure selected the

Table 5. REGRESSION EQUATION (Category Calculation)						
					EXAMPLE	
	R = 0.975,	R^2=0.951			Sample No.	
	Coefficient	Error	Std. Coef.	robability	1201	1212
microDeval, Coarse	0.093	0.024	0.044	0.000	14.1	20.8
PN Concrete	0.134	0.004	0.007	0.000	121	146
PN Granular	-0.035	0.009	0.002	0.000	100	100
Bulk Density	-4.110	0.298	0.003	0.000	2.821	2.603
Absorption	-0.323	0.191	0.060	0.092	1.73	2.919
			Calculated Category:		1.9	6.4

variables given in the table as significant variables. The Probability shows the significance of each of the variables. Magnesium sulphate test was found to be insignificant. The coefficients of the regression can be used in an equation to calculate the category classification of any aggregate based on the three variables by multiplying the test result by its coefficient. In Table 5, the sum of the products of such multiplication yields calculated categories of 1.9 (good to excellent) and 6.4 (fair) for samples 1201 and 1212 respectively. The samples come from two different pits.

DISCUSSION AND CONCLUSIONS

Multivariate statistical analysis is a valuable tool in assessing the relationship between tests, the suitability or efficacy of the test, and, most importantly, in classifying the aggregates. Rather than relying on the passing limits of any one or several tests, the response of the aggregate to a variety of tests together can be used as a more reliable means of classifying it. Several multivariate procedures can be used on the same data set, and one or more predictive durability, soundness, quality, etc. models can be developed based on those procedures. Factors (tests, properties) that combine to define a group of aggregates can be establish for a given sample set. The analysis becomes more reliable as more results are added to the database. The predictive models can be further refined by developing regional or provenance-specific models. The predictive models developed in this paper apply only to the region sampled, i.e., specifically, to aggregates derived from the Superior province of the Precambrian Shield of Ontario, since these rocks have a specific range of responses to the tests. Mixed Paleozoic/Precambrian gravels of southern Ontario will require a separate analysis based on the principles developed here. Likewise, quarried crushed stone from Paleozoic sources should also be treated as a separate database for predictive purposes. Conclusions applied to this data set are:

Geologic Influence:

1. The glacial origin of the gravel has a significant influence on its quality. River terrace, outwash, and ice-margin delta gravels were significantly better in quality than moraine, lake terrace, and kame gravels.
2. Provenance of the gravel, i.e., the geology of the region in the immediate up-ice direction also, as expected, had some influence. Any areas where volcanics dominated had a poorer material than the gneissic-granitic rock dominated areas.

Significance of Tests:

1. MicroDeval test correlates well with more tests than any other testing procedure. Magnesium sulphate test depends mostly on the pore properties of the sample. It is successful here mainly because it was performed on all samples by the same lab.
2. Cluster dendogram shows that $MgSO_4$ test is the most isolated, whereas PN tests, absorption, and microDeval tests from a common cluster, i.e., are somewhat interdependent. The only reason that $MgSO_4$ correlates at all is because the test was done by a single laboratory.

Aggregate Classification:

1. K-Cluster analysis is capable of sorting the individual samples into Excellent, Good, Fair and Poor categories based on the aggregated test scores. It is perhaps the most powerful technique in effectively classifying the aggregates.
2. Tree Analysis formulates group limits based on significant tests that can classify the aggregate.
3. Stepwise regression analysis can assign quality category to a source based on standard tests. The categorical variable can be an a priory assigned, or determined by K-Cluster analysis.

ACKNOWLEDGMENTS

The authors would like to acknowledge the valued contributions and support of the individual who aided in the preparation of this paper. We would like to thank Larry Wells and John Dixon of the MTO's Northwestern Region office and Chris Rogers of MTO's Soils and Aggregate section for permission to use the data for this analysis. We would also like to than Wayne Hurley, P.Eng. and Mike Fabius, P.Eng. of DST for reviewing the manuscript, as well as John Bociurko and Allison Stoddart of DST for their diligent work in compiling the laboratory test results.

REFERENCES

Bostock, H.S., 1991. Physiographic Subdivisions of Canada; *in* Geology and Economic Minerals of Canada, Geological Survey of Canada, Economic Geology Report No. 1, Ch. II, p.10-30

Barnett, 1991. Quaternary Geology of Ontario; *in* Geology of Ontario, Ontario Geological Survey Special Volume 4, Part 2, p1011-1090.

Hudec, P. P., 1997. Multivariate Statistical Methods in Evaluation of Concrete and Aggregate Properties; ACI SP 171-25, pp. 531-550

Johnson, M.D., Armstrong, D.K., Sanford, B.V., Telford, P.G., and Rutka, M.A., 1991. Paleozoic and Mesozoic Geology of Ontario; *in* Geology of Ontario, Ontario Geological Survey Special Volume 4, Part 2, p.907-1010.

Sutcliffe, R.H., 1991. Proterozoic Geology of the Lake Superior Area; *in* Geology of Ontario, Ontario Geological Survey Special Volume 4, Part 1, p.627-660.

Thurston, P.C., 1991. Archean Geology of Ontario: Introduction: *in* Geology of Ontario, Ontario Geological Survey Special Volume 4, Part 1, p.73-82.

Williams, R., 1986. Reasoning with Statistics, Holt, Reinhart & Winston, New York, NY

THE EFFECT OF AGGREGATE TYPE AND MIX DESIGN ON WET PAVEMENT SKID RESISTANCE

W. Cullen Sherwood, Department of Geology & Environmental Studies, James Madison University

David C. Mahone, Virginia Transportation Research Council, Retired

L. Scott Eaton, Department of Geology & Environmental Studies, James Madison University

INTRODUCTION

Providing skid resistant pavements is a high-priority goal of Virginia's Wet Accident Reduction Program (WARP). Research on pavement friction, begun in Virginia by Shelburne and Sheppe (1948), has continued to the present day. Shelburne and Sheppe mainly researched methods of measuring pavement friction but noted the role of aggregate type in providing skid resistance. Klein and Brown (1939) and Moyer (1959) also found that aggregate rock type affects pavement friction. Aggregate type affects pavement surface texture, and pavement surface texture is a critical factor in wet skid resistance (Mahone, 1975; Leu and Henry, 1978; Argawal and Henry, 1980; Henry, 1980; Henry and Saito, 1981; Yandell et al., 1982; Wombold et al., 1986; Glendon, 1988).

These early studies found that some aggregates were susceptible to polishing under traffic. Polished aggregates exhibited significantly lower wet skid resistance than those which remained unpolished under traffic wear. Later studies (Nichols, 1959; Sherwood, 1959; Sherwood and Mahone, 1970; Webb, 1970; Stutzenberger and Havens, 1958; Finney and Brown, 1959; Knill, 1959; McLean and Shergold, 1959; Shupe and Lounsbury, 1959; Gray and Renninger, 1960; Stephens and Goetz, 1961; Kummer and Meyer, 1967) ultimately determined that the polish susceptibility of mineral aggregates was related to the mineralogy and texture of the rock.

Based on early research findings and observations by the operating divisions, the Virginia Department of Transportation excluded certain polish-susceptible aggregates from Primary and Interstate roads by 1955. In Virginia, polish-susceptible aggregates are predominately the limestones and dolomites occurring in the Valley and Ridge area in the western part of the state. To date, Virginia is the only state to exclude polish-susceptible limestone aggregates as coarse aggregate in primary and interstate surface mixes.

This report identifies and characterizes Virginia's nonpolishing aggregates in terms of their wet skid resistance, in order to provide information which can be applied to Virginia's Wet Accident Reduction Program (WARP). The Virginia *Road and Bridge Specifications* (1991) states, "The term 'non-polishing aggregate' shall mean aggregate that the Department has determined will result in a surface of acceptable skid resistance when it is used and exposed as part of a wearing surface." Most of the "non-polishing aggregates" produced in Virginia are composed predominately of hard, durable silica or silicate minerals. Selected manufactured materials such as slag and expanded shale have also proved to be nonpolishing. However, several studies (Nichols, Dillard and Alwood, 1956; Webb, 1970; Runkle and Mahone, 1977) together with data from routine skid testing in Virginia have indicated that some nonpolishing aggregates are superior to others in imparting road surface friction. An important objective of this study was to rate the polish-resistance of the state's various nonpolishing aggregates.

Information on asphalt mix design was included in the database in order to investigate the influence of mix design on skid resistance.

Some of the earliest studies on skid resistance recognized that surface texture affects pavement friction (Shelbourne and Sheppe, 1948; Moyer and Shupe, 1951). Later Stutzenberger and Havens (1958), Kummer and Meyer (1967), and Webb (1970) among others used the terms "microtexture" and "macrotexture," to describe the elements of pavement surface texture which most affect skid resistance. Microtexture refers to asperities with wavelengths from 0.50 mm (0.020 in), while macrotexture describes asperities with wavelengths up to 0.50 mm (0.020 in) to 50 mm (2.00 in). Normally, asperity height is approximately one half of the wavelength.

MATERIALS AND METHODS

Identifying and Characterizing Nonpolishing Aggregates

During 1989 and 1990, a total of 57 sources producing nonpolishing aggregates within Virginia were identified and sampled. Material was taken from a minimum of two stockpiles to obtain a representative sample of the rock being mined. A search of the existing literature on Virginia geology, and contacts with geologists at the Virginia Division of Mineral Resources and industry sources, provided geologic information and other data on each aggregate source. Samples from each source were examined using hand specimen and microscopic techniques. The aggregates from the 57 quarries represented eighteen specific rock types. Table 1 provides brief lithologic descriptions of each type together with data on the number of quarry sources for each rock and the number of road sites skid tested.

Table 1

NUMBER OF SOURCES AND NUMBER OF SITES SKID TESTED FOR EACH AGGREGATE TYPE

NON-POLISHING AGGREGATE GROUPS		
Rock Type	Number of Quarry Sources	Number of Sites Tested
Aplite (Med. grained plagioclose feldspar & minor qtz.)	1	28
Arch Marble (Med. Grained, 78% calcite + micas & qtz.)	2	81
Basalt (Fine grained pyroxene & plagioclose)	3	86
Gravel Blends (Qtzite gravel with limestone fines)	2	10
Biotite Granite (Med. Grained, biotite-rich, slightly foliated)	2	42
Coastal Plain Gravels (Vein qtz. & qtzite, from alluvium)	2	18
Diabase (Fine med. Grained, pyroxene & plagioclose feld)	5	148
Fine Grained Granite (Fine to med. Grained >30% qtz.)	1	66
Greenstone (Metabasalt, fine grained, chlorite-rich)	1	39
Antietam Quartzite (White to gray, >99% qtz.)	1	11
Lovingston Granite (Med. grained granite & augen gneiss)	3	71
Metagraywacke (Metamorphosed impure sandstone & graywacke)	2	77
Metamorphic (Undifferentiated,foliation common)	3	62
Metavolcanic (Metarhyolites & metadacites, foliation common)	2	195
Petersburg Granite (Med. to coarse grained, orthoclase phenocrysts)	8	191
Slate (Fine grained, strongly foliated)	1	19
Triassic Hornfels (Baked siltstone from contact metamorphism)	1	49
Valley Gravels (Alluvial gravels, mainly Antietam qtzite)	2	53

ASTM E 274-90 Skid Tests

Following identification of the 18 types of nonpolishing aggregates produced in Virginia, an intensive program of skid testing was undertaken. The object of the program was to provide skid data for each of the 18 rock types sufficient to evaluate and compare their skid resistance. All testing was conducted on bituminous pavements in the Virginia primary road system during 1989-91. Test sites were limited to segments of highway a minimum of one mile in length, paved under a single contract. The small number of sites tested for materials such as Gravel Blends and Antietam Quartzite reflect the limited availability of these materials in primary roads.

All skid tests were run according to the standard ASTM E 274-90 procedure. A total of 1,246 sites were tested. All tests were run at a test speed of 40 mph and are identified in this work as SN40S for the smooth tire test, and SN40R for the ribbed tire test. Initially, 15 tests were run with both ASTM E 524-88 standard smooth and ASTM E 501-82 standard ribbed tires at each site. This number was later reduced to 7 tests per site with each type of tire. In addition to aggregate lithology, a number of other parameters for each skid test site were noted. These parameters included: location, mix design, placement date, skid date, lane average vehicle passes per day (LAVD), accumulated traffic (AT), and the ratio of smooth tire to ribbed tire skid test means.

Pavement Surface Macrotexture

Data from 105 sand patch measurements of macrotexture (ASTM E 965) were included in the database. Most of the sand patch tests were conducted in response to a request to investigate specific aggregates. Consequently, data on only 6 of the 18 lithologies were available. Multiple regression was performed on the data from the 105 sites where sand patch measurements of macrotexture were made to determine the effect of macrotexture on skid resistance for those pavements.

RESULTS

Skid test data from the 1,246 sites yielded considerable insight into existing conditions on Virginia's primary road system. As would be expected, traffic volumes for the test sites varied widely. LAVD varied from a low of 425 to a high of 20,936, with a mean of 3,263. AT ranged from 181,496 to 95,488,928 vehicle passes, with a mean of 6,291,494. Using these values for LAVD and AT, a mean age of 5.23 years for the pavements studied is indicated. Eight years is generally considered to be the average life for bituminous pavement surfaces in Virginia (C. S. Hughes, personal communication).

Results of the SN40S tests for the 1,246 sites ranged from 13 to 59 with an overall mean of 36 and a standard error of 7.8, while SN40R tests ranged from 26 to 69 with an overall mean of 47 and a standard error of 5.2 (Figures 1 and 2). Assuming that the test results conform to normal distributions, in the smooth tire tests 16.7% of the pavements should fall below an SN40S of 28 (one standard error below the mean), and 2.5% below an SN40S of 21 (two standard errors below the mean). In the ribbed tire tests, 16.7% of the pavements should fall below an SN40R of 42 (one standard error below the mean), and 2.5% of the tests below an SN40R of 37 (two standard errors below the mean).

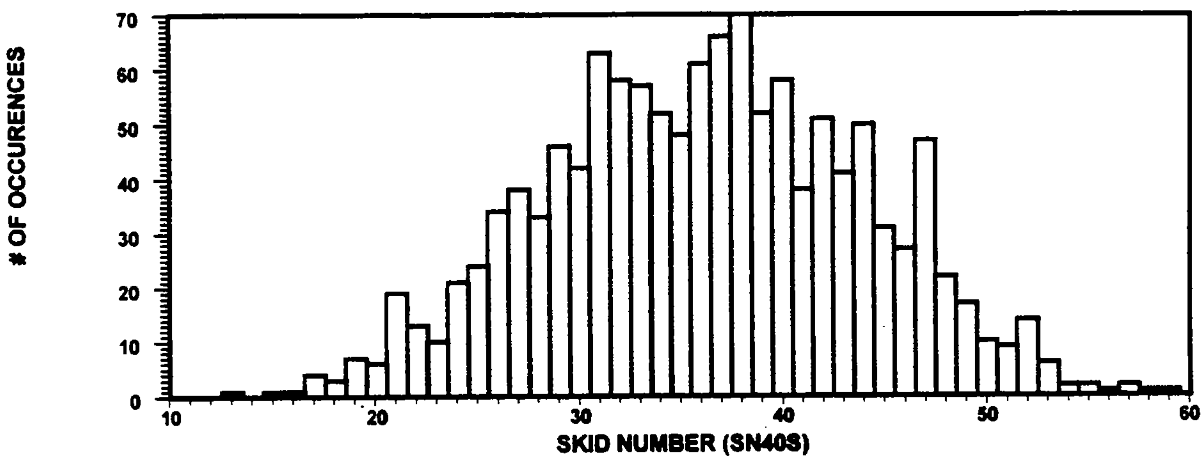

Figure 1. Distribution of skid numbers (SN40S) for tests run with the smooth tire.

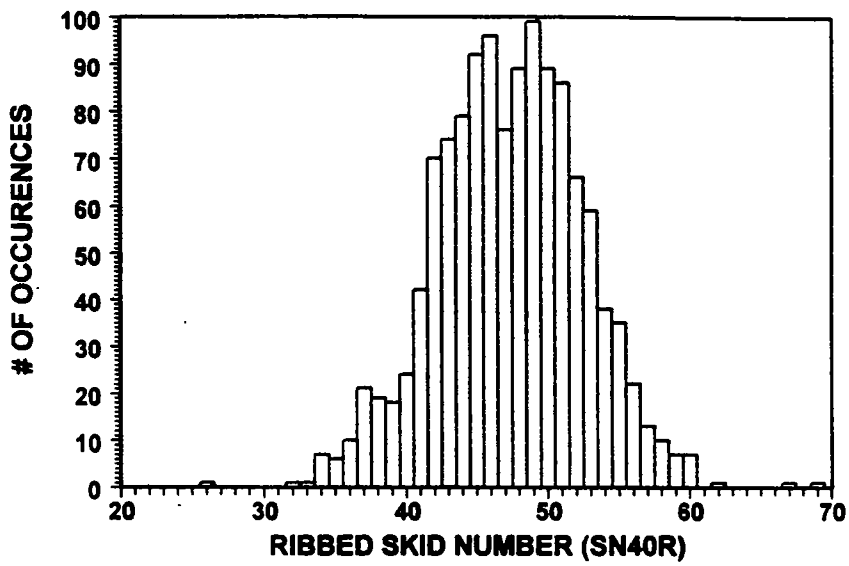

Figure 2. Distribution of skid numbers (SN40R) for tests run with ribbed tires.

The range and standard error values for smooth tires (SN40S) are greater than those for ribbed tires (SN40R). The smaller range for the ribbed tire data has been explained by Henry and Saito (1981) as a function of more effective water removal by ribbed tires, allowing greater tire-to-pavement contact on wet pavements. The greater range in the smooth tire data appears to indicate that smooth tires are more sensitive to small differences in wet pavement friction. This greater sensitivity to wet pavement conditions together with a desire to provide safe pavements under "worst case" conditions has led VDOT to use smooth tire data as a basis for Virginia's wet accident prevention program.

Aggregate Lithologies and SN40S values

As skid test data accumulated from the field it became evident that comparisons of the SN40S values for the different aggregate types would not be a simple matter. Aggregates from different parts of the state are exposed to significantly different volumes of traffic (Table 2). For instance, the LAVD means for the 18 nonpolishing groups ranged from a low of 1,610 for Slate to a high of 6,715 vehicles per day for Diabase. AT means exhibited an equally large range from a low of 2.4 million vehicle passes for Slate to a high of 9.9 million vehicle passes for Diabase. Values for the other 16 aggregate types occupied the broad range in between these two.

Table 2
SUMMARY OF LANE AVERAGE VEHICLES PER DAY (LAVD), ACCUMULATED TRAFFIC (AT), AND MEAN STOPPING DISTANCE NUMBERS (SN40S) AND STANDARD ERRORS FOR EACH AGGREGATE TYPE

AGGREGATE TYPE	MEAN LAVD	MEAN AT	MEAN SN40S	SN40S RANGE	STANDARD ERROR(σ)	SN40S MEAN MINUS 2σ
Aplite	1,737	2,611,036	35	21-48	8.45	18
Arch Marble	2,819	8,476,084	33	17-50	8.46	16
Basalt	2,697	4,479,681	37	18-52	7.86	21
Biotite Granite	3,127	5,393,060	34	16-43	5.79	22
Gravel Blends	2,029	5,877,554	38	30-49	5.39	27
Coastal Plain Gravel	1,068	5,444,883	44	31-58	6.50	31
Diabase	6,715	9,906,872	35	18-52	7.19	21
Fine Grained Granite	1,631	5,843,151	42	25-52	5.54	31
Greenstone	4,491	7,570,377	32	18-53	8.49	15
Antietam Quartzite	2,146	5,190,138	38	27-55	8.53	23
Lovingston Granite	2,517	3,112,880	41	19-54	6.86	27
Metagraywacke	2,691	5,965,203	34	15-47	7.15	20
Metamorphics	2,296	5,035,420	37	21-49	7.26	23
Metavolcanic	3,331	7,570,849	34	19-52	6.39	21
Petersburg Granite	3,308	6,044,563	35	17-59	5.84	21
Slate	1,601	2,400,642	32	17-49	6.82	18
Triassic Hornfels	2,618	3,924,126	34	24-52	8.50	17
Valley Gravel	2,505	5,600,897	43	23-57	7.47	29
Mean-All Tests	3,263	6,291,494	36			

Because of these significant differences in exposure to traffic, several techniques were employed to compare and evaluate the relative skid resistance of the aggregate types. Initially, SN40S means, standard errors, and the means minus two standard errors were computed for each group (see column 1 of Table 3). The five groups showing the highest values for mean SN40S minus two standard errors were Fine Grained Granite (31), Coastal Plain Gravel (31), Valley Gravel (29), Lovingston Granite (27), and Gravel Blends (27). The five groups projecting the lowest SN40S values were Greenstone (15), Arch Marble (16), Triassic Hornfels (17), Aplite (18), and Metagraywacke (20). Assuming normal distributions apply, 2.5 percent of the SN40S values for each aggregate type should fall below these values. An SN40S of 20 is used in Virginia's Wet Accident Reduction Program as a value below which pavement friction may not be acceptable.

Another common method of evaluating the skid resistance of an aggregate has been to test a number of pavements which have been exposed to a wide range of total vehicle passes, and plot the rate of decrease in SN40 as AT increases (Mahone and Runkle, 1972; Runkle and Mahone, 1977). However, research conducted in Great Britain (Salt, 1976) and elsewhere indicates that LAVD also has a strong influence in skid resistance. In order to test whether AT or LAVD correlated more strongly with SN40 values, correlation coefficients were calculated for SN40S vs. AT and SN40S vs. LAVD for each of the 18 aggregate types.

First order correlation coefficients were found to cover a wide range of values with R^2 ranging from 0.00 to 0.37 for AT, and 0.04 to 0.54 for LAVD (Table 5). Low R^2 values in most of the cases indicate that increases in AT and LAVD may not be the major causes of decreases in SN40S values.

Based on the higher R^2 values for LAVD, it was decided to utilize SN40S vs. LAVD data as a basis for further aggregate evaluation. SN40S vs. LAVD graphs were plotted for each of the eighteen aggregate types. First order least square curves along with parallel curves at one and two standard errors were computed and plotted. Finally a horizontal line at SN40S=20 was added. Figure 3, is an example of the graphs constructed for each of the eighteen aggregate types.

Figure 3 contains the SN40S vs. LAVD graphs for Diabase. The SN40S=20 curve intersects the two- and one-standard-error lines at 9,108 and 16,885 LAVD respectively. These LAVD values are among the highest in the study, indicating that Diabase maintains SN40S values of greater than 20 even under high volumes of traffic. Typically the SN40S values show high variability and relatively large standard errors which lower the LAVD values where the one- and two-standard-error curves reach SN40S=20. Even so, the mean LAVD of 6,715 for Diabase test sites is well below the 9,108 projected at two standard errors.

Column 2 of Table 3 lists the results of the graphs similar to Figure 3, constructed for all eighteen aggregate groups. The five aggregates projecting the highest LAVD values where the mean minus 2σ curve intersected the SN40S=20 line were Valley Gravel (11,506), Diabase (9,108), Lovingston Granite (9,061), Metavolcanics (7,488), and Greenstone (7,294). Those projecting the lowest LAVD values were Triassic Hornfels (1,916), Arch Marble (1,975), Slate (2,217), and Aplite (2,303). Only one aggregate group, the Arch Marble, showed a mean LAVD for the test population (2,819) to be higher than that projected at the intersection of the SN40S=20 line and the curve at two standard errors below the mean (1,975).

Next, multiple regression was performed on the whole test population using SN40S values as the dependent variable. Independent variables were aggregate rock type, LAVD, AT, Mixes I-2 and S-5, and date of placement. The resultant R^2 value was a relatively low 0.33. LAVD showed the strongest negative T value, indicating that high LAVD values correlate with low SN40S values. In order to rank the aggregate types, basalt was chosen as the comparison group. The choice of basalt was made because its mean SN40S value of 37 was closest to the total population mean. Column 3 of Table 4 contains the results of the rankings.

The lithologies testing most positive for T in column 3 of Table 3 (i.e. projecting higher SN40S values than Basalt) in the regression were Valley Gravel (+6.3), Fine Grained Granite (+3.9), Lovingston Granite (+3.8), and Diabase (+3.1). Aggregate Groups with T values exhibiting the most negative influence were Arch Marble (-3.1), Slate (-3.0), Greenstone (-2.5), Blends (-2.3), and Metamorpohics (-2.3).

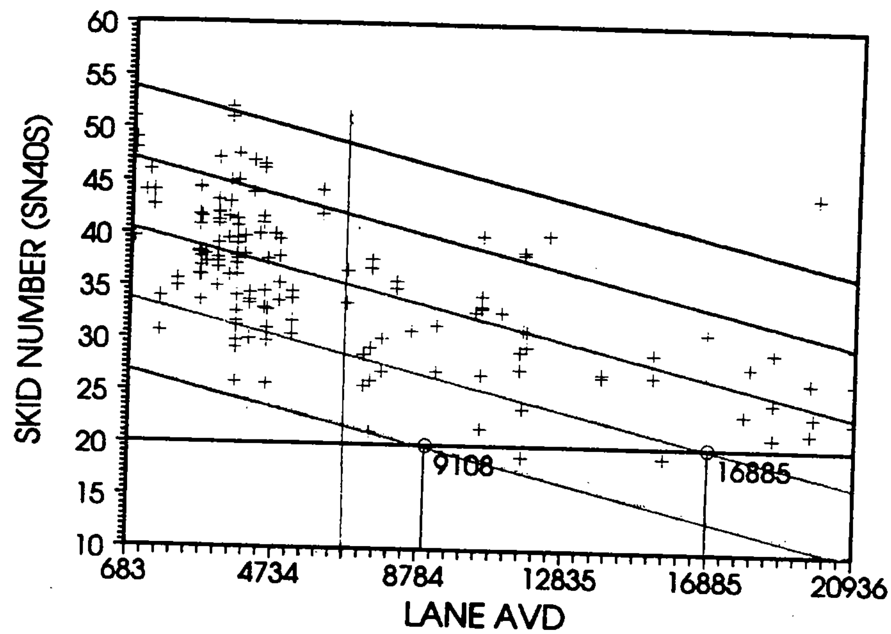

Figure 3. Skid numbers vs. lane average vehicles per day (LAVD) for Diabase. Parallel lines at one and two standard errors have been added.

Finally, multiple regression was performed on the data from the 105 sites where sand patch measurements of macrotexture were available. The correlation value increased to R^2=0.70 with macrotexture contributing a strongly positive T value of 8.82. These values clearly indicate that macrotexture is an important element in imparting skid resistance. However, sand patch data were available for only 6 of the 18 aggregate types (Table 3, column 4).

Table 3
SUMMARY OF THE RESULTS OF THE FOUR METHODS USED
TO EVALUATE THE RELATIVE SKID RESISTANCE OF THE AGGREGATE GROUPS.
IN EACH CASE THE COLUMNS REFLECT HIGHEST TO LOWEST SKID VALUES

SN40S VALUES MEAN -2σ		LAVD VALUES: -2σ Curve Intersects SN40S=20		Multiple Regression Total Population T Values		Multiple Regression T Values Using 105 Sand Patch Locations*	
Fine-Grained Granite	31.41	Valley Gravel	11,506	Valley Gravel	6.3	Fine Grained Granite	-2.23
Coastal Gravel	31.26	Diabase	9,108	Fine Grained Granite	3.9	Greenstone	-3.11
Valley Gravel	28.53	Lovingston Granite	9,061	Lovingston Granite	3.8	Biotite Granite	-3.18
Lovingston Granite	27.20	Metavolcanics	7,488	Diabase	3.1	Slate	-3.33
Gravel Blends	26.72	Greenstone	7,294	Coastal Gravel	2.3	Aplite	-3.74
Antietam Quartzite	23.24	Fine Grained Granite	6,882	Antietam Quartzite	1.5	Arch Marble	-4.40
Metamorphics	22.54	Antietam Quartzite	6,872	Biotite Granite	0.1		

Biotite Granite	22.19	Petersburg Granite	5,980	Basalt	0.0
Metavolcanics	21.23	Biotite Granite	5,831	Petersburg Granite	-0.6
Petersburg Granite	21.19	Coastal Plain Gravel	5,780	Metagraywacke	-1.3
Basalt	21.00	Gravel Blends	5,257	Aplite	-1.6
Diabase	20.98	Metagraywacke	4,598	Metavolcanics	-2.2
Slate	20.18	Metamorphics	4,587	Triassic Hornfels	-2.2
Metagraywacke	19.91	Basalt	4,479	Metamorphics	-2.3
Aplite	18.40	Aplite	2,303	Gravel Blends	-2.3
Triassic Hornfels	17.10	Slate	2,217	Greenstone	-2.5
Arch Marble	16.44	Arch Marble	1,975	Slate	-3.0
Greenstone	15.30	Triassic Hornfels	1,916	Arch Marble	-3.1

*Sand patch data was available for only six aggregate groups

Mix Design vs. Skid Resistance

Table 4 contains mean skid resistance values for pavements containing all of the mixes found in the skid test database. Note that the SN40S means computed for the I-2 and S-5 mixes are similar. No significant difference in skid resistance for the two most commonly used mixes can be inferred from these data. To investigate further, graphs were constructed showing SN40S vs. AT and Sn40S vs. LAVD, each containing all of the I-2 and S-5 data. Again, significant differences could not be identified. Finally, individual graphs of SN40S vs. AT and LAVD for I-2 and S-5 with each aggregate type were plotted in the same manner. Figure 4 is the graph for SN405 vs. AT for the Arch Marble.

The I-2 design generally incorporates significantly coarser aggregates than the S-5. Up to 37% of plus ½ in, material is allowed in an I-2 mix, while 100% of the aggregate must pass the ½ in sieve in the S-5 mix (Virginia Department of Transportation Road and Bridge Specifications, 1991).

Table 4

MEAN SKID NUMBERS AND TRAFFIC DATA FOR ALL MIXES IN THE TEST POPULATION

	S-3	S-5	I-2	S-6	URBAN[a]	ST[b]	SS[c]	SS/B[d]	LATSU/C[e]
Lane Avd	3,812	3,762	2,778	6,375	3,030	1,306	1,940	1,368	2,568
Accumulated Traffic	6,709,595	8,223,842	4,643,765	7,125,249	2,572,138	2,681,696	3,979,259	3,536,964	154,061
Smooth Mean	30	36	37	36	31	37	38	34	43
Ribbed Mean	45	47	48	44	44	45	47	48	50

a. Urban Mix b. Surface Treatment c. Slurry Seal C d. Slurry Seal B e. Latex

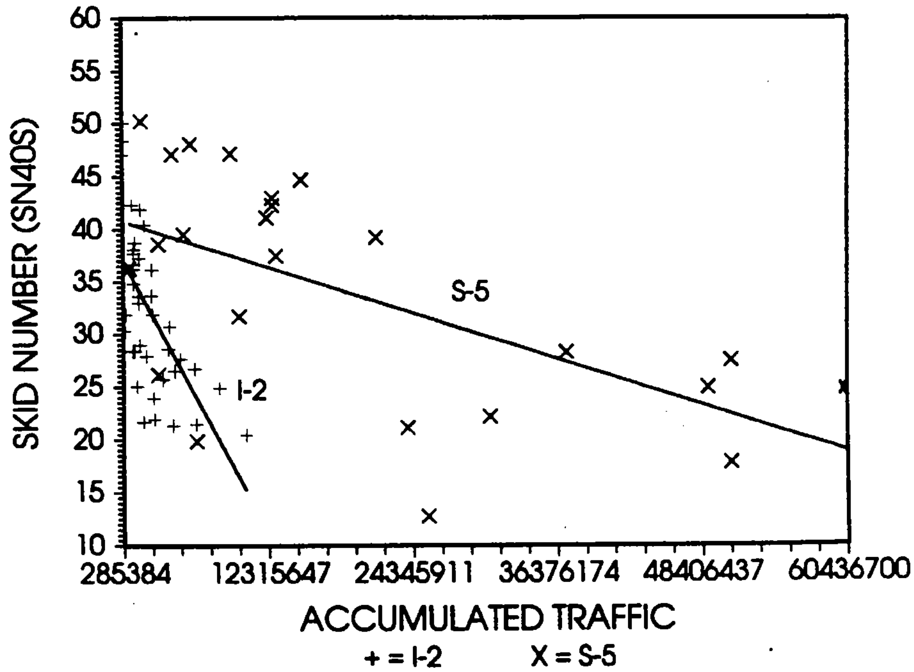

Figure 4. Skid numbers (SN40S) vs. accumulated traffic for I-2 and S-5 mixes containing Arch Marble aggregate

While the differences in the Arch Marble curves shown in Figure 4 were the most dramatic, in every case but one as AT increased the I-2 curve showed a greater downward slope than the S-5 curve. The lone exception was Valley Gravel, where the slope differences were insignificant. Even in cases where the initial I-2 SN40S values at low AT were higher than the S-5 values, the greater slope of the I-2 curve carried it to lower SN40S values as AT increased.

Using all of the individual I-2 and S-5 mix curves plotted for SN40S vs. AT for each aggregate type, SN40S values at 1 million, 4.4 million and 8.8 million vehicle passes were estimated. At one million vehicle passes I-2 mixes projected slightly higher SN40S values than S-5 mixes. As accumulated traffic increased to 4.4 million and 8.8 million, S-5 skid numbers assumed the higher values. These trends appear to indicate that during the early stages, I-2 mixes are more skid resistant than S-5 mixes. However, as the pavement ages beyond one million AT, S-5 mixes project higher skid numbers.

Pavement Macrotexture as Measured by the Sand Patch Method

Over the course of the study, 105 sand patch ASTM E965 tests were conducted, on pavements containing six lithologies (see Table 3) mostly in response to requests to investigate specific aggregates. Mean depths ranged from 0.49 mm (0.019 in) for Slate and Biotite Granite to 0.97 mm (0.038 in) for Fine Grained Granite. For situations requiring a high level of skid resistance, Salt (1976) recommended a minimum macrotexture depth of 1.00 mm (0.039 in).
Compared to Fine Grained Granite, the macrotextures exhibited by the other five aggregates are relatively low. Three of the five consistently ranked low in skid resistance (Table 3). Figure 5 illustrates the relationships between macrotexture depth and skid numbers for smooth and ribbed

tires for Aplite. Typically, the difference between the smooth and ribbed SN40 curves were found to decrease as macrotexture depth increases.

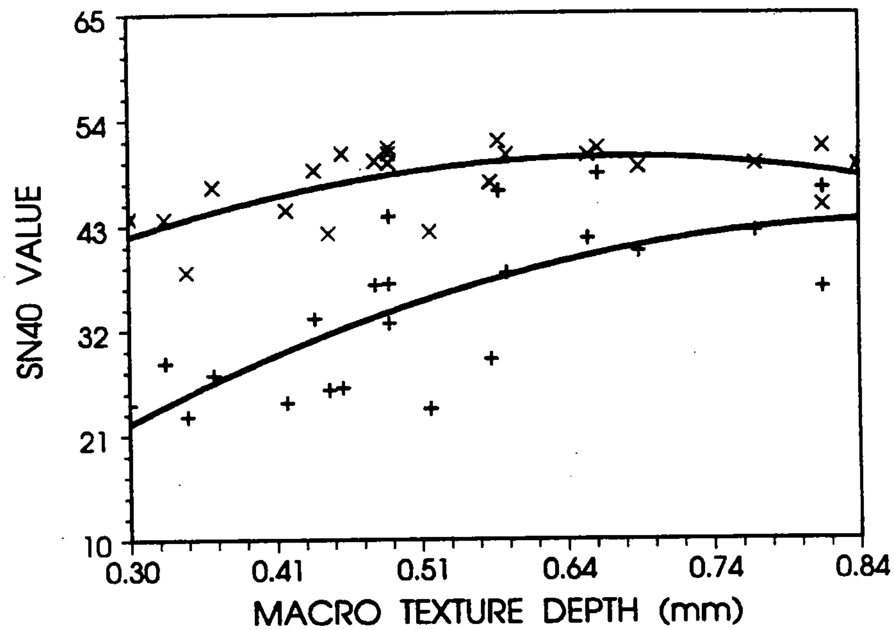

Figure 5. SN40 values vs. macrotexture depth for pavements containing Aplite aggregate. += smooth tire data. += ribbed tire data.

DISCUSSION

Skid Resistance of Various Aggregates

Table 3 shows clearly that certain aggregate lithologies tend to fall near the top of each ranking, indicating high relative skid resistance. Other groups consistently fall near the bottom, indicating relatively low skid resistance. Because of the high variability in the test population, the relative ranking in any one of these columns might be open to serious question. However, some aggregates consistently rank high or low.

Aggregates exhibiting generally high rank are Valley Gravel, Fine Grained Granite, Lovingston Granite, Coastal Gravels, and Diabase. Valley and Coastal Gravels are composed of a mixture of crushed and uncrushed quartz and quartzite gravels. The materials are hard and durable, showing little wear even under heavy traffic. While Fine Grained Granite and Lovingston Granite rank highest of the granites, Biotite Granite and Petersburg Granite also project relatively high SN40S values. The mixture of hard granular quartz and softer minerals produces differential wear and surface renewal in granites, which enhances skid resistance (Webb, 1970). Diabase is a very tough rock composed of intergrown feldspars and pyroxenes which resists wear under traffic.

Aggregates which consistently rank relatively low in skid resistance are Arch Marble, Triassic Hornfels, Slate, and Aplite. Greenstone is rather inconsistent, falling near the top of two columns and near the bottom of the remaining two columns.

SN40S data on the remaining eight aggregate groups tend to be distributed between the high and low members. These aggregates consistently exhibit levels of skid resistance near the mean for the whole test population. Included in this middle group are two granites (Biotite Granite and Petersburg Granite), three types of metamorphic rocks (Metavolcanics, Metagraywacke, and Undifferentiated Metamorphics), Gravel Blends, Antietam Quartzite, and Basalt.

The four aggregates projecting the lowest skid resistance exhibit some properties which might logically account for their relatively low tire-pavement friction values. Slate and Arch Marble are strongly foliated rocks, high in micas. Aggregates produced from the crushing of foliated rocks tend to assume flat, platy shapes with smooth, reflective faces. In addition, the Arch Marble contains high levels of calcite, a relatively soft mineral. Why the remaining two aggregates, Triassic Hornfels and Aplite, exhibit only fair skid resistance is less clear. Triassic Hornfels is a fine grained, dense, uniform rock and Aplite is composed predominately of feldspar. While feldspars are harder than calcite and micas, they are softer than quartz and may cleave under stress. Uniformity of hardness in the minerals of an aggregate, if the minerals are softer than quartz, may not be the optimum condition for maintaining a high level of skid resistance (Webb, 1970). The uniformity of the Aplite and the Triassic Hornfels may preclude surface renewal and make them susceptible to polishing if traffic is sufficiently heavy.

It appears that if Virginia is to consistently maintain high levels of wet accident safety in the face of increasing traffic, some LAVD limitations may be required for the use of Arch Marble, Aplite, Slate, and Triassic Hornfels.

Mix Design and Pavement Macrotexture

Comparison of the relative skid resistance of I-2 and S-5 mixes showed a more rapid loss of skid resistance for I-2 mixes than for S-5 mixes as accumulated traffic increased, for all aggregate types except Valley Gravel. This reduction was attributed to aggregate wear. In particular, large platy particles of Arch Marble and Slate in I-2 mixes tended to be oriented parallel to the pavement surface, resulting in low aggregate relief and smooth foliation or cleavage planes in the aggregate coming in contact with the tire. The results of these tests suggest that when platy aggregate is used, S-5 mixture would provide better long-term skid resistance than I-2.

Only a limited number of sand patch tests of pavement macrotexture were made, and these tests did not encompass all aggregate types. Consequently, findings from the sand patch tests are not conclusive, but it seems reasonable to hypothesize an association between the low macrotexture depth of Aplite, Arch Marble, Slate and Hornfels and their low skid resistance (Table 3). Again, logical explanations for this effect might be accelerated wear due to high contents of relatively soft minerals, or the preferred flat orientation of platy aggregate particles. Certainly, macrotexture appears to be a critical element in providing wet pavement skid resistance, and further research appears to be needed to design bituminous pavements to ensure greater macrotexture for the life of the pavement.

CONCLUSIONS

1. On the basis of field observations and laboratory analyses, the aggregates from Virginia's 57 producers of nonpolishing material are found to represent 18 different lithologies.

2. Skid test results for the total test population of 1,242 sites showed a mean SN40 of 36 and a standard error of 7.8 for smooth tires, and a mean SN40 of 47 with standard error of 5.2 for ribbed tires.

3. Mean values for accumulated traffic (AT) and lane average vehicles per day (LAVD) for the eighteen aggregate lithologies varied widely. AT ranged from 2.4 million for Slate to 9.9 million for Diabase. LAVD varied from 1,610 for Slate to 6,715 for Diabase. These large differences preclude simple comparisons of mean skid numbers (SN40S) for the different aggregate groups.

4. In an effort to rank the relative skid resistance of the 18 aggregates SN40S data were treated using four different methods. These were: 1) determining the SN40S value at each group mean minus 2 standard errors, 2) determining the LAVD value where a two standard error line projects to an SN40S of 20, 3) ranking the aggregate group T values from most positive to most negative through a multiple regression analysis incorporating the whole test population, and 4) ranking six of the aggregate types by multiple regression analysis where sand patch macrotexture data from 105 test sites were available. Based on these four methods of data treatment, five aggregates, Valley Gravel, Fine Grained Granite, Lovingston Granite, Coastal Plain Gravels, and Diabase, consistently ranked relatively high in skid resistance, while four aggregates, Arch Marble, Triassic Hornfels, Slate, and Aplite, ranked consistently low.

5. Only one lithology, the Arch Marble, showed a mean LAVD (2,819) higher than that projected at the intersection of the SN40S=20 line and the curve at two standard errors below the SN40S mean (1,975). This difference could mean that more than 2.5 percent of the pavements containing Arch Marble would show SN40S values below 20.

6. The two mix designs, I-2 and S-5, used most extensively in Virginia over the last two decades showed no overall statistical difference in SN40S values when the whole test population was considered.

7. When skid numbers (SN40S) for I-2 and S-5 mixes were plotted vs. accumulated traffic (AT) for each aggregate type, I-2 curves usually started at higher SN40S values than S-5 curves, but showed a greater negative slope. This indicates that the initial skid resistance of I-2 is higher but drops more rapidly as accumulated traffic increases, especially for platy aggregates. Consequently, when platy aggregates are used, S-5 mixtures could be expected to provide a higher level of long-term skid resistance than I-2 mixtures.

8. Macrotexture depth, as measured by the sand patch method, showed a higher correlation with skid number (SN40S) than any other factor investigated.

9. As macrotexture depth increased, the differences between smooth and ribbed tire skid numbers diminished. The finding that smooth tires are more sensitive at low macrotexture depth supports the use of SN40S values as a standard measure of skid resistance.

REFERENCES

1. Argawal, S. G., & Henry, J. J. (1980). Experimental investigation of the transient aspects of hydroplaning. *Transportation and Road Research Record,* 788, 15-22.
2. Finney, E. A., & Brown, M. G. (1959). *Relative skid resistance of pavement surfaces based on Michigan's experience.* First International Skid Prevention Conference Proceedings, Part 21, pp. 435-457.
3. Glendon, D. E. (1988). *Evolution of smooth vs. ribbed friction test tires as a means of measuring macrotexture of pavements.* (Report No. FHWA/IN/RD-89-2). West Lafayette, IN: Indiana Department of Highways, Division of Research.
4. Gray, J. E., & Renninger, F. A. (1960). Limestones with excellent nonskid properties: *Crushed Stone Journal*, 35, 6-11.
5. Henry, J. J. (1980). Use of blank and ribbed test tires for evaluating wet pavement friction. *Transportation Research Record,* 788, 1-6.
6. Henry, J. J., & Dahir, S. H. (1979). Effects of textures and aggregates that produce them on performance of bituminous surfaces. *Transportation Research Record*, 712, 44-50.
7. Henry, J. J. & Saito, K. (1981). Skid-resistance measurements with blank and ribbed tires and their relationship to pavement texture. *Transportation Research Record*, 946, 38-43.
8. Klein, K. M., & Brown, W. J. (1939). *Skid-resistant characteristics of Oregon pavement surfaces.* (Tech. Rept. No. 39-5). Oregon State Highway Dept.
9. Knill, D. G. (1959). Petrographical aspects of the polishing of natural roadstones. *Journal of Applied Chemistry*, 1, 28-35.
10. Kummer, H. W., & Meyer, W. E. (1967). *Tentative skid-resistance for main rural highways.* (National Cooperative Highway Research Program Report 37). Highway Research Board.
11. Leu, M. C., & Henry, J. J. (1978). Prediction of skid resistance as a function of speed from pavement texture measurements. *Transportation Research Record,* 666, 7-
12. Mahone, D. C. (1975). *An evaluation of the effects of tread depth, pavement texture, and water film thickness on skid number-speed gradients.* (Report No. VHTRC 75-R40). Charlottesville, VA: VHTRC.
13. Mahone, D. C., & Runkle, S. N. (1972). Pavement friction needs. *Highway Research Record*, 396, 1-11.
14. McLean, D. J., & Shergold, F. A. (1959). *The polishing of roadstones in relation to their selection for use in road surfaces.* First International Skid Resistance Conference Proceedings, Part 2, 497-506.
15. Moyer, R. A. (1959). *A review of the variables effecting pavement slipperiness.* First International Skid Prevention Conference Proceedings, Part 2, 411-433.

16. Moyer, R. A., & Shupe, J. W. (1951). *Roughness and skid resistance measurements of pavements in California.* Bulletin 37, Highway Research Board.

17. Mullen, W. G. (1974). Prediction of pavement skid resistance from laboratory tests. *Transportation Research Record*, 523, 40-50.
18. Nichols, F. P. (1959). *Further studies on skid resistance of Virginia pavements.* First International Skid Prevention Conference Proceedings, Part 2, 461-468.
19. Nichols, F. P. Jr., Dillard, J. H., & Alwood, R. L. (1956). *Skid resistant pavements in Virginia.* Bulletin 139, 35-59. Highway Research Board.
20. Runkel, S. N., & Mahone, D. C. (1977). *Relationships between skid numbers, paving materials and mix design, and accumulated traffic.* (Report No. VHTRC 77-R57). Charlottesville, VA: VHTRC.
21. Salt, G. F. (1976). Research on skid-resistance at the transport and road research laboratory (1927-1977). *Transportation Research Record*, 341, 1-10.
22. Shelburne, T. E., & Sheppe, R. L., (1948). *Skid resistance measurements of Virginia pavements.* Research Report 5-B. Highway Research Board.
23. Sherwood, W. C. (1959). *A study of the crystallization and mineral content of some Virginia limestones with possible relationship to their skid resistance performance.* Progress Report 1, Charlottesville: Virginia Highway Research Council.
24. Sherwood, W. C., & Mahone, D. C. (1970). Predetermining the polish resistance of limestone aggregates. *Highway Research Record,* 341, 1-10.
25. Shupe, J. W., & Lounsbury, R. W. (1959). *Polishing characteristics of mineral aggregates.* First International Skid Prevention Conference Proceedings, Part 2, 509-536.
26. Stephens, J. E., & Goetz, W. H. (1961). *Effects of aggregate factors on pavement friction.* Bulletin 302, 99. 1-17. Highway Research Board.
27. Stutzengerger, W. J., & Havens, J. H. (1958). *A study of the polishing characteristics of limestone and sandstone aggregates in regard to pavement slipperiness.* Bulletin 186, 58-81. Highway Research Board.
28. Virginia Department of Transportation. (1987). *Road and Bridge Specifications.* Richmond: VDOT.
29. Virginia Department of Transportation. (1991). *Road and Bridge Specifications.* Richmond: VDOT.
30. Webb, J. W. (1970). *The wearing characteristics of mineral aggregates in highway pavements.* Report No. 70-R7. Charlottesville: Virginia Highway Research Council.
31. Wombold, J. C., Henry, J. J., & Hegmon, R. R. (1986). Skid resistance of wet weather accident sites. In Pottinger & Yager (Eds.), *ASTM STP 929, the tire pavement interface,* 47-60. Philadelphia: ASTM.
32. Yandell, W. D., Tanerrananon, P., & Zankin, W. (1982). *Predicion of tire-road friction from surface and tread rubber properties.* ASTM STP 793. Philadelphia: ASTM.
33. Zoeppritz, H. P. (1976). An overview of European measuring methods and techniques. *Transportation Research Record*, 621, 75-82.

Grid-Based Model for Prediction of Debris Flow Susceptibility: Applied to the Appalachian Valley and Ridge, Spruce Run Mountain, Giles County, Virginia

Christopher L. Rupe and Kimbell L. Knight
crupe@runet.edu, klknight@runet.edu
Radford University
Radford, Virginia

ABSTRACT: Recent advances in Geographic Information Systems (GIS) have allowed the creation of better models for predicting the susceptibility of an area to natural hazards. The advantage of GIS in these types of applications is its ability to manipulate large amounts of data over large areas. This paper presents the use of ARC/INFO GRID software to create a model for predicting the susceptibility of 30 meter grid-cells to debris flows using information gathered by the investigators as well as information readily available through other sources. The study area is located in the Valley and Ridge physiographic province of Virginia and consists of folded and faulted sedimentary rocks of Paleozoic age. Spruce Run Mountain is a doubly plunging syncline that allows for evaluation of similar lithologies for different slope aspects. The model is loosely based on Level I Stability Analysis (LISA) software developed for forested uplands by the U.S. Department of Agriculture Forest Service. LISA uses the infinite slope equation, which can calculate factor of safety values for shallow surficial slope failure. Because LISA uses large irregularly shaped polygons, which result in imprecise values for its variables, it must use a complex Monte Carlo simulation technique to calculate probabilities of failure rather than actual factor of safety values. The model described here uses smaller, regularly spaced grid cells. The engineering properties of varying soil types, based on the Soil Conservation soil survey; and the slope morphology and hydrodynamic flow characteristics, based on the digital elevation model (DEM) of the study area are determined for each grid-cell. Each grid-cell is then evaluated independently in order to produce a relative factor of safety. The final product is a map delineating areas of higher susceptibility to debris flows, which can be useful to highway departments when evaluating slope stability for existing as well as proposed roads.

INTRODUCTION

Debris flows have long been a phenomenon associated with the western regions of the United States, including the Rocky Mountains and the Pacific Northwest. Furthermore, with the recent occurrences of extremely powerful El Niño weather patterns, the public has been reacquainted with the destructive power of this natural hazard. It has become almost commonplace to see houses and highways being destroyed by thick blankets of mud and boulders during periods of very heavy rainfall. However, it is not generally appreciated that similar scenes of destruction occur in the Appalachians of the Eastern United States.

We need only to look back a few years to see proof that the Appalachians are indeed susceptible to this type of erosion. Madison County, Virginia, fell victim to over

1,000 debris flows on June 27, 1995. This resulted from a severe storm, which produced as much as 30 inches of rain in some areas of the county (Morgan and others, 1997). There were also more than 1,000 slope movements recorded on the days of November 3-5, 1985, in the mountainous areas southeast of Elkins, West Virginia and north of Hot Springs, Virginia. This event was also a result of heavy rain (Jacobsen and others, 1989). And the most infamous event in the Appalachians occurred due to Hurricane Camille in 1969 with more than 1,000 debris flows contributing to heavy loss of life in Nelson County, Virginia (Gryta and others, 1989).

These Appalachian debris flows point out two major concerns for the people of the Appalachian Highlands throughout the Mid-Atlantic states. First of all, the factors leading up to major debris flow events are rare, but when they do happen, the damage to an area can be quite extensive. The second point is that debris flows can occur not only in the Blue Ridge physiographic province (Madison County, 1995 and Nelson County, 1969) but also in the Valley and Ridge, west of the Blue Ridge (Virginia and West Virginia, 1985).

Land-use planners and highway geologists in these regions need to be aware of areas that are susceptible to debris flows in order to make sound judgments as to the proper zoning of real estate or the alignment of highways. Other concerns may include major projects such as power line routing or landfill siting. All these activities require the delineation of areas that may be susceptible to debris flows. Consequently, debris flow susceptibility and hazard maps can be invaluable in making major decisions as to the use of land when such costly projects are being considered.

This paper describes a technique that shows promise to be able to successfully predict those areas in the Appalachians most susceptible to the shallow soil-bedrock interface slope failure that initiates most debris flows. This technique uses a grid-based Geographic Information System (GIS) to deductively incorporate readily available data such as soil maps and Digital Elevation Models (DEM) into the infinite slope stability equation. The results of an initial model that successfully predicts the debris flow susceptibility of Spruce Run Mountain in Giles County, Virginia, are described.

METHODS OF DEBRIS FLOW PREDICTION

The prediction of debris flows may include any or all of the following: susceptibility, hazard, vulnerability, or risk prediction. Debris flow susceptibility indicates the relative likelihood of a debris flow occurring in an area as opposed to somewhere else. Debris flow hazard indicates the probability of failure during a given period of time and requires a detailed chronology of previous flows. Debris flow vulnerability and risk relate more directly to the consequences to the entire area affected by a flow (Mejia-Navarro and others, 1994).

The method detailed in this paper can be used to predict the relative susceptibility an area has to being the focus or site of initiation of a debris flow. While the techniques used here may also be used as an important component in vulnerability and risk assessment, they predict only where a debris flow is likely to begin and not the path of destruction that it might follow.

Debris flow prediction is usually presented in the form of maps that display an area's susceptibility, hazard, vulnerability, or risk. A significant problem with constructing these types of maps is the variety and complexity of the spatial data required for their construction. For instance, the model used by this study to calculate the susceptibility of an area to a debris flow must handle ten potentially different variables.

Geographic Information Systems are computer hardware/software systems that excel at managing and analyzing many layers (or variables) of spatially related data. The advantages of using a GIS-based computer model in a debris flow study are numerous. Perhaps the most important advantage is that the analyst is able to handle the large amounts of data required for larger study areas while not having to sacrifice on the complexity of the mathematical algorithms required. Another advantage is that spatially related data (soil and geologic maps, digital elevation models) from many sources with varying map projections can be easily incorporated into the study. GIS also facilitates the repeat testing and readjustment of the model as new data or better algorithms are discovered.

Debris flow or landslide predictive modeling studies using GIS generally take one of two routes. Many investigations develop debris flow susceptibility algorithms inductively, based on those variables thought to be influential, such as slope, slope aspect, soil properties, geology, and hydrology (Gupta and Joshi, 1990; Carrara and others, 1991; Mejia-Navarro and others, 1994; Gao and Lo, 1995). Variables are statistically weighted based on where debris flows or landslides have been mapped. Other investigations begin deductively with mathematical slope stability models thought to represent the physical processes responsible for slope failure (Hammond and others, 1992; Jibson and others, 1998; Kohler, 1998).

STUDY AREA

The grid-cell debris flow susceptibility model is presently undergoing testing in the Valley and Ridge of southwestern Virginia by comparing sites predicted to be susceptible with sites where debris flows have occurred. Spruce Run Mountain in Giles County, Virginia, was an excellent candidate for the initial tests. Spruce Run Mountain is a small doubly plunging syncline held up by Silurian sandstones that circle the top of the mountain and is surrounded by Paleozoic carbonates and shales in the valleys. The uniformity of lithologies around the varying orientation or aspect of the mountain provides for a test of this possible factor. The mountain has also been carefully mapped previously for colluvium including debris flows and contains at least forty-four debris flow/fan like areas of varying size. There are also areas for comparison that are relatively free of debris flow/fans.

METHODOLOGY

The infinite slope equation has been used to predict debris flows successfully for some time by the U.S. Department of Agriculture, Forest Service, in the forms of deterministic (DLISA) and probabilistic (LISA) DOS-based computer models (Hammond and others, 1992; Kohler, 1998; *see* http://forest.moscowfsl.wsu.edu/4702/reports/biblio.html for annotated bibliography). DLISA and LISA are menu-driven and require the manual input of data for each area calculated. Probably due to the needs of the Forest Service for assessing the slope stability of burned or cleared tracts of woodland, DLISA and LISA look at generally large, irregular polygonal areas.

The infinite slope equation used in DLISA, LISA and for this study is:

$$\text{Factor of Safety} = \frac{C_r + C_s' + \cos^2\alpha\,[q_o + \gamma(D-D_w) + (\gamma_{sat}-\gamma_w)D_w]\tan\phi'}{\sin\alpha\cos\alpha[\,q_o + \gamma(D-D_w) + \gamma_{sat}D_w]}$$

where: C_r = tree root strength, lb/ft^2
C_s' = effective soil cohesion, lb/ft^2
α = slope of the ground surface, degrees
q_o = tree surcharge, lb/ft^2
γ = moist soil unit weight, lb/ft^3
D = total soil depth-vertical, ft
D_w = saturated soil depth-vertical, ft
γ_{sat} = saturated soil unit weight, lb/ ft^3
γ_w = unit weight of water, lb/ ft^3
ϕ' = effective angle of internal friction, degrees

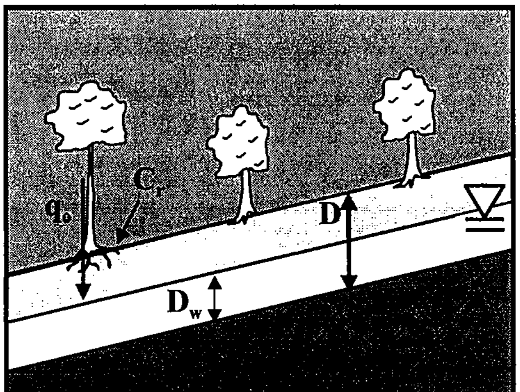

(after Hammond and others, 1992)

Figure 1. Diagram of Soil Surface above weathered bedrock with variables from factor of safety equation.

This version of the infinite slope equation includes factors such as tree root strength and tree surcharge that often play important roles in the stability of slopes in the forested mountains of the Appalachians (Figure 1). The most critical variables determining stability within the equation are ground slope and the ratio of D_w/D (Hammond and others, 1992). At least two deficiencies exist in LISA's use of the infinite slope model. The first is the lack of variables relating to a slope's aspect or spatial orientation. A mountain's aspect may play an important role in determining the varying orographic effects of the rainfall responsible for triggering debris flows. Secondly, topography will have an impact on D_w/D values. Concave topography tends to funnel and concentrate water during a rain event, increasing D_w/D values, which will reduce stability within channels. Convex topography sheds water, decreasing D_w/D, which will increase stability on ridges. LISA assumes a uniform range of values for a polygon no matter what the topographic variation within the polygon.

In theory, if values for all the variables are well know, the infinite slope model can be used with DLISA to predict the stability of the shallow surficial material where most debris flows are initiated. In practice, most of the variables for large irregular tracts of land are only known imprecisely and DLISA is not intended to be used to calculate the factor of safety. Its main use is to back calculate the other variables in the equation from an assumed factor of safety value. LISA deals with this uncertainty by using not a single value but the predicted probability distribution functions of each variable within a polygon to calculate 1,000 randomly derived factor of safety values, from which the probability of failure can be calculated.

This study uses the infinite slope stability equation to deductively calculate the relative factor of safety of regularly spaced 30 meter grid-cells. This grid-cell based model is not intended to predict the actual factor of safety of a location, but it may be used to suggest which areas will be more prone to failure under extreme conditions such as a major rainfall event. The advantages of using grid-cells as opposed to the generally much larger polygons used by LISA include the increased certainty of the values of the various variables within the smaller grid cells. For instance, LISA must use a probability density function to express the wide range in α, the slope of the ground surface, for its large irregular polygons. On the other hand, the technique described here uses a 30 meter DEM available from the United States Geological Survey to calculate the slope for each 30 meter grid-cell much more precisely. As a result, debris flow susceptibility has been successfully predicted without the need for probability density functions and Monte Carlo simulations. In addition, using a GIS with grid-cell capabilities such as ESRI's ARC/INFO allows for the automatic input of entire layers of values, such as an entire grid of soil attributes, without the need for the polygon-by-polygon manual input required by LISA.

The grid-based debris flow susceptibility model developed here (Figure 2) makes use of two data sources often available without cost, DEM's and soils maps. Digital Elevation Models are available from the United States Geological Survey at a number of resolutions for most areas of the United States and may be downloaded from the Internet. Most grid-based GIS have a function that easily converts DEM's into ground slope α values. ARC/INFO's GRID also has a set of hydrology modeling functions that provide for the more realistic modeling of the topographical effects on D_w/D.

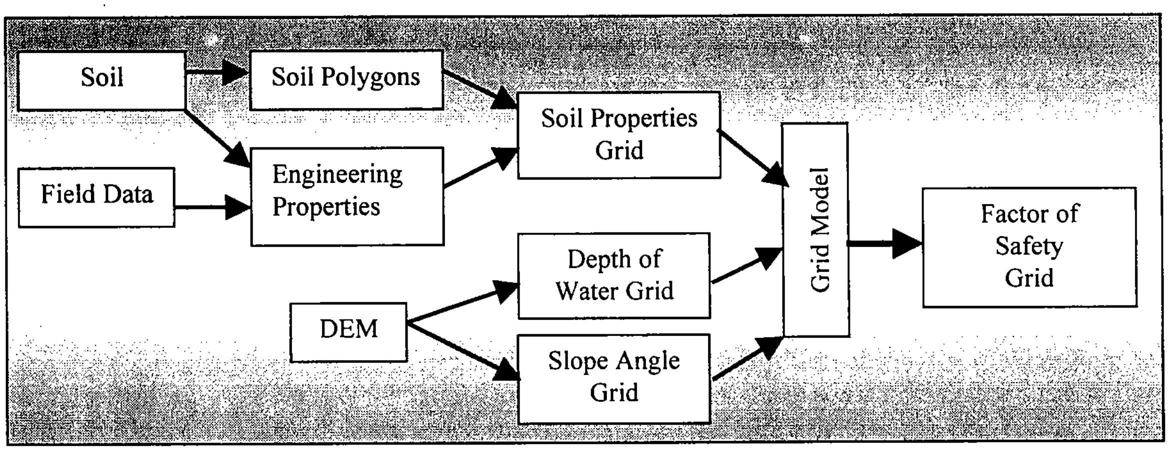

Figure 2. Flow chart of modeling process.

Many areas like Virginia have soil reports available from the United States Department of Agriculture (USDA, 1985). Maps included with these reports generally consist of soil polygons layered on top of aerial photographs, which can be rectified into the same projection as the DEM's. Soil polygons include a number of attributes which can then be used to obtain reasonable values for C_s', ϕ', γ_{sat}, D, and γ with the help of tables contained in the LISA documentation (Hammond and others, 1992). Fieldwork can of course be used to refine this data set.

ARC/INFO's GRID package contains a powerful algorithm writing routine that was then used to combine the separate grid-cell layers for each of the variables into the infinite slope equation to calculate the factor of safety. The factors of safety values calculated in this fashion are not meant to be taken literally. Most debris flows occur during extreme rain events where D_w/ D undergoes significant changes related to the topographic position of each grid-cell. Although the model used here accounts for some of the topographic variation in D_w/ D values and probably reflects the relative values for each grid-cell fairly accurately, it does not calculate values based on actual expected rainfall amounts and rainfall rates. However, by mapping only the relative factor of safety, this model should show those grid-cells most likely to exhibit slope failure during a given rain event.

RESULTS

The various soil types within the study area are represented in the Soil Conservation Service Soil Survey by polygons drawn over the aerial photograph mosaic of the study area. These polygons were digitized and transformed into real world coordinates as seen in Figure 3. The polygon coverage was then converted to a 30 meter grid of cells representing the soil types as well as their respective attributes. Each cell then contains all of the values for the soil that it represents.

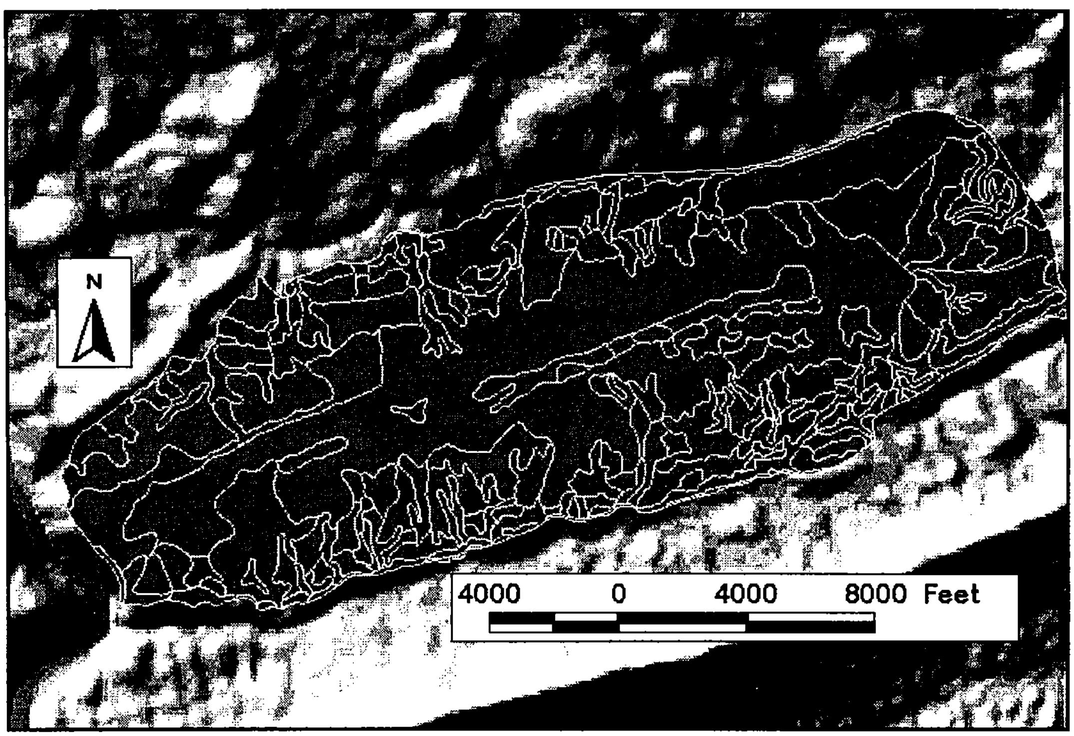

Figure 3. ARC/INFO polygon coverage of study area. Each polygon delineates areas digitized from the Soil Conservation Service Soil Survey.

The DEM is also a 30 meter grid with each cell containing a value representative of that area's elevation above mean sea level. This grid was used to model the slope angle of each grid cell. ARC/INFO has a built-in routine that calculates the slope angle for each cell. This gives each cell an α value for use in the infinite slope equation.

Additionally, the DEM was used in determining values for the depth of groundwater for each grid cell. There is a function in ARC/INFO that allows the calculation of the number of cells that would drain into each cell. The cells with higher values are given higher values of groundwater depth. The initial conditions of the model were set at a water content of 20%. This value was then adjusted according to its flow accumulation up to a maximum value of 100%, which would represent saturated conditions and the initiation of sheet runoff.

Figure 4 is a grid representing the ratio of the saturated soil depth to the total soil depth. It can be seen here that the model is giving grid cells positioned closer to the natural surface drainage higher values of saturated soil depth. This allows cells within the same soil polygon to have varying values for hydrological conditions and more realistically models the distribution of water in the phreatic zone during times of heavy rainfall. Areas on a slope that are subject to elevated pore pressures can now be effectively evaluated within the infinite slope equation. Previous models of this type would consider each polygon or terrain unit to have the same hydrological properties regardless of spatial position.

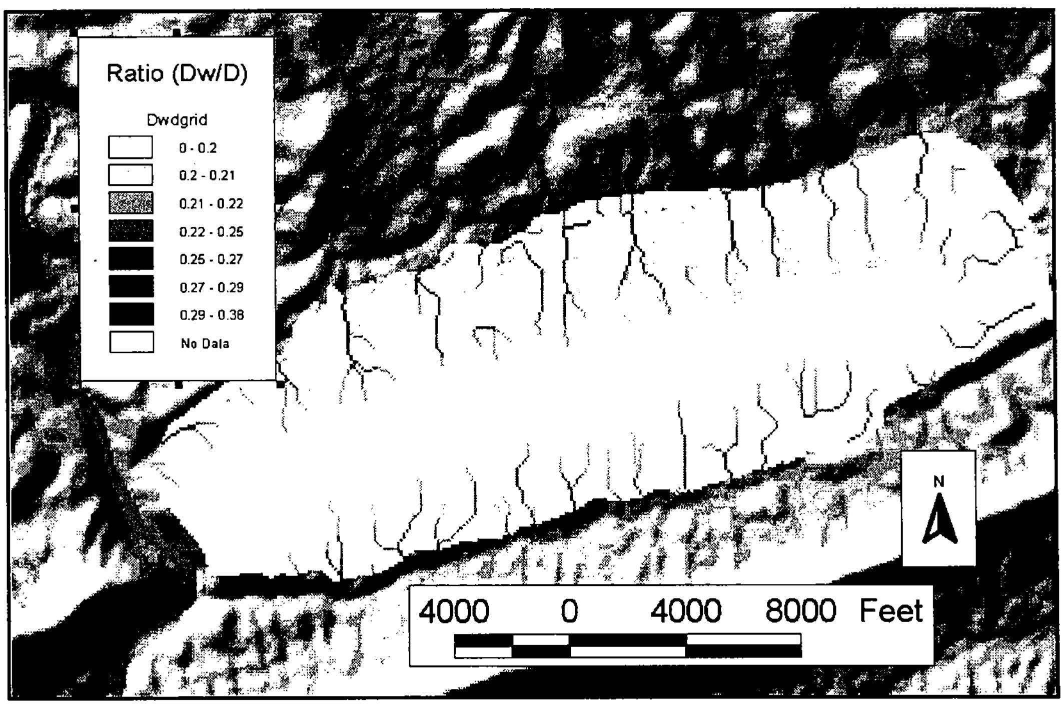

Figure 4. Grid of the ratio between the saturated soil depth and total soil depth.

The grids for water depth and soil properties were then incorporated into the grid-based model along with the slope grid. The model output is a 30 meter grid containing the calculated factor of safety for each grid cell (Figure 5). Again, it should be stated that

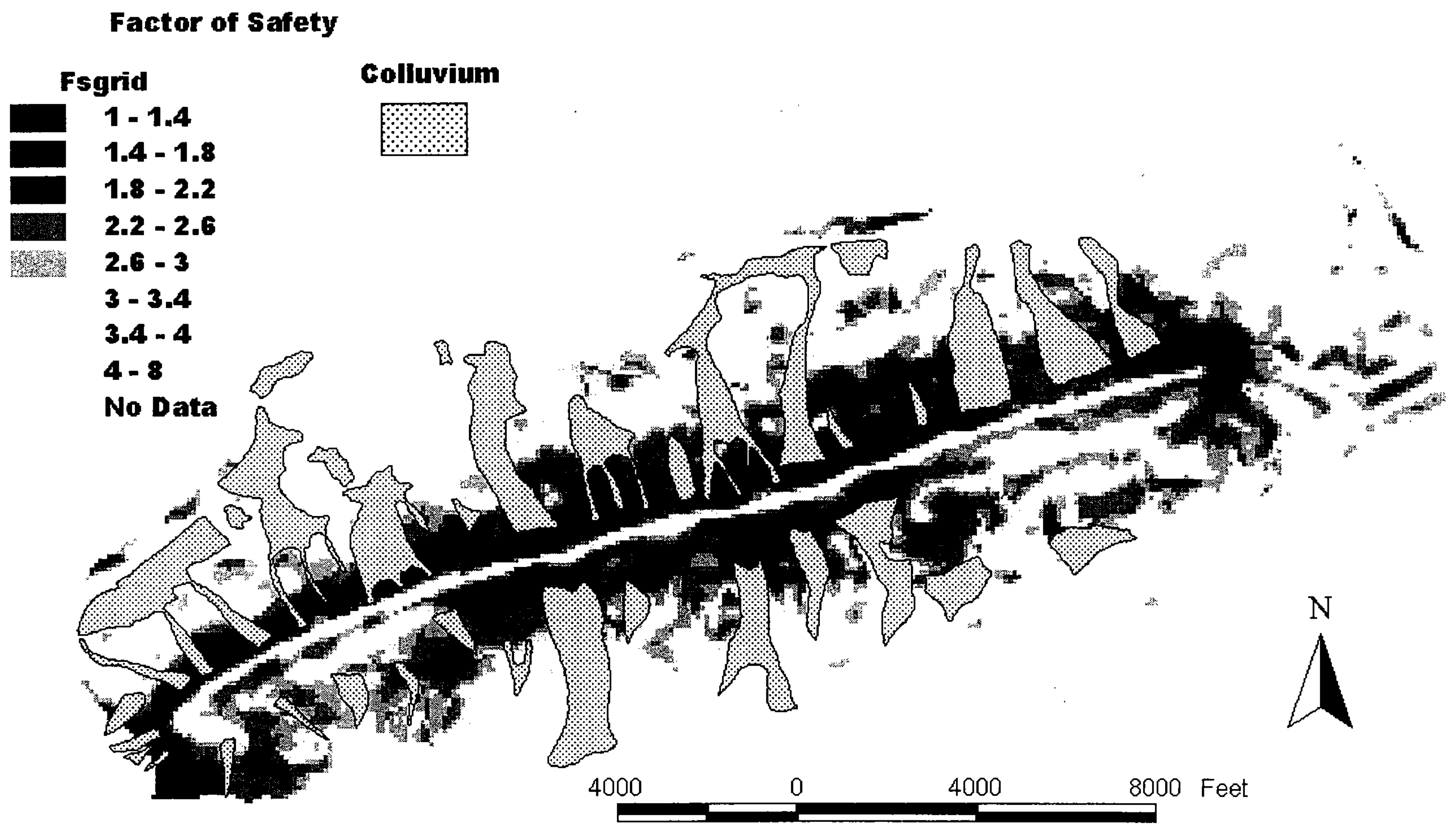

Figure 5. Model output of values for factor of safety with mapped colluvium and fan deposits.

these values should be evaluated relative to the other cells in the area. The areas with the lower factor of safety values are expected to be less stable than those areas with relatively higher values. Consequently, if a debris flow were to occur it is more likely that it would initiate within an area having a lower factor of safety.

The factor of safety grid was then evaluated against the areas previously mapped as colluvium and fan deposits on the geologic map of Giles County (Schultz and others, 1986). There is a correlation between the areas that were designated as less stable and the colluvium (Figure 5). Also, the areas that were relatively more stable generally matched up with areas where no colluvium was mapped. This is a promising sign when considering the fact that landslide inventories have been used in the past to evaluate the performance of a susceptibility model (Carrara and others, 1991).

As with any computer model, the proper background is essential to the correct interpretation of the results. The complex processes involved in the occurrence of debris flows are not fully understood, therefore it is expected that any model will have limitations that should be understood by the operator. The results of the initial run yielded no cells that were determined to be unstable. When considering the study area involved, these results are reasonable, as no debris flows have been recorded in this area in recent times.

There are several factors that make this model attractive. First of all, it is based on an algorithm that has proven to be effective in evaluating slope stability. The LISA program has been used for almost a decade in these types of projects (Koler, 1998). In addition, the grid-based model gives a more realistic evaluation of a slope while using data that is readily available and easily obtained. Finally, planning commissions and highway departments can use the model for initial studies of debris flow susceptibility over larger areas in less time and at lower cost.

REFERENCES

Carrara, A., Cardinali, M., Detti, R., Guzzetti, F., Pasqui, V., and Reichenbach, P., 1991, GIS techniques and statistical models in evaluating landslide hazard: *Earth Surface Processes and Landforms*, Vol. 16, pp. 427-445.

Gao, J. and Lo, C.P., 1995, Micro-scale modelling of terrain susceptibility to landsliding from a DEM: a GIS approach: *Geocarto International*, Vol. 10, No. 4, pp. 15-30.

Gupta, R.P. and Joshi, B.C., 1990, Landslide hazard zoning using the GIS approach-A case study from the Ramganga Catchment, Himalayas: *Engineering Geology*, Vol. 28, pp. 119-131.

Gryta, J.J., and Bartholomew, M.J., 1989, Factors influencing the distributions of debris avalanches associated with the 1969 Hurricane Camille in Nelson County, VA: *Geological Society of America Special Paper 236*, pp. 15-28.

Hammond, C.; Hall, D.E.; Miller, S.; and Swetik, P., 1992, *Level I Stability Analysis (LISA) Documentation for Version 2.0*: U.S. Department of Agriculture, Forest Service, Intermountain Research Station; General Technical Report INT-285, Ogden, UT, 190 p.

Jacobson, R.B., Cron, E.D., and McGeehin, J.P., 1989, Slope movements triggered by heavy rainfall, November 3-5, 1985, in Virginia and West Virginia, U.S.A.: *Geological Society of America Special Paper 236*, pp. 1-13.

Jibson, R.W., Harp, E.L., and Michael, J.A., 1998, A method for producing digital probabilistic seismic landslide hazard maps: an example from the Los Angeles, California area: *U.S. Geological Survey Open-File Report 98-113*, 17 p.

Koler, T. E., 1998, Evaluating slope stability in forest uplands with deterministic and probabilistic models: *Environmental & Engineering Geoscience*, Vol. IV, No. 2, pp. 185-194.

Mejia-Navarro, M., Wohl, E.E., and Oaks, S.D., 1994, Geological hazards, vulnerability, and risk assessment using GIS: model for Glenwood Springs, Colorado: *Geomorphology*, Vol. 10, pp. 331-354.

Morgan, B.A., Wieczorek, G.F., Cambell, R.H., and Gori, P.L., 1997, Debris-flow hazards in areas affected by the June 27, 1995 storm in Madison County, VA: *U.S. Geological Survey Open-File Report 97-438*, 14p.

Schultz, A.P., Stanley, C.P., Gathright, T.M.II, Rader, E.K., Bartholomew, S.E., Lewis, S.E., and Evans, N.H., 1986, Geologic Map of Giles County, VA.: Virginia Division of Mineral Resources Pulication 69, 1 plate, scale 1:50,000

United States Department of Agriculture, 1985, Soil survey of Giles County, Virginia; southern and central parts: Soil Conservation Service, United States Department of Agriculture, 136p

Evaluation of a Suspected Ancient Mass Movement Using Electrical Resistivity

W. T. Dean, ATS International, Inc., Christiansburg, VA
C. F. Watts, Institute for Engineering Geoscience, Radford University, Radford, VA
W. J. Seaton, ATS International, Inc., Christiansburg, VA

ABSTRACT

The Virginia Department of Transportation (VDOT) has proposed new locations for U.S. Routes 29 and 460 near Lynchburg, Virginia. The proposed routes will require numerous bridge piers for the crossing over Little Opossum Creek near Lynchburg, Virginia. Several of the proposed bridge piers are located on what has been identified by some as an area of ancient mass movement.

Stereoscopic analyses of aerial photographs and observations of surficial colluvial soils revealed the presence of the possible mass movement on the west side of Little Opossum Creek. At that location, the creek bends sharply around the fan-shaped feature in an otherwise linear stretch of creek bed. This suggests a mass movement that filled the former stream channel deflecting the stream around the toe. The deflection resulted in greater erosion and steepening of the eastern bank, which in turn caused several younger landslides on the east side of the stream visible as scarps on the air photographs.

Numerous test borings were conducted over the feature by VDOT contractors, most of which encountered auger refusal at depths of approximately 10 meters. Only two borings were advanced to a greater depth of 23 meters before encountering refusal. The shallow auger refusal in most of the borings was interpreted by other parties involved with the project to indicate shallow bedrock beneath the colluvial soils and not evidence of mass movement.

A limited electrical resistivity survey of one line was conducted gratis at the site to help evaluate whether the auger refusal was the result of competent in-situ bedrock or the result of transported rock blocks and slabs resting within an area of ancient mass movement. Electrical resistivity defines the characteristic of a material to limit or resist the flow of an electric current. Changes in resistivity can be used to determine changes in lithology such as stratigraphic contacts. The resistivity profile was conducted trending directly east-west through the locations of four previous borings. The profile extended from the bank of the creek over the crest of the fan and into a north-south trending draw. The profile was approximately 162 meters long. A uniform electrode spacing of 6 meters was applied to a dipole-dipole array.

The results from the resistivity profile reveal the bedrock over the eastern portion of the feature and exposed near the creek to have a resistivity value of approximately 5000 ohm-meters. The data indicate that a significant resistivity boundary, marked below by these 5000 ohm-meter readings and above by lesser resistivity values, dips slightly westward from the creek over the eastern 60 meters of the profile. The dip of the boundary then increases sharply to the west, passing below the depth of measurement approximately 70 meters west of the creek bank. The western 90 meters of the profile show resistivity values that are generally less than 2000 ohm-meters, which is often indicative of highly fractured and weathered rock or soil. This

interpretation of the resistivity data suggests that only the two deepest borings actually encountered bedrock, and that the bedrock resides at a much greater depth than suggested by the remaining boring data. Hence, the data provide evidence that the feature is the result of mass movement, perhaps a rock block slide.

An alternative hypothesis has been suggested in which the lower resistivity values on the west side may be indicative of a fault zone. The low values could result from the higher porosities and generally weak rock conditions caused by shearing and imbrication of a rock mass during faulting. Additional resistivity survey lines are required to further clarify this issue.

INTRODUCTION

Stereoscopic analyses of aerial photographs and observations of surficial colluvial soils revealed the presence of a possible large mass movement located on the west side of Little Opossum Creek near Lynchburg, Virginia. At that location, the creek bends sharply around a fan-shaped feature in an otherwise linear stretch of creek bed (Figure 1). This suggests that the mass movement filled the former stream channel deflecting the stream around the toe. The deflection resulted in greater erosion and steepening of the eastern bank, which in turn caused several younger landslides on the east side of the stream visible as scarps on the aerial photographs (Watts and Whisonant, 1998).

Numerous test borings were conducted over the feature by the Robert B. Balter Company (Balter), most of which encountered auger refusal at depths of approximately 10 meters. Only two borings in the vicinity of B-5 were advanced to depths as great as 23 meters before encountering refusal. The shallow auger refusal in most of the borings was interpreted by other parties involved with the project to indicate shallow bedrock beneath the colluvial soils, which would be inconsistent with a large colluvial mass movement at the site.

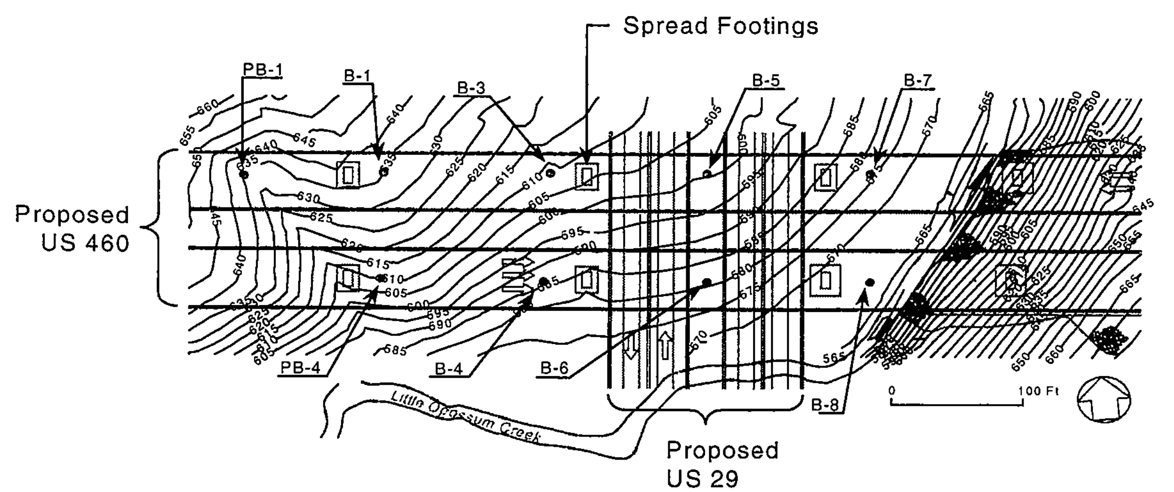

Figure 1. Locations of new proposed highway routes, proposed spread footings, and test borings on the suspected mass movement feature.

SITE GEOLOGY

The site is located in the western Piedmont province of the Appalachian Mountains. The bedrock observed in the creek bed is of the Candler Formation. The Candler Formation is a foliated dark gray to greenish gray phyllite and schist composed of quartz, muscovite, chlorite, and chloritoid. The Candler Formation occasionally also exhibits quartzite and marble layers. In addition, numerous hydrothermal quartz veins can be observed.

The Candler Formation, in the vicinity of the site, has been intensely sheared within a major Appalachian tectonic zone, the Bowens Creek fault. The Bowens Creek fault is mapped immediately east of the of the ridge line that lies east of Little Opossum Creek (Henika, 1997). The bridge crossing is located within the shear zone of the Bowens Creek fault. The fault and its associated shear zone have a trend of approximately north 50 degrees east. Because of the intense deformation associated with Bowens Creek fault, the Candler Formation at the site is a mylonite, a sheared and pulverized metamorphic rock with a strongly lineated mineral fabric.

ELECTRICAL RESISTIVITY SURVEY

METHODOLOGY

Electrical resistivity is a medium property that defines the characteristic of a material to limit or resist the flow of an electrical current. The flow of electric current usually occurs not within the earth materials themselves, but through the water that exists in soil pores and rock fractures. Therefore, the primary factors influencing the resistivity of materials include grain size, porosity, clay content, water saturation, and the ionic strength of the pore water. Electrical resistivity provides high-density data that reveals subsurface features such as the soil-bedrock interface, water table, geologic structure, and voids.

Resistivity surveys are conducted by inducing a current into the ground between two electrodes, and measuring the potential at other electrodes (Figure 2). Numerous configurations of electrode placement are commonly employed, each with unique data characteristics. By convention and for data handling purposes, the current electrodes are identified as B and A, and the potential electrodes are defined as M and N.

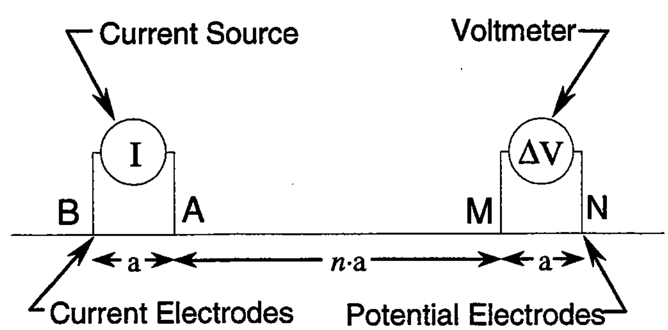

Figure 2. Schematic diagram of the dipole-dipole array.

The configuration utilized for this study is the dipole-dipole array (Figure 2). A current is applied to two adjacent electrodes positioned a predetermined distance apart (distance a). The voltage across two other electrodes is measured simultaneously with the applied current. The two sets of electrodes are always spaced distance a apart and the distance between the current and voltage electrodes is always a multiple of a ($n \cdot a$). As the value of n increases and the electrodes are moved farther apart, the deeper the sampling depth of the resistivity.

FIELD APPLICATION

An electrical resistivity survey was conducted to identify the soil-bedrock interface at the site. Resistivity data were collected over a profile by utilizing a multi-electrode system consisting of 28 electrodes connected by a multi-conductor cable. Electrode spacing was uniform at 6 meters. Measurements were initiated at one end of the line and incrementally moved through the electrodes until readings had been taken at every position along the line. The value of n was then increased to add additional resistivity readings at greater depths in the subsurface.

One resistivity survey line was applied to the site, trending directly east-west from the creek bank over the crest of the fan-shaped feature and into a small north-south trending draw (Figure 3). The profile passes through Balter borings B-1, B-3, B-5, and B-7 instead of trending northwest through the axis of the feature. This orientation was chosen so that the boring data could provide control to the interpretation of the resistivity, and for direct comparison of the resistivity results to the boring logs.

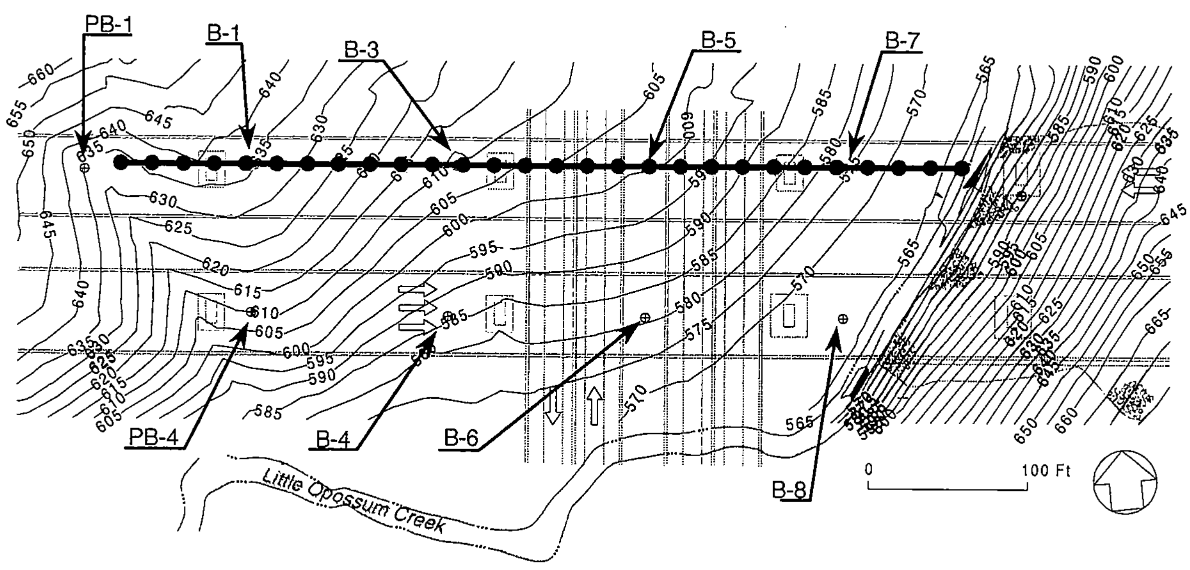

Figure 3. Location of the resistivity profile line applied to the site, dots represent electrodes.

DATA INTERPRETATION

Using the apparent resistivities for this profile, linear inversion techniques were applied to the data. Linear inversion modeling fits the measured data to an earth model. The inversion modeling then requires calculating apparent resistivity from the earth model for comparison to the measured data. If the comparison is within specified limits, the earth model can be accepted as an approximation of subsurface conditions. The root mean squared error (RMS error) between the measured and calculated apparent resistivities for the profile was 0.19. Details of the inversion process may be found in Loke and Barker (1996).

The results from the resistivity profile and the borings confirm the presence of the surficial colluvial deposit. Furthermore, bedrock exposed in and near the creek exhibit resistivity values of 5000 ohm-meters. A significant resistivity boundary, marked by these 5000 ohm-meter readings below and lesser values above, dips slightly westward from the creek over the eastern 60 meters of the profile. The dip of the boundary then increases sharply to the west, passing below the depth of measurement approximately 70 meters west of the creek bank. The western 90 meters of the profile show resistivity values that are generally less than 2000 ohm-meters, which is indicative of fractured or highly weathered rock or soil. These results imply that only the two deepest borings, at B-5, actually encountered bedrock, and that the bedrock resides at a greater depth than suggested by the remaining boring data. Hence, the resistivity data provide evidence that the feature is the result of mass movement, perhaps a rock block slide.

An alternative hypothesis has been suggested in which the lower resistivity values on the west side may be indicative of a fault zone. The low values could result from the higher porosities and generally weak rock conditions caused by shearing and imbrication of a rock mass during faulting. Additional resistivity survey lines are required to further clarify this issue.

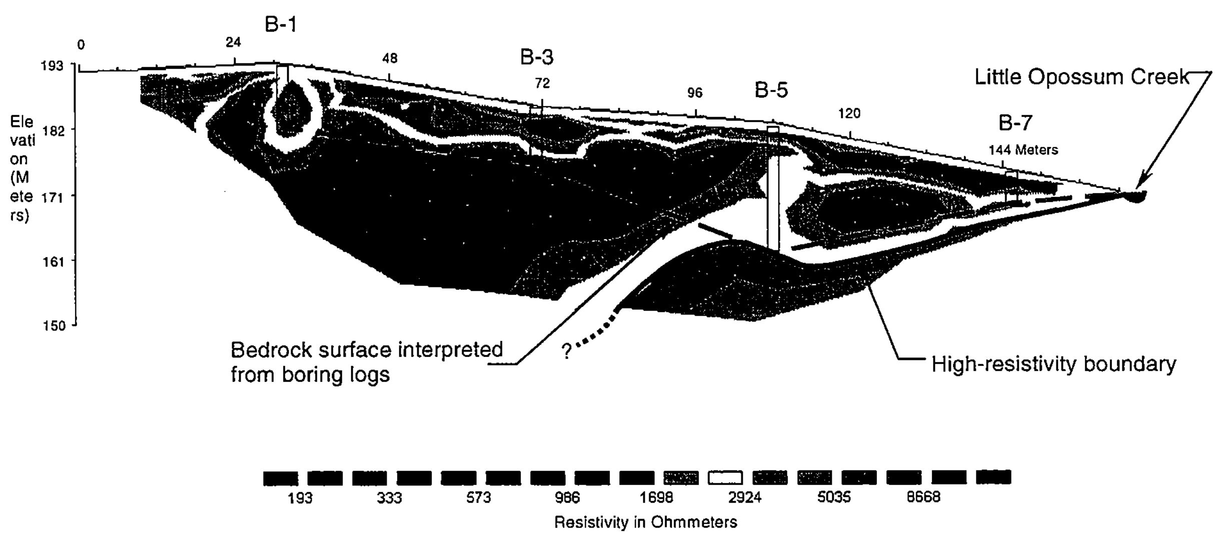

Figure 4. Resistivity profile comparing the soil-bedrock interface interpreted from the boring logs to the high-resistivity boundary.

CONCLUSIONS

Electrical resistivity is an emerging technology for investigating subsurface conditions. At Little Opossum Creek near Lynchburg, Virginia, the technology was applied to evaluate subsurface materials in an attempt to ascertain whether auger refusal was the result of competent in-situ bedrock or the result of transported rock blocks and slabs resting within an area of ancient mass movement. The electrical resistivity imaging provided evidence that the study area represents an area of mass movement. A second hypothesis has been suggested in which the overlying low resistivity values may be indicative of a fault zone. In that a limited electrical resistivity survey of only one line was conducted gratis, where three or four lines would normally be utilized, additional resistivity lines are needed to more adequately map the shape and extent of the feature.

REFERENCES

Henika, W.S., 1997. *Geologic Map of the Roanoke 30 X 60 Minute Quadrangle*, Virginia Division of Mineral Resources, Charlottesville, Virginia.

Loke, M.H., and R.D. Barker, 1996. *Rapid least-squares inversion of apparent resistivity pseudosections by a quasi-Newton method*, Geophysical Prospecting, Vol. 44, No. 1, Pages 131-152.

Watts, C.F., and R.C. Whisonant, 1998. *Slope stability study, Rt. 460 and Rt. 29 bridge sites over Little Opossum Creek*, Institute for Engineering Geosciences, Department of Geology, Radford University, Radford, Virginia.

A RECONNAISSANCE SURVEY OF HAZARD POTENTIAL OF SLOPE MOVEMENTS ALONG THE KARAKORAM HIGHWAY NORTHEASTERN PAKISTAN

Abdul Shakoor
Department of Geology, Kent State University, Kent, Ohio 44242

ABSTRACT

The Karakoram Highway, known as the world's highest and the most difficult road ever built, is a 500 mile (800 km) long road that links Islamabad, the capital of Pakistan, to the Xinjiang Province in China. It took 25,000 workers nearly 20 years to construct the Karakoram Highway which cuts across three major ranges including some of the world's highest mountains, and ascends from an elevation of 5000 ft (1515 m) near Thakot to over 16,000 ft (4800 m) near Khunjerab Pass at the Chinese border. Twenty-nine million cubic yards of rock had to be moved during the construction phase of this highway which first runs along the Indus River from Thahkot to Gilgit and then along the Hunza River from Gilgit to the Chinese border.

Landslides and other forms of slope failure have been the most serious problem along the Karakoram Highway both during and after its construction. Over 1000 people died during the construction of this road, mostly due to landslides and rock falls. Since its opening to heavy traffic in1979, it has seldom been free from obstruction caused by landslides, many of which resulted in fatal accidents. The presence of a large variety of highly-jointed rock types, loosely deposited glacial sediments, extremely high and steep slopes, melt water from glaciers, poor construction and maintenance methods, and occasional occurrence of large earthquakes are the important factors that contribute to slope failures along the Karakoram Highway. Rock falls, plane failures, wedge failures, toppling, slumps, debris slides, debris flows, and mudflows are all common along the highway. The largest and the most devastating failures, however, occur in the glacial deposits.

INTRODUCTION

This paper briefly reviews the various types of slope movements that affect the Karakoram Highway in northeastern Pakistan. It also evaluates the hazard potential of these movements, especially the very large failures that occur in the glacial material. The paper is based on a reconnaissance survey that was undertaken to evaluate the problem of slope instability in general and, therefore, stability of individual sites is not discussed.

The Karakoram Highway is a 500-mile (800-km) long road that links Islamabad, the capital of Pakistan, to the Xinjiang Province in China. It basically follows the old Silk Route to China from west that consisted of a footpath linked together with rope bridges. The highway first runs along the Indus River from Thakot to the well-known town of Gilgit, and then along the Hunza River to Khunjerab Pass at the Chinese border.

Pakistan's army engineers initiated the construction of the Karakoram Highway along the Silk Route in 1959. In 1965, China offered to help and started construction from their border. At one time, there were as many as 10,000 Chinese working beside

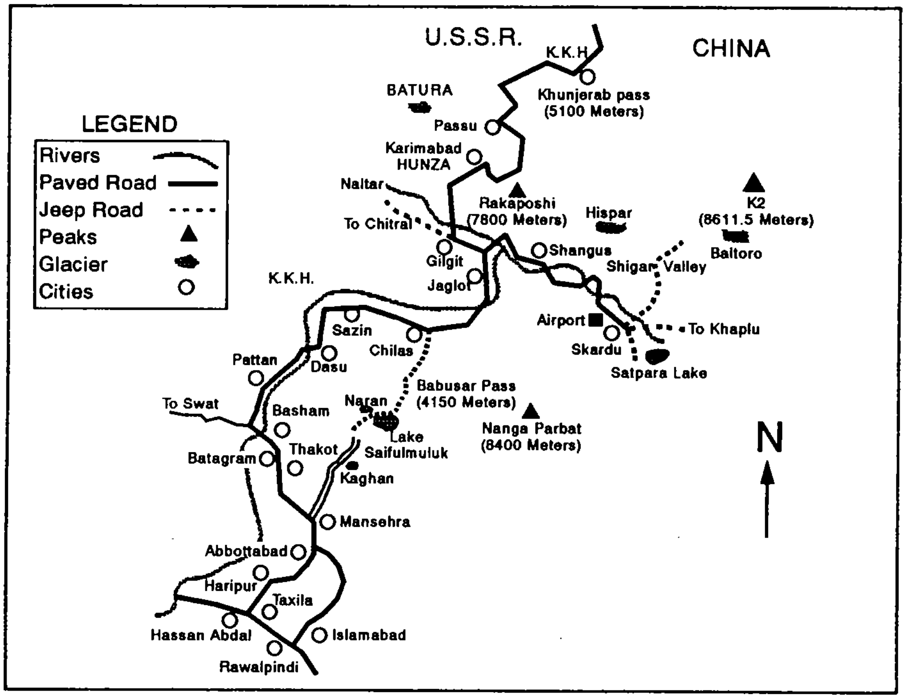

Figure 1: Location of the Karakoram Highway, northeast Pakistan.

15,000 Pakistanis (Wood, 1981). It took nearly 20 years to construct this highest and the most difficult road ever built. Twenty-nine million cubic yards (22 million cubic meters) of rock had to be shifted during the construction stage (Wood, 1981). The highway cuts across the three major ranges: the Himalayas, the Karakoram, and the Hindukush. The completed highway ascends from an elevation of 5000-ft (1515 m) near Thakot, to over 16,000-ft (4800 m) near Khunjerab pass at the Chinese border. The highway is a two-lane, heavy traffic road with a pavement width of 20-ft (6m). The gradient is 5 percent and the 70 bridges along its length are 24 ft (7.3 m) wide (Civil Engineering, April, 1979).

THE LANDSLIDE PROBLEM

Landslides and other forms of slope failure have been the most serious problem along the Karakoram Highway both during and after its construction. Over 1000 people died during the construction phase of this road, mostly due to landslides and rock falls (Wood, 1981). Since its opening in 1979 to heavy traffic, it has experienced numerous slope failures, many of which resulted in fatal accidents. At present, there are a number of active slides along the highway some of which are over 4 miles (6 km) long.

During the construction stage, blasting operations caused many large rockslides. A rockslide at Kamila in 1976 killed 25 Chinese workers (Wood, 1981). In 1977, 15 million tons of debris emerged as a glacial avalanche from a side valley near the village Shishkat in northern Hunza. In three days, a 7.5-mile (12-km) long reservoir had formed that submerged the newly finished "Friendship Bridge" just upstream from the dam. A new bridge and a long diversion had to be constructed. Damming of the area rivers by giant landslides, and subsequent flooding caused by breaching of these dams, is also a major problem in the area (Shroder, 1989).

TYPES OF SLOPE MOVEMENTS AND ASSOCIATED HAZARDS

Rock falls, plane failures, wedge failures, toppling, slumps, debris slides, debris flows, debris avalanches, and mudflows are the common types of slope movement along the Karakoram Highway. The largest and the most devastating failures occur in the glacial deposits. Examples of some of these modes of failure and their hazard potential are presented below.

Rock Falls

Rock falls are a common mode of failure along the Karakoram Highway where overhangs are present as a result of uncontrolled blasting. Extremely large and dangerous overhangs are present where the road has been cut through vertical cliff faces in the form of a half tunnel (Figure 2). The square-shaped block in the overhang in Figure 2 weighs over 10 tons and can be extremely hazardous if it falls. The size and frequency of such rock falls depends on the spacing of discontinuities in the overhangs as well as on the strength characteristics along the discontinuities.

Rock falls are also common where the highway has been excavated through extensive fields of morainal deposits and where boulders weighing several tons are poised half out of the steeply dipping cut slopes, ready to fall (Figure 3). Such cuts are quite common in the Hunza Valley. Loose boulders also fall out of the residual soils where they cover the cut slopes (Figure 4).

Rock falls are a particularly hazardous type of slope failure because of their speed and suddenness of occurrence (Peckover and Kerr, 1979; Barrett and White, 1991; Wyllie, 1991). The cost of combating rock falls is also generally quite high.

Plane Failures

Plane failures occur when discontinuities "daylight" on the slope face, strike more or less parallel to it, and dip more steeply than the friction angle along the discontinuity surfaces (Hoek and Bray, 1981). Examples of plane failure can be seen all along the Karakoram Highway. Figure 5, taken approximately 15 miles (25 km) north of Thakot, shows three well-developed sets of discontinuities, two of which (marked A & B) are very susceptible to plane failures. Figures 6-a and 6-b also show potential sites for plane failures approximately 50 miles (80 km) north of Gilgit. The failures at these sites can be quite hazardous because the road is narrow and there is no provision of a shoulder.

Wedge Failures

Wedge failures occur when discontinuities strike across the slope face. For a wedge failure to occur, the line of intersection of the two discontinuities forming the wedge must daylight on the slope face and must dip more steeply than the friction angle along the discontinuities (Hoek and Bray, 1981). Figure 7 is an example of a wedge failure from the Hunza Valley. The failed block in this case has already been cleared away. Wedge failures along the Karakoram Highway were found to be less frequent than the plane failures.

Figure 2: A large overhang with significant potential for hazardous rock falls.

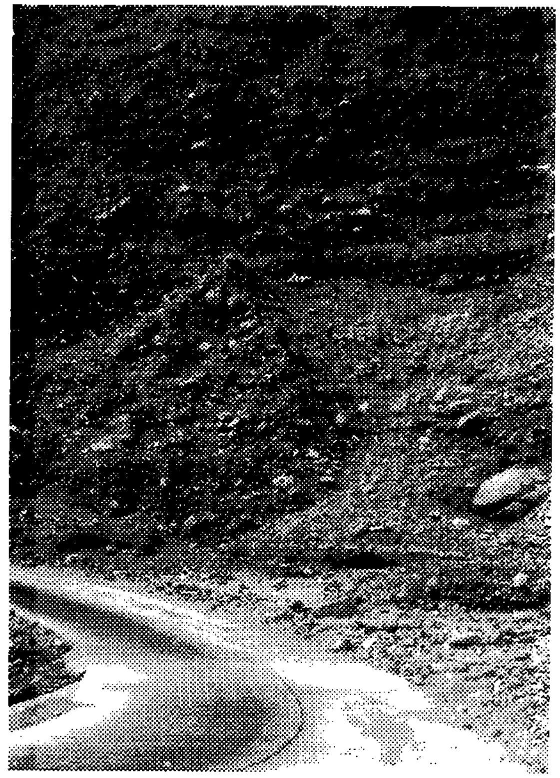

Figure 3: Loosely embedded boulders ready to fall from a steep cut made through a morainal deposit in Hunza Valley.

Figure 4: Boulders in residual soil that can spontaneously roll down and cause serious accidents.

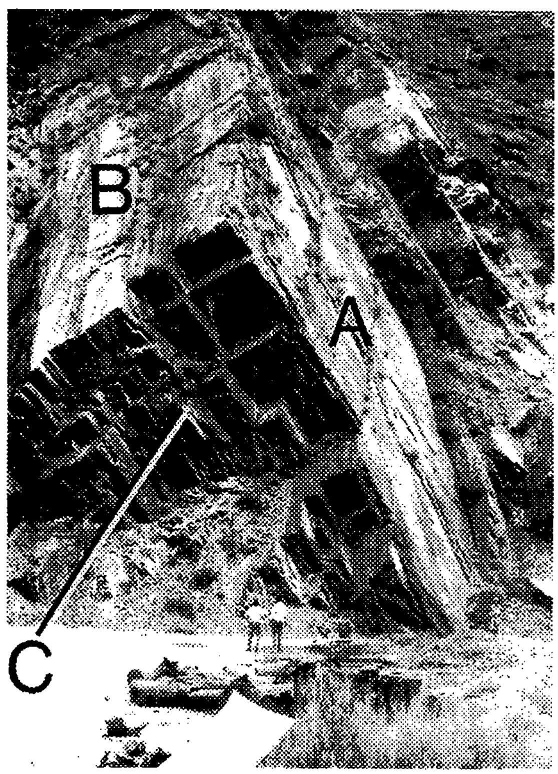

Figure 5: The three well-developed sets of discontinuities at this site represent potential for plane failures along discontinuities A and B, and toppling failure along discontinuity set C.

Figure 6a: Example of potential plane failures in Hunza Valley. Notice the presence of gravel and boulders of glacial origin covering the cut slope.

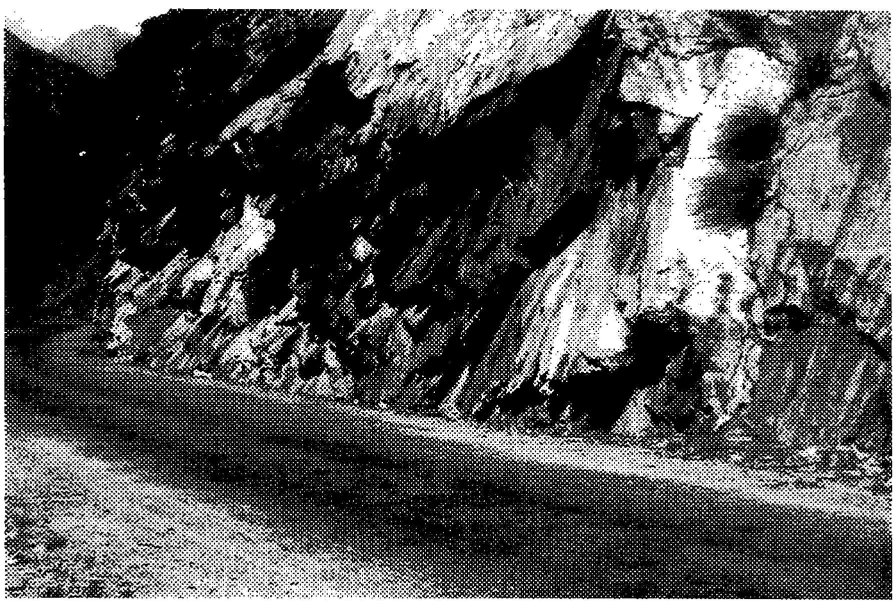

Figure 6b: Example of potential plane failures in Hunza Valley. Because of the absence of a shoulder at this site, the plane failures can be very hazardous.

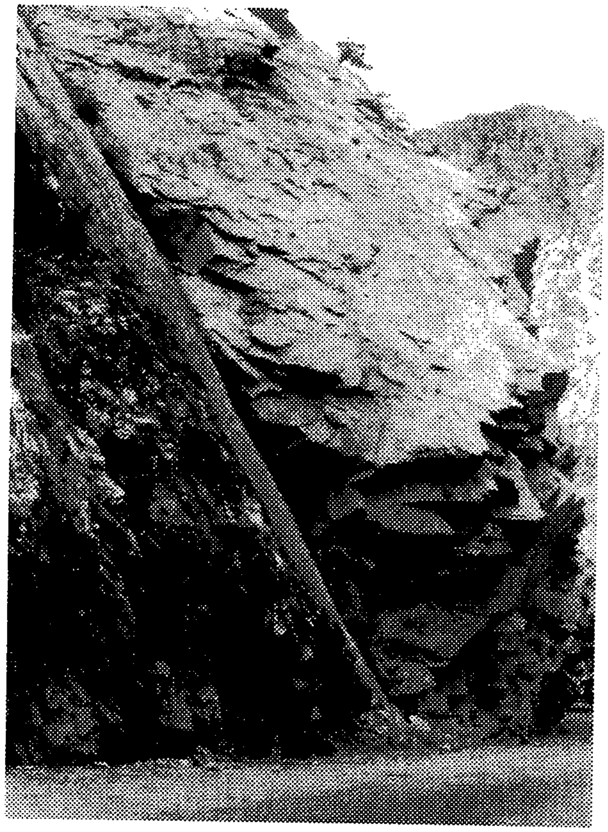

Figure 7: Example of a typical wedge failure in Hunza Valley.

Toppling

Toppling involves rotation of rock blocks whose height is much greater than their width. Toppling occurs when one set of discontinuities dips into an excavation with another set of closely spaced discontinuities perpendicular to it, but dipping away from the slope face.

The requirement for toppling to occur is that the weight vector should fall outside the base of the block or W/H ratio should be less than *tan* θ, where W and H are width and height of the rock block, respectively, and θ is the inclination of the discontinuity on which the blocks are sitting (Hoek and Bray, 1981). In Figure 5, discontinuity C dips away from the roadcut and is, therefore, conducive to toppling type of failure. Toppling was observed to be the least common mode of failure along the Karakoram Highway.

Slumps

Slumps, or circular failures, are very common along the highway. Slumps occur where close jointing and extensive weathering has changed the bedrock to a soil-like material. Figure 8 is a good example of a slump failure that resulted in the collapse of a large section of the road and the adjacent retaining wall. The site is located about 20 miles (36 km) north of Thakot. At a nearby site, the movement in a highly jointed and weathered rock is jeopardizing the safety of a small bridge (Figure 9). Slump failures of varying sizes are also quite common where slopes are covered with residual soils or where the road has been cut through glacial material.

Figure 8: A slump failure in an embankment of a highly weathered rock, 20 miles (36 km) north of Thakot. The failure resulted in collapse of the adjacent retaining wall.

Figure 9: The safety of a bridge is jeopardized by movement in the highly fractured and weathered abutment rock about 20 miles (36 km) north of Thakot.

Debris Slides, Debris Flows, Debris Avalanches, Mudflows

The Karakoram Highway traverses active scree slopes at many places, especially in the Hunza Valley where highly jointed, sheared, and foliated metamorphic rocks (slates and schists) are common. Here the over-steepened slopes above or below the road have been left to re-establish their gradients, destroying the road in the process. The scree continuously moves downslope as debris slides or as debris flows depending upon the water content (Figure 10). Where steepness of gradient further adds to the mobility of the moving mass, debris flows change to debris avalanches. Several very large and hazardous debris flows and debris avalanches in the Hunza Valley (Shishkat, Sarat, Ganesh, Yal Pari, and Shitan Pari failures) have been mapped and described by Khan et al. (1986). Debris flows are also common in steep-gradient streams, which cut through weathered and closely jointed rocks. Figure 11 shows an active debris flow that keeps blocking the road periodically in the Thakot-Besham area.

Mudflows occur at some places in the Hunza Valley where glaciofluvial or residual soils contain abundant sand, silt, and clay size material, and where large quantities of rain and meltwater infiltrate the material through tension cracks. The mudflows at Jaglot Gah and Ghammessar in the Hunza Valley, as described by Fayaz et al. (1985), are good examples.

Slides in Glacial Materials

In Hunza Valley, the Karakoram Highway frequently cuts through glacial and glaciofluvial material deposited by side-valley glaciers. Some of these cuts are over 4 miles (6 km) long and most of them are very steep (Figure 3). The glacial material in these cuts is extremely heterogeneous in nature and consists of variable size boulders

Figure 10: Yal Pari slide in Hunza Valley representing an active scree slope and a debris slide.

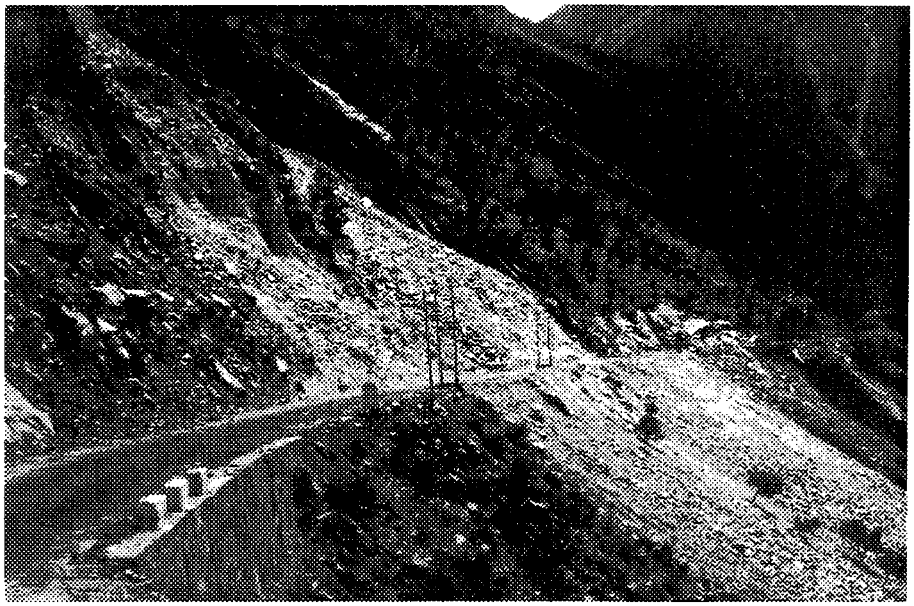

Figure 11: An active Hunza debris flow that follows a stream channel in the Thakot-Besham area

embedded in a matrix of gravel, sand, silt, and clay. At many places, the material extends up to the snouts of the existing glaciers and, therefore, abundant quantities of meltwater seep directly into this material in the spring season. In addition, rainwater freely enters the material through tension cracks that have developed as a result of previous movement. The development of high pore pressure during the wet season causes some of the largest and the most devastating slope movements to occur in the glacial material. Depending upon the conditions prevalent at a particular time, these movements can occur as slumps, earthflows, debris flows, mudflows, avalanches, or as falls of loose boulders.

Figure 12 shows a slope failure in glacial material near Jaglot Gah, Hunza Valley that takes various forms depending on the quantity of water available. The continual movement of the material frequently blocks the road at this site and has forced its location closer to the Hunza River. Figures 13 and 14 are other examples of large-size slope failures in glacial material. The movement in glacial material is not only hazardous but also a perpetual and expensive problem for the Frontier Works Organization of Pakistan, which is responsible for the maintenance of the road.

CAUSES OF SLOPE MOVEMENT

The slope instability problems listed in the previous sections exist because many engineering techniques such as tunneling, benching, pre-splitting, rock bolting, provision of adequate drainage, provision of shoulder and wide catchment ditches, safe back-slopes, and stabilization by vegetation were not incorporated in the design of this very important, but dangerous, highway. Lack of sufficient funds, difficulty of moving heavy equipment into the area, and sometimes lack of expert help could have been the reasons for the non-engineered slopes.

Glacial moraines and meltwater from glaciers are probably the most important factors contributing to slope movement along the Karakoram highway. In northern

Hunza, several glaciers fed by the heavy snows of the main Karakoram range advance annually to within 2000-ft (600 m) of the Hunza River. The loose, unconsolidated, and heterogeneous nature of the morainal material deposited by these and the previous glaciers, coupled with the abundance of meltwater available, results in some of the

Figure 12: A large (300 m), active slope failure in glacial material near Jaglot Gah,, Hunza Valley. The unpaved section of the road at this site indicates the active nature of slope movement.

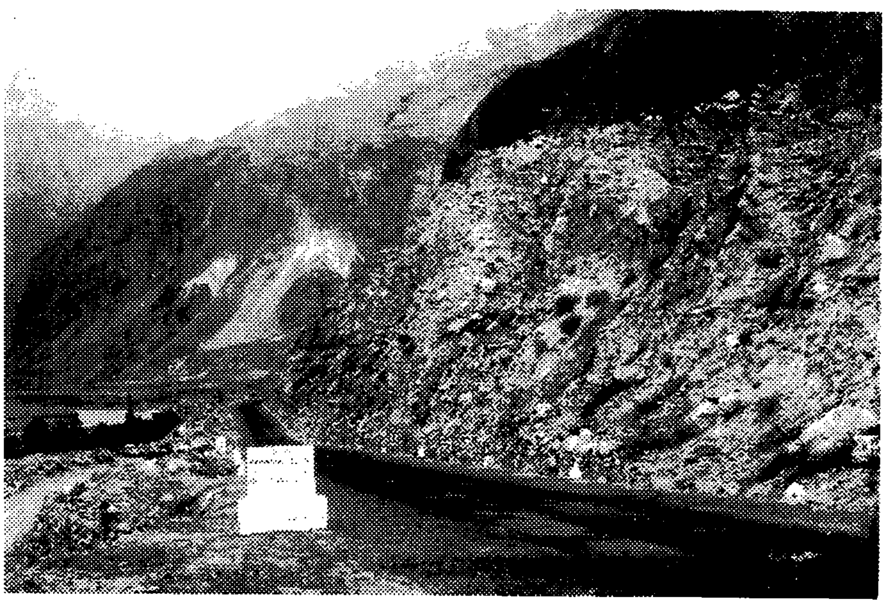

Figure 13: A 550 m long slope failure in glaciofluvial material in Hunza Valley, locally known as the Rahimabad slide.

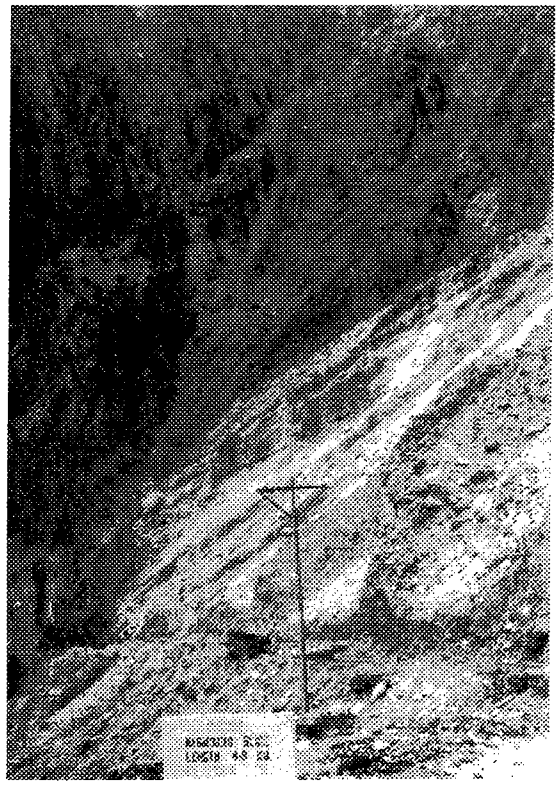

Figure 14: A very large (4-9 km), active slope failure in glaciofluvial material near Nasarabad, Hunza Valley.

largest debris flows in the area. Between 1973 and 1974, the meltwater stream from Batura Glacier (Figure 1) changed its course and shifted about 1000 ft (300 m), removing a section of the highway embankment. Similarly in the summer of 1980, the debris deposited by the meltwater from the Ghulkin Glacier, south of Batura, buried the road under 7-10 ft (2-3 m) of boulders up to 3 ft (I m) in diameter (Wood, 1981). This resulted in relocation of the road closer to the Hunza River. Shroder (1989) has reviewed the role of glaciers in causing geologic hazards along the Karakoram Highway.

Earthquakes are another factor that contribute to slope instability in the region. During the Pattan earthquake in 1975, several long sections of the highway collapsed. The earthquake also released many large boulders from the mountainsides that came tumbling down the steep slopes and destroyed the highway. Because of their momentum, such large boulders can be extremely hazardous to both life and property.

Since the river runs close to the highway, undercutting by the river, or by the tributary streams, is another cause for the collapse of highway sections at many places. The slump failure in Figure 8 is partly due to undercutting by the tributary stream below.

CONCLUDING STATEMENT

The frequent occurrence of all types of slope failures along the Karakoram Highway is a major problem that needs immediate attention. An important reason why the landslide problem continues is that proper attention has not been paid to investigate the stability of specific sites and to the design of appropriate remedial measures required at these sites. In spite of the numerous slope failures that occur along the highway every year and the serious hazard they pose to the traffic, no detailed study has been undertaken by personnel experienced in slope stability investigations. The previous studies by Fayaz et al. (1985) and Khan et al. (1985, 1986) are qualitative in nature and do not analyze the stability of individual sites. If the Karakoram Highway is to serve its intended purpose, such a study is imperative.

REFERENCES

Barrett, R.K. and White, J.L., 1991, Rockfall Prediction and Control: in Hamabley, D.F., editor, Proceedings, National Symposium on Highway and Railroad Slope Maintenance, 34th Annual Meeting, Association of Engineering Geologists, Chicago, Illinois, pp. 23-40.

Civil Engineering, April 1979, World's Highest Highway Through Himalayas Links China to Pakistan: News Letter, American Society for Civil Engineers, p. 58.

Fayaz, A., Khan, K.S.A., and Latif, M., 1985, Mudflows and Avalanches Along the Karakoram Highway: Information Release No. 247, Geological Survey of Pakistan, Engineering Geology Branch, Islamabad, 28 p.

Fayaz, A., Latif, M., and Khan, K.S.A., 1985, Landslides Evaluation and Stabilization Between Gilgit and Thakot Along the Karakoram Highway: Information Release No. 253, Geological Survey of Pakistan, Engineering Geology Branch, Islamabad, 49 p.

Hoek, E. and Bray, J.W., 1981, Rock Slope Engineering: The Institution of Mining and Metallurgy, London, 358 p.

Khan, K.S.A., Fayaz, A., Latif, M., and Wazir, A.K., 1986, Rock and Debris Slides Between Khunjerab Pass and Gilgit Along the Karakoram Highway: Information Release No. 72, Geological Survey of Pakistan, Engineering Geology Branch, Islamabad, 56 p.

Peckover, F.L. and Kerr, J.W.G., 1977, Treatment and Maintenance of Rock Slopes Along Transportation Routes: Canadian Geotechnical Journal, Volume 14, pp. 487-507.

Shroder, J.F., Jr., 1989, Hazards of the Himalaya: American Scientist, Volume 77, No. 6, November-December, pp. 564-573.

Wood, R.M., September 1981, Highway to the Top of the World: New Scientist, U.S.A., pp. 656- 658.

Wyllie, D.C., 1991, Rockslope Stabilization and Protection Measures: in Hamabley, D.F., editor, Proceedings, National Symposium on Highway and Railroad Slope Maintenance, 34th Annual Meeting, Association of Engineering Geologists, Chicago, Illinois, pp. 41-64.

1997 California Storm Damage
The Gorda Landslide

by

John D. Duffy

805-549-3663

t5mail.jduffy@trmx3.dot.ca.gov

and

Mike Finegan

805-549-3194

t5mail.mfinegan@trmx3.dot.ca.gov

California Department of Transportation
50 Higuera Street
San Luis Obispo, California 93449

The Gorda landslide, located along State Route 1 at the town of Gorda, occurred on January 2, 1997 following sustained periods of heavy rainfall. The landslide occurred within a large Quaternary landslide causing 300 meters of roadway to move downslope. Additionally, localized concentrations of water in the northern end of the slide supersaturated two masses which burst downslope as debris flows completely removing the roadway and roadway prism. The slide was 215 meters wide and extended downslope 100 meters. Subsurface monitoring indicated the slide plane to be 20 meters below grade. The debris flows scars are approximately 10 meters wide and have scoured out a 15 meter deep steeply incised channel. Site geology consists of predominantly highly sheared and fractured serpentinite surrounded by metamorphosed rocks mostly derived from sandstones and shales. The sheared and fractured serpentinite possesses a low degree of plasticity. The investigation consisted of thirteen mud rotary borings, material sampling, laboratory testing, instrumenting the site with slope inclinometers and time domain reflectometry (TDR) instrumentation, field mapping, and eight seismic refraction lines. A 192 meter long thirty meter high wall soldier pile tieback wall was constructed to repair the roadway and mitigate against future failures. Spencer's Method for a specified failure surface was used in the design and indicated an effective friction angle of 28 degrees and 9.0 kPa of cohesion best represented the existing conditions. Standard Penetration Test (SPT) correlations indicated a friction angle of 31 degrees. Seventy four piles and 306 ground anchors were used in the retaining wall design.

Introduction

The landslide, along State Route 1 at the town of Gorda, occurred on January 2, 1997 following sustained periods of heavy rainfall. Gorda and Highway 1 in this area are located within a large Quaternary landslide. This Quaternary slide is dormant but a portion of the slide had re-activated. Since the road's construction, portions of the roadway had been creeping downslope with the slide. This movement was most pronounced during above average rainfall years.

The winter of 1996/1997 produced unusually high precipitation. Antecedent rainfall was well above average and individual storm events were of long duration and high intensity. These weather patterns caused groundwater levels to rise significantly and surface soils to become saturated.

The combination of a Quaternary slide, above average rainfall, and geologic setting compromised the stability of the area. The unusually high concentration of water, into this marginally stable Quaternary landslide, increased pore water pressures which in turn reduced shear strength causing the landslide to move. In this manner the slide creeped downslope taking the road with it. Additionally, localized concentrations of water in the northern end of the slide supersaturated two masses which burst downslope as debris flows.

General Site Conditions

The slide is approximately 215 meters wide and extends downslope approximately 100 meters, The headscarp occurs approximately 10 meters upslope from the roadway. Subsurface data indicates the slide plane, within the northern portion of the slide, is approximately 20 meters below the original grade, becoming shallower southward to approximately 14 meters below original grade. Field mapping indicates a slide plane dipping 18 degrees. The debris flows scars are approximately 10 meters wide and have scoured out a 15 meter deep steeply incised channel.

The toe the slide is creeping and spilling over the bluffs. From the toe the slide plane is inclined 18 degrees upslope to the intersection of slope inclinometer movement. This inclination corresponds with slide plane exposures observed and mapped in the debris flow areas.

General Geologic Setting and Subsurface Conditions

The geologic unit at the site is described as ultra basic intrusive rocks surrounded by rocks of the Franciscan Formation. The ultra basic intrusive rocks are predominantly highly sheared and fractured serpentinite while those of the Franciscan Formation are metamorphosed rocks which have been mostly derived from sandstones and shales. The sheared and fractured serpentinite possesses a low degree of plasticity. When below the water table most of its shear strength is lost, resulting in landslides that flow even in areas of low slope angles.

Seismicity and Liquefaction Potential

Several faults are located in the vicinity of the project site. The fault which has the greatest potential to influence this site is the San Gregorio. The maximum credible Richter Magnitude for the San Gregorio Fault as determined by Caltrans is 7.5. The maximum credible acceleration in rock is 0.65g (gravity) according to the Caltrans attenuation curves. The 3 m (10 feet) to 24.4 m (80 feet) Design Force Coefficient Curve is appropriate at this site.

Field and Laboratory Investigation

The investigation consisted of subsurface drilling, material sampling, laboratory testing, instrumenting the site, field mapping, and geophysical studies. All of this information was used to determine the nature, extent, and properties of the subsurface materials.

Subsurface operations

Thirteen mud rotary borings were installed in the project area. Nine of the borings were installed at road level along the proposed wall lay out line. Three borings were installed upslope of the roadway within the headscarp and one boring was installed below the roadway. Target depths for all the drilling operations were formation contacts and sound competent bedrock. Hole depths varied between 20 and 61 meters.

Material Classification

During the drilling operations all materials were sampled and classified. The Unified Soil Classification System (USCS) was used for categorizing soils. Soil descriptions were based upon conventional methods from visual inspection (i.e., soil type, color, texture, cementation, consistency / relative density, etc.). Rock was classified and described by conventional methods from visual inspection (i.e., Rock type, color, degree of weathering, relative hardness, structure, etc.) and measurement of RQD (Rock quality designation).

Field and Laboratory Testing

Sampling techniques consisted of bag samples, SPT samples, 50 mm push samples, and core samples. Bulk bag samples were obtained from formation outcroppings. Standard penetration test (SPT) samples and continuous core samples were obtained from the rotary borings. Bulk samples were tested for Atterberg limits, gradation and moisture content. SPT tests provided blow count values for material strengths, visual inspection of the material, and provided material for Atterberg Limit tests. Continuous core samples were used for detailed material descriptions and rock discontinuity measurements. Push samples obtained from outcrops were used for triaxial tests to determine material strengths. These tests were conducted in saturated conditions with consolidating stresses bracketing field overburden pressures.

Instrumentation

Four of the fourteen rotary borings installed in the landslide were instrumented with piezometer pipe. This instrumentation is used to measure groundwater levels and in some instances can be used to determine depth of sliding.

Two borings installed above the road, four borings within the road, and one boring below the road were instrumented with slope inclinometers (SI's). Slope inclinometers are used in earth masses to obtain a profile of horizontal earth movement through a potential or active failure zone. An inclinometer installation is comprised of a special casing grooved to control orientation, from which a profile of slopes is obtained using a pendulum measuring device which measures tilt.

Two borings installed above the road, two borings along the road, and one boring below the road were installed with Time Domain Reflectrometry (TDR) instrumentation. TDR is used in earth masses to identify potential or active failure zones. TDR consists of a cable tester, which when connected to the coaxial cable, will identify bends or breaks in the cable and at what depth they occur.

All tension cracks were marked and dated with spray paint. In this way measurements were made to monitor head scarp recession. Head scarp recession can be an indicator of landslide movement.

Geologic Mapping

Utilizing published geologic maps and aerial oblique photographs, the project area was examined in the field "on foot" to accurately map the surface geology. Both site and regional geology were mapped. This information was used in conjunction with subsurface boring data to develop stratigraphy within the project area. Structure contour maps, stratigraphic columns, and landslide limits were generated from this information.

Seismic Refraction Studies

Eight seismic lines were run as part of a seismic refraction study to determine a bedrock profile. This work was performed on the roadway and below the slopes. A 12-channel, signal enhancing seismograph was used for this investigation. Energy was introduced into the ground by detonating small explosive charges. The approximate depth of investigation was below existing and proposed road grades.

Geologic Features of Engineering and Construction Significance

Figure 1 presents a cross section through the thickest part of the landslide and is assumed worst case where the mitigating structure would be the largest. The slope morphology along this section is very revealing. Below the roadway, where there is little human disturbance, the toe and body of the slide are clearly evident. Above the roadway human construction has modified some landslide features but overall the head and headscarp are evident. The headscarp is approximately 100 meters in slope length. Connecting these surface features with slope inclinometer and boring data delineates the probable Quaternary slide zone. Using this information we constructed a model of the proposed mitigation - a tie-back retaining wall - on the section. From this model it is clear that the tie-back tendons will most likely pass through the Quaternary slide zone and be bonded in Franciscan Formation serpentinite.

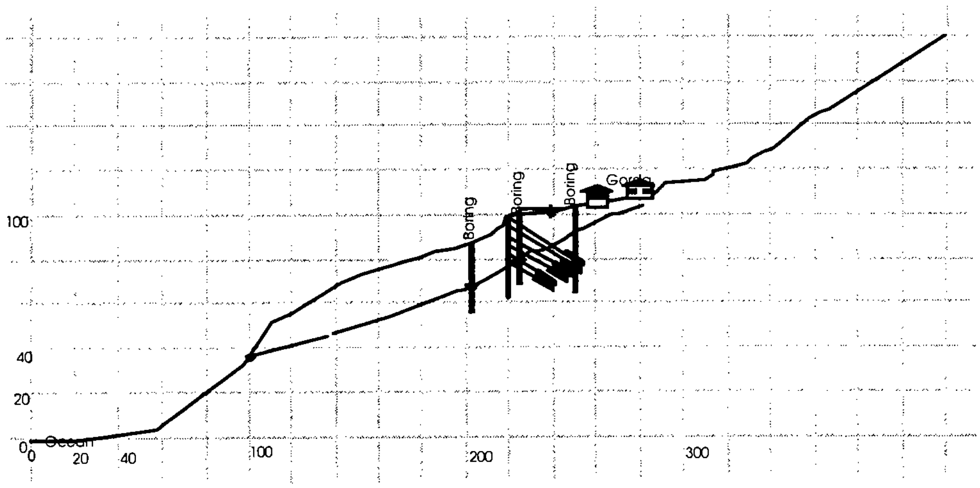

Figure 1: General Cross Section Delineating Borings, Slide plane and Relative Wall Location.

The large headscarps indicate that the slide has moved significantly and as a whole has reached a state of equilibrium. Smaller slides, occurring within the larger slide, continue to occur within the mass. These slides are what we have been experiencing since the opening of the roadway and most recently during the 96/97 storms.

Retaining Wall Recommendations

A tieback retaining wall was recommended for this site. The retaining wall up is 30 meters tall and 190 meters in length. The wall layout line was 10 meters left of original centerline to allow wall construction to proceed while maintaining a minimum of one lane of traffic.

A cross section through the critical landslide section was used to determine shear strength parameters along the sliding surface. Shear strength of the slide plane was back calculated using Spencer's Method for a specified failure surface. Based on the slide geometry and ground water levels shown on the typical cross section, an effective friction angle of 28 degrees and 9.0 kPa of cohesion was found to best represent the existing conditions. A moist unit weight of 18.8 kN/m3 and saturated unit weight of 19.6 kN/m3 with a phreatic water surface was used in the analysis. Ground water levels were determined based on open piezometer levels, field observations, and seismic refraction results.

Standard Penetration Test (SPT) correlations show a friction angle of 31 degrees for the fill and in place Quaternary landslide deposits. This value should be used for all in place and proposed fill in front of and behind the wall. Although SPT blow counts in the weathered Franciscan Formation closely approximate the blow counts in the overlying material, it is felt that these results are unreliable. Due to the varying degrees of shearing and decomposition within the Franciscan Formation, the strength parameters based on back analysis of the slide plane were used in the design of the Soldier pile wall.

Ground anchors used in the retaining wall have a minimum unbonded length to 5 meters beyond both the recent and Quaternary failure planes. This will place the bonded zone into the serpentinite. Because of the varying degrees of weathering within the serpentinite, an ultimate transfer load of 146 kN/m (10 kips/foot) is recommended. This value is comparable to values used for loose to medium dense sand and gravel. A maximum bonded length of 12 meters was also recommended. Testing has shown that bonded lengths greater than 12 meters will not significantly increase anchor capacity. Tieback unbonded length was determined with an inclination of 25 degrees down from horizontal. Unbonded lengths are presented for one to six levels of tiebacks with the top row of tiebacks 2.25m down from the top of wall and 3.3m spacing for all other levels. The maximum distance from the lowest level of tiebacks to the bottom of the wall is 4.25m. Tieback level T1 is the top level.

	Unbonded Lengths (meters)					
Number of Tieback Levels	T1	T2	T3	T4	T5	T6
6	38	34	30	22	18	14
5	34	30	26	18	14	
4	30	26	18	14		
3	26	18	14			
2	22	14				
1	18					

Minimum pile tip embedment below the failure surface 10 meters left of the layout line are listed for the given number of levels of tiebacks and axial service level loads. A 900 mm (36") diameter drilled hole backfilled with concrete was used for the analysis. A 3 meter thick zone of decomposed serpentinite is uniformly present within and below the slide plane. This very soft, saturated zone was ignored when determining the axial load capacity.

Number of Tieback Levels	Service Level Axial Load	Minimum Pile Embedment Below Failure Surface

6	3225 kN (725k)	12.0 m
5	2669 kN (600k)	10.5 m
4	1957 kN (440k)	8.5 m
3	1334 kN (300k)	7.0 m

Due to predominantly sheared and fractured nature of the serpentinite, conservative values were used for the uniaxial compressive strength of the rock. A value of 500 psi was used for the serpentinite. The method presented in the Transportation Research Board (TRB) Manuals for the Design of Bridge Foundations for bearing capacity of drilled shafts socketed in rock was used when determining pile tip elevations. Piles are assumed to obtain their axial capacity in side resistance only, negligible pile settlement is anticipated.

Recompacted slopes in front of the retaining wall are 1:1.5 (V:H) or flatter. The slopes in front of the wall were considered meta-stable and are not be counted on for passive resistance. Depending on future ground water levels, this material will continue to slide. For this reason no pipes or other facilities be located within this fill

Conclusions or Summary

For what its worth.

LAST CHANCE AND WILSON CREEK WALL LANDSLIDES, DEL NORTE COUNTY, CALIFORNIA

By
TIMOTHY J. BECK
California Department of Transportation
5900 Folsom Blvd., Sacramento, CA 95819

ABSTRACT

A 1.6 kilometer (1 mile) long section of U. S. Route 101 in Del Norte County has been damaged by landslide activity on a regular basis since completion in 1923. This segment of the highway was built on the western flank of a ridge adjacent to the Pacific Ocean. The ridge is composed of a chaotic mix of shale and sandstone, mapped as Franciscan assemblage. The Last Chance and Wilson Creek Wall landslides have coalesced to cover 81 hectares (201 acres) of the ridge.

The northern portion of the Last Chance landslide is very active and the roadway requires almost continuous maintenance. At the northern side-scarp the highway sometimes drops several feet in a day. An initial study of the site in 1993/1994 identified a landslide complex that consisted of the active slide and a larger, apparently dormant, slide to the south. Inclinometer data from the center of the active slide indicated that the failure plane was 30 to 38 meters (100 to 125 feet) below the roadway.

Field studies in 1998/1999 identified tension cracks at the head of the southern portion of the slide. Previously considered dormant; it is now thought to be active. Slide movement is apparently episodic and is only active in heavy rainfall years. Pavement cracks, mapped in 1998/1999, and air photo interpretations were used to extend the 1993/1994 slide boundary to the south.

The Wilson Creek Wall Landslide is of roughly equal size, just south of the Last Chance Landslide. The slide was mapped based on tension cracks, scarps (both fresh and eroded), and closed depressions observed during recent field work. The field observations were augmented with geomorphic interpretations from the air photos.

The movement on both slides appears to be triggered by heavy rainfall and high surf. Infiltration of rainfall causes elevated groundwater levels which increase the driving forces on the slides. High surf causes increased erosion at the toes of the slides removing buttressing material, thus reducing the resisting forces. Air photos show that an area of no vegetation along the sea cliffs has greatly increased in recent years. This area is assumed to be undergoing mass-wasting resulting in removal of material from the toes of these slides.

Monitoring installations (inclinometers, piezometers, and TDR installed to a depth of 100 meters) are planned for the slides. Monitoring might continue three to five years in order to unambiguously determine the depths to the slide planes. A tunnel or realigning the highway are possible alternatives for stabilizing the road.

INTRODUCTION

The Last Chance and Wilson Creek Wall landslides are located about 10 miles south of Crescent City (See Figure 1), in the southwest corner of the Childs Hill 7.5 minute quadrangle. The elevation of the roadway at this site is approximately 215 to 260 meters

(700 to 850 feet). Most of the area is covered with a dense growth of redwood, douglas fir, spruce, and alder with a thick undergrowth of ferns and berry vines.

In 1894 a county road was built across "Last Chance slide," as it is known locally. In 1923 State Route 1 was built on the same alignment. The highway, connecting Crescent City and Eureka, is known as the Redwood Highway. In the early 1930s when the California Division of Highways was planning to widen and straighten the road, Last Chance slide was described as being "expensive to maintain because of the extremely unstable formation" (Comly, 1932). At that time consideration was given to realigning the highway on the east side of the ridge to avoid Last Chance slide. This option was rejected because of the high cost and the damage it would do to an adjacent state park. Widening and straightening the highway was completed in 1935. In the early 1960's this route became U. S. Highway 101. In 1993/1994 the California Department of Transportation (Caltrans) initiated a Project Study to determine stabilization strategies for Last Chance Slide. A further Project Study was conducted in 1998/1999.

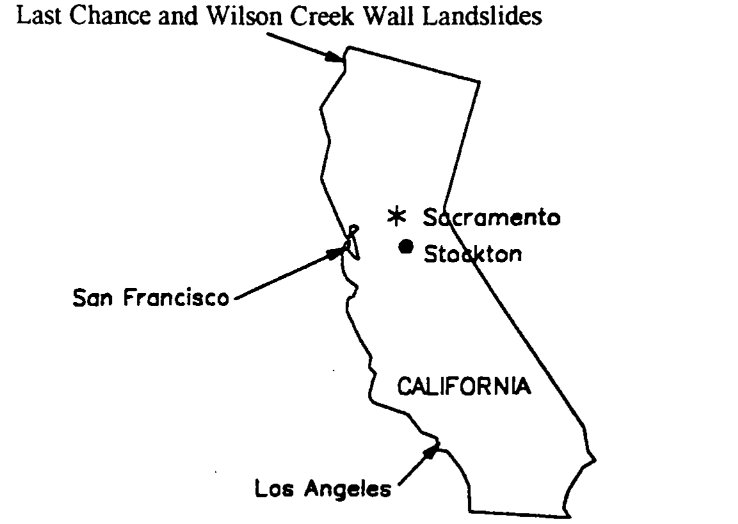

Figure 1. Location of Last Chance and Wilson Creek Wall landslides.

This portion of the highway is located in Del Norte Coast State Redwood Park. In the late 1910's and early 1920's, the Save the Redwoods League was very active in collecting money, donating property, and lobbying the State Park Commission to establish this park. It was one of the first state parks in California, established in 1925. One of the functions of the highway was to provide access to the park (Knight, 1931).

GEOLOGY

The study area is located in the northern portion of the California Coast Range Geologic Province. The Franciscan assemblage is the main geologic unit in this province. The Franciscan is characterized by extreme structural disorder and high-pressure metamorphism. Many geologists considered it the type example of accretionary complex formed by subduction (Blake and Jones, 1981). Approximately 60 miles offshore is the Cascadia Subduction Zone where the Gorda Plate is being forced under the North American Plate.

The Franciscan rocks are prone to landsliding due to their structural disorder and the active tectonics of the area. In 1984 the California Division of Mines and Geology published landslide mapping of the Childs Hill 7.5 minute quadrangle, Del Norte County, California (Davenport, 1984). The Last Chance Grade area was mapped as a debris slide slope, sculpted by numerous debris slides.

LAST CHANCE LANDSLIDE

The 1993/1994 Caltrans investigation identified a large deep-seated landslide complex at Last Chance Slide. Some results from that investigation were published previously (Kane and Beck, 1994). The 1998/1999 Caltrans study identified additional geologic and landslide features. The updated Geologic Map is shown in Figure 2. As mentioned previously, the rocks that underlie this site are a chaotic mix of shale and sandstone, mapped as Franciscan assemblage (map unit KJf). These rocks are intensely fractured, sheared, and weathered to a depth of 15 meters (50 feet). A major joint set appears to strike parallel to the ridge and dip 40 to 50 degrees toward the ocean.

Northern Portion of Last Chance Landslide

The northern portion (map unit Qlsn) of the Last Chance Slide is very active. The road requires almost continuous maintenance, it sometimes drops several feet in a day. The slide has enveloped approximately 17 hectares (43 acres) of the ridge. This slide appears to be composed of at least three translational/rotational blocks with a debris flow snaking up the middle. As the two lower blocks move forward the upper block is left unsupported and moves in behind the other two. The three blocks appear to move as intact masses. During the rainy season the materials (soil, rock fragments, downed trees, etc.) in the debris flow track lose almost all shear strength and flow downhill toward the ocean. Two inclinometers were installed in 1994 in the center of the active landslide area, along the roadway. The data indicated that the failure plane is 30 to 38 meters (100 to 125 feet) below the roadway.

Southern Portion of Last Chance Landslide

The 1993/1994 study also identified a larger, apparently dormant portion of Last Chance Slide (map unit Qlss). Field studies in 1998/1999 identified tension cracks at the head of this portion of the slide. For that reason it is now considered an active/reactivated landslide as defined by Cruden and Varnes (1996). The movement was probably triggered by 4 years of above-average rainfall from 1995-1998 (See Figure 3). Movement on this slide apparently stops for long periods, as indicated by the absence of tension cracks and the overgrown scarps observed during 1993/1994 study. Prior to 1995, there was a period of below normal rainfall for least 10 years when this portion of the slide was probably dormant.

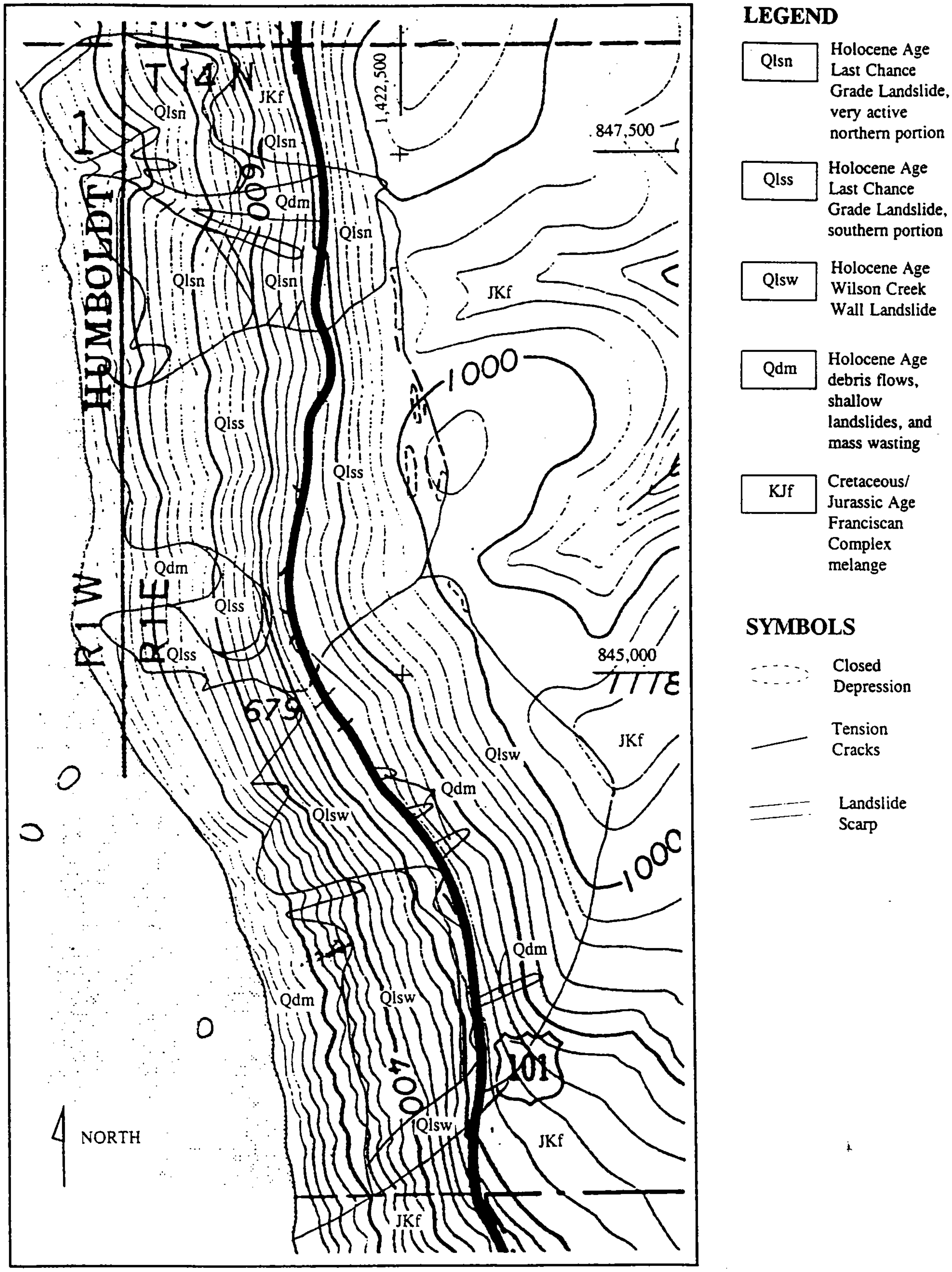

Figure 2. Geologic Map of Last Chance and Wilson Creek Wall landslides

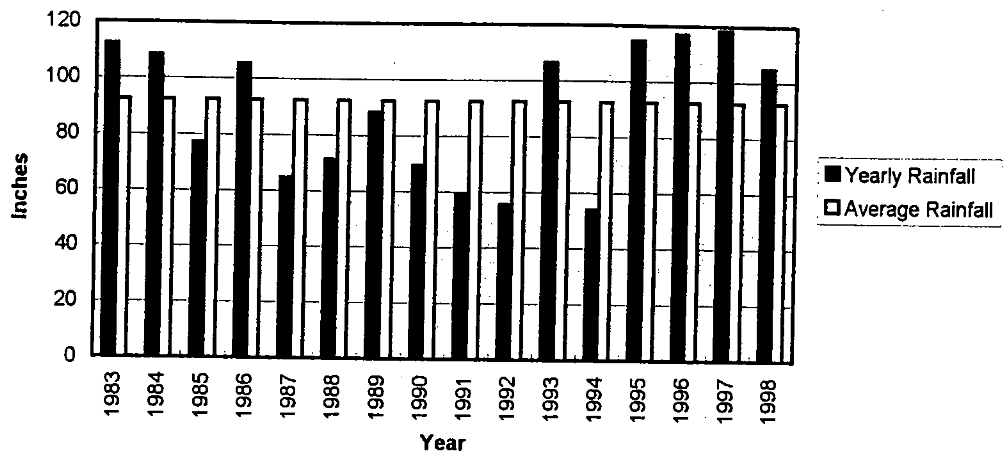

Figure 3. Rainfall Totals at Last Chance and Wilson Creek Wall landslides

The slide boundary was extended to the south based on observations, including cracking and a grade change in the roadway, made during the 1998/1999 investigation. Recent aerial photographs, flown on September 10, 1998, were used to make geomorphic interpretations which were considered in the boundary change. This portion of the slide has enveloped approximately 24 hectares (60 acres) of the ridge. A series of large closed depressions along the ridge-top are evidence that this slide has a large translational movement component to it. The depth to the failure plane was assumed to be 38 to 75 meters (125 to 250 feet) below the roadway. The depth assumption was based on the size of the slide and the failure plane depth measured at the northern portion of the slide. That assumption will be verified by installing slope monitoring equipment.

WILSON CREEK WALL LANDSLIDE

Another large landslide (map unit Qlsw) was identified during the 1998/1999 investigation just south of the Last Chance Slide. The Wilson Creek Wall Landslide (named for the purposes of this paper) has enveloped approximately 40 hectares (98 acres) of the ridge. The slide was mapped based on tension cracks, scarps (both fresh and eroded), and closed depressions observed during the recent field work. The field observations were augmented with geomorphic interpretations from the air photos. The depth to the failure plane is assumed to be similar (38 to 75 meters) to the Last Chance Slide. The Wilson Creek Wall, a tie-back soldier pile wall, was constructed along the roadway at the southern side of the slide. The wall was constructed 1991 and started showing signs of distress in 1997. The southern portion of the wall was displaced past the northern portion. It appears that the slope above the wall moved forward and placed the wall in compression. The slide movement was probably triggered by the period of heavy rainfall from 1995 to 1998 (See Figure 3).

SUMMARY

High surf, along with heavy rainfall, appears to trigger the movement on both slides. Infiltration of rainfall causes elevated groundwater levels increasing the driving forces on the slides. High surf causes increased erosion at the toes of the slides removing buttressing material, thus reducing the resisting forces. The 1998 air photos show that the area of no vegetation along the sea cliffs has greatly enlarged since the previous air photos were taken in 1993. This area (map unit Qdm) is assumed to be undergoing mass-wasting which is removing material from the toes of these slides.

ROADWAY STABILIZATION ALTERNATIVES

The usual methods of stabilizing landslides, that is, unloading, de-watering, and buttressing, are inappropriate due to the location and size of these slides. Unloading the head of the slides would only be effective temporarily because the ocean would continue to remove the toes. Buttressing the toes of the slides would be difficult and costly because of the rugged terrain, the ocean would make access to the toes difficult, the size of the slides would require a massive amount of material to buttress them, and the buttresses would have to be armored against the erosive action of the surf. Dewatering the slope would also be difficult and expensive because of the rugged terrain and the size of the slides.

For the reasons mentioned above, the roadway stabilization strategy should change the alignment to avoid the slides. There are at least two alternatives for changing the road alignment to avoid both slides. Realign the highway in a tunnel excavated behind the slide plane or realign the road on the east side of this ridge. Combinations of these alternatives could also be used to stabilize the roadway.

Tunneling conditions will be difficult at this site. The Franciscan assemblage behind these slides is known as block-in-matrix rock or bimrock (Medley and Lindquist, 1995). The blocks are hard to very hard sandstone. The matrix is soft to very soft, sheared shale. A tunnel boring machine would probably not be suitable for this site. The drill and blast excavation method would most likely be required. Zones of heavy groundwater flows would also be encountered.

Realigning the highway on the east side of the ridge would also encounter difficulties. The 1984 California Division of Mines and Geology landslide mapping indicates there are numerous landslides on the eastern slope of this ridge (Davenport, 1984). Realigning the highway must also avoid impacting the unique environment of the old growth redwoods in the state park.

No stable ground was identified in the southern portion of the study area. The unstable ground probably extends to Wilson Creek. The Caltrans is currently evaluating the stability of that portion of the highway.

CONCLUSIONS

In 1998/1999 Caltrans identified a large scale, deep-seated landslide complex that included Last Chance and Wilson Creek Wall landslides. Portions of these landslides were apparently dormant for 10 years or more. These slides are a case history for the time-dependent aspect of slope stability. Most engineering projects do not allow for the luxury of monitoring a marginally stable slope for a number of years. Therefore, caution should be exercised when planning engineering projects that impact or are impacted by "dormant" landslides.

REFERENCES

Blake, M. C., and Jones, D. L., 1981. "The Franciscan Assemblage and Related Rocks in Northern California: A Reinterpretation" in *The Geotectonic Development of California*, W. G. Ernst, Editor. Prentice-Hall, Inc., Englewood Cliffs, N. J. 07632.

Comly, H. S., 1932. "Report on the Routing of the State Highway from Wilson Creek to Crescent City in Del Norte County" California Department of Public Works, Division of Highways.

Cruden, D. M., and Varnes, D. J., 1996. "Landslide Types and Processes" in *Landslides, Investigation and Mitigation*, Special Report 247, A. K. Turner and R. L. Schuster, Editors. Transportation Research Board, National Academy Press, Washington, D. C.

Davenport, C. W., 1984. "Geology and Geomorphic Features Related to Landsliding, Childs Hill 7.5' Quadrangle, Del Norte County, California" California Department of Conservation, Division of Mines and Geology, OFR 84-7 S.F., scale 1:24,000.

Kane, W. F., and Beck, T. J., 1994. "Development of a Time Domain Reflectometry System to Monitor Landslide Activity" in *Proceedings, 45th Highway Geology Symposium*, S. F. Burns, Editor.

Knight, E., 1931. "The Del Norte Coast State Park" Sierra Club Bulletin.

Medley, E., and Lindquist, E. S., 1995. "The Engineering Significance of the Scale-Independence of some Franciscan Melanges in California, USA" in *Proceedings of the 35th U. S. Symposium on Rock Mechanics*, J. K. Daemen and R. A. Schultz, Editors.

Soil Nail and MSE Wall for Stabilization of the Elbow Fill Slide, Snake River Canyon, Wyoming

John P. Turner[1], Wayne G. Jensen[1], John R. Wolosick[2], and Mark Falk[3]

Abstract

Reconstruction of US Highway 26-89 through Snake River Canyon in Wyoming required stabilization of the Elbow Fill Slide and an effective means to support the overlying roadway. A request for design/build proposals resulted in construction of a soil nail wall at the Elbow site. This was the first soil nail wall project for the Wyoming DOT. In cooperation with the Federal Highway Administration, the wall was designated an "Experimental Feature" and an instrumentation and monitoring program was undertaken. Instrumentation includes slope inclinometers for measuring wall deformations and strain gauges attached to the soil nails for the purpose of evaluating mechanisms of load transfer from the ground to the structural components of the wall.

Objectives of the study are to: (1) provide verification of wall performance, especially pertaining to control of landslide movements and resulting damage to the roadway, (2) evaluate field load transfer to the soil nails compared to the loads assumed for design purposes, and (3) evaluate the construction and cost viability of soil nailing as a slope stabilization system, for the purpose of utilizing soil nails in similar, future projects.

This paper summarizes the site conditions, design aspects, and construction of the soil nail wall. Performance of the wall, based on field observations of ground movements and load transfer in soil nails, is described and discussed.

Background and Site Conditions

US Highway 26-89 through Snake River Canyon in northwest Wyoming is a two-lane road constructed in 1947. The entire 24-mile section through the canyon is under reconstruction so that it can accommodate increased traffic volumes and be brought up to current design standards. Most of this route is in a narrow corridor between the Snake River and steep mountainous terrain. One of the most narrow portions of the route is a section approximately 1000 ft long at milepost 131.8 near a point where the Snake River makes a nearly 90 degree bend, with flow changing from a southerly to a westerly direction, as shown in Figure 1. This large bend is locally termed the "Elbow".

---

[1] Dept. of Civil & Architectural Engineering, University of Wyoming, Laramie, WY 82071
[2] Hayward Baker, Inc., 419 Crossville Rd., Suite 101, Roswell, GA 30075
[3] Engrg. Geologist, Wyoming Dept. of Transportation, P.O. Box 1708, Cheyenne, WY 82002

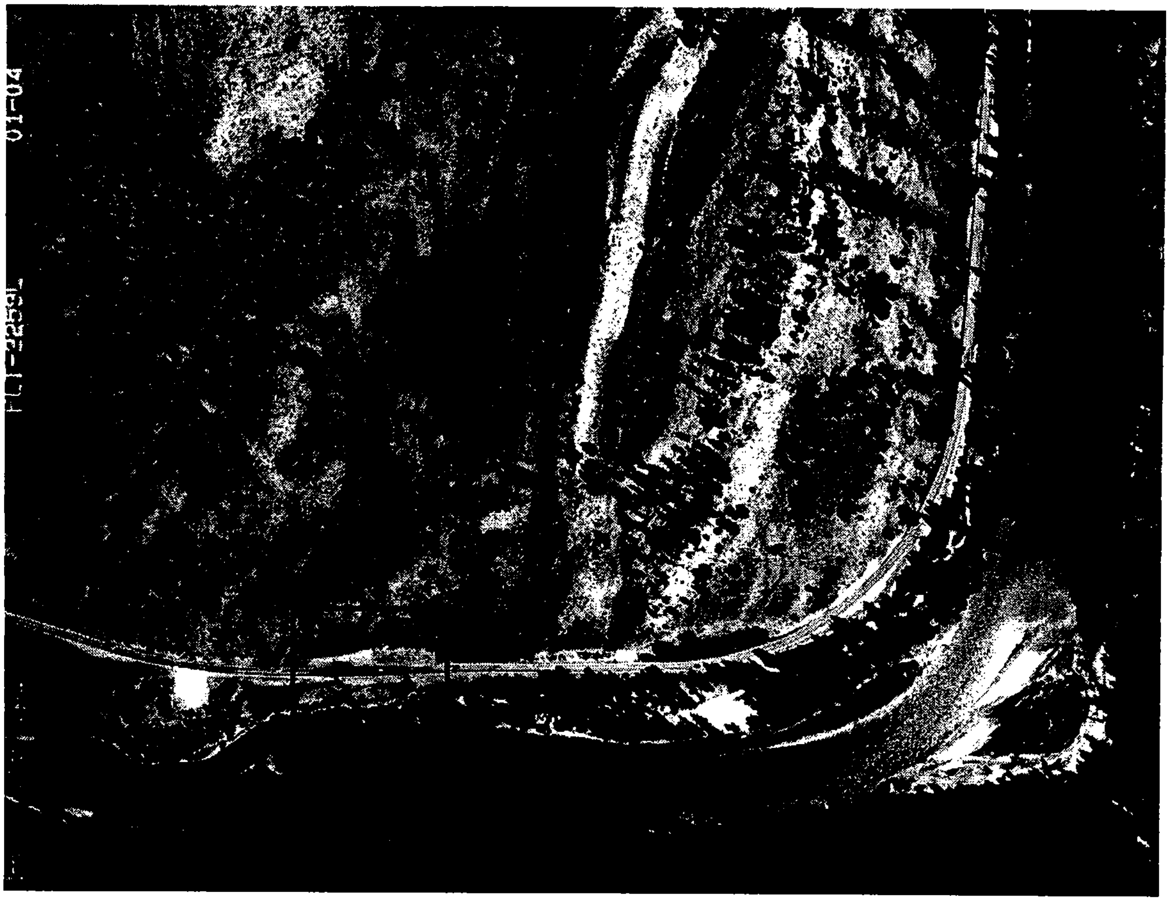

Figure 1. The Elbow site, with slide area outlined in box.

Geological Setting

From the "Elbow" to the west end of Snake River Canyon at Alpine, the Snake River cuts through Paleozoic and Mesozoic sedimentary rocks of the Wyoming-Idaho Overthrust Belt (Love and Christiansen, 1985). This physiographic region is characterized by northward trending low-angle thrust faults along which thousands of feet of marine sedimentary rocks were displaced eastward about 50-150 million years ago. This thrust faulting has resulted in outcrops of the various formations being repeated through this section of the canyon (Albee, 1968). In addition, the river is cutting through the ridges in a direction generally parallel to the dip of the beds (west). This combination of downcutting by the Snake River and repetition of formations has led to geotechnical problems wherever the roadway intersects certain rock units which are particularly prone to landslides.

The geomaterials involved in many of the slope stability problems in the canyon are associated with the Cretaceous Bear River Formation. The upper and lower portions of this formation consist of weathered and decomposed clay shales which are very moisture sensitive (high plasticity, expansive, low shear strengths). Throughout the canyon there are numerous landslides and mudflows within the Bear River Formation or in colluvial and residual soils derived from rocks of the Bear River Formation. Some of the slides in this formation that have resulted in significant roadway damage in recent years include Wolf Mountain Slide, Blue Trail Slide (Turner et al. 1998), Deer Creek Slide, and the Elbow Slide.

The Elbow Slide

The existing roadway through the Elbow section consists of two 11-ft wide travel lanes with virtually no shoulders. The new roadway will consist of two 12-ft travel lanes and 8-ft wide shoulders. To widen the template of the road, significant amounts of cutting and filling would be required. However, two conditions at the Elbow location limit the amount of cut and fill that is possible. First, the Snake River at this site has changed course within the past 10 years and began to erode the toe of the highway embankment. This erosion created a situation in which the 65-ft high fill slope became marginally stable. The resulting slow-moving landslide is designated the "Elbow Slide" and extends from its toe at the Snake River approximately 400 ft RTCL of the existing roadway to approximately 1200 ft LTCL above the road. Arcuate cracks in the roadway indicating this instability appeared in 1996, although no large displacements have been observed. The slide has caused continual minor road damage for several years, generally requiring patching once or twice a year since it was first recognized.

Secondly, the unstable fill lies adjacent to a slowly creeping large landslide which extends approximately 1500 ft above the roadway. At approximately station 20+200 there is a contact between the active Elbow Slide in the Lower Bear River Formation and potentially unstable interbedded shale in the Upper Gannett Group. Initially, the proposal was to cut into the backslope to move the road away from the migrating river. However, it was determined that cutting into the backslope could possibly trigger movement in the ancient landslide complex within the Gannett Group. Considering this restraint, a consultant investigating this slide in 1989 recommended that the roadway be moved as far toward the river as possible, to avoid all cutting through this area and to create a toe berm to resist movement of the slide (Chen-Northern, 1989). In addition, this template required installation of some type of retaining structure to provide the additional required roadway width. Specifically, this plan necessitated the building of retaining walls out toward the river in the narrow section from station 20+150 to 20+410.

A further challenge was recognized when the geotechnical investigation revealed very poor foundation conditions for placement of a wall. It was determined that the existing embankment would not provide adequate support, and building a wall without some type of foundation improvement would increase the risk of a slope failure below the wall. Furthermore, the road had to remain open to at least single lane traffic during construction. This restriction precluded simply removing the poor material and replacing it with a standard reinforced embankment.

In September 1997, the Wyoming Department of Transportation issued a request for proposals (RFP) soliciting a design/build solution to this wall and foundation problem.

A proposal from Hayward Baker, Inc. was selected as the preferred alternative. The proposed design consisted of a system of tiered soil nail walls combined with a mechanically stabilized earth (MSE) wall. Soil nailing is a construction technique in which passive, tension-resisting elements are installed in the ground to create a reinforced soil mass in-situ. The reinforced soil mass provides lateral and/or vertical support for excavations or slope stabilization and acts to resist ground movements. Reinforcing elements (or nails) typically are steel bars which can resist tensile, bending, and shear stresses. Nails may be driven directly into the ground, or placed in a drilled hole and grouted along their entire length. The basic design concept for soil nailing is that earth pressures and external loads are transferred directly to the nails in the form of tensile forces. Nail forces are then transferred into the surrounding soil through friction mobilized at the soil/nail interfaces.

In the proposed design, a lower soil nail wall varying in height from 6-10 ft with 40 ft long soil nails would reinforce the existing embankment and act as the foundation for the MSE wall. An upper soil nail wall varying in height from 13-25 ft with soil nails extending 33 ft into the slope would provide support for the existing roadway during and after construction of the MSE wall. The MSE wall would consist of geogrid-reinforced backfill and modular block facing. The MSE wall would provide the additional width needed for the new roadway. The final configuration results in the roadway being supported partly by the upper soil nail wall and partly by the MSE wall. Figure 2 shows a typical section through the proposed soil nail and MSE wall.

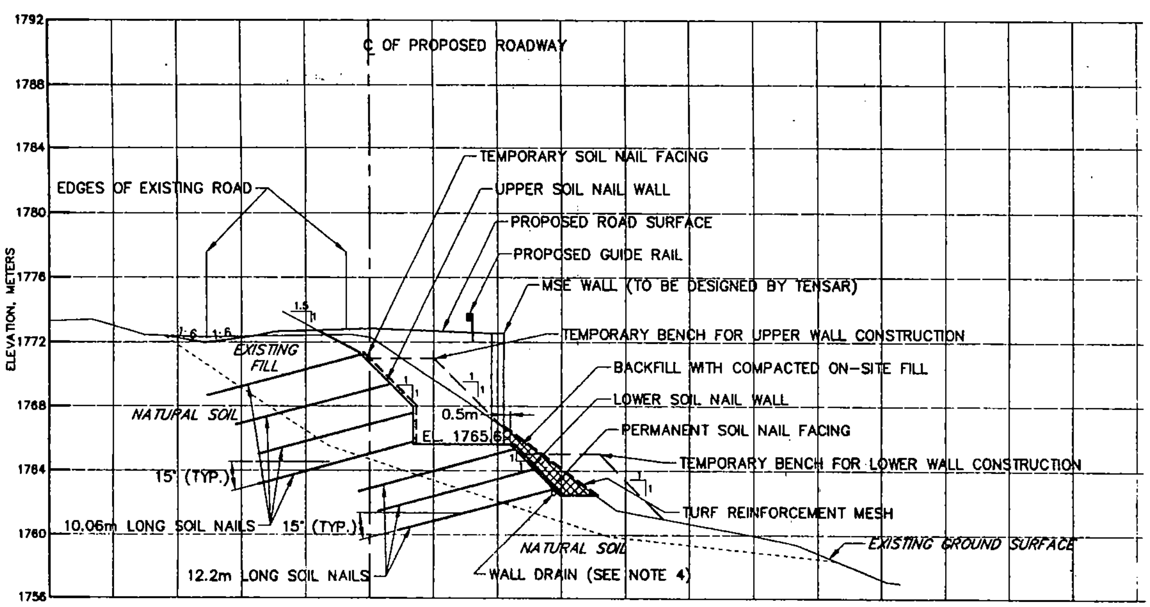

Figure 2. Typical section, soil nail details, and facing details.
(Source: Plan and Profile of State Highway, Alpine Jct.-Hoback Jct., Elbow Section)

Summary of Design

As summarized by Juran and Elias (1991) the basic steps involved in soil nail wall design are as follows:

1. For the specified structural geometry, ground profile, and boundary loadings, estimate working nail forces and location of the potential sliding surface.

2. Select the reinforcement type and verify local (or internal) stability at each reinforcement level, that is, verify that nail resistance is sufficient to withstand the estimated working forces with an acceptable factor of safety.

3. Verify that global stability of the nailed-soil structure and the surrounding ground is maintained during and after excavation with an acceptable factor of safety.

4. Estimate the system of forces acting on the facing and design the facing for specified architectural and durability criteria.

5. For permanent structures, select corrosion protection relevant to site conditions.

6. Select the drainage system for groundwater piezometric levels.

The soil nail and MSE wall at the Elbow was proposed by Hayward Baker, Inc., Atlanta, GA, with engineering design services provided by D'Appolonia Engineers. Preliminary design geometries such as shown in Figure 2 were based on ground profiles, traffic loading, and assumed failure planes derived from the RFP issued by WYDOT and based on WYDOT and consultants site investigations (Step 1). A cross section of the existing subsurface conditions at Station 20+350 is shown in Figure 3. The site is underlain by fill (sand, gravel, and cobble layers or SGC) overlying colluvium (clay and sandy clay layers) to bedrock, which consists of Bear River Formation shale. The failure surface at Station 20+350 is believed to be at the contact between the SGC materials and underlying clay layers. Strength properties assumed for design purposes were as follows: existing fill (SGC layers): $\phi = 29$ degrees, cohesion = 3 kN/m^2; native soil (clay and sandy clay layers): $\phi = 31$ degrees, cohesion = 4 kN/m^2; MSE backfill: $\phi = 33$ degrees, cohesion = 33.5 kN/m^2.

For both local and global stability analyses (Steps 2 and 3), estimates of nail pullout capacity are required. Pullout resistance is provided by side resistance (or friction) at the nail/soil interface, which is the sum of the ultimate unit shearing resistance (τ_u) acting over the surface area of the interface and given by:

$$\tau_u = \gamma h \tan \delta \qquad (1)$$

where γ = soil unit weight, h = overburden height above the nail, and δ = interface friction angle. Although several researchers have attempted to develop rational methods or empirical correlations with in-situ tests to evaluate the interface friction angle, the current state of practice is to estimate nail pullout capacities from field experience. Field pullout tests are then conducted at the job site to verify these values for final design, or to make changes if necessary. For the Elbow site, ultimate unit side resistances were assumed to be 6 psi in the existing fill materials (SGC) and 15 psi in the natural soils underlying the fill (clay and sandy clay layers).

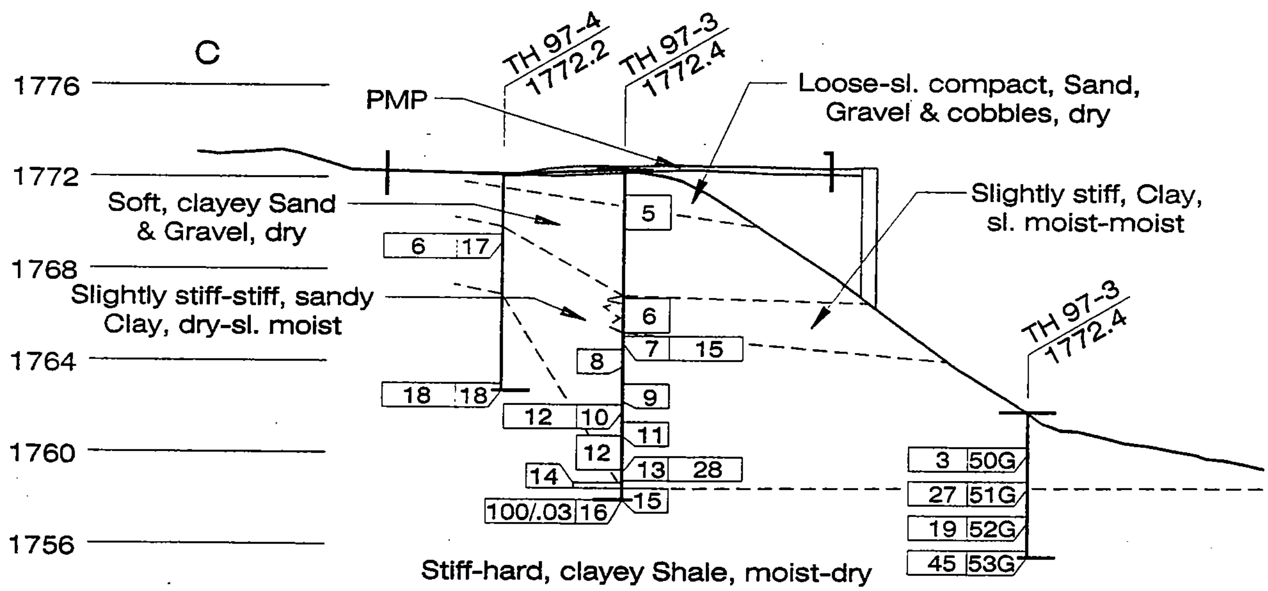

Figure 3. Site conditions at Station 20+350, Elbow Section (Source: WYDOT 1997).

Analysis of internal stability (Step 2) is based upon estimating the tensile forces generated in the nails during construction and for in-service conditions. The limiting factors that are considered in analyzing working loads in individual nails include (1) tensile strength of the nail tendon, (2) pullout capacity of the nail, and (3) the grout-tendon bond strength (FHWA, 1996). The steel bars used as nail tendons are selected to provide adequate tensile strength, based on yield stress of the steel. For the Elbow soil nail walls, these internal stability parameters were analyzed using the SNAIL computer program (Caltrans, 1991) and the Load Resistance Factor Design (LRFD) method as specified in the FHWA soil nail wall design manual (FHWA, 1996). These analyses resulted in the design parameters summarized in Table 1.

Table 1. Summary of Design for Internal Stability

Wall	Nail Length (ft)	Grouted Nail Diameter (in)	Horizontal Nail Spacing (ft)	Bar Size and Tensile Capacity
Upper	33	6	7	#8 47.1 kips
Lower	40	6	6	#10 73.6 kips

Global stability analysis of soil nail walls (Step 3) is accomplished by applying traditional limit equilibrium methods for slope stability. Although several different procedures may be used, all involve analyses which take into account the shearing, tension, and/or pullout resistance of the nails crossing the potential failure surface. Differences between the various methods involve assumptions about the shape of the failure surface (circular, bi-linear, parabolic, etc.) and the nature of interaction between the nails and surrounding soil (whether tension only or tension, shearing, and bending resistance of the nails are taken into account). For the Elbow walls, the computer program UTEXAS2 (Edriss and Wright, 1987) was used to analyze global stability, assuming circular failure surfaces, tension only in the nails, and using the nail parameters summarized in Table 1. The target factor of safety for global stability was 1.5. Final analyses of several sections along the wall yielded global factors of safety against slope failure ranging from 1.5 to 1.7 (D'Appolonia 1998).

Facing design (Step 4) must account for structural, architectural, and durability requirements. Since the upper wall will be covered by a permanent MSE wall, the upper wall facing is considered temporary and was designed under the assumption that it would not be required to carry long-term loads. The temporary facing consists of three layers of welded wire fabric overlying a layer of woven geotextile to prevent local sloughing of soil until the MSE wall is constructed. The lower wall was designed with a permanent facing. Analysis of punching shear and flexure at the nail/facing connection resulted in a design which consists of 8.5-inch thick shotcrete (4000 psi) reinforced by W4.0 x W4.0 welded wire fabric. In addition, at each nail the facing is reinforced with two, 3-ft long #5 bars in the vertical direction and two continuous #5 bars in the horizontal direction to act as walers. The permanent facing was then covered by compacted backfill soil and erosion protection matting. Since neither soil nail wall facing will be exposed once construction is completed, architectural considerations were not relevant.

Corrosion protection (Step 5) included the use of epoxy coated steel bars for the soil nails and providing adequate cover of shotcrete for the wire mesh in the permanent facing of the lower wall. Drainage features (Step 6) include geocomposite drainage sheets behind the permanent facing and plastic drainage pipes at the bottom of the lower wall extending from behind the facing through the overlying fill.

Construction

Construction began on August 15, 1998. Because this area is in designated critical habitat for bald eagles, construction is prohibited during eagle mating season, considered to be between February 15 and August 15. The soil nail walls were completed in early December, 1998. Due to weather and environmental restrictions, it wasn't feasible to begin building the MSE wall upon completion of the soil nail walls. Construction of the MSE wall is scheduled to begin on August 15, 1999, again to comply with bald eagle habitat restrictions. The Elbow wall is part of a 5-mile long reconstruction project which is scheduled for completion by October 31, 1999.

Soil nailing was selected for this project because it was determined to be more economical, based on construction costs, than a soldier pile and drilled and tensioned tieback anchor system. Soil nails were installed at 15 degrees from horizontal. Each soil nail consisted of epoxy-coated 1-inch diameter (upper wall) or 1-1/4-inch diameter (lower wall), GR75 deformed steel bars. The bars were placed in 7-inch diameter drill holes and grouted using neat cement grout.

Soil nails were installed using hydraulic powered drill rigs with rotary drilling techniques including tri-cone roller bits and/or down-the-hole-hammer drilling tools (Figure 4). Typically, compressed air was used as the flushing medium for the drill cuttings. The drilling was often difficult when boulder fill and talus were encountered. The soil nails were installed by placing the steel bars directly in boreholes whenever possible. However, when caving conditions were encountered, the holes were drilled using steel casing, and the nails were placed within the casings. The casings were then withdrawn, and neat cement grout, consisting of portland cement and water (water/cement ratio of 0.45) was injected from the bottom of the hole using tremie tubes, filling the drill hole from the bottom up. The steel casings were then withdrawn as the drill holes were kept filled with grout.

The lower wall, which was constructed first, is located approximately 30 ft below the roadway elevation, and is 725 ft (221 m) long. The lower wall contains approximately 308 soil nails, 40 ft (12.2 m) in length and spaced at 4 ft (1.2 m) vertically and 6 ft (1.8 m) horizontally. The facing for the lower wall consists of reinforced shotcrete, 8.5 inches in thickness. The bottom of the lower wall is located approximately 42 ft (13 m) below roadway level and a few meters above the Snake River. Figure 5 shows a nail in the lower wall being proof load tested. Note the wire mesh, shotcrete, and geocomposite sheet drains. Final plans call for the lower wall to be buried in a structural fill, so that it is not seen in the final configuration of the slope stabilization system.

The upper wall is located just below the elevation of the existing roadway, and extends to an elevation of about 25 ft (8 m) below the existing roadway elevation. The upper wall is 743 ft (226.4 m) in length along the road. The wall contains 418 soil nails that are 33 ft (10 m) in length. The spacing of the nails is 5.5 ft (1.68 m) horizontally and 7 ft (2.13 m) vertically. Since the upper wall will be buried by the MSE wall, the facing was designed as a temporary measure, and consists of three layers of heavy welded wire fabric over a woven geotextile (Figure 6). A 23-ft wide horizontal bench, where the modular block wall will be placed, currently separates the two walls. The modular wall will consist of

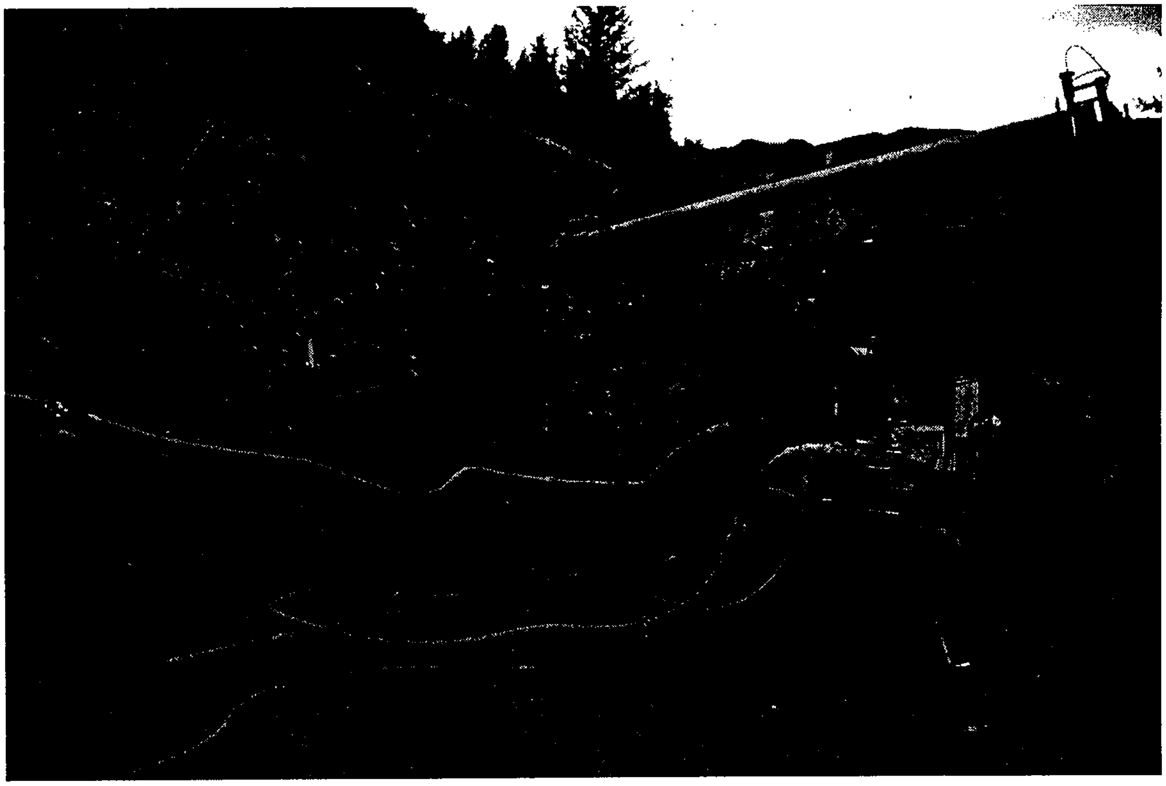

Figure 4. Drilling soil nails for lower wall.

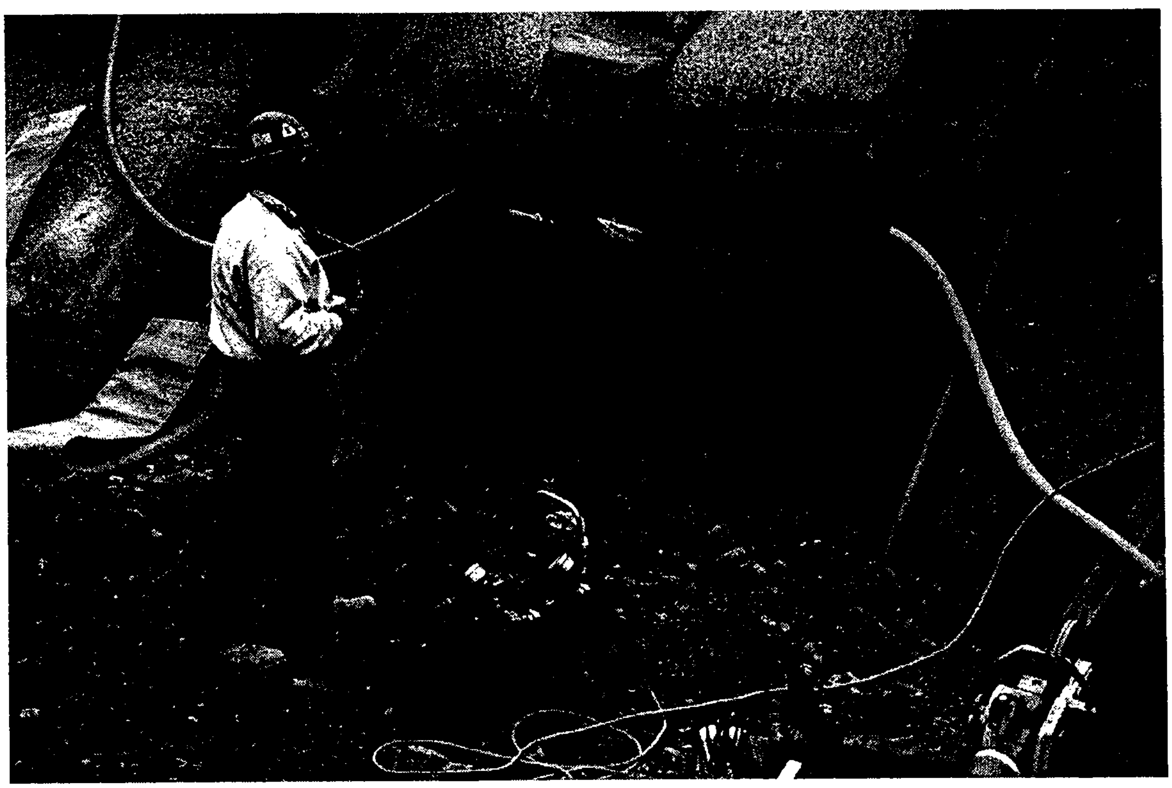

Figure 5. Proof load test on soil nail.

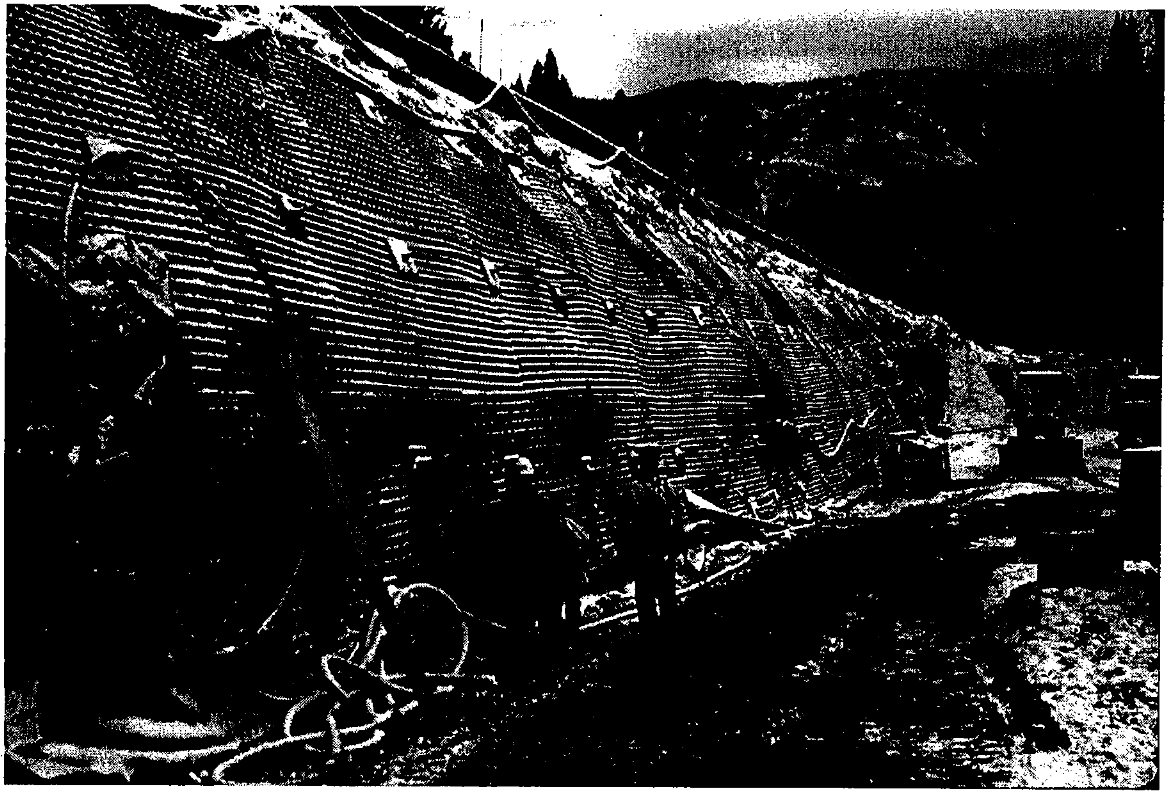

Figure 6. Temporary facing, upper soil nail wall.

Keystone Compact blocks and geogrids with select backfill. The modular block wall will be up to 25 feet in height and will total 12,000 square feet.

Instrumentation and Monitoring

The soil nails at one vertical section (Station 20+350) are instrumented with vibrating wire strain gauges attached to the steel bar of each nail. Strain gauges are oriented at the three o'clock position with respect to the vertical axis of the nail cross-section as shown in Figure 7. Placement of the strain gauges at this position is intended to minimize the potential for bending interference and maximize the possibility of measuring pure axial strain, as utilized by Thompson and Miller (1990) in a similar application.

At Station 20+350, the upper wall has four nails arranged slightly off vertical and the lower wall has three nails arranged in a similar manner (Figure 6). The four instrumented nails in the upper wall have five strain gauges welded to each nail, with the gauges evenly spaced along the length of each nail. The three instrumented nails in the lower wall have four evenly spaced strain gauges welded to each nail. Strain gauges are being monitored electronically using a datalogger and two multiplexers housed in a protective box. The monitoring installation is powered by a solar panel and battery. Stored data are downloaded to a laptop computer for analysis. Following installation, it was found that

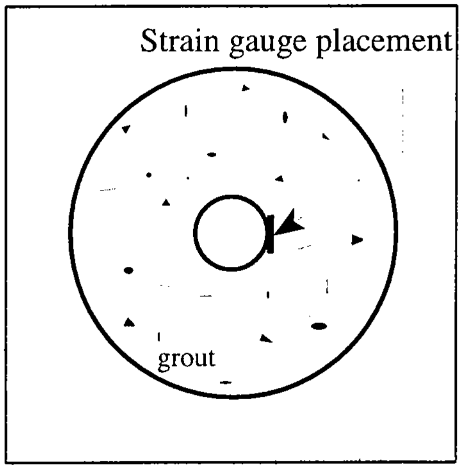

Figure 7. Cross Section of Soil Nail with Strain Gauge Location

the strain gauges in the lowermost soil nail are not providing any output signals. It is not known whether the lead wires were damaged during installation or if some other malfunction occurred.

Two slope inclinometer casings were installed at locations where they will ultimately extend through the MSE wall and the lower soil nail wall. At the present time, the casings extend from the bench above the lower wall down through the lower wall and into bedrock. One casing is close to the west end of the wall (Station 20+205) and the other is at the location of the instrumented nails (Station 20+350) at the east side of the wall. Ground deformation is currently being monitored at these locations to determine if slope movements occur before placement of the MSE wall, and will continue to be monitored during and after construction of the MSE wall. Figure 8 is a view of the site as it appeared in December, 1998, shortly after construction of the soil nail walls was completed and the inclinometer casings were installed.

The data collection system is currently programmed to read each strain gauge twice daily and store all measurements. Monthly visits to the site by UW researchers are being made to download strain gauge readings and to take slope inclinometer readings.

Interim Results

Because construction of the wall is not completed, monitoring and analysis of the instrumentation data will not be completed and available until two years after completion of the MSE wall. Results presented herein are considered preliminary and subject to final interpretation. Slope inclinometer measurements are shown in Figure 9. The readings

Figure 8. View of the Elbow site looking east, showing completed soil nail walls. Slope inclinometer installation at Station 20+205 is in the foreground.

shown indicate movements which occurred from the time the casings were installed (11 December, 1998) through 13 March, 1999. At both installations, movements are small, on the order of a few millimeters. These readings indicate that the soil nail walls are effectively controlling slope movements, at least over the limited time since the inclinometer casings were installed. The critical time for ground movements at this site normally occurs in late spring, when snowmelt, high precipitation, and high water levels in the Snake River combine to create high driving forces, high pore water pressures, and toe erosion.

Monitoring of tensile forces developed in the steel bars of the nails provides an opportunity to compare service tensile loads to those assumed in the design. Measured and assumed tensile forces are presented in Table 2. In the upper wall, the top two rows of nails exhibit tensile loads that are slightly above the maximum values assumed for design purposes, while the bottom two rows show maximum tensile forces close to or below the design assumptions. In the lower wall, nails for which measurements are available exhibit tensile forces well below those used for design. Considering the many factors that determine the actual load carried by an individual nail, the measured nail forces are quite reasonable. Discrepancies between assumed and actual loads can be attributed to natural variability, inaccuracies inherent in estimating nail loads using generic material property data, and highly simplified material models (FHWA, 1996).

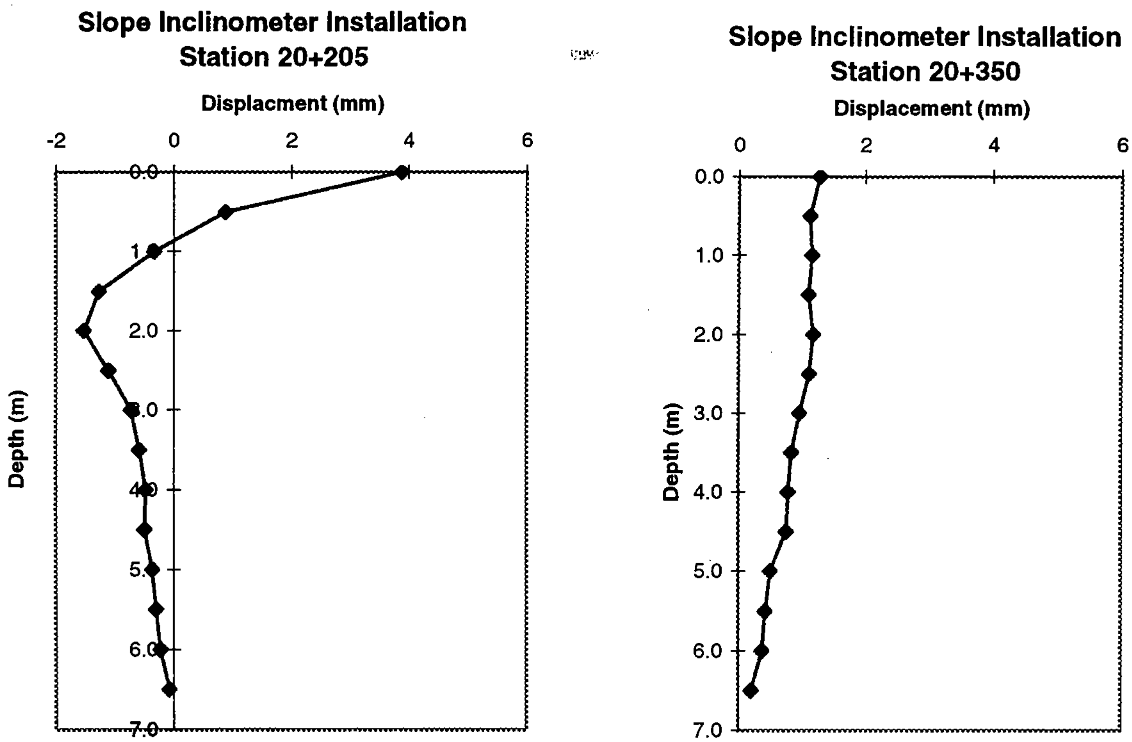

Figure 9. Slope inclinometer measurements of lateral deformation measured between 12/11/98 and 3/13/99.

Table 2. Measured maximum nail tensile forces versus design values.

Soil Nail Row		Design Maximum Tension kips (kN)	Maximum Tension Inferred from Strain Gauges, kips (kN)
(Top)	1	21.3 (95)	23.3 (103.6)
	2	22.9 (101.7)	24.4 (108.7)
	3	21.2 (94.3)	15.6 (69.4)
	4	12.5 (55.7)	12.4 (55.2)
	5	53.8 (239.7)	39.0 (169.2)
	6	57.3 (255.1)	29.7 (132.0)
(Bottom)	7	52.2 (232.1)	no reading

Summary and Conclusions

A combined soil nail and MSE wall provides a practical and cost-effective solution to the difficult site conditions posed by roadway reconstruction and widening at the Elbow fill slide. Problematic conditions at this site include a marginally stable fill which has undergone slope movements and caused continual roadway damage since 1996, a potentially unstable and large ancient landslide which prohibits cutting into the backslopes, poor foundation conditions for construction of retaining walls, and limited space between the Snake River and the roadway alignment. The solution selected for this site was to underpin the existing roadway with a soil nail wall to allow construction of an MSE wall which will eventually support a widened roadway. The poor foundation conditions were addressed by first constructing a lower soil nail wall which will serve as a foundation for the MSE wall. Soil nailing has the added advantage of providing constructibility in limited access space while allowing the road to be open to traffic. These technical and constructibility factors led to the selection of soil nailing combined with an MSE wall for the Elbow site.

Because the Elbow wall is the first application of soil nailing for a WYDOT project, an instrumentation and monitoring program was implemented, consisting of strain gauges attached to the steel bars of the nails at one vertical section of the wall and slope inclinometer installations at two locations. Interim results reported herein indicate that slope movements since construction of the soil nail walls are minimal and tensile forces mobilized in the nails are within the values assumed for design. Continued monitoring before, during, and after construction of the MSE wall will allow the investigators to assess mobilized nail forces for a combined soil nail/MSE wall system. In addition, no soil nail wall constructed at an active slide has been instrumented, monitored, and reported in the literature, according to Holtz and Schuster (1996). This research should provide valuable information for designing soil nail walls for similar applications.

Acknowledgments

The authors would like to thank the Wyoming Department of Transportation for the opportunity to participate in this unique project. Mike Hager and Jim Dahill of the WYDOT Geology Branch were particularly helpful. Brad Campbell of D'Appolonia was the design engineer for the Elbow soil nail walls and generously shared his expertise and design calculations with the authors. Mr. John King of Seismic Imaging installed the strain gauges and data acquisition equipment. The authors express their sincere thanks to all of these individuals.

References

Albee, H.F. (1968). "Geologic Map of the Munger Mountain Quadrangle, Teton and Lincoln Counties, Wyoming", *GQ-705*, U.S. Geological Survey.

Caltrans (1991). "A User's Manual for the SNAIL Program", California Department of Transportation, Office of Geotechnical Engineering, Sacramento, CA.

Chen Northern Inc. (1989). "Report of Geotechnical Investigation, Alpine Junction-Hoback Junction", Project No. 88-638.

Edriss, E., Jr., and Wright, S.G. (1987). "UTEXAS2 Slope Stability Package", prepared for U.S. Army Corps of Engineers.

D'Appolonia (1998). "Final Design Summary and Calculations Brief, Soil Nail Walls, Elbow Section, Lincoln County, Wyoming", Project No. 973109A, prepared for Hayward-Baker, Inc., Roswell, GA.

FHWA (1996). "Manual for Design & Construction Monitoring of Soil Nail Walls", *Publication No. FHWA-SA-96-069R*, U.S. Department of Transportation, Federal Highway Administration, Washington, D.C.

Holtz, R.D. and Schuster, R.L. (1996). "Stabilization of Soil Slopes", Ch. 17 in *Landslides: Investigation and Mitigation, Special Report 247*, edited by A.K. Turner and R.L. Schuster, Transportation Research Board, National Academy Press, Washington, D.C., pp. 439-473.

Juran, I. and Elias, V. (1991). "Ground Anchors and Soil Nails in Retaining Structures", Chapter 26 in *Foundation Engineering Handbook*, 2nd Edition, edited by H.-Y. Fang, Van Nostrand Reinhold, New York, pp. 868-905.

Love, J.D., and Christiansen, A.C. (1985). Geologic Map of Wyoming, U.S. Geological Survey, scale: 1:500,000.

Turner, J., Hasenkamp, R., and Wolosick, J. (1998). "Micropile and Tieback Reinforced Walls for Landslide Stabilization, Snake River Canyon, WY", *Proceedings*, 49th Highway Geology Symposium, Arizona DOT, Prescott, AZ.

Thompson, S.R. and Miller, I.R. (1990). "Design, Construction, and Performance of a Soil Nailed Wall in Seattle, Washington", *Design and Performance of Earth Retaining Structures, Geotechnical Special Publication No. 25*, edited by P.C. Lambe and L.A. Hansen, ASCE, New York, NY, pp. 629-643.

SLOPE FAILURE REMEDIATION
USING
GEOGRID REINFORCEMENT

By:

B. Dan Marks, Ph.D., P.E.
Chief Geotechnical Consultant/Vice President
S&ME, Inc.
44 Buck Shoals Road, Suite G-9
Arden, North Carolina 28704
(828) 687-9080

50TH ANNUAL HIGHWAY GEOLOGY SYMPOSIUM
Hotel Roanoke & Conference Center
Roanoke, Virginia
May 20 – 23, 1999

SLOPE FAILURE REMEDIATION USING GEOGRID REINFORCEMENT

INTRODUCTION

Construction of airports in mountainous physiographic and geologic provinces requires massive excavation and fill placement. Prominent ridgelines are typically excavated by blasting, and sidehill embankments are constructed over natural slopes to provide sufficient area for airport development. While this method of construction is commonplace in mountainous areas, geologic conditions at the Tri-State Airport in Huntington, West Virginia are such that typical mountainous construction methodology must be supported by sound geotechnical engineering evaluations, analyses, and design.

Subsurface conditions at the Tri-State Airport generally consist of variable depth residual soils overlying interbedded sandstone and shale formations. Residual soils are typically deeper and consist of moderate to highly plastic fine to medium sandy silty clays where the upper parent bedrock stratum is shale. Conversely, residual soils are typically shallower and consist of silty fine to medium sands where the upper parent bedrock stratum is sandstone. As such, the depth of the residual soil above partially weathered bedrock is typically directly related to the weathering resistance characteristics of the parent bedrock.

Existing geologic conditions result in geotechnical engineering complexities with most projects where sidehill embankments must be constructed. Variability in weathering resistance characteristics of sandstone and shale formations coupled with the presence of steep natural drainage features create irregular excavation/embankment (cut to fill) contacts. As such, sidehill embankments typically vary significantly in volume, depth, and lateral extent over short distances as these natural drainage features are filled with embankment material. In addition, natural drainage features often contain seeps or springs where groundwater flows from more pervious sandstone in the interbedded sandstone/shale geologic profile.

Materials excavated from prominent ridgelines that are reused for sidehill embankment construction consist of a mixture of residual soils (sands and clays), shale, and sandstone. The silty fine to medium sand residual soils and the sandstone bedrock materials provide excellent embankment fill materials. The fine to medium sandy silty clay residual soils and shale materials are less desirable embankment fill materials. However, these less than desirable embankment fill materials must be incorporated into the sidehill embankments since wasting of these materials would be economically prohibitive.

Although excavated shale can typically exhibit very hard and seemingly durable characteristics when initially excavated, most shales weather and/or deteriorate rapidly, particularly in the presence of water. Incorporation of deleterious shale into general embankment fill placed within natural drainage features containing seeps or springs results in moisture accumulation and significant shear strength reduction. Without proper consideration of shear strength loss of shale materials during geotechnical engineering analyses and embankment design, instability of sidehill embankment slopes is often the result. Since embankment sections are more massive in natural drainage features and the presence of seeps and springs is more likely within the natural drainage features, the areas of embankment instability and prevalent locations of embankment slope failures are within the natural drainage features. Sidehill embankment slopes intermediate of natural drainage features are typically stable because of the reduced volume of the sidehill embankments.

PROJECT BACKGROUND

During the period of 1976 to 1978, an embankment slope failure occurred along the Service Road near Building No. 8 at the Tri-State Airport in Huntington, West Virginia. The embankment slope failure, which involved an estimated 5000 to 6000 cubic yards of embankment fill material during the initial failure, removed a portion of the Service Road. Since failure occurred in an area where the Service Road could be realigned, the slope failure was not repaired. The failure mass increased in volume to about 8000 cubic yards and continued to move over the next fifteen to seventeen years. Construction debris and waste soil and aggregate materials were continually placed on the headscarp of the failure area which aggravated the progressive failure condition. In 1981, the West Virginia Department of Transportation conducted a subsurface exploration program within the embankment slope failure area. Findings of this subsurface exploration program revealed that this slope failure was within a natural drainage feature; however, no remedial slope failure design was developed.

On or about January 14, 1993, an embankment slope failure involving about 7000 cubic yards of material occurred along the Service Road adjacent to Building No. 6 occupied by D-G Airways, Inc. This failure resulted in closure of the Service Road and partially undermined foundations of Building No. 6. Slope movement in this area reportedly began about November, 1992 when approximately two inches of subsidence was observed along the Service Road in the failure area. Over the next two months the Service Road subsided an additional twelve to eighteen inches. Coarse aggregate base stone was placed in the failure area to level the Service Road.

At or about the same time as the larger slope failure, a small embankment slope failure occurred beyond the original Service Road embankment slope failure at Building No. 8. This small embankment slope failure involved an estimated 1000 cubic yards of material. The headscarp of this slope failure encroached to the outside edge of the Service Road pavement and received little attention from maintenance personnel.

On or about Thursday, January 21, 1993, the author of this paper was contacted and provided photographs of the failure area, building foundations, and cracks within the floor slab of Building No. 6. Subsequent to review of the provided information and discussions with Mr. Larry Salyers, Tri-State Airport Manager, S&ME, Inc. recommended that aircraft be removed from Building No. 6 on Friday, January 22, 1993 until such time that an on-site inspection of the structure could be made. Inspections of the failure areas and Building No. 6 were made on Monday, January 25, 1993. At that time S&ME, Inc. recommended that normal aircraft maintenance and repair operations could continue in Building No. 6 in areas away from the structurally distressed (cracked) floor slab adjacent to the Service Road embankment slope failure.

During inspection of the slope failure areas, limited topographic survey data were obtained to allow initiation of the geotechnical engineering analyses associated with development of remedial slope failure repair alternatives. In addition, boreholes for the subsurface exploration program were located within and adjacent to the embankment slope failures. The subsurface exploration program was initiated on January 26, 1993 and completed by January 28, 1993. A detailed inspection of Building No. 6 was made on January 26, 1993 during which time a detailed mapping of all cracks and other structural distresses was completed. This detailed inspection was followed by the installation of crack monitor gages at selected critical locations to monitor potential future movement of the structure.

REMEDIAL SLOPE REPAIR ALTERNATIVES

On February 18, 1993, three alternative remedial repair schemes with cost estimates were presented for consideration by the Tri-State Airport Authority, and representatives of the Federal Aviation Administration (FAA) and the West Virginia Department of Transportation. These alternative remedial repair schemes were presented for consideration based upon adequacy to maintain stability, constructibility, and economics. The three alternative remedial repair schemes consisted of the following: 1) a geogrid-reinforced embankment; 2) a shot-rock buttress stabilized embankment; and 3) a soldier-beam and lagging retaining structure. The West Virginia Department of Transportation had suggested Alternative No. 3 (soldier-beam and lagging wall) as a remedial repair scheme during the exploration of the original embankment slope failure in 1981.

The geogrid-reinforced embankment remedial repair alternative consisted of the use of uniaxial geogrid reinforcement so that the exterior embankment slopes could be reconstructed to about 1.5:1 to 2:1 (horizontal to vertical). The geogrid-reinforced embankment section provided for an extensive subdrain and blanket drain system to collect and remove groundwater seepage and infiltrating surface water to reduce the potential for saturation of the embankment fill material.

The shot-rock buttress stabilized embankment remedial repair alternative consisted of a more nearly conventional method of slope failure repair. This alternative consisted of the construction of a durable sandstone shot-rock buttress and a reconstructed embankment section with exterior slopes of 2.5:1 (horizontal to vertical). The shot-rock buttress stabilized embankment section provided an extensive subdrain and blanket drain system to reduce the potential for saturation of the embankment fill material as a result of groundwater seepage and infiltrating surface water.

The soldier-beam and lagging retaining structure remedial repair alternative consisted of the construction of a steel H-pile soldier-beam and timber lagging retaining wall at about the one-third height of the slope and backfilling the reconstructed embankment with an exterior slope of 2:1 (horizontal to vertical). This remedial repair alternative provided an extensive subdrain and blanket drain system to protect the embankment fill material from potential saturation.

Engineer cost estimates for the three remedial repair alternatives were approximately as indicated below:

Alternative No. 1 (Geogrid Reinforcement)	\$1.1M to \$1.2M
Alternative No. 2 (Shot-Rock Buttress)	\$1.2M to \$1.4M
Alternative No. 3 (Soldier-Beam & Lagging)	\$1.3M to \$1.6M

Subsequent to presentation of the alternatives, the Tri-State Airport Authority with concurrence of FAA and the West Virginia Department of Transportation selected the geogrid-reinforced embankment as the most desirable remedial repair alternative. The geogrid-reinforced embankment remedial repair alternative was subsequently bid at approximately \$1,100,000.00.

DESIGN AND CONSTRUCTION

On May 10, 1993, the Design Geotechnical Investigation Report was issued for preparation of the construction plans and specifications. The methodology utilized in the geotechnical engineering analyses associated with design of the geogrid-reinforced embankment consisted of providing adequate factors of safety (1.4 to 1.5) against potential slope failures for an exterior embankment slope of 1.5:1 (horizontal to vertical) while providing a recommended design slope of 2:1 (horizontal to vertical) to increase resistance to surface runoff erosion.

The required primary geogrid reinforcement was specified to be a uniaxial geogrid composed of a minimum of 97.5 percent high-density polyethylene and two percent carbon black. The geogrid was required to have a minimum tensile modulus of 50,000 pounds per foot and a long-term allowable design strength of 1600 pounds per foot. Geogrid meeting these specification requirements was Tensar UX1400HT. Secondary geogrid reinforcement was required within the outer five feet of the embankment slope face where the primary geogrid reinforcement spacing exceeded two feet. The secondary geogrid reinforcement was Tensar BX1100 which is a biaxial geogrid used to increase the stability of the face of the embankment slope and to provide additional resistance to surface erosion.

The geogrid-reinforced embankment section was divided into four zones with each zone being eighteen feet in height at the maximum embankment section. The height of the upper zone

(Zone 4) was variable according to the actual height of the embankment section. The length of geogrid in Zone 1 and Zone 2 (bottom 36 feet) was 49 feet which is one-half the roll length. The bottom zone (Zone 1) had nine layers of geogrid at two feet vertical spacing. The spacing of geogrid in Zone 2 was increased to three feet with the spacing of geogrid in Zone 3 increased to five feet. Two to three layers of geogrid were used in Zone 4 as the embankment height varied and geogrid layer spacing was adjusted for utilities. The secondary geogrid spacing varied from 1.5 to two feet beginning in Zone 2.

The blanket drain system consisted of a minimum three-foot thick layer of No. 57 stone encapsulated by Trevira 1120 nonwoven geotextile. The blanket drain extended beneath the entire bottom width of the new embankment section. The subdrain system which extended upward behind the embankment fill material at the contact of excavated natural material consisted of a two-foot thick layer of No. 57 stone encapsulated in Trevira 1120 nonwoven geotextile. Seepage and infiltrating groundwater intercepted by the subdrain system was collected in a six-inch diameter perforated Schedule 80 PVC pipe extended to a solid outlet pipe.

During construction of one of the maximum geogrid-reinforced embankment sections near Building No. 6, the very hard durable sandstone stratum encountered at auger refusal in some of the soil test borings was found to extend laterally into the embankment section further than anticipated. As such, excavation for placement of appropriate lengths of the geogrid could not be made without blasting prior to excavation of the sandstone. In order to preclude the need for blasting, the configuration of the embankment section was altered to allow for bearing of the new embankment section on the sandstone stratum and steepening a section of the embankment slope to 1.5:1 (horizontal to vertical). Because of the methodology used in the geotechnical engineering analyses leading to design of the geogrid-reinforced embankment, the embankment configuration changes were made without any interruption in the project construction.

Project construction was completed in October, 1993 at a cost of about $900,000.00. These geogrid-reinforced embankment remedial repairs are performing well after about six years since completion of construction. This project was awarded a Consulting Engineer Council of North Carolina Engineering Excellence Award in 1994.

CONCLUSIONS

Remedial repair of the Service Road embankment slope failures at the Tri-State Airport in Huntington, West Virginia coupled with the successful application of geogrid-reinforced embankments and geogrid-reinforced earth retaining structures on other projects have led to the following conclusions relative to the utilization of geogrid reinforcement on airport projects.

1. Geogrid reinforcement of embankments and earth retaining structures provides an economically beneficial and favorably constructable alternative for the design of over-steepened embankment sections in new projects and remedial repair of failed embankment slopes.

2. Geogrid reinforcement of embankments provides maximum flexibility during construction to allow alteration of embankment configurations and other field changes without interruption of project schedules and construction progress.

3. Geogrid reinforcement analyses, evaluations, and designs must be conducted by geotechnical engineers having experience with the behavior of both natural materials and geosynthetics.

4. The author considers the application of geosynthetics in civil engineering projects to be the most significant development in geotechnical engineering in the past fifty years. However, the author cautions that the application of geosynthetics is not to be viewed as a "quick fix" or remedy for the solution of all geotechnical problems and adverse geological conditions.

ACKNOWLEDGEMENTS

The author of this paper and S&ME, Inc. would like to take this opportunity to extend our appreciation to Mr. Larry Salyers, Airport Manager at Tri-State Airport, the Tri-State Airport Authority, and Delta Airport Consultants, Inc., Project Engineer for this project. Without the support of the individuals and organizations, this project would not have been such an award-winning achievement.

I-279 Landslide Repair

by

F. Barry Newman, P.E., Geotechnical/Structural Group Manager, GAI Consultants, Inc., Monroeville, Pennsylvania.

and

William R. Adams, Jr., Ph.D., P.E., P.G., District Geotechnical Engineer, District 11-0, Pennsylvania Department of Transportation, Pittsburgh, Pennsylvania

ABSTRACT

I-279 is a major four-lane artery connecting downtown Pittsburgh, Pennsylvania with its northern suburbs and other key highways to the north. The highway was constructed through hilly terrain resulting in several deep rock cuts and embankment fills to heights of about 100 feet. The construction occurred at the level of the cyclothemic Pennsylvanian age rocks of southwestern Pennsylvania.

Shortly before the completion of I-279, a 300-foot wide landslide occurred in the slope of a 70-foot high embankment. The highway was not immediately affected, but the embankment had to be repaired. This paper describes the geology of the landslide, the exploration, the instrumentation, and the permanent tied-back soldier beam and lagging retaining wall used to stabilize the slope.

INTRODUCTION

The location of the landslide that occurred in June 1989 along the west facing fill slope of I-279, a major four-lane artery connecting Pittsburgh in southwestern Pennsylvania and its northern suburbs, is shown on Figure 1. The landslide did not immediately affect the highway, but required repair to prevent progression into the highway.

Figure 2 shows a plan of the failed area within the 70-foot high west facing slope of the side-hill embankment. The head scarp of the landslide was about 2 to 6 feet high and easily observable. The toe of the movement was not clearly defined because it was within a wooded area beyond the right-of-way. Minor surface cracking from heaving in the toe area was the only visible indication of movement of the toe.

The embankment slope had been in place less than a year when it failed. Although the failure occurred following a relatively wet period, the failure was puzzling because the construction plans required that the toe of the embankment be constructed using rock fill and that all of the embankment fill be keyed and benched into rock. In addition, the fill compaction was monitored and tested. Therefore, an exploration of subsurface conditions was initiated to determine what caused the failure and how to repair it.

GEOLOGY

The highway was constructed in an area underlain by the cyclothemic sedimentary rock strata of the Pennsylvanian age Conemaugh Group including rocks from the lower portion of the Casselman Formation and upper portion of the

Glenshaw Formation. These strata are relatively flat-lying and are composed primarily of claystone (including Pittsburgh red bed) and shale, with lesser amounts of siltstone and sandstone. Winters(1) found that the weak claystone unit known as the Pittsburgh red bed is its thickest (~60 feet) in this portion of Allegheny County. The Ames limestone which is the thin upper unit of the Glenshaw Formation is present below the embankment. The Morgantown sandstone of the Casselman Formation is exposed in the cut slope above the level of the landslide on the east side of I-279. The site is located approximately one half mile northwest of the axis of the southwesterly plunging Mt. Nebo syncline and the strata dip gently to the southeast. Figure 3 from Wagner (2) shows the geologic column at the landslide.

Soils derived from weathering of these rock strata tend to be residual on hill tops and colluvial on the hill sides and at the toes of the slopes. Figure 4 shows the topography prior to construction of the highway. The lower portions of the slope contains remnants of prehistoric landslides which are typical of the region and a contributor to the problem. The colluvial soils derived from weathering of the Pittsburgh red bed claystone are notoriously landslide-prone and contained weak slickensided shear planes with low residual shear strengths. Gray (3) and Hamel (4) give detailed discussions of these types of colluvial soils.

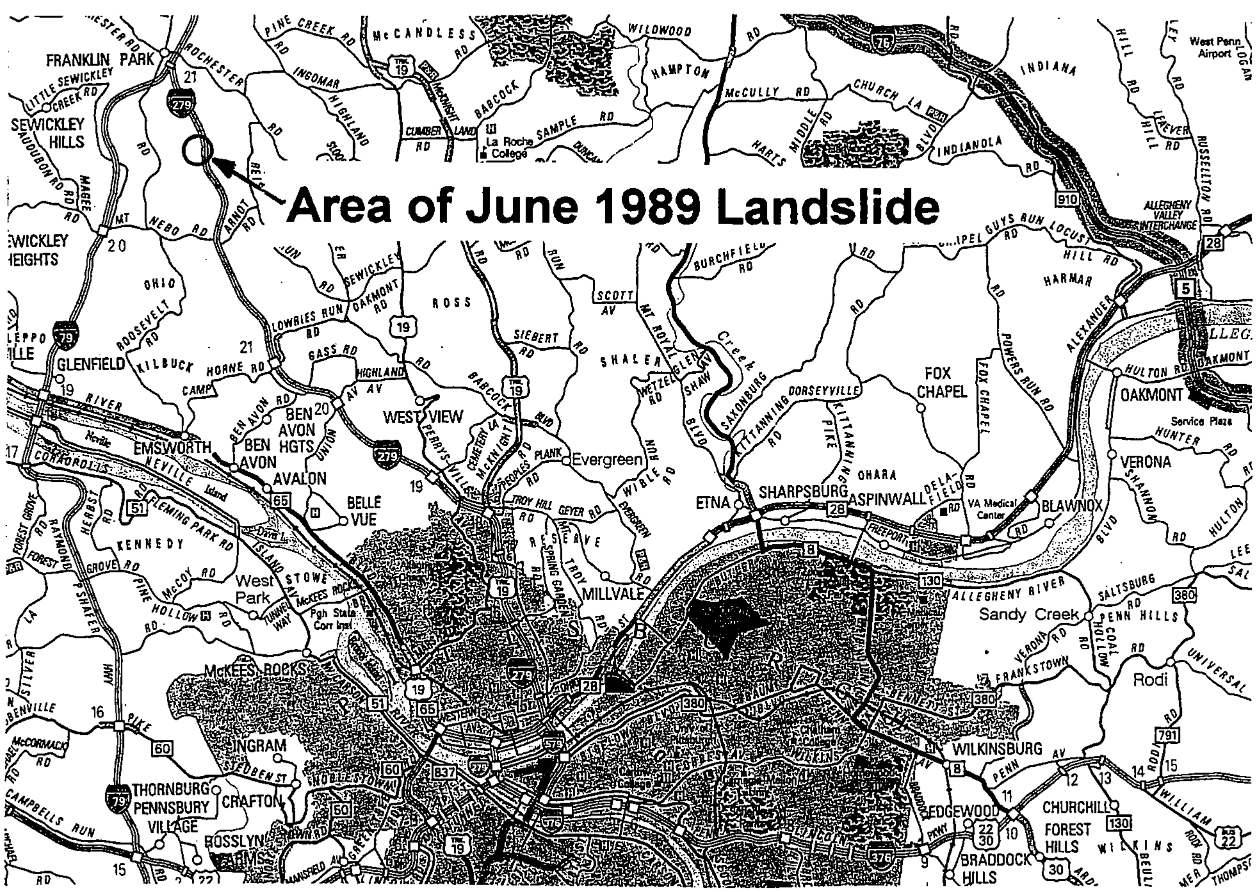

Figure 1 - Location of Landslide

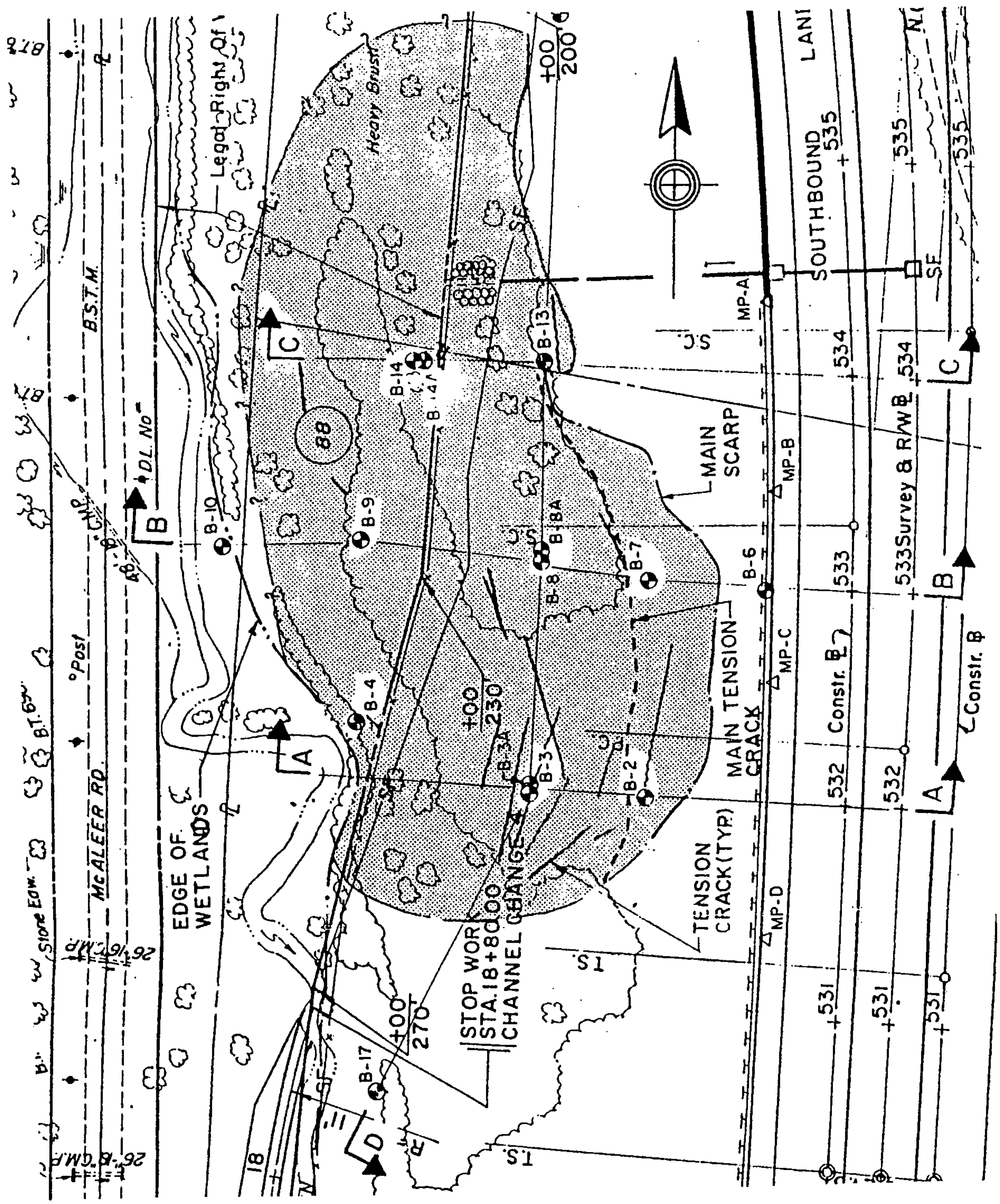

Figure 2 - Plan of Landslide Area and Borings

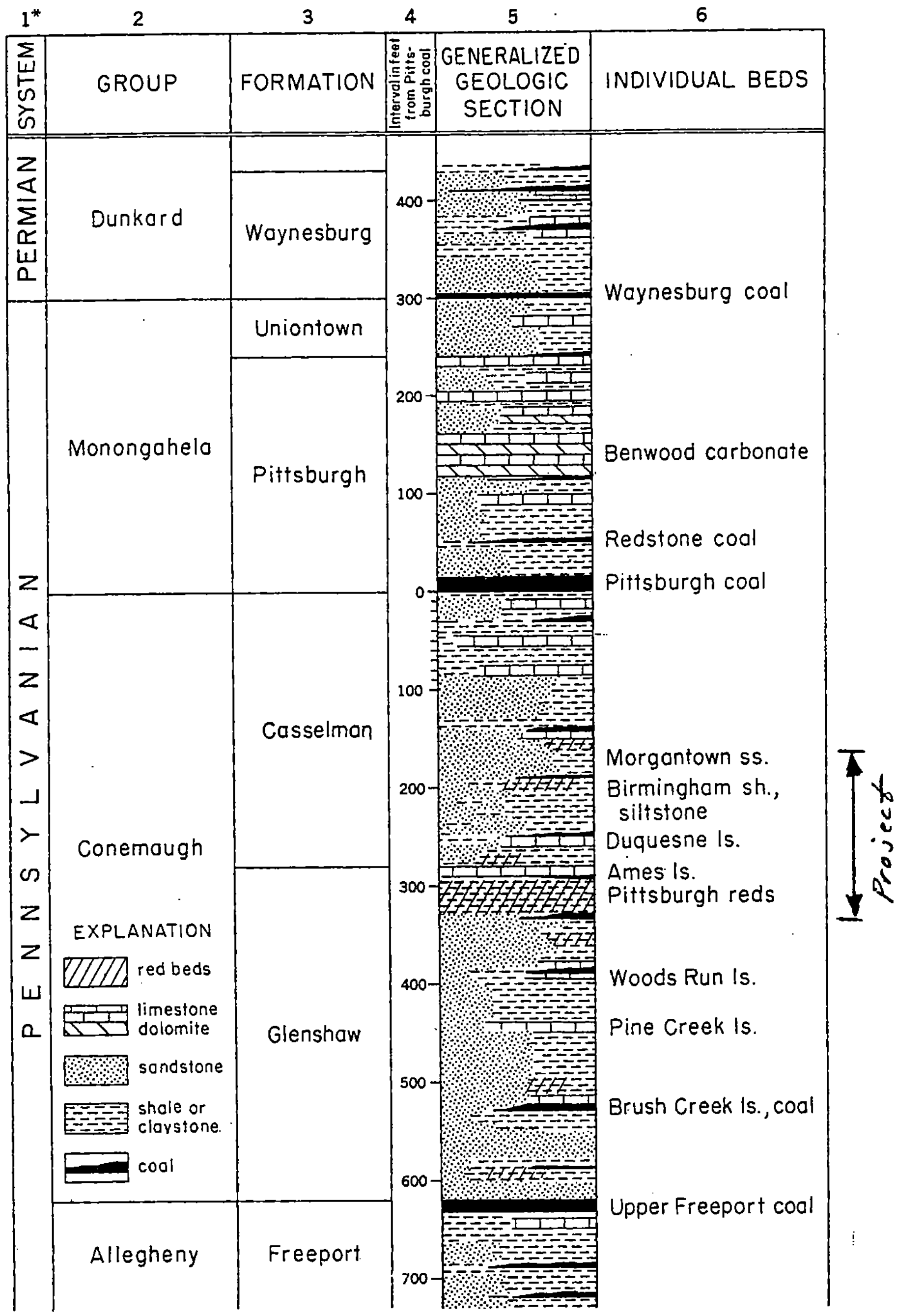

Figure 3 - Geologic Column of Rocks in Allegheny County (Reference 2)

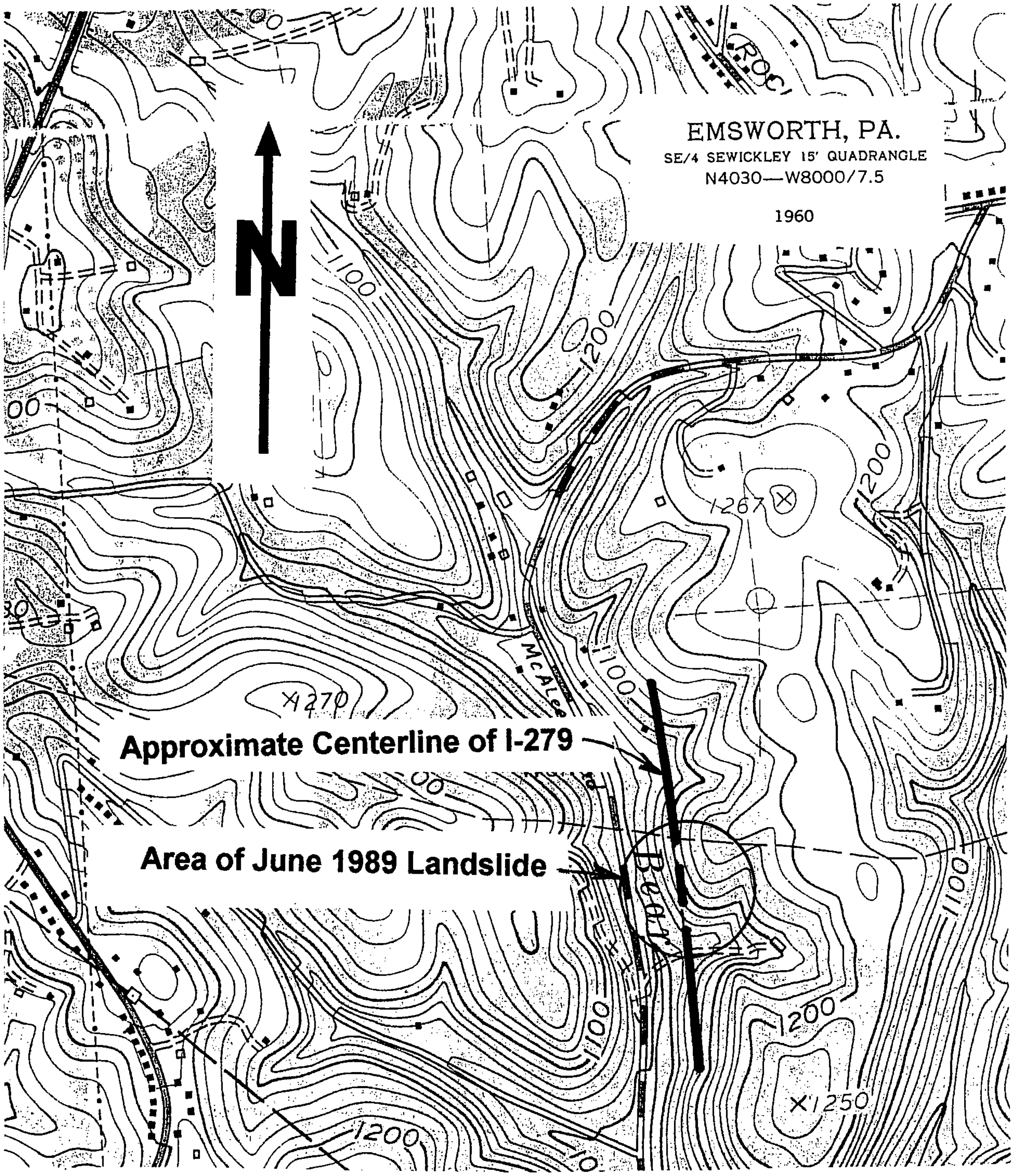

Figure 4 - Topography Prior to Construction I-279

GEOTECHNICAL EXPLORATIONS

Fifteen exploration borings were made at the locations shown on Figure 2 to determine subsurface conditions for evaluating the landslide. The borings were continuously sampled according to ASTM D 1586 (standard penetration test) through soil and were cored into rock sufficiently to define the full geologic column affecting the landslide. Slope inclinometer casings with open pop rivet holes were installed in each boring using sand backfill so that the casings could be used to monitor ground movements and ground water levels. Shelby tube samples of soil were obtained for laboratory testing.

The borings confirmed that the embankment fill was well compacted and consisted primarily of cohesive soil with rock fragments. However, the fill was not keyed into rock and thick deposits of colluvium were found below the toe of the embankment fill. In addition, the lower portion of the embankment was composed of a mixture of cohesive soil with rock fragments and was not a rock fill as originally specified.

Figure 5 shows the geologic section through the center of the landslide. It indicates that the toe of the embankment is resting on a massive wedge of colluvium. It also shows the presence of a layer of decomposed rock below the fill. Claystone is the parent rock under the lower two thirds of the slope. The decomposed rock weathered from claystone is a very stiff clay. Borings 6, 7, and 8 all confirmed that the embankment fill was not keyed and benched into rock nor was it keyed as deeply into the slope as proposed on the construction cross sections (see Figure 5). Although ground water was encountered, it was not exceptionally high, and in fact, was at an appropriate level for the natural conditions prior to embankment construction.

The inclinometer data obtained over a few weeks defined the location of the base of the landslide as shown on Figure 5. It clearly indicated that the failure occurred along the base of the colluvium and partially within the decomposed claystone.

STABILITY ANALYSES

Laboratory direct shear testing determined that the colluvium-decomposed claystone interface had a residual angle of shearing resistance (ϕ') of about 14 degrees with zero cohesion. Testing also showed that the massive colluvial wedge above the failure zone had a residual angle of shearing resistance of 30 degrees. The compacted embankment fill was assigned an angle of shearing resistance of 35 degrees.

Stability analyses were performed using computerized software for the modified Bishop method of analysis. The results of the stability analyses indicated a stability factor of safety of 1.0 for the as-built slope using the measured ground water levels.

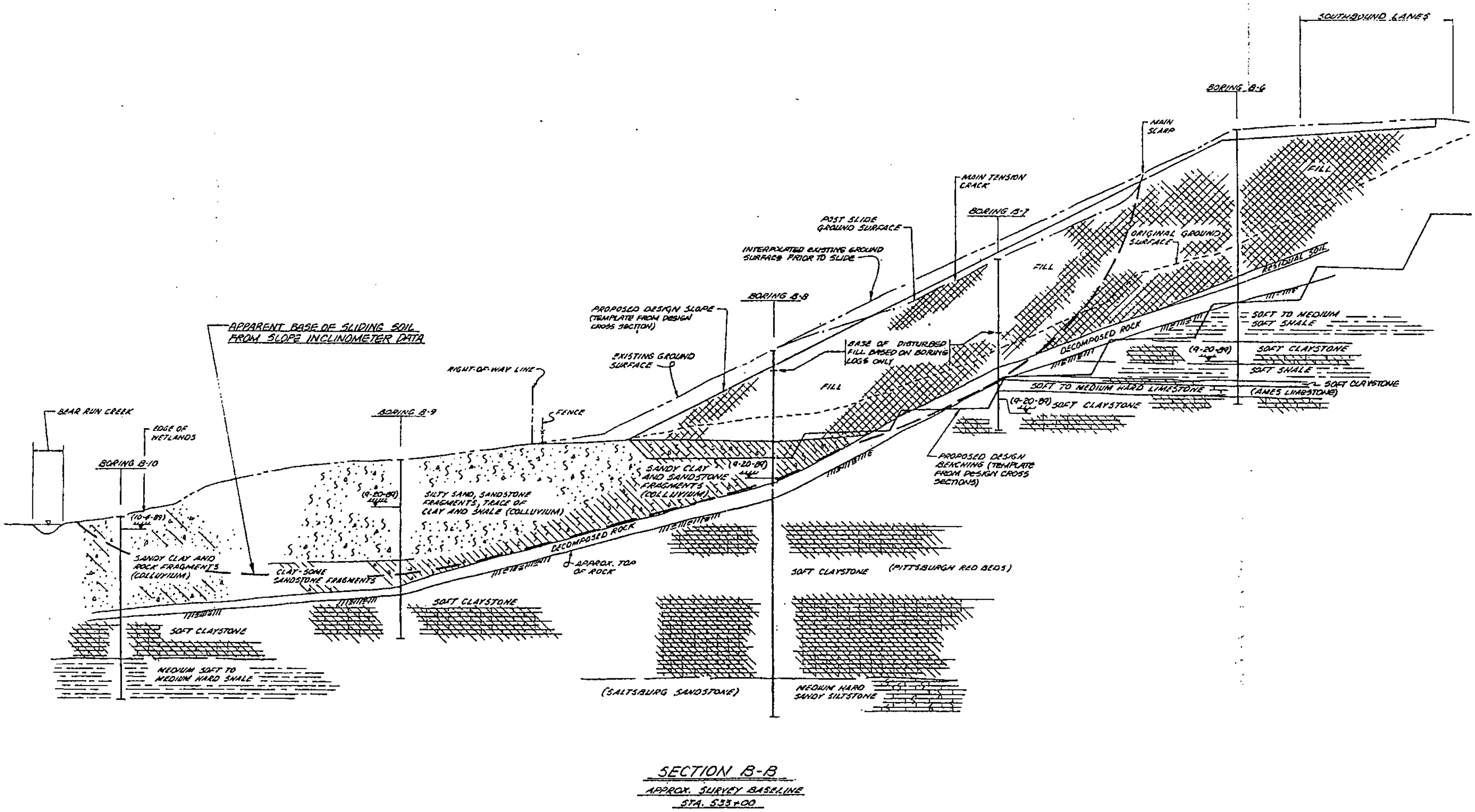

Figure 5 - Section B-B Through Center of Landslide

CAUSE OF LANDSLIDE

Once the subsurface conditions were clearly identified and the analyses were completed, it was concluded that the landslide occurred because the embankment was not keyed into rock as originally planned, but was built over decomposed claystone and weak slickensided colluvial soils which showed topographic evidence of prehistoric movement. While the unusually high precipitation that occurred immediately prior to the failure may have triggered the failure, the failure would have eventually occurred anyway because of the weak foundation support for the large embankment. The lack of a rock fill toe in the embankment fill was probably not a factor because the natural soil remaining below the embankment would have inhibited drainage from springs anyway.

OPTIONS FOR REPAIR

Several options for repair were evaluated. Initially it was thought that a buttress would be an economical repair method, but a protected wetlands was identified in the wooded area beyond the toe of the embankment that limited the available space to construct a buttress. The buttress would also require raising a state roadway for several hundred feet and enclosing a stream. It was not economically feasible to overexcavate the landslide and properly key the embankment into rock while maintaining the operation of the highway. Since lack of drainage was not the primary factor causing the landslide, enhancement of drainage which is sometimes an economical repair option was of no value in this case. Drilled-in slope reinforcement was considered, but was not found to be the most economical solution.

The option found to be the best relative to site constraints and overall technical reliability and economy was a combination of regrading of the embankment slope and a tied-back solder beam and lagging retaining wall. Key features of the design are shown on Figure 6. The stability of the slope in the lower portion of the embankment was improved by removing the driving weight of the upper portion of the embankment. The stability of the road was maintained by installing the permanent tied-back wall.

The lateral extent of the repair was also a consideration. The location of the top of rock is shallower to the north and deeper to the south where the embankment transitions from a side hill fill to a valley fill. Stability analyses indicated that future landslides were possible further to the south of the existing landslide. Therefore, although the planned repair extended to just beyond the limits of the current landslide, the southern portion of the design was prepared so the repair could be extended to the south, if needed.

The wall was designed using an apparent rectangular earth pressure distribution based on the "at rest" lateral earth pressure coefficient instead of the "active" earth pressure coefficient. This was because the wall is permanent and long-term creep of the cohesive soils behind the wall may transition to pressures corresponding to the at-rest condition.

The anchors and foundations for the wall were all extended into rock to assure global stability of the installation. The anchors were all tested to a safety factor of 1.5. The design of the wall was redundant so that one anchor could completely fail and the wall would remain stable by transferring load to other nearby anchors. There was sufficient space to maintain four-lanes of traffic on I-279 while constructing the repair by temporarily shifting traffic one lane-

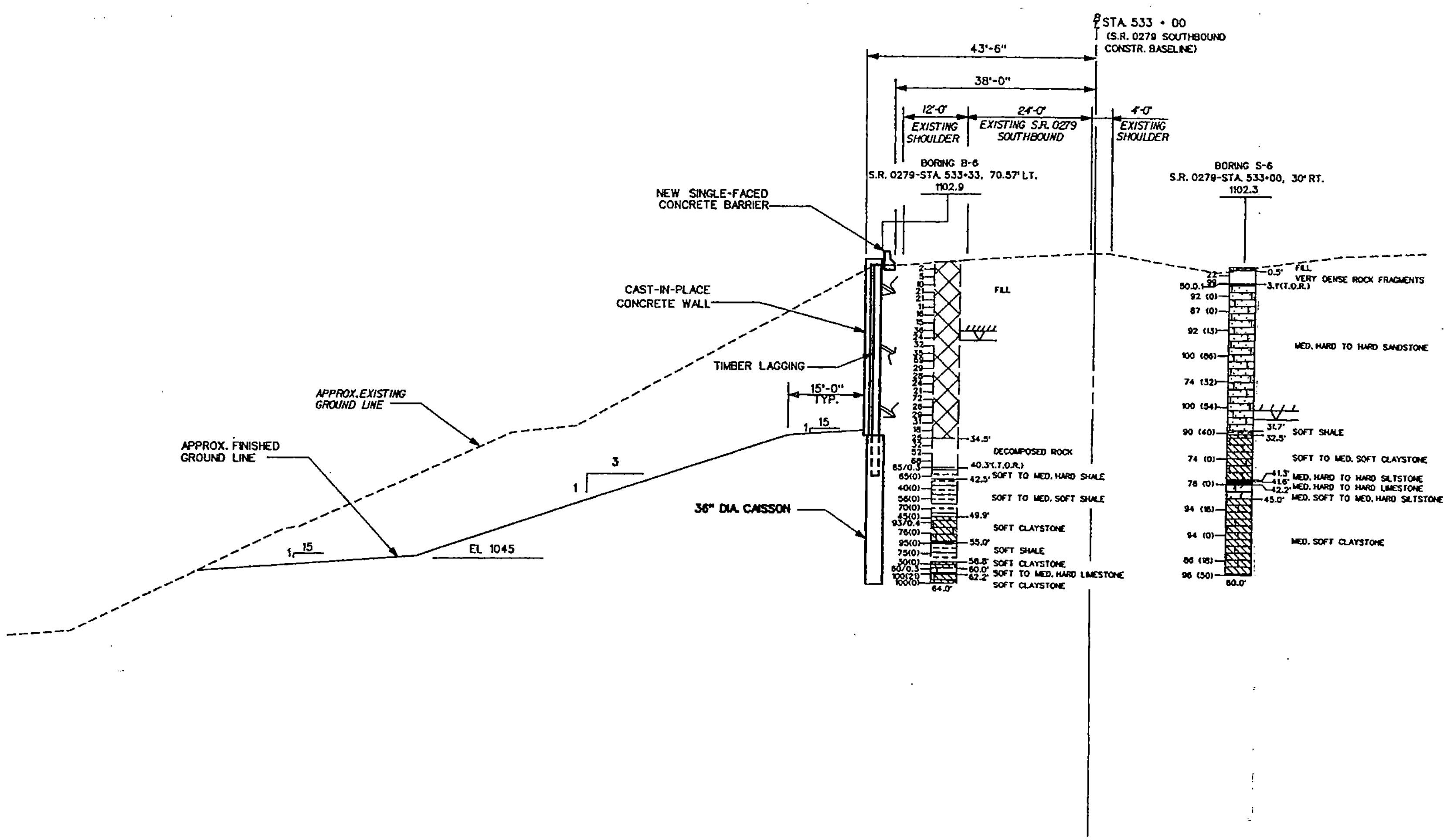

Figure 6 - Regraded Slope and Tied-Back Wall Through Center of Landslide

width away from the slope. Load cells and slope inclinometer casings were provided to monitor performance of the system, and the data indicates satisfactory performance over about 4 years since the completion of the repair.

LESSONS LEARNED (AGAIN)

This landslide could have been prevented at two critical stages of the project. Initially, the potential for the landslide might have been detected during the geotechnical exploration conducted for the highway design. Unfortunately, the prehistoric movement was not identified, a boring was not drilled in the area where the failure occurred, and the original exploration did not detect the potential for a problem at this location. Nevertheless, the design did include provisions to prevent the failure from occurring by requiring that the embankment to be keyed into rock and by making provisions for drainage from natural springs.

The second critical stage for prevention of the landslide was during construction. If the entire embankment (including the toe) had penetrated the decomposed rock and had been keyed into rock, the landslide would not have occurred. Unfortunately, those observing the exposed subgrade materials concluded that the embankment was keyed in "well enough" even though the embankment was not keyed into rock. It was found that if the embankment was built exactly to the construction template shown on the drawings, it would still probably have failed because of the significant amount of colluvium present below the toe of the embankment.

If the field personnel responsible for determining the suitability of material supporting the toe of the embankment had sufficient technical knowledge of the local geology, they would not have allowed the embankment to be built on materials other than rock in this side-hill fill situation. They would know that low-strength slickensided surfaces are likely to be present near the top of rock. Thus, subsequent projects in this District attempt to include more thorough geotechnical explorations during the design stage and have required on larger project that subgrades for fills be evaluated by an engineering geologist or a geotechnical engineer in an attempt to detect problems of this type and correct them before they become failures.

REFERENCES

1. Winters, Dermit M., "Pittsburgh Red Beds Stratigraphy and Slope Stability in Allegheny County, Pennsylvania," (MS. Theses), University of Pittsburgh, Pittsburgh, Pennsylvania, 1972.
2. Wagner, Walter R., et al. "Geology of Pittsburgh Area", Report G59, Pennsylvania Geological Survey, Harrisburg, PA, 1970, Page 46.
3. Gray, Richard, E., Ferguson, Harry F., and Hamel, James V., "Slope Stability in the Appalachian Plateau of Pennsylvania and West Virginia," Rockslides and Avalanches, Part II-Engineering Sites, B. Voight, ed., Developments in Geotechnical Engineering, Vol. 14B, Elsevier North-Holand, Inc., New York, NY, 1978.
4. Hamel, James V. "Geology and Slope Stability in Western Pennsylvania," Proceedings of the ASCE Spring Convention, Pittsburgh, PA, April 24-28, 1978.

ROCK SLOPE ENGINEERING AND MANAGEMENT PROCESS ON THE CANADIAN PACIFIC RAILWAY

A.J. Morris, P.Geol., Engineering Geologist, Canadian Pacific Railway
D.F. Wood, P.Eng., Rock Engineer, David F. Wood Consulting Ltd.

ABSTRACT

The safe operation of a major railway line through mountainous terrain has been a continual challenge for the Canadian Pacific Railway (CPR) since the "Last Spikes" were driven in 1885 at Craigellachie, British Columbia, and at Jackfish, Ontario, completing the transcontinental railway. In 1976, an empty coal train hit rocks on the track, derailed and fell onto the Trans-Canada Highway near Spences Bridge, British Columbia, killing both engineers. Because of this accident, the Canadian Transportation Board ruled that an evaluation be undertaken of the stability of all rock cuts along the CPR and to prioritize sites where stabilization work was required. An initial slope inventory was conducted in both Western and Eastern Canada, detailed stability assessments were made of each site, priorities were established, and stabilization programs carried out.

Data collected during this evaluation became the basis for, what has become, a sophisticated database system used to store, evaluate and manage rock slope information obtained system wide. Considerable development in the method of slope prioritization has been accomplished, taking into account the potential hazard and consequences of a rock fall related incident together with the rock fall data and stabilization history for a given slope. The system used today by CPR to prioritize slopes combines an inspection rating with a required action and is the primary tool used in the CPR Rock Slope Engineering and Management Process. Components of the process include Planning, Inventory and Record Keeping, Inspection and Reporting, Stabilization Measures and Program Review.

INTRODUCTION

CPR manages rock slopes along over 750 miles of track from Vancouver to Calgary, over 650 miles of track in Northern Ontario and nearly 70 miles of track in upper New York State, incorporating a total of over 2500 man made excavated rock cuts throughout 20 subdivisions. A program of rock cut inspections, stability assessments and priority ratings for each slope is conducted on a regular basis by qualified rock slope specialists. Results generated from inspections together with all relevant historical information are used to plan short term (annual) and long term (over several years) stabilization programs. Once a list of work sites is finalized, cost estimates are made, contract specifications are written, and the stabilization work is tendered to pre-qualified private contractors.

The engineering and management of rock slopes on the CPR has been defined in an internal company Directive (1997) as "an organized process for the monitoring and investigation of rock slope behaviour, for the planning, design and implementation of rock slope mitigative measures, all for the purpose of contributing, at the lowest economic cost to the company's service requirements for safety, delivery and environmental protection." This is accomplished through the following processes:

- Planning – to identify short term and long term objectives
- Inventory and Record Keeping – of all rock slope information essential to effective management
- Inspection and reporting – including annual inspection of all slopes by professionals on a regular basis to determine priority ratings, and by track maintenance personnel during routine track inspections; construction inspections, rock fall inspections, detailed assessments and follow-up inspections.
- Stabilization measures – or mitigation undertaken through regular planned program construction work based on a priority system or due to emergencies or additional requirements obtained through detailed assessments.
- Program Review - undertaken annually to assess the program effectiveness and to identify possible improvements.

The key component of the process is the inspection rating system from which priority sites are identified and required actions are specified that define the time frame in which remedial work should be carried out.

INSPECTION RATING SYSTEM

History

The Canadian Pacific Railway initiated the first Priority evaluation of rock slopes along the mainline throughout British Columbia in 1976 after a Canadian Transportation Board ruling that such an evaluation shall be undertaken to prioritize sites where slope stabilization is required. This ruling came about after the deaths of two CPR locomotive engineers from a derailment caused by a rock fall at Mile 74.9 on the Thompson Subdivision. Golder Associates, geotechnical consultant engineers, were given the task of collecting pertinent information for each slope in order to establish priority stabilization sites and plan work programs.

The process used by Golder included the following four phases to establish Priority sites and the stabilization work required:

- Phase I - initial slope inventory;
- Phase II - detailed stability assessments for each site; slopes were prioritized using a rating system from A (highest probability of failure) to E (lowest probability);
- Phase III - detailed site specifications; and
- Phase IV - completion reports for the stabilization programs.

Data collected during this evaluation became the basis for, what is now, a sophisticated database system used to store, evaluate and manage rock slope information system-wide. Since 1976, information on rock fall incidents, mitigative measures, inspections and priority ratings has been collected annually on a consistent basis for British Columbia and Alberta, and since about 1994 for Ontario and New York State. Since 1994, considerable development in the method of prioritizing slopes has been accomplished, taking into account the potential hazard and consequences of a rock fall related incident. A system for statistical evaluation of rock falls is combined with previous work history and inspection data to aid in the planning for both short term and long term work programs. The current system used to prioritize rock slopes combines an inspection rating with a required action as described below.

Inspection Ratings and Required Actions

The observations made for each slope are used to assign an **inspection rating,** which describes the potential for rock falls, and to specify a **required action** which defines the time frame in which remedial work should be carried out. The assigned ratings are checked for consistency with previous year's ratings. Figure 1 illustrates the relationship between the rating and the required action.

Figure 1: Inspection Ratings and Corresponding Actions

		REQUIRED ACTIONS						
		Limit service Work within 1 month	Work in current year	Follow-up inspection	Work in 1-2 years	Lock-blocks/ ditch	Long term	No action
INSPECTION RATING	Urgent	X		X		X		
	Priority		X	X	X	X		
	Observe						X	X
	OK							X

Definition of Inspection Ratings and Required Actions

The observations made at each slope are used to assign an **inspection rating,** which describes the rock fall potential, and a **required action,** which defines the time frame for remedial work. The following is a description of the inspection ratings.

Urgent Rating

This inspection rating is restricted to sites where a potential rock fall hazard could cause a derailment and/or serious injury to personnel, and failure may occur within the next few weeks or months.

The possible actions following an **Urgent** rating are as follows. First, service below the slope should be limited, with this action normally being implemented as soon as practicable after the urgent condition is observed. The service limits could be a slow order, halting traffic, or having a watchman on site until the area is stabilized. A detailed follow-up inspection would then be carried out to determine stability conditions more accurately. A follow-up inspection would normally be carried out within one week to determine if the Urgent rating was justified and recommend an appropriate action. If stabilization work were required, it would be carried out within a specified time, which will not exceed one month, depending on the severity of the condition. If there is an adequate ditch at the site, the work may be limited to ditch cleaning.

Priority Rating

The **Priority** rating is used at sites where there is evidence of movement or change in conditions from the previous year's observations. It is also used where the volume of potential failure material is large enough and the material unstable enough that it could reach the tracks and cause derailment or injury.

There are three possible actions following a **Priority** rating.

- Firstly, the site could be scheduled for work that could be added to the current year's stabilization program; the required work may be limited to ditch cleaning.

- Secondly, a detailed follow-up inspection could be carried out within about three months to more accurately assess stability conditions and recommend an appropriate course of action.

- Thirdly, the site could be added to the list of sites considered for stabilization work over the following 1 - 2 years.

Observe Rating

The **Observe** rating is used at sites where potential instabilities exist that could impact the tracks, and where some deterioration in stability conditions is noted, such as loosening of blocks or minor raveling. Usually this specific area will be observed in each subsequent inspection for a change in condition. Where possible, a photograph of the potential instability should be taken each year from the same location to help document and assess any changes.

There are two possible actions following an **Observe** rating. First, no further action may be required. Second, the site could be added to the list of sites considered for long term stabilization. Long-term sites require a substantial stabilization program to provide long term protection against rock falls. Typical work might include a rock fall catch ditch excavation, extensive rock bolting, shotcreting, slide fence installations, or Lockblock installations.

OK Rating

This inspection rating is used at sites where no potential instability could impact the tracks, or, where some slope movement is observed but there is minimal risk of failure at present. The only action arising out of this rating is No Action.

PLANNING

On an annual basis, meetings are held between CPR Geotechnical Staff and Consultant Specialists involved directly in program management, generally soon after annual rock slope inspections have been completed, to plan both short-term stabilization requirements for the following year's program as well as long-term or 4 to 5 year plans for stabilization projects. Sites requiring short-term stabilization work by contract during the upcoming year are selected from those meeting one or more of the following criteria:

1) Any sites that were included in the previous year's work program but were not completed either for budgetary or operational reasons;
2) Priority sites identified during the annual inspection two years prior, where action was recommended in 1-2 years that were not included in the previous year's work program;
3) Priority sites identified during the previous year's annual inspection where action was recommended in 1-2 years;
4) Any other Priority site identified either during previous inspections or because of recent Follow-up inspections or detailed site assessments of recent rock fall locations; or
5) Any sites rated as "Follow-up" during the current year's inspections that after field investigation were re-rated as current year sites.

Sites for which stabilization requirements cannot be determined without detailed geotechnical investigations, surveying or design work are rated during the inspection process as "Long Term". The required design and stabilization measures cannot usually be completed in one field season because of following reasons:

1) The required work involves several construction stages;
2) Detailed design investigations must be completed prior to any construction;
3) Operational restraints such as availability of track time, track personnel are restrictive; or
4) Budgetary restraints prevent completion.

In addition to site selection, considerations such as personnel requirements and available budgets are planned on an annual basis.

INVENTORY AND RECORD KEEPING

The primary tool used for managing all relevant rock slope information is the CPR rock slope database which has been built upon the original 1976 inventory of all CPR rock cuts. In 1985, a dBase database was used to track rock fall records as part of the rock slope stabilization program. In 1993, the database was converted to Paradox and expanded. In addition to rock fall records, it now includes descriptions of rock cuts and tunnel portals, annual inspection observations, slope ratings and required actions and summaries of stabilization work performed. The database is continuously up-dated as new information becomes available. By organizing the data in a format that can be easily searched and sorted, the database has become an integral part of the planning and management of the stabilization program. Once inspections have been completed, the most recent Priority ratings are used in the planning of short-term and long-term stabilization programs.

The database is updated throughout a given year with the following information:

1) Descriptions of each site, identifying its "type" as either a slope, tunnel, bridge, retaining wall etc.
2) Rock fall reports from each subdivision, system wide. Figure 2 shows the number of rock falls for 1998, as well as over a five year period and a 24 year period for five subdivisions.
3) Annual inspection report information for each subdivision, including Priority ratings, required actions and comments for every documented rock cut in every subdivision.
4) Results of Follow-Up inspections, which could change the Priority rating assigned during an annual inspection.
5) Construction and stabilization information including actual work completed or not completed for each site where current year stabilization work was planned.

INSPECTION AND REPORTING

Annual Inspections

A schedule for the annual rock slope inspections across the CPR system is drawn up very early in the year so that the appropriate arrangements can be made. Inspections are made by helicopter in those subdivisions having the highest and most active slopes as well as along the track from a high rail vehicle. Other subdivisions are inspected from the track only. Most mainline and active rock fall locations are inspected annually, while other, less active slopes are inspected once every two years.

Information is gathered for each rock cut using a database-generated rock slope inspection form. Using the database, information including the last recorded rock fall, geology notes, cut height, the most recent Priority rating, required action and the last year stabilization work was carried out is shown on the form, see Figure 3. Space is provided for observations, an inspection rating and required action. A photographic record is also kept of rock cuts with evidence of instabilities from year to year, allowing for visual comparisons over time.

Figure 2: Total Reported Rock Falls B.C. and Prairie Districts 1998

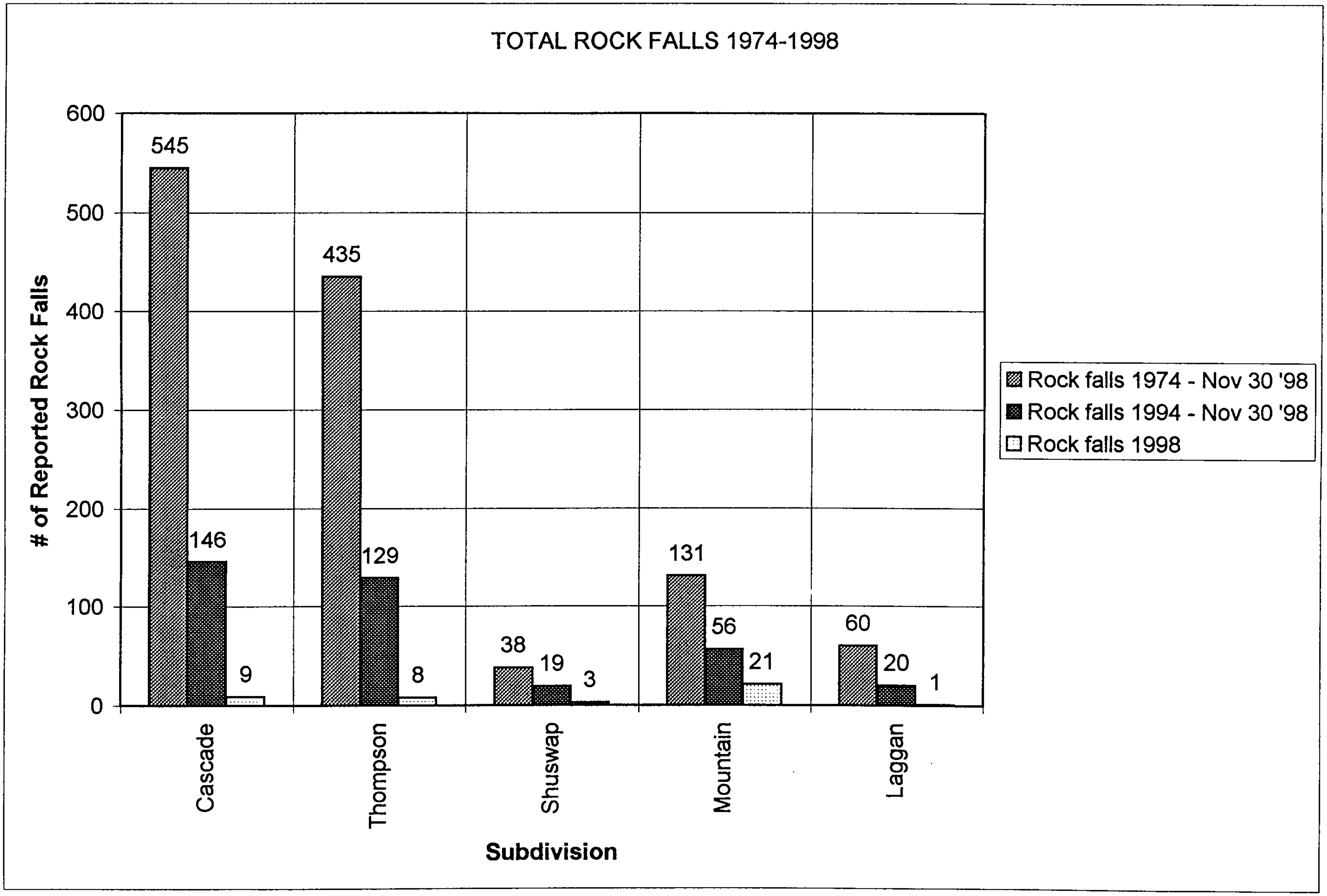

Figure 3: Rock Slope Inspection Form

ROCK SLOPE INSPECTION

Inspected by: Subdivision: Mountain Pg.: 1 Inspection Date: April 6, 1999

Mile	Site Type	Height (m)	Site Records	Observation	Insp. Rating	Required Action
31.90	☐ **Cut** ☐ **Nat. Slope** ☐ **Fill** ☐ **Slide Fence** ☐ **Drainage** ☐ **Wall** ☐ **Tunnel** ☒ **Bridge**	**Cut Max.** **Cut-N:** **Cut-S:** **Nat. Slope:**	**Last Rock Fall:** Last Work Year: 1997 Cut Notes / Geology: *Shale – low strength, horizontal bedding with spacing of ¼"-2".* ***1998 OK No Action*** ***Due to the nearly horizontal orientation of shale beds, small pieces tend to occasionally drop from crown.***	**Photo:**	☐ Urgent ☐ Priority ☐ Observe ☐ OK	☐ Follow-up ☐ Current Year ☐ Limit Service ☐ 1-2 Years ☐ Long-term ☐ Lockblocks ☐ Clean Ditch ☐ No Action
31.00	☐ **Cut** ☐ **Nat. Slope** ☐ **Fill** ☐ **Slide Fence** ☐ **Drainage** ☐ **Wall** ☐ **Tunnel** ☐ **Bridge**	**Cut Max.** ***180*** **Cut-N:** **Cut-S:** **Nat. Slope:**	**Last Rock Fall: 1986** Last Work Year: 1993 Cut Notes / Geology: *Inspect Mile 30.9 – 31.1. Potential of large rock block falls is high. Frequent rock falls – rock and mud flow at Mile 31.0 took out track. Bedded phyllite rock. Some hard layers and blocks.* ***1998 Observe Long-term*** **West Portal: excavate rock starting at tunnel to create catchment area, and extend excavation to the west into talus area. In 1997, catchment berm created in talus.**	**Photo:**	☐ Urgent ☐ Priority ☐ Observe ☐ OK	☐ Follow-up ☐ Current Year ☐ Limit Service ☐ 1-2 Years ☐ Long-term ☐ Lockblocks ☐ Clean Ditch ☐ No Action
31.20	☐ **Cut** ☐ **Nat. Slope** ☐ **Fill** ☐ **Slide Fence** ☐ **Drainage** ☐ **Wall** ☐ **Tunnel** ☐ **Bridge**	**Cut Max.** ***30*** **Cut-N:** **Cut-S:** **Nat. Slope:**	**Last Rock Fall: 1992** Last Work Year: 1993 Cut Notes / Geology: *Tunnel portal plus 45 m (150 ft). Periodic rock falls. Adverse jointing near top. Potential toppling failure.* *85 deg. (120 deg) 75 deg (030 deg) jointing. Horizontally bedded phyllite rock.* ***1996 Observe Long-term*** ***A* follow-up inspection. Long-term: deepen ditch and scale***	**Photo:**	☐ Urgent ☐ Priority ☐ Observe ☐ OK	☐ Follow-up ☐ Current Year ☐ Limit Service ☐ 1-2 Years ☐ Long-term ☐ Lockblocks ☐ Clean Ditch ☐ No Action

A target date for completion of inspection reports for mainline subdivisions has recently been set at two weeks after the inspection. This is to ensure that the inspection results can be distributed to track personnel in a reasonable time if priority or urgent sites were observed, and to give CPR District personnel adequate time for planning stabilization programs.

A typical report includes a definition of inspection ratings and required actions; tables of inspection ratings, required actions and observations for each site, identified by subdivision and mileage; descriptions of each site with priority ratings; selected site photographs, summary of rock falls and long term stabilization sites.

Construction Inspections

During the course of annual contract stabilization work, inspections of the work progress and site conditions are carried out on a regular basis either by geotechnical consultants or by CPR geotechnical staff. Stability requirements are determined and recommendations made for stabilization measures such as scaling, rock bolt or rock dowel installation, concrete buttressing or shotcrete etc. Formal site reports are required for these inspections.

In all CPR rock slope stabilization contracts, the contractor is required to complete a "Daily Work Report" form, summarizing the personnel, equipment and materials used for work during a particular day. The CPR representative on site (usually the flagman) also supplies information on actual track time available and hours worked on the track that day. At the completion of the work at a particular site, this information is used to summarize the work completed in a "completion" report.

Rock Fall Report Inspections

Track maintenance personnel patrol the track routinely. They report any signs of recent slope activity if observed. A CPR rock fall report is generally submitted if a rockfall is discovered on or adjacent to the track and there is concern that there may be additional instabilities. Similarly, when rockslide detectors or rockfall detectors are triggered and repaired by Signals and Communications personnel, a report is submitted. An example of a typical rock fall report is shown in Figure 4.

Provision is provided on the rock fall report form to request an inspection within a specified time frame. Inspections are carried out either by CPR geotechnical staff or consultant specialists. Once the inspection has been made a formal site inspection report is required to be submitted to CPR describing observations and recommended actions.

Figure 4: Rock Fall Report

SEND TO: MOR0007,GOL1010 COPIES: MAC0015,OM01220,MTM,JON

REPORT OF ALL ROCK FALLS, ROCK SLIDES, MUD SLIDES & SNOW SLIDES WHICH CAUSE OR MAY CAUSE: A DERAILMENT, DAMAGE, INJURY OR DELAY TO ANY TRAIN, ROLLING STOCK, EQUIPMENT, WORK SECTION/CREW, EMPLOYEE OR OTHER PERSON.

1. DISTRICT: B.C. District
2. SUBDIVISION: Cascade
3. MILEAGE: 10.50
4. DATE: November 22/23, 1998
5. TIME: After 13:00 Nov. 22/98.
6. WEATHER CONDITIONS:
 a) AT TIME OF OCCURRENCE(Snow,Rain,Dry,Temp) Moderate rain, 4 c.
 b) 24 HRS.PRIOR TO OCCURRENCE(Condition,Temp)Heavy rain, 4 c.

7.a) TYPE OF FALL/SLIDE(Rock,Mud,Tree,Snow) Rock.
 b) LOCATION OF FALL/SLIDE(Track,Ditch) North side, edge of ballast section.
 c) SIZE OF FALL/SLIDE(Feet,Cu.Yd.,Tons) 5 boulders, total 3 cubic metres.

8.a) DELAYS TO TRAIN MOVEMENTS(Hrs.,Mins.) Nil
 b) HAS A SLOW ORDER BEEN PLACED? ( ) Y (X) N
 c) IF YES, WHAT SPEED?

9.PARTICULARS OF ANY DAMAGE TO TRAIN/INJURY TO PERSONS: (X) nil

10.a) TIME TO CLEAR FALL/SLIDE(Hrs.,Mins.) N/A
 b) EQUIPMENT USED (BTMF forces,Contractor)

11.ORIGIN OF SLIDE/FALL(Loc'n.,Ht.above track) Boulders dislodged from tree line approximately 100 ft. up slope.

12.a) IS THERE MORE LOOSE MATERIAL ON THE SLOPE? (?) Y (?) N
 Two boulders at tree line that may eventually fall as the soil is eroded.
 b) IF YES, HOW MUCH (Cu.Yd.,Tons) Approx. 2 cubic metres total.

13.a) IS THERE A CATCHMENT DITCH AT THE SITE? (X) Y ( ) N
 Natural depression.
 b) IF YES, HOW WIDE AND DEEP? Roughly 14 ft. wide x 2 ft. deep.
 c) HAS THE DITCH BEEN CLEANED OUT? ( ) Y ( ) N
 Will use a backhoe to place fallen rock and ditch a burm, sometime this week.
 d) IS THERE A SLIDE FENCE AT THE SITE? ( ) Y (X) N
 e) IS THERE A RETAINING WALL AT THE SITE? ( ) Y (X) N

14.IS AN IMMEDIATE SITE INVESTIGATION REQURIED? ( ) Y ( ) N
 Mr. Frank Seki inspected, Monday Nov. 23/98.
 IF NO, IS AN INVESTIGATION REQUIRED IN 1WK?( ) 1MO?( ) 1YR?( )

COMPLETED BY:		INFORMATION PROVIDED BY:	
Name:	Victor L. Tome'	Name:	Frank Seki
Title:	A.T.M.S.	Title:	Geotechnical Engineer,
Location:	Haig B.C.	Location:	Golder Associates
Date:	November 23, 1998	Date:	November 23, 1998

Detailed Assessments and Follow-Up Inspections

Detailed stability assessments and follow-up inspections are generally required when more field information is needed to further evaluate the inspection rating of a site and to finalize stabilization design requirements. These inspections are usually carried out by senior engineering personnel or specialists. The results of a follow-up inspection could lead to a re-rating of a slope. A formal report is required for all follow-inspections.

All of the inspections described above will have an effect on the final site selection for a given year's stabilization program.

STABILIZATION MEASURES

Mitigation or stabilization measures are determined for each of the priority sites selected for work either as part of the annual, short-term program or a long-term program, which may take several years to complete. Sites rated as Urgent are generally not considered part of program work, as more immediate measures are required.

Short-Term Programs

Rock slope stabilization work on an annual basis is considered a short-term program. Work sites are selected using the Priority Ratings as described above, stabilization methods chosen and cost estimates made for the work in each subdivision. An estimate is made of the number of work days required and the materials needed at each site. Annual contracts are tendered for work in each CPR District based on the estimated quantities. Operating from an annual budget, all costs for Engineering and CPR's own forces must be estimated based on the amount of stabilization work in the year's program. Figure 5 shows part of a typical estimating spreadsheet describing the work required at each location for a CPR annual work program.

Typically, the types of stabilization measures employed during an annual work program include hand scaling, machine scaling, rock bolt and dowel installation, shotcreting, concrete buttressing, Lockblock wall construction and ditch excavation.

Long-Term Programs

Rock stabilization programs considered long-term are generally those that involve mitigative work over several years due to the size and cost of the recommended measures. They are sites that require careful planning, engineering design and high level approvals but are primarily aimed at eliminating a potential high hazard location to improve operating conditions.

Typical types of long-term stabilization work include major ditch widening and slope excavation, rock fall catchment fences, rock fall sheds or major rock bolting and shotcreting.

PROGRAM REVIEW

An annual audit of the rock slope engineering program is conducted to evaluate how each of the processes was implemented across the system. Tables summarizing the effectiveness of inspections, inspection ratings, rock fall inspections, construction inspections, follow-up inspections, construction activity and status of long term stabilization sites are produced and used as planning aids for the following year.

Using this review process, full closure is brought to the management process, allowing for the next year's rock engineering program to proceed with all of the data and benefits accrued from the previous years' program. This process becomes a built-in procedure of monitoring and continuous improvement to ensure that the Canadian Pacific Railway's rock slopes are managed effectively and efficiently.

Rockfall Hazard Remediation along Ontario Highways

Stephen A. Senior, P. Eng., Ministry of Transportation Ontario*

Abstract

The Canadian Shield, one of the oldest eroded mountain ranges in North America, dominates the physiography of Ontario. Highway construction through this region has required excavations in granitic rock masses close to 30 metres in height. Pre wall controlled blasting methods and weathering have combined to create conditions in which ravelling and ice jacking are the dominant failure mechanisms.

New planning initiatives are carried out by the Ontario Ministry of Transportation (MTO) to identify short and long term objectives for managing rockfall hazards in Ontario. Long term investigations are based on the recently developed Rock Hazard Rating System for Ontario. This system was adopted after initial trials of the Oregon DoT's Rockfall Hazard Rating System was found to have limited application to Ontario's physiography and bedrock conditions. Some development aspects of the Ontario rating system are discussed.

Despite long term planning and priority management strategies, the requirement to address particular hazards may be influenced by outside agencies. Two case histories along Highway 17 on the east shore of Lake Superior are given where this has occurred. Field inspections carried out by rockfall hazard specialists to confirm conceptual stabilization designs have resulted in various engineering solutions to reduce or remove the potential hazards. The final procedure is sometimes arrived at by considering criteria outside those suggested from a rock engineering viewpoint.

Introduction

Ontario's geological setting is a much older, stable environment with significantly less relief than the tectonically active mountainous region of the continent's west coast. Elevations within the province range from 60 to 600 metres above sea level but generally do not exceed 300 metres (Magni, 1984). Almost two thirds of Ontario's 21,000 km of highways are constructed through Precambrian bedrock where many of the roadside rock excavations do not exceed 15 m in height. Along the east shore of Lake Superior they are generally higher but are seldom greater than 30 metres.

Many of the rock cuts of northern Ontario were built prior to the adoption of wall control blasting methods. As a result, they consist mainly of blocky, often overblasted, and heavily fractured rock faces. While most of the excavations are largely stable, they are still prone to ravelling and ice jacking that continually deposit small volumes of rock in roadside ditches and shoulder areas. Where these failure mechanisms become more progressive, larger rock volumes may fail, overspilling onto the pavement.

MTO is responsible for the construction and maintenance of highways and rock cuts. In the past, rockfall hazards were dealt with through maintenance operations or highway construction and rehabilitation programs. Because of the lower face heights, solutions consisted almost exclusively of scaling and trimming. Prior to the introduction of wall controlled blasting specifications in the early 1980's, only two projects are documented where engineered reduction measures were required. The first occurred in 1961 at Haviland Bay on Hwy 17, 27 km north of Sault Ste. Marie in response to a massive slope failure involving more than 760 m^3 (~2000 tonnes) of rock. The second project was constructed on a 27 m high rock cut in 1974 on Hwy 101, 8 km east of Wawa. This contract included the first Ontario installation of

---

* Engineering and Materials Research Office, Downsview, ON, Canada M3M 1J8

suspended wire mesh (966 m^2) to control errant rockfall as an alternative to excavation or highway realignment. Up until the 1990's, no other major stabilization projects requiring detailed rock engineering analysis have been constructed.

Within the last 10 years, MTO has significantly changed its approach to dealing with rockfall hazards. Outsourced project management has lead to greater involvement of the private-sector and the use of rockfall hazard specialists. Through the evolution of improved rockfall management policies, MTO has developed a rockfall hazard rating system as well as completed several significant rockfall hazard mitigation projects. The remainder of this paper will briefly review the Ontario rating system and highlight two projects along the east shore of Lake Superior. This area is one of the most rugged and scenic parts of the province formed from Precambrian granitic batholiths that rise hundreds of metres above the surrounding land.

Ontario's Rockfall Hazard Rating System

MTO's review of rockfall hazard policy and construction standards was initiated in 1992 following a fatal traffic accident involving a rock slope failure on Highway 401 near Kingston, Ontario. Although the failure site had been identified for remedial treatment years earlier, there was no indication or record that any work had ever been carried out. This tragedy highlighted MTO's lack of a systematic approach to managing rockfall hazards and prompted a policy review to improve and correct this situation. As the basis for conducting this review, MTO selected the Rockfall Hazard Rating System (RHRS) sponsored by the US Federal Highways Administration. This system, based on publications by Brawner and Wyllie (1975) and Wyllie (1987) and further developed through extensive data on more than 3,000 rock slopes by the Oregon Department of Transportation (Pierson et al, 1990), applies a balanced approach to hazard evaluation including such factors as traffic frequency, speed, site distance, and roadway geometry as well as rock mechanics slope stability factors.

The first field application of the RHRS in Ontario was along highways within MTO's northern Region (12,000+ lane-km) where a preliminary survey identified about 200 Class A, or highest risk category sites. MTO awarded a consultant assignment to Franklin Geotechnical Limited to carry out detailed hazard scores and provide preliminary treatment recommendations and costs. It was not intended to make any substantial modifications to the existing RHRS. During the detailed RHRS rating, it became apparent that the system presented several limitations that were particularly due to the exponential 3^x weighting. For example, observations of slope height could not be effectively applied since the difference between a 5 m and a 15 m high face (which covers a significant percentage of Ontario highway rock cuts) changed the RHRS score by less than 1%. Careful estimation of slope height became unnecessary, yet clearly a 15 m cut is significantly more hazardous and more expensive to treat. As each parameter was further analysed, it was found that only six of its ten parameters made a meaningful contribution to the final ratings of Ontario's rock cut conditions. Overall, the RHRS was so insensitive that it was decided that the Ontario version of RHRS should abandon the use of the 3^x weighting system. Since this amounted to a major change in the definition of RHRS, further shifts in modifications were allowed where these modifications appeared beneficial.

One major area that was deemed to be of benefit was inclusion of parameters relating to the types of failure mechanisms common to Ontario rock cuts. What appeared to be missing from RHRS was a measure of intensity of jointing (block size or RQD), face looseness (joint aperture), or height of water table as a percentage of face height. All three of these parameters are considered fundamental in assessing the risk of ravelling, ice-jacking, and similar modes of rock face instability. From more than 400 analyses conducted during the course of this study, the following types and frequencies of potential failure mechanisms were identified: ravelling (25%), toppling (23%), overhang (15%), ice-jacking (11%), block roll (11%), 2D sliding (8%), and 3D sliding (2%) (Franklin and Senior 1997a). In contrast, RHRS does not recognise ravelling as an independent failure mechanism and evaluates it in the same manner as sliding. This is inappropriate because the probability of occurrence of ravelling and sliding are dependant on quite different rock mass characteristics.

The revised system, termed RHRON (Rockfall Hazard Rating System for Ontario), shown schematically in Figure 1, includes all but one of the original RHRS parameters ("water table height" replaces "seepage"). Five new parameters were added and most of the original parameters have been to some extent redefined. For example, based on index measurements and descriptions, joint shear strength has been linked to peak friction angle as required for stability calculations using Barton's non-linear shear strength criterion. Also, "difference in erosion rates" (durability) has been expressed in terms of slake-durability index that allows a forecast of erosion rates (Franklin, 1983, Shakoor and Rodgers, 1992). New RHRON parameters include: the total quantity of unstable rock; face looseness; crest angle (ratio of slope height to width of ditch plus shoulder); and "overspill", an estimate of how much of the road will become blocked by the rockfall.

RHRON includes four "factors" corresponding to obtaining answers to the basic questions and criteria shown in Table 1. During the preliminary rating, each factor is rated on a scale from 0 (good) to 9 (bad) and the ratings are averaged and converted to a percentage. The detailed rating procedure of RHRON is defined identically in that it also gives equal weight to magnitude, instability, reach, and consequence but employs a more comprehensive set of observations in arriving at each factor. The detailed rating also gives equal and separate attention to the three main categories of instability mechanism: ravelling, sliding, and erosion types.

Table 1. Ontario Rockfall Hazard Ratings System Factors

Factor	Question	Assessment Criteria
Magnitude	How much rock is likely to become unstable? How much potential energy would be released?	Volume and mass of rock; height, and velocity and energy of fall.
Instability	How unstable is the material? How likely and how frequent are rockfall events?	Instability mechanisms; face looseness and irregularity; rock quality; shear strength; joint roughness, filling, persistence, and orientation; rock durability and strength; water pressure; seismic accelerations; severity of freeze-thaw process.
Reach	What are the chances of this rock reaching the pavement? How much of the pavement will be blocked?	Kinetic energy - height of fall; size and shape of debris; presence of launching features; ditch width and depth; history and evidence of previous falls
Consequences	How serious are the consequences of the blockage?	Traffic density, rockfall visibility, speed limit, and stopping distance; pavement width.

To obtain reproducible results, each parameter and its range has been carefully specified as well as the distribution of values within this range. For example, the quantity of potentially unstable rock is defined as the total in-place volume that would be removed if the face were to be given the minimum mechanical scaling required for stability. For cases where scaling is inappropriate, this is replaced by the total in-place volume of all potential slides or falls. Full range is defined as 1 to 100 m^3, corresponding to ratings 0 and 9 (2-cycle logarithmic scale).

Further details of RHRON are published in Franklin and Senior 1997(b). A field procedures manual has also been produced complete with appropriate definitions and instructions (Franklin, 1977). Data sheets are available to allow for preliminary ratings, route logs, site segmentation (hazard segments), treatment selection, and cost estimation. An Excel spreadsheet has also been developed to calculate rating values and to determine relative indexing. Sites may be ranked according to greatest hazard rating or indexed according to cost per unit of hazard reduction. Either rank or index values may be used to assign hazard treatment priorities. MTO is now in the process of applying RHRON throughout the province following successful deployment within MTO's northern Region.

Case History: Agawa Bay Hill, Highway 17

A contract was completed in 1996 for the stabilization of a 24 m high vertical rock cut on the westbound lanes of Highway 17 on Agawa Bay Hill, 2 km north of the Agawa River (Fig 2). This site had been identified as problematic for many years and the construction of a west bound truck climbing lane (WBTCL) originally seen as a benefit, eliminated any existing rockfall catchment and increased the risk to the motorist.

In the fall of 1992, a contractor was completing the WBTCL that had been designed between the existing original pavement shoulder and the rock cut. No rock excavation had been included and the resulting section left approximately one metre between the toe of the rock face and the edge of the shoulder. The Ministry of Labour (MOL) had concerns with loose rock endangering workers adjacent to rock face and had made notice that the contractor was not in compliance of the Occupational Health and Safety Act (regulations for construction projects). Specifically, "the walls of an excavation shall be stripped of loose rock or other materials that may slide, roll, or fall upon a worker", and "the walls of an excavation cut in rock shall be supported by rock anchors or wire mesh if support is necessary to prevent the spalling of loose rock". The MOL inspector also pointed out that under the regulations for Mines and Mining Plants: "the vertical height of the working face shall not be more than 25 metres". It was indicated to the contractor and MTO that the "danger area" would be a horizontal distance equal to the vertical height of the rock face. Fortunately, MOL had only chosen this site to apply their regulations, as there are many rock cuts throughout the area to which similar orders could have been given.

An inspection of the site by MTO identified the immediate need for scaling along with a large wedge shaped mass with the potential for sliding failure. The contractor performed hand scaling across the rock face and successfully removed a significant quantity of loose rock fragments. Removal of the larger mass was beyond the capability of equipment on hand and was not completed at this time. The scaling work satisfied the MOL who rescinded their work order so that the final paving of the WBTCL (and ditch) could be completed.

Shortly after this incident, the MOL issued an "Order to Comply" against the MTO District Engineer. This order required MTO to "cause a professional engineer to undertake a comprehensive geotechnical assessment" of five selected rock cuts (including Agawa Bay Hill) and to issue a report indicating the "slope failure potential and recommended measures to ensure their long term stability". Considerable discussion ensued regarding the mandate and jurisdiction of MOL with respect to highway safety. Although MOL acknowledged their responsibility was protection of workers within the "danger zone", MTO unsuccessfully argued their responsibility for addressing rockfall hazards and the compliance order remained. Nonetheless, MTO regarded the Agawa Bay Hill site as a priority and conducted a detailed study as an extension to the findings of the previous contract.

Initial recommendations included several options (Table 2), each one addressing the existing problems to different degrees. (This site has also been subject to long term seepage problems that result in significant ice build-up on the crest and face of the slope in the winter months. While reassessing the hazards at the site, it was discovered that the new WBTCL had to be closed to traffic for at least two months during the winter due to the ice problem. In some years, this ice build-up had been so significant that a blasting contractor had been hired to remove the excess.) Following MTO's recommendations, an independent rockfall hazard consultant (Franklin Geotechnical Ltd.) was also requested to review the Agawa Bay Hill rock cut for an independent assessment.

Table 2. Preliminary options for hazard treatment at Agawa Bay Hill rock cut.

	Overview	Cost estimates
1	rock bolting, 1800 m^2 of suspended wire mesh , 85 m^3 trim blasting,	$164,000
2a	excavate rock cut to standard clear zone - 5.65 m clearance(12,877 m^3), remove and replace asphalt steel beam guardrail	$1,027,000
2b	rock excavation to provide 9.0 m clear zone and standard 250 mm ditch, remove and replace asphalt steel beam guardrail	$1,976,000
2c	rock excavation (25,755 m^3) to provide 9.0 m clear zone increased 900 mm ditch, remove and replace asphalt, steel beam guardrail	$2,082,000
3	realign road - additional 12 m to existing 23 m of R.O.W. required, 11,276 m^3 rock excavation/ 581 m^3 rock fill	$1,412,000
4	realign road and profile, culvert replacement, 20,380 m^3 rock excavation	$2,164,000
5	per consultant's recommendations: rock bolts, drainage, shotcrete (540 m^2)	$220,000

At the Agawa site, the major instability identified was ravelling along the western edge of the face. As such, no factor of safety could be assessed for this mechanism and the final analysis was left to "engineering judgement". Slope instability was assigned a "slight to moderate risk against the occurrence of rockfall" by the consultant. To alleviate the risk, the consultant offered a design that addressed a low probability, medium to large rockfall, i.e., 10m high by 10m long by 2m thick falling 10m from the face. The option of draped mesh was not recommended because of the absence of any adequate ditch and shoulder. Instead, the consultant's recommendations called for an application of shotcrete and rock bolts to eliminate the ravelling problem.

The final design package included the consultant's recommendations for rock stabilization. Final quantities included provisions for manual scaling (40 hours), shotcrete (400 m^2), rock bolts (55), and rock drain holes (100). The contract also included trimming of the large rock wedge. As a final precaution against the ice build-up hazard and to increase protection against errant rockfall, the design also include the removal of the truck climbing lane up to the western end of the rock cut, a total distance of about 1.1 km. The contract package was awarded for the bid price of $360,120 (including pavement removal). Design elements are illustrated in Figure 3. Overall, few problems were encountered with specifications, no items varied more than 15% from the original quantities, and all work was completed within the allotted 30 working days. This site is currently being monitored to document the performance of the rock stabilization measures.

Case History: Alona Bay Hill Rock Cut, Highway 17

Highway 17 crosses Alona Bay at the location of a scenic lookout over eastern Lake Superior. Travelling westward the highway climbs for about 2 kilometres up the east flank of Alona Bay Hill. At the top, the highway passes through a 25m vertical rock cut on the south side of the pavement for about 220 metres (station 15+520 to station 15+740). The rock face at this location has been the site of numerous failures due to near vertical intersecting joints, undermining and insufficient ditch catchment. Figure 2 identifies the site location and offers a glimpse of conditions prior to1993.

A contract in 1993 for this location, had called for the extension of an existing eastbound truck-climbing lane (EBTCL) from station 15+050 to 15+500 with a 200 metre taper ending at station 15+700 (within the area of the Alona Bay Hill rock cut, see Figure 3). During construction, the lane extension was revised and the taper end changed to station 15+500. By implementing this change, the expected rock excavation had been deemed unnecessary for roadway requirements leaving the poor rock face conditions untouched. The contractor had pre-drilled portions of the cut during the late winter months of 1994 and made the decision to continue with the rock excavation. This operation was halted in May 1994 when the MOL issued a stop work order to the contractor for working near the crest without appropriately designed safety equipment. Following discussions with MOL, the contractor was allowed to resume work on the rock cut. The previously drilled area was blasted and removed but the contractor had decided to abandon the remaining excavation, leaving the rock face beyond station 15+635 incomplete. The contractor then moved operations to the removal of approximately 250 m^3 of overhanging rock wedges in an area of progressive recurring failure (vicinity of station 15+700). This work was completed with a backhoe working from the pavement elevation.

Following the completion of this contract in late 1994, attention over this site remained. In September 1995, a member of the public (geologist working for a private mining firm) had expressed concern over this site to the District Engineer. At the same time, the local maintenance patrol had noted that, in their opinion, rockfalls at Alona Bay Hill had increased following the extension of the EBTCL. A site visit was made to review conditions and assess priority of the work. MTO's focus at this time was directed to resolving the outstanding MOL compliance order against five other sites further to the north as well as resolving stabilization design of the Agawa Bay Hill rock cut. (The MOL compliance order did not include the Alona Bay Hill site.)

The initial review of the Alona Bay Hill rock cut identified four zones along the face where different treatments could be applied. Preliminary recommendations included a program of scaling and trimming to remove a significant portion of untreated minor hazards, particularly those located near the crest as well as smaller blocks along the face. This approach would deal with immediate hazards only and would require an annual review of the site to document and identify progression of new hazards as well as a regular inspection by a competent scaling contractor (3-5 year cycle). These recommendations were forwarded in view of the imminent work at Agawa Bay since it would have been possible, from a scheduling perspective, to include both sites under the same contract. However, MTO eventually decided that this contract would deal strictly with the Agawa site without the addition of any other rock cuts. The recommendations for Alona Bay were placed on hold pending future construction projects in the area.

In early 1997, the Alona Bay Hill rock cut was considered for inclusion in the work plans for an upcoming contract to the south of the Montreal River. This project was to be managed as a Total Project Management (TPM) assignment whereby consultant services would be hired for site survey, site evaluation and recommendations, contract package preparation, and construction administration for engineering services. Under this initiative, an Expression of Interest (EOI) was released by MTO to elicit responses from private industry. Requests for proposals were delivered to those consultants who qualified for the TPM assignment as per the evaluation of the EOI. David F. Wood Consulting Ltd was retained by the prime consultant responsible for the TPM assignment. A site assessment was carried out and the following options for Alona Bay Hill rock cut were proposed:

Option 1: This option addressed stabilization of the existing excavation through local trim blasting, scaling, rock bolting, and buttressing. Considerations for future application of shotcrete and/or suspended wire mesh were suggested as post construction add-ons, pending the outcome and success of the initial work. The consultant recognized that face stabilization through this type of program would require ongoing maintenance in the form of annual ditch cleanout and a thorough scaling revisit every ten years.

Option 2: This option considered increasing available ditch catchment volume and shape through the addition of a Jersey barrier wall and ditch excavation in addition to the measures included in Option 1. Installation of the barriers along the edge of pavement would require a minor highway realignment to allow for a minimum 4 metre wide ditch. It was estimated that this would provide approximately 60% retention of rock fall material. A scaling program similar to Option 1 would be required.

Option 3: This option proposed highway realignment away from the rock face to increase rock fall catchment. Rock excavation would be required along the opposite rock face that is less than half the height of the hazard rock cut. This alternative would allow for the extension of the EBTCL as well as incorporation of a full clear zone width to reduce the need for maintenance scaling and/or ditch cleanout. However, highway geometry would require the creation of a reverse curve alignment on a moderately steep grade along with construction of steep fills.

Option 4: This option was for the continuation of the rock excavation abandoned under contract 93-226. This would remove the potential wedge failure blocks through station 15+700 as well as additional weathered and fractured surface rock. The expected results would include increased overall stability and a reduced maintenance schedule (scaling assumed every 10 years). Results would be dependent on the quality of drilling and blasting.

These options offer two main approaches to the problem at hand - short term vs. long term solutions. The simplest short-term solutions of scaling, trimming, buttress support etc. lead to high maintenance costs whereas the long-term solution requires a higher initial capital outlay. To compare each of these options on an even basis, a 30-year lifecycle costing was developed by the consultant and is shown in Table 3.

Table 3. Alona Bay Hill rock cut - Lifecycle cost estimates (Wood, 1998)

Option		Initial Cost ($)*	Maintenance Cost ($) (present value)	30 year Total Cost ($)	Remarks
1	Trim blasting, scaling, bolting, shotcrete, wire mesh	165,870	113,130	279,000	Includes $50,000 expenditure every 5 years for 30 years
2	Trim blasting, scaling, bolting, shotcrete, wire mesh, and jersey barrier	200,000	110,000	310,000	Includes $5,000 expenditure every year for 30 years; plus $50,000 in each 10 year period (10 & 20 years)
3	Alignment shift away from hazard rock face	447,000	---	447,000	No maintenance costs allocated
4	Cut back existing slope at 1:4	316,000	43,900	360,000	Includes $50,000 expenditure in each 10 year period (10 & 20 years)

*unit costs based on data presented by Franklin (1977)

The consultant recommended the simplest, most cost-effective solution - Option 1, taking into account the continual maintenance requirements and the associated risks of potentially continual, albeit reduced rockfall. New fallout design criteria for ditch fallout capacity (Pierson et al, 1994) indicated that the existing ditch met the criteria for somewhat less than 30% retention. Improvement to about 60% retention could be obtained by the addition of jersey barriers for a moderate incremental cost as indicated under Option 2. This improvement may not alter the maintenance situation and in fact could increase such costs by having to remove the barriers for ditch cleanout. The benefit of Option 2 is the added overspill protection against an unpredicted rockfall.

Final design quantities and specifications were attached to the contract, which also included 17.8 km of pavement reconstruction. Design details are shown in Figure 3. The final design package items were: trimming (170 m^3); mechanical scaling (350 hours); shotcrete (220 m^2); rock bolts (43); rock drain holes (20); concrete buttress (90 m^3); and suspended wire mesh (1200 m^2). The inclusive bid price for these stabilization elements in the successful bid was approximately 8% of total contract bid. The contract was awarded and completed in 1999.

Summary

MTO has developed a rockfall hazard rating system based on the evaluation of more 200 high-risk sites in northern Ontario. The RHRON system includes parameters that are sensitive to the physiography, geology, and blasting methods used in construction of highway rock cuts throughout the Canadian Shield. It is expected that this system will be applied over the entire province and used for long term rockfall hazard management decisions. Individual sites will always require detailed planning to meet both long and short term objectives.

Two case histories (Agawa Bay and Alona Bay) involving relatively high rock cuts on Highway 17 along the eastern edge of Lake Superior have been presented. Both these cases illustrate how long term approaches do not necessarily win out under the influence of external pressures as both sites were revisited within 3 years of construction. These projects also illustrated a number of technical design options that were considered. At the Agawa site, initial costs were most influential, whereas at the Alona site, ongoing maintenance was included in the overall life cycle costing.

References

Brawner, C.O. and D. Wyllie, 1975. Rock Slope Stability on Railway Projects, in Proceedings of the American Railway Engineering Association Regional Meeting, Vancouver, B.C.

Franklin, J. A., 1997. RHRON - Ontario Rockfall Hazard Rating System: Field Procedures Manual, Franklin Geotechnical Ltd Report G785.3 prepared for Ministry of Transportation Ontario

Franklin, J. A., 1983. Evaluation of Shales for Construction Projects - an Ontario Shale Rating System, Ministry of Transportation & Communications, Ontario, Report RR229.

Franklin, J. A. and S. A. Senior, 1997a. Rockfall Hazards - Strategies for Detection, Assessment and Remediation, Proceedings, Engineering Geology and the Environment, Marinos, Koukis, Tsiambos, and Stournaras (Eds.), Balkema, Rotterdam

Franklin, J. A. and S. A. Senior, 1997b. The Ontario Rockfall Hazard Rating System, Proceedings, Engineering Geology and the Environment, Marinos, Koukis, Tsiambos, and Stournaras (Eds.), Balkema, Rotterdam

Magni, E. R., 1984. Rock Cut Stability along Ontario Highways, Proceedings, 4th International Symposium on Landslides, Toronto, Ontario.

Pierson, L. A., S. A. Davis, and T. J. Pfieffer, 1994. The nature of rockfalls as the basis for a new fallout area design criteria for 0.25:1 slopes. Research Report SPR 5287. Oregon Department of Transportation.

Pierson , L. A., S. A. Davis, and R. Van Vickle, 1990. Rockfall Hazard Rating System Implementation Manual, Report FHWA-OR-EG-90-01, Oregon State Highway Division, Engineering Geology Group.

Shakoor, A. L. and J. P. Rodgers, 1992. Predicting the Rate of Shale Undercutting along Highway Cuts. Bulletin of the Association of Engineering Geologists, Vol. 29 No. 1, pp 61-75.

Wood, D. F. (1998). Report to Northland Engineering (1987) Limited on Rock Mass Conditions for WP 272-90-00, Highway 17, Alona Bay, Ontario, David F. Wood Consulting Ltd.

Wyllie, D., 1987, Rock Slope Inventory System; in Proceedings of the Federal Highway Administration Rockfall Mitigation Seminar, F.H.W.A. Region 10, Portland, OR.

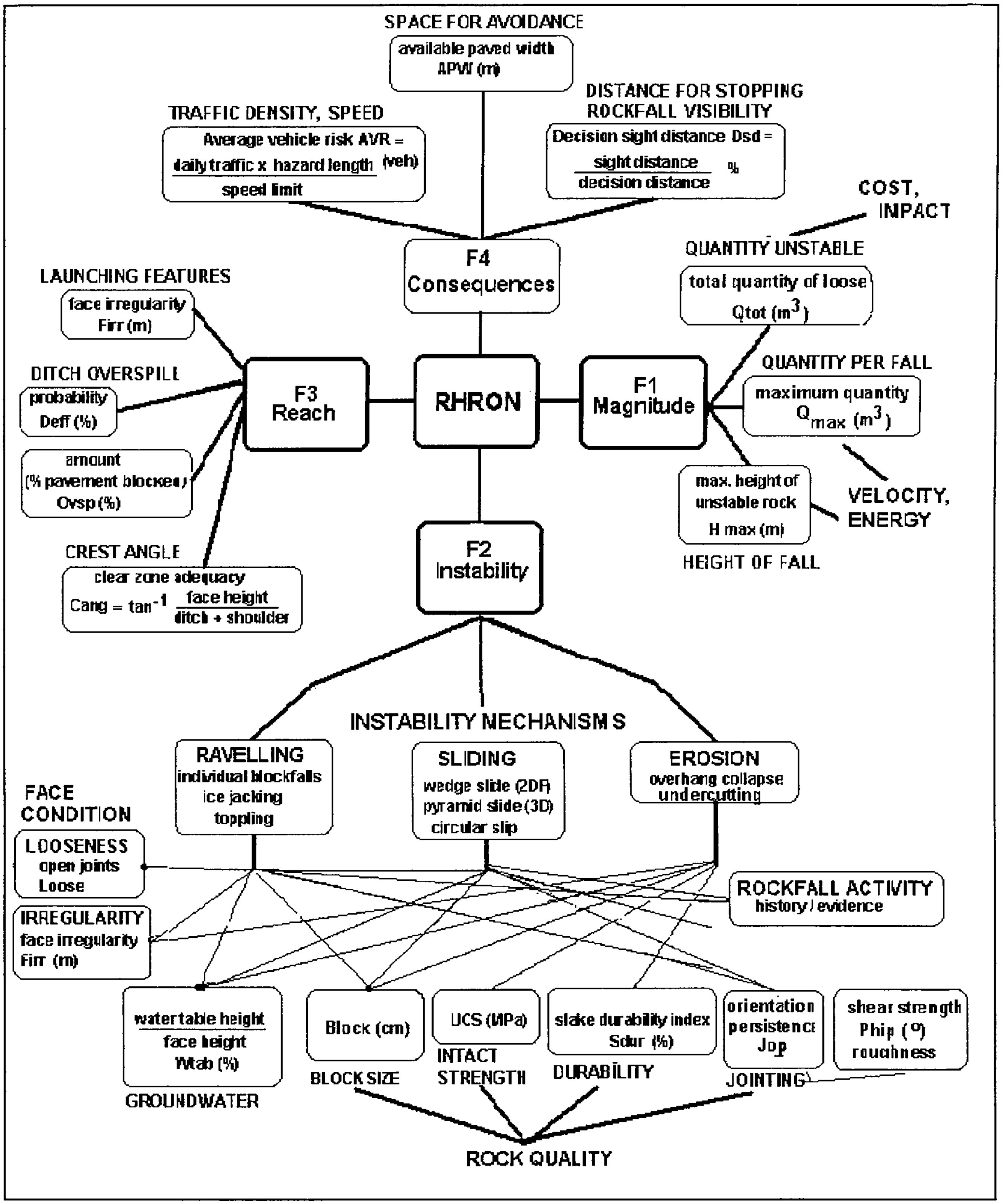

Figure 1. Schematic layout of Ontario Rockfall hazard rating System

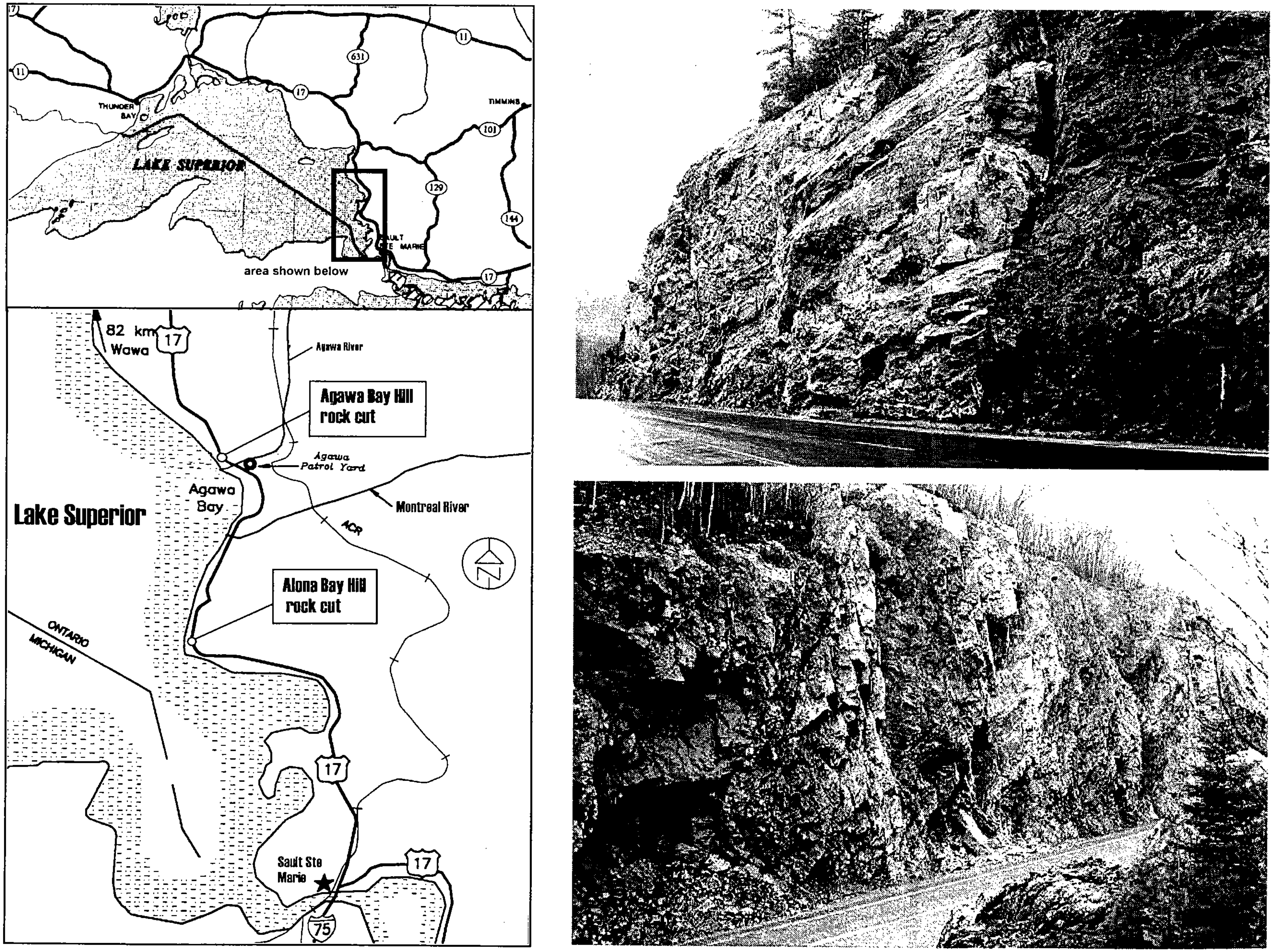

Figure 2. Locations and photographs of Agawa Bay Hill rock cut (upper rigth) and Alona Bay Hill rock cut (lower right)

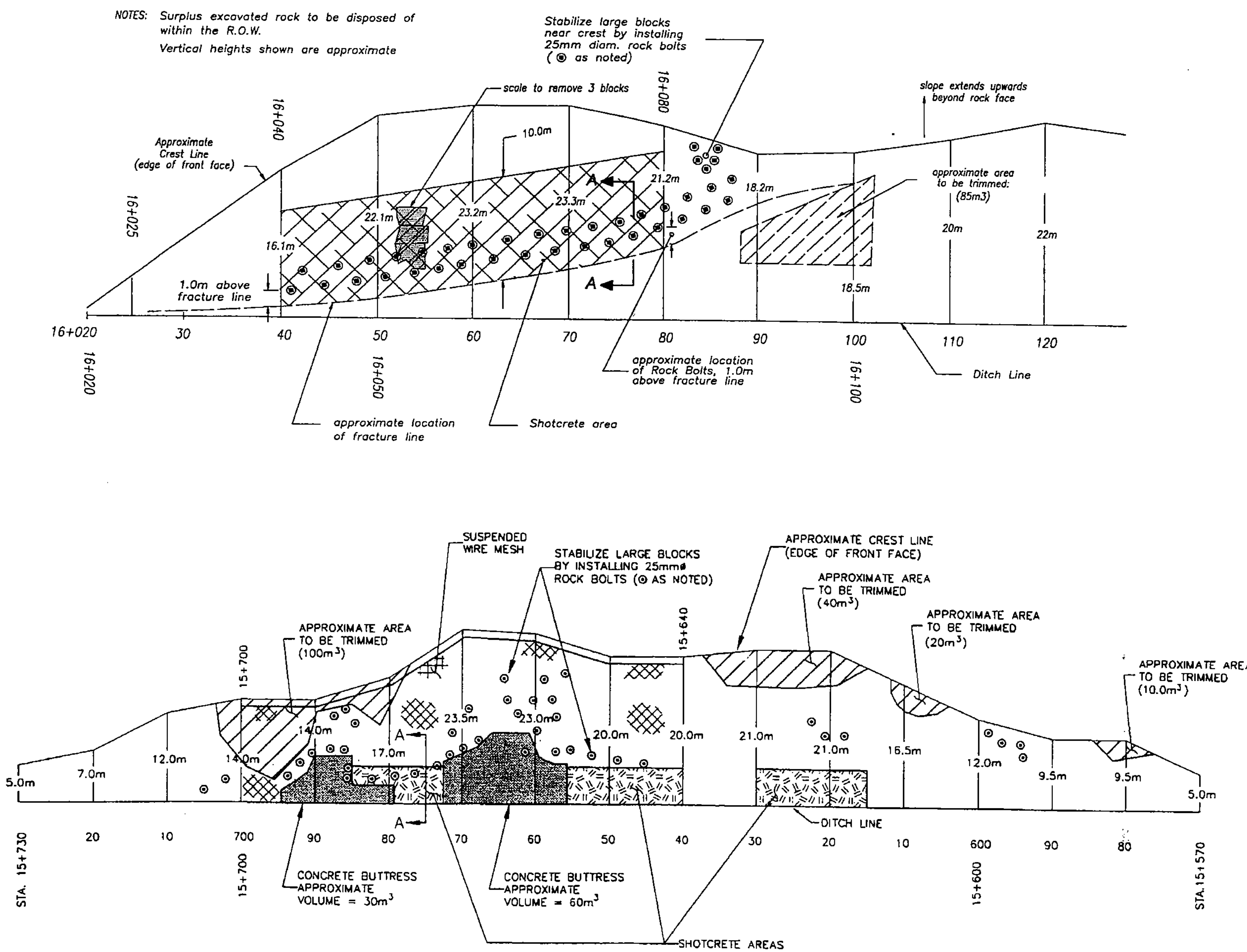

Figure 3. Contract drawings for Agawa Bay (upper) and Alona Bay (lower) rock cuts detailing rock hazard mitigation measures.

Design and Construction of Major Cuts on US 460 in Virginia

Presented to

Highway Geology Symposium
50th Anniversary Meeting
May 1999

Written by

James M. Sheahan, P.E.
Chief Geotechnical Engineer
HDR Engineering, Inc.
Pittsburgh, PA
(Tel: 412-497-6039; e-mail: jsheahan@hdrinc.com)

Stan L. Hite, P.E.
Assistant State Materials Engineer
Virginia Department of Transportation
Sandston, VA
(Tel: 804-328-3108; e-mail: hite_sl@vdot.state.va.us)

Sam Graybeal
District Geotechnical Engineer
Virginia Department of Transportation
Bristol, VA
(Tel: 540-669-9953)

Introduction

US Route 460 crosses the entire State of Virginia from Norfolk on the east to the point where it crosses into Kentucky just north of Breaks, Virginia (Figure 1). The 10-mile section from Deel to Harmon Junction in Buchanan County is one of the few remaining sections in the state that is not four lanes wide. Most of the construction for this segment is on or adjacent to, the existing two-lane facility through a narrow valley between the Levisa Fork River and homes, businesses and steep mountainous terrain. A railroad on the other side of the river servicing coal-handling facilities is located in this major coal mining region. US Route 460 is heavily traveled by private and commercial traffic including many coal-hauling trucks. The Town of Grundy is situated along this segment. Virginia Route 83 intersects Route 460 in Grundy and both routes are coincidental until Route 83 diverges to the south at Vansant. HDR prepared designs for this segment of Route 460 under a contract with the Virginia Department of Transportation. Line segments were designated Sections 501, 502, 505 and 506.

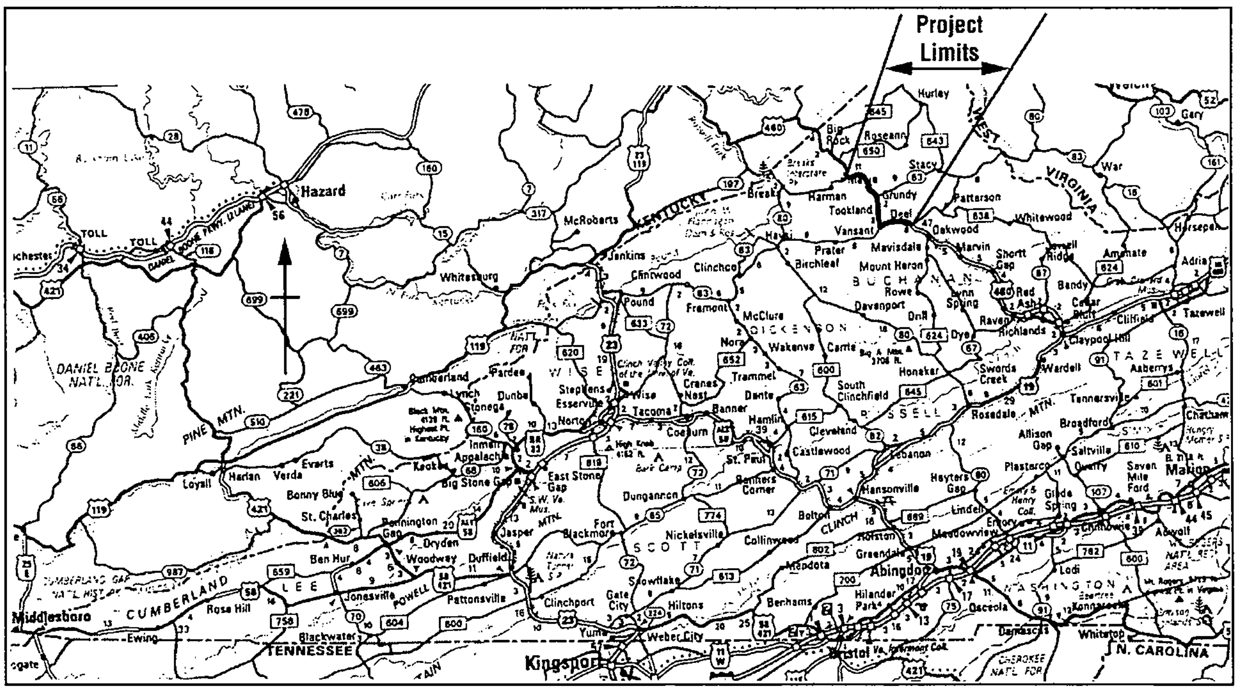

Figure 1 - Project Location Map

There is a difference in elevation of over 2000 feet between the valley floor and the steep slopes leading up to the mountain ridges. The project includes eleven rock cuts ranging in height from 100 to 400 feet and a number of embankments or retaining walls. There are few readily available areas for wasting excavation, and there are no temporary detour routes available; therefore, traffic has to be maintained during construction.

Construction of Section 502 was completed in 1997 and Section 501 construction began in 1998 but has not yet been completed. Sections 505 and 506 will be constructed in the future.

This paper describes the investigation and design process used for cuts on the project with emphasis on a 400-foot high cut constructed in Section 502.

Geology of the Project Area

The project lies within the Appalachian Plateau Physiographic province. Surface rocks are of Lower and Middle Pennsylvania Age and are from the Norton Formation (Figure 2). The rock sequence consists primarily of persistent sandstones with interbedded siltstone, claystone, shale and coal. Major units include the Council and McClure sandstones. Nolde (1984) reports that there are twenty named coal seams in the area, seven of which have been commercially mined. In ascending order the five mined coal seams in the Norton Formation are the Raven (Red Ash) No. 1, Kennedy, Lower Banner, Splash Dam and Hagy. All of these seams are above the valley floor. The Pocahontas No. 3 coal seam is the most important commercial seam in the area. It is located near sea level about 1200 feet beneath the valley.

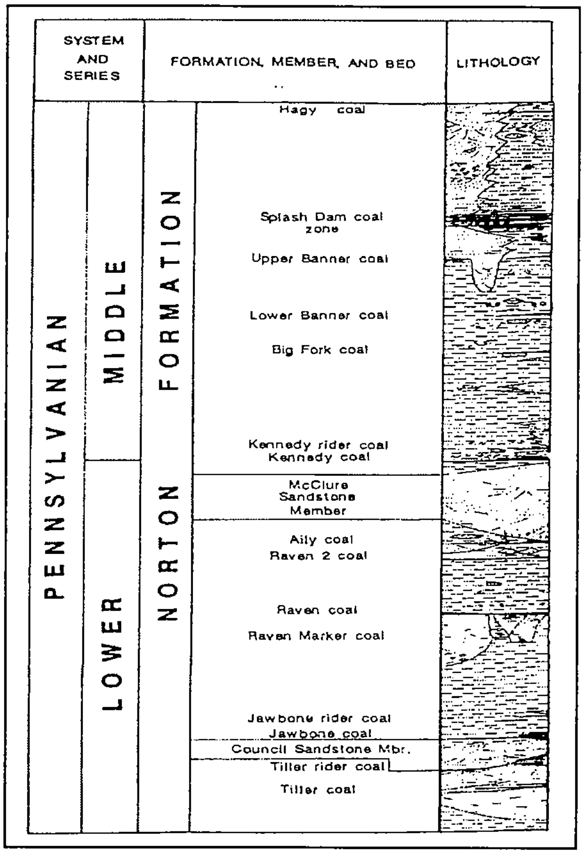

Figure 2 - Geologic Column

Structurally, the regional dip of these formations is toward the northwest at about 35 to 70 feet per mile although local folding is sometimes more pronounced. Figure 3 shows structure contours on the Splash Dam coal seam in the area of Sections 501 and 502. The dip appears to be steepest in the area from Deel to Vansant where it is about 170 feet per mile. The Pine Mountain Anticline, which trends southwest to northeast, crosses the Levisa Fork River about 4 miles north of Route 609, while the north-south trending Middleboro Syncline is located several miles south of the project. There are three known faults in the area but all are outside the project area. A minor fault was found in the formations adjacent to the railroad tracks near the

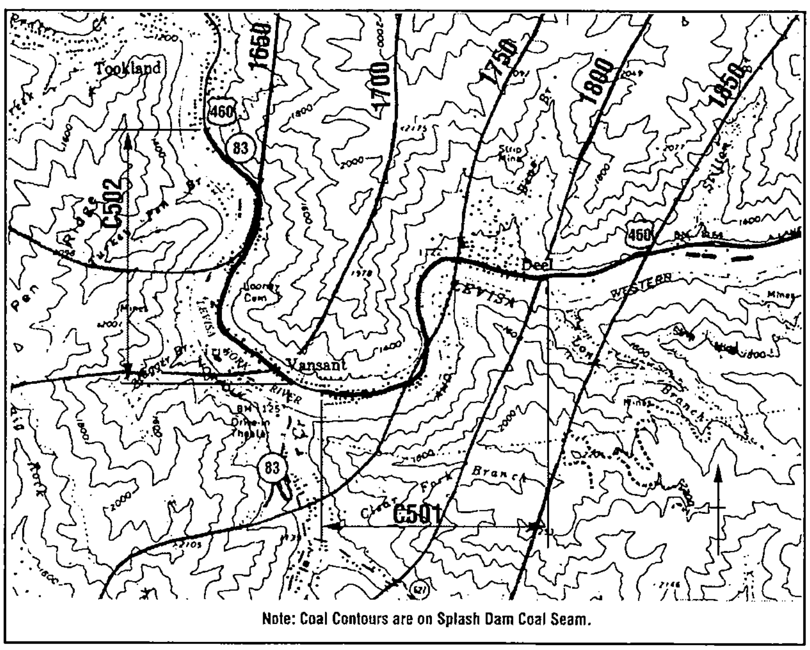

Figure 3 - Geologic Structure Map for Sections 501 and 502

intersection of Routes 83 and 460 but it does not influence the project. A geologic profile was developed for the alignment using borings, exposures and other geologic data. Figure 4 shows the profile for Sections 501 and 502. Similar profiles were developed for Sections 505 and 506. Major cuts in each section were designated by section number and letter, e.g., Cut 501A, 501B.

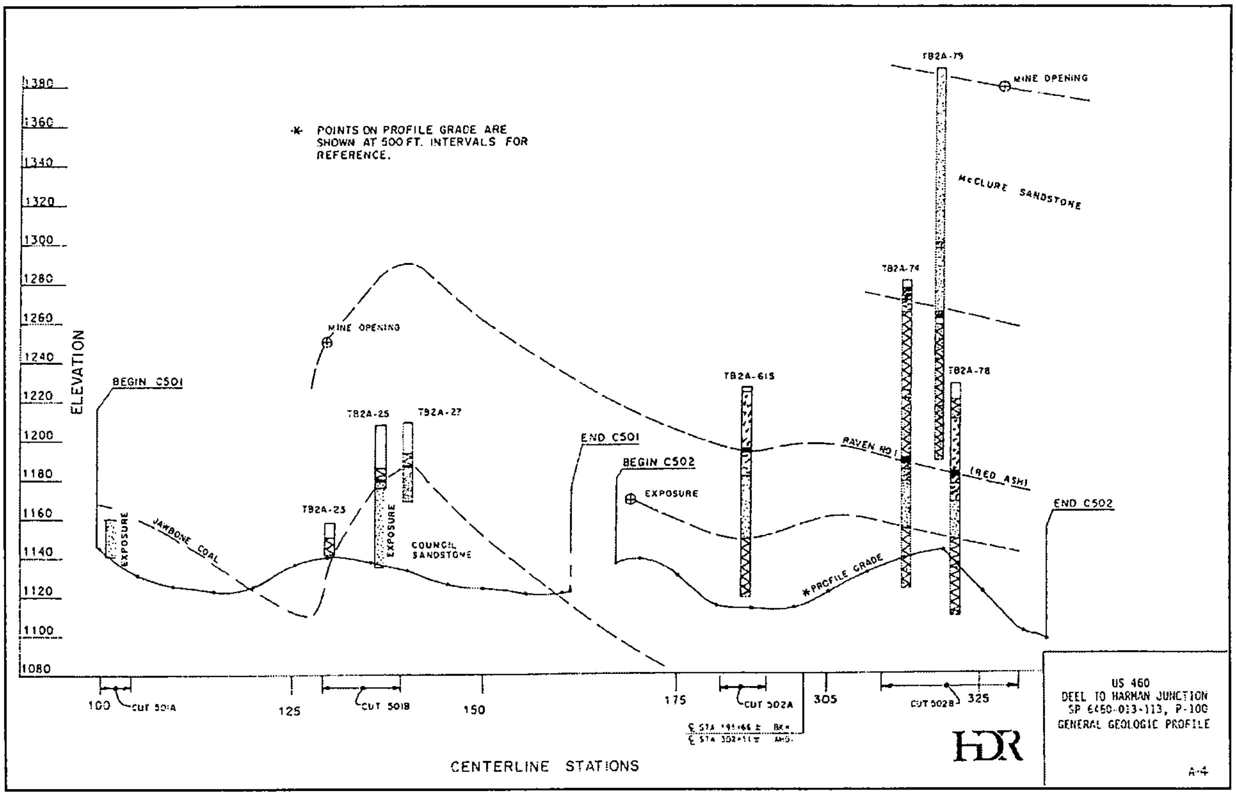

Figure 4 - Geologic Profile for Sections 501 and 502

A significant factor in the development of overburden is the erosion and differential weathering of shales and siltstones underlying harder sandstones as the Levisa Fork River was downcutting through these formations. As the shales and siltstones deteriorated, undercutting the sandstones, stress relief joints were intercepted causing rockfalls. The resulting heterogeneous colluvium contains boulders, shale and rock fragments in various stages of weathering. These colluvial formations are usually found on the shale formations that separate prominent sandstones. Nests of boulders are sometimes found in deeply eroded gullies or on hillsides. In some areas colluvium still remains on the mountainsides just below the massive sandstone exposures, or is lodged in steep ravines on the hillsides. In either location it is susceptible to rapid, unpredictable movement or debris slides, particularly during wet periods.

Design Phase

Borings were generally located at intervals of about 200 feet along the alignment and were used in conjunction with exposures and previous geologic mapping to establish a geologic profile as well as to obtain information on the quality and extent of soil and rock. At least one boring was drilled in each major cut, and some horizontal borings were drilled to examine joint spacing. A considerable amount of care was taken during setup of the program to minimize property damage and coordinate with property owners. For this reason and because access to some sites above the existing road posed safety concerns, a helicopter was used to move on and off some of the sites. Three different drilling subcontractors worked simultaneously on the full project to complete 278 borings. One contractor coordinated helicopter services to move as many as six of the ten drill rigs used by the three firms. This resulted in a very efficient use of the helicopter.

Rock Quality Designation (RQD) values for much of the rock in the major cuts were above 75 percent and rock could be classified as "Good to Excellent" (Deere, 1963). Unconfined compressive strength and wet/dry slaking durability tests were performed on representative samples from these formations. In this test, core samples were alternately soaked for eight hours then oven-dried for eight hours at 110°F for five cycles. Unconfined strength test results for siltshales and sandy shales ranged from approximately 2,000 to 5,000 psi while sandstones and some siltstones ranged from about 10,000 to 15,000 psi. However, durability tests showed that some of the siltshales were susceptible to slaking and would deteriorate to thin chips within the five wet-dry cycles. Sandy shales and sandstones showed little or no effect in slaking tests.

Numerous rock exposures were logged and the orientations of 619 rock discontinuity surfaces were measured at these exposures over the length of the project. In each case the strike, dip and condition of the surface were noted. Table 1 summarizes the distribution of the measured dip angles. Results show that two-thirds were steeper than 75 degrees (1/4:1 slope) and over 90 percent were steeper than 64 degrees (1/2:1). This distribution was essentially the same within each construction section over the length of the project and was similar to those reported by Nolde (1984) for geologic studies in the area. Horizontal borings and field observations indicated that joints were moderately to closely spaced (1' to 10').

Table 1
Distribution of Measured Dip Angles on Discontinuities

Construction Section	Total Measurements	Distribution of Measured Dip Angles		
		<64°	64° to 75°	>75°
501/502	189	25 (14%)	46 (24%)	118 (62%)
505	230	6 (3%)	54 (23%)	170 (74%)
506	200	10 (4%)	51 (26%)	139 (70%)
Totals	**619**	**41 (7%)**	**151 (24%)**	**427 (69%)**

The effects of discontinuities on each rock cut were evaluated using methods described in Hoek and Bray (1981).

Cut 502B is approximately 1700 feet long and over 400 feet high from grade to the top of the finished slope. It represents the most significant cut on the project. Existing Route 460 was located at the base of the existing hillside where a siltshale had been eroding beneath a sandstone (Photo 1).

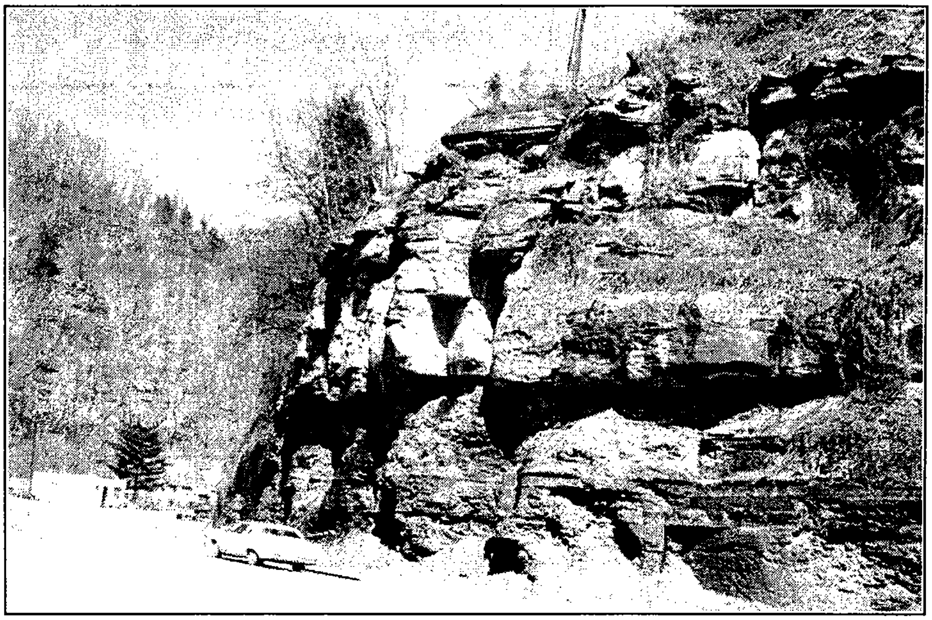

Photo 1 - Shale Undercutting Sandstone near Cut 502B

Poles representing the 97 measured discontinuities at this cut were plotted on a spherical projection and representative "poles" were selected based on the contouring of the pole plots. Figure 5 shows the discontinuity plot and Figure 6 shows the discontinuity frequency contour plot for the 97 poles. Four representative poles were selected from this plot (DP-1 through DP-4), and planes representing cut slopes of 1/4:1 and 1/2:1 were superimposed on projections (Figure 7). Due to the curvature of the alignment in the area, a range of cut slope bearings was used in the analysis.

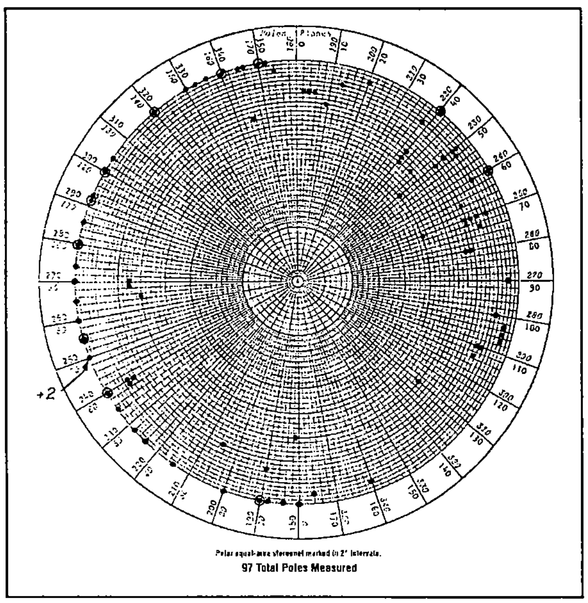

Figure 5 - Plot of Poles for Measured Discontinuities at Cut 502B

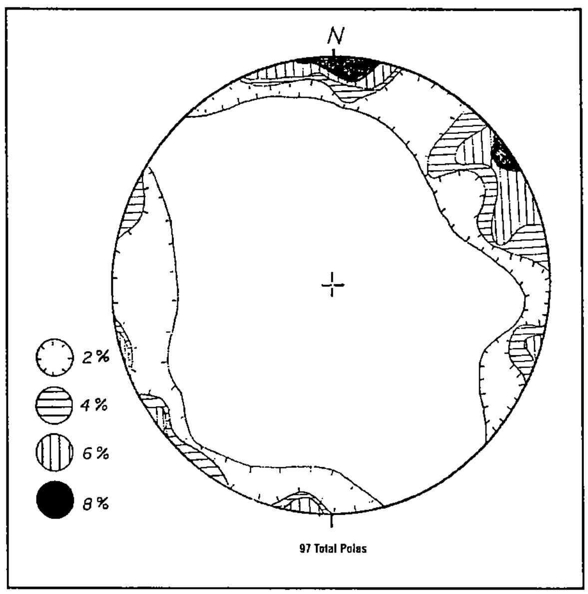

Figure 6 - Contour Plot of Discontinuity Frequencies at Cut 502B

Results suggested a small chance of plane failure with 1/2:1 slopes for those discontinuities that would be parallel to the cut face and a slightly greater chance with 1/4:1 slopes. This would be consistent with data in Table 1. However, not all of the measured discontinuities were parallel to

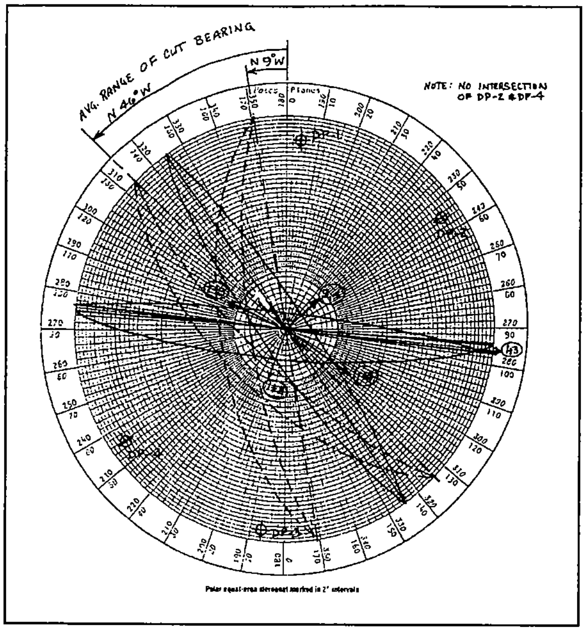

Figure 7 - Analysis of Discontinuity-Cut Slope Interaction at Cut 502B

the intended cut slope orientation, suggesting that the number of potential plane failures should be limited. Plots suggest wedge failures with 1/2:1 cut slopes should be negligible while there was some chance they might occur with 1/4:1 slopes for certain cut bearings. Results also suggested the potential for toppling was minor. Several cut slope designs were considered including a benched configuration with different slope ratios in formations and a single slope ratio for the entire cut. Alternate designs included the use of slopes as flat as 1:1 in shales subject to deterioration and 1/2:1 slopes in sandstones, with and without benches at changes in lithology. Excavation quantities increased as flatter slopes and benches were used. The selected slope design included 1/4:1 slopes with a "fall bench" at road level and 20-foot wide intermediate benches at lithology changes from less weather-resistant to more weather-resistant formations, e.g., at the top of shale formations underlying sandstone formations. Fall bench dimensions were patterned after studies presented by Ritchie (1960) for what has been referred to as a Washington Ditch. An additional, intermediate bench was placed in the McClure sandstone because it was so high in the cut, is so massive (more than 100 feet thick) and may contain some fractured zones based on some boring information. It was intended that these features would provide an economical design while controlling the risk of potential for rockfalls that might reach the roadway. Pre-splitting was specified for finished slopes to minimize fracturing at the face. A number of special provisions were included in the contract to control impacts on traffic and blasting activity in this area with many businesses and residences nearby. Figure 8 on the next page shows the Cut 502B design section.

Rockfall simulation was conducted using the Colorado Rockfall Simulation Program (CRSP) with special emphasis on possible falls from the McClure sandstone. Results suggested the benched cut would likely catch falls that might occur or slow them as they moved down slope. Simulations with a slope that had some weathering of benches and debris on the benches suggested the falls would still likely be caught in the fall bench, if it is maintained.

Construction Phase

The contractor for the project was Elmo Greer and Sons, Incorporated from Kentucky. His initial work included a pre-blast survey of nearby homes and businesses. A concrete barrier and fence assembly was installed at road level to provide some separation of traffic from potential falls (Photo 2); in addition, a trench approximately 50 feet wide and 15 feet deep was excavated in the middle-to-lower section of the slope to catch excavated material. Trees cleared from the slope were placed against the downslope side of the trench to improve the barrier while trees below the trench were allowed to remain uncut. Excavated material was pushed off the high slope into the trench where it was loaded by a Hitachi Model 1100 excavator into trucks

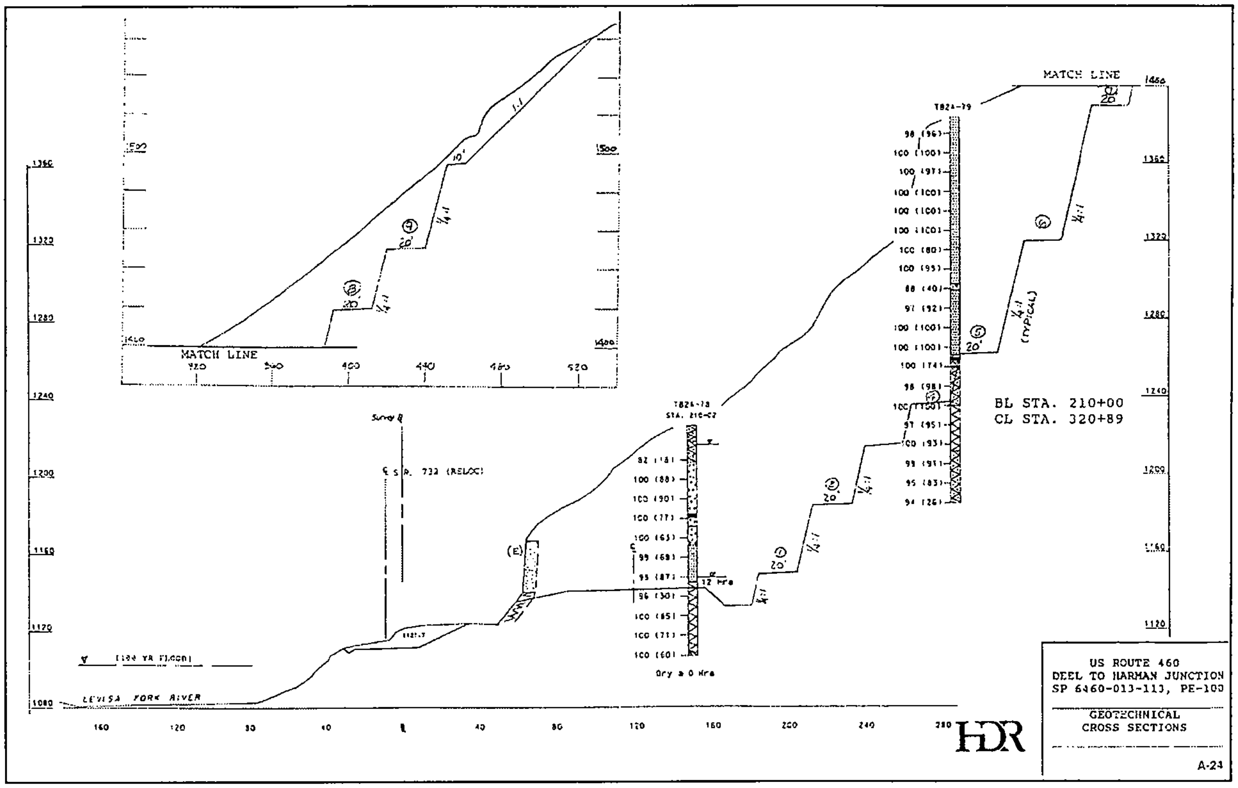

Figure 8 - Design Cross Section of Cut 502B

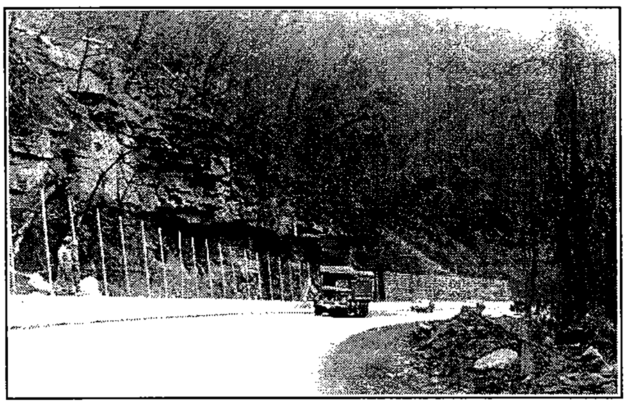

Photo 2 - Construction Fencing at Road Level

(6-wheel drive Volvo Model 435s and CAT Model 777s) and taken to the waste area. Blasting was not allowed during periods when school was in session, during rush hour (4 to 6 PM) or at night. Maintenance of traffic was very difficult. Traffic could not be stopped from 7 to 9 AM and 4 to 6 PM. Traffic was always stopped during blasting and was not allowed to proceed again until the contractor had made an inspection of the blast area in the slope. Much of the heavy excavation was made at night when traffic was minimal. A few boulders did roll onto existing Route 460 after blasting, and some were large enough to require additional traffic delays while they were broken down into manageable sizes; but these occasions were very limited. Three times these falls damaged a 14-inch water line under the shoulder of the road. This line was to be relocated subsequently. On one occasion, some softball-sized rock fragments were thrown from the hillside by a blast and caused some damage to autos in a nearby parking lot.

The waste area was located in a gully on the opposite side of the Levisa Fork River. Access required crossing Route 460 and the river. Temporary pipes were placed in the river after obtaining a permit for a low-water crossing from the US Army Corps of Engineers. More than a million cubic yards of

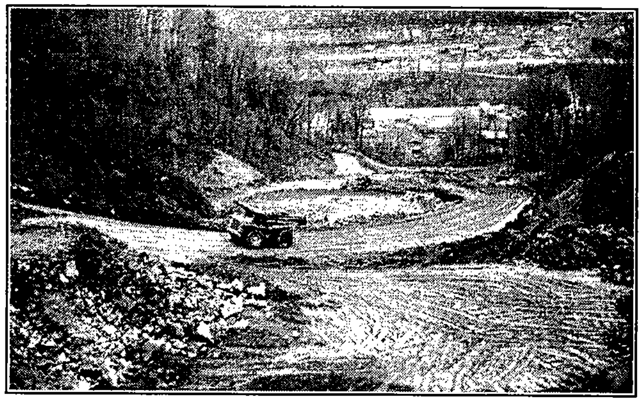

Photo 3 - Cut 502B with Excavation Near Grade **Photo 4 - Waste Area Across Levisa Fork River**

waste was placed in this area. Photos 3 and 4, respectively, show the excavation for Route 460 as it approaches grade and trucks moving up the steep grade in the waste area.

A mine opening was found in the Kennedy coal seam just above the McClure sandstone. A minimum 10-foot thickness of rockfill was placed in the entrance, and this was grouted after placing 6-inch diameter pipe through the rockfill to prevent the buildup of water behind the backfill. No drainage was observed at the time the opening was encountered.

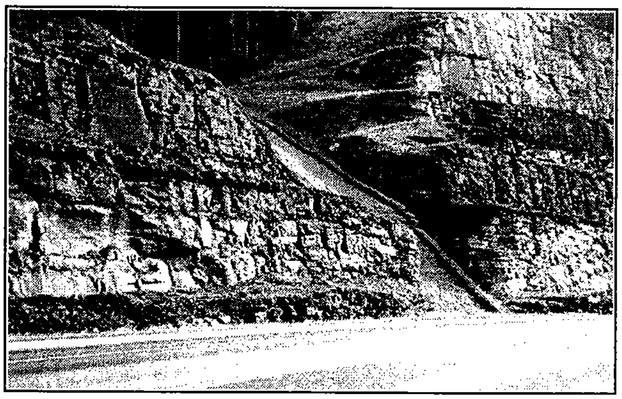

Photo 5 - Gabions in Channel Between Cut Sections

Cut 502B actually consists of two cuts separated by a large drainage gully. A gabion-lined channel was constructed to handle significant drainage flows through that gully. Individual baskets were installed at the bottom of the channel to act as energy dissipators. Photo 5 shows the channel at its completion.

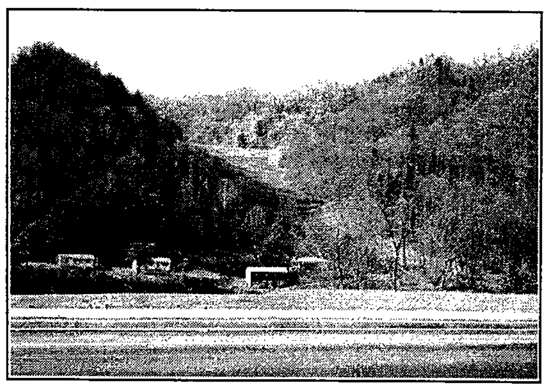

Photo 6 - Completed Waste Area

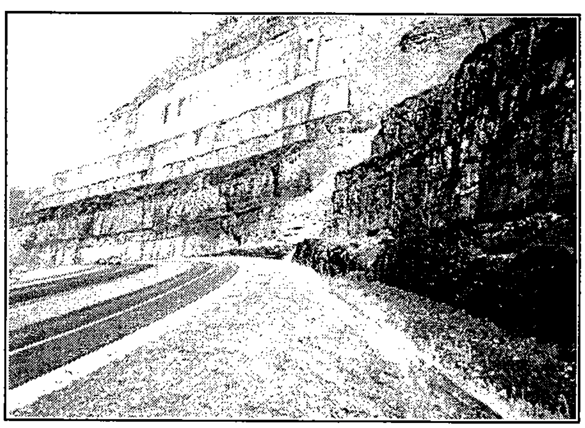

Photo 7 - Fall Bench at Base of Completed Cut.

Photo 6 shows the waste area after it was seeded and closed, and Photo 7 shows the fall bench at the base of the cut. It can be cleaned if debris collects with time.

Summary

The construction of four lanes for US Route 460 through the mountainous sections of western Virginia will require many significant rock cuts as well as retaining walls and embankments within a narrow river valley and must be constructed while traffic flows are maintained. The slope designs will consider the geology of the site as well as constructability issues. A major cut (shown in Photo 8) has been successfully completed on the first construction section. Blasting damage was not significant, and traffic was maintained with minimal interruptions even with excavation equipment hauling across US 460 to the waste area.

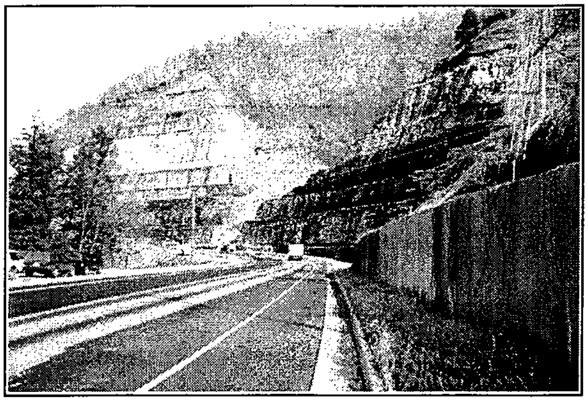

Photo 8 - Completed Cut 502B

Bibliography

Deere, D. U. (1963), "Technical Description of Rock Cores for Engineering Purposes," *Rock Mechanics Engineering Geology,* Volume 1, pp 18-22.

Hoek, E. and Bray, J. W. (1981), *Rock Slope Engineering*, The Institution of Mining and Metallurgy, London.

Nolde, Jack E., Martin L. Mitchell and Joan K. Polzin (1984), *Geology of the Prater and Vansant Quadrangles*, Virginia Department of Mineral Resources Publication 52, Department of Conservation and Economic Development, Division of Mineral Resources.

Ritchie, A. M. (1963) "Evaluation of Rockfall and Its Control," Highway Research Board, Highway Research No 17, pp 13-28

ROCK SLOPE ENGINEERING IN COMPLEX GEOLOGY

JENKINS BY PASS

ABSTRACT

By
Earl Wright, P.G. Engineering Geology Section

Kentucky Department of Highways

The US 23 project originated February 17, 1966, when Cecil Hatter, Kentucky's Assistant Director of Design, signed a letter of agreement with the Virginia Department of Transportation to meet at the state line with a new four-lane highway. Numerous construction problems were encountered due to changes in environmental and highway geometric design standards. The 1975 design plans had to be modified for 1998 standards. The new highway cost approximately $53.3 million and was officially opened September 28, 1998.

INTRODUCTION

Pine Mountain is a 125-mile long, 2,000 –foot – high ridge that runs across southeastern Kentucky. The ridge was formed by the Pine Mountain thrust fault that is the easternmost expression of the Appalachian Valley and Ridge physiographic province. The surface trace of the fault varies from north 55 degrees east to north 60 degrees east and the dip of beds is approximately 25 to 30 degrees to the southeast. The Russell Fork Fault defines the northeast end of the thrust fault at Elkhorn City and the southeast end of the thrust fault is the Jacksboro Fault near Jellico, Tennessee. The fault surface moved horizontally along the Devonian Shale, but broke more steeply upward through stronger beds to create the overthrust fault in the valley immediately north of Pine Mountain. The strata on the north flank of Pine Mountain include the dipping strata of Devonian to Pennsylvanian Age. The crest of the mountain is capped by a hard sandstone and conglomerate, which consists of more than 90% quartz grains. Pine Mountain is dissected at several locations by transverse faults, which usually uplifts weaker shales that weather and result in Gaps in the ridgelines. The old section of roadway went through the Pound Gap fault section that had a displacement of 140 feet.

DESIGN OF THE CUT

Overall, cuts generally exceeded 300 feet in depth. The average cut slope lifts was 40 feet high and the angle of the cut slope varied according to the lithology type, geometry of the structural discontinuities, and the slope orientation. The 18 foot intermediate benches were intended to be horizontal to avoid the possibility of concentrating runoff and creating severe erosion problems. In some sections, where possible, the rock was removed along the bedding plane when the dip was into the roadway. Near the foot of the mountain, the cut slopes in the Grainger Formation were modified to remove benches that were anticipated to be ineffective. The Grainger formation contained a large percentage of slaking shale with interbedded weak sandstone beds and the cut slope was changed to a 1V:2H slope with a wider roadside ditch bench.

Strata north of the overthrust are generally flat lying sandstones, siltstones, shale and coal beds in the Breathitt Formation of Pennsylvanian Age. Strip and abandoned underground coal mines are present through the northern part of the project. The abandoned mines were sealed and millions of gallons of water accumulated in the down dip sections. Underground mines presented numerous stability and drainage problems. In some sections the contractor stabilized the area under the roadway by blasting the roof rock to collapse the mine and then recompacted the top five feet.

HISTORY

A general history of the project covers approximately 32 years. The project was initiated on February 17, 1966 when Cecil Hatter, Kentucky's Assistant Director of Design, signed a letter of agreement with the Virginia Department of Transportation to meet at the state line with a new four-lane highway. Kentucky's Geotechnical Branch became involved in 1968. Planning and design work started in 1977. Haworth, Meyer and Bolin, an engineering design firm in Frankfort, KY provided a corridor study, which included six alternate sites. Doug Piteau and Associates from British Columbia completed a detailed engineering geology report and a corridor very close to the existing roadway was selected. Piteau and Associates mapped the accessible exposures of bedrock and provided descriptions and distribution of various rock types, including strike and dip of the formations, faults and joints. Based on the field investigation, core holes were proposed at critical locations. Fuller, Mossbarger, Scott and May of Lexington KY cored 14 holes where exposures were limited. The Department's Geotechnical Branch drilled a final subsurface plan to identify unstable areas in colluvium deposits. Haworth, Meyer and Bolin provided the surveying and prepared the final set of plans. The Federal Highway Administration granted an exception for the Department to use a 7.5% grade due to the short distance from the base to the top of the mountain.

Four contractors submitted bids for the project in September 1995. Bizzack Inc. was the low bidder for the 2.8 mile project, which was awarded for approximately $41.2 million. The rock excavation bid price was $3.12 per cubic yard and in some areas where unexpected excavation with excessive hauling distances, the price was $4.65 per cubic yard (for 205,000 cu. yards). Rock bolts were bid at $40.00 per linear foot with a pull test for $14.00 each. The contractor worked on three levels, maintained traffic, and used day and night shifts (some under adverse weather conditions) in order to meet the completion date.

CONSTRUCTION PROBLEMS

Numerous problems were encountered during construction and some required change orders. Complications occurred at the top of the mountain when a local church group removed approximately 40 feet of the sandstone cap to provide a level lot to build a church, school, and playground. This exposed a flat surface for water to seep into bedding planes of a sandstone, which dipped directly into the Virginia section of roadway. The grade of Kentucky's section undercut Virginia's roadway by 50 feet and also undercut the approach road to the church property. This was considered to be a high-risk area and a rock bolting program was proposed to utilize various lengths of bolts to avoid bedding plane failures. The bolts varying from 30 to 60 feet were installed and grouted according to specifications outlined in the F.H.W.A. Manual.

Sites for waste material were extremely limited near the mountaintop, however, the contractor was able to use some of the rock to construct a new approach to the church property. One other small area was available, but due to being on the down dip side of Pine Mountain, side hill fill conditions had to be avoided. The contractor did make a vertical cut through overturned beds at the foot of the mountain to shorten haul distances to a large waste area. This waste area was designated to be included in the Jenkins golf course and rocks were not allowed in the top six inches.

When rock excavation in the Glen Dean limestone section (Upper Newman) was made solution features filled with wet clay presented a foundation problem for the trucks hauling rock to the waste area. The contractor had to clean out the soft areas and refill with rock to prevent the trucks from getting stuck or turning over. In the Newman Limestone section, large vertical solution features 50-60 feet deep were encountered. They contained stalactites along with flowstone deposited on the walls of the openings. Some of the openings extended below the ditch line and could be present under the roadway. The department elected to remove the debris, inspect the openings and refill with rock to provide support. The cave sections were refilled with rock to prevent accidents due to an "attractive nuisance". Ditch lines were fully grouted to prevent surface water from getting below ground.

In Payne Gap, a box culvert was designed to take US 119 under US 23; however, the excavation was to be located in an extremely unstable part of the thrust fault. The alignment of the structure was modified to be constructed in a rock fill section, which was chocked in on both sides. This change amounted to approximately $800,00 in savings.

Several approach roads were modified to provide acceptable grades. One approach was changed from 16% to a flatter grade by widening an intermediate bench and taking local traffic through a rock cut. A new ramp on KY 805 was added during the construction phase by change order and the cost was approximately $1,000,000.

CHANGE ORDERS

The largest change order (about $2 million) was for stabilization of rock in an old quarry section where the formation had numerous cave systems and the formation deteriorated after original design recommendations were made. Approximately $1.1 million was required to modernize pavement design to match the remaining corridor. Additional road signs and lighting cost $1 million and removal of hazardous waste from service station's leaking gas tanks cost $1.1 million. After the addition of approximately $12.1 million to the bid price, the total cost of the project was about $ 53.3 million.

DETAILED GEOLOGY INFORMATION

The publication "Geology of the Pound Gap Roadcut, Letcher County, Kentucky" was offered at the 1998 Annual Field Conference of the Kentucky Society of Professional Geologist held on September 25th and 26th, 1998. This publication contains excellent Geology descriptions and is the end result of a study by fifteen scientists and several university classes. The publication is available from the Kentucky Geological Survey in Lexington, Kentucky. The Kentucky Society of Professional Geologists has designated this cut as its first "distinguished geologic site".

Kentucky Governor Paul Patton officially opened the road on September 28, 1998.

Controlled Removal of Unstable Overhanging Rock above Roadway and Hydro Power Facility, Horse Mesa Dam, Salt River Canyon, West of Phoenix, Arizona

Kenneth M. Euge, R.G., Geological Consultants, Inc., Phoenix, Arizona
Peter M. Kandaris, P.E., Salt River Project, Phoenix, Arizona

INTRODUCTION

During the early 1990's a series of rock falls resulted in extensive damage to the left abutment and spillway of Horse Mesa Dam in central Arizona. During the course of dam repair work and associated geologic evaluations, the investigators and dam operator discovered an unstable overhanging rock outcrop below the outfall of the left spillway chute. This condition endangered the main access road and hydro-power generation facility. Water discharge through a damaged spillway gate had eroded supporting rock fragments and exposed the potentially dangerous condition. Dam operators requested the technical support team to formulate and execute a rock removal plan that would keep the site safe and in operation during this process.

FACILITY AND BACKGROUND

Horse Mesa Dam is a 305-foot high concrete thin-arch structure located in a steep and narrow canyon on the Salt River 65 miles northeast of Phoenix, Arizona (Figure 1). The facility was constructed by the Salt River Valley Water Users' Association during 1924-27 and formed a 245,138 acre-foot reservoir named Apache Lake. A number of structure modifications have been performed on the dam and its facilities since original construction. In particular, the left and right spillway aprons and structures were modified in 1936 by the US Bureau of Reclamation. A 100MW pumpback-generation unit and penstock were constructed in 1970, and were located adjacent to and slightly upstream of the left spillway chute.

The modified reinforced concrete left spillway chute is 87 feet wide and varies from 55 to 68 feet in horizontal length. Water is discharged from three 26-foot wide radial gates at a crest elevation 1891 feet (MSL). The downstream lip of the chute has a flat departure angle with a dipping cross section that drops from elevation 1850 feet to 1863 feet. This spillway lip extends out from the shear rock face from 0 to 16 feet in various locations.

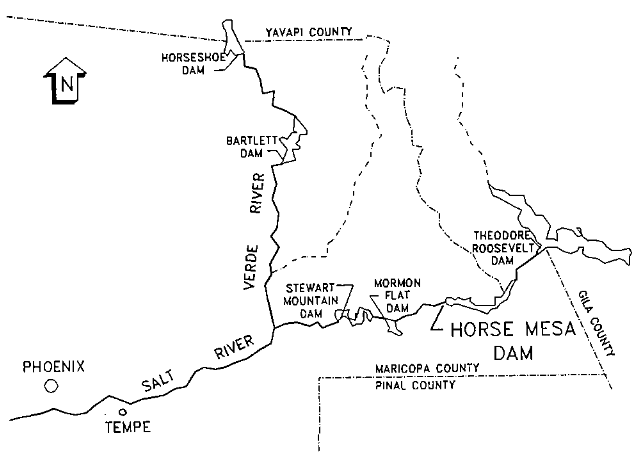

Figure 1 – Horse Mesa Dam location map

The lower access road to the hydro facility is at an average elevation of 1670 and is directly below the left spillway chute. During heavy releases, the discharge water is carried over the road and hydro facilities, falling into the tailrace plunge pool at normal water surface elevation of 1665. At low flows the release waters fall directly onto the access road, eroding fill soils down to the underlying rubble boulders and rock. For this reason, the left spillway is only operated at high discharge rates. A Bureau of Reclamation report from 1955 noted that deterioration of rock masses below spillway aprons should be expected unless discharges are directed away from impacting the underlying cliffs. In the Bureau's opinion, previous undercutting along rock mass joints and flow banding contacts was probably caused by water flows during spillway discharges (Nickell, 1955).

SITE CONDITIONS

Through continual mass wasting, rockfalls and slides have occurred periodically at and around the left abutment of Horse Mesa Dam during construction of the dam and during its operation. These rockfalls have resulted in damage to the spillway gates and equipment, the dam crest bridge, access roads, and other operations equipment. Raveling of small rock fragments and debris have been reported almost continuously from this area. A detailed summary of the site rockfall history has been provided in previous work (Euge, et al., 1994).

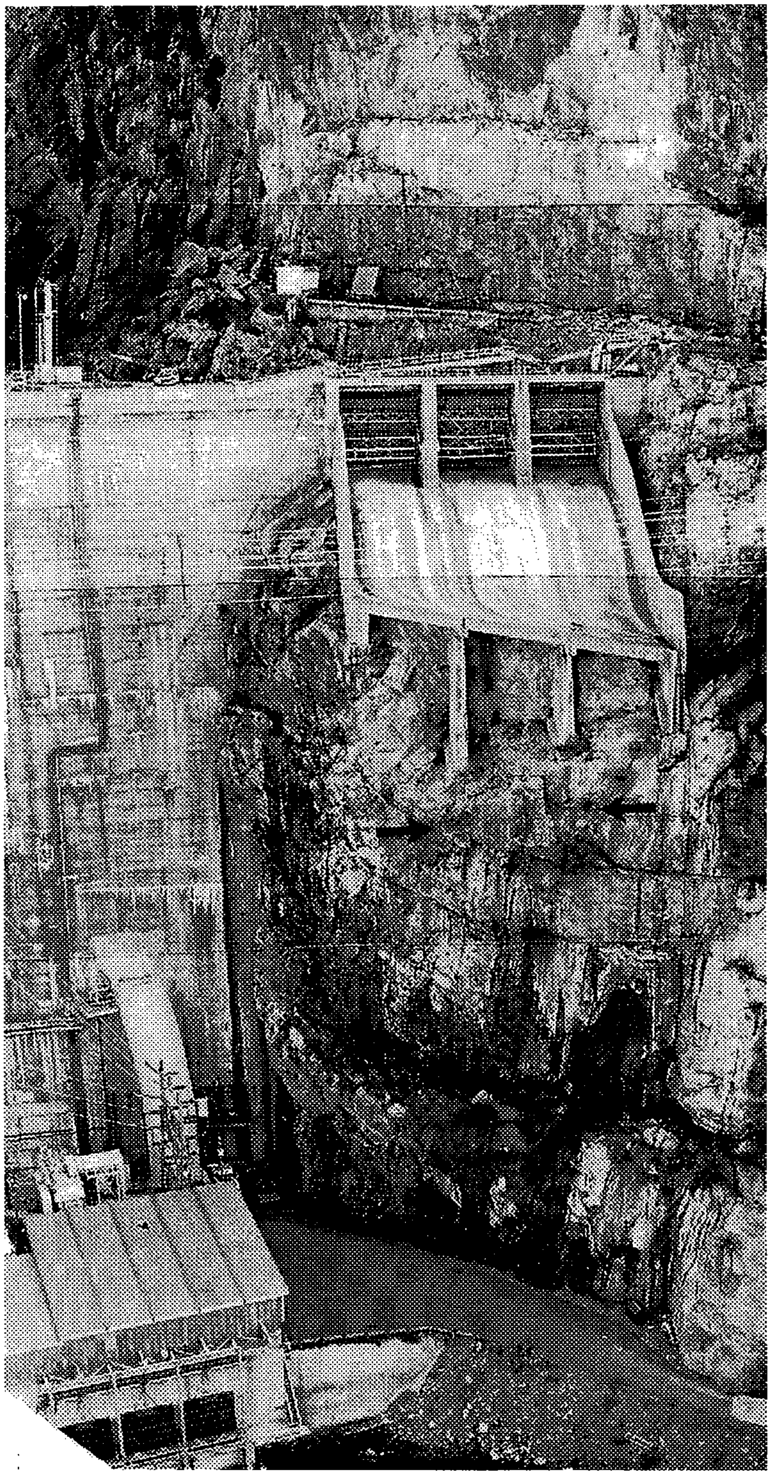

Figure 2 – View of left abutment spillway damage following 12/92 rockfall. Note overhanging rock below spillway chute. Powerhouse and penstock lower left view.

On December 5, 1992, a rockfall originated from a high, near vertical slope adjacent to and above the left spillway (Figure 2). One hundred-fifty to three hundred cubic yards of fragments ranging from gravel size to boulder about 20 feet in diameter choked the spillway approach channel, damaged spillway radial gates and gate operating mechanisms, rendering the spillway inoperable. The damage to the gates resulted in a small discharge through the spillway that primarily flowed across and down the cliff directly below the spillway chute. Though the water level was reduced and gate repairs were made over the following nine months, periodic small discharges from the spillway did occur.

By the fall of 1993, dam operators began to notice a nominal 20-foot wide by 30-foot high overhanging rock outcrop just under the center of the left spillway outfall chute. This same outcrop had also been identified by the investigators during an earlier overall site rockfall hazard assessment (GC, 1992). Joints on both sides and underneath the rock appeared to be opening, with rock fragments washed clean to the point where the mass appeared to overhang the access road below with little support (Figure 3). These conditions caused in the facility operators to request its geological consultant to perform the following professional services:

- Perform a rockfall hazard assessment of the overhanging rock formation;

- Provide rock removal options and recommendations, including the most probable trajectories from a controlled drop of the rock mass with corresponding impact energy and rollout data;
- Assist in the design of access road and hydro facility protection systems.

ROCKFALL ANALYSIS

GEOLOGY

The general geology of the rockfall site consists of a sequence of Tertiary age volcanic and volcanoclastic rock units. Horse Mesa Dam is founded on bedrock described as a sequence of dacite flows of rhyolitic appearance (Ransom, 1935) or rhyodacite (GC, 1992). The rock is a light pinkish brown on fresh surfaces. It color is attributed to the microcrystalline groundmass that contains euhedral to anhedral crystals of feldspar, biotite, and hornblende. Some glass shards are also present. The rock is siliceous to intermediate composition with about 50 percent k-feldspar, 20 percent plagioclase feldspar, less than 5 percent quartz, and the balance composed of mafic minerals.

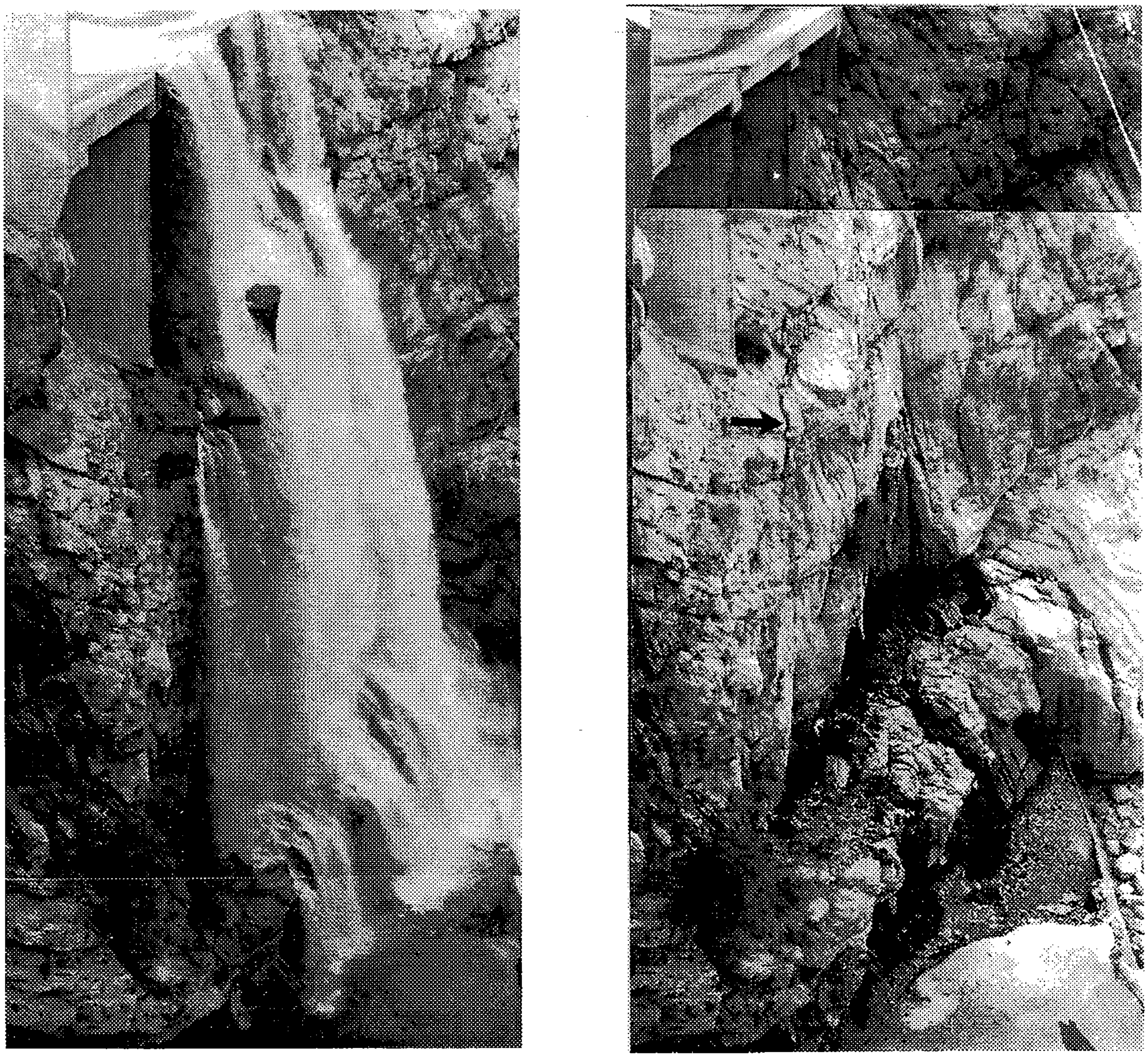

Figure 3 – (a) Spillway discharge onto rock overhang. Note fissure in center view; access road and bedrock shelf in bottom view. (b) Same view as 3a following discharge. Note open tension crack behind unstable rock overhang.

The rhyodacite is broken by numerous discontinuities, including flow banding and joint sets that directly affect rock slope stability. Flow banding, striking N 50° W and dipping 30° to 35° NW, defines discrete lava flows within the rock mass that are inclined at low to moderate angles. There are several crosscutting, high angle, moderately close (one foot) to wide (ten feet) spaced joint sets that partition the rock into orthogonal and wedge shaped blocks. Rock fragment shape and sized are consistent with the joint spacing and their continuity. The principal joint sets are continuous throughout the slope. Stereographic analysis of joint orientation data identified three prominent joints sets, many of which daylight directly out of the north facing slope below the spillway chute (Euge et al, 1994). Bulk rock density of the rhyodacite, averaging about 148 pounds per cubic foot, was used as an input parameter to the rockfall simulations.

INVESTIGATION

Site access as one of the most significant restrictions to completing the geological analysis of the rock slope. Other constraints were experienced during the course of the investigation, including:

- Very limited available geological information directly from the rock overhang area;
- No access directly to the slope.

Because of the danger from spillway flows and continued rockfalls, the field investigation of the rock overhang was accomplished by remote inspection. No rock climbing was allowed. Direct examination of the rock fall area limited to accessible rock outcrops above and adjacent to the spillway chute. The owner, because of limited access, safety concerns, and time constraints, prohibited mobilization of sampling equipment to the overhang area. The investigation of the rock face was primarily based upon photographic analysis complemented with previous geologic site reports, historical records, and professional experience working in difficult terrain.

ROCKFALL MODEL & CHARACTERIZATION

Primary rock structure (flow banding) and secondary joints and fractures provide planes of weakness within the rock mass that form potentially unstable blocks especially when combined with the high-relief terrain and very steep slopes at this site. Stresses within the rock mass (induced by dam construction and reservoir loading) cause localized tensional strain displacements forming cracks and opening. Rock surfaces exposed to this process are then subject to chemical weathering, water infiltration, freeze-induced heaving, and erosion that eventually produce rockfalls ranging in size from gravel to large boulders.

The rockfall area below the left abutment spillway was characterized using visual examination of:

- Steep slope sections, barren cliffs, and overhangs;
- Extensive, continuous, and open adversely oriented joints, fractures, flow banding and weak zones;
- Scars of previous rockfalls on the slope face and the appearance of the scars related to the degree of desert varnish, or weathering patina, formed on the rockfall scars;
- Observed offset or displaced blocks, eye witness report of rock movement, and historical documentation.

The general appearance of the slope appeared to indicate a rockfall could originate from almost any point on the slope face. However, based on the visual examination of the slope during small discharges from the spillway, a large rock block below the spillway lip appeared to have the greater propensity to fail than other areas of the slope. A flow band discontinuity defined the basal plane along which the rock block had been displaced laterally about one to two feet. Near vertical joints define the breakaway planes behind the block along which separation was occurring. During a discharge from the spillway, water was observed flowing into the tension crack behind the block and exiting along the basal plane and slope face where the tension cracks daylighted. The addition of water to the area appeared to cause additional lateral displacement that raised concerns that rockfall was imminent.

Profiles of the slope section were constructed of what appeared to be the more critical area slope sections for rockfall modeling (Figure 4). The rock is about 105 to 115 feet above the roadway. A 10 to 15-foot wide bedrock shelf is located about 30 feet above roadway grade. The distance from the toe of slope to the powerhouse and tailrace is about 75 feet. Initial interpretations of the site profiles indicated that the trajectory of the rock block (if the block remained intact during its fall) would cause the block to impact the bedrock shelf. If that occurred, it was anticipated that the block would fragment into various sizes reducing the mass kinetic energy. Also, because the surface of the bedrock shelf is inclined toward the powerhouse, it was expected that the rock fragments would have sufficient angular momentum to reach the powerhouse and tailrace with damaging impacts.

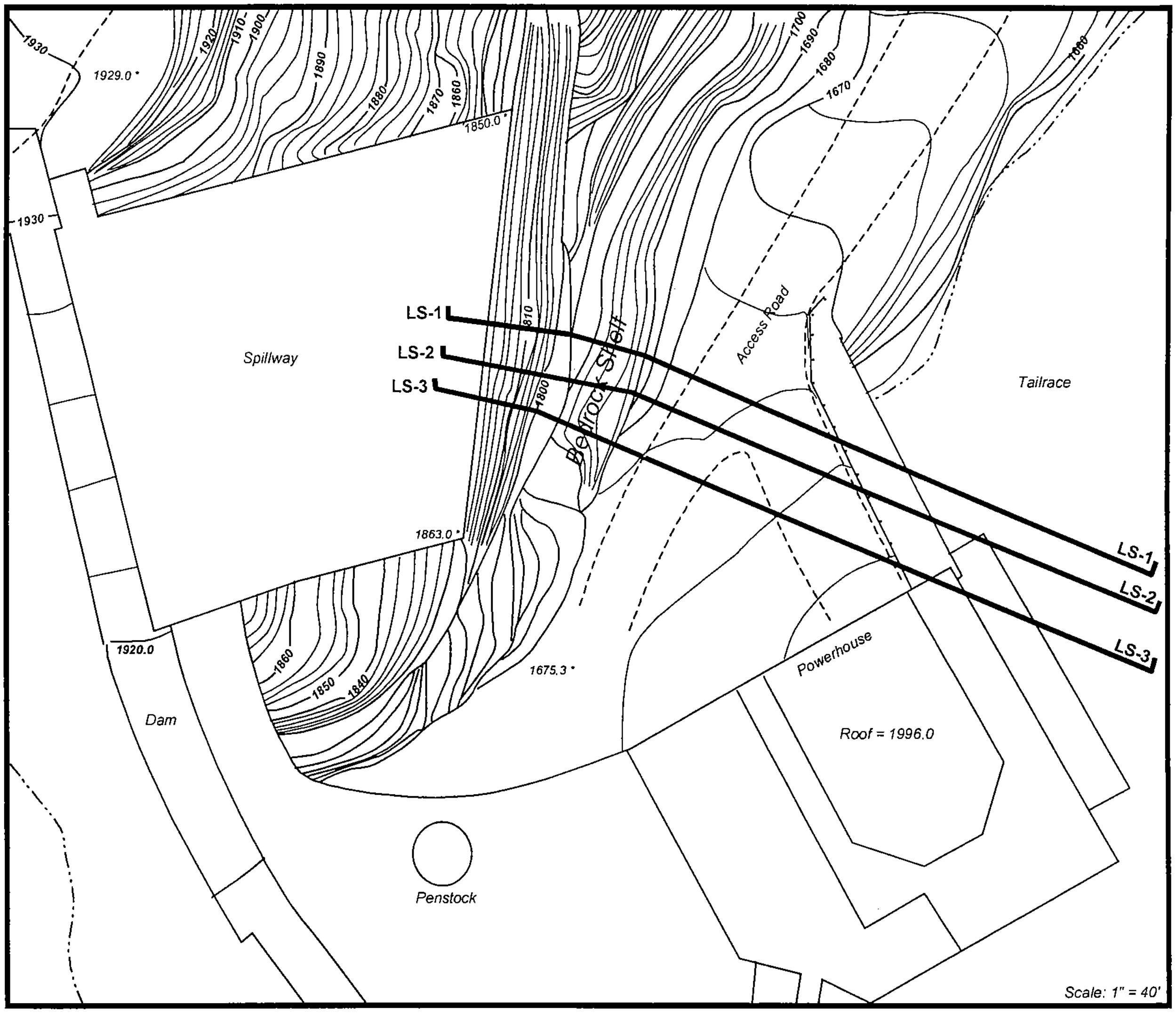

Figure 4 – Site plan depicting rockfall analysis profile alignments and dam site facilities.

The Colorado Rockfall Simulation Program (CRSP) developed by the Colorado Department of Highways was used to perform the rockfall analysis to verify (or refute) preliminary interpretations and to assist with the design of a rockfall protection system. The analysis included:

- Simulations encompassing the selected profiles, anticipated trajectory, and impact limit deduced from careful examination of the site topographic maps;
- Comparison simulations for the existing conditions and with the rockfall protection system incorporated into the analysis;

- Modeling the simulated rockfalls with different rock sizes based on the anticipated sizes of rock fragments that might be generated with the rock is dropped.

The results of the worst case CRSP simulation using various sizes of rock fragments are summarized in Table 1 (typical case is shown in Figure 5) The following description characterizes the results of the rockfall simulations used to predict path, impact point, bounce height, and kinetic energy of the rock dropped from below the left spillway:

- All of the rock, either intact or as fragment, will drop vertically to impact the bedrock shelf above the access road;
- Fragments will bounce across the access road about 25 to 30 feet away from the toe of slope toward the tailrace or powerhouse;
- Beyond 25 to 30 feet from the toe of slope, the rock fragments will continue to roll along their path until they impact the powerhouse or drop into the tailrace.

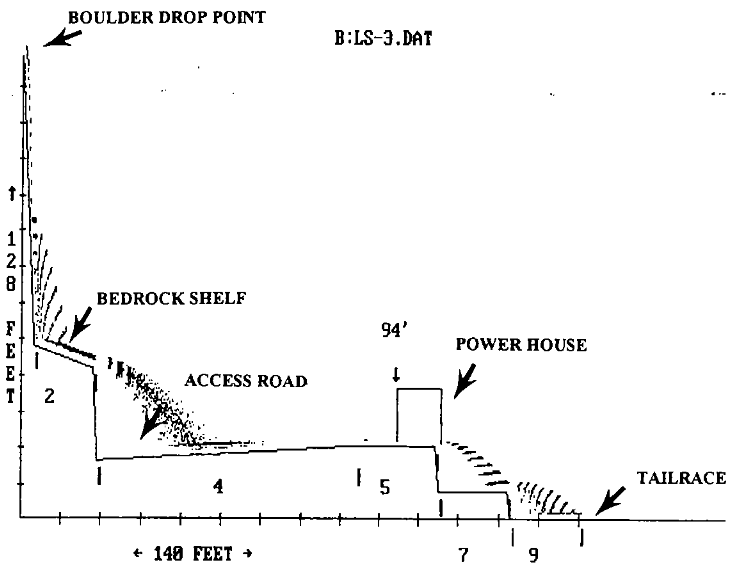

Figure 5 – Typical CRSP rockfall simulation profile

Table 1: Results of Worst Case CRSP Rockfall Protection System Design Analysis

Rock Size/Weight (feet) / (pounds)	Average Velocity @ Analysis Point (feet per second)	Bounce Height @ Analysis Point (feet)	Kinetic Energy (foot-pounds	Percent Fragments Impacting Powerhouse/Tailrace
10 x 10 / 116,190	16	0 (rolling)	878,700	100
10 x 5 / 58,100	16	0 (rolling)	327,700	100
5 x 5 / 14,525	11	0 (rolling)	81,920	30
5 x 22 / 7,260	11	0 (rolling)	45,390	24
22 x 2 / 1,450	11	0 (rolling)	3,270	3

MITIGATION MEASURES

The consultant analysis indicated that the most probable trajectories of the dropping rock mass were either downstream of the hydro facilities or toward the powerhouse. With a high probability, it was predicted that most of the debris would impact on the access road before bouncing toward the main powerhouse building. The analysis also predicted that large intact rock fragments would impact the powerhouse or tailrace unless some form of rockfall protection was employed. A rock net mitigation system was designed to reduce impact energy and contain any bouncing or rolling rock fragments larger than 8 inches in diameter. A secondary system would be placed to protect sensitive equipment from small rock fragments that could possibly ricochet off of the fallen rocks or from impacts on the steep cliff face.

For the purpose of establishing the design criteria for rock net capacities, it was assumed that the rockfall would be initiated with the entire outcrop intact. However, fragmentation of the block would occur on impact with either the bedrock shelf or the access road. The rock was expected to fragment because of the relatively close spacing of incipient fractures and joints in the rock mass. Therefore, the rock net fence was designed to accommodate at least 200,000 foot-pounds of impact kinetic energy. The location of the rock net fence was selected along a line at a distance at least 30 feet from the powerhouse beyond where the rock fragments ceased bouncing and started to roll.

The following elements were incorporated as mitigation (Figure 6):

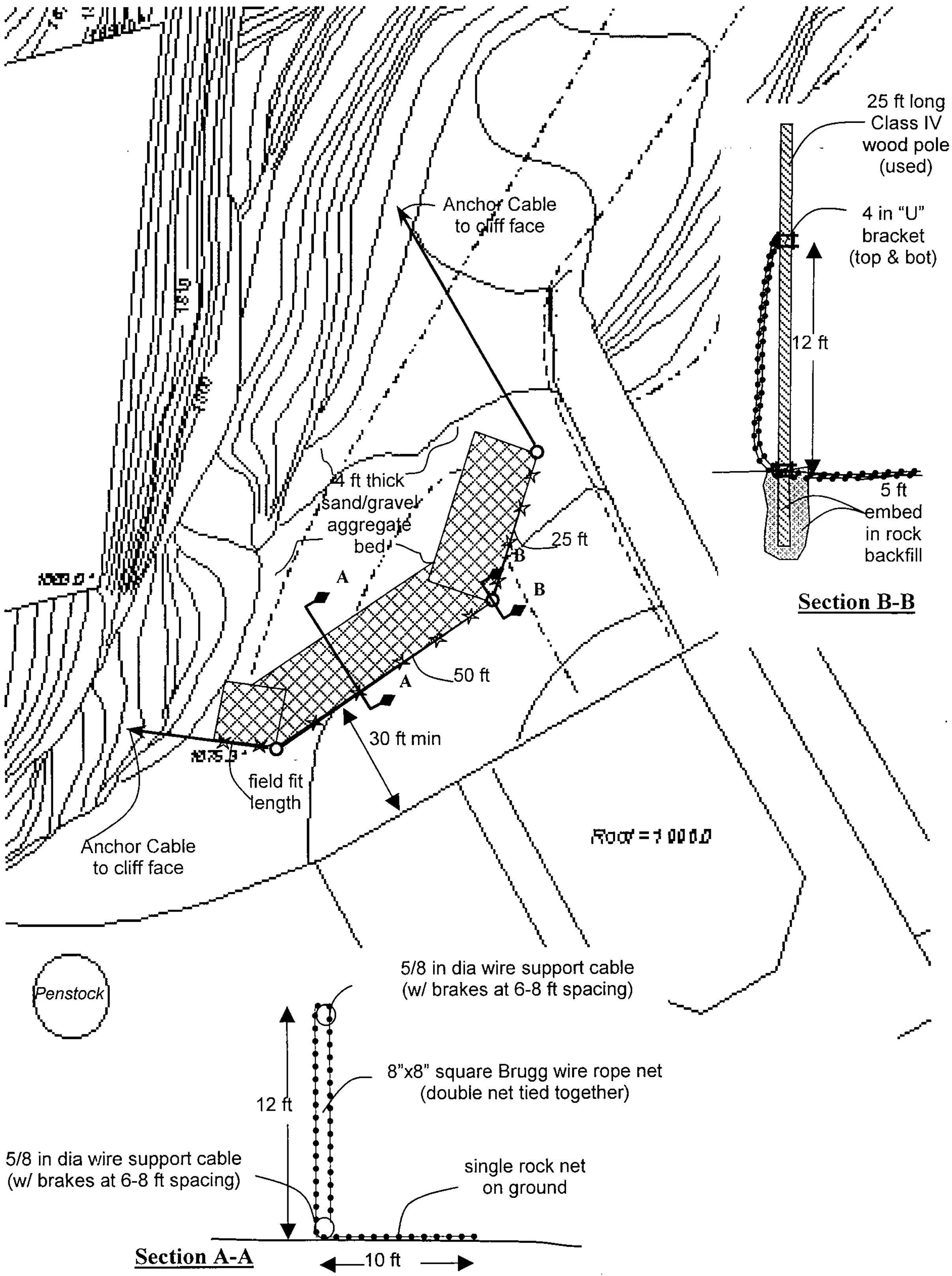

Figure 6 – Temporary rockfall mitigation system: Rock net plan and details.

- A minimum 4-foot thick sand/gravel aggregate bed placed on the access road to function as an energy absorbing cushion;
- Placement of a rock net fence no closer than 30 feet from the powerhouse walls. A temporary, double 10-foot high protection rock net fence supported with wood power poles and breaker cables anchored into the face of the cliff. The double rock net hung loosely to ground level and then was extended along the ground surface 10 feet from the fence toward the toe of slope;
- One-inch thick plywood sheets placed around the penstock and sensitive electric equipment on and near the powerhouse.

A time-and-materials contract was issued to Edward Kraemer & Sons to execute the plan. The scope of work included removal of the fractured rock outcrop below the left spillway, removal of all loose hazardous rock fragments, installation of the mitigation system, cleanup of all debris and removal of the mitigation measures. The dam operator would furnish all materials including wire rope, Brugg cable netting panels, Brugg cable braking devices and wood poles.

RESULTS

The mitigation system was installed in early November 1993. After a series of unseasonably frequent rainstorms, it was decided that the work should proceed before the end of the month. The contractor coordinated rock removal activities with a professional rock scaling company. The work site was not accessible to motorized equipment. All work had to be performed from the downstream lip of the spillway, with personnel and equipment hand-lowered via safety harnesses to a stable ledge above the overhanging rock.

The contractor's initial concept was to loosen the remaining rock supports with hand-operated pneumatic jackhammers, then insert wedges to move the rock mass laterally. It was thought that this process would cause the rock to tumble off the cliff into the mitigation system. After three days of effort, only one small rock fragment (roughly 8 feet in diameter) had fallen. More rainstorms and cold weather were expected, so rock removal activities were accelerated. The wedging system initially employed by the contractor proved inadequate in delivering enough force to displace the rock overhang.

It was determined that the jackhammers could carve enough room behind the rock overhang for the installation of a small hydraulic load jack. A 150-ton capacity hand-pumped hydraulic jack with an 6-inch stroke was place in a fissure behind the rock mass. Once the maximum limit of throw was achieved, small cobbles and boulders were hand placed into the gap. The device was retracted, lowered farther down into the opening, and then re-loaded to push the overhanging rock out further. This method worked rapidly - after three cycles the whole rock mass toppled over the cliff.

The rock mass impacted the bedrock shelf and then directly onto the sand/gravel cushion, fracturing into smaller pieces validating the rockfall simulations and assumptions used in the analysis. Rock fragments either bounded harmlessly into the dam tailrace or were captured by the rock net system that was designed to clamshell and encapsulate the larger rock fragments. Several steel cable breaks installed on the anchored support cable substantially reduced impact energy at the net. Small fragments that reached the powerhouse caused no damage and only a road guardrail adjacent to the tailrace required any subsequent repairs. Two of the wood pole supports fractured during impact, but did not inhibit the system from functioning as designed. Clean up work was rapidly completed and the access road to the site was restored within a day (Figure 7).

CONCLUSIONS

Careful planning and execution of the investigation and analysis program resulted in the formulation of practical, buildable rockfall protection system design. The close interaction between the Salt River Project, the consultant, and the contractor throughout the project resulted in the successful installation and operation of the temporary rockfall protection system.

- The successful investigation program was accomplished using proven techniques that had been used previously at Horse Mesa Dam to evaluate and successfully predict rockfall events. The techniques included local knowledge of geology, site and area conditions, evaluating archival data, and performing a site geological reconnaissance using experienced professionals.
- The Colorado Rockfall Simulation Program (CRSP) can be used to accurately predict slope mass-wasting characteristics at a confined site and assist with the design of practical rockfall mitigation measures, as confirmed by the controlled rockfall above the access road and powerhouse at Horse Mesa Dam.
- Rockfall mitigation systems functioned as designed and were successful in protecting the hydro facility and access road from significant damage. The site remained operational throughout the process and the access road was opened to traffic within 24 hours after rock removal was performed.

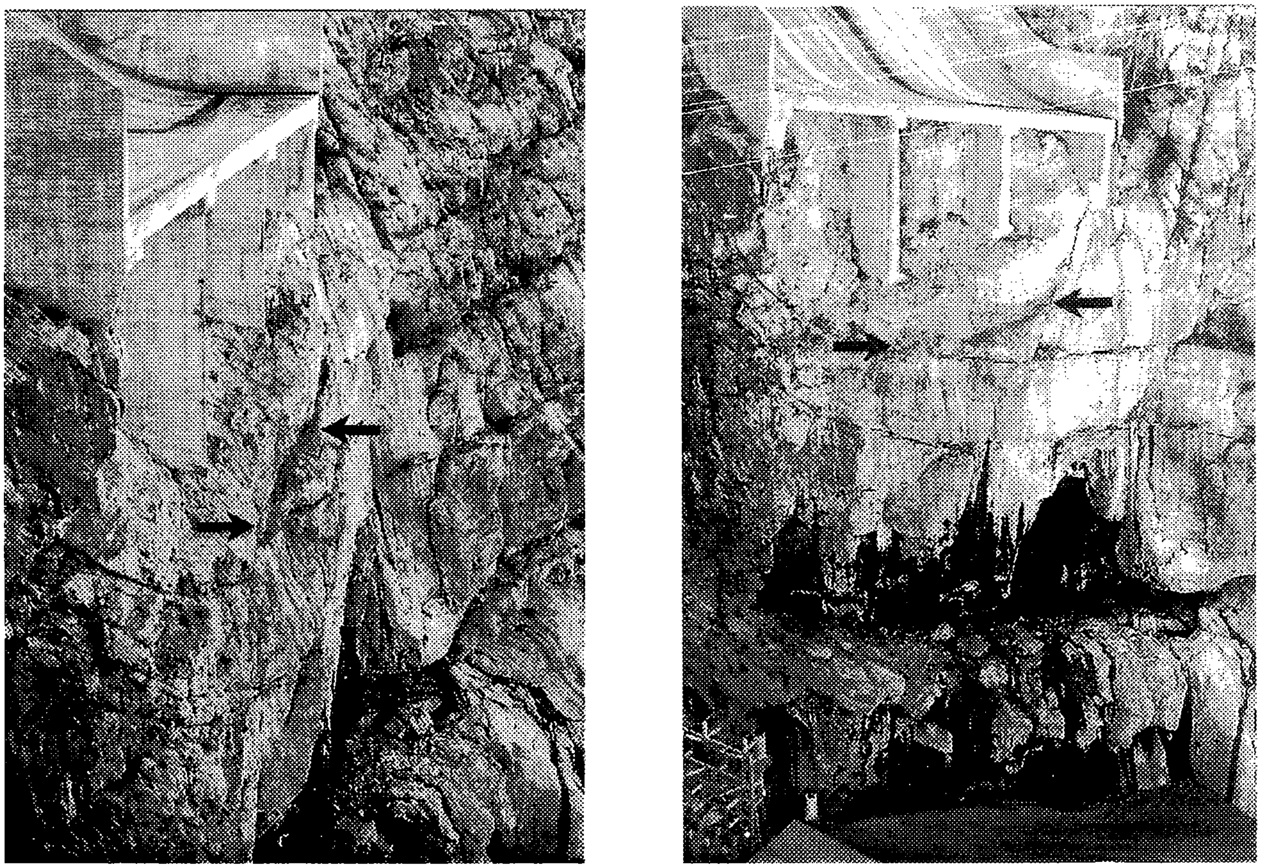

Figure 7 – Profile view (a) and elevation view (b) of rock slope following removal of rock overhang.

REFERENCES

Euge, H.M., Wright, R.S. and Kandaris, P.M. 1994, Mitigation of rockfall-induced damage to improve safety at Horse Mesa Dam, Salt River, Arizona. Dam Safety Modification and Rehabilitation: 149-164. USCOLD: Denver.

Geological Consultants (GC) 1992, (consultant report) Horse Mesa Dam left abutment rock slide hazard evaluation, Consultant Report No. 91-036, Salt River Project Microfilm File No. CE-345.

Nickell, F.A. 1955, Horse Mesa damsite – Salt River – Arizona, US Bureau of Reclamation memo report to Chief Engineer.

Ransom, F.L. 1935, (consultant report) Geological report on spillway conditions at Mormon Flat and Horse Mesa Dams, Arizona, Salt River Project File No. D-A7.5/1935.03 (MF-A7.5 & HM-A7.5).

The MP 5.9 Rockslide
Emergency Clean-up, Design and Construction

Christopher A. Ruppen, P.G., Michael Baker Jr., Inc., Beaver, Pennsylvania

ABSTRACT

Conrail's Mon Line in Pittsburgh Pennsylvania carries about 30 trains per day on double tracks. Approximately 1.3 million tons of freight travels this line per week. It is the heaviest traveled line in southwest Pennsylvania and a critical link in Conrail's Pennsylvania double stack route. As the line passes through downtown Pittsburgh, it is situated on a narrow shelf excavated from the base of the southern valley wall along the Monongahela river. On May 22, 1997, a deteriorated retaining wall at the base of a 400 foot high rock cut collapsed. This allowed the entire rock face to fail along an existing valley stress relief joint and completely covered both tracks with 1500 tons of rock. A train approaching the slide made an emergency stop and halted approximately 100 feet before the slide. Conrail was forced to reroute trains over a long detour in order to accommodate double stacked "land/sea" containers while emergency repairs commenced.

Initial response consisted of removing the slide material to reopen the tracks. Local contractors responded with excavators and trucks and worked around the clock to remove material and uncover the tracks. Of principle concern during the removal phase was to remove material that posed an immediate threat to trains and construction personnel but to avoid removing material that might destabilize larger masses of rock. Geologists worked closely with the contractors as excavation progressed to guide excavation of a temporary slope that allowed the outside track to be reopened to traffic within eight hours and the inside track to be reopened within a few days.

Collapse of the wall left a soft claystone unit at the base of the cut exposed to weathering. Loss of strength in the claystone allowed failure of the entire rock face after collapse of the wall. In order to prevent weathering and loss of strength further back into the claystone, perhaps triggering another rock slide, remedial measures were required and had to be completed prior to the heavier rail traffic which occurs in the fourth quarter for the Christmas shipping season. Several different replacement wall designs were evaluated for ease of construction and cost. A reinforced concrete wall cast directly against the exposed rock face was selected for design. Multi-strand tiebacks were installed through the wall to provide restraint for potential future slides and horizontal drains were installed to reduce hydrostatic pressure in the valley stress relief joints behind the exposed face.

Construction involved rock slope scaling of loose material from the face, shotcrete repairs to overhangs in the face, and construction of the wall while maintaining traffic on the outside track. Construction was completed in November 1997.

This paper presents the relationship between the site geology and the observed failure mechanism, the remedial alternatives considered and the final design and construction for this project.

INTRODUCTION

On May 22, 1997, a major rockslide occurred onto the Consolidation Rail Corporation's Monongahela Line at Milepost 5.9. This line, comprised of two tracks, is Conrail's heaviest traveled line in Southwestern Pennsylvania and a critical link in Conrail's Pennsylvania double stack system. The rail corridor parallels the southside of the Monongahela River, located on an area locally known as the Conrail shelf. This shelf is positioned at the base of Mt. Washington, an approximate 400 foot high rock slope, carved by the Monongahela River with some older man made excavations occurring at the base of the slope to allow space for the rail condor. The rockslide occurred between the Ft. Pitt Bridge (Interstate I-279) and the Monongahela Incline.

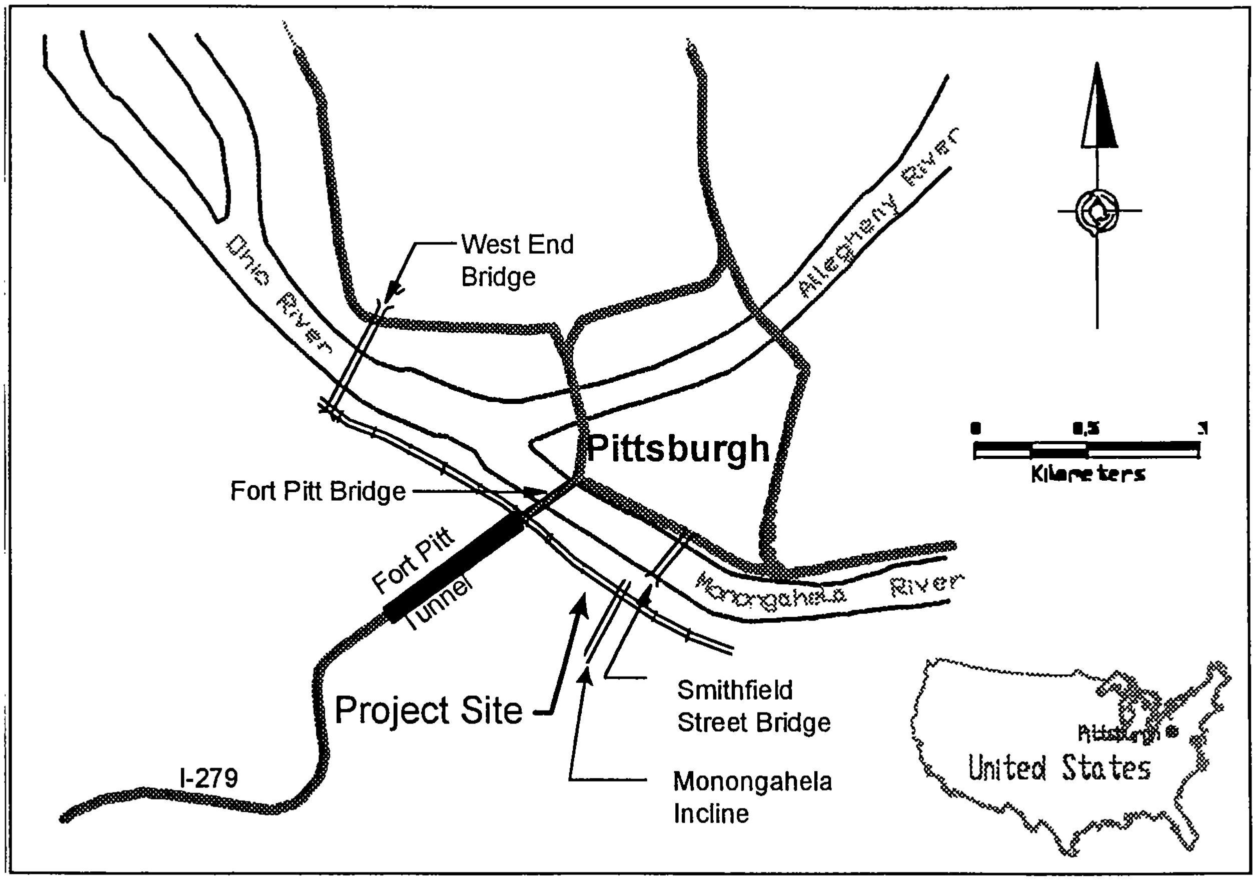

Figure 1 - Site Location Map

The slide activated without warning at approximately 11:00 a.m. on May 22, 1997 and occurred as one quick movement. Both of Conrail's tracks were buried almost immediately under major rock debris and trees. A train approaching the slide went into emergency and stopped without incident approximately 100 feet from the slide. Emergency clean-up of the slide began almost immediately. Luckily, two contractors, Baker Mellon Stuart and Mosites Construction Company had heavy excavating equipment working in the area and were able to mobilize quickly to clear the river side track (Track #1). This track needed to be uncovered and quickly repaired in order to clear three trains which were dead ended because of the rockslide. Once these three trains were cleared, the track was again closed and work commenced around the clock to remove the rockslide. Three excavators and one hoe ram worked approximately 30 hours to remove the slide mass. An estimated 1500 tons of rock was excavated and trucked from the slide location. All work occurred under the guidance of geologists to provide input into how to safely excavate the failed material and to attempt to minimize any further damage to the remaining rock slope.

Once this emergency clean-up was complete, an emergency design was prepared to provide a more permanent repair to allow safe operation of the railroad. This emergency design was completed and bid in a few short weeks. The contract was awarded to Brayman Construction Company, with all work occurring and completed during the summer of 1997. The work consisted of rock slope safety scaling, on-slope shotcrete work, construction of a new anchored retaining wall to replace the failed section, and concrete and shotcrete rehabilitation of the remaining toe of Mt. Washington retaining wall (old railroad wall).

LOCAL GEOLOGY AND THE FAILURE MECHANISM

Pittsburgh is positioned on the Appalachian Plateau, in an area maturely dissected by the Ohio, Monongahela and Allegheny Rivers and their tributaries. This dissection and incision by the rivers has formed steep sided valley walls, often exposing over steepened bedrock out crops. Bedrock within this portion of the Plateau typically consists of flat lying to very shallowly dipping sedimentary rocks represented by cyclic sequences of sandstones, siltstones, limestone, claystones, shales and coals.

The local stratigraphy consist of members of the Pennsylvanian age lower Monongahela and upper Connemaugh Groups, specifically within the Casselman Formation. Mt. Washington, at this location, is represented by the Duquesne coal, limestone and claystone unit at railroad grade overlain by the Birmingham sandstone unit up through the Pittsburgh coal near the top of Mt. Washington. See Figure 2- Stratigraphic Cross Section. This section consists of typically thicker sandstone and siltstone units (Birmingham, Morgantown and Connellsville) with each underlain by soft, thin coal and claystone units (Duquesne, Wellersburg and Clarksburg) respectively. These softer units underlying the sandstones tend to decompose relatively quickly and develop deep weathered zones, and in many cases more closely exhibit soil on their exposed face. Large overhangs and loss of support in the basal portions of the sandstones are common features within the slope.

The other key component to the local geology and this slope is the well developed valley stress relief joints which generally parallel the Monongahela and Ohio Rivers. Experience with this slope had identified well developed joint sets with the primary joint oriented parallel to the river valley. Based on visual observations along the length of this slope and a limited amount of drilling for various anchor installations, some general conclusions were developed regarding the joints. In the sandstone units, the first joint is typically generally present eight to twelve feet into the slope. (See Figure 3 - Anticipated Failure Mechanism.) The condition of this joint varies from very tight; bedrock to bedrock contact; to being open twelve inches or greater. Soil infilling was common in the open joints. A parallel joint, positioned another eight to twelve feet into the slope was also common. The condition of the second parallel joint was generally tighter than the outermost joint.

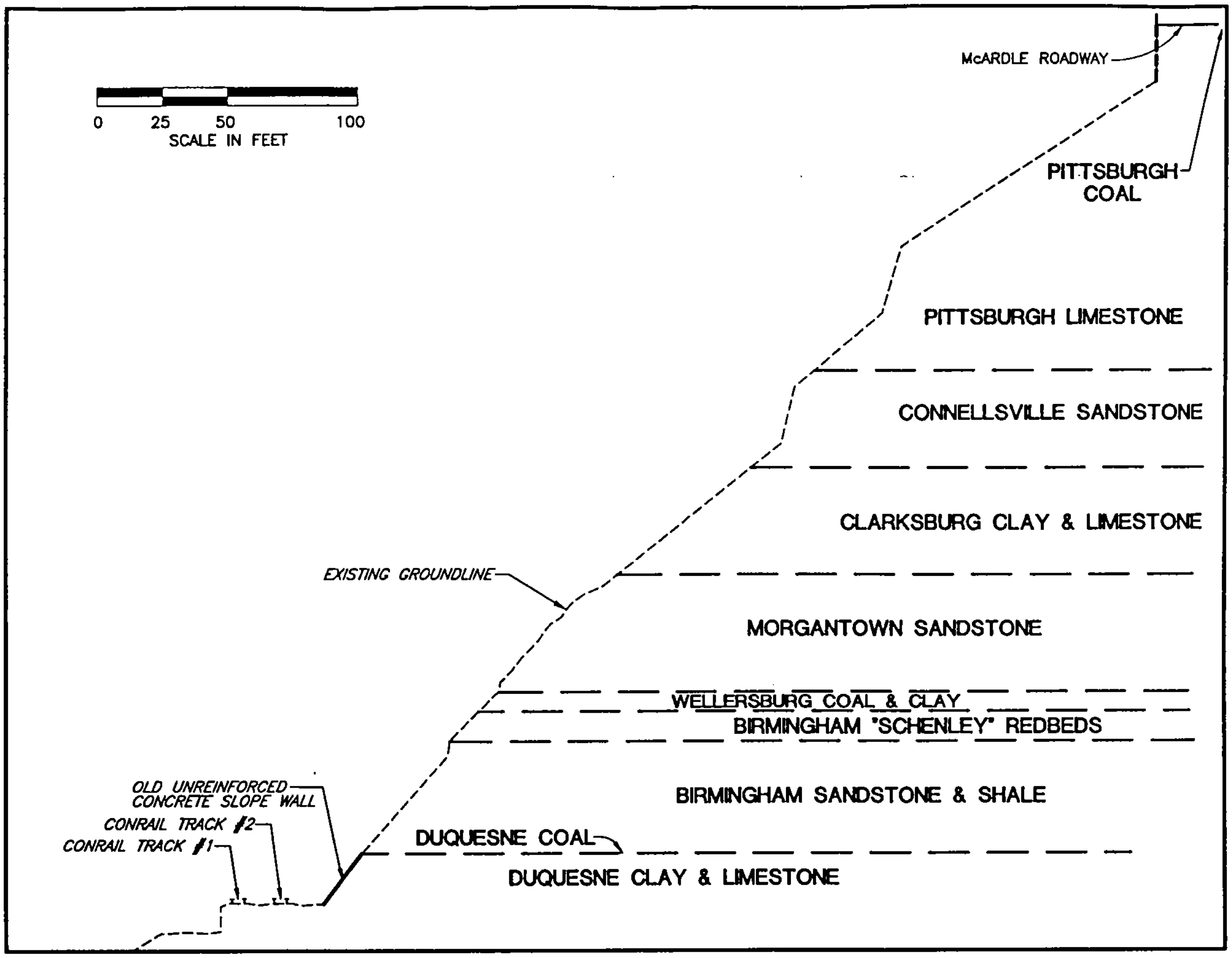

Figure 2 - Stratigraphic Cross Section

The rockslide appeared to have occurred as a very large block failure along a valley stress relief joint in the Birmingham sandstone. It did not topple but rather, fell vertically after the claystone supporting it translated outward along a somewhat circular failure surface. Due to past movement and weathering of the Duquesne claystone, an old sloped , unreinforced concrete retaining wall positioned at the toe of the slope was incapable of providing support or weathering protection to the claystone. Therefore, it is concluded that deep weathering of the claystone occurred to the point that the claystone experienced significant loss of shear strength and was providing very little support to the overlying sandstone. This combined with the well developed valley stress relief joints in the Birmingham, allowed the failure to occur along the stress relief joint and daylight through the Duquesne claystone at the toe of the slope. Although, this slide is smaller in size, the failure mechanism is very similar to the perceived failure mechanism for the Brillant Cut Failure which occurred on March 20, 1941 along the Allegheny River near Pittsburgh. (Philbrick, 1953, 1960; Ackenheil, 1954; Hamel 1969, 1972) This slide was also suspected to fail along valley stress relief joints through weaker claystones and clayshales at the toe of the slide and adjacent to the railroad. See Figure 3 - Anticipated Failure Mechanism. The entire rockslide was most likely activated by an increase in groundwater pressure as a result of rainfall that occurred during the prior week. Rainfall measured during the month of May placed this month in the top ten highest recorded rainfall months for the Pittsburgh area.

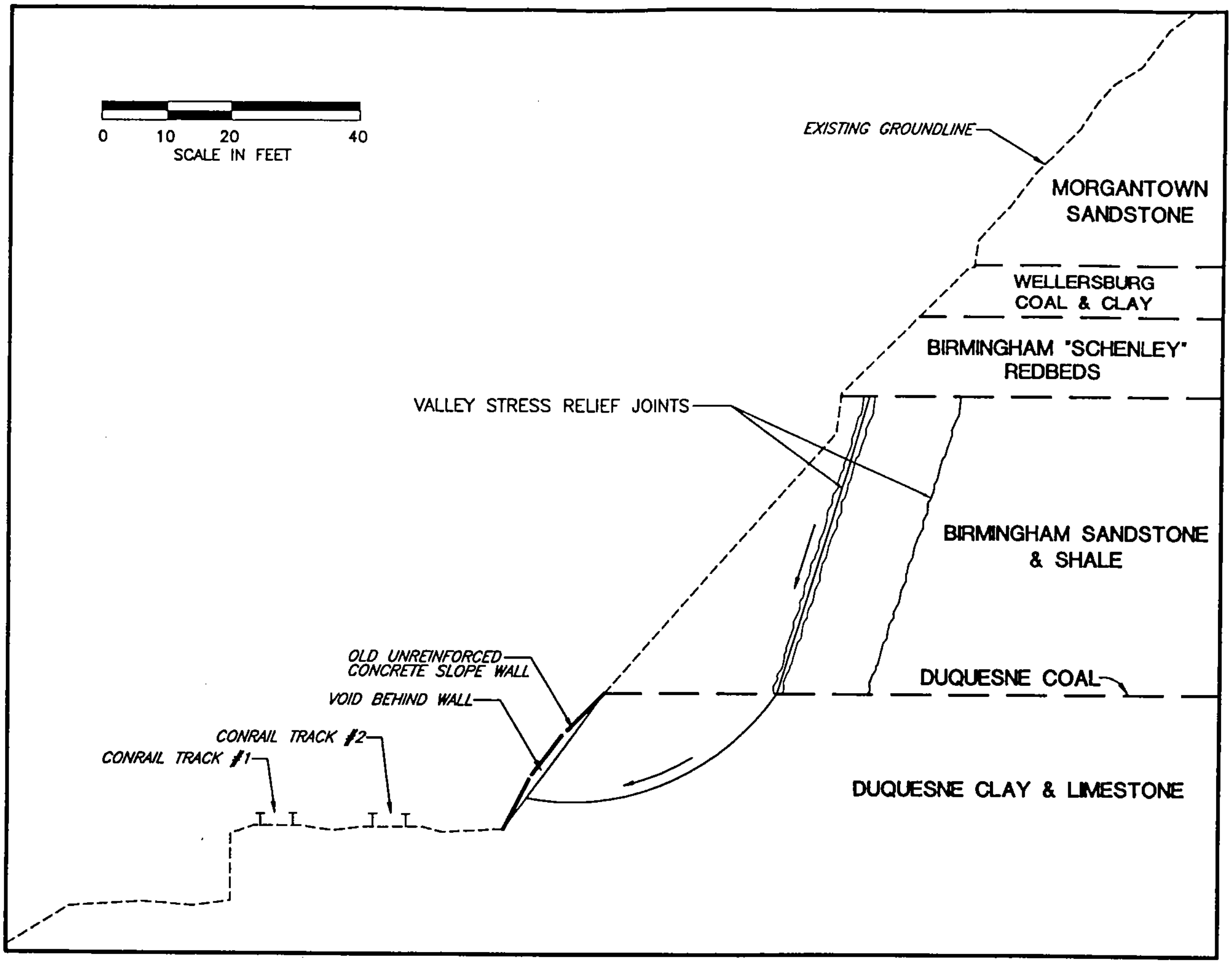

Figure 3 - Anticipated Failure Mechanism

EMERGENCY REMEDIAL DESIGN

The emergency remedial design consisted of three principal parts: The design of a 300 foot long retaining structure at the base of Mt. Washington to replace the failed wall, rehabilitation design of 1000 lineal feet of adjacent old railroad wall and on slope remediation consisting of safety scaling and shotcrete protective facings.

REMEDIAL WALL DESIGN

Design of a retaining structure at the base of the slope to replace the failed wall was undertaken first. The three principal objectives of this design were to:

- Cover the existing soft Duquense claystone unit at the base of Mt. Washington to limit further deterioration of the rock strength due to weathering. This was accomplished by extending the wall to a height such that the entire soft claystone was covered by the completed wall.

- Buttress existing overhangs at the base of the Birmingham sandstone and shale to prevent local failures in this unit. This was accomplished by providing a sloped cap on the wall that extends to the bottom of all overhangs.

- Increase the shearing resistance along a plane similar to the one that resulted in failure of the existing wall such that a factor of safety of 1.5 was provided. This was accomplished by providing tensioned tie backs that act to increase the normal force on the shear plane and to resist sliding. The required tie back force was determined by assuming the soft claystone had degraded to a point such that its strength was equal to that which existed at the time of failure of the existing wall. The design load and tie back spacing were determined such that a factor of safety of 1.5 against sliding failure would result. This calculation assumed that water pressure on the failure plane does not extend above the top of the soft claystone unit. This assumption is based on providing horizontal drains into the bedrock to relieve any water pressure that might develop in the Birmingham sandstone and shale and within the next valley stress relief joint.

  Covering the exposed claystone was intended to greatly reduce the rock strength loss due to weathering, however, strength loss will still occur due to the presence of fractures and groundwater in the rock mass. Therefore, an analysis was made to determine the factor of safety of the wall system when the cohesion in the rock mass has been reduced to zero and the tie backs have been stretched to their breaking point (ultimate load case). The resulting factor of safety for this extreme case was slightly greater than one, thus the design was considered acceptable.

To accomplish these objectives, four alternative wall designs were considered. See Figure 4 - Alternative Wall Designs.

These alternatives consisted of a Cast In Place Tied Buttress, Precast Tied Buttress, Tied Back Soldier Pile Wall and a Sheet Pile Tied Buttress. Based on the urgency required for construction, availability of materials, clearance restrictions of construction equipment required to maintain rail traffic and cost, Option 1.a., the Cast In Place Tied Buttress was selected.

The wall measured 300 feet in length with panel heights of 20 and 30 feet depending on the existence of overhangs in the Birmingham sandstone. A minimum of 15 feet of horizontal clearance was maintained from centerline of Track 2 to the new wall at rail elevation. The toe of the wall was placed below the future ditch line to limit undermining of the wall by storm flow in the ditch. 8,000 cubic yards of concrete were used to construct the wall and the cap.

The wall included tieback anchors with a design load of 240 Kips. Three rows of anchors were utilized in the 30 foot wall panels and two rows in the 20 foot panels. The capacity was met with seven - 0.6 inch diameter strands. A 30 foot long stressing length and a 45 foot long bond length was

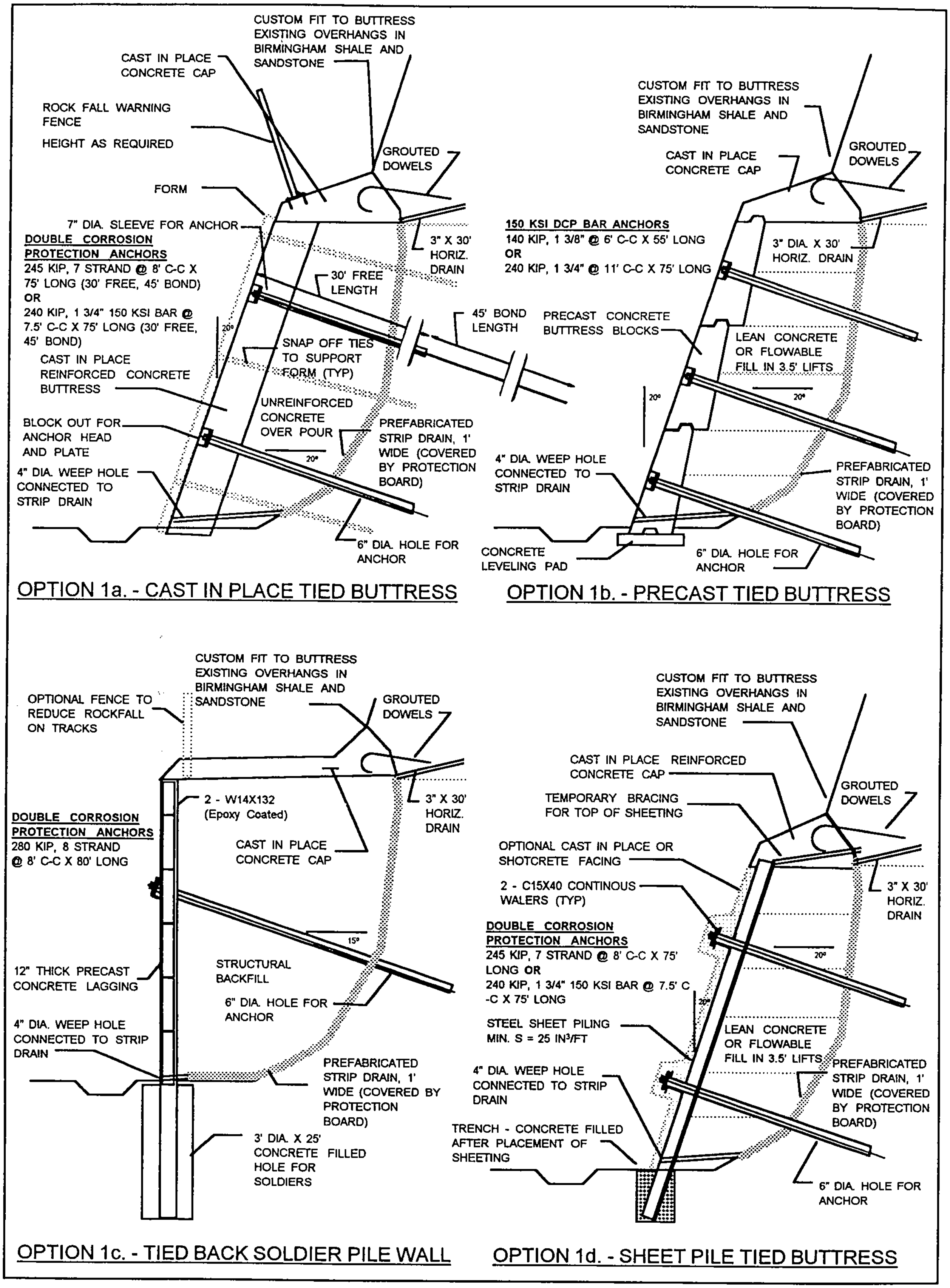

Figure 4 - Alternative Wall Designs

provided to develop the design capacity. A design bond stress of 25 psi and a hole diameter of six inches was used to determine the bond length. The tieback was specified to be double corrosion protected to provide a design life on the order of 75 years. A total of 90 anchors were installed in the 300 foot long new wall. All new wall construction occurred under very restrictive clearances with at least one track and generally both tracks in service.

REHABILITATION OF ADJACENT EXISTING WALLS

The existing walls adjacent to the rockslope remained in place. The remaining walls totaled approximately 1,000 feet in length and ranged in height from 14 to 36 feet. Based on the history of the railroad, the walls were estimated to be close to 100 years old. Due to the age, the walls were in various stages of deterioration. In fact, some wall panels exhibited signs of significant movement. This movement was considered indicative of an imminent failure similar to the rockslide which occurred on May 22. Because of this, two repair schemes were developed for the remainder of the existing wall.

In areas where no movement of the existing wall or rock above the wall has been observed, cosmetic repairs were made to deteriorated face of the wall. The repair consisted of removing the deteriorated concrete, securing a reinforcing grid to the face with grouted dowels and covering the face with six to nine inches of shotcrete. Drainage of the wall was improved by installing sand filled weep holes drilled through the wall and outleted by strip drains.

In areas where movements have resulted in distress to the existing wall or where rock conditions above the wall indicate that the rock mass may already be mobilized, repair consisted of a cast-in-place tied back buttress and facing against the existing wall, identical in design to the rockslide wall. An additional 90 anchors were installed in the cast-in-place rehabilitation wall sections.

Of the 1,000 lineal feet of rehabilitated walls, approximately half of the length was rehabilitated with the cast-in-place tied buttress wall and half were rehabilitated with the shotcrete option. Over 8,000 cubic yards of concrete were placed to complete this work. The fact that 50% of the walls required the anchored wall section is indicative of the well developed stress relief joints and the decomposition of the claystone at the base of the slope.

ON-SLOPE REMEDIATION

On-slope remediation consisted of safety scaling and construction of shotcrete protective facings. In order to safely construct the proposed wall and perform the repairs of the existing wall, the slope above the work area had to be first scaled to remove loose and/or unstable material. This work was detailed on photo mosaics and provided as part of the construction plan set. The use of colored, full size annotated photo mosaics to convey the design was a very useful tool and eliminated much of the guess work by the contractor. The scaling work occurred by rope from the top of the slope down and also from a man lift to clean the brow at the top of the Birmingham sandstone (top of the rockslide). Scaling operations were halted when a train approached within a specified distance of the work site to ensure the track was clear for safe rail passage. This required close communication between approaching trains, railroad flagman and on-slope personnel.

Due to the development of significant overhangs in the Birmingham sandstone unit, several shotcrete protective facings were constructed to buttress the overhangs and slow down the weathering and undercutting in this unit. They consisted of 25 foot long dowels drilled and grouted into the rockslope. The dowels support a reinforcement cage which was shotcreted in place. Temperature expansion mesh was placed in the outer 3 inches of the shotcrete.

SUMMARY AND CONCLUSIONS

A rockslide of this nature, disabling a critical link corridor, required an expedited response not only for the initial clean-up, but also for the follow-on emergency remedial design and construction. A response of this type effectively restored and maintained rail transportation due to the cooperation and efforts of the owner, geotechnical and structural engineers, geologists and contractor.

Due to the stratigraphy of alternating sequences of massive sandstones underlain by weaker claystones and coals, this type of failure can be expected on over steepened natural slopes, especially when influenced by well developed valley stress relief joints. Since this rockslide occurred at the base of a high natural rockslope, the selected remedial design appears to have been appropriate to slow down the weathering of the weaker claystone unit at the toe of Mt. Washington while also providing an adequate buttress to decrease the likelihood of a similar rockslide at this location.

REFERENCES

Ackenheil, A.C., 1954. A Soil Mechanics and Engineering Geology Analysis of Landslides in the Area of Pittsburgh, Pennsylvania. Ph.D. Thesis, Univ. of Pittsburgh, Pittsburgh, Pa.

Elliott, G. M. & C. A. Ruppen 1995. Mitigating Landslide/Rockfall Hazards - A Quantitative Evaluation of Risk Reduction. Proc. 46th Highway Geology Symposium: 14 pp.

Ferguson, H. F. 1967. Valley Stress Release in the Allgheny Plateau. Bull. Assoc. Engr. Geol. 4:63-71.

Ferguson, H. F. & J. V. Hamel 1981. Valley Stress Relief in Flat-Lying Sedimentary Rocks. In K. Akai et al. (Eds), Weak Rock: 1235-1240. Rotterdam: Balkema.

Hamel, J.V. 1998. Mechanism of Pleistocene Rock Slides Near Pittsburgh, Pennsylvania. Int. J. Rock Mech. & Min.Sci.: in press.

Hamel, J. V., G. M. Elliott, J. D. Lasko, & C. A. Ruppen 1998. Rock Slope Risk Assessment, Pittsburgh Airport Busway. In M. Sivakumar & R. N. Chowdhury (eds), Environmental Management: 971-979. Amsterdam: Elsevier.

Hamel, J.V., 1969. Stability of Slopes in Soft, Altered Rocks. Ph.D. Thesis, Univ. of Pittsburgh, Pittsburgh, Pa. (No. 70-23, 232- Univ. Microfilms, Ann Arbor, Mich.)

Hamel, J. V., 1972. The slide at Brilliant Cut. In: E.J. Cording (Editor), Stability of Rock Slopes, Proc., 13th Symp. On Rock Mechanics, Univ. of Illinois, Urbana, Ill., 1971. American Society of Civil Engineers, New York, N.Y., pp. 487-510.

Philbrick, S.S., 1953. Design of Deep Rock Cuts in the Conemaugh Formation. Proc. 4th Symp. On Geology as Applied to Highway Engineering. State Road Commission of West Virginia, pp. 79-88.

Philibrick, S.S., 1960. Cyclic Sediments and Engineering Geology. Proc., 21st Int. Geol. Congr., Part 20, pp. 49-63.

Flexible Wire Rope Net Barriers For Debris Flow Protection: A Review of Installations to Date

Erik J. Rorem
Brugg Cable Products, Inc.
Vancouver, WA

50th Annual Highway Geology Symposium
Roanoke, VA
May 20th – 23rd, 1999

ABSTRACT

Since initial testing of Flexible Wire Rope Net Barriers for debris and mud flow applications in 1996, several such systems have been installed in the field to mitigate actual debris and mud flow hazard sites in Washington state and California. Each of these installed systems is unique in design to the specific site in question, including variations in height, kinetic energy rating, and foundation and anchoring conditions. The intent of each system is to stop the majority of mud and debris contained in small to moderate sized mud/debris flows, helping to prevent them from flowing onto the adjacent roadways below. In addition to preventing immediate hazards to motorists, they are also intended to reduce or eliminate the need for emergency road closures and emergency cleanup, as well as possible damage to the roadways. The capability for the barriers to be readily partially disassembled in order to permit cleanout of accumulated debris on a scheduled and controlled basis was a desired feature with each of these sites.

An overview will be presented on each of these field installations, with emphasis on design features, construction, performance to date, and maintenance requirements and procedures.

INTRODUCTION

Mud and debris flows can result in significant public or private property damage, can represent hazards to motorists and individuals, and can result in extended or repeated road closures. Unusually heavy rainfall coupled with ever-progressing development have put the topic of mud and debris flows at the forefront of the public eye in recent winters. These factors have contributed to the need for a barrier that can effectively and cost efficiently provide protection against these events while providing ease of cleanout and maintenance.

In 1996, Brugg developed a flexible debris flow protection barrier based on tests conducted at the USGS Debris Flow Flume facility near Blue River, Oregon. From the results of these tests, modifications were made to the GeoBrugg Flexible Wire Rope Net Barrier making it appropriate for stopping small to moderated sized mud and debris flows. Though the basis for the design is a system intended to stop rockfall events, with modifications, these systems can effectively stop mud and debris flows with a minimum of required maintenance. Since the 1996 tests and development of the Mud & Debris Flow Barrier, several such systems have been and are in the process of being installed in actual field locations.

Each of the systems described herein is a variation from a standard rockfall barrier design, with modifications made to the system based on that learned during the debris flow tests of 1996 at the USGS flume. In addition to the infrastructural modifications made to each of these systems to make them appropriate for stopping debris, each system uses 1" mesh chain link mesh instead of the standard 2" mesh chain link used for rockfall barriers. The testing conducted in 1996 confirmed that the mesh used on the barrier needs to be small enough to prevent solids from passing through the barrier, but not so small as to restrict the passage of water. The 1" mesh chainlink has proven to optimize this balance.

INSTALLATIONS

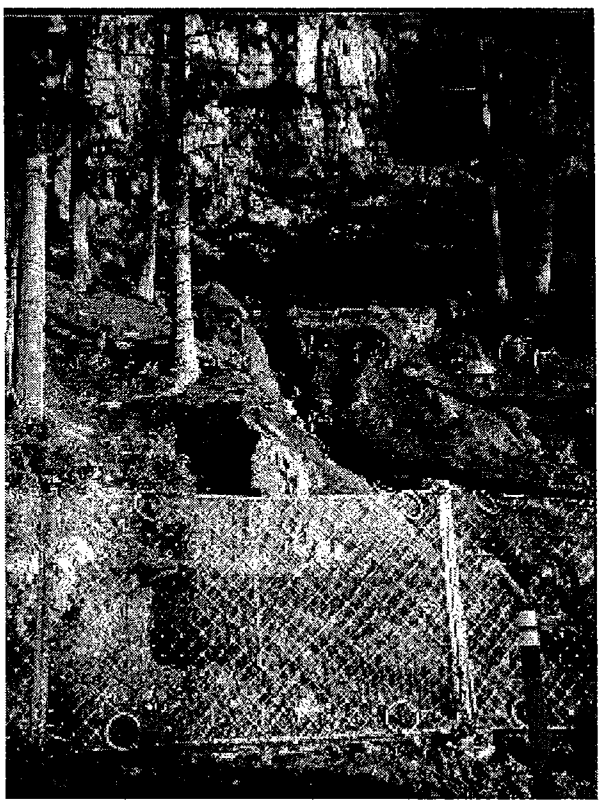

Figure 1 – Stella, WA site overview.

Stella, WA; Wash. State Rte. 4

This project site is located along the Columbia River on the north side of Washington State Route 4 at milepost 50, near the small town of Stella just west of Longview, WA. This site has had a history of sheet flow and rapidly moving, fluid and channeled mudflows creating a hazard to motorists, a maintenance nuisance and even water quality issues with the Columbia River. On numerous occasions, mudflows have required road closures for extended time periods, with no reasonable detours. For these reasons, Washington State Department of Transportation decided to mitigate the problem with a slope drainage program together with a GeoBrugg Debris Flow Barrier.

The barrier for this site was installed as a FHWA "experimental feature," with the intention of evaluating the construction, field performance, maintenance performance and mitigation effectiveness of the barrier.

The system is 141 feet (43 meters) long and 12 feet (3.66 meters) high. This system is based on the 129 ft-ton (350 kJ) rockfall protection barrier design, with the following modifications for debris flow: an increase in the number of friction braking elements, an increase in the number of upslope tieback anchors from each post, and an increase in the anchor pullout strengths of each tieback and lateral anchor.

Since construction completion in November 1997, there has been only one small mudflow event. Soon after installation, the barrier was impacted by 4 to 5 yd^3 of channelized mudflow consisting of a very fluid and fine-grained mud.

Though some mud did flow under the bottom of the nets and into the ditch below, nearly all the mud was retained by the barrier with none reaching the roadway. The energy associated with this mudflow impact was insignificant relative to the system capacity, with no noticeable effect on the system. However, much larger events are anticipated in the future. In the absence of this barrier, this small flow may have resulted in a temporary road closure until such time the mud could be cleared from the roadway by maintenance crews.

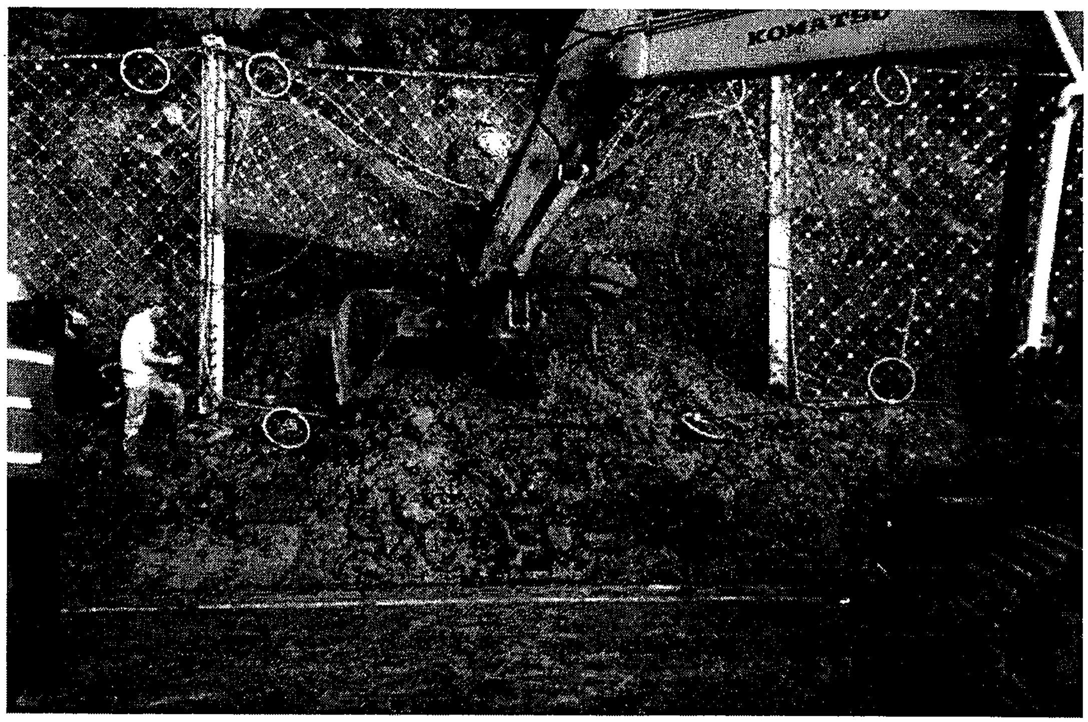

Figure 2 – Stella, WA site cleanout operations.

Within days of the mudflow event, cleanout operations were undertaken to determine the best methodology for cleanout and evaluation of the ease of maintenance. To clean out the mud behind the barrier, the seam rope connecting the bottom half of the affected net panel was removed. After the bottom half of this net was lifted up and temporarily attached to the top support rope, an excavator was then used to remove the debris. Though the entire cleanout process took about 3 hours to complete, subsequent cleanout events will be faster since this initial cleanout event was a learning event.

Laguna Beach, CA; California State Route 133

This project site is located along California State Route 133 at milepost 1, in the town of Laguna Beach, CA. This site has had a history of mud and debris flow originating from the cut slope and above on the natural slope creating a hazard to motorists, and a maintenance nuisance. For these reasons, the California Department of Transportation (Caltrans) decided to mitigate the problem with a GeoBrugg Debris Flow Barrier.

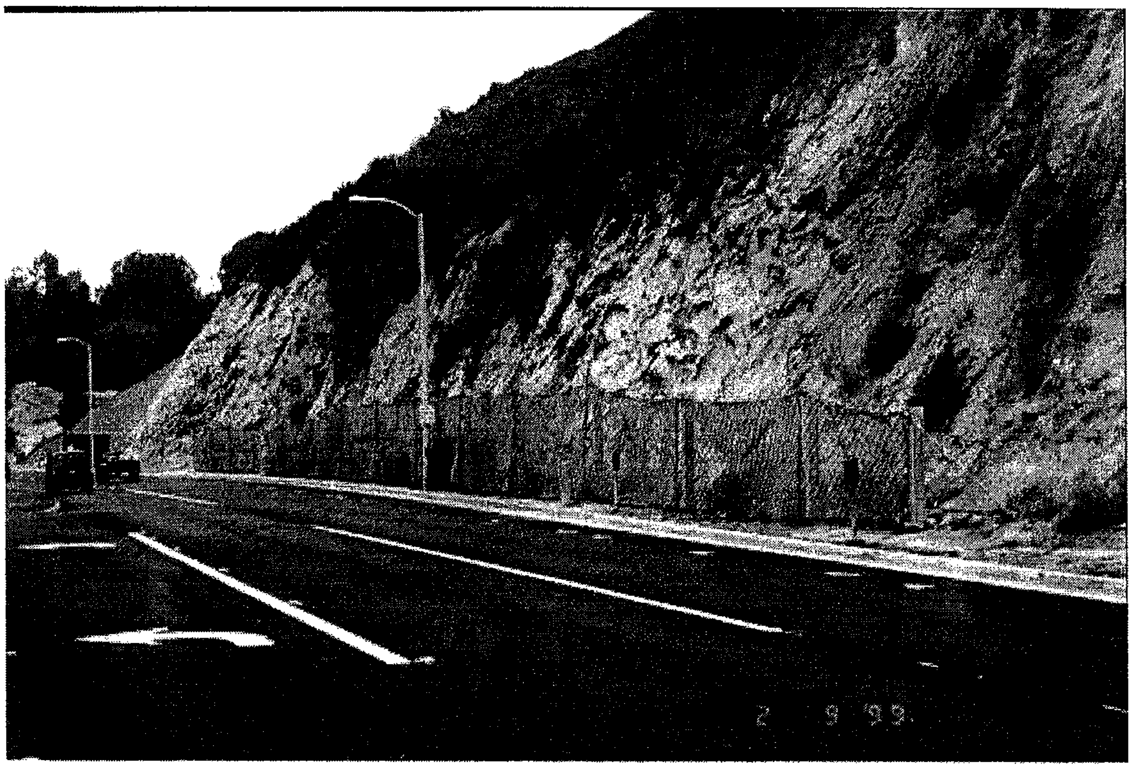

Figure 3 – Laguna Beach, CA. One of several debris flow barriers.

The system is 537.9 feet (164 meters) long in several separate sections and ranges in height from 6.56 feet (2.0 meters) to 9.84 feet (3.0 meters) high. This system is based on the 74 ft-ton (200 kJ) rockfall protection barrier design, with modifications for debris flow.

This site is located in the tourist town of Laguna Beach, with various art galleries, restaurants and shops immediately across the roadway from the problem slopes. For these reasons, the following extra measures were taken to minimize the aesthetic impact of this installation: painting of the posts to match surrounding earth materials, using a PVC coated chainlink colored to match the surrounding earth materials, and sloping the tops of the nets to visually "soften" the geometry of the barrier.

Since construction completion in June 1998, there have been no mudflow events impacting the barriers. However, during installation earlier in the year, the barrier was impacted by flows consisting of rapidly moving and fluid mud, debris and rock. These flows were a result of the winter 1998 storms that ravaged Laguna Beach and the surrounding area. Since the 1" chainlink mesh had not yet been attached to the wire rope nets of the barriers, some mud did flow through the wire rope nets and onto the roadway, though the barrier retained all larger rocks. The energy associated with these mudflow impacts was insignificant relative to the system capacity, with no noticeable effect on the system. However, much larger events are anticipated in the future.

Orinda, CA; California State Route 24

This project site is located along California State route 24 at milepost 1.8, in the town of Orinda between Oakland and Walnut Creek, CA. This site has had a history of large, rapidly moving debris flows during storm events creating a hazard to motorists, road closures and a maintenance nuisance on this major arterial route in the Bay Area.

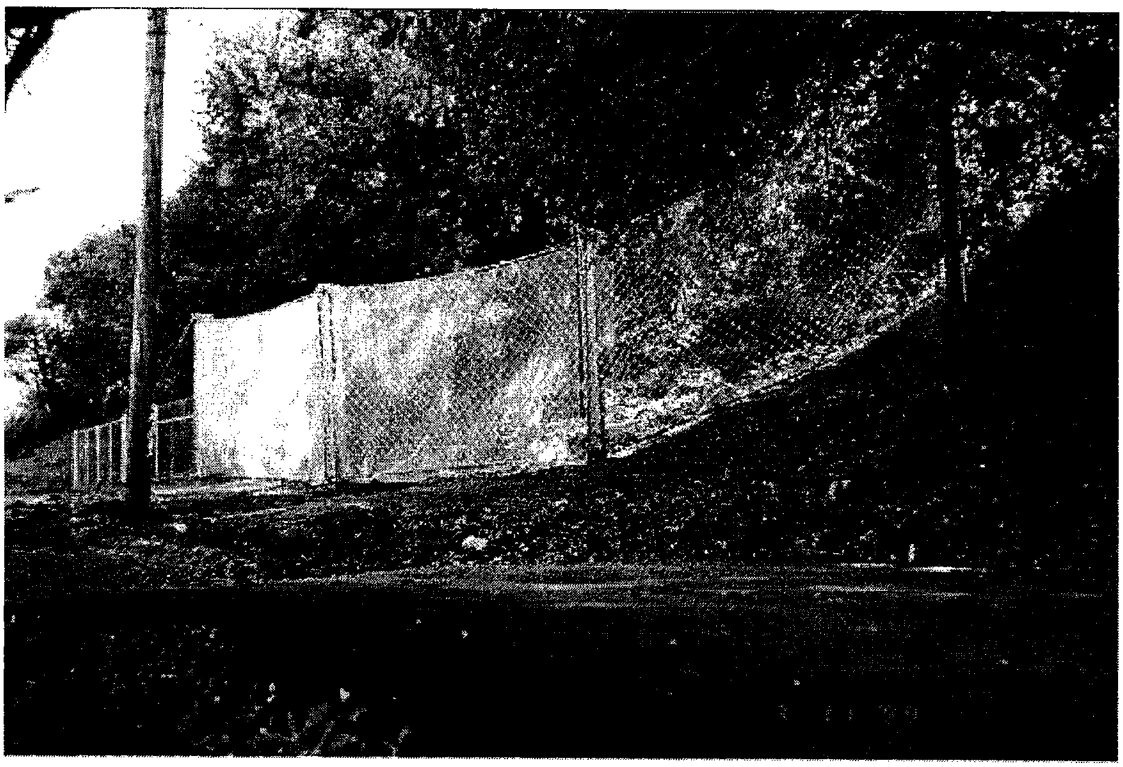

Figure 4 – Orinda, CA debris flow barrier.

The California Department of Transportation (Caltrans) decided to mitigate this problem with a GeoBrugg Debris Flow Barrier. The system is 59.04 feet (18 meters) long and 12.0 feet (3.66 meters) high. This system is based on the 180 ft-ton (488 kJ) rockfall protection barrier design with modifications for debris flow. Since the elevation along the barrier alignment changes significantly, wire rope nets with angled corners were fabricated in order to achieve a proper configuration.

Caltrans personnel anticipate that a very large debris flow beyond the barrier capacity could impact the barrier. For this reason, the barrier alignment was placed at an oblique angle to the flow channel, with the intention for the barrier to deflect the debris away from the road into a collection area, and also to reduce the total effect of the impact with the barrier. It is possible that in such a large event, significant barrier damage could be experienced; though most if not all debris should be kept from reaching the roadway.

Since construction completion in May 1998, no mud or debris flows have impacted the barrier. However, conditions in the debris source area are such that with time and enough water, a large debris flow could impact the barrier.

Pacific Palisades, CA; West Palisades Drive

This project site is located along West Palisades Drive, in the Pacific Palisades area of Los Angles, between Malibu and Santa Monica, CA. This site is characterized by a large global landslide adjacent to the roadway. Though mitigation of the global failure is ultimately desirable, due to property and right of way issues such measures are not currently feasible. In the meantime, mitigation was needed for the smaller mud and debris flow and rockfall problems generating from the surface of the larger landslide. Though smaller in nature, these smaller flows and rockfalls still represented a significant hazard to motorists, a maintenance nuisance, and potential for road closures with no detour options or alternate route into the area.

One alternative barrier that was considered for this project was a timber-lagging wall commonly used in the Malibu area. However, since the City of Los Angeles would ultimately be responsible for maintenance of the barrier, City officials preferred the Geobrugg barrier design due to the amenability for cleanout of accumulated debris. For these reasons, consultants working for the property owner, insurance company and City of Los Angeles decided to mitigate the problem with a GeoBrugg Debris Flow Barrier.

The system is 384 feet (117.07 meters) long and 15 feet (4.57 meters) high. This system is based on the 295 ft-ton (800 kJ) rockfall protection barrier design using ring nets instead of woven wire rope nets, with modifications for debris flow. Since all system components were increased in size and because of the redundancy in function for many of the components, this system was assigned a design load of 350 ft-tons (950 kJ), with an ultimate load capacity far beyond this level.

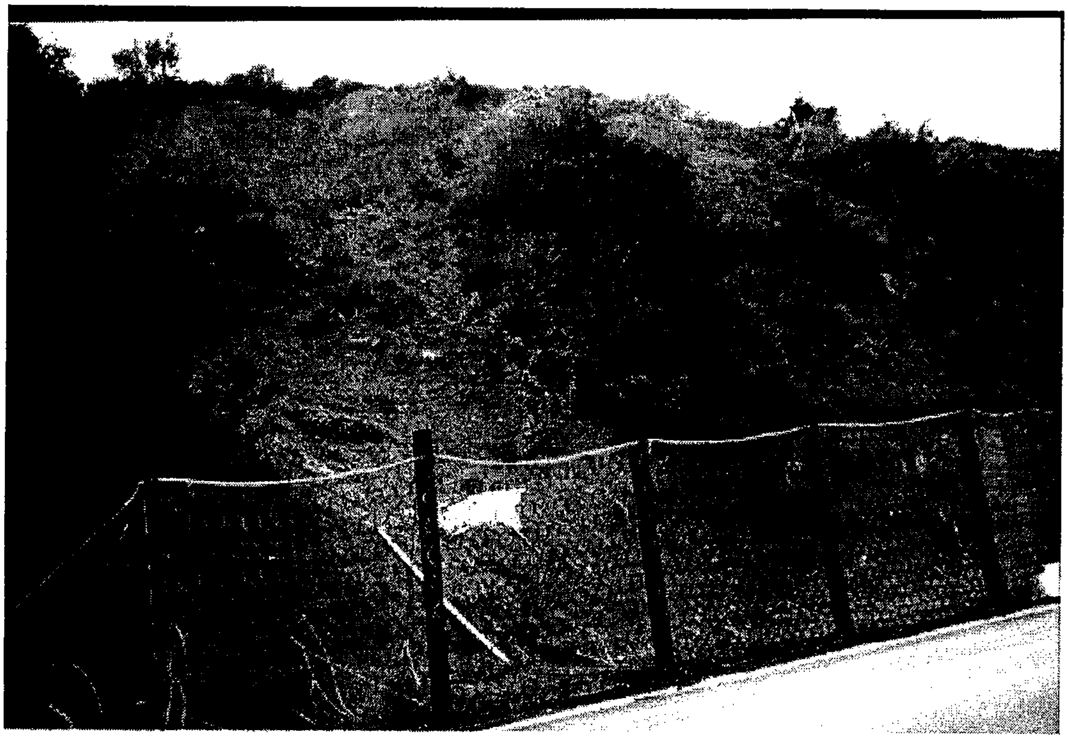

Figure 5 – Pacific Palisades, CA debris flow barrier.

It is possible that a very large debris flow with a large volume of solids could impact this barrier, possibly resulting in damage to the barrier. However, because the site geometry allowed for a large catchment area, much of the debris should deposit in the area behind the barrier, limiting the amount of debris impacting the barrier. In any case, the barrier will completely retain most debris flows, and all anticipated rockfalls without requiring repair, and in the worst case scenario prevent an extended road closure and reduce potential hazard to motorists.

Since construction completion in October 1998, there have been no mud or debris flow events impacting the barrier, though there have been several small rock impacts.

Hoodsport, WA; Washington State Route 101

This project site is located along Washington State Route 101 at milepost 331.5, adjacent to the Hood Canal area of Puget Sound, near the town of Hoodsport, WA. Removal of large trees and vegetation from the steep glacial till slope adjacent to the roadway has resulted a history of sheet flow and shallow debris flows ranging in size from 10's to several 100's of square yards of material, with relatively low velocity. These flows represent a hazard to motorists and a motel on the opposite side of the road, as well as a maintenance nuisance. On numerous occasions, mudflows have required road closures for extended time periods, with no reasonable detours. For these reasons, Washington

State Department of Transportation (WSDOT) decided to mitigate the problem with a GeoBrugg Debris Flow Barrier.

The system is 639.6 feet (195 meters) long and 12 feet (3.66 meters) high. This system is based on the 74 ft-ton (200 kJ) rockfall protection barrier design, with modifications for debris flow.

This system is currently under construction with an expected completion of May 1999.

Waddell Bluffs, CA; California State Route 1

This project site is located along California State route 1 at milepost 37, north of Santa Cruz, CA. This site has had a history of very frequent rockfall, representing a significant hazard to motorists. Thus, the California Department of Transportation decided to install a Geobrugg rockfall protection barrier at this site, with installation in May 1997.

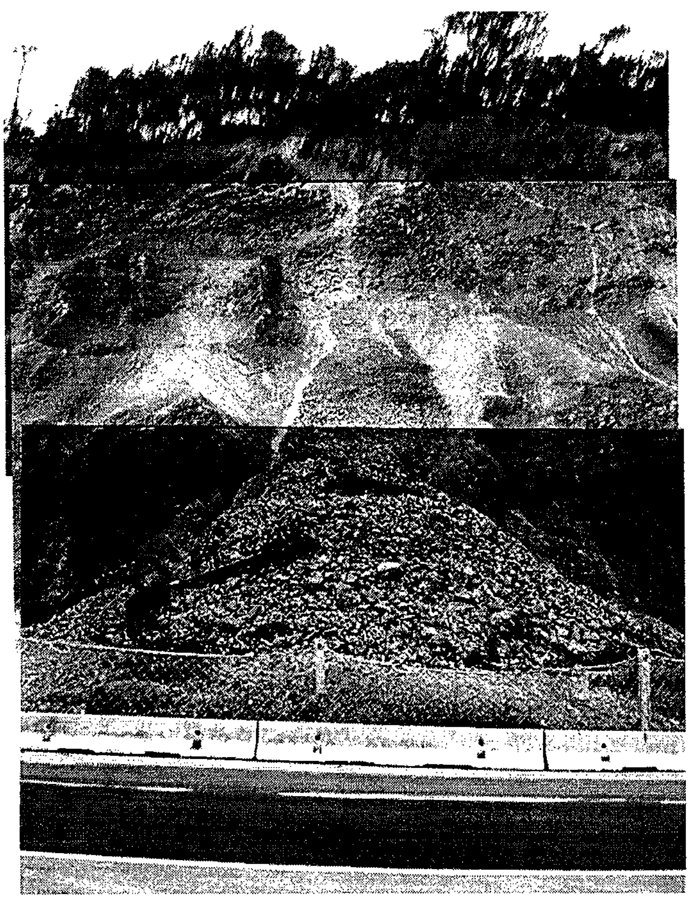

Figure 6 – Waddell Bluffs, CA rockfall barrier with retained rock and mud.

The system is 3,200 feet (975.6 meters) long in two separate sections with a height of 8 feet (2.44 meters), and a 74 ft-ton (200 kJ) design load. Though this system is not specifically designed as a debris flow barrier, some design modifications were made to the rockfall system design that resulted in an ability to stop mud and debris.

Throughout the winter of 1997/1998 numerous rockslides and mudflows impacted the barrier, ranging in size from 300 to 500 yd^3. Caltrans has estimated that these impacts to be above 222 ft-tons (600 kJ), well beyond the even the ultimate capacity of the barrier. Material including mud, trees and other debris in these slides and flows was completely retained with minimal damage to the barrier.

This event illustrates the effectiveness of the use of flexible barriers for retaining large debris movements, and the use of 1" chain link mesh for retaining fine-grained solids.

SUMMARY

The intent of these systems is to stop and retain the majority of mud and debris contained in small to moderate sized mud/debris flows, helping to prevent them from flowing onto the adjacent roadways below. The debris collected in the nets can then be removed relatively easily on a scheduled and controlled basis by maintenance crews.

Though the systems can stop a significant volume of material and even repeated flows without cleanout between flows, this is of course limited by the volume capacity upslope from the nets. Once the nets are completely full, excess flow material or subsequent flows may pass over or around the nets. Consequently, a system will need to be monitored during heavy rains to ensure it has not been filled with mud and debris.

There are still many unknowns with respect to defining the magnitude and character of expected mud/debris events at any site, and thus precisely predicting the limits of debris containment system performance is difficult. Though we cannot reliably predict the amount of material or kinetic energy that will impact the system, we can design systems that should be capable of withstanding the forces associated with the estimated volumes up to a limit.

As with any mitigation measure, these debris flow barriers are not intended to eliminate all risk associated with debris flow with 100% certainty, but rather to significantly reduce risk. Though this system is still somewhat experimental, with proper application the barriers will help prevent immediate hazards to life and property, the need for emergency road closures and emergency cleanup, and damage to roadways.

REFERENCES

DeNatale, J. S.. Fiegel, G. L., Iverson, R. M., Major, J. J., LaHusen, R. G., Duffy, J. D. and Fisher, G. D. (1997), "Response of Flexible Wire Rope Barriers to Debris-Flow Loading" Proceedings of the First International Conference on Debris-Flow Hazards Mitigation.

Thommen, R. A. and Duffy, J. D. (1998), "Testing and Application of Flexible Wire Rope Netting Barriers to Retain Mud & Debris Flow" Proceedings of 49th Annual Highway Geology Symposium, pp. 195-202.

Duffy, J. D. (1998), "Performance Review of Rockfall Mitigation Measures" Proceedings of 49th Annual Highway Geology Symposium, pp. 76-83.

Advances in Highway Slope Stability Instrumentation

By

WILLIAM F. KANE

***KANE* GEOTECH, INC.**

P.O. Box 7526

Stockton, CA 95267-0526

TIMOTHY J. BECK

California Department of Transportation

5900 Folsom Blvd., Sacramento, CA 95819

ABSTRACT

Many options are available for monitoring unstable highway slopes. These range from inexpensive, short-term solutions to more costly, long-term monitoring programs. The location of many unstable slopes has created a need for systems that can be accessed remotely and provide immediate warning in case of a failure. Advances in electronic instrumentation and telecommunications make it possible to monitor these slopes economically.

Available electronic instrumentation includes piezometers, electrolytic bubble inclinometers and tiltmeters, and time domain reflectometry (TDR) for sensing changes in slope conditions. This instrumentation can be used in the field by technicians, or remotely by dataloggers and telemetry. By combining instrumentation types, a full array of stability parameters can be gathered. Computer software is available to quickly plot data allowing immediate assessment of the situation.

Several case studies in California illustrate where these technologies were implemented. The use of a technological advance like TDR alone can provide a robust array of data. Budget constraints limited the monitoring of a landslide along the San Andreas fault in San Mateo County to one conventional probe inclinometer and four exploration holes. Instead, the inclinometer was not used and all five holes were instrumented with TDR. This allowed determination of the sequence and extent of the failure. In another case study, TDR was used to locate the depth of a landslide in Mendocino County.

A potentially unstable slope above a sand pit next to Interstate 15 in Riverside County was instrumented using piezometers and TDR. Data on movement and groundwater levels was monitored by cellular phone and modem 350 km away. A soldier pile wall in Santa Cruz County was instrumented with an extensometer and tiltmeter. Data was collected daily by cellular phone. An alarm circuit in the unit notified geotechnical personnel by pager if threshold movements were exceeded. A large landslide in Monterey County employed electrolytic bubble inclinometers in conjunction with a 180 m TDR cable. Threshold movement of the slope triggered a page notifying personnel of changed conditions at the site.

INTRODUCTION

Landslide monitoring involves determining certain parameters and how they change with time. The two most important parameters are groundwater levels in the slope and movement. Movement involves depth of failure plane(s), direction, magnitude, and rate. Depending on the complexity of the problem, one or all of these variables are desired. Piezometers allow the determination of water levels; inclinometers and tiltmeters allow determination of direction and rate, and to some extent, failure plane location; extensometers provide an indication of magnitude; and TDR allows determination of failure plane depth.

Conventional slope monitoring utilizes several methods or a combination of methods. This includes surveying to track the movements of targets on the slope surface, extensometers which record the movement of a wire firmly attached to the slope, and inclinometers. Inclinometers are the most common means of long-term monitoring of slopes.

Critical facilities adjacent to many unstable slopes has created a need for monitoring systems which can provide immediate warning if movement occurs. Advances in telecommunications and electronic instrumentation make it possible to economically monitor slope movements from a distance. Many types of sensors and data transmission systems are available. Several systems were installed in Central and Northern California using extensometers, tiltmeters, inclinometers, and TDR. Telemetry was by either cell phone or hard wire phone. Power was provided by rechargeable lead/acid batteries and solar panels.

There are many manufacturers of the various instruments described in this paper. The authors do not specifically endorse any of these products. Design philosophies and suitability to particular problems vary. Readers are urged to investigate all opportunities before purchasing any instrumentation.

INSTRUMENTATION FOR LANDSLIDE MONITORING

The critical data that are required from a slope monitoring program are the water level(s) in the slope and the depth and rate of movement. There is a wide array of instrumentation used, ranging from simple, mechanical devices to sophisticated electronic equipment.

WATER LEVELS

The usual method of monitoring water levels in a slope is to drill and case a borehole. The water surface is located by dropping a measuring tape down the boring. While useful for simple water table situations, and where monitoring can be done on an infrequent basis, other methods may be more desirable. These methods involve the use of more sophisticated instruments which may be mechanical or electrical.

Vibrating Wire Piezometers

A vibrating wire piezometer, Figure 1, works on the same principle as tuning a guitar or piano (Slope Indicator Company, 1994). A steel wire is stretched over a distance. The wire is set to vibrating by "plucking" it with an electromagnetic field. The natural frequency of the wire is a function of the tension in it. By reducing or increasing tension in the wire, the frequency becomes lower or higher. The frequency of vibration can be sensed by the electromagnetic coil and this is output to a readout device.

One end of the wire is attached to a diaphragm that is deforms by water pressure entering through a porous tip. An increase in water pressure, reduces the tension in the wire by deforming the diaphragm inward. The magnetic coil in the piezometer "plucks" the wire to

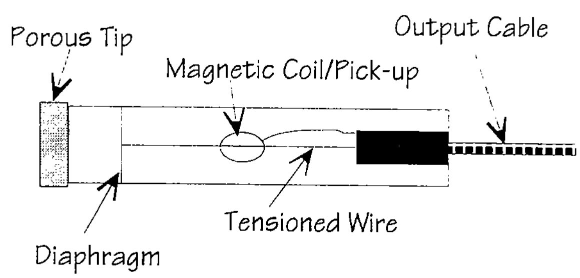

Figure 1. Schematic of vibrating wire piezometer.

vibrate it. The wire is plucked using variable excitation frequencies and then allowed to return to its natural frequency. The magnetic coil then becomes a sensor which is used to "count" the number of vibrations. The output signal is then converted into units of pressure or head. Two piezometers are considered ideal. One should read atmospheric pressure and the other downhole pressure. By subtracting the atmospheric from the downhole pressure, the true water level can be obtained.

MOVEMENT

Inclinometers and tiltmeters are commonly used to monitor slope movement. These instruments use two basic types of sensors. Force balance accelerometers are used in probe inclinometers (Dunnicliffe, 1993). Electrolytic bubbles are used in tiltmeters and "in-place" inclinometers. Probe inclinometers require manual operation. Tiltmeters and "in-place" inclinometers, when coupled with a datalogger, can be used for continuous monitoring. It is also possible to string several force balance inclinometers together in a casing to make an "in-place" inclinometer.

Electrolytic Bubble Inclinometers "In-Place" and Tiltmeters

An electrolytic level is similar to an ordinary "bull's eye" level. The fluid in this level, however, is an electrical conductor. Also in the level vial are three electrical nodes, Figure 2. One node is located at the base of the vial (B), and two are located on the top (A and C) at an equal distance from Node B. An electrical current is applied to the nodes and the resistance through the fluid is measured. As the vial tilts clockwise the resistance between A and B increases, and the resistance between B and C decreases. The change in resistance can be measured, and is directly proportional to the angle of tilt.

Extensometers

Extensometers often use a steel wireline firmly implanted on the slope face. Movement of the slope pulls a weight along a track. The amount and rate of movement can then be measured.

Extensometers can also use potentiometers to measure movement. Much like the rheostat controls of a model electric train, the extensometer uses a variable resistance mechanism to measure the amount of expansion. A moveable arm makes an electrical contact along the fixed resistance strip as shown in Figure 3. The circuit's resistance is based on the position of the slider arm on the resistance strip. A regulated DC current is applied and the output voltage corresponds to the amount of expansion and ground movement.

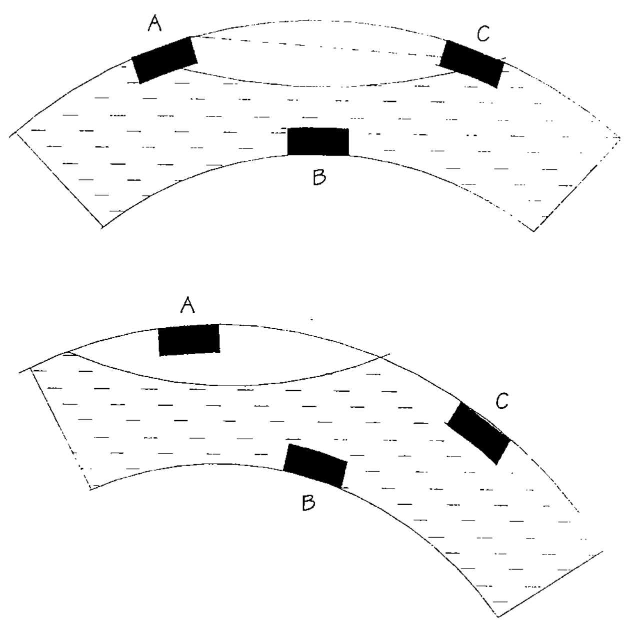

Figure 2. Schematic of electrolytic bubble. See text for explanation.

Time Domain Reflectometry (TDR)

Time domain reflectometry (TDR) is a new approach to monitoring slope movement (Kane and Beck, 1994, 1996a, 199b; Mikkelsen,1996; O'Connor and Dowding, 1999). Originally developed to locate breaks and faults in communication and power lines, TDR can be used to locate and monitor the locations of slope failures. This technology uses coaxial cable and a cable tester.

The basic principle of TDR is similar to that of radar. The cable tester sends an electrical pulse down a coaxial cable grouted in a borehole, Figure 4. When the pulse encounters a break or deformation in the cable, it is reflected. The reflection shows as a "spike" in the cable signature. The relative magnitude and rate of displacement, and the location of the zone of deformation can be determined immediately and accurately. The size of the spike increase correlates with the magnitude of movement. A laptop computer is connected to the tester and cable signatures are written to disk for future reference.

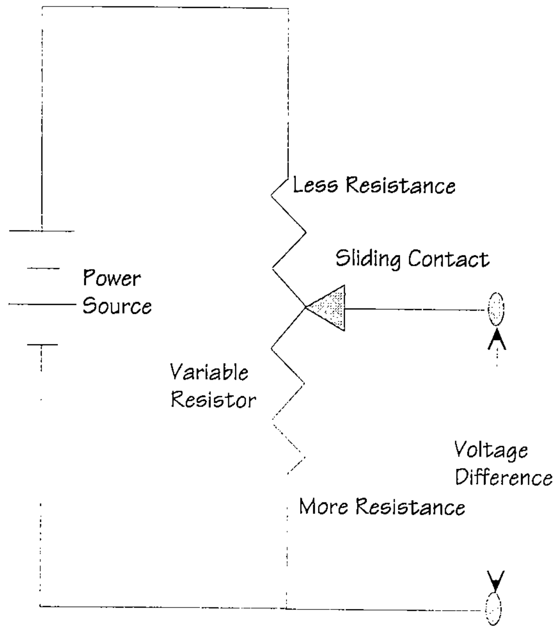

Figure 3. Schematic diagram of variable resistance potentiometer as used in an extensometer.

REMOTE DATA ACQUISITION COMPONENTS

The remote data acquisition equipment includes a datalogger, multiplexer, communication devices, and a power source. In addition, software is necessary to program and interact with the datalogger. Many different manufacturers and equipment exist. Only the equipment used in the case studies are described here. The reader is urged to investigate other manufacturers and approaches.

DATALOGGER

A datalogger is a essentially a small computer CPU/voltmeter with memory. It is programmed to do certain tasks. The Campbell Scientific CR10X logger used for this work can be programmed to output specified voltages over certain durations, read voltages, and store values (Campbell Scientific, Inc., 1997). It can also be programmed to do calculations and store the results such as converting the readings of a piezometer to feet of head.

Instruments are wired to connections, or "ports," on the logger. Control ports and excitation ports can be programmed to output voltages at certain times to turn on peripheral equipment, such as cell phones or cable testers,. Other ports are wired to the sensors and are used to measure output voltages.

MULTIPLEXER

A multiplexers allows many sensors to be attached to a single datalogger. The multiplexer is wired to a single set of ports on the datalogger. A set of contacts in the multiplexer switches between each sensor

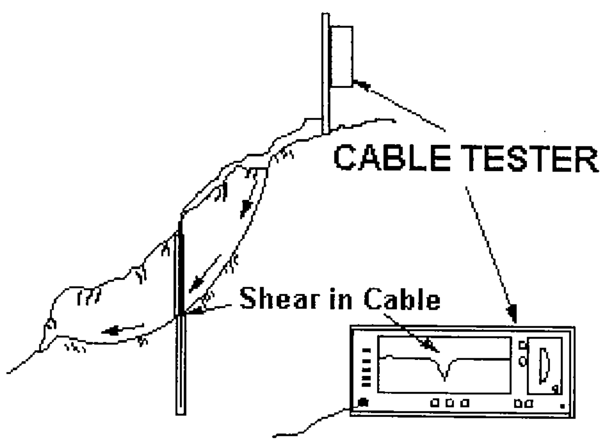

Figure 4. Deformed cable resulting in signature "spike" on cable tester screen.

attached to it. The data is collected sequentially by the logger. Multiplexers can even be multiplexed to each other creating the ability to read a very large number of instruments. To read more than one TDR cable a multiplexer for this purpose, such as a Campbell Scientific SDMX50 which has 8 connectors for TDR cables, must be used.

COMMUNICATIONS

Communications with the datalogger can be by several means. "Hardwired" telephone lines are best, but not always available. Cellular and satellite telephones can be used as well as conventional and spread-spectrum radios. A telephone line only requires a modem to transmit data and receive instructions. The other methods require modems and cell phones and/or radio transceivers.

POWER

Power requirements vary depending on the number of instruments and the communications device. Ideally, power is available at the site but that is often not the case. A small system with a phone line and one or two sensors requires only a small rechargeable gel-type battery. A large system with cellular phone and cable tester requires a 12 V deep cycle marine battery. The battery is recharged by regulated solar panels.

SOFTWARE

Specialized software is required to process the raw data. When TDR cables are read, signatures can be digitized and downloaded to a laptop computer when using Tektronix, Inc. software (Tektronix, 1994). Plotting several TDR signatures on the same plot requires the user either write a specialized spreadsheet or use a commercially available program such as TDRPlot (Kane and Parkinson, 1998). Piezometer data is best viewed with a spreadsheet. Electrolytic bubble tiltmeters and inclinometers used in the work described here were plotted using TBASEII (AGI, 1998).

In order to program and communicate with the datalogger Campbell Scientific developed PC208W (Campbell Scientific, Inc., 1998). The program allows the user to write code for datalogger control; contact the remote station, either automatically or manually; monitor instrument readings; and download data.

CASE STUDIES

The 1998 El Niño storms of January and February caused a large number of landslides in California (CDMG, 1998; USGS, 1998). Repair of these landslides required immediate action in often hazardous conditions. At some locations, the relative ease and cost-effectiveness of TDR allowed the determination of the depth to the shear plane. At other locations, remote automated monitoring was required during construction to assure the safety of workers and the general public. The locations of the sites described below are shown in Figure 5.

MUSSEL ROCK LANDSLIDE, SAN MATEO COUNTY

Continued long-term movement of the Mussel Rock Landslide necessitated its repair. Repair measures required determining the location of the depth to the failure. Initial plans called for a site investigation of five borings and the installation of a single inclinometer to monitor movement. Because of the cost advantages of TDR, it was decided instead to use TDR cables in all five borings. The TDR was monitored periodically for a fraction of the cost of monitoring the single inclinometer hole. Because five borings were monitored, the depth and areal extent of the slide plane was determined.

Figure 6 contains example of TDR signatures from two cables. Note that failure began at the lowest of the two, B-15 and then progressed to B-18. Cable B-19 showed a similar pattern indicating progressive movement of the slide slices up the slope. Cables B-16 and B-17 showed no change, thus locating the head and toe of the slide as shown in Figure 7.

HIGHWAY 1, MENDOCINO COUNTY

A portion of California Highway 1 crosses a landslide complex approximately 200 m (650) wide. In November 1997, a coaxial cable was grouted in a borehole at the site. The boring encountered relatively weak soil on top of competent rock. The slide complex became active as the winter rains infiltrated into the slide mass. The cable deformed at a depth of 6.4 m (21 ft), as shown in Figure 8. This is the soil/rock interface. A second cable was installed in the slide later that winter. It failed accurately located the depth to the shear zone. to detect any movement probably because the slide had stopped moving. The TDR installation accurately located the depth to the shear zone.

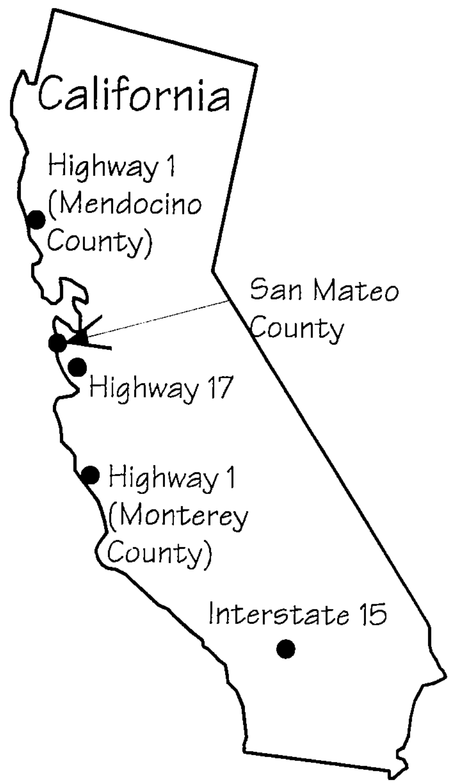

Figure 5. Location map of case studies.

INTERSTATE 15, RIVERSIDE COUNTY, CALIFORNIA

Over-steepened slopes in a sand pit adjacent to Interstate 15 in Riverside County, led the California Department of Transportation (Caltrans) to install a monitoring system.

Two TDR cables 52 m (170 ft) deep and two vibrating wire piezometers were installed between Interstate 15 and the pit. A remote data collection system was also installed. It included a datalogger, piezometer signal conditioner, a multiplexer to attach the two TDR cables, and a cell phone and modem for data transmission. Power was supplied by a 12 V deep cycle marine battery and 20 W regulated solar panel. Because the cell phone requires significant current, it could not be kept on at all times.

The system was programmed to read the two piezometers every morning, calculate the head of water present in the slope, and store the values in memory. It then turned on the cable tester and sequentially accessed and digitized the cable signatures from the TDR installations. After data collection the cell phone was turned on and a computer in Sacramento about 350 km (218 mi) away dialed the cell phone number and downloaded the data. The piezometer data was plotted using a spreadsheet program and the TDR data with TDRPlot. Data was collected for over a year before the system was removed for installation at another site.

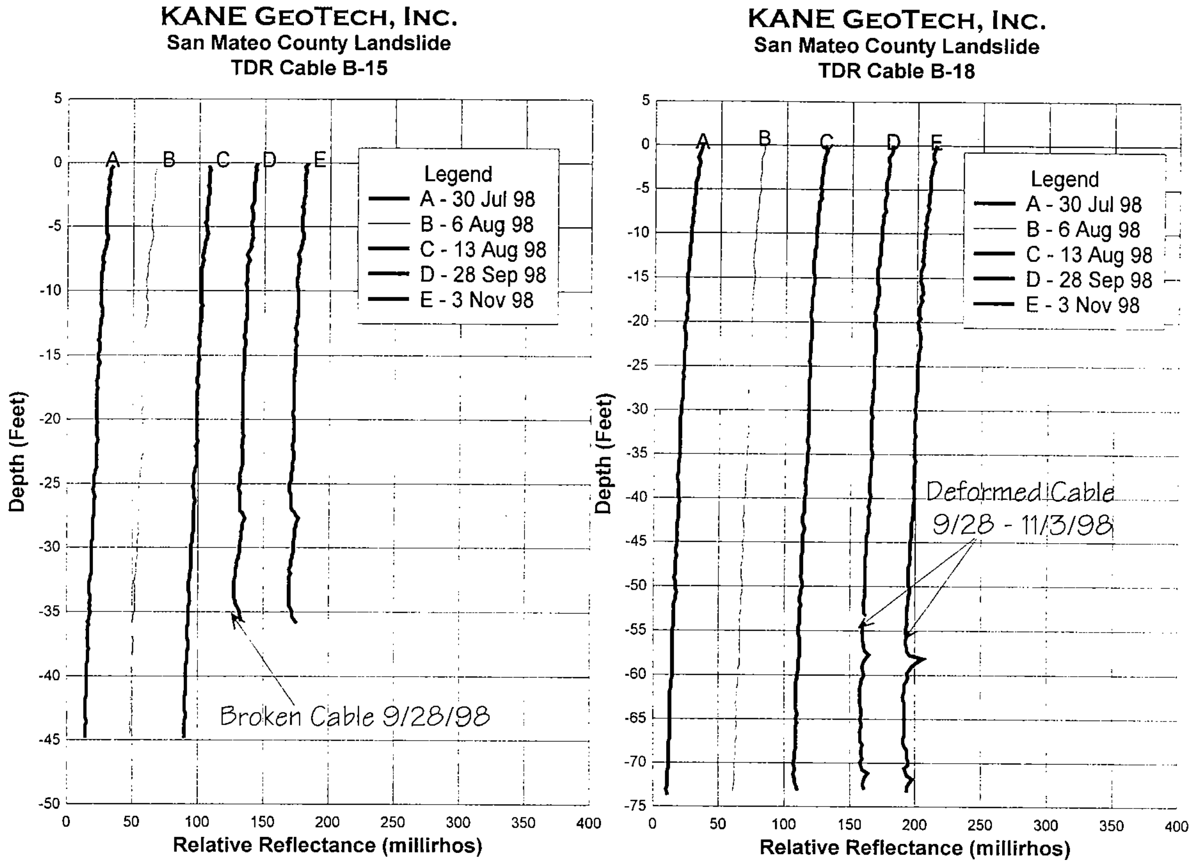

Figure 6. TDR cable signatures from San Mateo County.

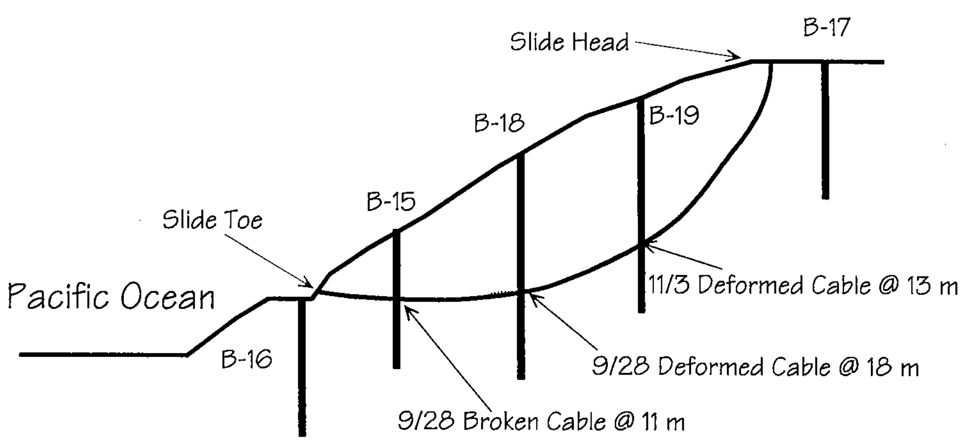

Figure 7. Cross-section of San Mateo County landslide showing dates and locations of cable damage.

HIGHWAY 17, SANTA CRUZ COUNTY, CALIFORNIA

In January 1998, a landslide/debris flow destroyed a small Santa Cruz County road adjacent to California Highway 17. Caltrans constructed a soldier pile wall at the head of the slide to protect Highway 17 from future movement. Caltrans was concerned that progressive failure at the head scarp would jeopardize the wall stability.

A monitoring system consisting of a datalogger, cell phone, and phone dialer was installed. The system monitored a clinometer attached to the wall, and the movement of an extensometer anchored to the wall and embedded at the head of the scarp. The datalogger was programmed to monitor both instruments and determine if a threshold movement was reached. If the threshold was exceeded, the phone dialer immediately notified personnel by means of pagers. The system also was automated to download data everyday to an office computer.

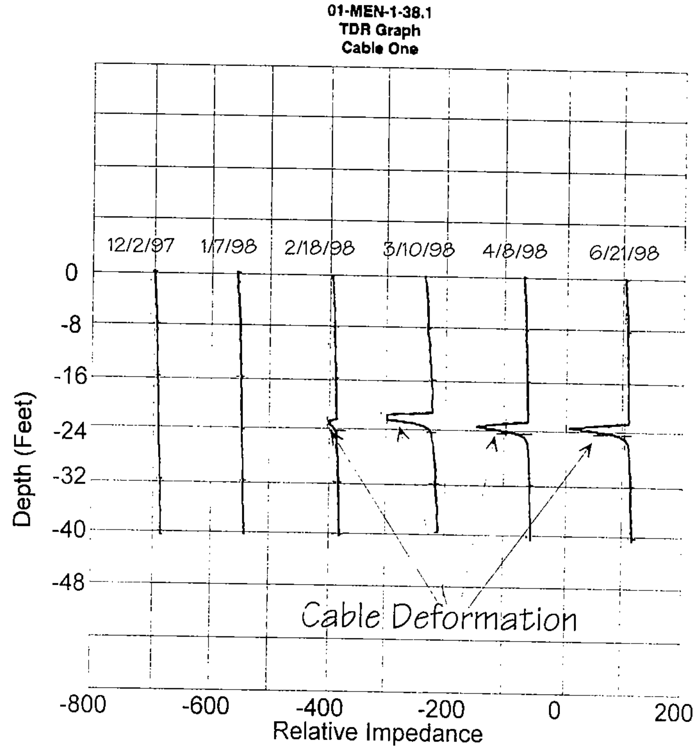

Figure 8. TDR cable signatures from Mendocino County.

STATE HIGHWAY 1, MONTEREY COUNTY, CALIFORNIA

Numerous slides along California Highway 1 in San Luis Obispo and Monterey Counties closed portions of the road throughout the winter of 1998. Grandpa's Elbow Landslide in Monterey County was a reactivation of a older, much larger landslide complex. To protect motorists and clean-up crews, Caltrans instrumented the slide with four downhole, in-place inclinometers attached to a TDR cable in a 200 ft borehole. The inclinometers were placed at the 150 ft, 100 ft, 50 ft, and 10 ft . Any movement of the slide changed the tilt of the inclinometers and triggered a warning by phone dialer and hard-wire telephone line. The system could also be monitored remotely by computer and modem.

Soon after installation, slight movement of the inclinometers triggered the telephone dialer and personnel were paged. TDR cable readings showed the development of a spike in the cable at a depth of 9 m (30 ft) indicating movement, Figure 9. Observation of tension cracks in the ground surface verified the fact that some movement had taken place.

CONCLUSIONS

The huge advances in electronic technology, coupled with rapidly falling prices, make remote monitoring cost-effective and a powerful tool in slope stability work. Instrumentation is available that will provide much of the information necessary, not only to monitor slopes but to obtain some of the necessary parameters for mitigation and remediation.

ACKNOWLEDGMENTS

The authors would like to thank Jeff Schuyler and Gary Holzhausen of Applied Geomechanics, Inc., Santa Cruz, California, for their technical assistance in using many of the sensors described in this paper. Caltrans District 5 geotechnical personnel Ron Richman, John Duffy, Wade Hoon, and Sarah Conner were very helpful in ideas and implementation.

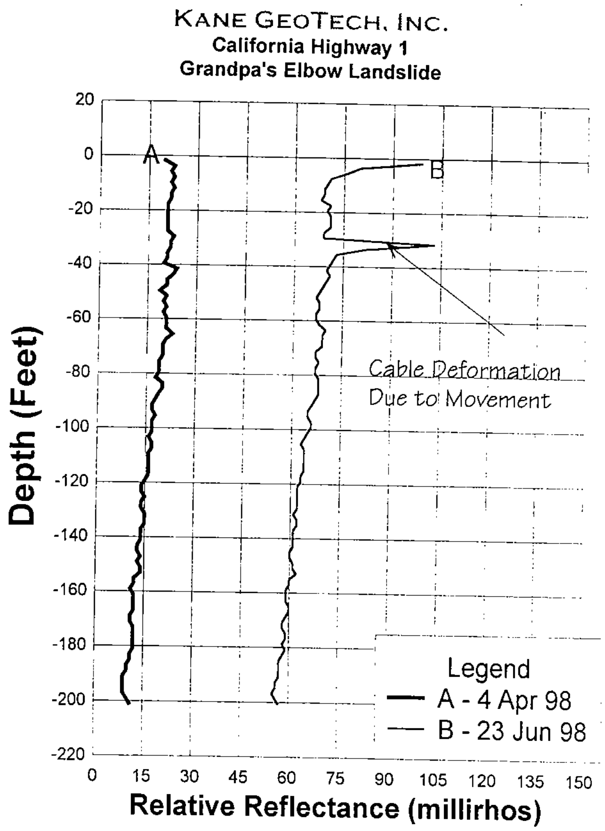

Figure 9. TDR cable signatures showing deformation which activated alarm circuit.

REFERENCES

AGI (Applied Geomechanics, Inc.) (1998). TBASEII User's Manual. Applied Geomechanics, Inc., Santa Cruz, California.

Campbell Scientific, Inc. (1997). "CR10X Measurement and Control Module Operator's Manual." Revised 5/97, Campbell Scientific, Inc., Logan, UT.

Campbell Scientific, Inc. (1997). "PC208W Datalogger Support Software Instruction Manual." Revision: 5/97, Campbell Scientific, Inc., Logan, UT.

CDMG (California Division of Mines and Geology) (1998). "Landslide Reports from Various State Offices Between February 3,1998 and April 30,1998." California Division of Mines and Geology Web Page, http://www.consrv.ca.gov/dmg/minerals/98landslide/24.htm.

Dunnicliffe, John (1993). *Geotechnical Instrumentation for Monitoring Field Performance.* John Wiley & Sons, Inc., New York.

Kane, W.F. and Beck, T .J., 1994, Development of a time domain reflectometry system to monitor landslide activity: *Proceedings*, 45th Highway Geology Symposium, Portland, OR, p. 163-173.

Kane, W.F., and Beck, T .J. (1996a). "Rapid Slope Monitoring." *Civil Engineering*, American Society of Civil Engineers, New York, 66(6), 56-58.

Kane, W.F. and Beck, T. J. (1996b). "An Alternative Monitoring System for Unstable Slopes." *Geotechnical News*, 14(3), 24-26.

Kane, W. F., and Parkinson, W. A. (1998). "Remote Landslide Monitoring Including Time Domain Reflectometry." Short Course Manual, KANE GeoTech, Inc., Stockton, CA.

Mikkelsen, P. E. (1996). "Field Instrumentation." in Turner, A. K., and Schuster, R. L.. *Landslides. Investigation and Mitigation.* Special Report 247, Transportation Research Board, National Academy Press, Washington, DC.

O'Connor, K. M., and Dowding, C. H. (1999). *GeoMeasurements by Pulsing TDR Cables and Probes*. CRC Press, Boca Raton, FL.

Slope Indicator Company (1994). *Applications Guide.* 2nd Edition, Slope Indicator Company, Bothell, WA.

Tektronix, Inc. (1994). "1502B Metallic Time Domain Reflectometer Operator Manual." 070-6266-01 Textronix, Inc., Redmond OR.
USGS (United States Geological Survey) (1998). "El Niño and Recent Landslides." United States Geological Survey Web Page, http://geohazards.cr.usgs.gov/elnino/elninols.html.

ROCK SLOPE ANALYSIS USING INTERACTIVE VISUAL SOFTWARE

By Joshua H. Cole[1] and Matthew Mauldon[2]
[1]Graduate Research Assistant, [2]Associate Professor, Department of Civil and Environmental Engineering, University of Tennessee, Knoxville, TN.

ABSTRACT

Interactive software can aid in the analysis of rock slope stability in two main ways: first, by automating long and involved calculations, thus saving time and minimizing human error and second, by providing rapid visual feedback on how changing input parameters affects stability. In this way, the rock slope engineer can quickly get a feel for the factors critical to the problem at hand and the software thus becomes an effective learning tool, in addition to being an analysis tool.

Three interactive computer programs which aid in the stability analysis of rock slopes have recently been developed at the Institute for Geotechnology, University of Tennessee, Knoxville under a research project funded by the Tennessee Department of Transportation. These programs are entitled *PlaneSlip*, *WedgeSlip*, and *RockSlip* and are collectively known as the *ROCKSLIP* package. *PlaneSlip* and *WedgeSlip* implement limiting equilibrium solutions for plane and wedge slides, respectively, while *RockSlip* implements an energy method to analyze the stability of curved or multi-plane failure surfaces. Application of these programs to the analysis of rock slopes in East Tennessee and Alabama will be demonstrated.

These programs allow the user to adjust interactively the discontinuity geometry, slope geometry, water pressure, friction angle, cohesion, and slope reinforcement. Water pressure in *PlaneSlip* and *RockSlip* is governed by the combination of two parameters: the height of water in a tension crack and a parameter called drainage impedance, which controls the permeability of the discontinuities. In *WedgeSlip* there is an input value for the average water pressure on each plane which can be specified by the user or set to a default value based on slope geometry. Screen displays of the slope cross section and stereographic projections of the slope geometry and discontinuity data change in real time as the user adjusts the variables.

INTRODUCTION

Rock slope failures are a recurrent problem for many highways in the United States. In particular, the Appalachian Region and the Rocky Mountain Region are two of the most susceptible areas for rock slope instability. Expansion of highway systems into these geologically complex domains has heightened the need for more extensive analysis techniques. The need for continued maintenance of rock slopes is also increased in these situations due to the potentially fatal hazards that rock slope failures present to motorists (Moore, 1986). In order to analyze these rock slopes with greater accuracy and speed , a family of computer programs has recently been developed at the University of Tennessee, Knoxville, under a research project funded by the Tennessee Department of Transportation. These programs are entitled *PlaneSlip*, *WedgeSlip*, and *RockSlip* and are collectively known as the *ROCKSLIP* package. The importance of user-friendliness and a practical screen setup has been the focus of all the programmers involved in this project. Visual Basic 5.0 Professional Edition© has been used to develop the most recent versions of the programs. The use of this 32-bit developing environment has allowed a compact and eye-pleasing design for all the programs. All the programs are *Windows* based applications and compatible with *Windows 95/98/NT.* Another goal in designing these programs has been the implementation of "real-time learning" features through the auto-redraw function (found in *PlaneSlip* and *WedgeSlip*). This paper summarizes the work done on this project and describes the three computer programs.

The original impetus behind this project was the need to implement a new rock slope stability analysis method for slopes consisting of folded rock geometries. Since the failure surface in such cases is essentially a series of planes (>2), limiting equilibrium analysis yields an indeterminate answer for these slopes. A method based on potential energy was developed for stability analysis in folded rocks. This analysis technique was adapted into a computer program entitled *RockSlip*. As time progressed, programs to analyze other basic rock slope geometries were developed. *WedgeSlip* and *PlaneSlip* were the results of this effort.

PROGRAM FEATURES

The following is a list of key program features found in the *ROCKSLIP* package:

- **Units of Measurement** - All three programs allow for the use of two different measuring systems, fps (English) and SI (Metric).
- **Auto-Redraw** - Included in *PlaneSlip* and *WedgeSlip*. The *auto-redraw* function enables the user to change key parameters and see, in "real-time", how these changes affect the slope's stability.
- **Rockbolts** - The effects of rock reinforcement (rock anchors or rockbolts) are included in *PlaneSlip* and *WedgeSlip*. Parameters such as number, orientation, tensile and shear capacity, minimum embedment length and horizontal spacing can be defined for the rock reinforcement.
- **Examples** - Included in *PlaneSlip* and *WedgeSlip*. Several example problems are included under the pull-down menu "Data", which are based on published results.
- **Water Level** - Included in *PlaneSlip* and *RockSlip*. The height of water in the tension crack controls the magnitude of water pressure acting on the slope.
- **Drainage Impedance** - Included in *PlaneSlip* and *RockSlip*. A parameter entitled "drainage impedance" has been incorporated into the program, which allows the user to change the pressure distribution behind the slope by varying the drainage conditions along the sliding plane and at the toe of the slope.
- **Tension Crack Angle** - Included in *PlaneSlip*. The angle of the tension crack can be adjusted. This is a feature that has not been included in much of the previous work on rock slopes (e.g., Hoek & Bray, 1981).
- **Graphical Output** - *WedgeSlip* incorporates several diagrams (including upper and lower hemisphere stereographic projections, cross section and variables diagram) which aid the user in grasping the physical scenario. Different quantities can be plotted on the stereographic projections, such as normal and dip vectors. The removable wedge, as determined by block theory, can also be highlighted (available for lower hemisphere projections only).
- **Water Pressure** - Included in *WedgeSlip*. The effects of water pressure on wedge stability are also accounted for with the average water pressure parameters (one value for each plane).
- **Y2K Compliant** - *PlaneSlip*, *WedgeSlip* and *RockSlip* include no reference to date and are therefore fully Y2K compliant.

ASSUMPTIONS

PlaneSlip

The following assumptions are made for the analysis of a plane slide. All are based on Hoek & Bray (1981), except for the assumption concerning water pressure:

- The sliding surface and the tension crack strike parallel to the slope surface.

- Water enters the sliding surface along the base of the tension crack and seeps along the sliding surface, escaping at atmospheric pressure where the sliding surface daylights in the slope face. This is the case when there is no drainage impedance at the toe of the slope. If drainage is impeded then the water pressure distribution on the sliding surface is modified according to the amount of impedance.

- All forces are assumed to act through the centroid of the sliding mass. This implies that there are no moments created by the forces acting on the block. This assumption is not the case in most plane slides, but the error introduced by ignoring the moments is negligible (Hoek & Bray, 1981).

- The shear strength of the sliding plane is defined by the Mohr-Coulomb criterion:

$$\tau_f = c + \sigma_f' \tan\phi \tag{1}$$

  where τ_f = shear stress at failure, c = cohesion, σ_f' = effective normal stress at failure, and ϕ = friction angle.

- A slice of unit thickness is considered and it is assumed that release surfaces are present so that there is no resistance to sliding at the lateral boundaries of the failure.

WedgeSlip

The following assumptions are made for the analysis of a wedge slide (due to Hoek & Bray, 1981):

- All forces are assumed to act through the centroid of the sliding mass. This implies that there are no moments created by the forces acting on the block. This assumption is not the case in most wedge slides, but the error introduced by ignoring the moments is negligible (Hoek & Bray, 1981).

- The shear strength of the sliding planes is defined by the Mohr-Coulomb criterion.

RockSlip

The following assumptions are made when the potential energy model is implemented:

- Each contact face of the rock block is assumed to have a normal stiffness of k_n, whereas the previously published work employed a uniform spring stiffness constant for all contact surfaces.

- The block itself is assumed to be undeformable, deformation occurring only at the contact faces.

- The block is acted upon by an active resultant force $\boldsymbol{R}$, which includes self weight, and may include other forces.

- An important assumption is that the frictional shear stresses act parallel to the direction of sliding only (Hoek and Bray, 1981; Chan and Einstein, 1981). This is a standard assumption in limiting equilibrium analyses.

- An elastic, conservative system is assumed to determine the distribution of normal forces that minimizes the potential energy of the system. These normal forces will then allow the stability to be determined.

- A local coordinate system is defined with the Z axis parallel to the fold axis and X and Y in the plane orthogonal to the fold axis.

- Each plane has a length L_i in the XY plane, and since this is a prismatic block, the other dimension of the contact plane will be taken as a unit length in the Z (fold axis) direction.

LIMITING EQUILIBRIUM

The term "limiting equilibrium" means that the forces tending to induce sliding exactly balance the forces resisting sliding. Thus, one must define an index which describes the relationship between driving and resisting forces for each geometric and mechanical situation in a rock slope. This is traditionally done using an index called the *Factor of Safety* (FS), defined as the ratio of the total resisting force to the total driving force. For plane sliding with no reinforcement, the equation for calculating the FS is as follows (Hoek & Bray, 1981) (see Appendix I for definition of variables).

$$\mathrm{FS} = \frac{\mathrm{cA} + (\mathrm{W}\cos\psi_\mathrm{p} - \mathrm{U} - \mathrm{V}\sin\psi_\mathrm{p})\tan\phi}{\mathrm{W}\sin\psi_\mathrm{p} + \mathrm{V}\cos\psi_\mathrm{p}} \qquad \textbf{(2)}$$

The previous equation includes the effects of water pressure but does not address the effects of rock reinforcement. If rockbolts or cables are installed, then the equation is modified as follows (see Appendix I for definition of variables).

$$\mathrm{FS} = \frac{\mathrm{cA} + (\mathrm{W}\cos\psi_\mathrm{p} - \mathrm{U} - \mathrm{V}\sin\psi_\mathrm{p} + \mathrm{NT}\cos\beta)\tan\phi + (\mathrm{NS}/\mathrm{SH})}{\mathrm{W}\sin\psi_\mathrm{p} + \mathrm{V}\cos\psi_\mathrm{p} - \mathrm{NT}\sin\beta} \qquad \textbf{(3)}$$

For wedge sliding, under gravity, the equation for calculating the Factor of Safety is as follows (see Appendix I for definition of variables).

$$FS = \frac{N_1^{'} \tan\phi + N_2^{'} \tan\phi + c_1 A_1 + c_2 A_2}{W \sin\psi_i} \tag{4}$$

If rock bolts are included the factor of safety equation is modified as follows (Note that N_i' is the effective normal force, equal to N_i - $u_i A_i$) (see Appendix I for definition of variables).

$$FS = \frac{[N_i^{'} + N_i^{'} + NT\cos\beta]\tan\phi + NS + (c_1 A_1 + c_2 A_2)}{W\sin\psi_i - NT\sin\beta} \tag{5}$$

POTENTIAL ENERGY MINIMIZATION

RockSlip deals with failures involving multiple or curved sliding surfaces. The analysis procedure, which was originally developed for stability analysis in folded rocks, is based on minimization of potential energy. For a detailed explanation of the potential energy minimization method please refer to Mauldon and Ureta (1996) and Mauldon, Arwood and Pionke (1998). Due to the lengthy mathematical formulations involved, an explanation of the method will not be presented here.

WATER FORCE

PlaneSlip

The water force is calculated in three separate parts depending on the conditions at the toe of the slope. If the toe is free to drain, the water pressure distribution is that shown in Figure 1 (note that z_w is the depth of water in the tension crack). If drainage at the toe of the slope is completely impeded then the pressure head continues to increase with depth and the pressure distribution is the same as the free draining case with an additional triangular pressure block acting perpendicular to the sliding plane (Figure 2). If drainage at the toe of the slope is partially impeded then the pressure distribution will vary based on the amount of drainage impedance (ξ). An intermediate pressure distribution is shown in Figure 3.

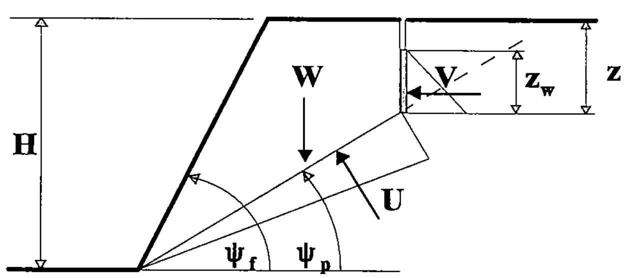

Figure 1. Generalized cross-section of a plane slide with no drainage impedance at the toe of the slope. (ξ = 0%)

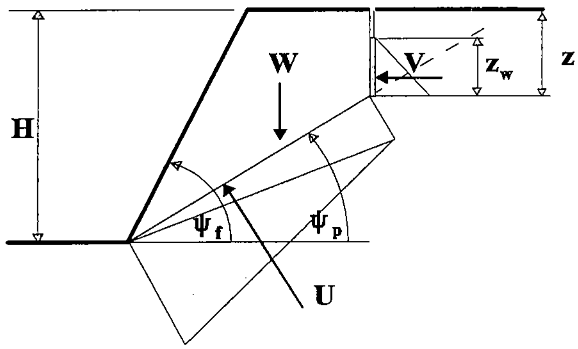

Figure 2. Generalized cross-section of a plane slide showing assumed water pressure distribution with complete drainage impedance at the toe of the slope. (ξ = 100%)

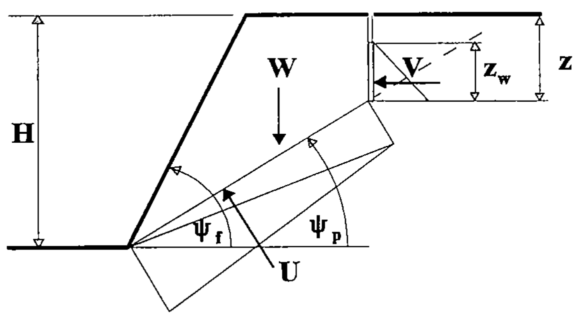

Figure 3. Generalized cross-section of a plane slide showing assumed water pressure distribution with partial drainage impedance at the toe of the slope. (ξ ≈ 50%)

WedgeSlip

The water force is calculated as the average pressure on each plane times the area of each plane. The formula used to calculate the average water pressure on each plane is taken from Hoek & Bray (1981). It is assumed that the distribution on each plane is tetrahedral. The formula for the average pressure on each plane is as follows:

$$u_1 = u_2 = \frac{1}{3} \times \left(\gamma_w \times \frac{H}{2}\right) = \frac{(\gamma_w \times H)}{6} \qquad (6)$$

RockSlip

The same basic principles used in *WedgeSlip* are utilized in the calculations. The major difference is that the volume calculation in *RockSlip* is much more complicated and requires Gaussian Numerical Integration to obtain. The parameter z, height of water level in tension crack, and drainage impedance are included in the "Outcrop" form and can be modified according to the water level and drainage conditions of the slope.

ROCKBOLTS

PlaneSlip

PlaneSlip considers rockbolt reinforcement based on the number, spacing, capacity and orientation of the bolts, all of which are input by the user. The orientation of the rockbolts is defined by the angle, θ, that the rockbolts make with the normal to the face. This angle is easily measured in the field and is also the type of information that needs to be conveyed to a driller who is installing the rockbolts. However, in calculations it is easier to use the angle, β, the bolts make with the normal to the failure plane (See Figure 4). Note that β can be calculated indirectly from the dips of the face and failure plane and the angle, θ. The following is the formulation of β that is used in the *PlaneSlip* computer code:

$$\beta = \psi_f - \psi_p - \theta \tag{7}$$

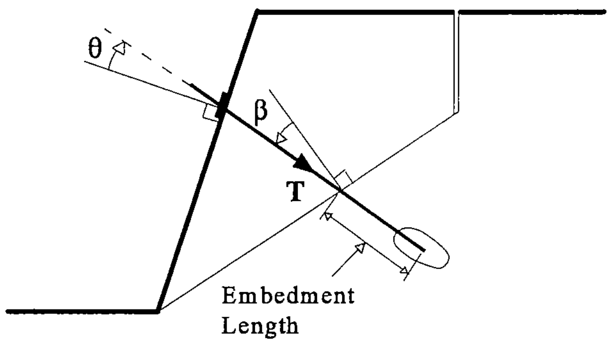

Figure 4. Plane slide schematic defining the orientation of a rock bolt or cable.

In *PlaneSlip*, rockbolts are shown penetrating the slope face first and then the failure plane (See Figure 5). The user specifies the minimum embedment length (Figs 4 and 5). If a bolt embedment length is less than the specified minimum, it is drawn as a dashed line and omitted from the stability calculations.

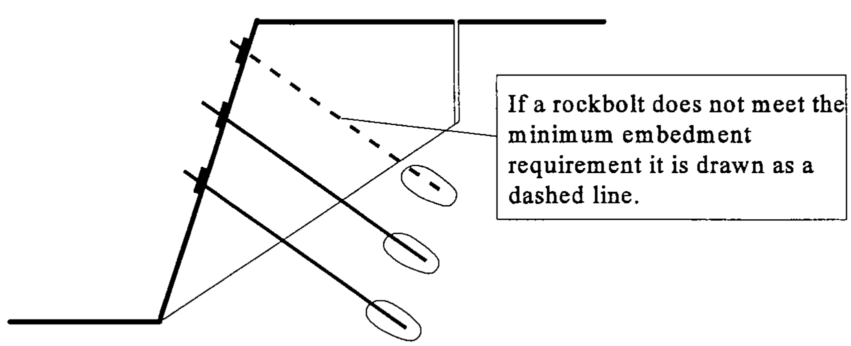

Figure 5. Plane slide schematic showing the number of rockbolts.

If rockbolts are to be installed in the top face of the slope, β will be related to θ by a different equation.

$$\beta = \psi_t - \psi_p - \theta \qquad \textbf{(8)}$$

All quantities are the same except for ψ_t, which is the dip of the top face instead of the front face. *PlaneSlip* only shows rockbolts which penetrate the slope face, but rockbolts in the top face can be modeled accurately as bolts in the slope face by ensuring that β is the correct value (Figure 6). This requires some caution when entering the value for θ. First calculate β based on the assumption that the rockbolts will be in the top face (i.e. use equation 8). Then insert this value into equation 7 to obtain the proper input value for θ.

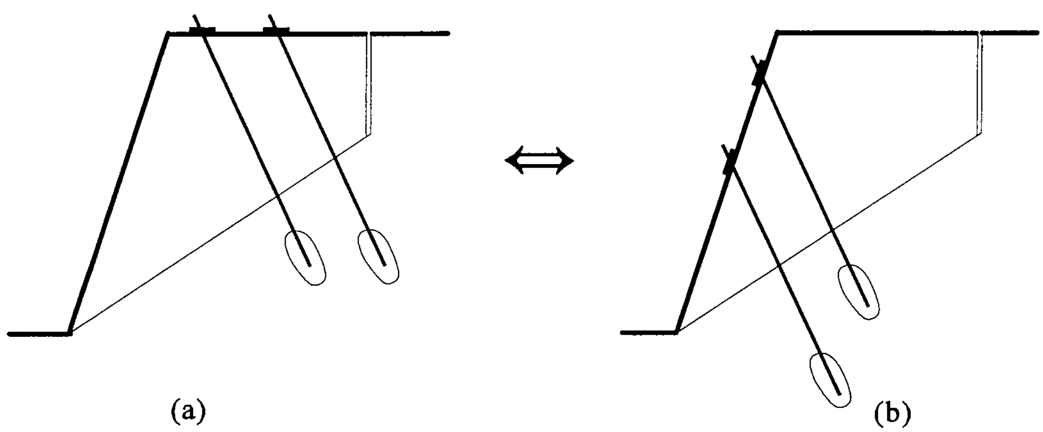

Figure 6. **a. Rockbolts in the top face equivalent to**
b. Rockbolts in the slope face.

WedgeSlip

There is debate over how rockbolts enhance the factor of safety of a rock slope. One viewpoint is that rockbolts add exclusively to the resisting force. Another possibility is that the components of the rockbolt force are split between the two, with the normal component adding to the resisting force and the shear component decreasing the driving force. Since it is impossible to determine the exact loading and movement sequence in a rock slope, the choice of which assumption to use becomes arbitrary (Hoek & Bray, 1981). *WedgeSlip* assumes that the normal component adds to the resisting force and the shear component decreases the driving force when calculating the factor of safety. In the case of wedge failure, the plunge of the line of intersection takes the place of the dip of the sliding plane when calculating the rockbolt angle.

EXAMPLES

The following section presents some example screen outputs from each of the programs. The examples from *PlaneSlip* and *WedgeSlip* are based on data from a limestone quarry in Alabama. The example in *RockSlip* is from Scott Arwood's Thesis site in Biltmore, Tennessee.

PlaneSlip

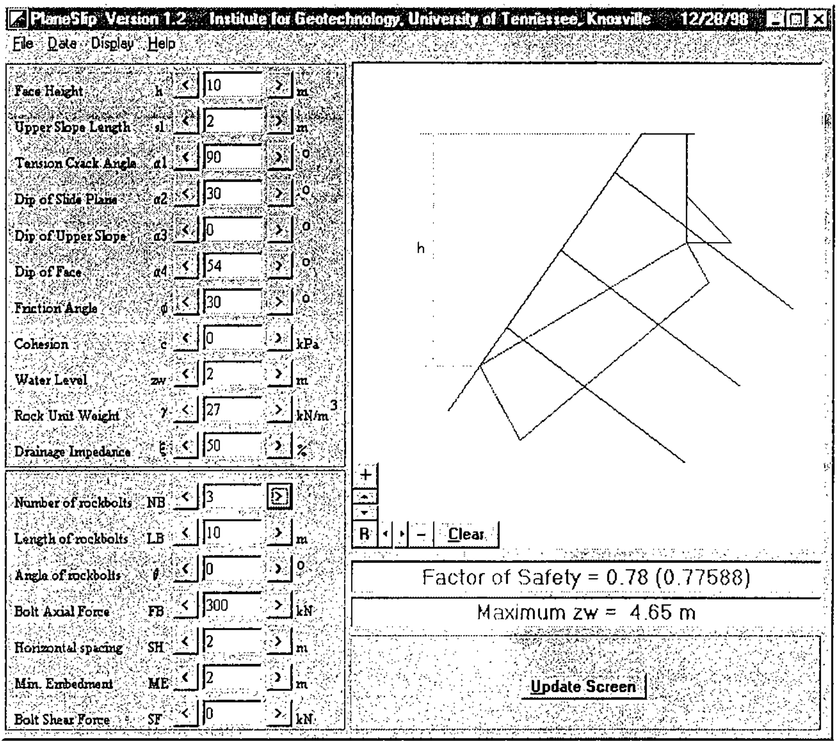

Figure 7

WedgeSlip

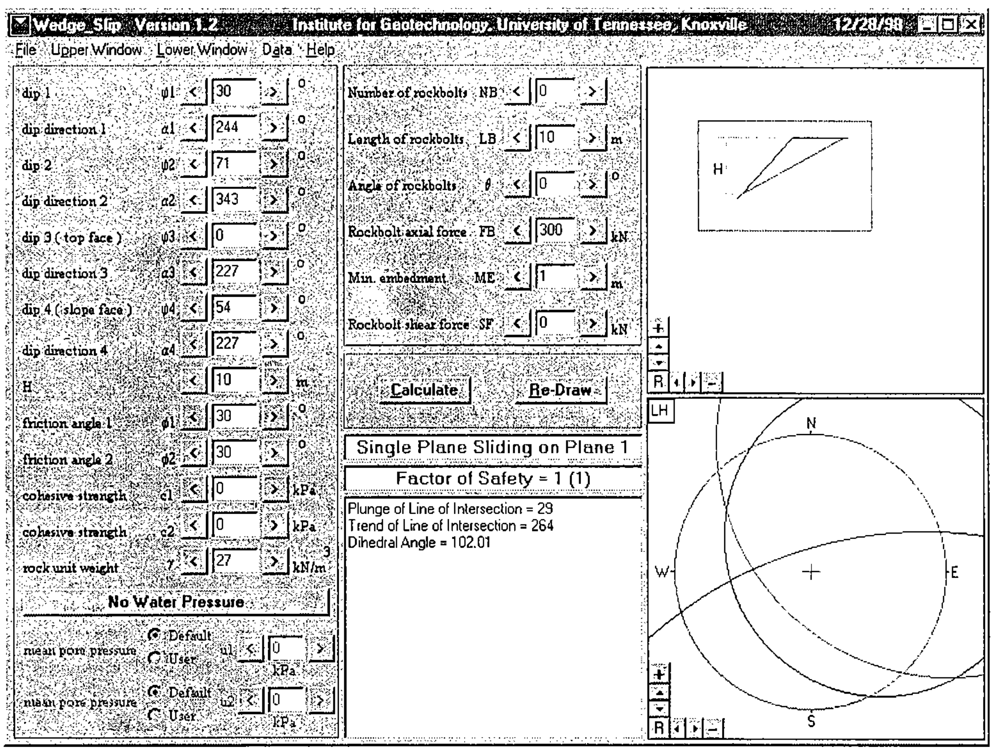

Figure 8

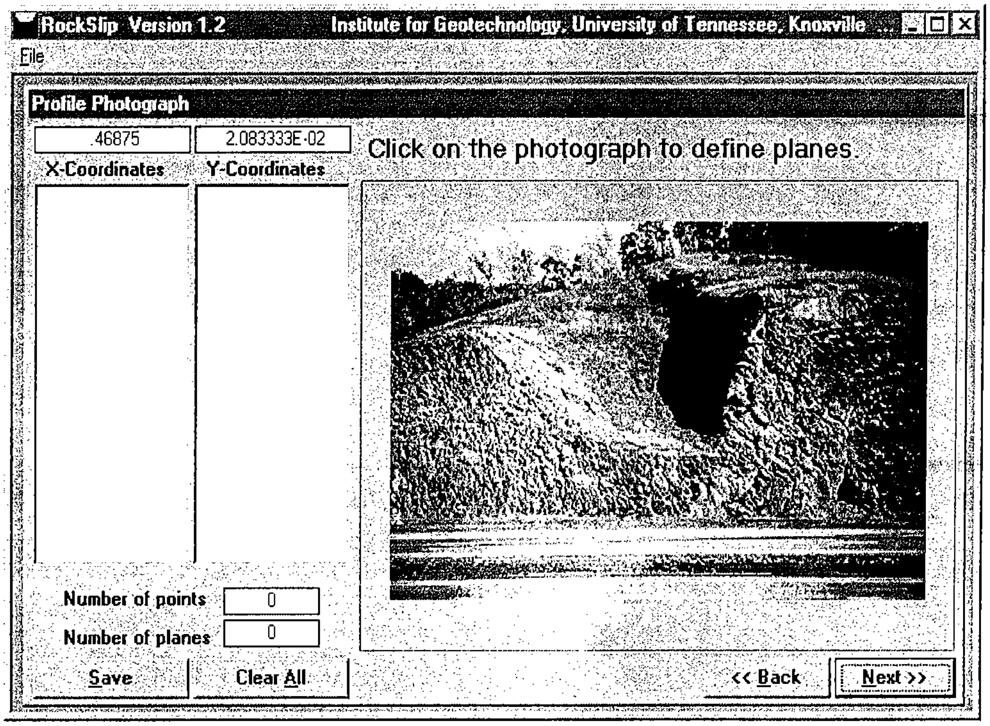

Figure 9

CONCLUSIONS

A family of three computer programs, entitled *ROCKSLIP*, has been developed to rapidly assess the stability of a wide variety of rock slope configurations. The user-friendly setup of each program allows the user to quickly analyze the particular slope geometry at hand.

Several features make these programs unique and powerful tools in the workplace. The auto-redraw function serves as a flexible and practical design tool, making it possible for professionals in the rock engineering field to perform complex studies, such as sensitivity analyses, and for students to better visualize the orientations of each physical component of the slope. An effort to better model the effects of water pressure has resulted in a parameter entitled "drainage impedance". This parameter allows the user to adjust the drainage conditions at the toe of the slope. The effects of cohesion, water pressure and friction angle are also accounted for. Rockbolt reinforcement can be added to the analysis. Number, length, orientation, tensile and shear strength and minimum embedment can all be adjusted depending on the type of rockbolt and the installation procedure used.

The contents of this paper summarizes the work done on this project and describes the three computer programs that have been designed. There is still need for further planning and development of methods for the analysis of rock slope failures throughout Tennessee (especially Eastern Tennessee) and other states. Further development of the *ROCKSLIP* family of programs is underway. For updates please visit the *ROCKSLIP* website at:

http://www.engr.utk.edu/research/geo/institute/research/rsupdate.htm

ACKNOWLEDGEMENTS

The programs described in this paper were developed under a research project funded by the Tennessee Department of Transportation. The writers thank Harry Moore and Saieb Haddad of the Division of Materials and Tests for their support and insight. The writers also wish to thank the previous students and scholars that have worked on this project: Jorge Ureta, Scott Arwood, You Li and Yen-Yit Chan.

REFERENCES

Chan, H.C., Einstein, H.H. (1981). "Approach to Complete Limit Equilibrium Analysis for Rock Wedges - The Method of Artificial Supports." *Rock Mechanics*. 14, 59-86.

Cole, J.H. (1998). "Computer Assisted Analysis of Rock Slope Stability." Master's Thesis (in progress), Dept. of Civil & Environmental Engineering, University of Tennessee, Knoxville.

Hoek, E., Bray, J.W. (1981). *Rock Slope Engineering*, Revised 3rd ed., Institution of Mining and Metallurgy, London, England.

Mauldon, M., Arwood, S., Pionke, C.D. (1998). "Energy Approach to Rock Slope Stability Analysis", *Journal of Engineering Mechanics, ASCE*, Vol. 124, No. 4, 395 - 404.

Mauldon, M., Ureta, J. (1996). "Stability Analysis of Rock Wedges with Multiple Sliding Surfaces." *Geotechnical and Geological Engineering*. 14, 51-66.

Moore, H.L. (1986). "Wedge Failures along Tennessee Highways in the Appalachian Region: Their Occurrence and Correction." *Bulletin of the Association of Engineering Geologists*, Vol. 23, No. 4, 441 - 460.

Turner, A.K., Schuster, R.L. (1996). *Landslides: Investigation and Mitigation*, Transportation Research Board Special Report 247, National Academy Press, Washington, D.C.

APPENDIX I. NOTATION

PlaneSlip Variables

FS = Factor of safety;
c = Cohesion;
A = Area of failure surface;
W = Weight of sliding mass;
ψ_p = Dip of failure plane;
U = Uplift water force on failure plane;
V = Water force on tension crack;
ϕ = Friction angle;
N = Number of rockbolts with embedment length greater than the minimum;
T = Tensile force in rockbolts;
β = The angle the bolts make with the normal to failure plane;
S = Shear strength of rockbolts;
SH = Horizontal spacing of rockbolts;

WedgeSlip Variables

N'_i = Effective normal force on plane i; $N_i' = N_i - u_iA_i$;
ϕ_i = Friction angle of plane i;
c_i = Cohesive strength of plane i;
A_i = Area of plane i;
W = Weight of the wedge;
ψ_i = Plunge of the line of intersection of planes 1 and 2;
u_i = Average water pressure on plane i;
N = Number of rockbolts;
T = Tensile force in rockbolts;
β = Angle rockbolts make with normal to the failure plane;
S = Shear strength of rockbolts;

Discontinuity Orientation Measurements for Rock Slope Design in Western North Carolina

Hyuckjin Park and Terry R. West

Department of Earth and Atmospheric Sciences

Purdue University

West Lafayette, IN 47906-1397

Abstract

Data depicting the orientation of discontinuities are of paramount importance for rock slope stability studies. Most data are collected using linear sampling techniques, such as borehole fracture mapping and the detailed scanline method (outcrop mapping). However, data, acquired by such linear sampling techniques, are subject to bias, owing to the orientation of the sampling line. In order to reduce this bias, a weighting factor has been proposed by several researchers. Yet, in some cases such as steeply dipping joints or possibly gently dipping ones, the bias will not be significantly reduced when certain sampling orientations are involved. Simply stated, if the linear sampling orientation nearly parallels the discontinuity orientation, important fractures will be excluded. This phenomenon can cause serious misinterpretation of discontinuity orientation data because critical information is omitted.

In the current study, orientation data collected using the borehole fracture mapping method (vertical) were compared to those based on orientation data from the detailed scanline method (horizontal). Differences in results for the two procedures revealed a concern that a representative orientation of discontinuities was not accomplished. Equal-area, polar stereo nets were used to determine the distribution of dip angles and to compare the data distribution for the borehole method versus that for the scanline method.

Based on a field survey of a completed road cut, steeply dipping joints are quite common in the study area. However, most of these steeply dipping joints were omitted from the polar diagram using the borehole sampling technique, and differed significantly from the polar diagrams obtained from the author's field survey and scanline approach. This omission and bias yields a blind zone of absent data, due to the relative orientation of the borehole and the discontinuities (subparallel). This may yield significant loss of fracture data, overlooking important fracture orientations. Therefore, discontinuity orientation data must be evaluated relative to data from field exposures before analyzing that data set for slope stability purposes. Sampling methods must be devised which will minimize this sampling bias.

Introduction

Both the outcrop mapping method and the borehole sampling method are common procedures used to collect discontinuity characteristics, such as orientation, size, frequency and joint surface geometry. In particular, borehole methods can provide valuable information when the area of outcrop is limited and when a construction project requires the characteristics of discontinuities in the deep subsurface. In addition, there are a number of rock mechanics tests that can be conducted on drill cores and in boreholes. Therefore, many engineering projects include borehole drilling in the investigation stage and a great number of data and design parameters are provided and estimated based on results of borehole sampling even though the method involves major difficulties. One significant problem is that the core can rotate during drilling. Therefore, special sampling and analysis techniques are required to provide the true orientation of discontinuities. A second difficulty is that the core may be too small to measure discontinuity size. Core diameters are usually less than 100 mm, so it is difficult to acquire information on discontinuity length from widely distributed rock cores.

Compared to the borehole method, outcrop mapping has the advantage of involving a relatively large volume of rock, which enables the direct measurement of discontinuity characteristics. Additionally, geological and spatial relations between discontinuities are easily observed using this method. However, if rock faces are damaged by blasting or degraded by weathering, this method cannot produce good quality data. In addition, where outcrops are a significant distance from an access point or zone of interest, quality data are not easily obtained for objective and statistical analysis. Outcrop mapping methods most commonly used are the scanline and window sampling techniques.

Sampling Bias in Orientation Data from a Linear Survey

Orientations of discontinuities in a rock mass can be measured by the borehole method or from an exposed rock face. There have been many endeavors to obtain objective and representative orientations, based on measured data from those sampling methods. As one of the efforts, statistical analysis has been applied. This requires measuring a large number of discontinuities to provide orientation data for a rock mass. In outcrop mapping, especially the scanline method, all discontinuities that intersect a sampling line on the rock face are measured for statistical analysis. The sampling line or "scanline" is usually positioned on the rock face either vertically or horizontally. Next, the measured orientation data are evaluated statistically using a graphical presentation, hemispherical projection. For borehole sampling, all the discontinuities that intersect the borehole are included.

However, it should be noted that both the borehole and the scanline methods are linear sampling procedures and although the linear survey involves an objective sampling approach, a single, linear sampling regime will bias the orientation data. That is, the sampling line tends to intersect preferentially those discontinuities whose normals make a small angle to the sampling line (Priest, 1985). Terzaghi (1965) discussed this type of bias, proposing a geometrical correction factor based on the observed angle between the sampling line and the normal to a particular discontinuity. This bias was also discussed also by Baecher (1983), Kulatilake and Wu (1984), and Priest (1985).

Sampling Bias of Orientation Data Observed in This Study

The North Carolina Department of Transportation (NCDOT) provided most of the orientation data utilized in this research. Measurements of discontinuity orientations were accomplished by NCDOT personnel; the data were obtained from outcrop field mapping and borehole sampling. In the borehole mapping method, rock core was placed in a goniometer and reoriented, so the dip and dip direction of discontinuities could be recorded (Beard, 1997). The other set of discontinuity data was measured directly from outcrop.

As those data sets were acquired by two different linear sampling methods, the data might be biased by the orientations of the respective sampling lines. That is, the orientation of the sampling line in the borehole method is usually vertical and the scanline on the rock face is generally a horizontal directional line, so the data from borehole and outcrop could be affected by each direction of the sampling lines; vertical and horizontal respectively. Therefore, prior to identifying sets and determining representative orientation data to be utilized in a rock mass stability analysis, the sampling bias caused by different directions of sampling lines should be scrutinized and corrected for, if possible.

In order to compare the differences of orientation distribution, which were caused by different sampling lines, the measured orientations were plotted on two different equal–angle stereonets. Figure 1 (a) and (b) are lower hemisphere projections of discontinuity normals measured from borehole sampling and scanline sampling in Area 2 of Interstate-26 respectively. In Figure 1 (a), based on borehole sampling, note that there are a large number of poles of discontinuity normals near the center of the projection and very few poles are located near the circumference. In contrast many poles in Figure 1 (b) are located near the circumference but the poles are distributed uniformly as compared to Figure 1 (a). This phenomenon is caused by the sampling bias explained previously, so the borehole method gives preference to discontinuities showing a horizontal orientation, whereas vertical discontinuities are given preference in the scanline method.

To compare the two sets of stereonets before correcting any bias, without further processing, the orientation data were analyzed by clustering. This is appropriate, as any significant preferred orientations should be apparent as clusters of normals in a stereonet. The orientation limits for each set were identified by applying the clustering algorithm proposed by Shanley and Mahtab (1976), Mahtab and Yegulalp (1982), and Priest (1993). Figure 2 (a) and (b) are stereo projections of clustered discontinuity normals collected from borehole and scanline survey in Interstate-26 Area 2. As observed in Figure 2 (a) and (b), clustered sets in hemisphere projections are obviously different for the two stereonets. In Figure 2 (a), two discontinuity sets are shown with both having lower dip angles compared with the joint sets in Figure 2 (b). Joint set 1 (J_1) has a mean dip direction and dip value of 160/22 and joint set 2 (J_2) has 54/36. However, most joint sets in Figure 2 (b) have steep dip angles; J_1 (192/89), J_3 (50/86), and J_4 (118/83). Only J_2 has a low dip angle and this seems to be the same set as J_1 in Figure 2 (a). These significant differences are apparently due to missing discontinuity poles which would be located near the circumference in Figure 2 (a). In other words, the discontinuities whose dip angles are relatively steeper are selectively omitted when the orientations are measured by borehole sampling.

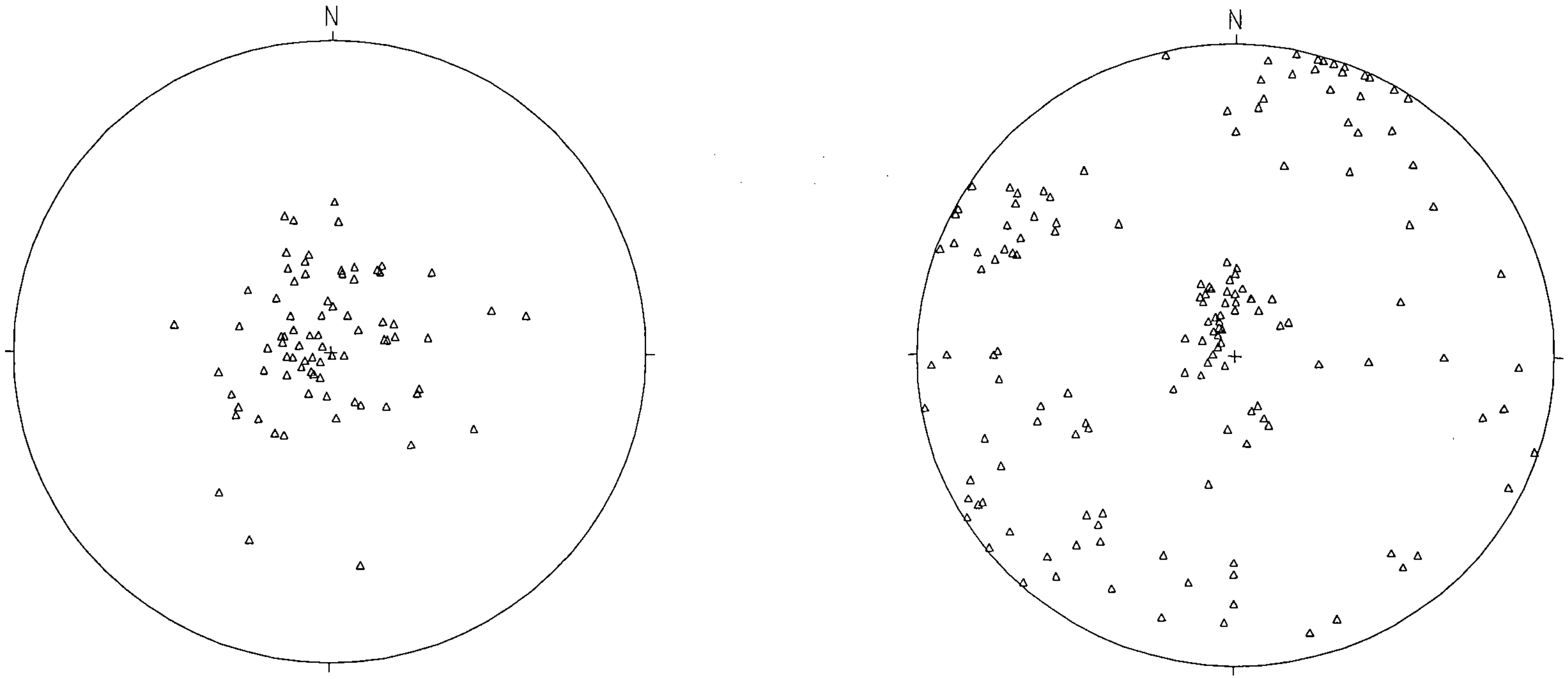

(a) (b)

Figure 1 Lower hemisphere projection of discontinuity normals measured by (a) borehole method and (b) scanline method in I-26 Area 2

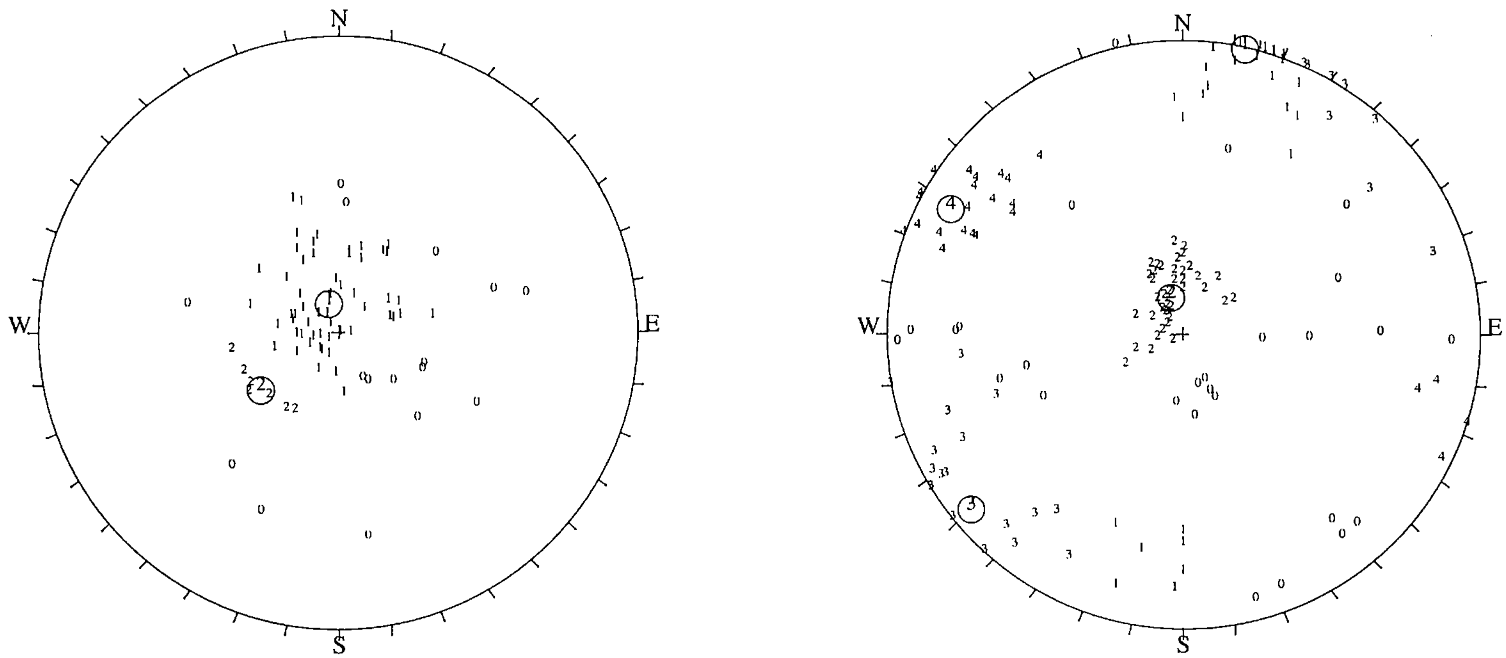

(a) (b)

Figure 2 Lower hemisphere projection of **clustered** discontinuity normals measured by (a) borehole method and (b) scanline method in I-26 Area 2

Contoured Equal-Area Polar diagram

The relationship between measurement methods and distributions of poles can be illustrated by polar diagrams (Terzaghi, 1965). Therefore, poles of the collected discontinuity normals are plotted on an equal-area polar diagram to analyze this relationship. Poles are uniformly distributed in an equal-area polar diagram if the joint surveys are performed on outcrops and the outcrops are numerous with a random orientation. In contrast, if the observations are made by the scanline method on a horizontal surface or the borehole method is used, joints with specific directions are not observed and unrecorded in the polar diagrams.

When α is considered as the acute angle between the discontinuity and the sampling line, the number of intersections between the sampling line and joints in a given spacing is proportional to the sine of angle α of intersection. In a polar diagram, the successive contours, starting from the direction of sampling line, can be drawn as the loci of poles of joints which intersect the sampling line at angle α such as sin α is 0.1, 0.3, 0.5, 0.7, and 0.9 respectively. Such lines are called isogonic (equal-angle) lines (Terzaghi, 1965). In some cases the relative densities of poles in the zones bounded by the isogonic lines lie within the ranges 0 to 1, 1 to 3, 3 to 5, 5 to 7, 7 to 9, and 9 to 10. Figure 3 (a) and (b) are idealized, contoured-diagrams of random joints observed on a horizontal outcrop and in a vertical drill hole, respectively. Therefore, for example, if discontinuities observed by the scanline method are plotted on Figure 3 (a), many more poles will be on the isogonic line for $\sin \alpha = 1.0$ (the circumference of the circle) than on the line for $\sin \alpha = 0.1$, which indicates the horizontal direction of discontinuity. This is because the steeply dipping discontinuities are collected selectively in the scanline method. Similarly, a large number of poles measured from the borehole are located on the isogonic line for $\sin \alpha = 1.0$ and few poles are located on the $\sin \alpha = 0.1$; in Figure 3 (b), a large number of poles are plotted near the center of circle, which is due to sampling bias.

Analysis of Measured Orientation Data

Figure 4 (a) and (b) are contoured polar diagrams of discontinuities sampled by the borehole method and the scanline method in Interstate 26 Area 2. As observed in Figure 4 (a), few poles of discontinuities are located on the circumference of the circle which means that steeper joints are omitted while others are recorded preferentially. There are no poles between the isogonic line for $\sin \alpha = 0$ and $\sin \alpha = 0.3$ in Figure 4 (a), that is, there are no poles whose dips range from 73° to 90° or all the poles whose dip angles range from 73° to 90° are omitted. However, in Figure 4 (b) the proportion of those poles whose dips lie between 73° and 90° is almost 52% of all discontinuities recorded from outcrops. Consequently, a large number of the steeply dipping discontinuities exist in the field but were not observed along the vertical sampling line. This fact was confirmed by the author's field survey and experience in this research area. A major difference exists which indicates that the two different orientations of sampling lines yield significantly different results. Therefore, after collecting joint orientation data, the feasibility of orientation data should be evaluated and sampling bias should be corrected for. In many cases, analysis of data and clustering are required to aid judgment and experience of the researchers in the project area.

Figures 5 (a) and (b) are stereo projections of clustered discontinuity normals for Interstate 26 Area 5. Figure 5 (a) is based on data obtained from the borehole sampling method and Figure 5 (b) is based on outcrop mapping. These two stereonets show different distribution results than shown in Figure 2 (a) and (b). To examine the distribution of dip angles, data were

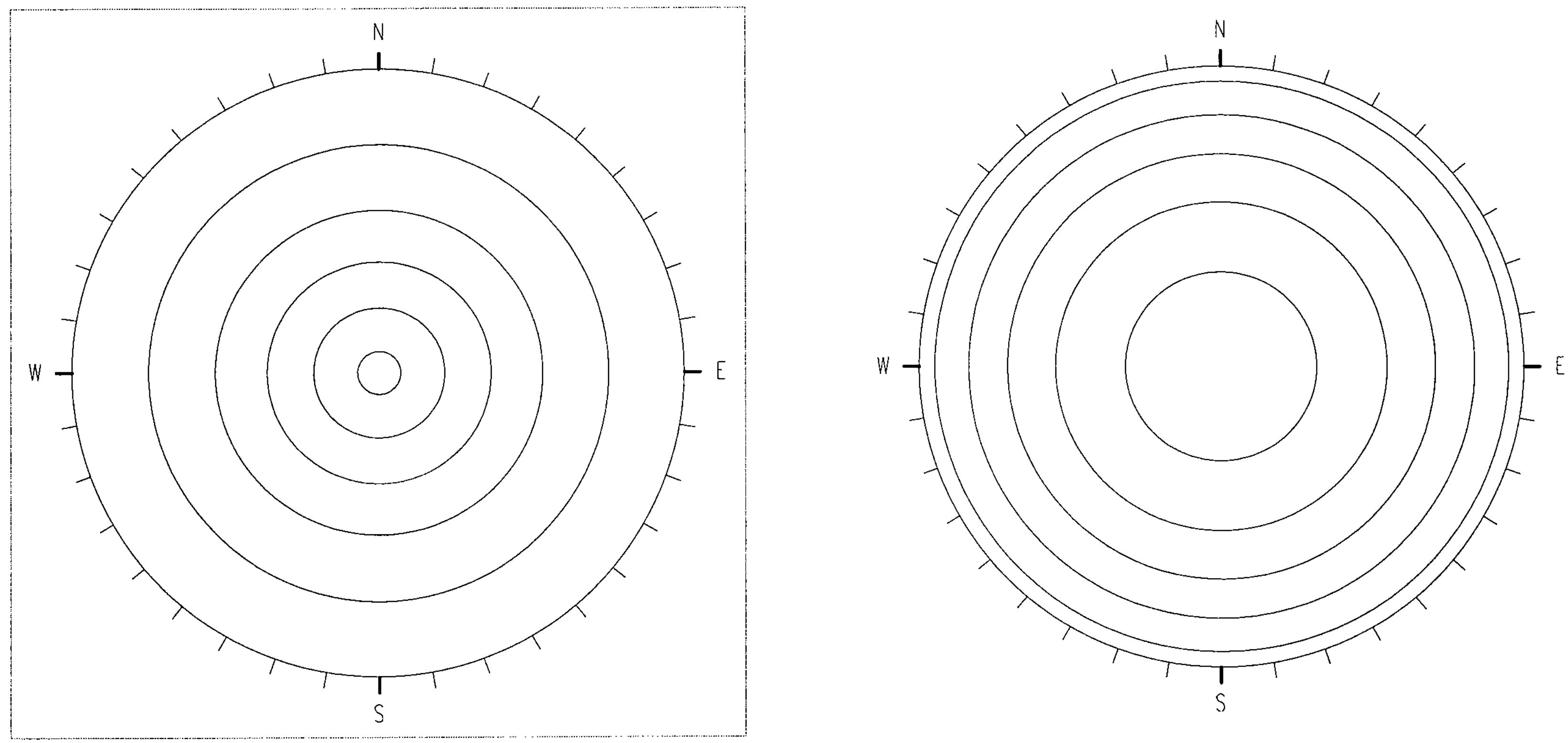

(a) (b)

Figure 3 Idealized contoured polar diagram of observation (a) on horizontal outcrop and (b) in a vertical drill hole (after Terzaghi, 1965)

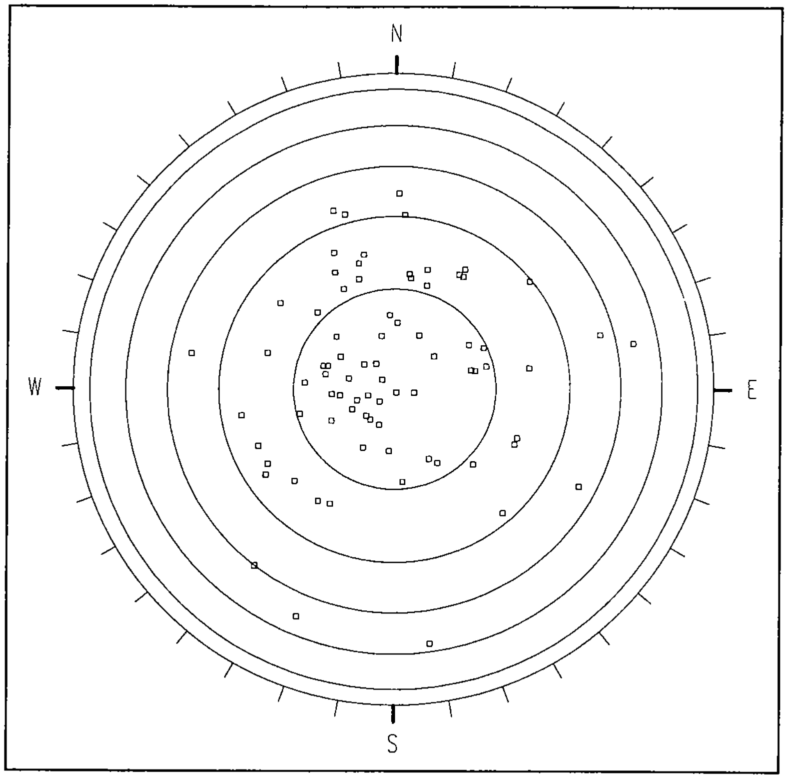

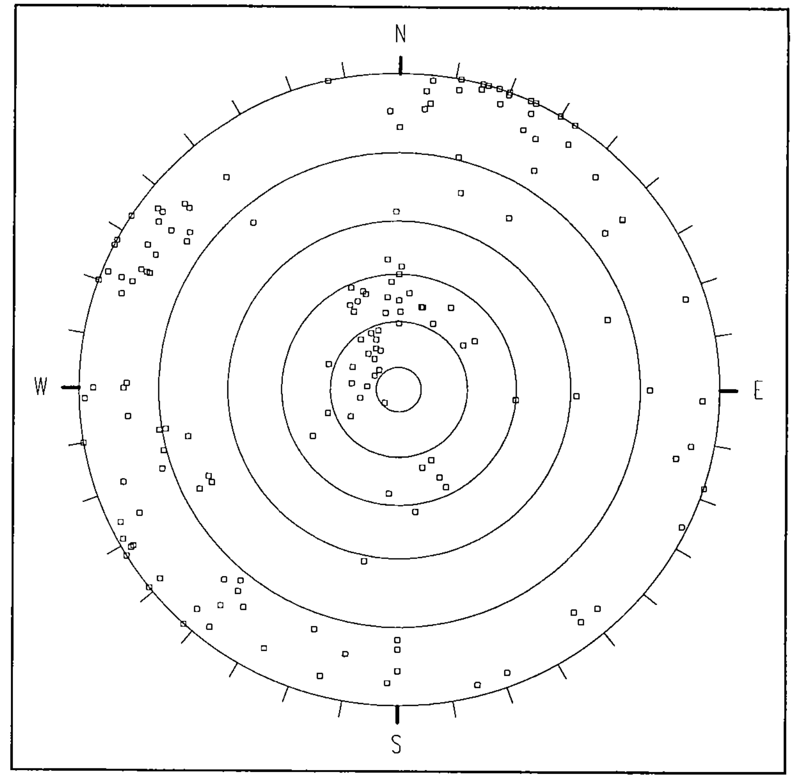

Figure 4 Contoured polar diagrams of discontinuity observed by (a) borehole method and (b) scanline method in I-26 Area 2

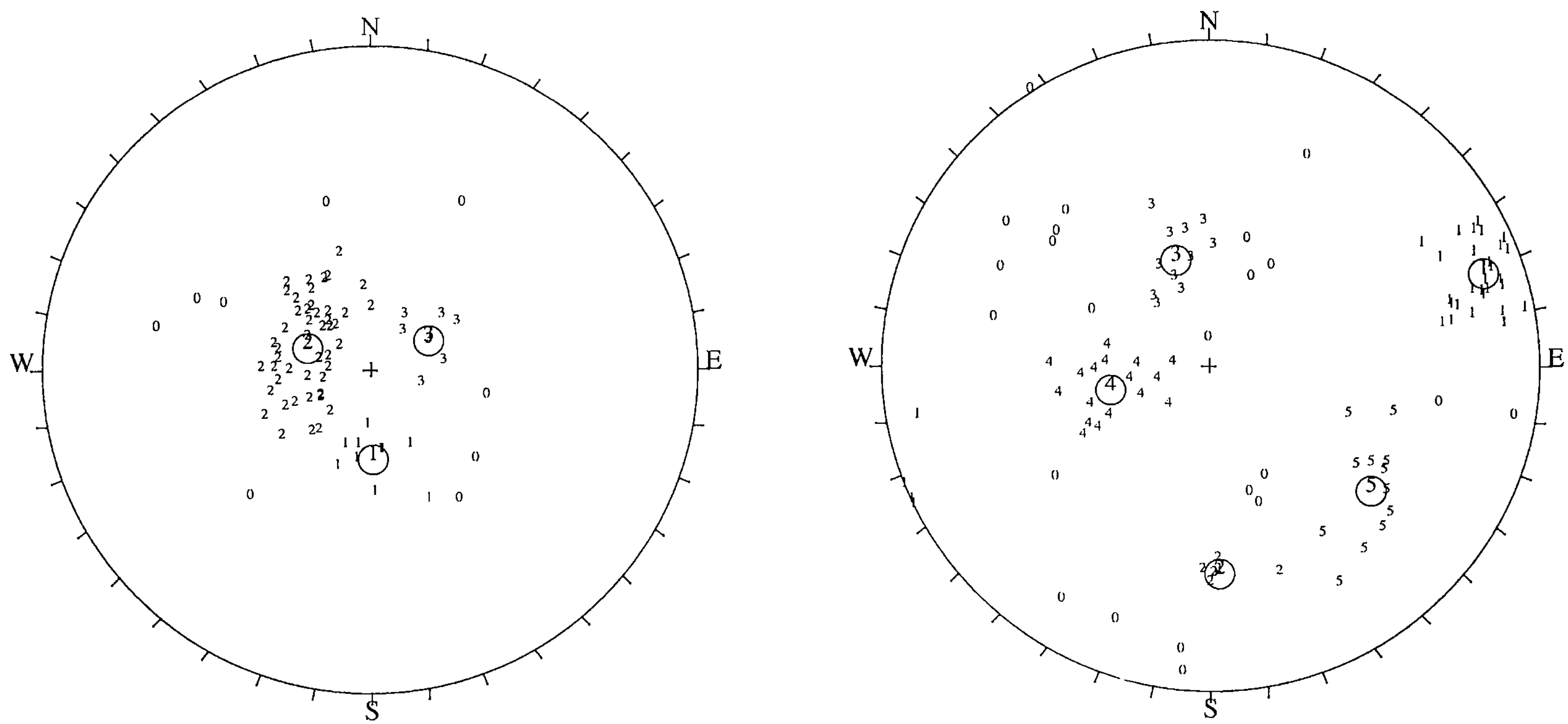

Figure 5 Lower hemisphere projection of clustered discontinuity normals measured by (a) borehole method and (b) scanline method in I-26 Area 5

plotted on contoured polar diagrams (Figure 6 (a) and (b)). In these diagrams, orientation data which lie nearly parallel to the sampling line will not likely be observed, as indicated by previous results. There are no poles with dip angles ranging from 70° to 90° in Figure 6 (a), however, the proportion of those poles is about 55% of all data in Figure 6 (b). Again the steeply dipping joints were not observed in borehole sampling. However, for the case of gently dipping discontinuities, the proportions of poles with dip angles less than 20° are 10% versus 4% in Figure 6 (a) and (b) respectively. This result is not as different as for the steeper poles, that is, based on the results of borehole sampling. The actual proportion of gently dipping joints is small so that the sampling result for the scanline method is more similar to borehole results in this region. Therefore, the outcrop mapping method does not contribute as serious a bias as does the borehole method. Consequently, data from outcrop mapping in this case are less biased than those obtained by borehole mapping.

Correction of Sampling Bias

The orientation sets can be delimited using clustering by applying a clustering algorithm mentioned in the previous section. However, results of the clustering process can be affected by sampling bias because bias removal reduces the sample size of discontinuities which have lower α values.

The weighting factor, *w*, is proposed by several researchers (Terzaghi, 1965; Goodman, 1976; Priest, 1985) to reduce the sampling bias. The concept of this factor is that the reduced sample size at the lower values of α can be compensated for, by assigning a higher weighting factor to those discontinuities sampled (Priest, 1993). The weighting factor is given by

$$w = \frac{1}{\sin \alpha} \qquad \alpha \langle 90^{\circ}$$

, where α is the acute angle between the discontinuity and sampling line and $\sin \alpha$ is given by the above equation. Priest (1993) suggested that this weighting would tend to balance the orientation sampling bias introduced by linear sampling for a large sample size.

The authors applied this weighting factor to orientation data to reduce sampling bias observed in orientation data from boreholes in Area 2 and Area 5. Therefore, all orientation data collected from boreholes were multiplied by this factor, then the corrected data were plotted on the stereonets and clustered by the same algorithm mentioned previously (Figure 7 and 8). However, the results of clustering the weighted data do not show any difference from those obtained by unweighted data. Consequently, the sampling bias in the borehole data was not significantly reduced by this weighting factor. In particular, bias of steeply dipping discontinuities and the measured orientation data seem to be too sparse to correct the bias in a joint survey. Therefore, another concept was considered to evaluate this concern.

The Concept of A Blind Zone

Terzaghi (1965) realized that the orientation data with small α angles to the sampling line are not observed and introduced the blind zone concept to explain these effects. She suggested that observations of joint orientation should be made at a moderately high angle, not less than about 30°, to prevent this effect. Goodman (1976) and McEwen (1980) subsequently estimated the size of the blind zone at 20°. Accordingly, any discontinuity within 20° to 30° from a

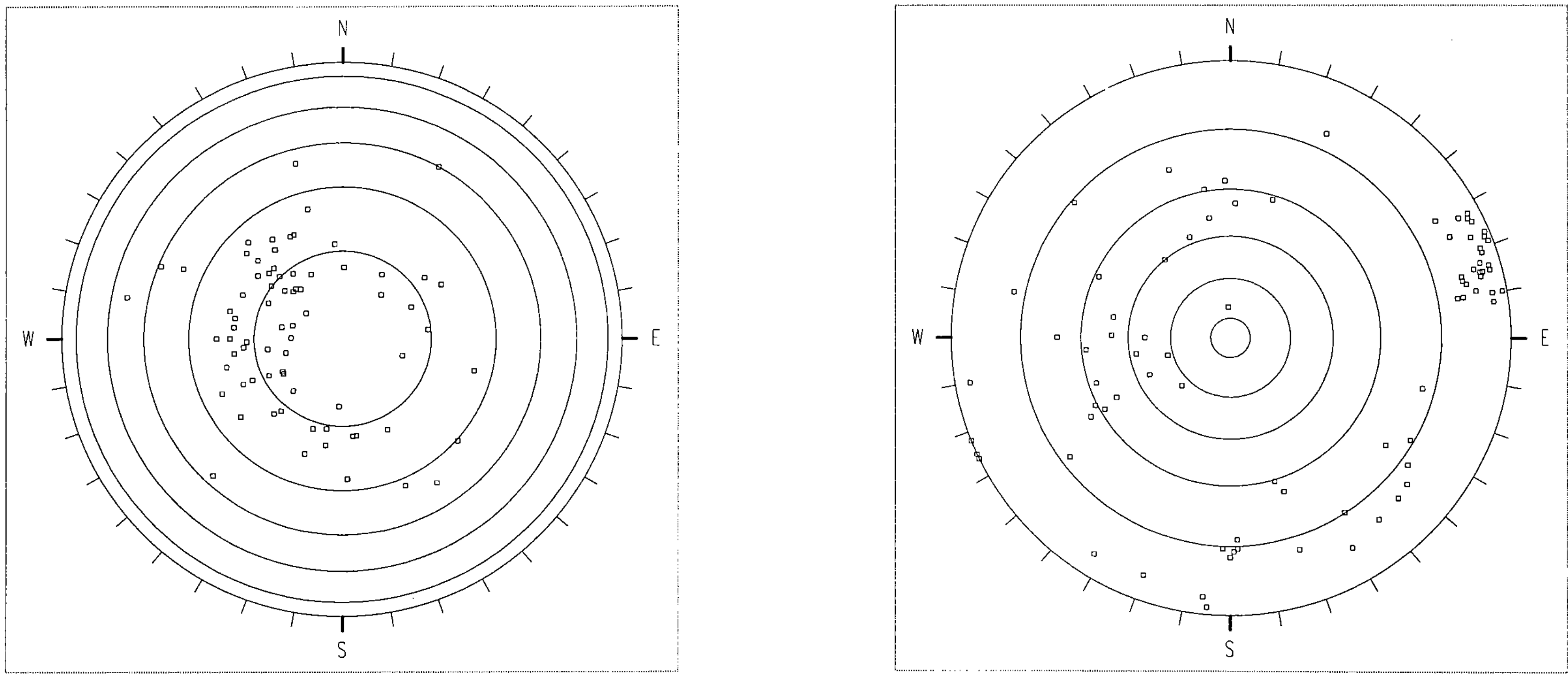

(a) (b)

Figure 6 Contoured polar diagrams of discontinuity observed by (a) borehole method and (b) scanline method in I-26 Area 5

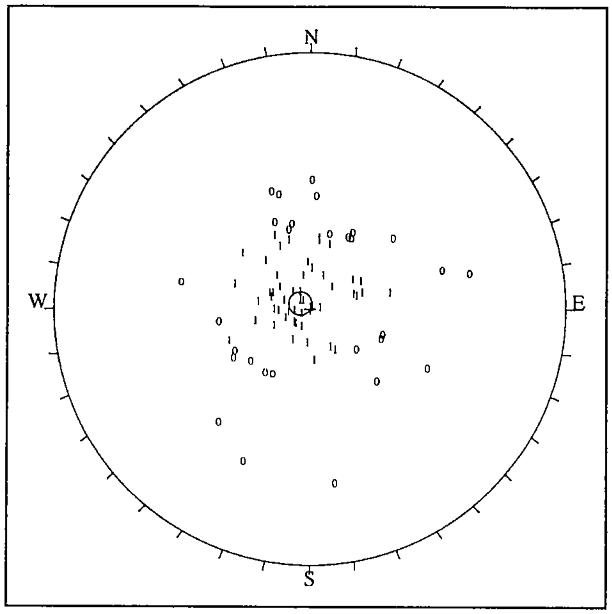

Figure 7 Lower hemisphere projection of discontinuity normals, weighted and clustered in Area 2

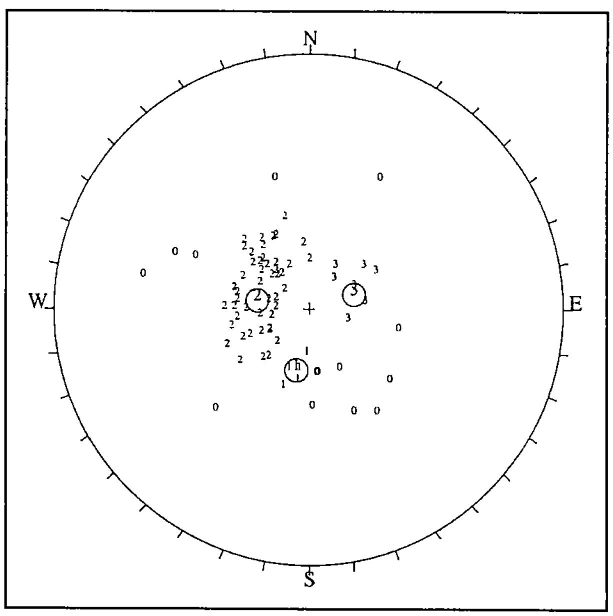

Figure 8 Lower hemisphere projection of discontinuity normals, weighted and clustered in Area 5

borehole would be in the blind zone of that borehole. . Therefore, the blind zone of borehole data on hemisphere projection can be applied to the stereonet by drawing a great circle 90° from the axial point of borehole. The zone is widened about ± 30° from the great circle on the stereonet. In contrast, the blind zone in outcrop horizontal mapping on the stereonet can be considered by applying a small circle of 30° from the center of stereonet. It should be noted that the blind zone does not depend on the data; it is instead a characteristic of the data source (i.e. a mapping surface or borehole) that affects the data (Yow, 1987). Yow (1987) proposed that the size of the blind zone depends on both α angle and random errors in orientation measurement, so the size of the blind zone increases as random measurement error increases. Although this concept of bias has been recognized in discontinuity mapping for several years, the specific sizes of the blind zones remains somewhat unclear.

Blind Zone for Measured Orientation Data

When plots of discontinuities on hemisphere projections are examined in this research, the size of the blind zone in borehole data seems to be about 30°. However, there are no poles within 20° of borehole direction in Figure 4 (a) and Figure 6 (a). Nonetheless, it can be widened to 30° because in Figure 4 (a), only 3 orientation data points (about 4 % of the total data) are within 30° from the borehole and in Figure 6 (a) only 1 data point (only 1 % of the total data) are in the same zone. By contrast, when the outcrop mapping data are considered, it does not appear that the measured orientation data from outcrop mapping contain a blind zone. This is because 46 orientation data points and 11 data points, about 30 % and 11 % respectively of their total data, occur within 30° to sampling line in Figures 4 (b) and 6 (b) respectively. Even if a 20° blind zone is considered, 23 and 4 data points occur in blind zones, respectively.

On the whole, a large number of discontinuities with dip angles ranging from 60° to 90° (that is, α angles ranging from 0° to 30° in borehole data) in the field area were not observed and consequently not recorded due to the blind zone. As discussed previously, this effect limited the application of the weighting factor and correction of sampling bias.

According to the author's field mapping and experience in the exposed rock cut, the dominant discontinuity sets typically have a steep dip angle of about 84°.. Therefore, based on this experience and previous analysis of orientation data, outcrop mapping is the more reliable source of orientation data for this research because of two reasons: 1) Results of the author's field experience and mapping are similar to the results of outcrop mapping by NCDOT. 2) As indicated in the previous section, for this location, orientation data from outcrop mapping are less biased than data from borehole sampling. For this reason, more emphasis was placed on orientation data for discontinuity sets obtained from outcrop mapping.

Validation of Discontinuity Orientation Data

To validate the orientation data provided by NCDOT, the authors surveyed and measured joint and foliation orientation data along a 100-ft road cut in the Interstate 26 area. About 100 orientation data values were collected using the detailed scanline method. As observed in Figure 9, the result of clustering, based on these measurements, is similar to that for NCDOT data except for joint set 3, Figure 10 which results from clustering based on NCDOT data. That is, the discontinuity normals that were clustered in joint set 3, Figure 10 did not show up and were not clustered into a set in Figure 9. A similar omission was observed in the plot of foliation

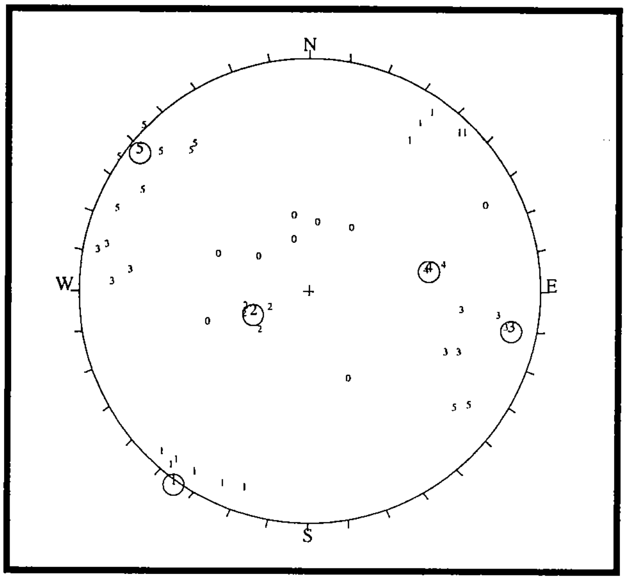

Figure 9 Lower hemisphere projection of clustered discontinuity normal for joints in I-26 Area 2 measured by authors

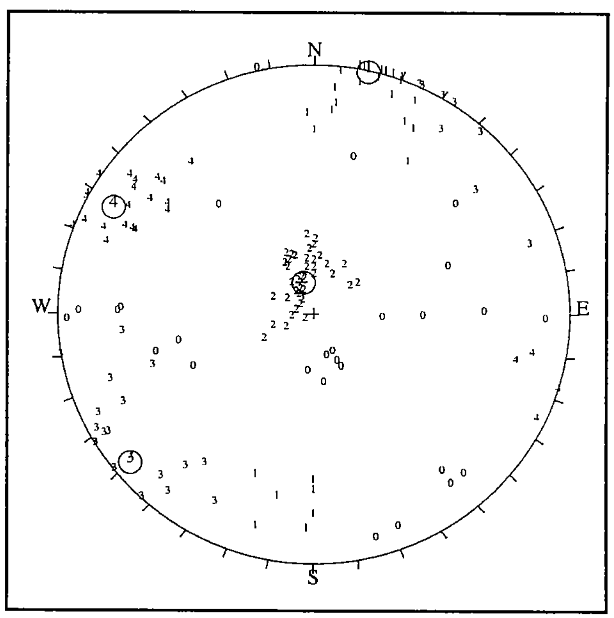

Figure 10 Results of clustering process of joint normals in I-26 Area 2

orientation data measured by the authors. Figure 11 shows the clustering results of foliation orientation data obtained by the authors in Area 2. Comparing Figure 11 to Figure 12, which is the clustering results of NCDOT foliation data in the same area, discontinuity normals did not plot around the dotted line in Figure 11. The attitude of joint set 3 in Figure 10, which does not appear in Figure 9, seems to occur along the direction of the dotted line in Figure 11. Therefore, omission of discontinuity normals in Figure 9 and 11 could be due to the same cause, that is, the blind zone. As author's measurements are based on the scanline method for the road cut showing a straight extension in one direction, all data are measured along the same scanline direction. This may give rise to the blind zone effect. A fact that tends to support this idea is that the scanline orientation corresponds to the direction of the dotted line. Terzaghi (1965) mentioned this possibility; "If there is a marked lack of balance in the distribution among outcrops, blind spot joints may be underestimated."

References

Baecher, G. B., 1983, Statistical analysis of rock mass fracturing. Journal of Mathematical Geology, 15, No. 2, 329-347

Beard, J., 1997, Parameters used for slope design of I-26 in North Carolina, Proceedings of 48th Highway Geology Symposium, Knoxville, Tennessee.

Goodman, R. E., 1976, Methods of Geological Engineering in Discontinuities Rocks. West, St.Paul, Minn.

Kulatilake, P. H. S. W. and Wu, T. H., 1984, Sampling bias on orientation of discontinuities. Rock Mechanics and Rock Engineering, 17, 243-253

Mahtab, M. A. and Yegulalp, T. M., 1982, A rejection criterion for definition of clusters in orientation data. Proceedings of the 22nd Symposium on Rock Mechanics, R. E. Goodman and F. E. Heuze eds., American Institute of Mining Metallurgy and Petroleum, New York, 116-123

McEwen, T. J., 1980, Fracture Analysis of Crystalline Rocks: Field Measurements and Field Geometrical Techniques. Institute of Geological Sciences, Harwell.

Priest, S. D., 1985, Hemispherical Projection Methods in Rock Mechanics, George Allen and Unwin, London.

Priest, S. D., 1993, Discontinuity Analysis for Rock Engineering, Chapman and Hall, London

Shanley, R. J. and Mahtab, M. A., 1976, Delineation and analysis of clusters in orientation data. Journal of Mathematical Geology, 8, No. 3, 9-23

Terzaghi, R. D., 1965, Source of error in joint surveys. Geotechnique, 15, 287-304

Yow, J. L., 1987, Blind zones in the acquisition of discontinuity orientation data. International Journal of rock Mechanics and Mining Sciences and Geomechanics Abstracts, 23, No.1, 19-28.

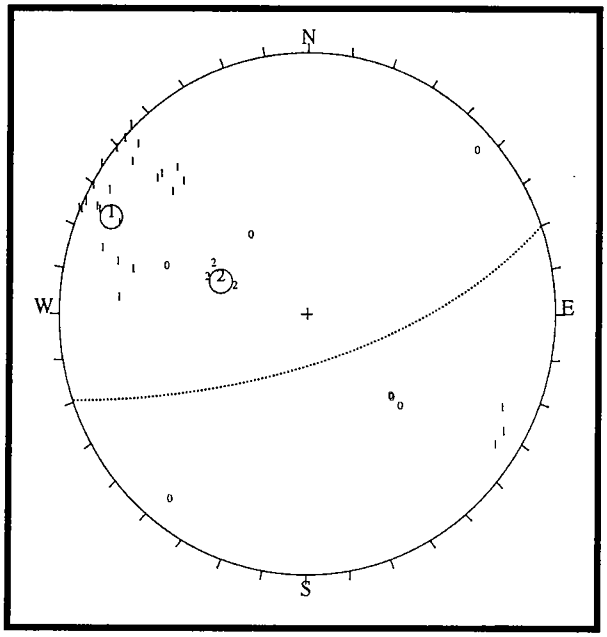

Figure 11 Lower hemisphere projection of clustered discontinuity normals for foliations in I-26 Area 2 measured by authors

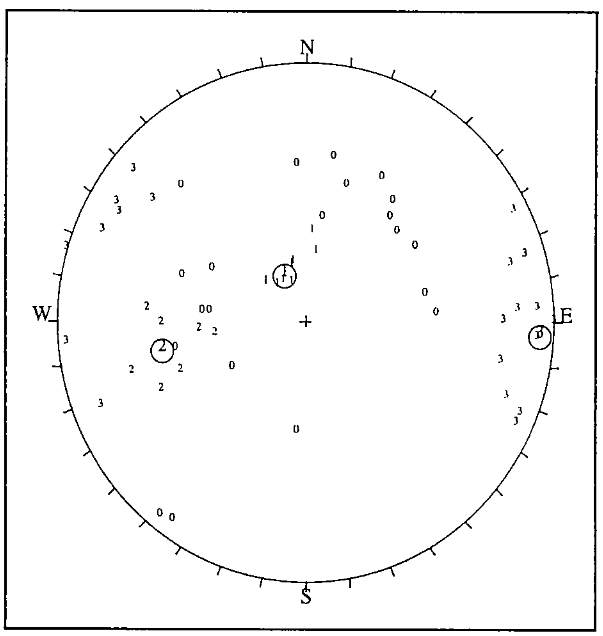

Figure 12 Results of clustering process of foliation normals in I-26 Area 2

ROCK FALL CONTROL TEST REPORT #1
RIFLE, COLORADO

Rick Andrew, Yenter Company
David Fry, Los Alamos National Laboratory
Robert E. Bookwalter, P.E., Chama Valley Producations, LLC, and Louis Berger and Associates

ABSTRACT

Between February 18 and March 18 of 1998, **Chama Valley Productions, LLC** of Chama, NM completed a rock fall control test with the assistance of the **Colorado Department of Transportation** and **Los Alamos National Laboraatory** at a test site located outside of Rifle, Colorado. The purpose of this test was to validate the design concepts of four different rock fall control fences. The fences were designed to withstand 30 ft-ton (81kJ), 80 ft-ton 217 kJ), 180 ft-ton (488kJ) and 250 ft-ton (678kJ) of kinetic energy from a single rock impact incident, with the capacity to withstand another impact of similar magnitude before major repairs are necessary. This report will detail the results of this test program.

The rock fall control fences that were tested are based upon a wire rope net panel that is constructed from a length of mesh rope, woven in a continuous pattern around a border rope. These net panels are extremely strong in resisting the tensile forces imparted to them by a rock fall incident.

The forces imparted to the net panels are transferred to a system of support rope configurations asttached to the net panels by a series of banding and seam rope. These forces are then transferred to energy dissipation devices located in the support ropes that absorb a majority of the energies from the rock fall impacts through material deformation and friction.

While these systems are similar in design to current unstallations available in the United States, **CVP** systems were tested using foundation designs, new energy dissipation device configurations, new support rope configurations and a new type of soil anchor. The new designs also increased the column spacing and the net panel heights from those used in prior testing programs. The goal of **CVP** during this test program was to validate the capacities of these new designs and to establish methods that would make installation of these system much more cost effective in both their manufacturing and in their installation. From the measurements and insights obtained during the test program with **CDOT** and **LANL**, these goals were realized.

GEOLOGY AND ENGINEERING CHALLENGES OF SOUTHWEST VIRGINIA

Edited by:

Daniel R. Gilliam and William S. Henika,

Virginia Department of Mines, Minerals and Energy
Division of Mineral Resources
Department of Geology
Institute for Engineering Geosciences
Radford University

Saturday, May 22, 1999

Contents

REVIEW OF FIELD TRIP AREA GEOLOGY

William S. Henika

This trip traverses the Appalachian fold and thrust belt westward along Interstate 81 and U.S.

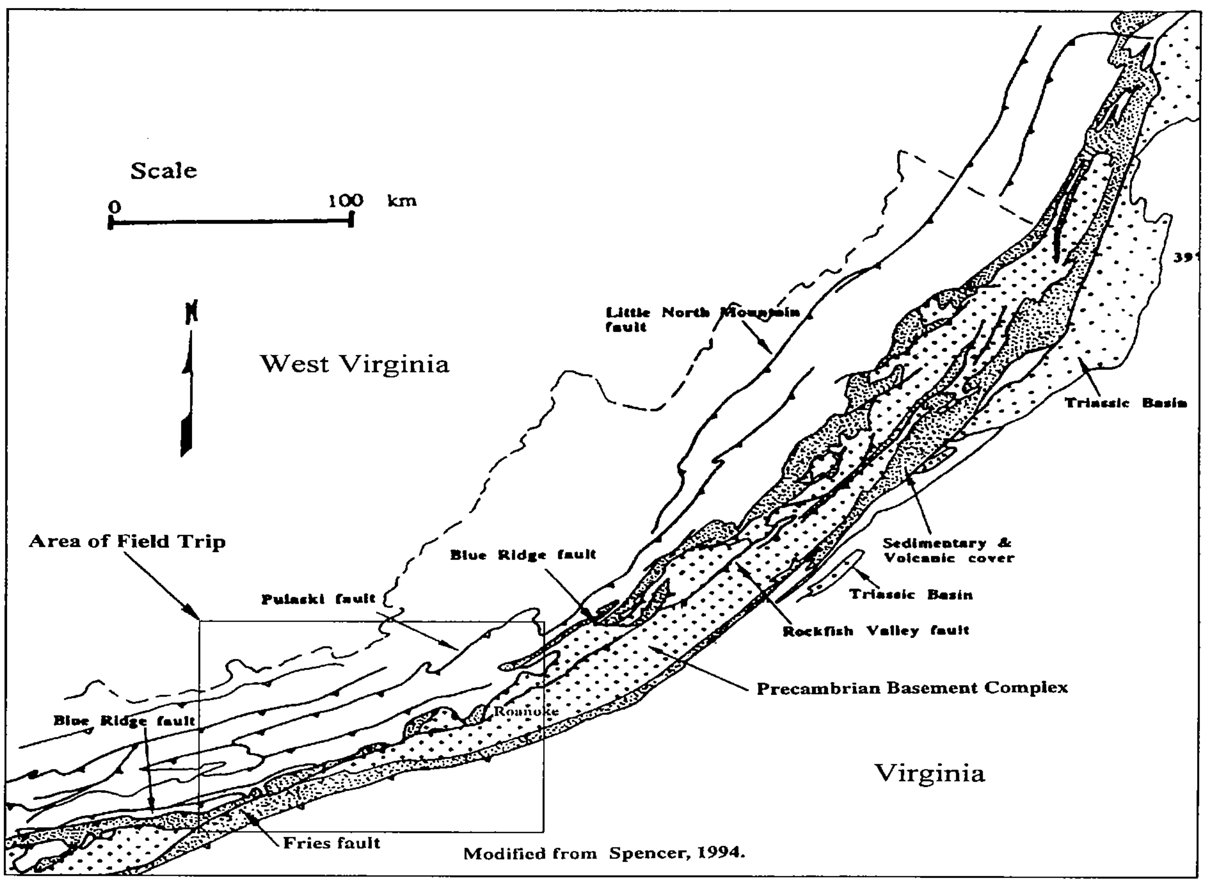

Figure 1. Regional Tectonic Map

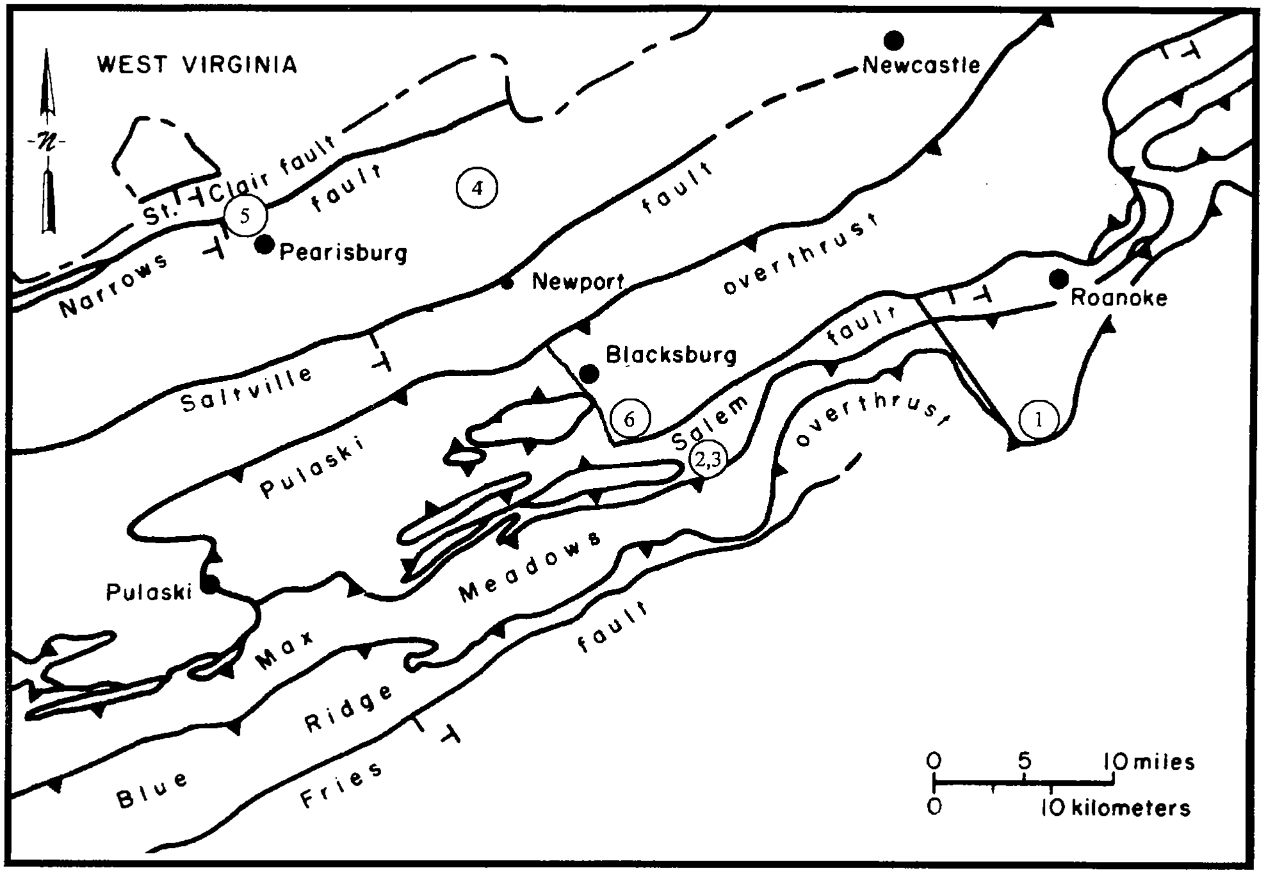

Figure 2. Tectonic map showing stops between Roanoke and Narrows, Virginia.

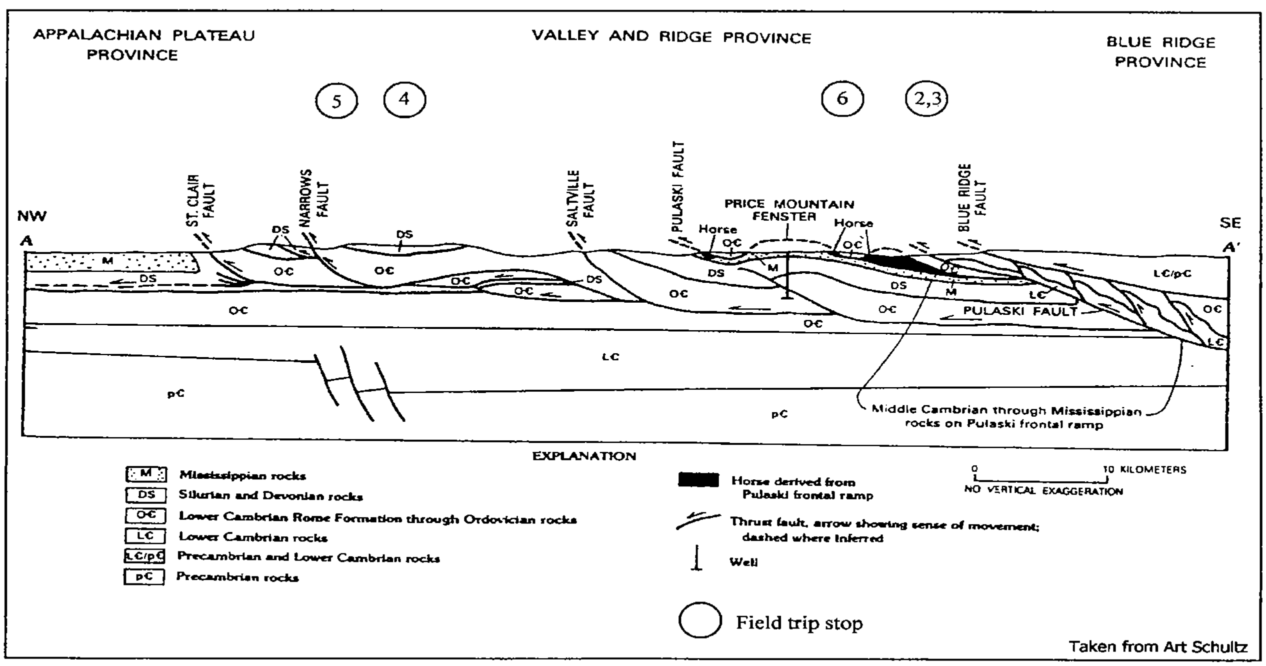

Figure 3. Cross section of field trip area.

Figure 4. Stratigraphic Units in the Roanoke and Radford 30 by 60 minute Quadrangles.

Mississippian	d	**Diabase**: coarse-grained plagioclase and pyroxene dikes.
	Mh	**Hinton Formation:** mudstone, siltstone, and fine to medium-grained sandstone.
	Mb	**Bluefield Formation**: sandstone and shale with interbedded mudstone and limestone.
	Mg	**Greenbriar Limestone**: fine-grained, interbedded with coarse bioclastic limestone and fine calcareous mudstone.
	Mmcu	**Maccrady Formation Upper**: interbedded siltstone, mudstone, and coarse conglomeratic sandstone.
	Mmcl	**Maccrady Formation Lower**: mottled mudstone and sandstone with thin coal beds.
	Mpru	**Price Formation Upper**: sandstone, siltstone, and mudstone, with thick coal beds.
	Mprl	**Price Formation Lower**: interbedded sandstone, siltstone, and mudstone with thick beds of coarse conglomerate.
	Mprc	**Cloyd Conglomerate**: very thick-bedded conglomerate at base of Price Fm.
Devonian	Dch	**Chemung/Foreknobs Formations**: mudstone, siltstone, sandstone, and conglomerate with fossil-debris beds.
	Db	**Brallier Formation**: claystone and mudstone with thin siltstone and fine-grained sandstone beds.
	Dm	**Milboro Formation**: black, fissile thin-bedded claystone and mudstone with disseminated sulfides.
	Dlrh	**Undivided Devonian**: Limestone, Rocky Gap Sandstone, and Huntersville Chert
Silurian	Stk	**Tonoloway Limestone**: thin-bedded argillaceous limestone and shale.
	Stk	**Keefer Formation**: medium sandstone and quartzite, minor siltstone and shale.
	Srh	**Rose Hill Formation**: reddish gray hematitic sandstone and shale.
	Stu	**Tuscorora Formation**: medium to coarse grained quartz sandstones.
Ordovician	Oj	**Juniatta Formation**: reddish-brown fined grained sandstone interbedded with minor reddish-gray shale.
	Omb	**Martinsburg Formation**: interbedded sandstone, shale, calcareous mudstone and limestone.
	Oem	**Eggelston Formation**: fine to medium grained sandstone and siltstone, thin bentonite beds. **Moccasin Formation**: interbedded maroon mudstone and gray limestone.
	Oba	**Bays Formation**: fine-grained quartzose sandstone, reddish-gray siltstone and sandstone; thin bentonite beds.
	Opl	**Paperville Shale**: dark gray to black laminated mudstone, interbedded siltstone and limestone.
	Oe	**Edinburgh Formation**: dark gray to black mudstone with abundant, coarse-grained limestone beds
	Olu	**Undivided Middle Ordovician Limestones**: argillaceous limestone near the top, middle cherty fossiliferous limestone, dolomitic limestone at base.
Cambrian	Oku	**Knox/Beckmantown Group**: (Knox) thick-bedded crystalline dolomite with nodules of light to dark-gray chert.
	Ob	(Beckmantown) thick to very thick bedded cherty dolomite and microcrystalline limestone.
	Ccr	**Copper Ridge/Conococheague Formations**: (Copper Ridge) very thick-bedded locally cross-bedded fine to medium-grained sandy dolomite, with oolite and sandstone marker beds near base and top
	Cco	(Conococheague) interbedded sandy fine-grained dolomite and with thinly laminated siliceous limestone and dolomite cycles.
	Cn	**Nolichucky Formation**: thin bedded argillaceous dolomite, interbedded with shale and flat-pebble conglomerate.
	Ce	**Elbrook Formation**: medium-bedded limestone and dolomite, interbedded with green to red laminated phyllite. Tectonic breccia common near base
	Ch	**Honaker Formation**: thin to very thick-bedded, fine-grained cherty dolomite.
	Cr	**Rome/Waynesboro Formations**: maroon green-yellow phyllitic mudstone with minor sandstone.
	Cwb	Massive bedded crystalline dolomite and thick karstic limestone interbeds.
	Cs	**Shady Formation**: dolomite, white to dark gray, medium to coarse grained, thick to very thick bedded.
	Cer	**Erwin/Antietam Formations**: fine to medium grained metamorphosed sandstone and quartzite, interbedded with phyllite.
	Ca	
	Ch	**Hampton/Harpers Formations**: dark gray to greenish-gray metamorphosed sandstone and phyllite. Locally mined ferruginous sandstone marker bed.
	Cu	**Unicoi Formation**: quartz-pebble conglomerate, metasiltstone and arkose, with metabasalt and tuffaceous interbeds near base.
Precambrian		**Basement Rocks:**
	Zad	Altered basalt and diabase dikes
	Zgd	Granitic gneiss
	Ybc	Megaporphyritic charnockite
	Yn	Nelsonite
	Yc	Charnokite
	Ybg	Biotite granitoid
	Yhm	Horsepen Mountain gneiss
	Ypg	Megaporphyritic granulite
	Ygb	Biotite granofels.

Highway 460 from the Blue Ridge at Roanoke to the Narrows of the New River (figure 1). The stops were selected to illustrate the interrelationships among stratigraphy, structure, geomorphology and soils development and their influence on engineering design and construction in the western portion of Virginia (figure 2).

The Roanoke Valley and New River Valley contain an aggregate thickness of Cambrian through Mississippi sedimentary strata in excess of 30,000 feet. These Paleozoic strata were deposited in a marginal marine basin from 500 million to about 300 million years ago. They were transported several tens of miles northwestward from the continental margin during a rotational tectonic plate collision event at the end of the Paleozoic Era and were fractured and rotated again during extension and igneous intrusion in the Mesozoic Era (figures 3 and 4).

Roanoke was developed within a large structural basin that lies along the southeastern boundary of the Valley and Ridge Province, inset along a major reentrant in the Blue Ridge thrust sheet. The northwestern side of the basin lies along the trace of the Salem fault (Figures 1, 2 and 6). This fault is a relatively older thrust fault that was tilted and uplifted by later imbricate faulting along the Pulaski thrust to the northwest and beneath the Catawba syncline block (Figures 6 and 7). Resistant Devonian and Silurian sandstone beds that were tilted and uplifted along imbricated thrust faults were later eroded to form the spectacular Allegheny Mountain Ridges that we will be crossing in the New River Valley west of Roanoke.

Along the southeastern boundary of the Roanoke Valley (Stop 1, Mill Mountain) imbricated segments of the Blue Ridge sole thrust separate resistant metamorphic rocks in the Blue Ridge Mountains from softer argillaceous rocks and limestones exposed on the valley floor (figures 3, 6 and 7). The great overthrust faults that cut rocks in the Blue Ridge and Valley and Ridge formed some 300 million years before the present during the Alleghanian continental collision. Water gaps that allowed the major streams to excavate the Valley and Ridge topography developed along lateral faults, ramps and extensional fractures that were locally intruded by mantle derived diabase dikes associated with the Mesozoic opening of the Atlantic Ocean Basin about 150 million years ago. Deeply eroded dikes, sills and a volcanic breccia plug penetrated fractures in the Potomac basin in Highland County beginning in the Eocene, (47 ma., Johnson, Jr. and others,1971). Thus the present day landscape is much younger than the Paleozoic folds and faults. The relief we see today did not evolve until the late Cenozoic, when uplift and erosion caused the New River, the Roanoke River and the James River to begin to rapidly excavate their basins along ancient tectonic structures. These are erosional mountains, roughly the same age as the Rockies. Recent research in geomorphology by scientists such as David Harbor at W&L and Daryl Granger at Purdue may be displacing much of the older geomythology previously published about the Appalachian area. Harbor describes the James and Roanoke Rivers as

Figure 5. View of Mill Mountain from the Blue Ridge Parkway

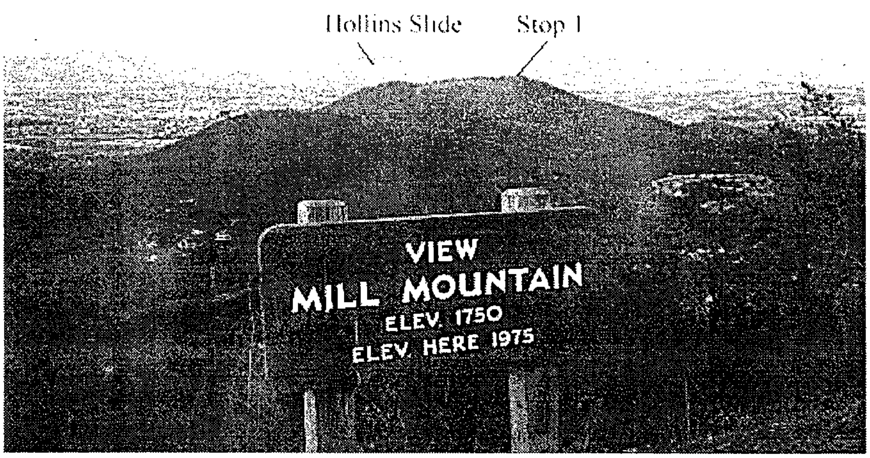

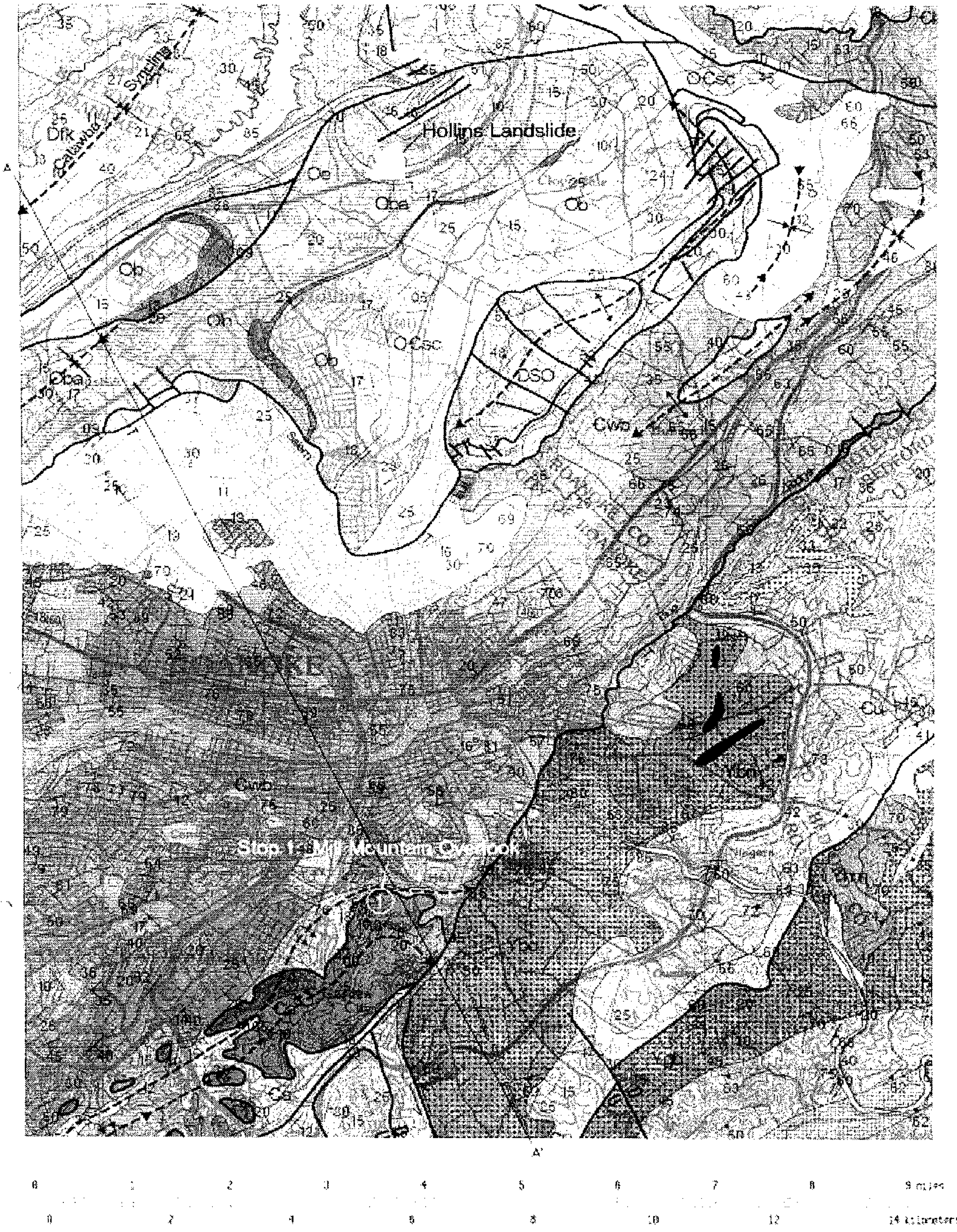

CONTOUR INTERVAL 20 meters

Figure 6. Geologic map of the Roanoke area showing Stop 1 (after Henika, 1997a).

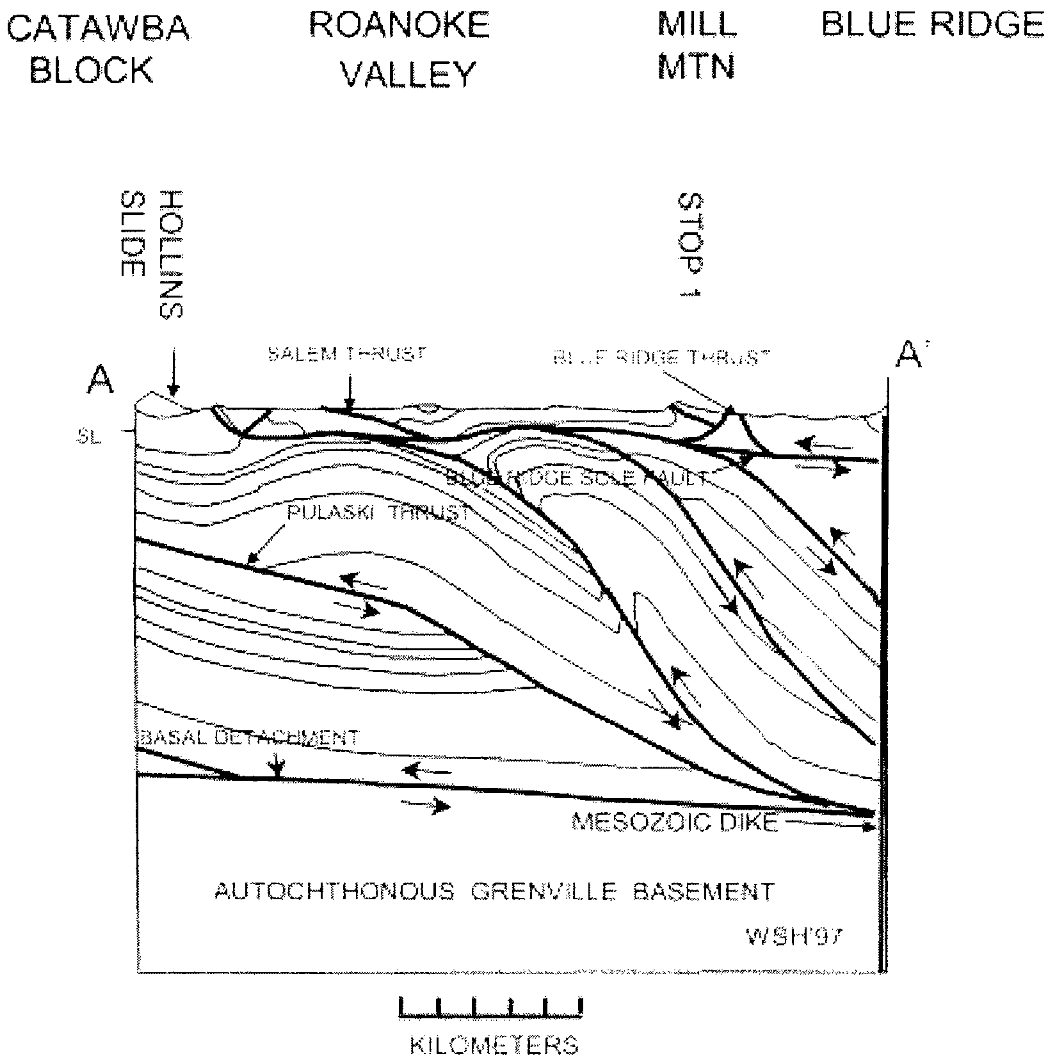

Figure 7. Cross section of the Roanoke area.

downcutting like "run-away locomotives" along their relatively direct courses to the coastal plain. Harbor and students have measured local erosion rates as high as 150 m/ma in the James basin (Harbor, 1998). Granger's work with cosmogenic dating of quartz cobbles buried in caves along the New River shows the New is cutting into the New River Plateau (some 350 m. above the Roanoke) at a sedate 20-30m./ma (Granger and others, 1997).

The local relief of about 800 meters between the crest of Poor Mountain and the upper Roanoke Valley (stops 2 and 3, near Elliston), could have formed in less than 6 million years if the 150m/ma rate was true. The previously accepted Appalachian erosion rate of 40 m/ma (Sevon, 1989) would yield a more conservative 20 million year old mountain front. The older date in this area seems to conform to Late Cenozoic, northwest-directed reverse faults recently discovered along the fall line in the Nottaway and Lower Roanoke Basins. These faults thrust Paleozoic and Precambrian metamorphic rocks of the eastern Slate belt over thick Pliocene sand and gravel deposits along the western edge of the Virginia Coastal Plain (Berquist and Bailey, 1998). One of our greatest challenges for Appalachian geologists during the next millennium may be to convince engineers and planners that the Appalachians are not just the worn-down roots of a Paleozoic overthrust mountain range. On the contrary, the Appalachians are a rapidly emerging chain with an active seismic history (Bolinger and Hooper, 1972), where detailed geological mapping and geotechnical studies are really needed for major projects.

ROAD LOG

Miles	Comments
	Leave rear of Hotel Roanoke (Wells & Jefferson) - Turn Right on Wells Avenue. Turn right on Williamson Road. Turn right on Elm Avenue and get in left lane. Turn left on Jefferson Street.
1.4	Turn left on Walnut Street which becomes Fishburn Parkway as it ascends Mill Mountain. Crossing first ledge of Antietam quartzite. Crossing slide area - note guardrail deformation. Slump structures are typical of residual soils formed on the Shady dolomite.
3.5	Turn right onto Mill Mountain Parkway.

4.3 **Stop 1.** Mill Mountain (figures 5, 6 and 7) is capped by the Antietam (Erwin) quartzite in a large outlier of the Blue Ridge thrust sheet now eroded back to the Blue Ridge Mountains on the southeast side of the Roanoke Valley. The Mill Mountain thrust sheet has been partly preserved on the gently dipping southeast anticlinal limb of the Crystal Spring anticline and in a synclinal trough to the southeast of Mill Mountain but may still be actively subsiding with the continued dissolution of carbonate rocks beneath the Blue Ridge thrust.

Crystal Spring is an important part of the Roanoke public water supply that emerges from a cavern at the foot of the mountain, about 800 feet below the overlook. It is part of an ancient karst aquifer system that was developed in fractured, cavernous Shady Dolomite beneath the Blue Ridge thrust fault. The fractures in the dolomite are recharged from above by rainwater percolating down through the highly permeable, fractured quartzite and thin, sandy soils developed above the Blue Ridge thrust fault in the mountains southeast of the spring.

Several large sinks that actually penetrated the Blue Ridge fault were the locus of extensive iron mineralization in quartzite breccias and as limonite nodules in the deep orange residual clay soils developed on the fractured dolomite below the fault. The main ore zone was exposed in more than a dozen open pit mines, some as large as 150 feet in diameter and 50 feet deep. These pits are accessible by foot or on horseback by following the Chestnut Ridge horse trail on the western side of the Parkway campgrounds southeast of Mill Mountain (Henika, 1997, a&b)

The deep residual clay soils developed in carbonate rocks are common along the lower slopes on Mill Mountain and other smaller outliers of the thrust sheet to the southwest of Mill Mountain. The clay-rich, residual soils have proven to be unstable in road embankments and shopping center parking lots. Several large slumps developed behind the Wall Mart lot at Hunting Hills Plaza and along the southbound lane of U.S 220 south of Roanoke (figure 8) have been stabilized by loading toe areas of the slumps with rip rap or building retaining walls with crushed stone gabions.

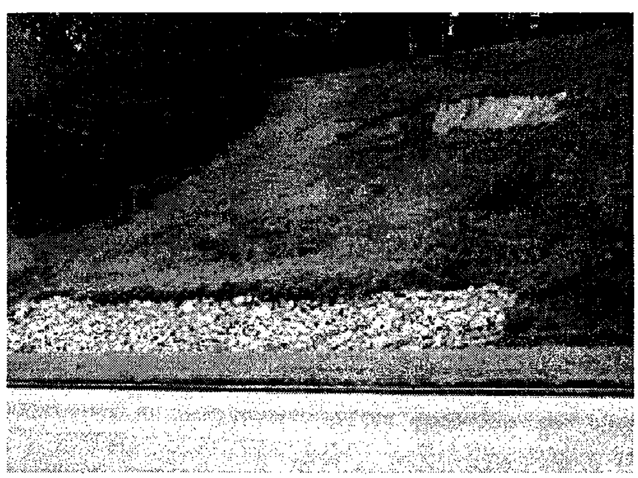

Figure 8. Rotational slump in Shady Dolomite residuum along Highway 220 S.

Large quartzite blocks and boulders left on the steep slopes above homes in the densely developed residential areas may constitute natural hazards. This is because of potential landslide development during intense rainfall events such as Hurricane Camille in 1969 (Williams and Guy, 1971), or seismic events similar to the 1924 temblor that sheared through a 16 inch cast iron water main above Crystal Spring, along the fault near the foot of the mountain (Woodward, 1934, and Bollinger and Hooper, 1972).

The largest landslide in the Roanoke area, known as the Hollins slide (figures 6, 7 and 9) was activated in the spring of 1962 when I-81 construction cut the lower slopes of Tinker mountain on the northwestern border of the valley (Spangler and others, 1964). The area that was devegetated during efforts to stabilize the slide is shown on the 1981 geologic map (Bartholomew, 1981). The slide area is just southwest of the weigh station visible along I-81 about 7.5 miles almost due north from the Mill Mountain overlook. A naturally stabilized (hyperbolic) slope can be seen on the northeast end of the large butte-shaped mountain capped by a thick section of Devonian and Silurian sandstone. The landslide developed on a similar slope facing the Interstate when the grade for the southbound lane undercut the base of a thick debris fan below the sandstone cliffs. The slide was nearly 2000 feet wide and extended some 800 feet north of the roadway. It took several years to stabilize the giant slide. Attempts to stop the movement by benching and draining the unconsolidated slide mass were initially unsuccessful and it was discovered that the slip plane was actually in the weathered Martinsburg shale beneath the debris fan. Stabilization was finally achieved by acquiring additional right of way and unloading the head of the slide by removing nearly 100,000 cu. yd. of rock and earth. A similar but much smaller slide developed northeast of the original when the new weigh station was built on the northeastern end of the mountain.

Proceed back to intersection of Fishburn Parkway/Walnut Avenue and Mill Mountain Parkway.

Figure 9. View of Tinker Mountain Showing Location of the Hollins Slide

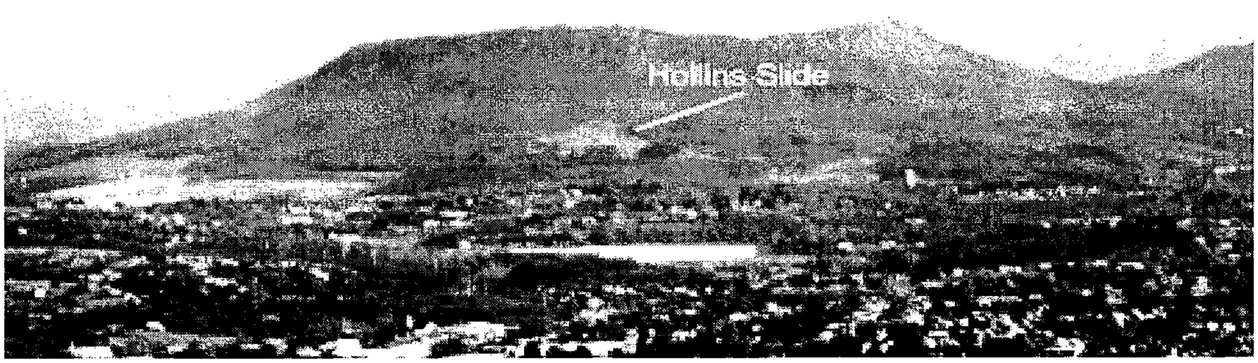

4.9 Turn left onto Fishburn Parkway/Walnut Avenue
6.10 Outcrop of Shady dolomite.
7.11 Cross Roanoke River.
7.12 Turn right onto Jefferson Street.
7.5 Turn right on Elm Avenue.
7.7 Turn left at the 581 junction.
13.5 Get in far-left lane for junction with I-81.
14.1 Bear left onto I-81 ramp and merge into traffic.
35.7 Take Dixie Caverns exit - Poor Mountain visible to the left
36.0 Turn left on Dow Hollow Road/State Road 940
36.2 Turn right on US 460/11 (West Main Street)
36.3 Turn right into Dixie Caverns parking lot.

Stop 2. Dixie Caverns. This is a small, well-decorated-commercial cavern developed in limestone interbedded with platy to thick-bedded dolomite of the Cambrian-aged Elbrook Formation (figures 3 and 10). The cavern has approximately 650 feet of passageways and contains a large room called the "Auditorium " which measures 70 feet wide and long and 60 feet high (Holsinger, 1975). The main passageways are parallel to and may be as close as 1500 feet to the northeast-trending breccia zone along the leading edge of the Salem thrust sheet. Cross passages are not at typical 90 degree joint intersections like many caves in the western Valley and Ridge but trend at 45 degree angles to the strike of bedding along the fault line (Bartholomew and others 1999, in press).

This angular relationship may reflect folding associated with complimentary shear directions or rotation of jointing and fracture cleavage along the fault line. Some small sinkhole subsidence in the recent past caused collapse of a portion of the northbound lane of the interstate roadway. The collapse areas developed about three thousand feet northeast of the entrance to Dixie Caverns in the same relative structural position along the leading edge of the thrust sheet as the caverns. Because of the fractured nature of the bedrock and its proximity to the Salem fault, this may continue to be a problem area. Return to West Main and turn right.

36.8 Turn left onto West River Road.
36.9 Cross Roanoke River.
37.1 Turn right at Spring Hollow access Road - View Spring Hollow dam.
37.3 Cross railroad tracks.
37.4 Spring Hollow Reservoir entrance gate.
37.9 Turn left, through gate and proceed to top of the dam.

Stop 3: Spring Hollow Reservoir – Spring Hollow Reservoir and the Clifford N. Craig Memorial Dam are located in the far western part of Roanoke County along the base of the northern slope of Poor Mountain. Spring Hollow Reservoir is a pump storage facility that impounds water pumped from the Roanoke River for storage and subsequent treatment for use as a potable water supply for the county. The reservoir is located in a side valley immediately south of the Roanoke River, and as such the environmental impacts normally associated with damming a river were minimized. The 243 ft high, 990 ft wide dam was named in memory of Clifford N. Craig, former utilities director for Roanoke County. The dam is a Roller Compacted Concrete (RCC) structure that was built using limestone quarried from the upper reaches of the reservoir area, and is the tallest RCC dam of its kind east of the Mississippi River.

The Spring Hollow Reservoir is sited in the Cambrian-aged Rome-Waynesboro formation on the Roanoke Valley thrust sheet (figures 3, 10 and 11). The Roanoke Valley fault is located about 3000 feet northwest of the dam and the Blue Ridge fault is about 9000 feet southeast of the dam (Bartholomew and others, 1999, in press). The Roanoke Valley thrust sheet is the major tectonic unit along the southeastern side of the Valley from the vicinity of Claytor Lake to the Glade Creek area near Montvale, (Henika 1997, Bartholomew and others 1999).

Prior to design and construction of the dam, an extensive geotechnical evaluation, including detailed geologic and hydrogeologic studies, was performed in an effort to evaluate the feasibility of siting the project in a karst terrain. Of primary concern was the potential for leakage from the reservoir valley through solution channels present in the carbonate rock.

The study area contains three major drainage basins, which are separated by parallel, north-south trending ridges, and includes the reservoir valley, Dry Hollow to the east and Cove Hollow to the west. Variably weathered and fractured dolomite, limestone, phyllite and argillite and metasiltstone bedrock of the Rome-Waynesboro Formation underlie the study area. Overall, strata in the vicinity of the reservoir trend in an east-west direction and dip steeply to the north. Groundwater flow in the reservoir area is generally through interconnected bedrock fractures and also through solution channels present in the carbonate rocks. Regional groundwater flow is in a northerly direction, toward the Roanoke River; however, lateral flow to the east and west occurs locally. Most carbonate units are strongly deformed into relatively tight similar folds, many of which are no longer intact but have been stretched to form boudinage structures. These large, spindle-shaped masses of carbonate have fracture and pressure-solution cleavage with open solution channels. This produces elongate, narrow but persistent areas characterized by rapid lateral groundwater movement along structural axes and cleavage as well as fault lines.

Geologic mapping of the reservoir valley and the adjacent valleys to the east and west revealed the presence of several fracture trends, with the most prominent fracture trend and the strike of the rock oriented in an east-west direction. As such, it was possible for groundwater flow to migrate laterally from a drainage way in one hollow to the next. Additionally, evidence of dissolution within the carbonate rock sequences, as well as several springs was observed in the central portion of the east side of the reservoir valley. Also, a topographic "bird's-foot" structure consisting of closely spaced, alternating ridges and valleys entered the east central portion of the reservoir valley at an oblique angle in the vicinity of the highest discharge springs.

To the east of the reservoir valley, and on strike with the "bird's-foot" structure, several sinkholes, a cave, and a sinking stream were documented during geologic mapping of the area. Fluoescein dye and chloride tracer tests later confirmed a hydraulic connection between Dry Hollow to the east, and the reservoir valley, with both surface and groundwater migrating westward into the reservoir valley drainage basin.

To the west, Cove Hollow is topographically and geologically similar the to reservoir valley, although there is a smaller quantity of water flow in the Cove Hollow stream than in the reservoir valley stream. The most significant feature in Cove Hollow is a drainage system that enters the valley obliquely from the southeast and closely resembles the "bird's-foot" structure observed in the reservoir area. The structure, which contains a series of small alternating ridges and drainageways trending along the strike of the bedrock, enters Cove Hollow from the east side of the valley and aligns along strike with the "bird's-foot" structure in the reservoir valley.

Based on both geologic and geomorphic evidence, it appeared that Dry Hollow was a more mature drainage basin than either Cove Hollow or the reservoir valley and as such had experienced a greater degree of weathering. As a result of the increased weathering, carbonate rocks in Dry Hollow had been exposed to dissolution processes for a greater period of time than the carbonates

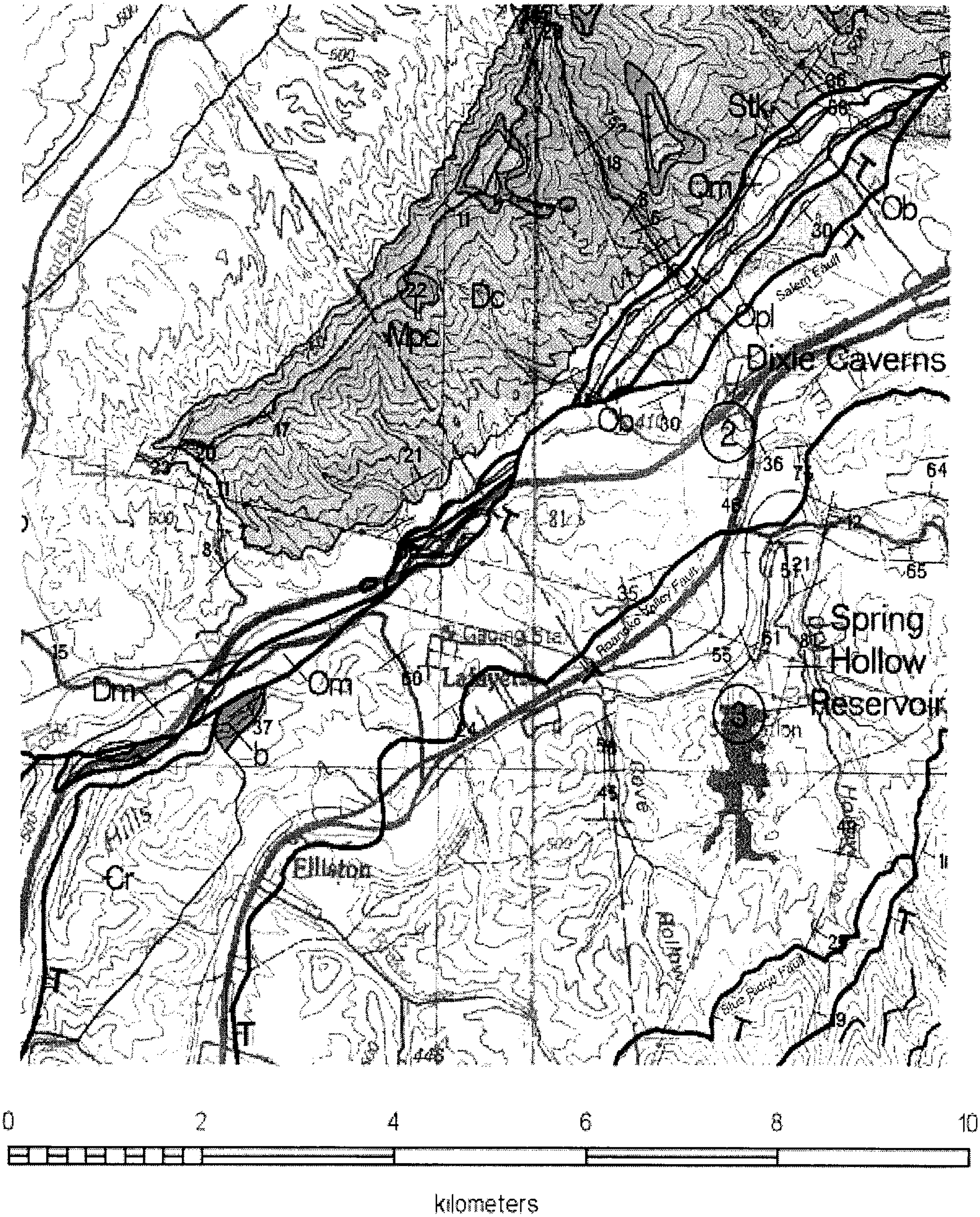

Figure 10. Geologic map of the Elliston area showing Stops 2 and 3 (after Bartholomew and others, 1999).

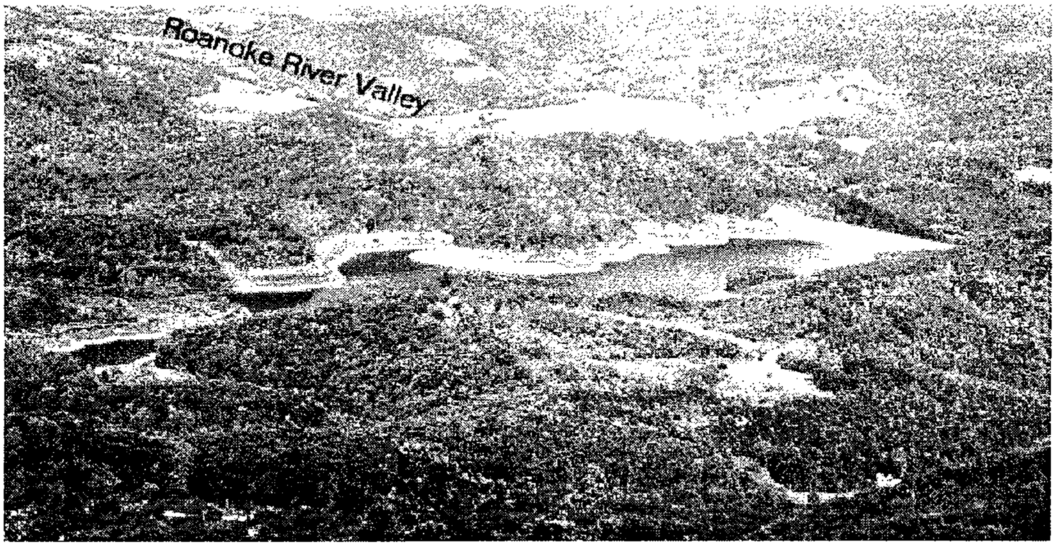

Figure 11. Spring Hollow Reservoir, Stop 3.

of the reservoir valley and Cove Hollow; thus resulting in the greater abundance of karst features. Prior to formation of the reservoir valley it is likely that the main tributary valley in the southeast portion of Cove Hollow was receiving significant groundwater flow from Dry Hollow through fractures and solution channels. Ultimately, this flow was captured as the reservoir valley eroded to the level of groundwater flow, eliminating the flow to Cove Hollow and leaving the creek bed in the "bird's-foot" drainage way dry.

Significant percentages, perhaps up to 50 percent, of the rock strata mapped in the study area were identified as limestone and dolomite. This is more typical of the Waynesboro Formation as mapped to the northeast of the Roanoke area (Butts, 1941 and Henika, 1981). Carbonate rocks are susceptible to dissolution, especially when highly fractured as at the project site. As such, the reservoir area was divided into three zones (Zones I, II, and III) that were identified according to differing geologic properties, especially with regard to degree of karst development and potential for leakage from the reservoir once it was under full head conditions.

Of the three zones identified Zone II, which included the high spring discharge area within the "bird's-foot" structure, was considered to be the most problematic with regard to the potential for leakage from the reservoir. Additionally, there was a good possibility that the dissolution identified on the east side of the reservoir valley also existed on the west side of the valley based on the likely flow of groundwater from Dry Hollow to Cove Hollow prior to formation of the reservoir valley. A grouting program based on the hydraulic connectivity between the reservoir valley and the adjacent drainages to the east and west, was developed and implemented prior to construction of the dam in order to reduce the potential for leakage from the reservoir along fractures and solution channels. To date, the grouting program has proven successful, with no major leakage observed from the reservoir to the adjacent drainages.

38.8 Turn left on West River Road.
38.9 Turn right at junction of US 460/11 and West River Road.
39.4 Turn left onto Dow Hollow Road.
39.6 Turn left onto I-81 access ramp.
41.9 Note tectonic slice of Tuscarora sandstone forms ridge along Salem fault.
42.2 Crossing Roanoke River channel diverted for I-81 construction.
42.5 Cross abandoned channel again.
42.7 Devonian shale cliffs form the footwall beneath Tuscarora sliver.

43.4 North Fork of the Roanoke River.
43.6 Ironto Road overpass - Dolomite cliffs to left form hanging wall.
44.1 Devonian shale exposed along footwall to Salem fault.
44.6 Semicircular escarpment to right is site of 1969 slide along Salem fault.
44.8 Outcrops of brecciated dolomite in tectonic zone at base of Pulaski sheet.
46.8 Outcrops of brecciated dolomite in tectonic zone at base of Pulaski sheet.
47.1 Outcrops of brecciated dolomite in tectonic zone at base of Pulaski sheet.
49.6 Future location of Smart Road junction with I-81.
51.4 Enter Crab Creek allochthon, note competent dolomite beds in this slice.
52.7 Take Exit 118 toward Blacksburg and bear right at end of access ramp.
53.3 Travelling west on US 460 toward Christiansburg/Blacksburg.
53.7 Note pinnacles and floaters behind Shelor Automotive.
54.2 Turn right onto US 460 bypass to Blacksburg, home of Virginia Tech.
57.7 At the intersection of US 460 and Route 114, view Price Mountain which is an anticlinal window in the Pulaski thrust sheet.
58.6 Rock cuts on left side of US 460, behind Wilco, are composed of leached Mississippian shale (Price Mountain Window) at its contact with the Cambrian Elbrook dolomite along the Pulaski fault trace.
59.7 Bear left at the US 460W bypass/460 Blacksburg Business interchange.
60.2 Maccrady shale within the Price Mountain Window in the left roadcut
60.4 Virginia Tech Corporate Research Center on the right. Pulaski fault on the NW side of the window passes beneath one of the buildings at CRC - as identified by Robin Reed 's subsurface investigation for the building.
60.9 Cross the Pulaski thrust fault - back onto the Pulaski thrust sheet.
66.5 Cross the Pulaski thrust fault onto the Saltville thrust sheet. Mississippian coal section of the Price Formation exposed and mined on the right.
68.0 We have been heading down section through the Mississippian strata. The base of the Mississippian section is delineated by the Cloyd Conglomerate, which is a ridge former in this area and was quarried for use as millstones. We are now headed down section through the Devonian Foreknobs Fm.
70.1 Nearing top of Gap Mountain - Keefer sandstone outcrops on right.
70.2 Rose Hill shale/sandstone outcrops on both sides of highway.
70.3 Tuscarora sandstone outcrops on both sides of highway.
70.4 Martinsburg Fm. outcrops along left side of highway.
72.6 Moccasin formation - Pink middle Ordovician limestone outcropping along right side of highway in the Clover Hollow anticline.
73.0 Turn right on Mountain Lake Road/State Road 700.
73.3 Old covered bridge preserved on left at Sinking Creek.
73.7 Outcrops of middle Ordovician limestone.
74.3 Knox dolomite outcrops in the core of Clover Hollow anticline.
75.2 Contact between Knox and middle Ordovician limestones.
76.4 Folded outcrop of Moccasin limestone, typical of Mid-level decollement.
78.7 Reedsville and Trenton Formations along right side of road.
80.3 Turn right into Mountain Lake Lodge Parking Lot for Stop 4: Mountain Lake.

Lunch break

Stop 4. Mountain Lake. Mountain Lake is an extremely interesting and unusual geologic feature. It is the only natural lake in the unglaciated Valley and Ridge province of the southern Appalachians (Mills, 1988). This lake is one of two natural lakes in the state of Virginia – the other is Lake Drummond in the Great Dismal Swamp of the Coastal Plain. Mountain Lake (figure 12) is located atop Salt Pond Mountain at an elevation of 3,860 feet, nearly 1,000 feet above the surrounding ridge tops and 2,000 feet above the New River less than six miles away (figure 13). The lake is underlain by a thick clastic sequence of upper Ordovician-lower Silurian rocks: the Martinsburg (Reedsville and Trenton), Juniata, and Tuscarora Formations, in ascending stratigraphic order. The Martinsburg and Juniata are interbedded shales and sandstones, whereas the Tuscarora is a very hard quartz

Figure 12. Mountain Lake Lodge.

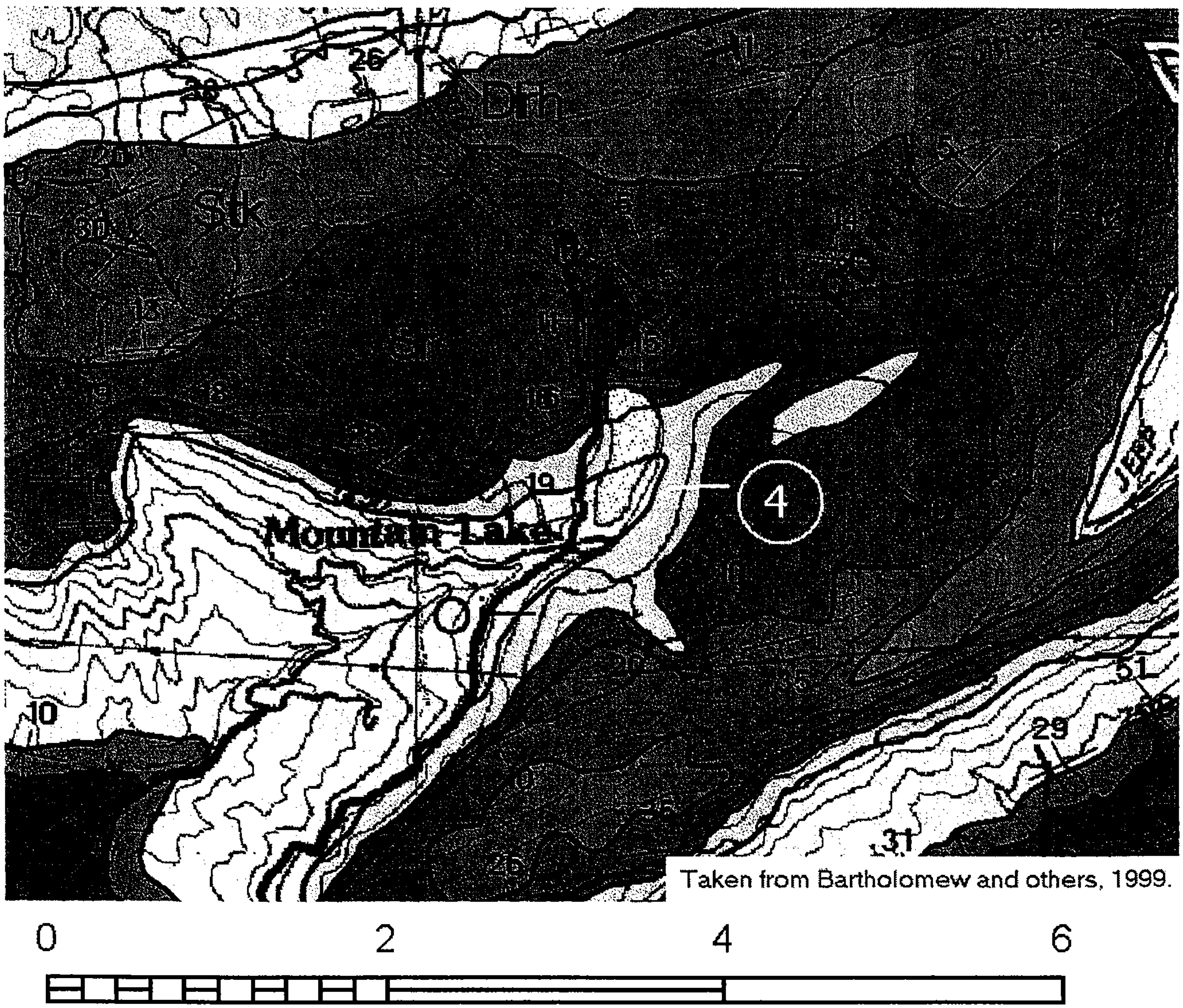

Figure 13. Geologic map of the Mountain Lake area.

arenite and a major ridge-former.

A number of modes of formation have been suggested for Mountain Lake, including solution activity, glacial or periglacial processes, volcanic events, meteorite impact, and even cows stomping around a salt lick on the mountain top (Dietrich, 1970; Frye, 1986). A more likely origin is damming of a typical stream valley by some sort of mass movement process, possibly involving slow transport of large blocks of Silurian sandstone by periglacial processes during the Pleistocene (Mills, 1988). Others (Whisonant and Watts, 1993; Cato and others, 1994) have suggested that a relatively rapid landslide, perhaps related to seismic activity, may have dammed the mountain stream. (Mountain Lake is located within the Giles County Seismic Zone, one of the major earthquake zones of eastern North America.)

Very recent work by Cawley and others (1999) contends that Mountain Lake is due primarily to vertical collapse in a proposed canyon-like feature developed along the Clinch-Juniata contact. Fracture trace analysis shows a large regional lineation feature associated with the north end of the lake. Sonar bathymetry and diving indicate this lineation to be expressed as a narrow open crevice in the deepest part of the lake. Evidently, as much as half of Mountain Lake's water mass may be escaping through this crevice. Cawley and others (1999) conclude that erosion of this crevice and periodic downsettling of overlying Clinch blocks are the principal mechanism of lake origin and water level control through time.

Leave parking lot and turn right on State Road 613 (Doe Creek Road).

85.1 Turn right onto US 460W and proceed toward Narrows.

89.8 Cross the New River - Highwall downstream is Knox Formation at the now abandoned dolomite quarry.

94.7 Cross the New River again and enter the Narrows Fault zone. Celco (cigarette filter factory) to the left has several high production water supply wells on its property. New Giles County PSA well (1,800 gpm+) located across the river to the north of the Celco plant.

96.0 **STOP 5. Narrows landslide or " the galloping highway".**

Strata: Units exposed in the active slide area: Devonian – Millboro Shale: Silurian – Keefer Sandstone and Rose Hill Formation; refer to the geologic map for other units.

Located along U. S. Highway 460 approximately 2 miles east of the Town of Narrows, the landslide affects the south-facing slope of Turnhole Knob (see geologic map).

Park on the right shoulder east of the landslide and walk along the highway westward to examine active sags and the underlying black shale (Millboro) in the drainage. On the slope above the highway, breakaway scarps, tension cracks, sag ponds, springs and seeps, and hummocky ground may be observed.

The first reported movement of the slide occurred in 1916 shortly after the Virginia Railway (now Norfolk Southern) was built. The ferry crossing New River at Bluff City was replaced with a bridge in 1940 and the existing road was improved. The landslide has been intermittenty active since April 1940.

Efforts to stabilize the landslide have had variable results. The earliest preserved attempt at stabilization was a stone retaining wall; a small portion is present at the east end of the slide along the railway. A grouting program from July 1950 through March 1951 may have contributed to the June 1951 movements by restricting the flow of groundwater. Grout from this program has recently surfaced near the eastern end of the railway cut. A concrete-beam retaining wall was constructed after 1951. Following major movements in 1971, a 400-foot-long Armco metal bin wall was constructed. Within 10 years this wall began to show signs of failure – tears in the sheet metal, sheared bolts, and piping gravel. In 1974 about 250,000 cubic yards of material was removed in an attempt to reduce the slope to 2:1 and reduce the overburden mass. Several attempts have been made to dewater the landslide with limited success; the most recent began in the Fall of 1997 and continued into January 1998. The Virginia Department of Transportation has spent more than $1,000,000 on remediation of this site.

Turnhole Knob is an overturned, footwall horse-block of the Narrows fault (see geologic map). The fault underlying the horse is in the Millboro Shale. Deformed rock in the fault zone may be seen along the drainage to the west of the landslide. The Huntersville Chert, including the Bobs Ridge Sandstone Member, is exposed on the east slope of Turnhole Knob. The Rocky Gap Sandstone outcrops at the crest of the knob. The dip slope and landslide are in the Keefer Sandstone. Most of the Rose Hill Formation rock has been hauled away. Between the Keefer and Rocky Gap Sandstones is the residual clay of the Tonoloway Limestone.

Observations over a number of years of the landslide debris indicate that only the Keefer and Rose Hill units are involved in the movement. Red sandstone blocks typical of the Rose Hill are found in the debris west of the large open cut. There is no evidence to suggest that rocks physically below the Keefer are involved in the landslide movements. I would suggest that the major slip plane is at or near the contact between the Keefer and the residual clay of the Tonoloway.

Debris movement appears to be related to construction activities that disrupt the toe of the slide and interfere with groundwater flow. The first reported movements occurred in 1916 shortly after construction of the Virginia Railway on the southernmost portion of the slide. Between 1916 and 1940 there is no record of movement, however there was no additional construction during this period. In 1940, with the building of the Celanese Corporation plant, construction of the bridge across New River to replace the ferry, and the upgrading of the road (present U. S. Highway 460), movement of the slide recurred and continues to the present.

The Narrows landslide is in the Giles County Seismic Zone which is centered at Pearisburg, 2.75 miles to the southeast of the landslide. More than a dozen landslides and megablock slides occur in Giles County (Schultz and others, 1986). Seismic activity has been suggested as the trigger for some megablock slides. The fault slice (horse) to the west (see geologic map) has a megablock slide. A megablock slide may have occurred on the Narrows landslide fault slice before New River undercut the slope toe.

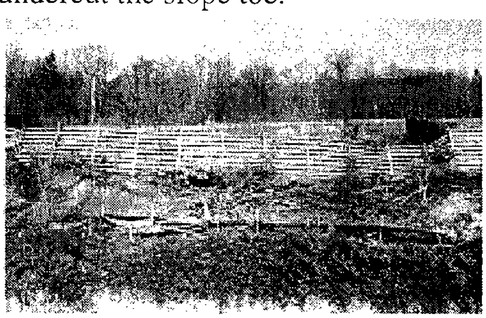

Figure 14. Armco bin wall, looking north. Note failures at extreme right (west) and left (east). Section between failures has moved several feet downslope.

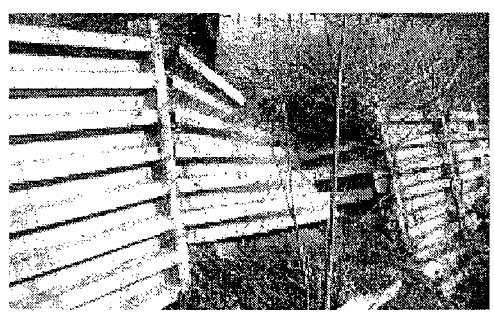

Figure 15. Detail photograph of western Armco bin wall failure.

Figure 16. Rotated, overturned block of Keefer Sandstone at road level.

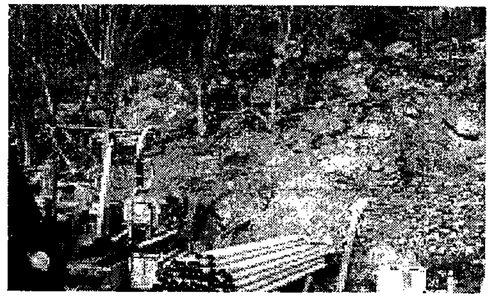

Figure 17. Horizontal drilling in an attempt to dewater the landslide (January 21, 1998).

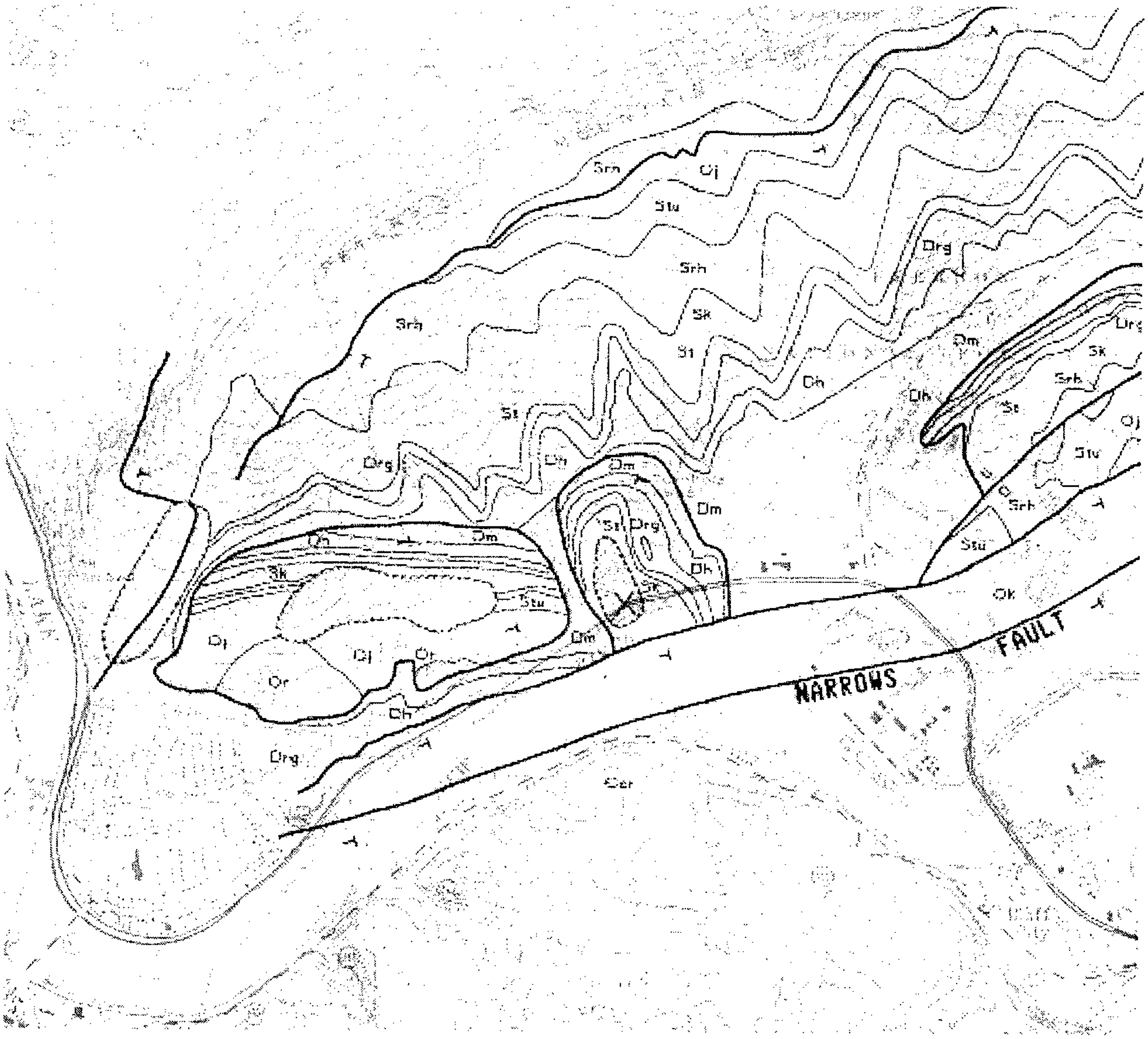

Figure 18. Geologic map of a portion of the Narrows quadrangle. Narrows landslide, dark gray area; **X** – marks the stop. Geologic units: Dm – Millboro Sh, Dh – Hunttersville Fm, Drg – Rocky Gap Ss, St – Tonoloway Ls, Sk – Keefer Ss, Srh – Rose Hill Fm, Stu – Tuscarora Fm, Oj – Juniata Fm, Or – Reedsville Sh, Ok – Knox Gr, Ccr – Copper Ridge Fm. Lighter gray areas - megablock slides.

98.1 Turn right on Route 61 at the stoplight.

98.2 Turn left on Route 61 across the New River.

98.6 Turn left on Route 100 in downtown Narrows

99.2 Leave Town of Narrows.

100.9 View the Narrows landslide to the left

102.1 New Giles County PSA well (1,800 gpm+) located to right.

102.5 Bear left to intersection of US Route 100 & 460.

102.6 Turn right on to US 460E.

106.7 Cross the New River again.

129.6 Exit US 460E to US 460 Business.

130.0 Turn left onto Merrimac Road

130.3 Merge from Merrimac Road to South Main Street and proceed to far right lane as quickly as possible.

130.5 Turn right on to Industrial Park Road.

130.6 Turn right on gravel driveway and proceed along Smart Road access road/test bed.

Stop 6: Virginia's Smart Road – Virginia's Smart Road, which will eventually connect Blacksburg with Interstate 81 near Ironto, is just part of a network of intelligent transportation systems that the Virginia Department of Transportation is in the process of developing for use in alleviating traffic congestion on Virginia's roadways. The first phase of the proposed six mile Smart Road, which is currently under construction in Blacksburg, Virginia, includes a 1.7 mile test bed which will be used as a research laboratory for intelligent transportation systems. Research will include the use of fiber optics and computers to monitor traffic flow, the effects of weather conditions on travel, and traffic counts. Additionally, scientists involved with the development and implementation of intelligent transportation system technology will research pavement durability, driver performance, and smart car technology.

Preliminary plans for the first phase of the Smart Road test bed, near Blacksburg, Virginia, included a vertical rock cut approximately 200 ft deep in a deformed and highly complex sequence of Cambrian-aged carbonates and shale displaced by the Salem Fault (figures 2 and 19). During the planning and design phase of the project between 1995 and 1997, geologic data collected from surface outcrops in the vicinity of the proposed roadway alignment indicated that the rock walls, if cut vertically, would be subject to potentially large rock slides. However, the data was not considered conclusive enough to alter the original plans and the project proceeded to the construction phase in the summer of 1997.

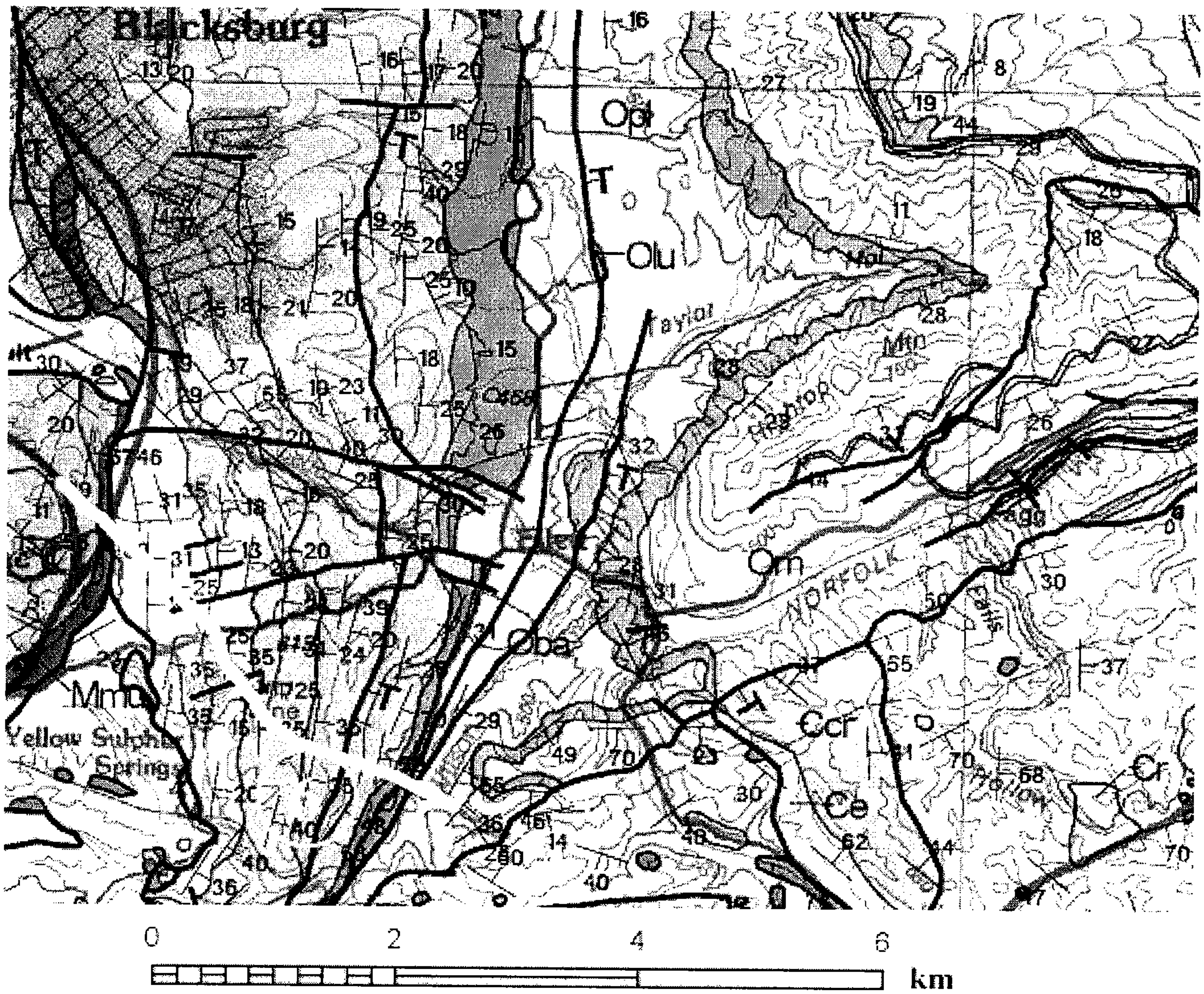

Figure 19. Geologic map of the Blacksburg area showing the location of Stop 6, Virginia's Smart Road Test Bed.

Original construction plans called for the uppermost bench of the roadcut to be constructed at a 2:1 slope, with the remainder of the planned roadcut to be constructed vertically. As construction progressed at the site, the contractor began to experience instability problems in the form of rock falls and rockslides. Due to concerns regarding the instability problems, a detailed rock slope stability investigation was initiated in July, 1998 to assess the potential for continued rock slides and rock falls within the Smart Road rock cut.

The initial slope stability evaluation performed by Radford University indicated that the rock walls would be subject to significant numbers of small to large-sized rock fall and rock slide events if constructed vertically as originally planned. The original analyses further indicated that laying the slope back to an angle of 60° would dramatically reduce the potential for hazardous rock fall and rockslide events. As construction has progressed at the site, excavation continued to expose numerous discontinuities within the rock walls that appeared to be repetitive throughout the extent of the excavation. Additionally, rock falls and rockslides continued to be observed during construction activities.

As a result of the continued stability problems, a design change of 1.5:1 was proposed and the discontinuity data collected during July 1998 for the initial evaluation were reevaluated for stability with respect to the design change.

The new analysis indicated that laying the slope back to the proposed angle of 1.5:1 (34°) would eliminate virtually all potential for hazardous rock fall and rock slide events from the numerous steeply dipping discontinuities on the left side of the roadcut. Of particular concern had been a series of steeply dipping joints that were repetitive throughout the extent of the cut and along which sliding had been observed during excavation. Figure 20 shows the steeply dipping joint face on the left side of the roadcut, prior to excavating the cut to final grade. Later excavation revealed more discontinuities of this type and orientation.

Stereonet analysis of the left side discontinuities indicated that the potential for both planar and wedge failures would be greatly reduced by laying back the slope to the proposed 1.5:1 angle. Note that the stereonet provided as Figure 21, generated with a cut slope dip orientation of 90°, indicates a large potential for planar failures on the left side of the cut if left in a vertical configuration. However, subsequent reanalysis of the slope according to the proposed design change of 34° indicated that virtually all potential for planar failures would be eliminated by laying the slope back, as shown in Figure 22. Although not included, stereonet analysis of wedge failure potential for the left side also indicated that laying the slope back would eliminate virtually all potential for wedge failures.

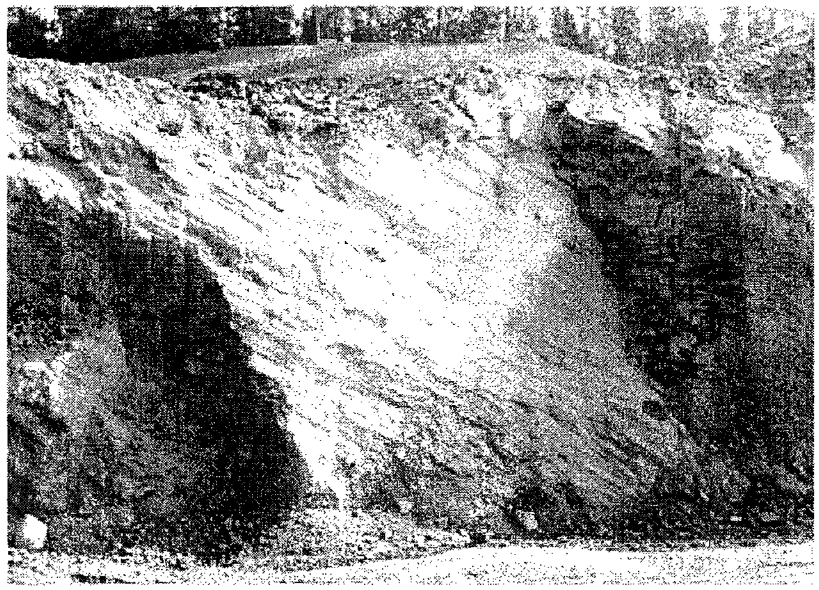

Figure 20. Steep discontinuities seen on left side of the Smart Road.

In addition to eliminating the potential for rock fall and rock slide events from the left side of the roadcut, laying back the slope to an angle of 1.5:1 would also eliminate the potential of planar-type failures on the right side of the roadcut. However, the right side of the roadcut would likely continue to be subject to varying magnitudes of rock fall and rockslide events due to a small group of potentially unstable rock wedges formed by shallowly intersecting sets of discontinuities as seen if Figure 23. These intersecting discontinuities, formed by bedding planes intersecting steeply-dipping joint sets, are surfaced with a smooth clay where exposed; laboratory testing provided a friction angle of 28° for these surfaces.

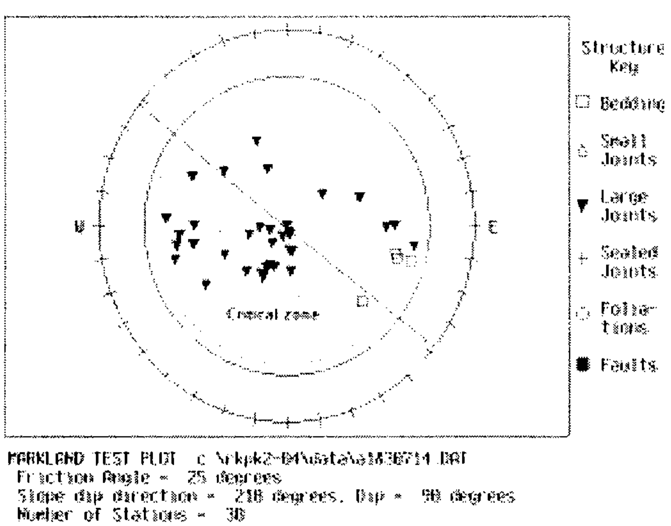

Figure 21. Stereonet plot of discontinuities taken from left side of Smart Road, cut slope dip = 90°.

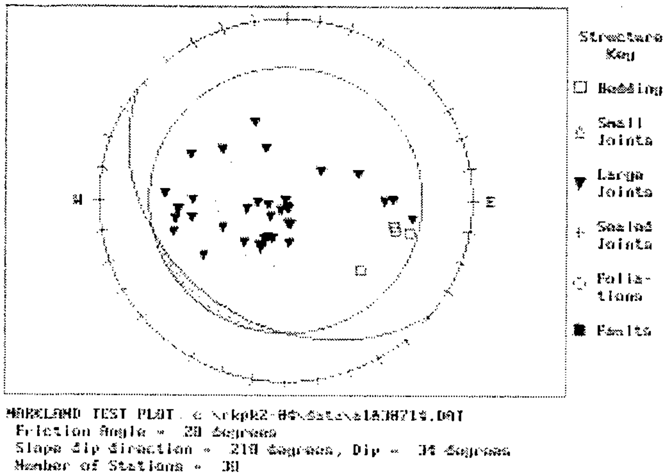

Figure 22. Stereonet plot of dixcontinuities taken from left side of Smart Road, cut slope = 34°.

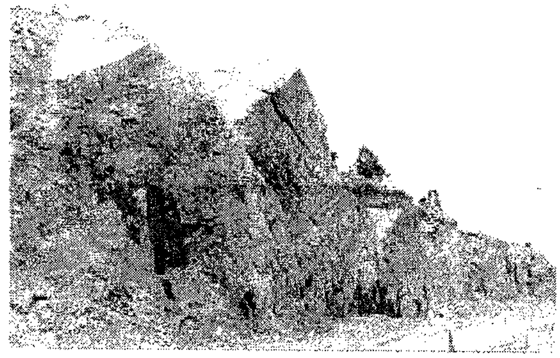
Figure 23. Sawtooth pattern formed by intersecting discontinuities on the right side of the Smart Road.

Figures 24 and 25 indicate stability conditions with respect to potential rock wedge failures as analyzed using stereonets on the right side of the cut; Figure 24 utilizes a 90° cut slope dip, and figure 25 utilizes a 34° cut slope dip. Potential rock wedge sliding is identified on the stereonet by the intersections with great circles representing clusters of discontinuities. If great circle intersections fall within the shaded critical zone, wedge failures are possible. In Figure 21, the wedge intersections of concern lie at the edge of the shaded critical zone in the northeastern portion of the stereonet and are considered to be likely failures at the 90°. However, it is noted that even if the slope is laid back to the proposed angle of 34°, the potential for wedge failures still exists. Safety factor calculations based on limiting equilibrium procedures using laboratory test data for the samples collected at the site indicated that the existing wedges would have safety factor values of 0.0 under saturated conditions (wedge

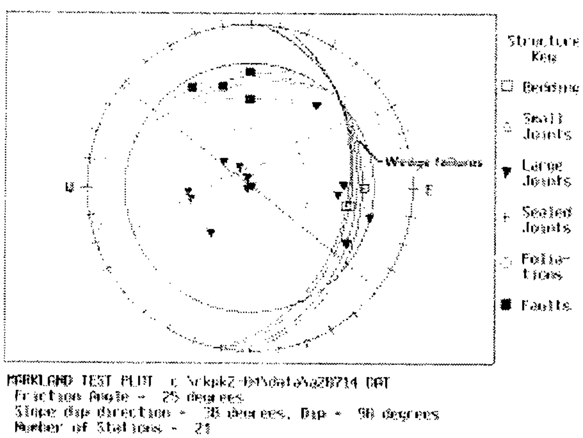

Figure 24. Stereonet showing wedges formed by intersecting great circles; taken from right side of Smart Road, cut slope dip = 90°.

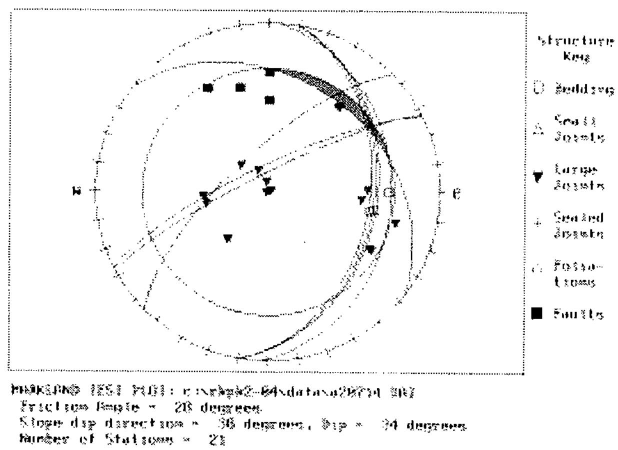

Figure 25. Stereonet showing wedges formed by intersecting great circles; taken from right side of Smart Road, cut slope dip = 34°.

floats) and 1.33 under dry conditions. Note that the positions of the intersection areas on the stereonet indicate that the axes of the wedges dip very gently, having angles of approximately 25°. As such, laying the slope back to an angle of 34° would not eliminate the potential for low angle wedge failures on the right side of the cut.

As of this writing, VDOT is currently in the process of laying back the left slope to an angle of 1.5:1. However, based on the slope stability analysis, it appears that the right side of the cut will continue to be subject to potential rockslides of various magnitudes. As such, VDOT plans call for the right side of the cut to be laid back to an angle of 2:1 (30°) with the likely addition of slope monitoring instrumentation for detection of potential slope movements.

REFERENCES CITED

Bartholomew, M.J., 1981, Geology of the Roanoke and Stewartsville quadrangles, Virginia, Virginia Division of Mineral Resources Publication 34, 23 p

Bartholomew, M.J., Schultz, A.P., Lewis, S.E., McDowell, R. C., and Henika, W.S., 1999, Bedrock Geologic Map of the Radford 30 by 60 minute quadrangle, Virginia-West Virginia, Virginia Division of Mineral Resources, Digital Publication (in preparation).

Berquist and Bailey, 1998, Late Cenozoic Faulting in the Fall Zone, Southeastern Virginia, Geological Society of America, Abstracts with Programs, v.30, no. 7, p. 126.

Bolinger, G.A., and Hooper, Margaret G., 1972, The Earthquake History of Virginia, 1900 to 1970: Virginia Tech Department of Geological Sciences, Blacksburg, Va., 85 p.

Butts, Charles, 1941, Geology of Appalachian Valley in Virginia, Virginia Geological Survey Bulletin 52, 566 p.

Cato, K. D., Gelinas, R., Kemppinen, H., and Amick, D., 1994, The genesis of Mountain Lake: A landslide dam origin (abs.): Assoc. of Engineering Geologists, 37th Annual Meeting, Williamsburg, VA, Program and Abstracts, p. 42.

Cawley, J. C., and Parker, B. C., 1999, New observations on the geomorphology and origins of Mountain Lake, Virginia (abs.): Geological Society of America Abstracts with Programs, v. 31, p. A-10.

Cooper, B. N., 1961, Grand Appalachian excursion: Virginia Polytechnic Institute Engineering Extension Series, Geological Guidebook No. 1, Blacksburg, 187 p.

Dietrich, R. V., 1970, Geology and Virginia: Virginia Division of Mineral Resources, Charlottesville, 213 p.

Frye, K., 1986, Roadside Geology of Virginia: Mountain Press Publishing Co., Missoula, MT, 278 p.

Granger, Darryl E.; Kirchner, James W.; Finkel, Robert C., 1997: Quaternary downcutting rate of the New River, Virginia, measured from differential decay of cosmogenic (super 26) Al and (super 10) Be in cave-deposited alluvium, Geology (Boulder), v. 25, n. 2, p. 107-110.

Harbor, D. J., 1998 River Incision produced by Punctuated Landscape Evolution in the Valley and Ridge of Virginia, in Geology of Eastern Rockbridge County, 28th Annual Virginia Geologic Field Conference Guidebook, Edited by N.H.Evans, Virginia Division of Mineral Resources, Charlottesville Va., p. 21-29.

Johnson, R.W., Jr., Milton, Charles, and Dennison, J.M., 1971, Fieldtrip to the igneous rocks of Augusta, Highland and Bath Counties, Virginia: Virginia Division of Mineral Resources Information Circ. 16, p.53.

Henika, W.S., 1981, Geology of the Villamont and Montvale quadrangles, Virginia: Virginia Division of Mineral Resources , Publication 35, 18 p.

———————, 1997a, Geologic Map of the Roanoke 30 by 60 minute quadrangle: Virginia Division of Mineral Resources Publication 148.

————————, 1997b, Economic and Environmental Geology across the boundary between the Blue Ridge and the Valley and Ridge near Roanoke, Virginia: 27th annual Virginia Geologic Field Conference Guidebook, Virginia Division of Mineral Resources, Department of Geological Sciences, Virginia Polytechnic Institute and State University, Blacksburg VA, 23 p.

Holsinger, J.R., 1975, Description of Virginia Caves, Virginia Division of Mineral Resources Bulletin 85, 450 p.

Martin, Ray E. and Werner, Stephen G., 1985, Preliminary Geotechnical Engineering Study, West County Reservoir, Roanoke County, Virginia: Schnabel Engineering Associates, Inc., Richmond, Virginia.

Mills, H. H., 1988, Surficial geology and geomorphology of the Mountain Lake area, Giles County, Virginia, including sedimentological studies of colluvium and boulder streams: U. S. Geological Survey Professional Paper 1469, 57 p.

Rader, E. K., and Gathright, T. M., II, 1985, Geologic map of the Narrows quadrangle, Virginia: Virginia Division of Mineral Resources Field Map File.

Samford, W. J., 1981, An investigation of the Narrows landslide, Giles County, Virginia [MS thesis]: Virginia Polytechnic Institute and State University, Blacksburg, 110 p.
Samford, W. J., 1983, Narrows landslide, Giles County, Virginia: Virginia Division of Mineral Resources, Virginia Minerals, v. 29, n. 4, p. 37-44.

Schultz, A. P., Stanley, C. B., Gathright, T. M., II, Rader, E. K., Bartholomew, M. J., Lewis, S. E., and Evans, N. H., 1986, Geologic map of Giles County, Virginia: Virginia Division of Mineral Resources Publication 69.

Spangler, D.P., Larew, H.G., and Meadors, G.S., 1964, The Hollins landslide on Interstate 81: Virginia Journal of Science, New Series, Vol. 15 no. 4, p. 335.

Watts, C. F., and Whisonant, R. C., 1994, Slope stability problems along highway cuts in the Virginia Valley and Ridge, *in* Schultz, A., and Henika, B., editors, Fieldguides to Southern Appalachian structure, stratigraphy, and engineering geology: Virginia Tech Department of Geological Sciences Guidebook No. 10, p. 229-248.

Whisonant, R. C., and Watts, C. F., 1993, Neotectonic investigations in the southeastern United States, Part I: Potential seismic triggering of giant bedrock landslides and suspected mass movements at Mountain Lake in the Giles County Seismic Zone, Virginia: Report prepared for Ebasco Services, Inc., Greensboro, NC, 62 p.

Williams,G.P., and Guy, H.P., 1973, Erosional and depositional aspects of Hurricane Camille in Virginia , 1969: U.S. Geological Survey Professional Paper 804, 80 p.

Woodward, H.P. 1932, Geology and Mineral Resources of the Roanoke area, Virginia: Virginia Geological Survey Bulletin 34, 172 p.

Appendix:

HGS Proceedings Availability List

HIGHWAY GEOLOGY SYMPOSIUM PROCEEDINGS
- Availability List -

Symposium/Date	Sponsor	Availability	Price
First (1950)			
Second (1951)			
Third (1952)		The First 10 Symposia "Proceedings" are contained in a 3 volume set.	
Fourth (1953)			
Fifth (1954)			
Sixth (1955)		A Limited Number of These Volumes are available at $20.00 a set.	
Seventh (1956)			
Eighth (1957)			
Ninth (1958)			
Tenth (1959)			
Eleventh (1960)	Florida State Univ. Tallahassee, Florida	Out of Print	
Twelfth (1961)	Univ. of Tennessee Knoxville, Tennessee	Out of Print	
Thirteenth (1962)	Phoenix, Arizona	Out of Print	
Fourteenth (1963)	Texas Highway Dept. College Station, Texas	Out of Print	
Fifteenth (1964)	Missouri Geol. Survey Rolla, Missouri	Out of Print	

Symposium/Date	Sponsor	Availability	Price
Sixteenth (1965)	Univ. of Kentucky Lexington, Kentucky	Out of Print	
Seventeenth (1966)	Iowa State Univ. Iowa State Hwy. Comm. Ames, Iowa	F. R. Glass*	$6.00
Eighteenth (1967)	Purdue University and Indiana Highway Commission	Professor Terry West Civil Engineering Dept. Purdue University West LaFayette, Indiana	
Nineteenth (1968)	West Virginia Geol. and Economic Survey	W. Virginia Geological and Economic Survey P. O. Box 879 Morganton, W. Va. 26505 (Circular 10)	$20.00
Twentieth (1969)	Univ. of Illinois	Out of Print	
Twenty-First (1970)	State Highway Commission of Kansas	Out of Print	
Twenty-Second (1971)	Oklahoma Geol. Survey and Oklahoma Dept. of Highways	Oklahoma Geological Survey University of Oklahoma Norman, Oklahoma	
Twenty-Third (1972)	Virginia Hwy. Research Council, Virginia Dept. of Highways	Highway Geologist Virginia Dept. of Highways Richmond, Virginia	
Twenty-Fourth (1973)	Wyoming State Highway Department	Out of Print	
Twenty-Fifth (1974)	North Carolina Dept. of Transportation	Out of Print	

Symposium/Date	Sponsor	Availability	Price
Twenty-Sixth (1975)	Idaho Transportation Department	R. G. Charboneau Chief Geologist Idaho Dept. of Highways P. O. Box 7129 Boise, Idaho 83707	
Twenty-Seventh (1976)	Florida Department of Transportation and Univ. of Florida	F. R. Glass*	$20.00
Twenty-Eighth (1977)	South Dakota School of Mines	Out of Print	
Twenty-Ninth (1978)	Maryland State Hwy. Administration and Maryland Geological Survey	Publications Dept. Maryland Geol. Survey 711 W. 40th Street Suite 440 Baltimore, Maryland 21314	$20.00
Thirtieth (1979)	FHWA at Portland, Oregon	F. R. Glass*	$20.00
Thirty-First (1980)	Bureau of Econ. Geol. Texas Dept. of Highways	F. R. Glass*	$20.00
Thirty-Second (1981)	Tennessee Department of Transportation	F. R. Glass*	$20.00
Thirty-Third (1982)	Colorado Dept. of Highways Colorado Geol. Survey USDA Forest Service	Colorado Geol. Surv. Dept. of Nat. Resources 1313 Sherman Street Denver, Colorado 80203	$20.00
Thirty-Fourth (1983)	Georgia Department of Transportation	F. R. Glass*	$20.00
Thirty-Fifth (1984)	California Dept. of Transportation San Jose State Univ.	F. R. Glass*	$20.00

Symposium/Date	Sponsor	Availability	Price
Thirty-Sixth (1985)	Kentucky Department of Transportation School of Civil Eng. Purdue University	F. R. Glass*	$20.00
Thirty-Seventh (1986)	Montana Department of Highways Montana Div. - FHWA	F. R. Glass*	$20.00
Thirty-Eighth (1987)	Pennsylvania Dept. of Transportation Engineer's Society of Western Pennsylvania	F. R. Glass*	$20.00
Thirty-Ninth (1988)	Utah Dept. of Trans. Utah Geological and Mineral Survey Brigham Young University	F. R. Glass*	$20.00
Fortieth (1989)	Alabama Highway Department	F. R. Glass*	$20.00
Forty-First (1990)	New Mexico State Hwy. and Transportation Dept. & New Mexico State Univ. Department of Civil, Agricultural and Geological Engineering	F. R. Glass*	$20.00
Forty-Second (1991)	American Society of Civil Engineers, American Inst. of Professional Geologists, NYSDOT, New York State Geological Survey	F. R. Glass*	$20.00
Forty-Third (1992)	Univ. of Arkansas Dept. of Civil Engineering, Arkansas State Highway and Transportation Department, Arkansas Geological Commission	F. R. Glass*	$20.00

Symposium/Date	Sponsor	Availability	Price
Forty-Fourth (1993)	Univ. of South Florida Dept. of Civil Engineering Florida Dept. of Transportation	F. R. Glass*	$20.00
Forty-Fifth (1994)	Portland State Univ. Oregon Dept. of Transportation Washington Dept. of Transportation Transportation Research Board	F. R. Glass*	$20.00
Forty-Sixth (1995)	West Virginia Geological and Economic Survey West Virginia Div. of Highways West Virginia University Transportation Research Board	F. R. Glass*	$20.00
Forty-Seventh (1996)	Wyoming Dept. of Trans. Wyoming Geological Survey	F. R. Glass*	$20.00
Forty-Eighth (1997)	Tenn. Dept. of Transportation Univ. of Tennessee: Dept. of Geological Sciences Institute for Geotechnology, Dept. of Civil Eng., Tenn. Division of Geology, Trans. Research Board	F. R. Glass*	$20.00
Forty-Ninth	Arizona Dept. of Transportation Materials Group Arizona Geological Survey Northern Arizona University, Dept. of Geology	F.R. Glass	$30.00

PLEASE NOTE: The price listed does not include the charge for postage and handling. These charges will be added to the price listed. Copies of papers are $5.00 each plus postage and handling.

* Highway Geology Symposium
c/o F. R. Glass
North Carolina Dept. of Transportation
Geotechnical Unit
P. O. Box 3279
Asheville, North Carolina 28802
(704) 298-7599